

**Earth Resources Earth R
rces Earth Resources Ea
Resources Earth Resou
arth Resources Earth Re
ces Earth Resources Ea
Resources Earth Resou
Earth Resources Earth F
rcer Earth Resources Ea
resources Earth Resource**

(NASA-SP-7041(63)) EARTH RESOURCES: A
CONTINUING BIBLIOGRAPHY WITH INDEXES (ISSUE
63) (NASA) 128 D N90-12091
CSCL 08B
Unclass
00/43 0243085

ACCESSION NUMBER RANGES

Accession numbers cited in this Supplement fall within the following ranges.

STAR (N-10000 Series) N89-20086 — N89-25112

IAA (A-10000 Series) A89-32451 — A89-43640

EARTH RESOURCES

A CONTINUING BIBLIOGRAPHY WITH INDEXES

Issue 63

A selection of annotated references to unclassified reports and journal articles that were introduced into the NASA scientific and technical information system and announced between July 1 and September 30 in

- *Scientific and Technical Aerospace Reports (STAR)*
- *International Aerospace Abstracts (IAA).*



National Aeronautics and Space Administration
Office of Management
Scientific and Technical Information Division
Washington, DC

1989

This supplement is available from the National Technical Information Service (NTIS), Springfield, Virginia 22161, price code A07.

INTRODUCTION

The technical literature described in this continuing bibliography may be helpful to researchers in numerous disciplines such as agriculture and forestry, geography and cartography, geology and mining, oceanography and fishing, environmental control, and many others. Until recently it was impossible for anyone to examine more than a minute fraction of the Earth's surface continuously. Now vast areas can be observed synoptically, and changes noted in both the Earth's lands and waters, by sensing instrumentation on orbiting spacecraft or on aircraft.

This literature survey lists 449 reports, articles, and other documents announced between July 1 and September 30, 1989 in *Scientific and Technical Aerospace Reports (STAR)*, and *International Aerospace Abstracts (IAA)*.

The coverage includes documents related to the identification and evaluation by means of sensors in spacecraft and aircraft of vegetation, minerals, and other natural resources, and the techniques and potentialities of surveying and keeping up-to-date inventories of such riches. It encompasses studies of such natural phenomena as earthquakes, volcanoes, ocean currents, and magnetic fields; and such cultural phenomena as cities, transportation networks, and irrigation systems. Descriptions of the components and use of remote sensing and geophysical instrumentation, their subsystems, observational procedures, signature and analyses and interpretive techniques for gathering data are also included. All reports generated under NASA's Earth Resources Survey Program for the time period covered in this bibliography are also included. The bibliography does not contain citations to documents dealing mainly with satellites or satellite equipment used in navigation or communication systems, nor with instrumentation not used aboard aerospace vehicles.

The selected items are grouped in nine categories. These are listed in the Table of Contents with notes regarding the scope of each category. These categories were especially chosen for this publication, and differ from those found in *STAR* and *IAA*.

Each entry consists of a standard bibliographic citation accompanied by an abstract. The citations include the original accession numbers from the respective announcement journals.

Under each of the nine categories, the entries are presented in one of two groups that appear in the following order:

IAA entries identified by accession number series A89-10,000 in ascending accession number order;

STAR entries identified by accession number series N89-10,000 in ascending accession number order.

After the abstract section, there are seven indexes:

subject, personal author, corporate source, foreign technology, contract number, report/ accession number, and accession number.

TABLE OF CONTENTS

	Page
Category 01 Agriculture and Forestry	1
Includes crop forecasts, crop signature analysis, soil identification, disease detection, harvest estimates, range resources, timber inventory, forest fire detection, and wildlife migration patterns.	
Category 02 Environmental Changes and Cultural Resources	4
Includes land use analysis, urban and metropolitan studies, environmental impact, air and water pollution, geographic information systems, and geographic analysis.	
Category 03 Geodesy and Cartography	6
Includes mapping and topography.	
Category 04 Geology and Mineral Resources	9
Includes mineral deposits, petroleum deposits, spectral properties of rocks, geological exploration, and lithology.	
Category 05 Oceanography and Marine Resources	15
Includes sea-surface temperature, ocean bottom surveying imagery, drift rates, sea ice and icebergs, sea state, fish location.	
Category 06 Hydrology and Water Management	17
Includes snow cover and water runoff in rivers and glaciers, saline intrusion, drainage analysis, geomorphology of river basins, land uses, and estuarine studies.	
Category 07 Data Processing and Distribution Systems	19
Includes film processing, computer technology, satellite and aircraft hardware, and imagery.	
Category 08 Instrumentation and Sensors	47
Includes data acquisition and camera systems and remote sensors.	
Category 09 General	64
Includes economic analysis.	
Subject Index	A-1
Personal Author Index	B-1
Corporate Source Index	C-1
Foreign Technology Index	D-1
Contract Number Index	E-1
Report Number Index	F-1
Accession Number Index	G-1

TYPICAL REPORT CITATION AND ABSTRACT

NASA SPONSORED
 ↓
 ON MICROFICHE

ACCESSION NUMBER → **N89-14479*#** Kansas Univ. Center for Research, Inc., Lawrence. ← **CORPORATE SOURCE**
 Radar Systems and Remote Sensing Lab.

TITLE → **INVESTIGATION OF RADAR BACKSCATTERING FROM SECOND-YEAR SEA ICE**

AUTHORS → GUANG-TSAI LEI, RICHARD K. MOORE, and S. P. GOGINENI

PUBLICATION DATE → Feb. 1988 67 p

CONTRACT NUMBERS → (Contract NASA ORDER W-16712; N00014-85-0200)

REPORT NUMBERS → (NASA-CR-180986; NAS 1.26:180986; RSL-TR-3311-7) Avail: NTIS ← **AVAILABILITY SOURCE**
 HC A04/MF A01 CSCL 08L ← **COSATI CODE**

The scattering properties of second-year ice were studied in an experiment at Mould Bay in April 1983. Radar backscattering measurements were made at frequencies of 5.2, 9.6, 13.6, and 16.6 GHz for vertical polarization, horizontal polarization and cross polarizations, with incidence angles ranging from 15 to 70 deg. The results indicate that the second-year ice scattering characteristics were different from first-year ice and also different from multiyear ice. The fading properties of radar signals were studied and compared with experimental data. The influence of snow cover on sea ice can be evaluated by accounting for the increase in the number of independent samples from snow volume with respect to that for bare ice surface. A technique for calculating the snow depth was established by this principle and a reasonable agreement has been observed. It appears that this is a usable way to measure depth in snow or other snow-like media using radar.

Author

TYPICAL JOURNAL ARTICLE CITATION AND ABSTRACT

NASA SPONSORED
 ↓
 ON MICROFICHE

ACCESSION NUMBER → **A89-12756*#** Michigan State Univ., East Lansing.

TITLE → **EVALUATING LANDSAT CLASSIFICATION ACCURACY FROM FOREST COVER-TYPE MAPS**

AUTHOR → W. D. HUDSON (Michigan State University, East Lansing) ← **AUTHOR'S AFFILIATION**

JOURNAL TITLE → Journal of Remote Sensing (ISSN 0008-2821), vol. 13, July 1987, p. 39-42. refs ← **PUBLICATION DATE**

CONTRACT NUMBER → (Contract NGL-23-004-083)

The use of complete enumeration in the form of photointerpreted forest cover-type maps to evaluate the accuracy of Landsat classifications was compared with assessments made directly from the aerial photography. A computerized, geographic information system was utilized to compare the Landsat classifications with the cover-type maps on a pixel-by-pixel basis. Error maps of pixels which were similarly misclassified by a variety of algorithms contained a larger number of errors than were verified from the aerial photography. For the two test sites studied, only 67 and 52 percent of the pixels which were originally considered to be in error were substantiated as being in error. Discrepancies between the two results were primarily caused by definitional difference between the cover-type maps and the Landsat classifications, especially with regard to minimum-type size and crown closure estimates of forest land.

C.D.

EARTH RESOURCES

A Continuing Bibliography (Issue 63)

OCTOBER 1989

01

AGRICULTURE AND FORESTRY

Includes crop forecasts, crop signature analysis, soil identification, disease detection, harvest estimates, range resources, timber inventory, forest fire detection, and wildlife migration patterns.

A89-33867*# National Aeronautics and Space Administration. John C. Stennis Space Center, Bay Saint Louis, MS.
MEASUREMENTS OF SHORT-TERM THERMAL RESPONSES OF CONIFEROUS FOREST CANOPIES USING THERMAL SCANNER DATA

J. C. LUVALL and H. R. HOLBO (NASA, Stennis Space Center, Bay Saint Louis, MS) Remote Sensing of Environment (ISSN 0034-4257), vol. 27, Jan. 1989, p. 1-10. refs

Thermal Infrared Multispectral Scanner (TIMS) data were collected over a coniferous forest in western Oregon. Concurrent radiosonde measurements of atmospheric profiles of air temperature and moisture provided inputs to LOWTRAN6 for atmospheric radiance corrections of the TIMS data. Surface temperature differences measured by the TIMS over time between flight lines were combined with surface radiative energy balance estimates to develop thermal response numbers (TRN). These numbers characterized the thermal response of the different surface types. Barren surfaces had the lowest TRN, whereas the forested surfaces had the highest. Author

A89-33873#
LARGE-AREA CROP MONITORING WITH THE NOAA AVHRR - ESTIMATING THE SILKING STAGE OF CORN DEVELOPMENT

K. P. GALLO (NOAA, Satellite Research Laboratory, Washington, DC) and T. K. FLESCHE (Purdue University, West Lafayette, IN) Remote Sensing of Environment (ISSN 0034-4257), vol. 27, Jan. 1989, p. 73-80. refs

The silking stage is an important event in the growth and development of the corn plant. Weather conditions at this stage can be critical to the final grain yield of the crop. Knowledge of the time of occurrence of the silking stage, as well as the weather conditions at that time, is important to individuals concerned with monitoring grain yield. Field observations provide estimates of crop development within the U.S.; however, these data are not readily available for other areas. A satellite-based method of monitoring the silking stage was developed and compared to ground-based estimates of the occurrence of the silking stage. Several vegetation indices, computed from weekly composites of visible and near-IR data of the NOAA AVHRR, estimated the occurrence of silking over large areas within one week of ground-based estimates. These indices may be the preferred method of estimating the occurrence of silking over large areas known to be predominantly planted with corn when reliable or representative ground-based estimates are unavailable. Author

A89-34947
MONITORING THE HALFA STEPPES OF CENTRAL TUNISIA USING LANDSAT MSS

JUERGEN VOGT (Trier, Universitaet, Federal Republic of

Germany) ITC Journal (ISSN 0303-2434), no. 2, 1988, p. 178-187. refs

Halfa steppes (perennial grass plains) cover extended areas of northern Africa. An expansion of agriculture and multiple exploitation have resulted in their severe degradation and reduction in area. An attempt to map - and thereby monitor - the halfa steppes of central Tunisia using Landsat MSS data is described. Author

A89-35584
SOUNDING OF CROP FIELDS BY NANOSECOND RADIO PULSES [ZONDIROVANIE SEL'SKOKHOZIAISTVENNYKH POSEVOV RADIOIMPUL'SAMI NANOSEKUNDNOI DLITEL'NOSTI]

V. I. KARPUKHIN, A. N. PESHKOV, and M. I. FINKEL'SHTEIN Radiotekhnika i Elektronika (ISSN 0033-8494), vol. 34, March 1989, p. 550-556. In Russian. refs

Results of ground-based and airborne remote-sensing studies of crop fields using nanosecond radio pulses are presented. It is shown that there exists a linear relationship between the arrival-time differences of pulses reflected from the boundaries of crop fields and their height. B.J.

A89-35865*# Naval Civil Engineering Lab., Port Hueneme, CA.
GEOBOTANICAL DETERMINATION OF AGGREGATE SOURCE MATERIAL USING AIRBORNE THEMATIC MAPPER IMAGERY
TIMOTHY MINOR (U.S. Navy, Naval Civil Engineering Laboratory, Port Hueneme, CA), DAVID MOUAT (Nevada, University, Reno), and JEFF MYERS (NASA, Ames Research Center, Moffett Field, CA) IN: Thematic Conference on Remote Sensing for Exploration Geology, 6th, Houston, TX, May 16-19, 1988, Proceedings. Volume 1. Ann Arbor, MI, Environmental Research Institute of Michigan, 1988, p. 147-158. refs

The possible use of vegetation to discriminate parent materials for suitability as aggregate source material is examined. Airborne Thematic Mapper data of two test sites representing potential alluvial and residual source areas in central California were analyzed. It is found that the most useful images were composites that included principal components bands and a Perpendicular Vegetation Index band. The image processing demarcated species compositional differences which characterized a shale site and revealed differences in an alluvial site caused by moisture stress due to aggregate size and sorting. R.B.

A89-35893#
A CLOSER LOOK AT THE PATRICK DRAW OIL FIELD VEGETATION ANOMALY

L. F. SCOTT, R. M. MCCOY, and L. H. WULLSTEIN (Utah, University, Salt Lake City) IN: Thematic Conference on Remote Sensing for Exploration Geology, 6th, Houston, TX, May 16-19, 1988, Proceedings. Volume 2. Ann Arbor, MI, Environmental Research Institute of Michigan, 1988, p. 529-538. refs

The Patrick Draw, Wyoming sagebrush/grassland community, which is paradigmatic of the effects on vegetation of hydrocarbon microseepage, is visible as a tonal anomaly on Geosat imagery due to both the lower density of sagebrush and interspace grass, and the dieoff of some of the sagebrush, thereby revealing bare soil. It is presently suggested that gas seepage is not the reason for the area's visibility on Geosat imagery; this is instead held to

01 AGRICULTURE AND FORESTRY

be due to the anaerobic conditions in the root zone and/or dissolved salts in the soil-water solution, as a result of increased precipitation during 1978-1983. O.C.

A89-35894*# Dartmouth Coll., Hanover, NH.

A LANDSAT THEMATIC MAPPER INVESTIGATION OF THE GEOBOTANICAL RELATIONSHIPS IN THE NORTHERN SPRUCE-FIR FOREST, MT. MOOSILAUKE, NEW HAMPSHIRE
PAUL J. TORCOLETTI and RICHARD W. BIRNIE (Dartmouth College, Hanover, NH) IN: Thematic Conference on Remote Sensing for Exploration Geology, 6th, Houston, TX, May 16-19, 1988, Proceedings. Volume 2. Ann Arbor, MI, Environmental Research Institute of Michigan, 1988, p. 541-550. refs
(Contract NASW-4049)

This investigation, in the northern spruce-fir forest at Mt. Moosilauke, NH, indicates that Landsat TM data can be used to distinguish between and map major vegetation zones. Principal components analysis can be used to reduce the dimensionality of the TM data; and in this simpler spectral space, it is easier to visualize the discrimination between major vegetation zones: the northern hardwoods zone, spruce-fir zone, fir zone, and alpine tundra zone. The moisture stress index highlights areas of heavy forest damage (fir waves), but does not correlate with low levels of damage in the mixed, background forest at Mt. Moosilauke. Care must be taken to avoid confusion between high-elevation climatically-stressed vegetation (normal krummholz forest) and damaged lower elevation forests, both of which have similar TM5/TM4 ratio values. Author

A89-37320

THE CONDITION OF NATURAL FEATURES AS RELATED TO THEIR INTRINSIC MICROWAVE AND IR EMISSION FIELDS [O VZAIMOSVIAZI POLIA SOBSTVENNOGO SVCH- I IK-IZLUCHENIIA PRIRODNYKH OB'EKTOV S IKH SOSTOIANIEM]

E. A. REUTOV (AN SSSR, Institut Radiotekhniki i Elektroniki, Moscow, USSR) Issledovanie Zemli iz Kosmosa (ISSN 0205-9614), Jan.-Feb. 1989, p. 70-76. In Russian. refs

The relationship between the condition of farming areas and their microwave and infrared emission fields is analyzed. The possibility of using remote microwave and IR radiometry data and meteorological information about air temperature to evaluate crop state is assessed. B.J.

A89-37949

THE DISCRIMINATION OF IRRIGATED ORCHARD AND VINE CROPS USING REMOTELY SENSED DATA

H. D. WILLIAMSON (New South Wales, University, Kensington, Australia) Photogrammetric Engineering and Remote Sensing (ISSN 0099-1112), vol. 55, Jan. 1989, p. 77-82. refs

Multispectral data recorded by a SPOT HRV sensor and an airborne Daedalus 1268 ATM sensor were analyzed for use in the monitoring of irrigated orchard and vine crops in the Riverland of South Australia. The spectral data were essentially two-dimensional and the additional bands and increased spatial resolution of the Daedalus 1268 ATM sensor over the SPOT HRV sensor did not provide useful additional information. An accuracy of 85 to 93 percent at the 95 percent confidence level was obtained for the classification of four orchard and vine crops using bands 2 and 3 of the SPOT HRV data. It is suggested that temporal data are required if the classification is to be extended successfully to include other crops and dryland farming areas. Author

A89-38969

THE INFLUENCE OF THE VIEWING GEOMETRY OF BARE ROUGH SOIL SURFACES ON THEIR SPECTRAL RESPONSE IN THE VISIBLE AND NEAR-INFRARED RANGE

JERZY CIERNIEWSKI (Poznan, Uniwersytet, Poland) Remote Sensing of Environment (ISSN 0034-4257), vol. 27, Feb. 1989, p. 135-142.

A89-39554* Jet Propulsion Lab., California Inst. of Tech., Pasadena.

MODELING AND OBSERVATION OF THE RADAR POLARIZATION SIGNATURE OF FORESTED AREAS

STEPHEN L. DURDEN, JAKOB J. VAN ZYL, and HOWARD A. ZEBKER (California Institute of Technology, Jet Propulsion Laboratory, Pasadena) IEEE Transactions on Geoscience and Remote Sensing (ISSN 0196-2892), vol. 27, May 1989, p. 290-301. Research supported by the U.S. Army. refs

To understand radar measurements of forested areas, the authors have developed a model of L-band (25-cm) microwave scattering from a forest. The forest floor is modeled as a rough dielectric surface above which is a layer of nearly vertical dielectric cylinders representing tree trunks. Above this layer is a second layer consisting of randomly oriented cylinders which represent branches. The authors identify several scattering mechanisms and calculate the corresponding Stokes matrices, which combine to give the total Stokes matrix and resulting polarization signature. It is found that this simple model permits accurate prediction of the polarization of the scattered waves and that additional mechanisms, including the effects of leaves and twigs, are not required for the 25-cm observation of the forests studied. The authors present measurements of the polarization signature acquired over a forested area and show comparisons with model calculations. I.E.

A89-39657

GEOBOTANICAL APPLICATION OF AIRBORNE THEMATIC MAPPER DATA IN SUTHERLAND, NORTH-WEST SCOTLAND

A. K. SARAF, A. P. CRACKNELL, and J. MCMANUS (Dundee, University, Scotland) International Journal of Remote Sensing (ISSN 0143-1161), vol. 10, March 1989, p. 545-555. refs

A89-39658* Science Applications International Corp., Washington, DC.

EFFECT OF METAL STRESS ON THE THERMAL INFRARED EMISSION OF SOYBEANS: A GREENHOUSE EXPERIMENT - POSSIBLE UTILITY IN REMOTE SENSING

R. SURESH, M. R. SCHWALLER (Science Applications International Corp., Washington, DC), C. D. FOY (USDA, Agricultural Research Service, Beltsville, MD), J. R. WEIDNER (Maryland, University, College Park), and C. S. SCHNETZLER (NASA, Goddard Space Flight Center, Greenbelt, MD) International Journal of Remote Sensing (ISSN 0143-1161), vol. 10, March 1989, p. 557-563. refs

Manganese-sensitive forest and manganese-tolerant lee soybean cultivars were subjected to differential manganese stress in loring soil in a greenhouse experiment. Leaf temperature measurements were made using thermistors for forest and lee. Manganese-stressed plants had higher leaf temperatures than control plants in both forest and lee. Results of this experiment have potential applications in metal stress detection using remote sensing thermal infrared data over large areas of vegetation. This technique can be useful in reconnaissance mineral exploration in densely-vegetated regions where conventional ground-based methods are of little help. Author

A89-40149

A PHENOLOGICAL DESCRIPTION OF IBERIAN VEGETATION USING SHORT WAVE VEGETATION INDEX IMAGERY

DANIEL LLOYD (Bristol, University, England) (Rutherford Appleton Laboratory, Meteorological Office, ESA, et al., Applications of AVHRR data: European AVHRR Data Users' Meeting, 3rd, Oxford, England, Dec. 16-18, 1987) International Journal of Remote Sensing (ISSN 0143-1161), vol. 10, Apr.-May 1989, p. 827-833. refs
(Contract NERC-GT/4/83/TLS/6/)

The phenology of Iberian vegetation is described using twelve full resolution Advanced Very High Resolution Radiometer short wave vegetation index images for the period April to October 1985 and 1986. The characteristics of the most appropriate vegetation classification scheme for use with these data are discussed. Author

A89-40150

MONITORING THE PHENOLOGY OF TUNISIAN GRAZING LANDS

P. J. KENNEDY (Reading, University, England) (Rutherford Appleton Laboratory, Meteorological Office, ESA, et al., Applications of AVHRR data: European AVHRR Data Users' Meeting, 3rd, Oxford, England, Dec. 16-18, 1987) International Journal of Remote Sensing (ISSN 0143-1161), vol. 10, Apr.-May 1989, p. 835-845. Research supported by NERC. refs

A89-41153

CROP IDENTIFICATION USING MERGED LANDSAT MULTISPECTRAL SCANNER AND THEMATIC MAPPER DATA - PRELIMINARY ATTEMPTS

MAZLAN HASHIM (Technological University of Malaysia, Johor Bahru) IN: 1988 ACSM-ASPRS Annual Convention, Saint Louis, MO, Mar. 13-18, 1988, Technical Papers. Volume 4. Falls Church, VA, American Congress on Surveying and Mapping and American Society for Photogrammetry and Remote Sensing, 1988, p. 11-20. refs

The main objective of this paper is to assess the crop classification accuracies using the merged TM-MSS data compared to their original data over a selected test site. The study also evaluates the separability of spectral signatures of the studied crops in the selected test site. Author

A89-41155

USING TEXTURAL MEASURES TO DISTINGUISH SPECTRALLY SIMILAR VEGETATION

BRADLEY C. REED (Kansas Applied Remote Sensing, Lawrence) IN: 1988 ACSM-ASPRS Annual Convention, Saint Louis, MO, Mar. 13-18, 1988, Technical Papers. Volume 4. Falls Church, VA, American Congress on Surveying and Mapping and American Society for Photogrammetry and Remote Sensing, 1988, p. 40-49. refs

Vegetation mapping schemes using remote sensing have experienced problems with classes possessing wide spectral responses and with dissimilar classes that have overlapping spectral responses. Vegetation that is not distinguishable spectrally may be identified by its textural attributes. In this study, textural and spectral data were merged in a hierarchical manner to map a portion of Everglades National Park. Only pixels with a high probability of belonging to a category were classified spectrally with remaining pixels classified using textural measures. Results indicate that caution should be used when employing texture measures and that classification accuracy can be improved only under certain conditions. Author

A89-43317

MONITORING IN MONERAGALA DISTRICT, SRI LANKA, WITH SPOT IMAGES

DICK VAN DER ZEE (International Institute for Aerospace Survey and Earth Sciences, Enschede, Netherlands) and JULIE A. COX ITC Journal (ISSN 0303-2434), no. 3, 1988, p. 260-271. refs

N89-22163*# Desert Research Inst., Reno, NV. Biological Sciences Center.

EXAMINATION OF THE SPECTRAL FEATURES OF VEGETATION IN 1987 AVIRIS DATA

CHRISTOPHER D. ELVIDGE /In Jet Propulsion Lab., California Inst. of Tech., Proceedings of the Airborne Visible/Infrared Imaging Spectrometer (AVIRIS) Performance Evaluation Workshop p 97-101 15 Sep. 1988

Avail: NTIS HC A11/MF A01 CSCL 08/2

Equations for converting AVIRIS digital numbers to percent reflectance were developed using a set of three calibration targets. AVIRIS reflectance spectra from five plant communities exhibit distinct spectral differences. Author

N89-22167*# Delaware Univ., Newark.

AVIRIS SPECTRA OF CALIFORNIA WETLANDS

MICHAEL F. GROSS, SUSAN L. USTIN (California Univ., Davis.), and VYTAUTAS KLEMAS /In Jet Propulsion Lab., California Inst.

of Tech., Proceedings of the Airborne Visible/Infrared Imaging Spectrometer (AVIRIS) Performance Evaluation Workshop p 128-133 15 Sep. 1988 Prepared in cooperation with California Univ., Berkeley

Avail: NTIS HC A11/MF A01 CSCL 08/2

Spectral data gathered by the AVIRIS from wetlands in the Suisun Bay area of California on 13 October 1987 were analyzed. Spectra representing stands of numerous vegetation types (including *Sesuvium verrucosum*, *Scirpus acutus* and *Scirpus californicus*, *Xanthium strumarium*, *Cynodon dactylon*, and *Distichlis spicata*) and soil were isolated. Despite some defects in the data, it was possible to detect vegetation features such as differences in the location of the chlorophyll red absorption maximum. Also, differences in cover type spectra were evident in other spectral regions. It was not possible to determine if the observed features represent noise, variability in canopy architecture, or chemical constituents of leaves. Author

N89-24015*# Florida Univ., Gainesville. Dept. of Engineering Sciences.

ADVANCED SPACE DESIGN PROGRAM TO THE UNIVERSITIES SPACE RESEARCH ASSOCIATION AND THE NATIONAL AERONAUTICS AND SPACE ADMINISTRATION Final Report, 1987-1988 Academic Year

GALE E. NEVILL, JR. Jun. 1988 264 p

(Contract NGT-21-002-080)

(NASA-CR-180450; NAS 1.26:180450) Avail: NTIS HC A12/MF A01 CSCL 06/3

The goal of the Fall 1987 class of EGM 4000 was the investigation of engineering aspects contributing to the development of NASA's Controlled Ecological Life Support System (CELSS). The areas investigated were the geometry of plant growth chambers, automated seeding of plants, remote sensing of plant health, and processing of grain into edible forms. The group investigating variable spacing of individual soybean plants designed growth trays consisting of three dimensional trapezoids arranged in a compact circular configuration. The automated seed manipulation and planting group investigated the electrical and mechanical properties of wheat seeds and developed three seeding concepts based upon these properties. The plant health and disease sensing group developed a list of reliable plant health indicators and investigated potential detection technologies.

N89-24685# Instituto de Pesquisas Espaciais, Sao Jose dos Campos (Brazil). Ministerio da Ciencia e Tecnologia.

MICROWAVE X-BAND RADIOMETRIC CHARACTERIZATION OF BRAZILIAN SOILS BY MEASUREMENT OF THE COMPLEX PERMITTIVITY

ULF WALTER PALME Jun. 1988 7 p Presented at IGARSS '88, Edinburgh, Scotland, 15 Sep. 1988

(INPE-4588-PRE/1319) Avail: NTIS HC A02/MF A01

The main activities and strategies in microwave radiometry are described for applications in agriculture in Brazil. Some relevant results regarding measurements of the complex permittivity (epsilon*) and estimates of emissivity for soils from tropical areas in function of soil moisture, at 10.62 GHz, are presented. Difficulties related to the measurement of epsilon* and mu* of important Brazilian soils (dielectric/ferromagnetic mixture) are highlighted. Author

N89-24687*# Michigan Univ., Ann Arbor. School of Natural Resources.

ESTIMATING POPULATION SIZE OF PYGOSCELID PENGUINS FROM TM DATA Final Report

CHARLES E. OLSON, JR., MATHEW R. SCHWALLER, and PAUL A. DAHMER (Environmental Research Inst. of Michigan, Ann Arbor.) Aug. 1987 45 p

(Contract NAS5-28755)

(NASA-CR-180081; NAS 1.26:180081) Avail: NTIS HC A03/MF A01 CSCL 06/3

An estimate was made toward a continent wide population of penguins. The results indicate that Thematic Mapper data can be used to identify penguin rookeries due to the unique reflectance

02 ENVIRONMENTAL CHANGES AND CULTURAL RESOURCES

properties of guano. Strong correlations exist between nesting populations and rookery area occupied by the birds. These correlations allow estimation of the number of nesting pairs in colonies. The success of remote sensing and biometric analyses leads one to believe that a continent wide estimate of penguin populations is possible based on a timely sample employing ground based and remote sensing techniques. Satellite remote sensing along the coastline may well locate previously undiscovered penguin nesting sites, or locate rookeries which have been assumed to exist for over a half century, but never located. Observations which found that penguins are one of the most sensitive elements in the complex of Southern Ocean ecosystems motivated this study. Author

02

ENVIRONMENTAL CHANGES AND CULTURAL RESOURCES

Includes land use analysis, urban and metropolitan studies, environmental impact, air and water pollution, geographic information systems, and geographic analysis.

A89-32756

DIRECT OZONE DEPLETION IN SPRINGTIME ANTARCTIC LOWER STRATOSPHERIC CLOUDS

D. J. HOFMANN (Wyoming, University, Laramie) *Nature* (ISSN 0028-0836), vol. 337, Feb. 2, 1989, p. 447-449. Research supported by NSF. refs

Balloon measurements of ozone and cloud particles in the lower stratosphere made at McMurdo Station, Antarctica, on September 9, 1988 are presented which indicate that the cloud particles are directly involved in ozone depletion in this region. The reductions in ozone appear to be correlated with high concentrations of smaller particles of about 0.2 micron radius which dominate the surface area density in the cloud. The observations suggest a high degree of spatial inhomogeneity of free chlorine, associated with lower stratospheric clouds, and are important in understanding ozone depletion in this region. C.D.

A89-34946

RURAL SETTLEMENT EXPANSION IN MONERAGALA DISTRICT, SRI LANKA

DICK VAN DER ZEE (International Institute for Aerospace Survey and Earth Sciences, Enschede, Netherlands) *ITC Journal* (ISSN 0303-2434), no. 2, 1988, p. 155-164. refs

Land use changes, farming systems, and land tenure systems are analyzed for the Moneragala district, a region of rapidly increasing population in Sri Lanka. The analysis is based on aerial photographs from 1956, the early 1970s, and 1982. Land use and land cover maps were digitized and put into a geographic information system for analysis. The observed changes in land use and land cover are described in detail and recommendations are made for preventing the sudden increase in population from permanently damaging the environment. R.B.

A89-38897 Los Alamos National Lab., NM.

SPACELAB 2 UPPER ATMOSPHERIC MODIFICATION EXPERIMENT OVER ARECIBO. II - PLASMA DYNAMICS

P. A. BERNHARDT (Los Alamos National Laboratory, NM), W. E. SWARTZ, M. C. KELLY (Cornell University, Ithaca, NY), M. P. SULZER (Arecibo Observatory, PR), and S. T. NOBLE (Rice University, Houston, TX) *Astrophysical Letters and Communications* (ISSN 0888-6512), vol. 27, no. 3, 1988, p. 183-198. Research supported by NASA and DOE. refs (Contract NSF ATM-85-21180)

Results are presented from an experiment performed on Spacelab 2 over Arecibo to study the neutral gas dynamics of supersonic flows in a rarefield atmosphere and to modify the plasma density by releasing chemically reactive vapors. Exhaust vapor

was released at an altitude of 317 km, where the plasma density was 300,000/cu cm. Observations were made with high resolution incoherent scatter radar. A localized depletion formed in the ionosphere. The depletion fell and eventually disappeared within the bottomside F-region ionosphere. The dynamics of the evolution of the depletion are discussed. Optical and radar data are compared, setting an upper limit of 3 percent for the branching ratio to produce O(D-1) from dissociative recombination of CO(2+) and electrons. R.B.

A89-39739

MONITORING THE GREENHOUSE EFFECT FROM SPACE

BHUPENDRA JASANI (Royal United Services Institute, London, England) *Space Policy* (ISSN 0265-9646), vol. 5, May 1989, p. 94-98. refs

The use of outer space observations to monitor global changes in the environment is examined. The greenhouse effect is described and satellites monitoring the earth's atmosphere are listed. Consideration is given to the proposed Earth Observation System to study long- and short-term weather and climatic changes using satellites and instruments on polar platforms. It is recommended that an international cooperative environmental monitoring program should be established. R.B.

N89-20534# Beleidscommissie Remote Sensing, Delft (Netherlands). Research Inst. for Forestry and Landscape Planning.

THE SUITABILITY OF REMOTE SENSING FOR SURVEYING AND MONITORING LANDSCAPE PATTERNS. VOLUME A: PILOT STUDY - LANDSAT IMAGERY. VOLUME B: PEPS PROJECT NO. 73 - SPOT IMAGERY

J. M. J. FARJON Feb. 1988 79 p Original contains color illustrations (BCRS-87-12-VOL-A/B; ETN-89-93871) Avail: NTIS HC A05/MF A01

The possibility of using LANDSAT Thematic Mapper and SPOT satellite imagery for land use mapping was studied. Image analysis and processing requirements, and the utilization of geographic information systems were investigated.

ESA

N89-20541# National Aerospace Lab., Amsterdam (Netherlands). Space Div.

LAND USE INVENTORY USING LANDSAT THEMATIC MAPPER IMAGERY TO STUDY ENVIRONMENTAL POLLUTION

F. B. VANDERLAAN, O. F. SCHOUMANS, and H. A. M. THUNNISSEN (Netherlands Soil Survey Inst., Wageningen.) 31 Aug. 1987 14 p Presented at the Willi Nordberg Symposium on Remote Sensing towards Operational Cartographic Application, Graz, Austria, Sep. 1987 (NLR-MP-87063-U; ETN-89-94042) Avail: NTIS HC A03/MF A01

The ability to obtain up-to-date information on agricultural land use from LANDSAT TM imagery by means of classification was investigated in a pilot study on a 50,000 ha area. The study was meant to supply information on agricultural land use that could not be obtained in other ways. Land use information was particularly required on the cultivation of maize and other crops, grasslands, coniferous and deciduous forest, and heather and grass-invaded heather. This information was to be used to investigate and to predict the effects of manure on soils, surface water, and ground water and the effects of national policies to solve the manure problems, caused by the rearing of large concentrations of animals in the part of the Netherlands studied. The accuracy of the results for the most important classes varies between 80 percent and over 95 percent. The result is due to the excellent quality and timing of the image, the ecological homogeneity of the area, and the spectral differentiation between the classes. ESA

N89-22189 Harvard Univ., Cambridge, MA.

ANTARCTIC OZONE: THEORY AND OBSERVATION Ph.D. Thesis

ROSS JAY SALAWITCH 1988 258 p Avail: Univ. Microfilms Order No.DA8901637

Observational data describing the phenomenology of the Antarctic ozone reduction are reviewed. Theories are presented to account for the observed ozone reductions while satisfying other available constraints. A discussion of the thermodynamic properties of solid phases containing HCl and HNO₃ is presented. The presence of clouds in the Antarctic stratosphere leads to the condensation and precipitation of HNO₃ and condensation and reaction of HCl. Both processes lead to the conversion of unreactive forms of chlorine to chlorine oxides, which participate in a sequence of chemical reactions that consume ozone. A chemical model that incorporates the influence of cloud catalyzed heterogeneous reactions is compared in detail to the interferometric measurements of HCl, ClONO₂, HNO₃, NO₂, and NO obtained over Antarctica. Model results are consistent with observed temporal trends of these species and reported trends for total column ozone. Loss of ozone is attributed to the catalytic influence of chlorine and bromine radicals in cycles. Constraints are then placed on the abundance of stratospheric bromine by the analysis of observations of OCIO over Antarctica. The diurnal variation of OCIO is consistent with 16 +/- 4 ppt of stratospheric bromine if a fraction of the overall ClO + BrO reaction proceeds through a channel resulting in the production of BrCl. Bromine levels in this range would contribute 20 percent of the total ozone loss. Finally, it is shown that the production of reactive chlorine oxides by heterogeneous processes depends on the initial concentration of HCl relative to the total amount of nitrogen oxides prior to the onset of condensation. Once HCl exceeds a critical value, the end products of the heterogeneous reaction are rapidly converted to chlorine oxide radicals. Dissert. Abstr.

N89-22192# Oak Ridge National Lab., TN.

**AIR POLLUTION EFFECTS FIELD RESEARCH FACILITY:
OZONE FLOW CONTROL AND MONITORING SYSTEM**

JIM A. MCEVERS, TERRY L. BOWERS (Westinghouse Electric Corp., Pittsburgh, PA.), and NELSON EDWARDS Jan. 1989 69 p

(Contract DE-AC05-84OR-21400)

(DE89-007922; ORNL/TM-10758) Avail: NTIS HC A04/MF A01

The Ozone Flow Control and Monitoring System was developed in 1986 for the controlled exposure of diverse plant species to various concentrations of ozone gas. Design, operation, and performance are described for the automated system for generation, distribution, sampling, analysis, and control of ozone gas for plant exposure. The system has proved to be reliable, easy to maintain, and flexible in adapting to exposure programs. System software is reliable, and the user interface (CRT keyboard) is easy to use, providing quick-glance viewing of overall exposure conditions. The capability to expose plants to ozone concentrations in multiples of the ambient ozone level has been added, and software improvements in the areas of system response and user input are planned. DOE

N89-22969# National Aeronautics and Space Administration, Washington, DC.

EARTH SYSTEM SCIENCE: A PROGRAM FOR GLOBAL CHANGE

1989 305 p Original document contains color illustrations (NASA-TM-101186; NAS 1.15:101186) Avail: NTIS HC A14/MF A01 CSCL 08/5

The Earth System Sciences Committee (ESSC) was appointed to consider directions for the NASA Earth-sciences program, with the following charge: review the science of the Earth as a system of interacting components; recommend an implementation strategy for Earth studies; and define the role of NASA in such a program. The challenge to the Earth system science is to develop the capability to predict those changes that will occur in the next decade to century, both naturally and in response to human activity. Sustained, long-term measurements of global variables; fundamental descriptions of the Earth and its history; research foci and process studies; development of Earth system models; an information system for Earth system science; coordination of Federal agencies; and international cooperation are examined. B.G.

N89-23982# National Aeronautics and Space Administration, John F. Kennedy Space Center, Cocoa Beach, FL.

REVIEW OF WILDLIFE RESOURCES OF VANDENBERG AIR FORCE BASE, CALIFORNIA

DAVID R. BREININGER (Bionetics Corp., Cocoa Beach, FL.) Jan. 1989 71 p

(Contract NAS10-10285)

(NASA-TM-102146; NAS 1.15:102146) Avail: NTIS HC A04/MF A01 CSCL 13/2

Wildlife resources are reviewed for purposes of developing a Base Biological Monitoring Program (BMP) for Vandenberg Air Force Base (VAFB) in Santa Barbara County, California. The review and recommendations were prepared by review of applicable scientific literature and environmental documents for VAFB, discussing information needs with natural resource management professionals at VAFB, and observations of base field conditions. This process found that there are 29 federally listed vertebrates (endangered, threatened, or Category 2) that occur or may occur in the vicinity of VAFB. There are also 63 other state listed or regionally declining species that may occur in the vicinity of VAFB. Habitats of VAFB represent a very valuable environmental resource for rare and declining wildlife in California. However, little information is available on VAFB wildlife resources other than lists of species that occur or are expected to occur. Recommendations are presented to initiate a long-term wildlife monitoring program at VAFB to provide information for environmental impact assessment and wise land use planning. Author

N89-23985# Jet Propulsion Lab., California Inst. of Tech., Pasadena.

ENVIRONMENTAL PROJECTS. VOLUME 3: ENVIRONMENTAL COMPLIANCE AUDIT Final Report

15 Sep. 1987 255 p

(NASA-CR-185019; JPL-PUBL-87-4; NAS 1.26:185019) Avail: NTIS HC A12/MF A01 CSCL 13/2

The Goldstone Deep Space Communications Complex is part of NASA's Deep Space Network, one of the world's largest and most sensitive scientific telecommunications and radio navigation networks. Activities at Goldstone are carried out in support of six large parabolic dish antennas. In support of the national goal of the preservation of the environment and the protection of human health and safety, NASA, JPL and Goldstone have adopted a position that their operating installations shall maintain a high level of compliance with Federal, state, and local laws governing the management of hazardous substances, asbestos, and underground storage tanks. A JPL version of a document prepared as an environmental audit of Goldstone operations is presented. Both general and specific items of noncompliance at Goldstone are identified and recommendations are provided for corrective actions. Author

N89-24749# Argonne National Lab., IL. Biological, Environmental and Medical Research Div.

THE RELATIONSHIP BETWEEN IN-LAKE SULFATE CONCENTRATION AND ESTIMATES OF ATMOSPHERIC SULFUR DEPOSITION FOR SUBREGIONS OF THE EASTERN LAKE SURVEY

BARRY M. LESHT and JACK D. SHANNON Mar. 1989 14 p (Contract W-31-109-ENG-38)

(DE89-009868; ANL-9009868) Avail: NTIS HC A03/MF A01

Estimated amounts of the total sulfur deposition at each of the 1798 lakes in the U.S. Environmental Protection Agency's Eastern Lake Survey, obtained by using the ASTRAP model, were compared with the survey measurements of in-lake sulfate concentration on a subregional basis. In general, the sample median in-lake sulfate concentration was qualitatively correlated with the sample median estimated total sulfur deposition, with in-lake concentration increasing with increased estimated deposition. Two subregions, 3A (southern Blue Ridge) and 3B (Florida), however, did not fit this relationship. In-lake sulfate concentrations were higher than expected in Florida and lower than expected in the southern Blue Ridge. Comparison of our modeled total sulfur deposition with estimated amounts of wet-only

02 ENVIRONMENTAL CHANGES AND CULTURAL RESOURCES

sulfate deposition were in good agreement in terms of subregional rank order. More detailed comparison of the magnitudes of the estimates was not done because others reported deposition in terms of the estimated population medians, obtained by using a weighting procedure based on alkalinity map class, instead of as sample medians and also used the weighting procedure to estimate the subregional median in-lake sulfate concentration. DOE

N89-24759# Naval Postgraduate School, Monterey, CA.
CORRELATION BETWEEN SATELLITE-DERIVED AEROSOL CHARACTERISTICS AND OCEANIC DIMETHYLSULFIDE (DMS)
M.S. Thesis
RICHARD A. SHEMA Dec. 1988 57 p Original contains color illustrations
(AD-A206179) Avail: NTIS HC A04/MF A01 CSCL 04/1

Since the turn of the century, the earth's climate has fluctuated between warming and cooling cycles. A warming cycle has been observed in the early 1900's. The rising global temperature has been attributed to CO₂ release from the burning of fossil fuels. The absorption of IR energy emitted from the earth, or greenhouse effect, brought concern that continued warming would melt polar ice caps and permanently change global climate. However, beginning in the mid-1940's, atmospheric cooling was observed. A possible contribution to the cooling trend is an increase in the numbers of relatively small aerosol particles. These particles are efficient scatterers of solar radiation. An increase in the number of scattering events causes a higher albedo, thereby creating a cooler planet. McCormick and Ludwig (1967) have presented arguments to show this relationship. Approximately forty years later, in the early 1980's, warming of the earth's climate again has been observed. GRA

03

GEODESY AND CARTOGRAPHY

Includes mapping and topography.

A89-33661
LASER SCATTERING PHENOMENOLOGY - BACKGROUND SIGNATURE CHARACTERIZATION AND PREDICTION
DAVID L. MEEKER (U.S. Army, Engineer Waterways Experiment Station, Vicksburg, MS) IN: Multispectral image processing and enhancement; Proceedings of the Meeting, Orlando, FL, Apr. 6-8, 1988. Bellingham, WA, Society of Photo-Optical Instrumentation Engineers, 1988, p. 141-154. refs

A laser scattering model has been developed to predict the laser signatures of various types of terrain backgrounds under selected weather conditions. Experiments have been conducted to calibrate the model, and the model has been integrated with terrain elevation data and land use maps to produce color displays that indicate terrain areas exhibiting high or low laser scattering. A comparison of the calibration data and the model output is made, and the differences are briefly discussed. C.D.

A89-34357* Louisiana State Univ., Baton Rouge.
MAPPING OF LANDSAT SATELLITE AND GRAVITY LINEAMENTS IN WEST TENNESSEE
DEMETRE P. ARGIALAS (Louisiana State University, Baton Rouge), RICHARD G. STEARNS (Vanderbilt University, Nashville, TN), and FIROUZ SHAHROKHI (Tennessee, University, Tullahoma) Journal of Aerospace Engineering (ISSN 0893-1321), vol. 1, April 1988, p. 74-87. Research supported by the Louisiana State University and U.S. Department of Health, Education, and Welfare. refs
(Contract NAS8-33218; USDA-A647-SCS00210)

The analysis of earthquake fault lineament patterns within the alluvial valley of west Tennessee, which is often made difficult by the presence of unconsolidated sediments, is presently undertaken through a synergistic use of Landsat satellite images in conjunction

with gravity anomaly data, which were quantitatively analyzed and compared by means of two-dimensional histograms and rose diagrams. The northeastern trend revealed for the lineaments corresponds to faults and is in keeping with reactivation of the Reelfoot rift near the Mississippi River; this suggests that deeper features, perhaps at earthquake focal depth, may extend to the land surface as Landsat-detectable lineaments. O.C.

A89-34945
VEGETATION AND LANDSCAPE OF KORA NATIONAL RESERVE, KENYA
PAUL E. LOTH (Food and Agriculture Organization, Harare, Zimbabwe) ITC Journal (ISSN 0303-2434), no. 2, 1988, p. 133-148. Research supported by the U.N. Environmental Program and National Museums of Kenya. refs

A89-34948
MAPPING COASTAL EVOLUTION IN SRI LANKA USING AERIAL PHOTOGRAPHS
UPALI WEERAKKODY (University of Ruhuna, Matara, Sri Lanka) ITC Journal (ISSN 0303-2434), no. 2, 1988, p. 188-195. Research supported by the International Institute for Aerospace Survey and Earth Sciences. refs

A89-34949
GROUND VERIFICATION METHOD FOR BATHYMETRIC SATELLITE IMAGE MAPS OF UNSURVEYED CORAL REEFS
DEBORAH KUCHLER (Mapping and Monitoring Technology Pty., Ltd., Townsville, Australia), WILLIAM BOUR, and PASCAL DOUILLET (Office de la Recherche Scientifique et Technique d'Outre-Mer, Centre de Noumea, New Caledonia) ITC Journal (ISSN 0303-2434), no. 2, 1988, p. 196-199. Research supported by the South Pacific Commission of New Caledonia. refs

A method is presented for the ground verification of 20 m resolution bathymetric image maps of relatively unknown and unsurveyed coral reefs. The method is based on the availability of a reef geomorphologic map and/or aerial photographs, radar and echo-sounder. The test site was located in the South Pacific on Tetembia Reef, northwest of Noumea, New Caledonia.

Author

A89-35840
ACCURACY ASSESSMENT OF A LANDSAT-ASSISTED VEGETATION MAP OF THE COASTAL PLAIN OF THE ARCTIC NATIONAL WILDLIFE REFUGE
NANCY A. FELIX and DARYL L. BINNEY (U.S. Fish and Wildlife Service, Arctic National Wildlife Refuge, Fairbanks, AK) Photogrammetric Engineering and Remote Sensing (ISSN 0099-1112), vol. 55, April 1989, p. 475-478. Research supported by the U.S. Fish and Wildlife Service. refs

A89-35856#
LANDSAT INTERPRETATION AND STRATIGRAPHY OF THE HUGOTON GAS FIELD (SOUTHWESTERN KANSAS) AND SURROUNDING AREAS
DONALD C. SWANSON and PATRICK J. SHANNON IN: Thematic Conference on Remote Sensing for Exploration Geology, 6th, Houston, TX, May 16-19, 1988, Proceedings. Volume 1. Ann Arbor, MI, Environmental Research Institute of Michigan, 1988, p. 37-45.

A89-35869#
LITHOLOGIC MAPPING IN EAST GREENLAND WITH LANDSAT THEMATIC MAPPER IMAGERY
J. THOMAS PARR (Analytic Sciences Corp., Reading, MA), RICHARD W. BIRNIE, H. RICHARD NASLUND, JENNIFER D. NICHOLS, and PATRICIA A. TURNER (Dartmouth College, Hanover, NH) IN: Thematic Conference on Remote Sensing for Exploration Geology, 6th, Houston, TX, May 16-19, 1988, Proceedings. Volume 1. Ann Arbor, MI, Environmental Research Institute of Michigan, 1988, p. 203-212.

Landsat Thematic Mapper data is being used in a collaborative study of the East Greenland Tertiary Igneous Province. The objectives are to use the imagery to map the plutonic bodies in this region as an aid to both improved understanding of rifting in

the North Atlantic, and to assessing the potential for economic deposits of strategic metals, such as chromium, platinum, and palladium. To accomplish these objectives a variety of image processing techniques are being used in conjunction with the collection of ground truth. During two field seasons investigations were conducted in the vicinity of the well-studied Skaergaard intrusion, which is being used as a test locality. During one of these seasons field spectra were collected with a Barringer Hand Held Ratiometric Radiometer. Interpretation of imagery from this high latitude site is complicated by subpixel snowcover, mineral staining, lichen cover, low sun elevation, and significant terrain relief.

Author

A89-35879#

APPLICATION OF LANDSAT THEMATIC MAPPER IMAGERY FOR LITHOLOGICAL MAPPING OF POORLY ACCESSIBLE SEMI-ARID REGIONS

A. PONTUAL (Open University, Milton Keynes, England) IN: Thematic Conference on Remote Sensing for Exploration Geology, 6th, Houston, TX, May 16-19, 1988, Proceedings. Volume 1. Ann Arbor, MI, Environmental Research Institute of Michigan, 1988, p. 339-348. Research supported by NERC. refs

The use of enhanced Thematic Mapper (TM) imagery in geological mapping would ideally produce consistent coverage of poorly accessible semiarid terrain, requiring only limited fieldwork. This study discusses two examples of how preexisting maps can be refined by study of the images (in one case), and how an interpretative map may be made using TM when no other detailed map existed. In both cases, fieldwork verified the image interpretation. Laboratory spectra of the weathered surfaces of the samples show trends that apparently correlate with those observed on the images.

Author

A89-35880#

TOPOGRAPHIC ANALYSIS OF THE ANDEAN HIGHLANDS USING THE LARGE FORMAT CAMERA

MATTHEW HERIC and KAYNE SMITH (Autometric, Inc., Alexandria, VA) IN: Thematic Conference on Remote Sensing for Exploration Geology, 6th, Houston, TX, May 16-19, 1988, Proceedings. Volume 1. Ann Arbor, MI, Environmental Research Institute of Michigan, 1988, p. 351-357. refs

The Oliva Range of the Andean Highlands in Chile and Argentina was analyzed using stereo imagery from the Space Shuttle Large Format Camera (LFC) obtained in October, 1984. The results were used to update the topographic features of a 1:500,000 scale map of the region. It is shown that the LFC photography provided topographic detail at a scale of 1:100,000 with a contour interval of approximately 150 m.

R.B.

A89-35882#

PHOTOLOGIC-GEOMORPHIC MAPPING PROVIDES CLUES TO STRUCTURAL FEATURES BENEATH GLACIAL TERRAIN

L. PAUL STOHL (Petroleum Information Corp., TGA Div., Littleton, CO) IN: Thematic Conference on Remote Sensing for Exploration Geology, 6th, Houston, TX, May 16-19, 1988, Proceedings. Volume 1. Ann Arbor, MI, Environmental Research Institute of Michigan, 1988, p. 373-382. refs

Geomorphic analysis is used to interpret aerial photographs of northern and central Ohio. It is shown that the methodology makes it possible to identify surface evidence of subsurface features in glacial deposits. The geomorphic method and the geological characteristics of the region are described. It is suggested that the method is advantageous for exploration studies in glaciated areas because it identifies features not readily apparent in a typical field mapping program.

R.B.

A89-35884#

FROM LARGE-SCALE TO SMALL-SCALE - ECONOMIC GEOLOGIC-GEOMORPHIC MAPPING USING AERIAL PHOTOGRAPHS AND LANDSAT IMAGES

STEPHANIE B. URBAN (Petroleum Information Corp., TGA Div., Littleton, CO) IN: Thematic Conference on Remote Sensing for

Exploration Geology, 6th, Houston, TX, May 16-19, 1988, Proceedings. Volume 1. Ann Arbor, MI, Environmental Research Institute of Michigan, 1988, p. 391-400. refs

Aerial photographs and Landsat images were used to map the basic structural and geomorphic characteristics of hydrocarbon-prospective areas. The programs discussed include the use of large-scale (1:40,000) aerial photographs were used to map a region of southeastern Colorado, mapping of an area in eastern China with 1:500,000 scale Landsat MSS imagery, and mapping the structural continuity of a region in Guatemala with 1:1,000,000 and 1:500,000 scale Skylab imagery. In all cases, the mapping successfully delineated structures and geomorphic anomalies which may have trapped hydrocarbons.

R.B.

A89-38583

GEOPHYSICAL GEODESY - THE SLOW DEFORMATIONS OF THE EARTH

KURT LAMBECK (Australian National University, Canberra, Australia) Research supported by CNES and Universite de Paris VI. Oxford and New York, Oxford University Press, 1988, 727 p. refs

The aims, theoretical principles, and experimental methods of geodesy are examined in a textbook for advanced undergraduate and graduate students of geology and geophysics. Chapters are devoted to geodetic concepts, the fundamental principles of geophysics, the hydrosphere and the atmosphere, terrestrial geodetic methods, satellite methods, lunar methods, radio interferometric methods, the earth gravitational field, crustal movements, and tides and the rotation of the earth. Diagrams, maps, graphs, photographs, and tables of numerical data are provided.

T.K.

A89-42787* Jet Propulsion Lab., California Inst. of Tech., Pasadena.

OPERATIONAL ASPECTS OF CASA UNO '88-THE FIRST LARGE SCALE INTERNATIONAL GPS GEODETIC NETWORK

RUTH E. NEILAN, T. H. DIXON, THOMAS K. MEEHAN, WILLIAM G. MELBOURNE, JOHN A. SCHEID, J. N. KELLOGG, and J. L. STOWELL (California Institute of Technology, Jet Propulsion Laboratory, Pasadena) (Society of Instrument and Control Engineers of Japan, IEEE, URSI, et al., Conference on Precision Electromagnetic Measurements, Tsukuba, Japan, June 7-10, 1988) IEEE Transactions on Instrumentation and Measurement (ISSN 0018-9456), vol. 38, April 1989, p. 648-651. refs

For three weeks, from January 18 to February 5, 1988, scientists and engineers from 13 countries and 30 international agencies and institutions cooperated in the most extensive GPS (Global Positioning System) field campaign, and the largest geodynamics experiment, in the world to date. This collaborative experiment concentrated GPS receivers in Central and South America. The predicted rates of motions are on the order of 5-10 cm/yr. Global coverage of GPS observations spanned 220 deg of longitude and 125 deg of latitude using a total of 43 GPS receivers. The experiment was the first civilian effort at implementing an extended international GPS satellite tracking network. Covariance analyses incorporating the extended tracking network predicted significant improvement in precise orbit determination, allowing accurate long-baseline geodesy in the science areas.

I.E.

N89-22174# Army Research Inst. for the Behavioral and Social Sciences, Alexandria, VA.

THE PRECEDENCE OF GLOBAL FEATURES IN THE PERCEPTION OF MAP SYMBOLS Final Report, May 1984 - May 1985

BEVERLY G. KNAPP Jun. 1988 99 p Prepared in cooperation with Army Research Inst. Field Unit, Fort Huachuca, AZ (AD-A203792; ARI-TR-803) Avail: NTIS HC A05/MF A01 CSCL 05/8

This research investigated the role of global precedence in visual perceptual processing. Researchers evaluated the effect of global features on the speed and accuracy of detecting map symbols. The global precedence position suggests that perception proceeds temporally, through stages, from the recognition of global

03 GEODESY AND CARTOGRAPHY

features to a more local, finegrained analysis of individual elements. The study was conducted to compare performance (speed and accuracy) in a symbol-alone condition with that in various symbol-plus-distractor conditions. Scaling techniques (Multidimensional Scaling Analysis and Hierarchical Cluster Analysis) were applied to an existing database of map symbols to categorize global (general) and local (detailed) features of the symbols. Following this, a detection task was performed to determine the level of interference in detecting target symbols of various global categories when distractor symbols were present. The response latency and accuracy measures from the detection study were analyzed using a one-way repeated measures ANOVA, followed by planned comparisons between target-distractor category means. The research shows that the response latency measure discriminates well among symbol-distractor conditions, but the accuracy measure does not. GRA

N89-23437# Federal Aviation Administration, Atlantic City, NJ.
LORAN C FIELD STRENGTH CONTOURS: CONTIGUOUS US
FRANK GARUFI May 1989 107 p
(Contract FAA-T0702-N)
(DOT/FAA/CT-TN89/16) Avail: NTIS HC A06/MF A01

The development of Loran C field strength contour plots for the contiguous United States (CONUS) is described. Various plots were developed which show Loran C field strength based on measured data, predicted data, and measured data augmented by predicted data. Measured data were taken from a data base formerly developed by the Federal Aviation Administration (FAA) Technical Center at the Atlantic City International Airport, N.J. Predicted data were generated by the Canadian Loran C propagation model. Field strength contour plots of the CONUS are a result of this project. It is concluded that the contours produced are realistic indicators of Loran C field strength for each of the CONUS transmitters. Also included in this report are atmospheric noise contours of the CONUS and Loran C coverage contours of the CONUS. Author

N89-23766*# Naval Ocean Research and Development Activity, Bay Saint Louis, MS.
KRMS (K-BAND RADIOMETRIC MAPPING SYSTEM) SSM/I
VALIDATION MARCH 1988 QUICK LOOK REPORT Technical
Note, 6-14 Mar. 1988

L. DENNIS FARMER, DUANE T. EPPLER, BRUCE HEYDLAUFF, and DAVID OLSEN Jan. 1989 44 p Prepared in cooperation with Naval Ocean Research and Development Activity, Hanover, NH and Naval Weapons Center, China Lake, CA
(NASA-CR-185320; NAS 1.26:185320; AD-A205606; NORDA-TN-385) Avail: NTIS HC A03/MF A01 CSCL 17/9

The primary objective of this mission was to provide high-resolution passive microwave imagery in support of the NASA SSM/I sea ice algorithm verification program. Four flights were flown, originating from Eielson AFB, Fairbanks, Alaska, over the Chukchi Sea, the Beaufort Sea, and the Bering Sea. The Ka-band Radiometric Mapping System (KRMS) was flown from 6 to 14 March 1988. Data were collected on each of four days during this period. This report provides the flight and navigation records required to reconstruct the missions. Flight racks, compiled from the primary navigation system, indicate areas of coverage. The system logs provide the sensor settings and pertinent flight data, such as altitude and ground speed. The navigation logs provide specifics as to location of data and time of collection. A flight track chart is provided for each day's mission. Several examples of KRMS imagery are also provided. GRA

N89-23941# Institut fuer Angewandte Geodaesie, Frankfurt am Main (Germany, F.R.).
REPORTS ON CARTOGRAPHY AND GEODESY. SERIES 1,
NUMBER 101 [NACHRICHTEN AUS DEM KARTEN- UND
VERMESSUNGSWESEN. REIHE 1, HEFT NR. 101]

1988 133 p In GERMAN; ENGLISH summary
(ISSN-0469-4236; ETN-89-93779) Avail: NTIS HC A07/MF A01

Hardware and software for graphic information systems; developments in the field of digital cartographic models; the status

of the topographic-cartographic information system ATKIS; and the use of digital urban maps in land information systems are presented. Developments in automatic digitizing of cadastral mapping; the ARC-INFO geographic information system; the universal photogrammetric-cartographic system PHOCUS; and the ANA Tech system for digitizing drawings and cadastral maps are discussed. Geocoded data sets of imaging satellites; the computer assisted layout of graphic settlement representations; the computer assisted generalization of buildings for the construction of digital landscape models; and computer assisted generalization of transport line representations were studied.

ESA

N89-23943# Institut fuer Angewandte Geodaesie, Frankfurt am Main (Germany, F.R.).

COMPUTER AIDED PRODUCTION OF A 1:25,000 RELIEF
MODEL OF BERLIN AND SURROUNDINGS
[RECHNERGESTUETZTE HERSTELLUNG EINES
GELAENDERELIEFS UND UMGEBUNG 1:25,000]

FRED CHRIST In its Reports on Cartography and Geodesy. Series 1, Number 101 p 17-22 1988 In GERMAN; ENGLISH summary

Avail: NTIS HC A07/MF A01

Developments in digital cartographic models, as well as the computer aided production of a three-dimensional relief model of Berlin and of a two-dimensional relief map of Berlin with hypsometric shadings are presented. ESA

N89-23944# Institut fuer Angewandte Geodaesie, Frankfurt am Main (Germany, F.R.).

THE OFFICIAL TOPOGRAPHIC-CARTOGRAPHIC
INFORMATION SYSTEM (ATKIS) OF THE GEODESY GROUP
OF THE LAENDER OF THE FEDERAL REPUBLIC OF
GERMANY: STATUS AFTER ONE YEAR OF DEVELOPMENT
[DAS ADV-VORHABEN ATKIS - STAND NACH EINEM JAHR
ENTWICKLUNGSARBEIT]

ROLF HARBECK In its Reports on Cartography and Geodesy. Series 1, Number 101 p 23-30 1988 In GERMAN; ENGLISH summary

Avail: NTIS HC A07/MF A01

The ATKIS topographic-cartographic system was extended with regard to its scientific bases, its resources, and the data model for storing the topographic information. Priority was given to the establishment of a digital topographic data set in the form of digital landscape models (DLM's). The feature type catalog, which serves to structure the landscape and define the contents of the DLM, is available as a draft version. Legal aspects of managing digital topographic data sets are dealt with. ESA

N89-23945# Institut fuer Angewandte Geodaesie, Frankfurt am Main (Germany, F.R.).

THE DIGITAL URBAN MAP AS A BASIS FOR A LAND
INFORMATION SYSTEM IN LOCAL ADMINISTRATION [DIE
DIGITALE STADTKARTE ALS GRUNDLAGE EINES
LANDINFORMATIONSSYSTEMS IN DER KOMMUNALEN
VERWALTUNG]

KARL HASLINGER In its Reports on Cartography and Geodesy. Series 1, Number 101 p 31-35 1988 In GERMAN; ENGLISH summary

Avail: NTIS HC A07/MF A01

The use of digital urban maps in land information systems is discussed. The complex task imposed by the increasing environmental demands is greatly facilitated by a land information system, in particular in urban areas where large batches of information with extremely complex interdependence in a very small area occur. Land information systems are based on a digital cadastre (legal representation) and on an urban map (natural and artificial representation); this division is advantageous because of administrative division of responsibility and of technical requirements of revision. The production and updating of urban maps using analytic photogrammetry (taking geodetic additions into consideration) combined with graphic coding, has many

advantages. The division of objects into dots, lines, network, and area allows their correlations to be described with descriptive data from specialized data bases. ESA

N89-23961* Michigan Univ., Ann Arbor. Radiation Lab.
MAPPING FREEZE/THAW BOUNDARIES WITH SMMR DATA
 B. W. ZUERNDORFER, A. W. ENGLAND, M. C. DOBSON, and F. T. ULABY 1989 28 p
 (Contract NAG5-852)
 (NASA-CR-184991; NAS 1.26:184991) Avail: NTIS HC A03/MF A01 CSCL 08/2

Nimbus 7 Scanning Multichannel Microwave Radiometer (SMMR) data are used to map daily freeze/thaw patterns in the upper Midwest for the Fall of 1984. The combination of a low 37 GHz radiobrightness and a negative 10.7, 18, and 37 GHz spectral gradient, Partial Derivative of Tb with Respect to f, appears to be an effective discriminant for classifying soil as frozen or thawed. The 37 GHz emissivity is less sensitive to soil moisture than are the lower frequency emissivities so that the 37 GHz radiobrightness appears to track soil surface temperature relatively well. The negative gradient for frozen ground is a consequence of volume scatter darkening at shorter microwave wavelengths. This shorter wavelength darkening is not seen in thawed moist soils. Author

N89-24060* Jet Propulsion Lab., California Inst. of Tech., Pasadena.

OBSERVATION MODEL AND PARAMETER PARTIALS FOR THE JPL GEODETIC GPS MODELING SOFTWARE GPSOMC
 O. J. SOVERS and J. S. BORDER 15 Dec. 1988 42 p
 (NASA-CR-185021; JPL-PUBL-87-21-REV-1; NAS 1.26:185021)
 Avail: NTIS HC A03/MF A01 CSCL 09/2

The physical models employed in GPSOMC and the modeling module of the GIPSY software system developed at JPL for analysis of geodetic Global Positioning Satellite (GPS) measurements are described. Details of the various contributions to range and phase observables are given, as well as the partial derivatives of the observed quantities with respect to model parameters. A glossary of parameters is provided to enable persons doing data analysis to identify quantities in the current report with their counterparts in the computer programs. There are no basic model revisions, with the exceptions of an improved ocean loading model and some new options for handling clock parametrization. Such misprints as were discovered were corrected. Further revisions include modeling improvements and assurances that the model description is in accord with the current software. Author

04

GEOLOGY AND MINERAL RESOURCES

Includes mineral deposits, petroleum deposits, spectral properties of rocks, geological exploration, and lithology.

A89-32988* Lunar and Planetary Inst., Houston, TX.
MEASURING THERMAL BUDGETS OF ACTIVE VOLCANOES BY SATELLITE REMOTE SENSING

L. GLAZE, P. W. FRANCIS (Lunar and Planetary Institute, Houston, TX), and D. A. ROTHERY (Open University, Milton Keynes, England) Nature (ISSN 0028-0836), vol. 338, March 9, 1989, p. 144-146. refs

Thematic Mapper measurements of the total radiant energy flux Q at Lascar volcano in north Chile for December 1984 are reported. The results are consistent with the earlier suggestion that a lava lake is the source of a reported thermal budget anomaly, and with values for 1985-1986 that are much lower, suggesting that fumarolic activity was then a more likely heat source. The results show that satellite remote sensing may be used to monitor the activity of a volcano quantitatively, in a way not possible by conventional ground studies, and may provide a method for predicting eruptions. C.D.

A89-33540* California Univ., Los Angeles.

COMPARISON OF FIELD-ALIGNED CURRENTS AT IONOSPHERIC AND MAGNETOSPHERIC ALTITUDES

H. E. SPENCE, M. G. KIVELSON, and R. J. WALKER (California, University, Los Angeles) (COSPAR and SCOSTEP, Plenary Meeting, 27th, Symposium on Multipoint Magnetospheric Measurement, 8th, Espoo, Finland, July 18-29, 1988) Advances in Space Research (ISSN 0273-1177), vol. 8, no. 9-10, 1988, p. 343-346. refs

(Contract NGL-05-007-004; NSF ATM-86-10858)

Using the empirical terrestrial magnetospheric magnetic field models of Tsyganenko and Usmanov (1982) and Tsyganenko (1987) the average field-aligned currents (FACs) in the magnetosphere were determined as a function of the Kp index. Three major model FAC systems were identified, namely, the dayside region 1, the nightside region 1, and the nightside polar cap. The models provide information about the sources of the current systems. Mapped ionospheric model FACs are compared with low-altitude measurements obtained by the spacecraft. It is found that low-altitude data can reveal either classic region 1/2 or more highly structured FAC patterns. Therefore, statistical results either obtained from observations or inferred from models are expected to be averages over temporally and spatially shifting patterns. Author

A89-33829

GEOS 1 OBSERVATIONS OF LOW-ENERGY IONS IN THE EARTH'S PLASMASPHERE - A STUDY ON COMPOSITION, AND TEMPERATURE AND DENSITY STRUCTURE UNDER QUIET GEOMAGNETIC CONDITIONS

C. J. FARRUGIA (Imperial College of Science and Technology, London, England), J. GEISS, H. BALSIGER (Bern, Universitaet, Switzerland), and D. T. YOUNG (Southwest Research Institute, San Antonio, TX) (COSPAR, IAGA, and SCOSTEP, Plenary Meeting, 27th, Symposium on Geospace Plasmas, 7th, Espoo, Finland, July 18-29, 1988) Advances in Space Research (ISSN 0273-1177), vol. 8, no. 8, 1988, p. 25-33. refs

Data are presented on the composition and the temperature (T) and density (N) distributions of the earth's plasmasphere ionic population, obtained from GEOS 1 thermal-ion data. In deriving the N and T of the ions, a novel technique was employed, which is based on the modulation of the count rates by the spacecraft's spin. It was found that, for the major ion species H(+) and He(+), the relative density abundance He(+)/H(+) value of several percent was fairly common; the H(+) and He(+) ions are generally in thermal equilibrium, with temperatures varying between 4000 and 15,000 K, with a tendency to increase with L value. A comparison of the thermal structure obtained with those obtained by the Plasma Composition Experiment on ISEE and the Retarding Ion Mass Spectrometer on DE 1 showed no systematic difference between the 'energy' techniques used in these studies and the present 'angular' technique. I.S.

A89-34003

USE OF AERIAL AND SPACE PHOTOGRAPHY FOR THE DETECTION OF FAULTS AND NEOTECTONIC MOVEMENTS IN CRIMEA AND THE AZOV COASTAL REGION [ISPOL'ZOVANIE AEROKOSMICHESKIKH SNIMKOV DLIA VYIAVLENIIA RAZLOMOV I NEOTEKTONICHESKIKH DVIZHENII KRYMA I PRIAZOV'IA]

I. I. CHEBANENKO, N. N. SHATALOV, L. S. BORISENKO, N. N. NOVIK, V. G. VERKHOVTSSEV et al. IN: Remote-sensing studies of present-day tectonic processes. Moscow, Izdatel'stvo Nauka, 1988, p. 12-16. In Russian. refs

A89-34004

DYNAMICS OF PRESENT-DAY GEOLOGICAL PROCESSES FROM REMOTELY SENSED DATA [DINAMIKA NOVEISHIKH GEOLOGICHESKIKH PROTSESSOV PO AEROKOSMICHESKIM DANNYM]

IA. G. KATS, A. I. POLETAEV, E. F. RUMIANTSEVA, and A. V. TEVELEV IN: Remote-sensing studies of present-day tectonic

04 GEOLOGY AND MINERAL RESOURCES

processes. Moscow, Izdatel'stvo Nauka, 1988, p. 20-27. In Russian. refs

Remotely sensed data on the dynamics of present-day exogenous and endogenous processes occurring at different depths and with different intensity and manifestations are discussed. Attention is given to the processes of continental-sediment accumulation at the Tedzhen and Murgab River deltas and the Amu-Daria River bed, deformation processes occurring in the Pamir-Alai region, and the deep-lying interactions of the Iranian and Turan platforms. It is noted that the presence of high-degree correlations among the lineament fields of the individual subregions of the Pamir-Alai region, the Gissar-Alai region, and the region of northern Pamir suggests that these regions belong to a single elongated dynamic zone. I.S.

A89-34005

INVESTIGATION OF THE RECENTLY FORMED IMBRICATE STRUCTURE OF THE SOUTHERN TIEN-SHAN USING SPACE PHOTOGRAPHS [IZUCHENIE NOVEISHEI CHESHUICHATOI STRUKTURY IUZHNOGO TIAN-SHANIA S ISPOL'ZOVANIEM MATERIALOV KOSMICHESKOI S'EMKI]

N. A. IABLONSKAIA IN: Remote-sensing studies of present-day tectonic processes. Moscow, Izdatel'stvo Nauka, 1988, p. 27-33. In Russian. refs

A89-34006

MORPHOSTRUCTURAL INTERPRETATION OF SPACE IMAGES AND THE RECONSTRUCTION OF THE RECENTLY FORMED STRESS FIELD IN THE ALTAI-BAIKAL REGION [MORFOSTRUKTURNAYA INTERPRETATSIYA KOSMICHESKIKH SNIMKOV I REKONSTRUKTSIYA NOVEISHOGO POLIA NAPRIAZHENII ALTAI-PRIBAIKAL'SKOGO REGIONA]

V. E. GONIKBERG IN: Remote-sensing studies of present-day tectonic processes. Moscow, Izdatel'stvo Nauka, 1988, p. 39-44. In Russian. refs

A89-34007

USE OF AERIAL AND SPACE METHODS FOR OBSERVATIONS AND STUDIES OF THE MORPHOLOGY AND KINEMATICS OF RECENT MOVEMENTS ALONG SOME FAULTS OF THE BAIKAL RIFT ZONE [ISPOL'ZOVANIE AEROKOSMICHESKIKH SREDSTV PRI IZUCHENII, MORFOLOGII I KINEMATIKI NOVEISHIKH DVIZHENII PO NEKOTORYM RAZLOMAM BAIKAL'SKOI RIFTOVOI ZONY]

N. V. LUKINA IN: Remote-sensing studies of present-day tectonic processes. Moscow, Izdatel'stvo Nauka, 1988, p. 45-52. In Russian. refs

A89-34009

STRUCTURAL STRESSES AND THE DIVISIBILITY INTO BLOCKS OF THE EARTH CRUST AS OBSERVED ON SPACE IMAGERY [STRUKTURNYE NAPRIAZHENIYA I BLOKOVAIA DELIMOST' ZEMNOI KORY, NABLIUDAEMYE NA KOSMICHESKIKH SNIMKAKH]

V. S. PONOMAREV IN: Remote-sensing studies of present-day tectonic processes. Moscow, Izdatel'stvo Nauka, 1988, p. 57-63. In Russian. refs

A89-34012

NEW DATA ON THE MORPHOSTRUCTURE AND GEODYNAMICS OF THE EASTERN MARGIN OF EURASIA [NOVYE DANNYE O MORFOSTRUKTURE I GEODINAMIKE VOSTOCHNOI OKRAINY EVRAZII]

A. P. KULAKOV IN: Remote-sensing studies of present-day tectonic processes. Moscow, Izdatel'stvo Nauka, 1988, p. 79-86. In Russian. refs

New findings on the morphostructure and geodynamics of the eastern margin of the Eurasian continent are discussed. Attention is given to morphological characteristics of individual gigantic central-type structures that envelop the continental margin and the depressions of adjacent Asian seas, and to processes responsible for their formation. It is emphasized that the

geodynamics of eastern Asia was affected significantly by tectonic movements induced by the earth rotation, which led to major dislocations in the eastern coastal region as well as to continental movements along the northwestern and northeastern dislocation zones. I.S.

A89-34016

DETERMINATION OF THE CHARACTER OF PRESENT-DAY VERTICAL MOVEMENTS FROM THE STRUCTURE OF SPACE IMAGERY [OPYT VYIAVLENIIA KHARAKTERA SOVREMENNYKH VERTIKAL'NYKH DVIZHENII PO STRUKTURE IZOBRAZHENIIA KOSMICHESKIKH SNIMKOV]

O. M. BORISOV and D. A. MAGZUMOVA IN: Remote-sensing studies of present-day tectonic processes. Moscow, Izdatel'stvo Nauka, 1988, p. 112-115. In Russian. refs

This paper describes structural features observed on remote images that can be correlated with particular topographical features on the earth surface, and, in particular, with the present-day vertical tectonic movements observed in a given region. Special consideration is given to the identification of tectonic settlements and of weak, moderate, moderately intensive, and very intensive uplifts in the regions of Tien-Shan, Pamir, the Turan Platform, and river valleys. The result of correlations of the structural types and their patterns identified on remote images with seismic maps of the observed regions made it possible to classify images of tectonic blocks according to the potential earthquake intensity characteristic for these blocks. I.S.

A89-34017

RECENT AND CURRENT GEODYNAMICS OF THE KYZYLKUM REGION AS DERIVED FROM SPACE IMAGERY [SOVREMENNAIA I NOVEISHAIA GEODINAMIKA KYZYLKUMSKOGO REGIONA V SVETE DANNYKH KOSMOSNIMKOV]

V. S. IUDIN IN: Remote-sensing studies of present-day tectonic processes. Moscow, Izdatel'stvo Nauka, 1988, p. 115-120. In Russian.

A89-34018

SEISMOGEOLOGICAL INTERPRETATION OF SPACE IMAGES OF THE REGION OF CAUCASIAN MINERAL WATERS [SEISMOGEOLOGICHESKAIA INTERPRETATSIYA KOSMICHESKIKH SNIMKOV RAIONA KAVKAZSKIKH MINERAL'NYKH VOD]

T. P. IVANOVA IN: Remote-sensing studies of present-day tectonic processes. Moscow, Izdatel'stvo Nauka, 1988, p. 124-132. In Russian. refs

A89-34196

CONCENTRIC STRUCTURES IN SOUTHERN TIEN-SHAN [KONTSENTRICHESKIE STRUKTURY IUZHNOGO TIAN-SHANIA]

V. V. BELOUSOV, ED. Moscow, Izdatel'stvo Nauka, 1988, 136 p. In Russian. No individual items are abstracted in this volume.

The nature and genesis of the concentric ovoid-type structures commonly found in the mountain ridges of East Fergana are discussed, and a close relationship is demonstrated between these structures and the major linear dislocations of the region. Attention is given to the geology and deep structures of the East Fergana area and to the results of earlier geological studies of this area, as well as to the comparative analysis of the East-Fergana structures and their genesis. The possible relationship between concentric structures and mineral deposits is discussed. Special consideration is given to the ovoid structures of the Alai, the Talas-Fergana fault zone, the Karasu-Mailisui zone, and southeastern Fergana, as well as to the East Alai ovoid megaanticlinorium. I.S.

A89-35851*

THEMATIC CONFERENCE ON REMOTE SENSING FOR EXPLORATION GEOLOGY, 6TH, HOUSTON, TX, MAY 16-19, 1988, PROCEEDINGS. VOLUMES 1 & 2

Conference organized by the Environmental Research Institute of

Michigan; Sponsored by Amoco Oil Co., ARCO Oil and Gas Co., NASA, et al. Ann Arbor, MI, Environmental Research Institute of Michigan, 1988, p. Vol. 1, 458 p.; vol. 2, 277 p. For individual items see A89-35852 to A89-35904.

Papers concerning remote sensing applications for exploration geology are presented, covering topics such as remote sensing technology, data availability, frontier exploration, and exploration in mature basins. Other topics include offshore applications, geobotany, mineral exploration, engineering and environmental applications, image processing, and prospects for future developments in remote sensing for exploration geology. Consideration is given to the use of data from Landsat, MSS, TM, SAR, short wavelength IR, the Geophysical Environmental Research Airborne Scanner, gas chromatography, sonar imaging, the Airborne Visible-IR Imaging Spectrometer, field spectrometry, airborne thermal IR scanners, SPOT, AVHRR, SIR, the Large Format camera, and multitimephase satellite photographs. R.B.

A89-35852#

BASIC CONCEPTS IN THE USE OF REMOTELY SENSED DATA FOR RESOURCE EXPLORATION

KEN M. MORGAN (Texas Christian University, Fort Worth) IN: Thematic Conference on Remote Sensing for Exploration Geology, 6th, Houston, TX, May 16-19, 1988, Proceedings. Volume 1. Ann Arbor, MI, Environmental Research Institute of Michigan, 1988, p. 1-10.

A review of the basic concepts of using remotely sensed data for resource exploration is presented as a guide for selecting computer enhancement and data integration techniques. Emphasis is placed on data collected by electromagnetic energy sensors. Topics include atmospheric and earth surface interactions, aerial photography, thermography, rada imaging, Landsat technology, and image processing. The processes for mapping lithology, lineaments, structures and tonal anomalies are described. Also, the integration of remote sensing data into a Geologic or Geographic Information System is discussed. R.B.

A89-35857#

HYDROCARBON POTENTIAL OF PART OF THE MARGIN OF THE TARIM BASIN FROM LANDSAT - A CASE HISTORY

JOHN L. BERRY (Shell Development Co., Houston, TX) and TAKASHI NISHIDAI (Japex Geoscience Institute, Akasaka, Japan) IN: Thematic Conference on Remote Sensing for Exploration Geology, 6th, Houston, TX, May 16-19, 1988, Proceedings. Volume 1. Ann Arbor, MI, Environmental Research Institute of Michigan, 1988, p. 49-63. refs

The structural geology and tectonics of the Tarim Basin in western China was determined from 50 Landsat MSS scenes. The photogeological techniques used to interpret the data are reviewed. The main geological features observed in the region are described in detail, including the tectonic setting, midbasin thrusting, the Kuqa depression, and the geology of the Kuruktag area. R.B.

A89-35859#

PETROLEUM EXPLORATION WITH AIRBORNE RADAR (SAR) AND GEOLOGIC FIELD WORK, SINU BASIN OF NORTHWEST COLUMBIA

JAMES M. ELLIS (Chevron Overseas Petroleum, Inc., San Ramon, CA) and LARRY L. DEKKER (Chevron Niugini Pty, Ltd., Port Moresby, Papua New Guinea) IN: Thematic Conference on Remote Sensing for Exploration Geology, 6th, Houston, TX, May 16-19, 1988, Proceedings. Volume 1. Ann Arbor, MI, Environmental Research Institute of Michigan, 1988, p. 79-89. refs

A89-35860#

IDENTIFICATION OF CROSS STRIKE DISCONTINUITIES IN THE APPALACHIAN BASIN AND IMPLICATIONS FOR HYDROCARBON EXPLORATION

IRA S. MERIN (to Geological Consultants, Fairfax, VA) IN: Thematic Conference on Remote Sensing for Exploration Geology, 6th, Houston, TX, May 16-19, 1988, Proceedings. Volume 1. Ann

Arbor, MI, Environmental Research Institute of Michigan, 1988, p. 93-102. refs

Landsat TM imagery of central Pennsylvania were analyzed for the selection of possible oil and gas producing areas. The methods used to interpret the data are summarized and the significance of the stress history for exploration is examined. The geological features which are indicative of hydrocarbon sites in the region are described. R.B.

A89-35868#

IMPLICATION OF PATTERNS OF FAULTING AND HYDROTHERMAL ALTERATION FROM LANDSAT TM IMAGES AND NHAP AERIAL PHOTOS TO MINERAL EXPLORATION AND TECTONICS OF THE VIRGINIA RANGE, NEVADA

AMY HUTSINPILLER COLLINS (Nevada, University, Reno) IN: Thematic Conference on Remote Sensing for Exploration Geology, 6th, Houston, TX, May 16-19, 1988, Proceedings. Volume 1. Ann Arbor, MI, Environmental Research Institute of Michigan, 1988, p. 185-198. refs

Landsat Thematic Mapper images and NHAP aerial photographs were analyzed for lineaments and alteration patterns in the Virginia Range, Nevada. Lineament trends correspond with tectonic patterns predicted by a model of northwest-trending, right-lateral shear and associated normal faulting along the Walker Lane. Lineament trends within altered areas vary depending on their location within the range, and generally correspond with reported trends of mineralization and predicted shear directions. Lineament junctions are twice as dense within altered areas as unaltered areas. Author

A89-35873#

LINEAMENT ANALYSIS FOR HAZARD ASSESSMENT IN ADVANCE OF COAL MINING

DOUGLAS C. PETERS, ROBERT A. SPEIRER, and VALOIS R. SHEA (U.S. Bureau of Mines, Denver, CO) IN: Thematic Conference on Remote Sensing for Exploration Geology, 6th, Houston, TX, May 16-19, 1988, Proceedings. Volume 1. Ann Arbor, MI, Environmental Research Institute of Michigan, 1988, p. 253-264. refs

Consideration is given to the use of lineament analysis to assess potential coal mine ground control hazards by estimating the relative degrees of risk associated with geologic structures. The analysis of processed remote sensing data and field studies show that surface lineaments match with fractures, fracture zones, paleochannels, and zones of ground control problems at the mine level. For two mines in Utah, approximately 80 percent of ground control problems were associated with the presence of lineament-controlling geologic structure. In addition, a 92 percent correlation was found between the number of roof falls and their proximity to lineaments for a mine in Alabama. R.B.

A89-35874#

APPLYING REMOTE SENSING TECHNOLOGY TO THE BUREAU OF LAND MANAGEMENT'S MINERAL MANAGEMENT PROGRAM

JAMES A. TURNER (U.S. Bureau of Land Management, Denver, CO) IN: Thematic Conference on Remote Sensing for Exploration Geology, 6th, Houston, TX, May 16-19, 1988, Proceedings. Volume 1. Ann Arbor, MI, Environmental Research Institute of Michigan, 1988, p. 269-282.

The use of high-resolution satellite imagery in mineral material resources management is demonstrated in a test study to identify and document authorized and unauthorized aggregate removal areas. Landsat TM and SPOT HRV imagery were rectified, enhanced, and merged to generate digital data filed and hard copy image maps for areas in Alaska, Nevada, and New Mexico. It is found that the satellite imagery is useful for monitoring the location and size of surface disturbances associated with mineral extraction. R.B.

A89-35881#

COMBINED REMOTE SENSING AND SURFACE GEOCHEMICAL SURVEY IN A DRIFT-COVERED AREA IN SOUTHEASTERN SASKATCHEWAN

ROBERT A. HODGSON (RAH Geological Consulting Services, Jamestown, PA), LYNDEN PENNER, and J. D. MOLLARD (J. D. Mollard and Associates, Ltd., Regina, Canada) IN: Thematic Conference on Remote Sensing for Exploration Geology, 6th, Houston, TX, May 16-19, 1988, Proceedings. Volume 1. Ann Arbor, MI, Environmental Research Institute of Michigan, 1988, p. 359-371. refs

An integrated remote sensing and soil gas geochemical survey was conducted near Estevan, Saskatchewan, demonstrating the feasibility of combining the two techniques for oil and gas exploration in drift-covered areas. It is suggested that the photolineament analyses should be performed prior to the geochemical survey in this type of study. Subsurface structural features determined from aerial photographs were combined with stratigraphic and hydrologic data to develop of geologic model to guide oil and gas exploration in the area. This model was used to design a geochemical sampling program. R.B.

A89-35886#

CONJUGATE SYNTHETIC NORMAL FAULTS AROUND THE GULF OF SALWA, SOUTHWESTERN QATAR, THE ARABIAN GULF

A. M. NOWEIR and I. A. EL-KASSAS (University of Qatar, Doha) IN: Thematic Conference on Remote Sensing for Exploration Geology, 6th, Houston, TX, May 16-19, 1988, Proceedings. Volume 2. Ann Arbor, MI, Environmental Research Institute of Michigan, 1988, p. 437-446. refs

Landsat MSS images and aerial photographs have undergone interpretation in order to delineate the spatial distribution of the Dam Formation outcrops in the southwestern corner of the Qatar peninsula. Attention is given to the southern tip of the northerly-plunged syncline of the Gulf of Salwa. The outcrops of the Dam Formation are found to be structurally controlled by a conjugate system of synthetic normal faults with small displacement. The principal set of normal faults extends NNW-SSE; the complex pattern produced by them may be due to a single episode of normal faulting. O.C.

A89-35887#

STRUCTURAL ANALYSIS OF THE WICHITA MOUNTAINS USING TM DATA FOR LINEAMENT MAPPING

XIANFANG HUANG (Beijing Research Institute of Geology, People's Republic of China), KEN MORGAN, and DAVID KOGER (Texas Christian University, Fort Worth) IN: Thematic Conference on Remote Sensing for Exploration Geology, 6th, Houston, TX, May 16-19, 1988, Proceedings. Volume 2. Ann Arbor, MI, Environmental Research Institute of Michigan, 1988, p. 451-460.

Both geophysical and TM data are presently used to map the lithology, lineaments, and structures of the Wichita Mountains; these, in virtue of their distinct mineralogies and textures, allow the identification of gabbros, rhyolites, and granites. A statistical analysis of 927 mapped lineaments shows a definite relationship between lineament orientation and tectonic stresses. An interpretation of the sequence of geologic events that is related to the opening of the aulacogen and is verifiable by field data is presented. An understanding of Wichita Mountain geologic conditions may be of significance to explorations of the Southern Oklahoma aulacogen. O.C.

A89-35889#

IDENTIFICATION OF MAGNESITE AND BAUXITE DEPOSITS ON LANDSAT IMAGERY, SOUTH INDIA

ASHOK KUMAR JOSHI (Syracuse University, NY) IN: Thematic Conference on Remote Sensing for Exploration Geology, 6th, Houston, TX, May 16-19, 1988, Proceedings. Volume 2. Ann Arbor, MI, Environmental Research Institute of Michigan, 1988, p. 475-483. Research supported by Syracuse University. refs

A89-35896*# Nevada Univ., Reno.

DISCRIMINATING LATE VOLCANIC DIFFERENTIATES COMMONLY ASSOCIATED WITH PRECIOUS METAL DEPOSITS, USING LANDSAT THEMATIC MAPPER IMAGERY

DAVID M. SPATZ and JAMES V. TARANIK (Nevada, University, Reno) IN: Thematic Conference on Remote Sensing for Exploration Geology, 6th, Houston, TX, May 16-19, 1988, Proceedings. Volume 2. Ann Arbor, MI, Environmental Research Institute of Michigan, 1988, p. 577-590. Research supported by NASA. refs

The magmatic differentiates emplaced late in volcanotectonic cycles (which when highly evolved commonly occur as domes, flow-dome complexes, and shallow intrusive porphyries) are typically more silicic and felsic than their earlier counterparts and exhibit unusually steep spectral curves from about 1.5 to 2.2 microns. This spectral characteristic emerges in the form of relatively high Landsat TM band 7 DN values and low 5/7 values, as well as dark-contrast or enhanced 5/7 images. These evolved late-phase differentiates are commonly associated both temporally and spatially with precious metal deposits, furnishing site-specific exploration targets as well as guides to caldera margins and other late-stage volcanotectonic structures. O.C.

A89-35897#

VISIBLE AND NEAR-INFRARED (0.4- TO 2.5-MICRONS) REFLECTANCE SPECTRA OF SELECTED MIXED-LAYER CLAYS AND RELATED MINERALS

J. K. CROWLEY and N. VERGO (USGS, Reston, VA) IN: Thematic Conference on Remote Sensing for Exploration Geology, 6th, Houston, TX, May 16-19, 1988, Proceedings. Volume 2. Ann Arbor, MI, Environmental Research Institute of Michigan, 1988, p. 597-606. refs

A89-37315

THE DEFINITION OF ISOMETRIC MAGMATOGENIC STRUCTURES ON SPACE IMAGERY [K PROBLEME KONTRASTNOSTI PROIAVLENIIA NA KOSMICHESKIKH SNIMKAKH IZOMETRICHNYKH MAGMATOGENNYKH STRUKTUR]

D. M. TROFIMOV, A. P. BORISIUK, and M. V. BORISIUK (Vsesoiuznyi Nauchno-Issledovatel'skii Geologorazvedochnyi Neftianoi Institut, Moscow, USSR) Issledovanie Zemli iz Kosmosa (ISSN 0205-9614), Jan.-Feb. 1989, p. 45-48. In Russian. refs

The dynamics of the movement of magmatogenic structures active at the relief-formation stage is examined with reference to two plutons of the Baltic Shield. Recent vertical-motion rates of these structures, determining their definition on space imagery, are calculated. B.J.

A89-39651

IDENTIFICATION AND ANALYSIS OF THE ALIGNMENTS OF POINT-LIKE FEATURES IN REMOTELY-SENSED IMAGERY. VOLCANIC CONES IN THE PINACATE VOLCANIC FIELD, MEXICO

G. WADGE and A. M. CROSS (NERC, Reading, University, England) International Journal of Remote Sensing (ISSN 0143-1161), vol. 10, March 1989, p. 455-474. refs (Contract NERC-F60/G6/12)

A89-39655

ALTERATION DETECTION USING TM IMAGERY - THE EFFECTS OF SUPERGENE WEATHERING IN AN ARID CLIMATE

B. J. AMOS and D. GREENBAUM (NERC, British Geological Survey, Nottingham, England) International Journal of Remote Sensing (ISSN 0143-1161), vol. 10, March 1989, p. 515-527. Research supported by the Overseas Development Administration. refs

A study has been made of the response on TM imagery of a suite of undisturbed sub-economic porphyry copper deposits occurring in the coastal desert of Peru. The deposits are associated with low-grade, mainly propylitic alteration but give rise to strong anomalies on a Landsat Thematic Mapper (TM) band-ratio image.

Field and mineralogical studies indicate that normal weathering within these alteration areas has been augmented by oxidation of sulphides and acid leaching of silicate minerals to produce clays and sulphates, including gypsum and natroalunite. It is this supergene assemblage, rather than the hypogene alteration minerals, that is responsible for the strong absorption in band 7 of the TM. Author

A89-41162

GEOLOGICAL APPLICATION OF SIR-A IMAGERY IN SOUTHERN IRAQ

JAWAD A. ZWAIN (Baghdad, University, Iraq), QASSIM A. ABDULLAH, and TAHREER A. MAJEED (Scientific Research Council, Space and Astronomy Research Centre, Baghdad, Iraq) IN: 1988 ACSM-ASPRS Annual Convention, Saint Louis, MO, Mar. 13-18, 1988, Technical Papers. Volume 4. Falls Church, VA, American Congress on Surveying and Mapping and American Society for Photogrammetry and Remote Sensing, 1988, p. 131-140. refs

SIR-A imagery was used to study the geology of an area in southern Iraq. This area covers three distinct geological provinces. The gently dipping sedimentary rocks of the southern desert in the southwest, the mesopotamian in the middle, and the foothills zone of the Zagros mountains in the east. The interpretation was executed on a positive image film at a scale 1/500,000 and enlarged image prints at a scale 1/125,000. Landsat images and air photographs were also used to compare some geologic features. The interpretation resulted in construction of three principal maps; structural lineament map, Lithostratigraphic map and Hydrological map. Lithostratigraphic units and structural lineaments could be demarcated with confidence on SIR-A image due to their different textural and morphologic expression. Drainage networks may be accurately located on SIR-A image due to the contrast of microrelief in the terrain. Author

A89-41167

STRUCTURAL ANALYSIS OF FRACTURING IN SINJAR ANTICLINE USING REMOTE SENSING TECHNIQUE

JAWAD A. ZWAIN and BALSAM S. MAJEED (Baghdad, University, Iraq) IN: 1988 ACSM-ASPRS Annual Convention, Saint Louis, MO, Mar. 13-18, 1988, Technical Papers. Volume 4. Falls Church, VA, American Congress on Surveying and Mapping and American Society for Photogrammetry and Remote Sensing, 1988, p. 181-190. refs

Jebel Sinjar represents an asymmetrical anticlinal fold located in northwestern Iraq. It forms the southern border of tectonically distinct folded zone. Structural analysis of directional distribution of fracture traces and lineaments interpreted on air and Landsat photographs was conducted. Structural and fracture trace maps were constructed. Different types of rose diagrams were also prepared. The study revealed that the directional properties of the fracture traces varies with different structural sectors of the anticline. A reasonable correlation could be obtained between the photogeological fracture traces and, the previously mapped joints and faults. This study demonstrated that air photos and remote sensing imagery can be an efficient tool in conducting structural investigation based primarily on the fracture trace analysis of folded areas. Author

A89-42149

MAGNETOMETER ARRAY STUDIES, EARTH STRUCTURE, AND TECTONIC PROCESSES

D. IAN GOUGH (Alberta, University, Edmonton, Canada) Reviews of Geophysics (ISSN 8755-1209), vol. 27, Feb. 1989, p. 141-157. Research supported by NSERC. refs

Results from magnetovariation fields recorded by two-dimensional arrays of magnetometers are reviewed. Particular attention is given to the conductive structures mapped and studied and their tectonic implications. Investigations of conductive structures under the Canadian Rockies and EMSLAB (electromagnetic sounding of the lithosphere and beyond) array results for Washington and Oregon are presented. The latter include a conductive strip beneath the Cascades volcanoes. K.K.

A89-42181* Joint Inst. for Lab. Astrophysics, Boulder, CO.

RATE OF CHANGE OF THE QUINCY-MONUMENT PEAK BASELINE FROM A TRANSLOCATION ANALYSIS OF LAGEOS LASER RANGE DATA

A. STOLZ, P. L. BENDER (Joint Institute for Laboratory Astrophysics, Boulder, CO), M. A. VINCENT (California Institute of Technology, Jet Propulsion Laboratory, Pasadena; Joint Institute for Laboratory Astrophysics, Boulder, CO), R. J. EANES, M. M. WATKINS (Texas, University, Austin) et al. Geophysical Research Letters (ISSN 0094-8276), vol. 16, June 1989, p. 539-542. Research supported by NBS. refs

Translocation studies of Lageos laser range data from Quincy and Monument Peak in California observed during 1984-1987 suggest that plate tectonic motion across the San Andreas fault system in the direction of the baseline between the two stations is uniform at a rate of $-30(+ \text{ or } - 3)$ mm/yr. Changes in the components of the baseline vector were inferred from repeat determinations using the solutions from successive 0.5-year intervals. The changes in the vertical and transverse components of the Quincy-Monument Peak baseline are $-0.4(+ \text{ or } - 5)$ mm/yr and $+14(+ \text{ or } - 5)$ mm/yr, respectively. The vertical component determinations attest to the height stability of the laser ranging method. Lageos measurements made from Quincy and Monument Peak before 1984 are inaccurate enough to limit their usefulness for plate tectonic studies. Author

A89-42795

THE BASELINE LENGTH CHANGES OF CIRCUMPACIFIC VLBI NETWORKS AND THEIR BEARING ON GLOBAL TECTONICS

KOSUKE HEKI, YUKIO TAKAHASHI, and TETSURO KONDO (Ministry of Posts and Telecommunications, Communications Research Laboratory, Kashima, Japan) (Society of Instrument and Control Engineers of Japan, IEEE, URSI, et al., Conference on Precision Electromagnetic Measurements, Tsukuba, Japan, June 7-10, 1988) IEEE Transactions on Instrumentation and Measurement (ISSN 0018-9456), vol. 38, April 1989, p. 680-683. refs

The baseline length changing rates predicted by plate motion models and those observed in global very-long-baseline interferometry (VLBI) are compared. A widely distributed 1979-1986 baseline length data set shows the rates to be in good agreement with the predictions. The deviations from the predicted rates, however, are found to have a negative correlation (significant at more than 99.99 percent by t-test) with the baseline lengths, as if the whole region were secularly contracting. The authors' analyses for 15 circumpacific and transpacific baselines in joint Japan-U.S. VLBI experiments since 1984 reproduce a similar apparent uniform contraction. I.E.

A89-43410

THE GEOMAGNETIC SPECTRUM FOR 1980 AND CORE-CRUSTAL SEPARATION

JOSEPH C. CAIN (Florida State University, Tallahassee), ZHIGANG WANG (State Seismological Bureau, Beijing, People's Republic of China), DAVE R. SCHMITZ (Univerzita Pavla Jozefa Safarika, Kosice, Czechoslovakia), and J. MEYER (Goettingen, Universitaet, Federal Republic of Germany) Geophysical Journal (ISSN 0955-419X), vol. 97, June 1989, p. 443-447. refs

The spectrum of a high degree spherical harmonic model of the geomagnetic field is analyzed to compute the constants for the core and crustal field contributions. Using a noise estimate of 0.091 nT sq at the mean Magsat radius of 6791 km , the values for the power reduced to the earth's surface show half the crustal power extrapolated to $n = 0$ compared with an $n = 23$ model, and a white noise depth of only 14 km below the mean surface. The core spectrum power is 30 percent less than previously estimated and becomes flat 80 km below the core-mantle boundary. The point where the energy density of the core and crustal components become equal at the earth's surface is $n = 14.2$. Author

04 GEOLOGY AND MINERAL RESOURCES

N89-20868# International Atomic Energy Agency, Vienna (Austria).

GEOLOGICAL DATA INTEGRATION TECHNIQUES: PROCEEDINGS

Sep. 1988 389 p Presented at the Technical Committee Meeting held in Vienna, Austria, 13-17 Oct. 1986 (DE88-705255; IAEA-TECDOC-472; CONF-8610449) Avail: NTIS (US Sales Only) HC A17/MF A01

The objectives of this Technical Committee are to bring together current knowledge on geological data handling and analysis technologies as developed in the mineral and petroleum industries for geological, geophysical, geochemical and remote sensing data that can be applied to uranium exploration and resource appraisal. The recommendation for work on this topic was first made at the meeting of the NEA-IAEA Joint Group of Experts on R and D in Uranium Exploration Techniques (Paris, May 1984). In their report, processing of integrated data sets was considered to be extremely important in view of the very extensive data sets built up over the recent years by large uranium reconnaissance programmes. With the development of large, multidisciplinary data sets which includes geochemical, geophysical, geological and remote sensing data, the ability of the geologist to easily interpret large volumes of information has been largely the result of developments in the field of computer science in the past decade. Advances in data management systems, image processing software, the size and speed of computer systems and significantly reduced processing costs have made large data set integration and analysis practical and affordable. The combined signatures which can be obtained from the different types of data significantly enhance the geologists ability to interpret fundamental geological properties thereby improving the chances of finding a significant ore body. This volume is the product of one of a number of activities related to uranium geology and exploration during the past few years with the intent of bringing new technologies and exploration techniques to the IAEA Member States. DOE

N89-21328*# Princeton Univ., NJ. Dept. of Geological and Geophysical Sciences.

HIGH RESOLUTION CHRONOLOGY OF LATE CRETACEOUS-EARLY TERTIARY EVENTS DETERMINED FROM 21,000 YR ORBITAL-CLIMATIC CYCLES IN MARINE SEDIMENTS Abstract Only

TIMOTHY D. HERBERT and STEVEN DHONDT *In* Lunar and Planetary Inst., Global Catastrophes in Earth History: An Interdisciplinary Conference on Impacts, Volcanism, and Mass Mortality p 74 1988

Avail: NTIS HC A11/MF A01 CSCL 08/3

A number of South Atlantic sites cored by the Deep Sea Drilling Project (DSDP) recovered late Cretaceous and early Tertiary sediments with alternating light-dark, high-low carbonate content. The sedimentary oscillations were turned into time series by digitizing color photographs of core segments at a resolution of about 5 points/cm. Spectral analysis of these records indicates prominent periodicity at 25 to 35 cm in the Cretaceous intervals, and about 15 cm in the early Tertiary sediments. The absolute period of the cycles that is determined from paleomagnetic calibration at two sites is 20,000 to 25,000 yr, and almost certainly corresponds to the period of the earth's precessional cycle. These sequences therefore contain an internal chronometer to measure events across the K/T extinction boundary at this scale of resolution. The orbital metronome was used to address several related questions: the position of the K/T boundary within magnetic chron 29R, the fluxes of biogenic and detrital material to the deep sea immediately before and after the K/T event, the duration of the Sr anomaly, and the level of background climatic variability in the latest Cretaceous time. The carbonate/color cycles that were analyzed contain primary records of ocean carbonate productivity and chemistry, as evidenced by bioturbational mixing of adjacent beds and the weak lithification of the rhythmic sequences. It was concluded that sedimentary sequences that contain orbital cyclicity are capable of providing resolution of dramatic events in earth history with much greater precision than obtainable through

radiometric methods. The data show no evidence for a gradual climatic deterioration prior to the K/T extinction event, and argue for a geologically rapid revolution at this horizon. Author

N89-21358*# Geological Survey, Lansing, MI.

THE CALVIN 28 CRYPTOEXPLOSIVE DISTURBANCE, CASS COUNTY, MICHIGAN: EVIDENCE FOR IMPACT ORIGIN

RANDALL L. MILSTEIN *In* Lunar and Planetary Inst., Global Catastrophes in Earth History: An Interdisciplinary Conference on Impacts, Volcanism, and Mass Mortality p 122-123 1988

Avail: NTIS HC A11/MF A01 CSCL 08/7

The Calvin 28 cryptoexplosive disturbance is an isolated, nearly circular subsurface structure of Late Ordovician age in southwestern Michigan. The structure is defined by 107 wells, is about 7.24 km in diameter and consists of a central dome, an annular depression and an encircling anticlinal rim. Seismic and geophysical well log data confirm that an intricate system of faults and structural derangement exists within the structure. Deformation decreases with depth and distance from the structure. U.S.G.S. topographic maps and aerial imagery show the structure is reflected as a subtle surface topographic rise controlling local drainage. Igneous or diapiric intrusion and solution collapse are rejected as possible origins for Calvin 28 on the basis of stratigraphic, structural and geophysical evidence. A volcanic origin is inconsistent with calculated energy requirements and an absence of igneous material. Although shock-metamorphic features are unidentified, microbreccias occur in deep wells that penetrate the structure. Morphology and structural parameters support an impact origin. Author

N89-21416* Miami Univ., FL. Dept. of Marine Geology and Geophysics.

NEOTECTONICS IN CENTRAL MEXICO FROM LANDSAT TM DATA Final Report

CHRISTOPHER G. A. HARRISON and CHRISTOPHER A. JOHNSON 15 Dec. 1988 136 p Original document contains color illustrations

(Contract NAS5-28745)

(NASA-CR-183416; NAS 1.26:183416) Avail: Issuing Activity CSCL 08/2

A summary is presented of results from a Thematic Mapper survey of neotectonics in central Mexico, dealing specifically with faulting and its relationship to volcanism there. The Mexican Volcanic Belt (MVB) is the dominant physiographic province in the study area. Late Miocene to Quaternary calc-alkaline volcanics of the MVB have been generated by active subduction of the Cocos plate beneath Mexico along the Middle America (Acapulco) Trench. The results firmly establish a link between deformation in the overriding plate (expressed as neotectonic activity) and the distribution and character of volcanism in the MVB. Volcanism appears to be controlled by tectonics at all scales from local to regional. The large variation in eruption styles along the MVB may be explained as the result of the influence of various tectonic domains created by differential movement of crustal blocks above a zone of magma production. In addition to the neotectonic synthesis, problems and questions regarding much older deformation may be addressed in unusual ways using the TM images. Examples are given. Author

N89-22255*# Geological Survey of India, Bangalore.

STRUCTURAL PATTERNS IN HIGH GRADE TERRAIN IN PARTS OF TAMIL NADU AND KARNATAKA

E. B. SUGAVANAM and K. T. VIDYADHARAN *In* Lunar and Planetary Inst., Workshop on the Deep Continental Crust of South India p 179-180 1988

Avail: NTIS HC A17/MF A01 CSCL 08/7

Detailed geological mapping in parts of Tamil Nadu and Karnataka has brought out vast areas occupied by highly deformed charnockite and high grade gneisses. These areas, similar to high grade shield terrains in other parts of the world have the impression of extensive tectonic reworking multideformation and polymetamorphism and are closely associated with layered ultramafics, shelf type sediments and different igneous events. In

OCEANOGRAPHY AND MARINE RESOURCES

Includes sea-surface temperature, ocean bottom surveying imagery, drift rates, sea ice and icebergs, sea state, fish location.

North Arcot and Charnapuri districts of Tamil Nadu and Kollegal taluk in Mysore district in Karnataka, charnockite is intensely cocolored with a supracrustal succession of layered ultramafics, pyroxene granulite, pink granulites, magnetite quartzite and khondalites. These areas have undergone five phases of deformation, five generations of basic dyke activities, four phases of migmatization and two periods of metallogeny. Geochronological data ranges from 2900 m.y. to 750 m.y. In working out the tectanostratigraphy of the above areas the basic dykes of different generations have served as major time markers. In addition, the persistent strike continuity of linear bands of pyroxene granulite, pink granulite and magnetite quartzite has been of great utility in using them as structural markers for bringing out the complex structural history in these areas. Author

N89-22263*# California Univ., Davis.

KINEMATICS AT THE INTERSECTION OF THE GARLOCK AND DEATH VALLEY FAULT ZONES, CALIFORNIA: INTEGRATION OF TM DATA AND FIELD STUDIES Final Report

KENNETH L. VEROSUB, ROLAND H. BRADY, III, and MICHAEL ABRAMS (Jet Propulsion Lab., California Inst. of Tech., Pasadena.) Mar. 1989 182 p (Contract NAS5-28754) (NASA-CR-184854; NAS 1.26:184854) Avail: NTIS HC A09/MF A01 CSCL 08/7

Kinematic relationships at the intersection of the southern Death Valley and Garlock fault zones were examined to identify and delineate the eastern structural boundary between the Mojave and the Basin and Range geologic terrains, and to construct a model for the evolution of this boundary through time. In order to accomplish this, satellite imagery was combined with field investigations to study six areas in the vicinity of the intersection, or possible extensions, of the fault zones. The information gathered from these areas allows the test of various hypotheses that were proposed to explain the interaction between the Death Valley and Garlock fault zones. Author

N89-24757*# Massachusetts Inst. of Tech., Cambridge. Dept. of Earth, Atmospheric and Planetary Sciences.

PLATE MOTIONS AND DEFORMATIONS FROM GEOLOGIC AND GEODETIC DATA Semiannual Report, 1 Jul. - 31 Dec. 1988

THOMAS H. JORDAN 24 May 1989 222 p (Contract NAG5-459) (NASA-CR-184987; NAS 1.26:184987) Avail: NTIS HC A10/MF A01 CSCL 08/7

The very long baseline interferometry (VLBI) measurements made in the western U.S. since 1979 provide discrete samples of the temporal and spatial deformation field. The interpretation of the VLBI derived rates of deformation requires an examination of geologic information and more densely sampled ground based geodetic data. Triangulation and trilateration data measured on two regional networks, one in the central Mojave Desert and one in the Coast Ranges east of the San Andreas fault, were processed. At the spatial scales spanned by these local geodetic networks, auxiliary geologic and geophysical data were utilized to examine the relation between measured incremental strain and the accommodation of strain seen in local geologic structures, strain release in earthquakes, and principal stress directions inferred from in situ measurements. VLBI data was also processed from stations distributed across the Pacific-North America plate boundary zone in the western U.S. The VLBI data were used to constrain the integrated rate of deformation across portions of the continental plate boundary in California and to provide a tectonic framework to interpret regional geodetic and geologic studies. Author

A89-32838

REMOTE SENSING OF OCEAN CHLOROPHYLL - CONSEQUENCE OF NONUNIFORM PIGMENT PROFILE

SHUBHA SATHYENDRANATH (Dalhousie University, Halifax, Canada) and TREVOR PLATT (Bedford Institute of Oceanography, Dartmouth, Canada) Applied Optics (ISSN 0003-6935), vol. 28, Feb. 1, 1989, p. 490-495. refs

Remote sensing of ocean color, applied to the estimation of chlorophyll (Ch) biomass is discussed for the case where the vertical phytoplankton pigment profile (PP) is nonuniform. Using a spectral model of reflectance, the consequences of vertical structure are evaluated by sensitivity analysis on a generalized PP. It is shown that the assumption of a vertically homogeneous Ch distribution can lead to significant errors (relative error exceeding 100 percent) in the estimation from satellite data of photic depth and total pigment content in the photic zone. The errors are shown to be functions of the parameters of the PP. It is further shown that, if the shape of the PP is known from independent data, the entire PP may be recovered from the satellite data by making slight changes in the existing algorithms for Ch retrieval. Author

A89-34011

IDENTIFICATION OF TECTONIC DISLOCATIONS UNDERNEATH LARGE WATER AREAS USING SPACE IMAGES [VYIAVLENIE TEKTONICHESKIKH NARUSHENII NA AKVATORIIAKH PO MATERIALAM KOSMICHESKIKH S'EMOK]

I. G. AVENARIUS and A. A. TRESHCHOV IN: Remote-sensing studies of present-day tectonic processes. Moscow, Izdatel'stvo Nauka, 1988, p. 74-78. In Russian. refs

This paper describes a method for the identification of tectonic dislocations on the sea floor, using space images of water areas covered with ice or clouds. The methodology consists of two stages, the first of which involves the detection of linear anomalies, while the second consists of a sorting process to identify lineaments among these anomalies. It is shown that a linear anomaly on remote images can be detected from the presence of a linear band devoid of clouds, an abrupt change in a cloud pattern, an elongated chain of clouds in an otherwise cloudless zone of sky, and/or a sharp thinning out of a cloud cover system. I.S.

A89-34878

INTERACTION BETWEEN NET SHORTWAVE FLUX AND SEA SURFACE TEMPERATURE

JOHN BATES and CATHERINE GAUTIER (California, University, La Jolla) Journal of Applied Meteorology (ISSN 0894-8763), vol. 28, Jan. 1989, p. 43-51. Research supported by the U.S. Navy. refs

Ocean surface shortwave irradiance estimates derived from GOES data with the model of Gautier and Frouin (1985) are compared to in situ measurements from research vessels and buoys as part of the Frontal Air-Sea Interaction Experiment. It is shown that the satellite method overestimates percentage cloudiness during fractional cloud cover and at large satellite viewing angles. An empirical relationship is developed to correct this overestimation. The estimates are correlated and used to study the influences and feedbacks between clouds and sea surface temperatures. The results show that in monthly mean correlations, there are more clouds and/or clouds with higher liquid water content over colder northern water than over warmer southern waters. It is concluded that the long-term mean cloudiness field may act in a positive feedback sense, keeping cold water from gaining heat. R.B.

05 OCEANOGRAPHY AND MARINE RESOURCES

A89-35686

METHODOLOGY FOR THE REMOTE SENSING OF FLUXES OF HEAT, MOISTURE, AND EFFECTIVE RADIATION IN THE OCEAN-ATMOSPHERE SYSTEM [METODIKA DISTANTSIONNOGO OPREDELENIIA POTOKOV TEPLA, VLAGI I EFFEKTIVNOGO IZLUCHENIIA V SISTEME 'OKEAN-ATMOSFERA']

IU. A. IL'IN, A. A. KUZNETSOV, and V. A. MALINNIKOV Geodeziia i Aerofotos'emka (ISSN 0536-101X), no. 3, 1988, p. 96-98. In Russian.

A89-35864#

USE OF SEABOTTOM MAGNETIC SUSCEPTIBILITY MEASUREMENTS IN HYDROCARBON EXPLORATION

R. H. BARTON, W. D. TOMLINSON (Tenneco Oil E&P, Houston, TX), and G. W. BARTINGTON (Bartington Instruments, Oxford, England) IN: Thematic Conference on Remote Sensing for Exploration Geology, 6th, Houston, TX, May 16-19, 1988, Proceedings. Volume 1. Ann Arbor, MI, Environmental Research Institute of Michigan, 1988, p. 137-145. refs

The design and construction of a magnetic susceptibility system capable of detecting magnetic variations in the offshore environment is discussed. The use of the system in hydrocarbon exploration was tested in the North Sea. The instrument is illustrated and its operation is described. The regional geology of the survey area determined by the system is presented. The results suggest that the variation in seabottom magnetic susceptibility is related to the position of subsurface faults. R.B.

A89-35907#

A REAL-TIME GLOBAL SEA SURFACE TEMPERATURE ANALYSIS

RICHARD W. REYNOLDS (NOAA, Climate Analysis Center, Washington, DC) Journal of Climate (ISSN 0894-8755), vol. 1, Jan. 1988, p. 75-86. refs

A global monthly sea surface temperature analysis is described which uses real-time in situ (ship and buoy) and satellite data. The method combines the advantages of both types of data: the ground truth of in situ data and the improved coverage of satellite data. The technique also effectively eliminates most of the bias differences between the in situ and satellite data. Examples of the method are shown to illustrate these points. Sea surface temperature (SST) data from quality-controlled drifting buoys are used to develop error statistics for a 24-month period from January 1985 through December 1986. The average rms monthly error is 0.78 C; the modulus of the monthly biases (i.e., the average of the absolute value of the monthly biases) is 0.09 C. Author

A89-35931#

SURFACE SOLAR IRRADIANCE IN THE CENTRAL PACIFIC DURING TROPIC HEAT - COMPARISONS BETWEEN IN SITU MEASUREMENTS AND SATELLITE ESTIMATES

CATHERINE GAUTIER (California, University, San Diego) Journal of Climate (ISSN 0894-8755), vol. 1, June 1988, p. 600-608. refs
(Contract NSF OCE-82-14791)

Results are presented from the Tropic Heat experiment (Eriksen, 1985) concerning solar radiation at the ocean surface. A simple radiative transfer model was used to calculate hourly and daily surface solar irradiance values from calibrated GOES visible brightness measurements. The resulting values are validated with in situ measurements. Measurements from the Pacific island of Hiva Oa are compared with the satellite-based estimates, showing that the island's topography influences the ocean environment, causing local, daily orographic cloud formation. It is concluded that the satellite-based estimates represent the oceanic conditions better than the island measurements. R.B.

A89-37571

GREATER GLOBAL WARMING REVEALED BY SATELLITE-DERIVED SEA-SURFACE-TEMPERATURE TRENDS
A. E. STRONG (NOAA, National Environmental Satellite, Data,

and Information Service, Suitland, MD) Nature (ISSN 0028-0836), vol. 338, April 20, 1989, p. 642-645. refs

An analysis is presented of satellite-derived SSTs for the period 1982-88. The results show that the global ocean is undergoing a gradual but significant warming of about 0.1 C per year. The trend obtained for the same period from conventional data sources is about half that magnitude. C.D.

A89-38766

BATHYMETRIC MAPPING WITH PASSIVE MULTISPECTRAL IMAGERY

WILLIAM D. PHILPOT (Cornell University, Ithaca, NY) Applied Optics (ISSN 0003-6935), vol. 28, April 15, 1989, p. 1569-1578. refs

(Contract N00014-87-K-6006)

Bathymetric mapping will be most straightforward where water quality and atmospheric conditions are invariant over the scene. Under these conditions, both depth and an effective attenuation coefficient of the water over several different bottom types may be retrieved from passive, multispectral imagery. As scenes become more complex - with changing water type and variable atmospheric conditions - it is probable that a strictly spectral analysis will no longer be sufficient to extract depth from multispectral imagery. In these cases an independent source of information will be required. The most likely sources for such information are spatial and temporal variations in image data. Author

A89-39062

MEAN TEMPERATURE IN A CLOSED BASIN BY REMOTE SENSING

A. LORIA, F. MANTOVANI, S. PUGNAGHI (Osservatorio Geofisico, Modena, Italy), L. PILAN, S. VINCENZI (CNR, Istituto per lo Studio della Dinamica delle Grandi Masse, Venice, Italy) et al. (Gruppo Nazionale per la Fisica dell'Atmosfera e dell'Oceano, Congress, 4th, Rome, Italy, June 22-24, 1987) Nuovo Cimento C, Serie 1 (ISSN 0390-5551), vol. 11 C, Sept.-Dec. 1988, p. 537-548. Research supported by CNR. refs

An example is presented of the water surface temperature determination using data collected in the thermal infrared from spacecraft platforms. The procedure utilized here is based on the remotely observed surface temperature implemented by a calibration point at which usual meteorological measurements are performed. The mean vertical temperature is obtained by the energy conservation equation applied at the calibration point. The results of a field determination on a large basin called the Comacchio Valley, situated in northern Italy, are reported. C.D.

A89-39372*

Jet Propulsion Lab., California Inst. of Tech., Pasadena.

OBSERVING OCEANIC MESOSCALE EDDIES FROM GEOSAT ALTIMETRY - PRELIMINARY RESULTS

LEE-LUENG FU and VICTOR ZLOTNICKI (California Institute of Technology, Jet Propulsion Laboratory, Pasadena) Geophysical Research Letters (ISSN 0094-8276), vol. 16, May 1989, p. 457-460. refs

Mesoscale eddies constitute the most energetic component of the variability of ocean currents. Sea level variations measured by the Geosat radar altimeter are used to study the spatial and temporal scales of the eddy motion. An attempt is also made to map the temporal evolution of the eddy field in the region of the Agulhas Current south of Africa, where the eddy motions are among the strongest in the world. The results demonstrate that Geosat has provided an unprecedented opportunity to map from space the temporal evolution of sea level variability associated with the energetic eddies in the ocean. Author

A89-39659

SEASAT ALTIMETRY AND THE SOUTH ATLANTIC GEOID. II - SHORT-WAVELENGTH UNDULATIONS

DOMINIQUE GIBERT, JEAN-LOUIS OLIVET (Institut Francais de Recherche pour l'Exploitation de la Mer, Plouzane, France), and VINCENT COURTILOT (Paris VI, Universite, France) Journal of

Geophysical Research (ISSN 0148-0227), vol. 94, May 10, 1989, p. 5545-5559. Research supported by CNRS. refs

Seasat altimeter profiles are used to recover the short-wavelength (25-100 km) undulations of the South Atlantic geoid by along-track filtering. The coordinates of Eulerian poles describing the finite relative movement between the South American and African plates were calculated from 22 regularly distributed FZs between 12 deg N and 47 deg S. Also, a map of the roughness of the geoid is presented and is compared to other maps of the region. R.B.

A89-40145

MESOSCALE VARIABILITY OF SEA SURFACE TEMPERATURE IN THE NORTH ATLANTIC

THOMAS VIEHOFF (Kiel, Universitaet, Federal Republic of Germany) (Rutherford Appleton Laboratory, Meteorological Office, ESA, et al., Applications of AVHRR data: European AVHRR Data Users' Meeting, 3rd, Oxford, England, Dec. 16-18, 1987) International Journal of Remote Sensing (ISSN 0143-1161), vol. 10, Apr.-May 1989, p. 771-785. refs (Contract DFG-SFB-133)

Analyses of mesoscale horizontal distributions of temperature were performed for an area of the North Atlantic using data from the NOAA-7 and NOAA-6 AVHRR. The zonal and meridional variance spectra have slopes between -1.4 and -2.5 with a clear maximum at -2.0. This is also true for the direction-dependent structure functions. The isotropic part of the variance spectra has a mean slope of -2.2 ± 0.17 at scales of 10-100 km. This lies between the slopes of -1 and -3 predicted by the theories of two-dimensional and geostrophic turbulence. In some cases there are significant maxima in the variance spectra at scales between 50 km and 250 km. Author

N89-20597# National Oceanic and Atmospheric Administration, Seattle, WA. Marine Environmental Lab.

BEAUFORT SEA MESOSCALE CIRCULATION STUDY: PRELIMINARY RESULTS

A. AAGAARD, C. H. PEASE, and S. A. SALO Jul. 1988 179 p (PB89-121693; NOAA-TM-ERL-PMEL-82; CONTRIB-1040) Avail: NTIS HC A09/MF A01 CSCL 08/3

The Beaufort Sea Mesoscale Circulation Study was initiated in the autumn of 1986 and included measurements of currents, winds, and ice velocities, as well as observations of state variables and nutrient distributions in the ocean and state variables in the polar atmosphere, principally between Barrow and Demarcation Point along the American Beaufort Sea shelf. The preliminary results from observations made during the first year of the project, including current velocity results from meters recovered through the ice in April 1987, hydrographic and nutrient sections completed in October 1986 and April 1987, wind velocity, air pressure and temperature records recovered continuously through the end of 1987, ARGOS buoy tracks through 1987, and a representative sample of analyzed weather maps during the first year are given. Data collection continued through April 1988. The total data set is extraordinary in the temporal and spatial extent of its synoptic coverage, and in the variety of its constituent measurements. The data set is also extremely large, and its full reduction and analysis will provide an exceptional opportunity for improving the understanding of the shelf circulation and its forcing, as well as conditions important to the marine ecology of the area. Author

N89-24014# GKSS-Forschungszentrum Geesthacht (Germany, F.R.).

IMAGING PROCEDURE OF UNDERWATER BOTTOM TOPOGRAPHY BY AIR AND SATELLITE IMAGES IN THE RANGE OF MICROWAVE AND VISIBLE ELECTROMAGNETIC SPECTRA Thesis - Bremen Univ. [ABBILDUNG VON SUBMARINER BODENTOPOGRAPHIE AUF LUFT- UND SATELLITENBILDERN IM MIKROWELLENBEREICH UND IM SICHTBAREN BEREICH DES ELEKTROMAGNETISCHEN SPEKTRUMS]

I. HENNINGS 1988 183 p In GERMAN; ENGLISH summary

(GKSS-88/E/41; ISSN-0344-9629; ETN-89-94411) Avail: NTIS HC A09/MF A01

The imaging mechanism of underwater bottom topography in coastal waters with strong (tidal) currents by real and by synthetic aperture radar is investigated. A theoretical model is presented which describes the radar cross-section modulation and is tested with radar data. As an example satellite images of an Earth terrain camera and of a synthetic aperture radar from the same sea area are analyzed. The imaging in the satellite photograph is direct sunlight specularly reflected from the sea surface (sunglitter radiance). ESA

06

HYDROLOGY AND WATER MANAGEMENT

Includes snow cover and water runoff in rivers and glaciers, saline intrusion, drainage analysis, geomorphology of river basins, land uses, and estuarine studies.

A89-33121

NEW EARTH OBSERVING PLATFORMS TO STUDY GLOBAL WATER, BIOLOGY

Aviation Week and Space Technology (ISSN 0005-2175), vol. 130, March 13, 1989, p. 46, 47, 49, 50.

Two Mission to Earth spacecraft are being developed under the Earth Observing System (EOS) program as part of the unmanned-platform segment of the U.S. Space Station program. The spacecraft are scheduled to carry instruments powerful enough to spot biological changes in small lakes. Factors affecting atmospheric composition as well as global temperature and weather parameters would be monitored by the Mission to Earth spacecraft. K.K.

A89-35937

SENSITIVITY OF 30-DAY DYNAMICAL FORECASTS TO CONTINENTAL SNOW COVER

JOHN E. WALSH and BECKY ROSS (Illinois, University, Urbana) Journal of Climate (ISSN 0894-8755), vol. 1, July 1988, p. 739-754. refs

(Contract NSF ATM-85-07782)

The sensitivities of 30-day forecasts to continental snow cover in North America and Eurasia were determined using several series of 30-day simulations with a global circulation model. For the eastern North America, the major effect of extensive snow cover was found to be a reduction of the near-surface air temperature in the vicinity of the snow anomaly; when snow cover is extensive, sea-level pressures are somewhat lower and precipitation amounts are somewhat higher offshore of the East Coast, while sea level pressures are generally higher inland. In a set of six March cases, positive anomalies of Eurasian snow cover were found to reduce air temperatures by at least several degrees C throughout the lower half of the troposphere in the region over and downstream of the snow anomaly; the 30-day forecast pressures for the Eurasian hemisphere varied with snow coverage in a manner consistent with the observed pressure fields of the same months. I.S.

A89-37319

ASSESSMENT OF THE PRESENT CONDITIONS OF LOWLAND LAKES OF CENTRAL ASIA USING THE INTERPRETATION OF SPACE PHOTOGRAPHS [OTSENKA SOVREMENNOGO SOSTOYANIYA RAVNINNYKH OZER SREDNEI AZII PO REZULTATAM DESHIFIROVANIYA KOSMICHESKIKH SNIMKOV]

O. S. NURIDDINOV (Gosudarstvennyi Nauchno-Issledovatel'skii i Proizvodstvennyi Tsentr Priroda, USSR) Issledovanie Zemli iz Kosmosa (ISSN 0205-9614), Jan.-Feb. 1989, p. 67-69. In Russian.

A89-41160

THE USE OF REMOTE SENSING AND GIS TECHNIQUES FOR WETLAND IDENTIFICATION AND CLASSIFICATION IN THE GARRISON DIVERSION UNIT-NORTH DAKOTA

LAURA B. HALL, RICHARD C. CLARK, JAMES D. VON LOH, JOANNE N. HALLS (Advanced Sciences, Inc., Lakewood, CO), MICHAEL J. PUCHERELLI (USBR, Denver, CO) et al. IN: 1988 ACSM-ASPRS Annual Convention, Saint Louis, MO, Mar. 13-18, 1988, Technical Papers. Volume 4. Falls Church, VA, American Congress on Surveying and Mapping and American Society for Photogrammetry and Remote Sensing, 1988, p. 91-101. refs

The Garrison Diversion Unit, Pick-Sloan Missouri Basin Program, North Dakota, is an irrigation, recreation, municipal, rural, and industrial water system development project. The evaluation of land cover, particularly wetlands, is in response to the mitigation and enhancement plan, which recommends that mitigation for project-related wetland impacts be implemented prior to losses of resources. It is noted that mitigation is to be carried out on an acre-per-acre basis, replacing lost wetlands with their ecological equivalent. K.K.

A89-41433* National Aeronautics and Space Administration. Lyndon B. Johnson Space Center, Houston, TX.

ANALYSIS OF SEASONAL CHARACTERISTICS OF SAMBHAR SALT LAKE, INDIA, FROM DIGITIZED SPACE SHUTTLE PHOTOGRAPHY

KAMLESH P. LULLA and MICHAEL R. HELFERT (NASA, Johnson Space Flight Center, Houston, TX) Geocarto International (ISSN 1010-6049), vol. 4, March 1989, p. 69-74. refs

Sambhar Salt Lake is the largest salt lake (230 sq km) in India, situated in the northwest near Jaipur. Analysis of Space Shuttle photographs of this ephemeral lake reveals that water levels and lake basin land-use information can be extracted by both the digital and manual analysis techniques. Seasonal characteristics captured by the two Shuttle photos used in this study show that additional land use/cover categories can be mapped from the dry season photos. This additional information is essential for precise cartographic updates, and provides seasonal hydrologic profiles and inputs for potential mesoscale climate modeling. This paper extends the digitization and mensuration techniques originally developed for space photography and applied to other regions (e.g., Lake Chad, Africa, and Great Salt Lake, USA). Author

A89-41434* Lockheed Engineering and Sciences Co., Houston, TX.

THE DECREASE OF LAKE CHAD AS DOCUMENTED DURING TWENTY YEARS OF MANNED SPACE FLIGHT

ROBERT R. J. MOHLER (Lockheed Engineering and Sciences Co., Houston, TX), MICHAEL R. HELFERT (NASA, Johnson Space Flight Center, Houston, TX), and JOHN R. GIARDINO (Texas A & M University, College Station, TX) Geocarto International (ISSN 1010-6049), vol. 4, March 1989, p. 75-79. refs

Space photography has been successfully used to extend the space remote sensing data base for environmental monitoring by a decade. In this study of Lake Chad, space photographs were digitized and registered to a topographic base map before water classifications were performed. From 1966 to 1985 over a 21,000-square-kilometer decrease in lake surface area was observed. Author

N89-20533*# Louisiana State Univ., Baton Rouge. Coastal Ecology Inst.

UTILIZING REMOTE SENSING OF THEMATIC MAPPER DATA TO IMPROVE OUR UNDERSTANDING OF ESTUARINE PROCESSES AND THEIR INFLUENCE ON THE PRODUCTIVITY OF ESTUARINE-DEPENDENT FISHERIES Final Report

JOAN A. BROWDER, L. NELSON MAY, ALAN ROSENTHAL (National Marine Fisheries Service, Miami, FL.), ROBERT H. BAUMANN, and JAMES G. GOSSELINK 20 Dec. 1988 188 p (Contract NAS5-28756)

(NASA-CR-183417; NAS 1.26:183417) Avail: NTIS HC A09/MF A01 CSDL 08C

The land-water interface of coastal marshes may influence the production of estuarine-dependent fisheries more than the area of these marshes. To test this hypothesis, a spatial model was created to explore the dynamic relationship between marshland-water interface and level of disintegration in the decaying coastal marshes of Louisiana's Barataria, Terrebonne, and Timbalier basins. Calibrating the model with Landsat Thematic Mapper satellite imagery, a parabolic relationship was found between land-water interface and marsh disintegration. Aggregated simulation data suggest that interface in the study area will soon reach its maximum and then decline. A statistically significant positive linear relationship was found between brown shrimp catch and total interface length over the past 28 years. This relationship suggests that shrimp yields will decline when interface declines, possibly beginning about 1995. Author

N89-22175# Army Cold Regions Research and Engineering Lab., Hanover, NH.

SNOWMELT INCREASE THROUGH ALBEDO REDUCTION

SAMUEL C. COLBECK Dec. 1988 14 p (AD-A204523; CRREL-SR-88-26) Avail: NTIS HC A03/MF A01 CSDL 08/12

Due to changing surface conditions, albedo decreases naturally as snow ages. The details of the melting processes have been investigated for some years and much is known about the effect of each process and the interactions among them. Albedo has attracted a lot of attention because of recent interest in snow-climate feedback, and the reduction in albedo by darkening agents has been studied and practiced extensively. Although much is known about albedo reduction, the optimum design for a field program to enhance snow melting requires too much information to be easily achievable. The relevant snow properties and processes are described here along with some field observations. Much research must still be done to provide guidelines for the use of snow darkening agents in any particular environment. GRA

N89-22183# Industrial Science and Technology Agency, Tokyo (Japan).

JAPAN'S SUNSHINE PROJECT 1987 ANNUAL SUMMARY OF GEOTHERMAL ENERGY R AND D

Apr. 1988 198 p In JAPANESE (DE88-756451; AIST-8804) Avail: NTIS (US Sales Only) HC A09

Results are reported on the geothermal energy research for 1987 in the Sunshine Project. Exploration methods and formation mechanism of fracture type reservoirs were studied together with the study of their productivity. Basic maps for regional resources evaluation were prepared for five regions in Japan and parameters were determined. Percussion drills and aerated mud excavation technique were developed. Damages in hydrothermal flow were investigated and materials were developed. Crushing and thermal extraction mechanism were analyzed by the pressurized water crushing experiments at a quarry. Results of field experiment on the hot rock mass were analyzed. Environmental conservation and multipurpose use of hot water were investigated. Wide area hydrothermal flow system was surveyed at three areas. High accuracy MT method was developed and its effectiveness was demonstrated. Data was compared and analyzed for the Sengan and Kurikoma areas, which differ in abundance to each other. For development of binary 10 MW class demonstration plant, a well was excavated and tested, downhole pumps were tested and improved, and the conceptual design was investigated for plant equipment. Researches were conducted on the production and recirculation mechanism of hot water and control of water flowout. DOE

N89-22280# Nansen Ocean and Remote Sensing Center, Solheimsvik (Norway).

NOAA (NATIONAL OCEANIC AND ATMOSPHERIC ADMINISTRATION) AVHRR (ADVANCED VERY HIGH RESOLUTION RADIOMETER) OBSERVATIONS DURING THE MARGINAL ICE ZONE EXPERIMENT, BETWEEN SPITZBERGEN AND GREENLAND, JUNE 7 TO 18 JULY 1984

Final Report

OEASTEN SKAGSETH, K. KLOSTER, K. BARTHEL, and O. JOHANNESSEN Jun. 1988 130 p

(Contract N00014-80-G-0003)

(AD-A204911; NRSCTR-6; NEPRF-CR-88-10) Avail: NTIS HC A07/MF A01 CSCL 04/2

The marginal ice zone (MIZ) is the region in which the polar air, ice and water masses interact with the temperate air and ocean masses. During MIZEX-84 an intensive effort was made to obtain an integrated data set including meteorology, oceanography and glaciology, using remote sensing as well as conventional in situ observation methods, in the MIZ between Spitzbergen and Greenland from 7 June to 18 July 1984. This report gives NOAA AVHRR (Advanced Very High Resolution Radiometer) satellite imagery near-visual and infrared overviews of the Fram Strait and the large-scale surrounding area. For near-visual imagery phenomena of particular interest, e.g., mesoscale vortices, the focus of attention is on off- and on-air circulation, island lee effects and synoptic low development. Features of special interest are noted and important small scale phenomena are enlarged if they are not prominent on the overview images. An appendix provides satellite images and surface charts showing day to day development over the MIZEX-84 area 7 June to 18 July. GRA

07

DATA PROCESSING AND DISTRIBUTION SYSTEMS

Includes film processing, computer technology, satellite and aircraft hardware, and imagery.

A89-33543

EXOS-C (OHZORA) OBSERVATIONS OF POLAR CAP PRECIPITATIONS AND INVERTED V EVENTS

T. MUKAI, T. OBARA, M. KITAYAMA, A. NISHIDA (Tokyo, University, Sagami-hara, Japan), and N. KAYA (Kobe University, Japan) (COSPAR and SCOSTEP, Plenary Meeting, 27th, Symposium on Multipoint Magnetospheric Measurement, 8th, Espoo, Finland, July 18-29, 1988) Advances in Space Research (ISSN 0273-1177), vol. 8, no. 9-10, 1988, p. 363-372. refs

By analyzing measurements of the precipitating electrons and ions obtained by the low-energy particle experiment on the semipolar-orbit satellite EXOS-C (launched in 1984), two issues are addressed. The first is the source of electrons forming the precipitation events observed as spikelike flux enhancements in the polar cap. Information derived from the conjugacy and the temperature is used to examine the adequacy of two possible sources, the plasma sheet and the solar wind. The second issue is the acceleration mechanism of the inverted-V electrons in the auroral region. The quantitative model of the field-aligned acceleration formulated by Lyons (1980) is compared with the observation, and fair agreement is found. Author

A89-33658

AN ALGORITHM FOR MACHINE-RECOGNIZING THE RIVER MOUTH AND MEASURING THE SEALINE FROM THE LANDSAT IMAGE

WENYI CHEN (Shandong University, Jinan, People's Republic of China) IN: Multispectral image processing and enhancement; Proceedings of the Meeting, Orlando, FL, Apr. 6-8, 1988. Bellingham, WA, Society of Photo-Optical Instrumentation Engineers, 1988, p. 64-68.

Recognition of the river mouth is the key to detect the coast line and to discriminate it from the river side. It is an essential step in automatic determining the coast length. To realize this the spatial information, the correlation between the boundary pixels, the curvature, and the curvature maximum must be taken into account. The algorithm proposed here has been used on some fractions of the seashore in North Shandong of China, and the results are satisfying. Author

A89-33664

MULTISPECTRAL TERRAIN BACKGROUND SIMULATION TECHNIQUES FOR USE IN AIRBORNE SENSOR EVALUATION

MICHAEL WEINBERG, RONALD WOHLERS, JOHN CONANT, and EDWARD POWERS (Aerodyne Research, Inc., Billerica, MA) IN: Multispectral image processing and enhancement; Proceedings of the Meeting, Orlando, FL, Apr. 6-8, 1988. Bellingham, WA, Society of Photo-Optical Instrumentation Engineers, 1988, p. 243-252.

A background simulation code called Aerie is discussed. Aerie is designed to reflect the major sources of IR background clutter that are of concern for the staring and scanning sensors being considered for various aircraft threat warning sensors. The Aerie characteristics are summarized, and the three-dimensional earth simulation procedures and the scene data base preparation Aerie uses are described. Some sample scenes generated by Aerie are shown. C.D.

A89-33684

REPRESENTATION AND RECOGNITION OF ELONGATED REGIONS IN AERIAL IMAGES

CHARLES A. LIPARI, CHARLES A. HARLOW (Louisiana State University, Baton Rouge), and MOHAN M. TRIVEDI (Tennessee, University, Knoxville) IN: Applications of artificial intelligence VI; Proceedings of the Meeting, Orlando, FL, Apr. 4-6, 1988. Bellingham, WA, Society of Photo-Optical Instrumentation Engineers, 1988, p. 557-567. Research supported by DMA. refs

The recent advances in model-based image understanding systems for aerial imagery have used intermediate-level interpretations of the low-level segmentations in terms of generic shape properties. This paper is concerned with those features recognizable in the context of having an elongated shape as evidenced from the planar point sets obtained from spectral classifications. The basic processing technique can be described as linear-strip point clustering, using the minimum spanning tree as a connectivity constraint. The algorithms are applied to classifications of suburban road networks. The major elongated regions are detected for the given strip width, and where connectivity can be established across any gaps in the segmentation. Author

A89-33872

A RASTER APPROACH TO POPULATION ESTIMATION USING HIGH-ALTITUDE AERIAL AND SPACE PHOTOGRAPHS

C. P. LO (Georgia, University, Athens) Remote Sensing of Environment (ISSN 0034-4257), vol. 27, Jan. 1989, p. 59-71. refs

A raster approach was used to extract residential building density data from remote sensing images on a grid cell by grid cell basis. The study used from National High Altitude photography (1:80,000 scale) and LFC photographs taken from the Space Shuttle (1:50,000 scale) of the area around Providence, Rhode Island. The maximum possible occurrence of residential units in each grid cell was determined with reference to dwelling unit sizes and existing census housing data. The actual percentage of residential buildings in each grid cell was estimated and translated into a population estimate. At census tract level, population estimates exhibited mean relative errors between + 2.50 and +6.94 percent in the aerial photography and between -8.24 and -13.64 percent in the LFC photography. R.B.

A89-33874*# Department of Agriculture, Beltsville, MD.

A NEW TECHNIQUE TO MEASURE THE SPECTRAL PROPERTIES OF CONIFER NEEDLES

C. S. T. DAUGHTRY (USDA, Remote Sensing Research Laboratory,

Beltsville, MD), K. J. RANSON (NASA, Goddard Space Flight Center, Greenbelt, MD), and L. L. BIEHL (Purdue University, West Lafayette, IN) Remote Sensing of Environment (ISSN 0034-4257), vol. 27, Jan. 1989, p. 81-91. refs
(Contract NAGW-799)

A technique that enables the measurement of reflectance and transmittance of narrow leaves or needles with spectroradiometers equipped with a light source and integrating sphere is described. Measurement procedures and formulas for optical property calculations are presented. A test of the techniques resulted in absolute reflectance differences of 3 percent or less when comparing optical properties measured for whole leaves and narrow strips cut from the leaves. Author

A89-33875* Arizona Univ., Tucson.

EVALUATING ATMOSPHERIC CORRECTION MODELS FOR RETRIEVING SURFACE TEMPERATURES FROM THE AVHRR OVER A TALLGRASS PRAIRIE

D. I. COOPER (Arizona, University, Tucson) and G. ASRAR (NASA, Washington, DC) Remote Sensing of Environment (ISSN 0034-4257), vol. 27, Jan. 1989, p. 93-102. refs
(Contract NAG5-389)

The effects of atmospheric attenuation on surface radiative temperatures obtained by the AVHRR over a tallgrass prairie area in the Flint Hills of Kansas are examined. Six atmospheric correction models developed primarily for sea-surface temperature studies are used to test their utility for retrieval of radiative temperatures over the land surface. An uncertainty of + or - 3.0 C was found for the AVHRR data, and used to evaluate the performance of a given model. When the difference between in situ and AVHRR surface temperatures was smaller than the uncertainty, the model was judged to be adequate. Among the six models evaluated, only the NOAA split-window model consistently adjusted the AVHRR surface temperatures within + or - 3.0 C of the in situ measurements. Author

A89-34001

REMOTE-SENSING STUDIES OF PRESENT-DAY TECTONIC PROCESSES [AEROKOSMICHESKOE IZUCHENIE SOVREMENNYKH I NOVEISHIKH TEKTONICHESKIKH PROTSESSOV]

V. G. TRIFONOV, ED. Moscow, Izdatel'stvo Nauka, 1988, 136 p. In Russian. For individual items see A89-34002 to A89-34018.

The application of remote sensing to the investigations of structures of recent origin and their contemporary geodynamics is discussed in the frameworks of theory and methodology. Results obtained by remote-sensing methodology on neotectonics and present-day geodynamics are presented for various regions on the territory of the USSR, including the Moscow Region, Crimea and the Caucasus, the Azov Coastal Region, the Altai-Saian and Baikal regions, Central Asia, the Pripiat' Basin, and the southern Arctic. Special consideration is given to the use of remote sensing to identify seismically active zones and the degree of seismic danger in these zones. I.S.

A89-34013

METHODS FOR INVESTIGATING SEISMICALLY ACTIVE ZONES USING REMOTE IMAGERY [AEROKOSMICHESKIE METODY IZUCHENIYA SEISMOAKTIVNYKH ZON]

V. G. TRIFONOV, V. I. MAKAROV, and S. F. SKOBELEV IN: Remote-sensing studies of present-day tectonic processes. Moscow, Izdatel'stvo Nauka, 1988, p. 87-100. In Russian. refs

Methods are described for estimating the degree of seismic danger in a given seismically active zone from criteria used for the classification of geological features on remote images. It is pointed out that the general character of the active-zone cross section is one of the major factors that determines the presence of a considerable tectonic stress. The predominance of incompetent beds (such as serpentines, clay shale, or loose precipitates) hinders the concentration of stress, while a predominance of competent beds promotes it. I.S.

A89-34014

AUTOMATED ANALYSIS OF LINEAMENTS FROM SPACE IMAGERY OBTAINED DURING SEISMIC STUDIES OF CENTRAL TIEN-SHAN [AVTOMATIZIROVANNYI ANALIZ LINEAMENTOV PO KOSMICHESKIM SNIMKAM PRI SEISMOTEKTONICHESKIKH ISSLEDOVANIYAKH /NA PRIMERE TSENTRAL'NOGO TIAN'-SHANIA/]

V. T. AKSENOV, I. G. GORDIENKO, S. I. GRADENKO, A. A. ZLATOPOL'SKII, G. N. IVANCHENKO et al. IN: Remote-sensing studies of present-day tectonic processes. Moscow, Izdatel'stvo Nauka, 1988, p. 100-104. In Russian. refs

A89-34015

THE USE OF SPACE IMAGERY FOR INVESTIGATIONS OF RECENT CRUSTAL DEFORMATIONS IN SOUTHERN IAKUTIA [ISPOL'ZOVANIE KOSMICHESKIKH MATERIALOV PRI IZUCHENII SOVREMENNYKH DEFORMATSIY ZEMNOI KORY NA IUGE IAKUTII]

A. F. PETROV, G. V. BOCHAROV, and N. N. ZAMARAEV IN: Remote-sensing studies of present-day tectonic processes. Moscow, Izdatel'stvo Nauka, 1988, p. 104-111. In Russian. refs

A89-34266*

Jet Propulsion Lab., California Inst. of Tech., Pasadena.

REVIEW AND STATUS OF REMOTE SENSING OF SEA ICE

FRANK CARSEY (California Institute of Technology, Jet Propulsion Laboratory, Pasadena) IEEE Journal of Oceanic Engineering (ISSN 0364-9059), vol. 14, April 1989, p. 127-138. refs

The status of obtaining geophysical observations through the interpretation of satellite data over sea ice is discussed. It is pointed out that the community working in this area has grown in size and sophistication over the last decade, that the connection between microscopic properties of ice and its microwave behavior is now being understood, and that a good deal of accurate satellite-derived information on sea ice can now be obtained. Areas of ongoing, as well as needed, work are outlined, especially in the understanding of first-year- and old-ice microwave properties, and it is pointed out that the efficient advance of remote sensing will require more active participation of scientists focused on in situ studies. I.E.

A89-34268

SEA-ICE CHARACTERIZATION MEASUREMENTS NEEDED FOR TESTING OF MICROWAVE REMOTE SENSING MODELS

DALE P. WINEBRENNER, LEUNG TSANG, BOHENG WEN, and RICHARD WEST (Washington, University, Seattle) IEEE Journal of Oceanic Engineering (ISSN 0364-9059), vol. 14, April 1989, p. 149-158. refs

The nature and accuracy of ice-characterization measurements needed to test two microwave backscattering models are clarified by examining the sensitivities of these models to variations in the geophysical parameters they require as input. First, the Bragg, or small perturbation, model for rough surface scattering, which appears appropriate for backscattering from new ice types at L-band, is considered. The sensitivities of this model to variations in the dielectric constant of the ice and to the power spectrum of surface roughness are examined. The dense-medium radiation-transfer model at X-band is considered for backscattering from air bubbles embedded in multilayer ice. The sensitivities of this model to air-bubble size, air-volume fraction, and dielectric loss in the ice are examined. Based on these sensitivities, quantitative characterization guidelines for model testing are discussed. I.E.

A89-34363

TAX - PROTOTYPE EXPERT SYSTEM FOR TERRAIN ANALYSIS

DEMETRE P. ARGIALAS and RAVI NARASIMHAN (Louisiana State University, Baton Rouge) Journal of Aerospace Engineering (ISSN 0893-1321), vol. 1, July 1988, p. 151-170. Research supported by Louisiana Department of Transportation and Louisiana State University. refs

The Terrain Analysis Expert, or 'TAX', is a rule-based expert

system that has been developed for the modeling interpretation logic involved in identification of landforms from aerial images. Knowledge of the geographic location of an image is used to arrive at hypotheses about the landform of the site manifested on the aerial image; these hypotheses were then established or rejected on the basis of the degree to which they matched between their landform pattern elements and those of the site. Site pattern elements were obtained interactively from the analyst, and a probabilistic method was designed for the handling of uncertainties in the observed pattern element values. O.C.

A89-34416* Jet Propulsion Lab., California Inst. of Tech., Pasadena.

IMAGE-ANALYSIS TECHNIQUES FOR DETERMINATION OF MORPHOLOGY AND KINEMATICS IN ARCTIC SEA ICE

MEEMONG LEE and WEI-LIANG YANG (California Institute of Technology, Jet Propulsion Laboratory, Pasadena) *Annals of Glaciology* (ISSN 0260-3055), vol. 9, 1987, p. 1-5.

SAR data have been used to study sea ice with respect to its motion and formation/deformation. With the prospect of the Alaska SAR Facility development in the near future, there is a great need for robust and efficient sea-ice analysis techniques. This paper presents a sea-ice motion analysis technique that can be used for: (1) local motion analysis of a selected ice patch, and (2) a global ice motion over the entire image area. In order to meet the operational speed requirement (over fifty images per day) a sea-ice motion analysis technique has been developed which requires very little human interaction. The proposed technique uses a subset of easily distinguishable features to predict global motion characteristics. The developed technique is applied to two pairs of SEASAT SAR images, one pair with a minor motion of 'ice pack' and another with a larger and discontinuous motion of 'fast ice'. The new approach enables the development of a set of computer-aided tools for feature selection and registration and the implementation of an optimal search strategy for automatic template matching via a motion prediction model. Author

A89-34706

ACCESSING REMOTE SENSING TECHNOLOGY - THE MICROBRIAN EXAMPLE

B. A. HARRISON, D. L. B. JUPP, P. G. HUTTON, and K. K. MAYO (CSIRO, Div. of Water Resources, Canberra, Australia) *International Journal of Remote Sensing* (ISSN 0143-1161), vol. 10, Feb. 1989, p. 301-309. Research supported by CSIRO and MPA International Pty., Ltd. refs

The development of the microBRIAN system, a PC compatible version of the BRIAN system (Jupp et al., 1985), is discussed. The system identifies remote sensing applications and provides access to the image processing and operational required for individual applications. The user requirements and range of applications of the system are examined. Consideration is given to the technology available for data analysis and the integration of the system with other data sets. R.B.

A89-34879

OBSERVATIONAL ANALYSES OF NORTH ATLANTIC TROPICAL CYCLONES FROM NOAA POLAR-ORBITING SATELLITE MICROWAVE DATA

CHRISTOPHER S. VELDEN (Wisconsin, University, Madison) *Journal of Applied Meteorology* (ISSN 0894-8763), vol. 28, Jan. 1989, p. 59-70. refs
(Contract NOAA-NA-84DGC0155)

Passive microwave observations from the NOAA polar-orbiting satellites are used to analyze 18 North Atlantic tropical cyclones between 1979 and 1985. An algorithm for estimating surface intensity is derived. Linear regression relationships are developed between the satellite-depicted horizontal temperature gradient of the upper-level warm core and the surface intensity measured by reconnaissance reports. Standard errors of estimate of 8 mb and 13 kts are found for surface pressure and maximum winds, respectively. It is shown that these errors may be reduced by including the effects of storm latitude, eye size, and surface-pressure tendency. R.B.

A89-35159

THEORETICAL ALGORITHMS FOR SATELLITE-DERIVED SEA SURFACE TEMPERATURES

I. J. BARTON, D. M. O'BRIEN (CSIRO, Div. of Atmospheric Research, Aspendale, Australia), A. M. ZAVODY (SERC, Rutherford Appleton Laboratory, Didcot, England), D. R. CUTTEN (Department of Defence, Defence Science and Technology Organization, Salisbury, Australia), and R. W. SAUNDERS (Oxford University, England) *Journal of Geophysical Research* (ISSN 0148-0227), vol. 94, March 20, 1989, p. 3365-3375. refs

The performances of several different atmospheric transmission models are compared by estimating the IR brightness temperatures measured by the NOAA 9 AVHRR for three standard atmospheres. Then, the computationally quickest of these models, the spectral band model, which was found to perform as well as the other models, is used to derive several preliminary prelaunch sea surface temperature (SST) algorithms for the ATS radiometer (ATSR). These algorithms, derived in the form of linear equations, show that a low-noise 3.7-micron channel is required to give the best satellite-derived SST, and that the design accuracy of the ATSR is achievable. I.S.

A89-35335#

RESEARCH ON SPECKLE BEHAVIOR IN SAR IMAGES [UNTERSUCHUNGEN ZUM SPECKLEVERHALTEN IN SAR-BILDERN]

F. HEEL, H. KIETZMANN, M. ZINK, and W. GOBLIRSCH (DFVLR, Institut fuer Hochfrequenztechnik, Oberpfaffenhofen, Federal Republic of Germany) (URSI and Informationstechnische Gesellschaft, Gemeinsame Tagung, Kleinheubach, Federal Republic of Germany, Oct. 3-7, 1988) *Kleinheubacher Berichte* (ISSN 0343-5725), vol. 32, 1989, p. 155-165. In German. refs

Seasat-SAR images of scenes with varying image contrasts, including the classes of sea surface, land, and urban regions, were studied in order to characterize the image speckle characteristics. The image amplitude distributions are determined using measurement data processed by a digital SAR processor. The least square error method is used to determine the functions resulting from the data distributions of the individual classes. The averages and standard deviations are calculated to determine the amount of agreement. The results are used to derive conclusions concerning the relationship of the object to the amount of speckle in the image. The significance of the results for speckle reduction is considered. C.D.

A89-35336#

PERFORMANCE ANALYSIS OF THE DFVLR REAL TIME SAR PROCESSOR FOR LOW SNRS [ANALYSE DER LEISTUNGSFAEHIGKEIT DES DFVLR ECHTZEIT-SAR-PROZESSORS BEI NIEDRIGEN SIGNAL/RAUSCH-VERHAELTNISSEN]

ALBERTO MOREIRA (DFVLR, Institut fuer Hochfrequenztechnik, Oberpfaffenhofen, Federal Republic of Germany) (URSI and Informationstechnische Gesellschaft, Gemeinsame Tagung, Kleinheubach, Federal Republic of Germany, Oct. 3-7, 1988) *Kleinheubacher Berichte* (ISSN 0343-5725), vol. 32, 1989, p. 167-176. In German. refs

A real-time azimuth processor was developed for the DFVLR's aircraft-borne Experimental SAR (E-SAR). The processor operates using an unfocused correlation procedure with a triangular function to suppress sidelobes. Measurements were conducted over sea and land using a transmit peak power of 50 W and a pulse width of 100 ns in the L-band. A satisfactory image quality was obtained with an SNR of 3-10 dB in the near range. Images processed with the triangular weighting showed far superior results for point targets and better image quality for photographs taken over nonhomogeneous regions. The system is suitable for many purposes, such as monitoring of oil pollution on the sea surface, where this SAR system can be implemented in small aircraft at reduced cost. C.D.

A89-35684

MULTISPECTRAL SPACE SURVEYS AND DATA PROCESSING [MNOGOZONAL'NYE KOSMICHESSKIE S'EMKI I OBRABOTKA INFORMATSII]

V. V. KISELEV, I. S. NENASHEV, I. K. ORLOV, G. A. SAVIN, and M. E. SOLOMATIN. *Geodeziia i Aerofotos'emka* (ISSN 0536-101X), no. 3, 1988, p. 81-84. In Russian.

Techniques for the processing of multispectral data from the Cosmos satellites are discussed. Particular attention is given to techniques of color image synthesis, and to the development of multispectral synthesizing devices. The application of digital techniques is examined. B.J.

A89-35837

AUTOMATED DTM VALIDATION AND PROGRESSIVE SAMPLING ALGORITHM OF FINITE ELEMENT ARRAY RELAXATION

URHO A. RAUHALA, DON DAVIS, and KEN BAKER (General Dynamics Corp., Electronics Div., San Diego, CA) *Photogrammetric Engineering and Remote Sensing* (ISSN 0099-1112), vol. 55, April 1989, p. 449-465. refs

The development of array relaxation algorithms of fast array algebra solutions for automated validation and progressive sampling of DTMs is discussed. Array algebra DTM techniques are reviewed. An array relaxation algorithm for a computational solution of general nonseparable and shift variant systems is introduced. Also, the generalization of the array relaxation algorithm to the array correlation technique of multiray global least-squares correlation is considered. R.B.

A89-35838

USING MULTISPECTRAL VIDEO IMAGERY FOR DETECTING SOIL SURFACE CONDITIONS

J. H. EVERITT, D. E. ESCOBAR, M. A. ALANIZ, and M. R. DAVIS (USDA, Agricultural Research Service, Weslaco, TX) *Photogrammetric Engineering and Remote Sensing* (ISSN 0099-1112), vol. 55, April 1989, p. 467-471. refs

The ability of multispectral video imagery to discriminate among various soil surface conditions is evaluated. Sets of seven multispectral images were acquired for five pans and three field plots with different soil surface conditions. Spectroradiometric reflectance measurements and digital video data were obtained from the plots. For the pan experiments, the best correlations between digital video and reflectance data were obtained for the green, red, and orange wavebands. For the field experiments, the best correlation was obtained for the MIR waveband. It is concluded that multispectral video imagery can be used successfully to differentiate among various soil surface conditions. R.B.

A89-35854#

SUCCESSFUL APPLICATIONS OF REMOTELY SENSED DATA FOR OIL AND GAS EXPLORATION

JOHN S. CARTER (Carter Exploration Co.; GeoTrac Energy Corp., Abilene, TX) and DAVID G. KOGER (Texas Christian University, Fort Worth) IN: Thematic Conference on Remote Sensing for Exploration Geology, 6th, Houston, TX, May 16-19, 1988, Proceedings. Volume 1. Ann Arbor, MI, Environmental Research Institute of Michigan, 1988, p. 19-25.

The use of Landsat MSS and TM data for gas and oil exploration on the Eastern Shelf of the Permian Basin is examined. Applications of the remote sensing data include the location of minor low-relief buried structure, minor faulting and fracture systems, and geochemically altered surface rocks and soils resulting from hydrocarbon microseepages. Examples are presented from several regions of Texas in which oil and gas drilling programs were developed using Landsat data. R.B.

A89-35855#

LOWERING THE COST OF EXPLORATION FOR INDEPENDENTS - HOW REMOTELY SENSED DATA AIDS IN THE SEARCH FOR OIL AND GAS

ARTHUR J. PYRON IN: Thematic Conference on Remote Sensing

for Exploration Geology, 6th, Houston, TX, May 16-19, 1988, Proceedings. Volume 1. Ann Arbor, MI, Environmental Research Institute of Michigan, 1988, p. 27-36. refs

Examples of cases in which Landsat imagery was applied for exploration by independent oil and gas companies are presented. The Landsat program and processes for analyzing Landsat data are reviewed. In each of the cases, the Landsat data was used to develop models of the tonal anomalies related to subsurface features in the region. The examples illustrate the use of Landsat data for choosing drilling sites in New Mexico, Arkansas, and the Middle East. R.B.

A89-35863#

GAS CHROMATOGRAPHIC AND SONAR IMAGING OF HYDROCARBON SEEPS IN THE MARINE ENVIRONMENT

V. T. JONES (Exploration Technologies, Inc., Houston, TX), J. C. WILLIAMS (Houston Area Research Council, TX), and R. J. MOUSSEAU IN: Thematic Conference on Remote Sensing for Exploration Geology, 6th, Houston, TX, May 16-19, 1988, Proceedings. Volume 1. Ann Arbor, MI, Environmental Research Institute of Michigan, 1988, p. 125-134. refs

The use of dissolved gas analysis systems to detect anomalous hydrocarbon concentrations in bottom waters is discussed. The use of a color imaging sonar system to provide color images of microseeps in the water column and the use of sniffer geochemical data to predict oil versus gas potential of subsurface reservoirs are examined. An example correlating marine seep data with hydrocarbons analyzed from dart cores is presented. R.B.

A89-35867*# Nevada Univ., Reno.

VEGETATION REFLECTANCE FEATURES IN AVIRIS DATA

CHRISTOPHER D. ELVIDGE (Nevada, University, Reno) IN: Thematic Conference on Remote Sensing for Exploration Geology, 6th, Houston, TX, May 16-19, 1988, Proceedings. Volume 1. Ann Arbor, MI, Environmental Research Institute of Michigan, 1988, p. 169-182. Research supported by NASA. refs

Equations for converting Airborne Visible-IR Imaging Spectrometer (AVIRIS) digital numbers to percent reflectance were developed using a set of three calibration targets. When converted to reflectance the following spectral features of vegetation can be observed in AVIRIS data: details in the pigment absorption region, the red edge, the NIR plateau, leaf water absorptions on the NIR plateau, leaf water absorptions, and lignocellulose absorptions. These results indicate that AVIRIS data will be quite useful in geobotanical remote sensing. Author

A89-35870#

HIGH RESOLUTION IMAGING OF GEOBOTANICAL ANOMALIES ASSOCIATED WITH SUBSURFACE HYDROCARBONS

NICHOLAS REID (Monitek, Ltd., Concord, Canada), A. IWASHITA (Earth Resources Satellite Data Analysis Center, Tokyo, Japan), YOICHIRO YAMASHITA (Japex Geoscience Institute, Inc., Tokyo, Japan), and KEITH THOMPSON (Recon Exploration, Inc., Dallas, TX) IN: Thematic Conference on Remote Sensing for Exploration Geology, 6th, Houston, TX, May 16-19, 1988, Proceedings. Volume 1. Ann Arbor, MI, Environmental Research Institute of Michigan, 1988, p. 213-223. refs

An inverted Gaussian model of red edge reflectance is presented for use in detecting vegetation stress associated with subsurface hydrocarbon anomalies from high resolution spectral measurements of vegetation reflectance. The model yields parameters for red edge shoulder height, the calculated reflectance minimum, and the Gaussian inflection point. The model was used to analyze images of an oil field in Michigan obtained with the airborne Programmable Multispectral Imager. Results are given from interpreting the imagery with respect to interstitial soil gas samples. R.B.

A89-35876#

THE APPLICATION OF HIGH RESOLUTION DIGITAL ELEVATION MODELS TO PETROLEUM AND MINERAL EXPLORATION AND PRODUCTION

ROBERT K. VINCENT, WILLIAM T. LEHMAN, RODNEY L. HENRY, JOHN D. HERMAN, MARK E. STIVERS (GeoSpectra Corp., Ann Arbor, MI) et al. IN: Thematic Conference on Remote Sensing for Exploration Geology, 6th, Houston, TX, May 16-19, 1988, Proceedings. Volume 1. Ann Arbor, MI, Environmental Research Institute of Michigan, 1988, p. 293-301. Research supported by DOE.

The types of image products that have been derived from two high-resolution digital elevation models (HRDEMs) of test sites in Alaska and California are described and illustrated. The production of the HRDEMs from SPOT stereo pair images, and the application of data derived from the HRDEMs to petroleum and mineral exploration are examined. The applications include the production of shaded relief images and elevation profiles, the calculation of structural dip direction, the creation of simulated perspective view images for line-of-sight determinations and drill site selection, and the overlaying of data from geophysical surveys, digitized maps, and various remote sensing platforms to create a Geographical Information System data base. R.B.

A89-35877#

ASSESSING AGGREGATE RESOURCE POTENTIAL IN THE CANADIAN SHIELD - A KNOWLEDGE-BASED APPROACH

J. K. HORNSBY (Intera Technologies, Ltd., Ottawa, Canada) and BILL BRUCE (Canada Centre for Remote Sensing, Ottawa) IN: Thematic Conference on Remote Sensing for Exploration Geology, 6th, Houston, TX, May 16-19, 1988, Proceedings. Volume 1. Ann Arbor, MI, Environmental Research Institute of Michigan, 1988, p. 313-325. refs

The application of remote sensing to the assessment of aggregate resource potential in a glaciated, shield-type environment is studied. An expert system was constructed to integrate Landsat TM, SPOT, Radar, and airborne photography data for an area in Canada at the western end of the Sudbury Basin. The knowledge-based approach used to develop the expert system is described and results are presented from geobotanical and landform interpretation and aggregate potential assessment. R.B.

A89-35883*# National Aeronautics and Space Administration. Lyndon B. Johnson Space Center, Houston, TX.

ASTRONAUT PHOTOGRAPHY OF THE EARTH - LOW COST IMAGES FOR RESOURCE EXPLORATION

CHARLES A. WOOD (NASA, Johnson Space Center, Houston, TX) IN: Thematic Conference on Remote Sensing for Exploration Geology, 6th, Houston, TX, May 16-19, 1988, Proceedings. Volume 1. Ann Arbor, MI, Environmental Research Institute of Michigan, 1988, p. 383-390. refs

Applications for photographs taken with handheld cameras by astronauts on the Space Shuttle are examined. The amount, types, and quality of photographs taken between 1981 and 1986 are described. Examples of these photographs and a portion of a map displaying the coverage of these photographs are presented. The possible use of handheld Space Shuttle photography in conjunction with Landsat mosaics for geologic exploration is discussed. R.B.

A89-35885#

APPLICATIONS OF AVHRR IMAGERY IN FRONTIER EXPLORATION

CHRISTOPHER A. LEGG (Royal Aerospace Establishment, National Remote Sensing Centre, Farnborough, England) IN: Thematic Conference on Remote Sensing for Exploration Geology, 6th, Houston, TX, May 16-19, 1988, Proceedings. Volume 1. Ann Arbor, MI, Environmental Research Institute of Michigan, 1988, p. 409-418. refs

Low-cost imagery from the AVHRR sensor on NOAA meteorological satellites can provide an overview of geologic structure as an aid to frontier exploration. Examples are presented to illustrate structural applications in arid and temperate climates. The split-window thermal infrared channels of the AVHRR permit crude thermal spectral observations in arid environments, enabling gross lithologic discrimination. Examples from a study area in

Morocco illustrate the use of the ratio between AVHRR channels 5 and 4 to discriminate silica-rich units from calcareous and argillaceous rocks. Author

A89-35888#

INTEGRATION OF LANDSAT TM, STREAM SEDIMENT GEOCHEMISTRY AND REGIONAL GEOPHYSICS FOR MINERAL EXPLORATION IN THE ENGLISH LAKE DISTRICT

M. D. FORREST (British Geological Survey, London, England) and A. E. HARDING (Royal Aerospace Establishment, National Remote Sensing Centre, Farnborough, England) IN: Thematic Conference on Remote Sensing for Exploration Geology, 6th, Houston, TX, May 16-19, 1988, Proceedings. Volume 2. Ann Arbor, MI, Environmental Research Institute of Michigan, 1988, p. 469-474. Research supported by the Department of Trade and Industry and NERC. refs

A89-35892#

IMPLEMENTATION OF BACKGROUND AND TARGET GEOBOTANICAL TECHNIQUES IN MINERAL EXPLORATION

J. K. HORNSBY, J. HARRIS (Intera Technologies, Ltd., Ottawa, Canada), B. BRUCE (Canada Centre for Remote Sensing, Ottawa), and A. N. RENCZ (Geological Survey of Canada, Ottawa) IN: Thematic Conference on Remote Sensing for Exploration Geology, 6th, Houston, TX, May 16-19, 1988, Proceedings. Volume 2. Ann Arbor, MI, Environmental Research Institute of Michigan, 1988, p. 511-521. refs

This paper reports on the implementation of both background and spectral geobotanical techniques in an area of zinc and gold mineralization in metasedimentary host rocks. The study area is located within the Grenville geological province. A geobotanical classification was produced of the area based on TM data and a digital terrain model combined with detailed ground surveys. Several anomalous areas were identified on the basis of the geobotanical classes and supporting geological data sets. The results demonstrate the synergistic value of the combined background and spectral geobotanical approaches to the application of remote sensing methods and data for mineral exploration in vegetated terrain. Author

A89-35895#

SATELLITE ALTIMETRY. II - A NEW PROSPECTING TOOL

BERT LUNDGREN and PER NORDIN (Petroscan, AB, Goteborg, Sweden) IN: Thematic Conference on Remote Sensing for Exploration Geology, 6th, Houston, TX, May 16-19, 1988, Proceedings. Volume 2. Ann Arbor, MI, Environmental Research Institute of Michigan, 1988, p. 565-575. refs

Geopotential method altimetry for offshore hydrocarbon-deposit remote prospecting seeks short-wavelength undulations of the mean sea level that are caused by density variations in the upper 10 km of the earth's crust. The geopotential method has been established to be well-suited for prospecting in areas with laterally-extended density contrasts; these greater-than-25 km density contrasts in sedimentary basins are usually caused by porosity variations, and can be distinguished from denser formations. Attention is given to a profile of observed altimeter data from GEOS-3 over the Norwegian Sea. O.C.

A89-35898#

USES OF THE SAS STATISTICAL PACKAGE FOR DIGITAL IMAGE ANALYSIS

R. VEENA MALHOTRA and THOMAS C. EAGLE (Dartmouth College, Hanover, NH) IN: Thematic Conference on Remote Sensing for Exploration Geology, 6th, Houston, TX, May 16-19, 1988, Proceedings. Volume 2. Ann Arbor, MI, Environmental Research Institute of Michigan, 1988, p. 635-644. refs

A maximum-likelihood cluster analysis has been performed on a 256-pixel x 240-line scene centered on Magadi Lake, Kenya, to demonstrate the application of SAS procedures to data used on the RIPS image-analysis system. The results thus obtained are compared with a supervised geological classification as well as with an unsupervised classification performed through SPEC DAT software on the RIPS image analyzer. The SAS analysis procedure

emerges as much more effective than conventional image-analysis software in the identification of lithologic units, due to its ability to handle the complete data set when defining clusters; the multidimensional graphics output of SAS further enhances the attractiveness of its use. O.C.

A89-35900#

RECONSTRUCTION OF IMAGERY OF FAULTED LANDSCAPES USING A PHOTO-OPTICAL TECHNIQUE

R. L. ANDERSON, A. FALCONER (Regional Centre for Services in Surveying, Mapping and Remote Sensing, Nairobi, Kenya), and W. L. SMITH (Decision-Science Applications, Inc., Arlington, VA) IN: Thematic Conference on Remote Sensing for Exploration Geology, 6th, Houston, TX, May 16-19, 1988, Proceedings. Volume 2. Ann Arbor, MI, Environmental Research Institute of Michigan, 1988, p. 653-662. refs

The application of remotely sensed image mosaics constructed directly onto film to various tectonic regions and problems in eastern and southern Africa is presently illustrated with the cases of the Gregory rift in Kenya and the Great Dike in Zimbabwe. The 'trimming' of images to fit seamlessly is accomplished by the use of masks to control the area of each image and to adjust that area's exposure. Landscape features that have been obviously disrupted by tectonic activity have been reconstructed by mosaicking in ways that permit the testing of landscape-evolution hypotheses as well as to graphically illustrate development stages. O.C.

A89-35902*# National Aeronautics and Space Administration. Lyndon B. Johnson Space Center, Houston, TX.

GEOLOGICAL APPLICATIONS OF THE SPACE STATION CORE PLATFORM

DAVID L. AMSBURY (NASA, Johnson Space Center, Houston, TX) IN: Thematic Conference on Remote Sensing for Exploration Geology, 6th, Houston, TX, May 16-19, 1988, Proceedings. Volume 2. Ann Arbor, MI, Environmental Research Institute of Michigan, 1988, p. 671-676.

The manned core platform of the Space Station will repeatedly provide observations of the tropical and subtropical parts of earth from about 500 km altitude in a 28.5 degree orbit. This orbit covers most of the landmasses in the Southern Hemisphere, half of the world ocean, and more than 120 nations. The platform can provide remote-sensing activities by means of: (1) sensors attached to structural members of the platform; (2) sensors deployed on one or more pointable platforms attached to structural members, or man-tended in separate orbits; (3) sensors operated from the resource nodes; (4) sensors operated through earth-viewing, optical-quality windows; and (5) hand-held cameras operated by crew members throughout the facility. Major applications of observations from the core platform in the exploration for and production of resources are discussed. Author

A89-35903#

DIGITAL DISPLAY OF SPOT STEREO IMAGES

T. H. LEE WILLIAMS and VIRGINIA THOMPSON (Cooperative Institute for Applied Remote Sensing, Norman, OK) IN: Thematic Conference on Remote Sensing for Exploration Geology, 6th, Houston, TX, May 16-19, 1988, Proceedings. Volume 2. Ann Arbor, MI, Environmental Research Institute of Michigan, 1988, p. 679-685.

A digital display system has been developed which allows on-screen stereo viewing of SPOT imagery; the left and right stereo images are alternated on the screen at a rate of 120/sec, thereby yielding 60 stereo views/sec with no visible flicker. The combination of an electronically-switched LCD screen and passive polarized viewing glasses accomplishes this presentation of left and right images to the viewer's left and right eye, respectively. The digital format allows radiometric matching and interactive tonal enhancement and convolution-filtering of the stereo image. O.C.

A89-35906

AUTOMATED RECOGNITION OF OCEANIC CLOUD PATTERNS. I - METHODOLOGY AND APPLICATION TO CLOUD CLIMATOLOGY

LOUIS GARAND (Department of the Environment, Atmospheric Environment Service, Dorval, Canada) Journal of Climate (ISSN 0894-8755), vol. 1, Jan. 1988, p. 20-39. Research supported by the Department of the Environment of Canada. refs (Contract NSF ATM-84-14467)

A scheme is presented for the automated classification of oceanic cloud patterns. Class discrimination is obtained from 13 features representing height, albedo, shape, and multilayering characteristics of the cloud fields. Two features derived from the two-dimensional power spectrum of the visible images proved essential for the detection of directional patterns and open cells. Based on the assumption of multinormal distributions of the features, a simple classification algorithm is developed. The generation of artificial samples yields a theoretical separability of 97 percent while the actual separability obtained on the training set is 95 percent. From 1020 independent samples, the separate verification of three expert nephanalysts indicates strict accuracy in 79 percent of the cases while there is agreement with their first or second choice in 89 percent of the cases. Author

A89-35912

SATELLITE DETECTION OF SAHARAN DUST - OPTIMIZED IMAGING DURING NIGHTTIME

MICHEL LEGRAND, KWAMI VOVOR (Universite Nationale de Cote d'Ivoire, Abidjan, Ivory Coast), and MICHEL DESBOIS (CNRS, Laboratoire de Meteorologie Dynamique, Palaiseau, France) Journal of Climate (ISSN 0894-8755), vol. 1, March 1988, p. 256-264. Research supported by CNRS. refs

The data of the ECLATS experiment (at Niamey, 1980) are used to study the daily variations of the sensitivity of ground temperature to atmospheric dustiness. In the presence of dust, ground temperature is lower during daytime and higher than normal during nighttime. During night, the influence of dust on ground temperature prevails over other factors. The sensitivity of temperature to dustiness is evaluated and used jointly with ECLATS aircraft soundings to assess the impact of atmospheric dust on the radiance measured by the Meteosat-I thermal infrared sensor. The results obtained demonstrate the ability of Meteosat to detect dust clouds during nighttime. A method of optimized imaging is described and applied to a case study. Author

A89-35926

A COMPARISON OF RADIATION VARIABLES CALCULATED IN THE UCLA GENERAL CIRCULATION MODEL TO OBSERVATIONS

BRYAN C. WEARE (California, University, Davis) Journal of Climate (ISSN 0894-8755), vol. 1, May 1988, p. 485-499. Research supported by NSF. refs

Spatial patterns of solar and thermal fluxes of radiation calculated by the UCLA general circulation model were compared to observations of the 1982-1983 El Nino for the December-February period. The observational data included estimates at the Pacific surface of the climatological averages of the net solar and thermal radiation, satellite observations of the climatological averages of planetary albedo and outgoing longwave radiation, and satellite observations of the anomalies of albedo and outgoing longwave. Results showed differences of up to 25 percent from the mean between the calculated and the observed climatological net solar radiation at the surface and planetary albedo. It was found that the model-generated El Nino anomalies of planetary albedo and outgoing longwave radiation agree with observations as to the position, but they underestimate the magnitudes by up to a factor of 4. I.S.

A89-36704* National Center for Atmospheric Research, Boulder, CO.

POLAR CAP DEFLATION DURING MAGNETOSPHERIC SUBSTORMS

J. J. MOSES (High Altitude Observatory, Boulder, CO), G. L.

SISCOE (California, University, Los Angeles), R. A. HEELIS (Texas, University, Richardson), and J. D. WINNINGHAM (Southwest Research Institute, San Antonio, TX) *Journal of Geophysical Research* (ISSN 0148-0227), vol. 94, April 1, 1989, p. 3785-3789. refs

(Contract NASA ORDER W-16320; NSF ATM-87-22962; NAG5-305; NAG5-306; NAS5-28712; F19628-84-N-0006)

The expanding/contracting polar cap model has been used to simulate DE-2 ion drift data during substorms as determined using the AL index. Of the 39 cases modeled, 57 percent required the opening of a nightside gap which maps to where reconnection occurs in the tail; 75 percent of the 16 recovery phase cases required a nightside gap, while only 29 percent of the 17 expansion phase cases required a nightside gap. On the basis of this result, it is concluded that if a nightside gap implies tail reconnection, then reconnection probably occurs after expansion phase onset and continues throughout most of the recovery phase of a substorm. Author

A89-37291* Miami Univ., Coral Gables, FL.

AEROSOL ANALYSIS WITH THE COASTAL ZONE COLOR SCANNER - A SIMPLE METHOD FOR INCLUDING MULTIPLE SCATTERING EFFECTS

HOWARD R. GORDON and DIEGO J. CASTANO (Miami, University, Coral Gables, FL) *Applied Optics* (ISSN 0003-6935), vol. 28, April 1, 1989, p. 1320-1326. refs

(Contract NAGW-273; NAS5-28798; N00014-84-K-0451)

A method for studying aerosols over the ocean using Nimbus-7 CZCS data is proposed which circumvents having to perform radiative transfer computations involving the aerosol properties. The method is applied to the CZCS band 4 at 670 nm, and yields the total radiance ($L_{sub t}$) backscattered from the top of a stratified atmosphere containing both stratospheric and tropospheric aerosols and the Rayleigh scattered radiance ($L_{sub r}$). The radiance which the aerosol would produce in the single scattering approximation is retrieved from ($L_{sub t}$) - ($L_{sub r}$) with an error of not greater than 5-7 percent. R.R.

A89-37318

A TECHNIQUE FOR APPLYING SPACE PHOTOGRAPHS TO SEARCH FOR ANTICLINAL OIL- AND GAS-TRAPS IN OROGENIC STRUCTURES OF THE TIEN-SHAN [METODIKA PRIMENENIIA KOSMICHESKIKH SNIMKOV DLIA POISKA ANTIKLINAL'NYKH LOVUSHEK NEFTI I GAZA V OROGENNYKH STRUKTURAKH TIAN-SHANIA]

A. D. BAKLANOV, D. A. TASHKHODZHAEV, and T. T. TADZHIEV (Institut Geologii i Razvedki Neftianikh i Gazovykh Mestorozhdenii, Tashkent, Uzbek SSR; Gosudarstvennyi Nauchno-Issledovatel'skii i Proizvodstvennyi Tsentr Priroda, USSR) *Issledovanie Zemli iz Kosmosa* (ISSN 0205-9614), Jan.-Feb. 1989, p. 59-66. In Russian.

A89-37321

PARAMETER OPTIMIZATION OF SYSTEMS FOR THE THERMAL MICROWAVE MAPPING OF THE EARTH'S SURFACE [OB OPTIMIZATSII PARAMETROV SISTEM RADIOTEPLOVOGO KARTOGRAFIROVANIYA POVERKHNOSTI ZEMLI]

A. P. PICHUGIN and S. A. SHILO (AN USSR, Institut Radiofiziki i Elektroniki, Kharkov, Ukrainian SSR) *Issledovanie Zemli iz Kosmosa* (ISSN 0205-9614), Jan.-Feb. 1989, p. 77-86. In Russian. refs

The paper examines the optimization of the parameters of thermal microwave mapping systems according to the criterion of data link capacity. The information content of this approach is evaluated on the basis of experimental spatial-frequency brightness-temperature spectra plotted for generalized surface types. B.J.

A89-37323

RADIOMETRIC CORRECTION OF AERIAL AND SPACE REMOTE-SENSING IMAGES [RADIOMETRICHESKAYA KORREKTSIYA AEROKOSMICHESKIKH IZOBRAZHENII]

A. S. BARYKIN (Vsesoiuznyi Nauchno-Issledovatel'skii Tsentr AIUS-Agroresursy, Moscow, USSR) *Issledovanie Zemli iz Kosmosa* (ISSN 0205-9614), Jan.-Feb. 1989, p. 94-102. In Russian. refs

A radiometric correction technique is described which can improve the recognition accuracy of landscape features when the reflectances of these features are compared with those of reference objects on the same image. Stochastic averages of the atmospheric optical thickness are used to approximate variations of the surface illumination and atmospheric transparency. Approximation errors are estimated, and the method is illustrated by an example. B.J.

A89-37324

METHODOLOGICAL ASPECTS OF THE AUTOMATION OF THE CALIBRATION AND PROCESSING OF SATELLITE MICROWAVE-RADIOMETER DATA [METODICHESKIE VOPROSY AVTOMATIZATSII KALIBROVKI I OBRABOTKI SPUTNIKOVYKH SVCH-RADIOMETRICHESKIKH DANNYKH]

A. B. AKVILONOVA, M. S. KRYLOVA, B. G. KUTUZA, B. Z. PETRENKO, V. P. SAVORSKII (AN SSSR, Institut Radiotekhniki i Elektroniki, Moscow, USSR) et al. *Issledovanie Zemli iz Kosmosa* (ISSN 0205-9614), Jan.-Feb. 1989, p. 103-114. In Russian. refs

A procedure for the computer-aided processing of satellite microwave-radiometer ground-track data is presented. Typical features of radiometer calibration with reference to two ground points are discussed, and a method for evaluating the influence of calibration errors on the accuracy of ocean-atmosphere brightness-temperature measurements is presented. Also considered is a procedure for the computer-aided identification of sites in the experimental data which correspond to the ground control points. B.J.

A89-37325

COMPUTER-AIDED SYNTHESIS OF TEXTURES SIMULATING THE EARTH'S SURFACE [MASHINNYI SINTEZ TEKSTUR, IMITIRUIUSHCHIKH ZEMNUIU POVERKHNOST']

G. A. ANDREEV, A. A. POTAPOV, T. V. GALKINA, A. I. KOLESNIKOV, T. I. ORLOVA (AN SSSR, Institut Radiotekhniki i Elektroniki, Moscow; Voronezhskii Gosudarstvennyi Universitet, Voronezh, USSR) et al. *Issledovanie Zemli iz Kosmosa* (ISSN 0205-9614), Jan.-Feb. 1989, p. 115-121. In Russian. refs

Several types of textures common to land covers are obtained using an autoregression synthesis model which uses the statistics of the underlying surfaces. The autoregression synthesis is characterized by a small number of parameters and moderate expenditures of CPU time. Experimental results indicate the high reliability of the simulation algorithm. B.J.

A89-37471

THE RATE OF GAS EXCHANGE BETWEEN THE OCEAN AND THE ATMOSPHERE USING MICROWAVE RADIOMETER DATA [SKOROST' GAZOOBMENA OKEANA S ATMOSFEROI PO DANNYM SVCH-RADIOMETRII]

V. B. LAPSHIN and I. G. RAGULIN (Gosudarstvennyi Okeanograficheskii Institut, Moscow, USSR) *Meteorologiya i Gidrologiya* (ISSN 0130-2906), March 1989, p. 113-115. In Russian. refs

A simple model is presented for calculating the rate of gas exchange between the ocean and the atmosphere using microwave radiometer data. The model is based on the experimental dependence of the ocean surface brightness temperature and the rate of gas exchange through the surface on the intensity of foaming. A synoptic analysis of the area studied is conducted and the data are compared with the results for wind and wave fields. R.B.

A89-37801#

EVALUATION OF GEOSAT ALTIMETER DATA WITH APPLICATION TO TROPICAL PACIFIC SEA LEVEL VARIABILITY

ROBERT E. CHENEY, BRUCE C. DOUGLAS, and LAURY MILLER (NOAA, National Geodetic Survey, Rockville, MD) *Journal of*

07 DATA PROCESSING AND DISTRIBUTION SYSTEMS

Geophysical Research (ISSN 0148-0227), vol. 94, April 15, 1989, p. 4737-4747. refs

Geosat altimeter measurements of sea level at ground track intersections and along collinear nests of profiles are used to evaluate the quality of Geosat data. A regional, precise surface of intersecting sea level profiles is constructed. The magnitude of the electromagnetic bias is determined. Also, sea level time series and anomaly maps are generated. It is concluded that Geosat data can determine sea level changes with a rms accuracy of about 4 cm for time scales of a month or longer. R.B.

A89-37808* Jet Propulsion Lab., California Inst. of Tech., Pasadena.

STATISTICAL GEOMETRY OF A SMALL SURFACE PATCH IN A DEVELOPED SEA

ROMAN E. GLAZMAN (California Institute of Technology, Jet Propulsion Laboratory, Pasadena) and PETER B. WEICHMAN (California Institute of Technology, Pasadena) Journal of Geophysical Research (ISSN 0148-0227), vol. 94, April 15, 1989, p. 4998-5010. refs

The fractal and marginal fractal regimes in surface geometry are studied. The basic notions of fractal geometry are applied to a small surface patch in a developed sea, corresponding to the equilibrium wave number spectrum. Topothesy, outer and inner boundaries of the fractal range, and a cascade pattern in surface geometry are discussed. Theoretical predictions of whitecap and foam coverage are presented. A fractal decomposition for a surface patch is developed based on the Karhunen-Loeve expansion. The resulting series formalizes the cascade process of constructing realization of a Gaussian random patch. The implications of the research for microwave remote sensing signatures are considered. R.B.

A89-37944

A DIGITAL MOSAICKING ALGORITHM ALLOWING FOR AN IRREGULAR JOIN 'LINE'

SUSANNE HUMMER-MILLER (USGS, Branch of Geophysics, Denver, CO) Photogrammetric Engineering and Remote Sensing (ISSN 0099-1112), vol. 55, Jan. 1989, p. 43-47. refs

Computer mosaicking of any type of digital images using intricate join lines can now be achieved through a simple algorithm. Prerequisites are two scenes, geometrically registered to each other and brightness-matched across the seam. The algorithm is used to define digitally every point of the join line in image space and to test each location to determine which scene brightness value should be used in the mosaic. An example is presented using daytime thermal IR data on the Arabian Peninsula from the NOAA-AVHRR satellite system. The mosaicking technique is simple, requires only minimal computation, and can be easily programmed on most minicomputers. Author

A89-37945

TWO-DIMENSIONAL SEAM-POINT SEARCHING IN DIGITAL IMAGE MOSAICKING

SHIREN YANG, LI LI, and PENG GAO (Chinese Academy of Sciences, Institute of Remote Sensing Application, Beijing, People's Republic of China) Photogrammetric Engineering and Remote Sensing (ISSN 0099-1112), vol. 55, Jan. 1989, p. 49-53.

Elimination of artificial edges in image mosaics is of importance for image interpretation and further processing. In this article, a two-dimensional seam-point searching algorithm is suggested where the grey-level difference in the vertical direction as well as in the horizontal direction is controlled. An algorithm for mosaics of multispectral images is also introduced. Experiments show that, with the method suggested, the artificial edges in the mosaics can be smoothed significantly. Author

A89-37946

A RASTER APPROACH TO TOPOGRAPHIC MAP REVISION

E. LYNN USERY (USGS, Rolla, MO) and R. WELCH (Georgia, University, Athens) Photogrammetric Engineering and Remote Sensing (ISSN 0099-1112), vol. 55, Jan. 1989, p. 55-59. refs

With the approaching completion of the U.S. Geological Survey's

1:24,000-scale mapping program for the conterminous U.S., map revision becomes a primary activity. Experimental techniques for map revision are being developed which require digitizing both map and photographic sources in a raster format, rectifying the resulting data to a common coordinate system, simultaneously displaying the digital map and photographic data, performing visual change detection, and manually updating the digital map data with an on-screen digitizing procedure. Updated image and line map output are generated from the raster data using a film-write device. Map revision performed completely in the raster domain achieves geometric accuracies sufficient to meet National Map Accuracy Standards at the 1:24,000 scale from 7-m-pixel data and 1:100,000 scale from 28.5-m-pixel data. Approximately 80 percent of the transportation and hydrography features are updated at the 1:24,000 scale from the 7-m-pixel raster data. Author

A89-37947

REFLECTANCE ENHANCEMENTS FOR THE THEMATIC MAPPER - AN EFFICIENT WAY TO PRODUCE IMAGES OF CONSISTENTLY HIGH QUALITY

F. J. AHERN (Canada Centre for Remote Sensing, Ottawa) and J. SIROIS (INTERA Technologies, Ltd., Ottawa, Canada) Photogrammetric Engineering and Remote Sensing (ISSN 0099-1112), vol. 55, Jan. 1989, p. 61-67. refs

The reflectance enhancement algorithm, originally developed for the Landsat MSS, has been found to be a reliable method for producing consistently high-quality photographic images from satellite data. Here, consideration is given to the algorithm and how it was adapted to TM data. Four enhancements have been developed for forestry applications for a range of biophysical and phenological conditions. The principal characteristics of these enhancements are described. Author

A89-37948

COMPARISON OF SATELLITE, GROUND-BASED, AND MODELING TECHNIQUES FOR ANALYZING THE URBAN HEAT ISLAND

JAMES A. HENRY, ORJAN F. WETTERQVIST, STEPHEN J. ROGUSKI (Florida, University, Gainesville), and STEVEN E. DICKS (Southwest Florida Water Management District, Brooksville, FL) Photogrammetric Engineering and Remote Sensing (ISSN 0099-1112), vol. 55, Jan. 1989, p. 69-76. Research supported by IBM Corp. and University of Florida. refs

This study compares six temperature patterns obtained from the Heat Capacity Mapping Mission satellite with a temperature pattern acquired using the auto-traverse technique and a thermal pattern predicted by a land-use-based simulation model called DYNASPACE for a region centered on Gainesville, FL. The satellite data reveal daytime heat islands of 5 to 6 C and early-morning magnitudes of up to 9 C. Highest temperatures during days and mornings were in the central business district (CBD), the university campus, and the airport. Other consistent thermal features in the satellite data were extensions of high temperatures to the north and east of the CBD and a stronger temperature gradient to the west of the CBD than to the east. All of these features were also apparent in the auto-traverse temperature pattern and were generally predicted by the DYNASPACE model. Author

A89-37950

CLUSTER ANALYSIS OF PINE CROWN FOLIAGE PATTERNS AID IDENTIFICATION OF MOUNTAIN PINE BEETLE CURRENT-ATTACK

PETER A. MURTHA and RAOUL J. WIART (British Columbia, University, Vancouver, Canada) Photogrammetric Engineering and Remote Sensing (ISSN 0099-1112), vol. 55, Jan. 1989, p. 83-86. Research supported by NSERC. refs

A89-38328

MARINE OBSERVATION SATELLITE-1 - FIRST YEAR IN ORBIT

HIROSHI HORIGUCHI, TATSUO MATSUEDA, TAKESHI MASUDA (National Space Development Agency of Japan, Tokyo), and SUSUMU YOSHITOMI (Space Communications Research Corp.,

Tokyo, Japan) IN: International Symposium on Space Technology and Science, 16th, Sapporo, Japan, May 22-27, 1988, Proceedings. Volume 2. Tokyo, AGNE Publishing, Inc., 1988, p. 2191-2196.

The orbital performance of Japan's first medium altitude experimental earth observation satellite, MOS-1, is described. This satellite was launched from the Tanegashima Space Center on February 19, 1987. During the first year of operation some minor problems arose, including the false execution of delayed command caused by single event upset of the command memory and safety attitude retraction due earth sensor malfunctioning. K.K.

A89-38332

DEVELOPMENT AND VERIFICATION OF OSAKA BAY SAMPLING MODEL BASED ON LANDSAT DATA

KATSUTOSHI KOUZAI (Kobe University of Mercantile Marine, Japan) and KIYOSHI TSUCHIYA (Chiba University, Japan) IN: International Symposium on Space Technology and Science, 16th, Sapporo, Japan, May 22-27, 1988, Proceedings. Volume 2. Tokyo, AGNE Publishing, Inc., 1988, p. 2217-2221. refs

An attempt was made to develop an improved methodology for selecting optimum water quality sampling locations on Osaka Bay through the use of Landsat MSS images. A multiple regression model with independent variables of resultant wind speed and degree days was used as a sampling model. It is found that the relationship between the mixed layer depth and the euphotic zone depth can be explained by the density prediction model. K.K.

A89-38333

DISCRIMINATION OF ROCKS AND HYDROTHERMAL ALTERED AREAS BASED ON LANDSAT TM DATA

KWANG HOON CHI, PIL CHONG KANG (Korea Institute of Energy and Resources, Seoul, Republic of Korea), and KIYOSHI TSUCHIYA (Chiba University, Japan) IN: International Symposium on Space Technology and Science, 16th, Sapporo, Japan, May 22-27, 1988, Proceedings. Volume 2. Tokyo, AGNE Publishing, Inc., 1988, p. 2223-2228. refs

An attempt is made to detect the hydrothermally altered zone via analysis of Landsat TM data together with the ground truth data on the spectral reflectance of rocks and pyrophyllite ore. The Seochangri region in the southeastern part of the Korean peninsula was used as a test site. A false color image of the band ratio can be used to identify a hydrothermal altered area. K.K.

A89-38334

ATMOSPHERIC CORRECTION OF SATELLITE MSS DATA IN RUGGED TERRAIN

S. UENO (Kyoto School of Computer Science, Japan) and Y. KAWATA (Kanazawa Institute of Technology, Japan) IN: International Symposium on Space Technology and Science, 16th, Sapporo, Japan, May 22-27, 1988, Proceedings. Volume 2. Tokyo, AGNE Publishing, Inc., 1988, p. 2229-2234. refs

The paper presents a method for evaluating the atmospheric effect in terms of the generalized scattering function in a vertically inhomogeneous and anisotropic scattering atmosphere bounded below by the horizontally inhomogeneous albedos of the ground surface. The atmospheric correction in rugged terrain (the topographic effect in a mountainous region) is discussed. Ways of nearly eliminating the atmospheric and topographic effects in rugged terrain are presented. K.K.

A89-38968*

WISCONSIN UNIV., MADISON. USING THE RADIATIVE TEMPERATURE DIFFERENCE AT 3.7 AND 11 MICRONS TO TRACK DUST OUTBREAKS

STEVEN A. ACKERMAN (Wisconsin, University, Madison) Remote Sensing of Environment (ISSN 0034-4257), vol. 27, Feb. 1989, p. 129-133. refs

(Contract NSF ATM-85-21214; NAS1-18272)

The radiative temperature difference between 3.7 and 11 microns (ΔT) is investigated as a possible method for tracking dust outbreaks. Theoretical calculations indicate that the technique would be most sensitive to dust loading during the day when the ΔT s are enhanced by reflection of 3.7-micron solar radiation.

The feasibility of tracking dust outbreaks is demonstrated by comparing satellite observations with surface estimates of visibility. Theoretical calculations also demonstrate the potential of inferring the dust layer optical depth from these spectral measurements.

Author

A89-38970*

KANSAS STATE UNIV., MANHATTAN. MEASURING AND MODELING SPECTRAL CHARACTERISTICS OF A TALLGRASS PRAIRIE

G. ASRAR, R. B. MYNENI, Y. LI, and E. T. KANEMASU (Kansas State University, Manhattan) Remote Sensing of Environment (ISSN 0034-4257), vol. 27, Feb. 1989, p. 143-155. refs (Contract NAG5-389)

This study was conducted to evaluate the diurnal and seasonal, spectral reflectance characteristics of burned and unburned areas of a tallgrass prairie, based on field measurements and models of radiation transport in plant canopies. Burning of the senescent vegetation, resulting from the previous years' growth, is a common management practice, which results in improved productivity and affects the succession of grass species. The burned and unburned grass canopies showed distinctly different, diurnal and seasonal, spectral reflectance characteristics in the visible and infrared regions of the spectrum. These were attributed to the differences in development of the two plant canopies and the azimuthal differences in sensor-sun-canopy positions during field measurements of spectral reflectance. The radiation transfer model properly simulated the diurnal spectral behavior of the two canopies. The simulated, seasonal, spectral reflectance values for the unburned grass canopy were greater than the measured ones, because of limitations in proper representation of the layer of senescent vegetation in the model. Author

A89-38971

A REFLECTANCE MODEL FOR THE HOMOGENEOUS PLANT CANOPY AND ITS INVERSION

TIIT NILSON and ANDRES KUUSK (AN ESSR, Institut Astrofiziki i Fiziki Atmosfery, Toravere, Estonian SSR) Remote Sensing of Environment (ISSN 0034-4257), vol. 27, Feb. 1989, p. 157-167. refs

An analytical reflectance model for a statistically homogeneous plant canopy has been developed. The most specific characteristics of the model are: (1) considering both the single and the multiple scattering of radiation in the canopy and on the soil and (2) accounting for the specular reflection of radiation on leaves and canopy hot spot. For the inversion of the model the technique suggested by Goel and Strebel (1983) has been applied. The reflectance model fits well the results of measurements both of the seasonal course of the nadir reflectance and of the angular distribution of the directional reflectance of the winter wheat and barley canopies. Author

A89-38972*#

NEW HAMPSHIRE UNIV., DURHAM. MODELING DIRECTIONAL THERMAL RADIANCE FROM A FOREST CANOPY

M. J. MCGUIRE (New Hampshire, University, Durham), L. K. BALICK (EG&G Energy Measurements, Inc., Las Vegas, NV), J. A. SMITH (NASA, Goddard Space Flight Center, Greenbelt, MD), and B. A. HUTCHISON Remote Sensing of Environment (ISSN 0034-4257), vol. 27, Feb. 1989, p. 169-186. Research sponsored by the U.S. Army. refs

The thermal vegetation canopy radiance model of Smith et al. (1981) is extended to account for the geometrically rough structure of a forest canopy. Fourier series expansion of a canopy height profile is used to calculate improved view facts which partially account for directional variations in canopy thermal radiance transfers. Predictions from the Smith model and the modified model are compared with experimental data obtained over a deciduous forest site in Tennessee. The results show that thermal radiance from a forest canopy depends on sensor viewing angle, solar position, and the degree of geometric roughness of the canopy surface. The maximum off-nadir angle variation in the original model was 1.6 deg C, compared with 4.4 C for the modified model.

R.B.

A89-39063

VALIDATION PROBLEMS FOR REMOTELY SENSED SEA SURFACE TEMPERATURE

G. DALU and G. L. LIBERTI (CNR, Istituto di Fisica dell'Atmosfera, Rome, Italy) (Gruppo Nazionale per la Fisica dell'Atmosfera e dell'Oceano, Congress, 4th, Rome, Italy, June 22-24, 1987) Nuovo Cimento C, Serie 1 (ISSN 0390-5551), vol. 11 C, Sept.-Dec. 1988, p. 589-607. Research supported by CNR. refs

A previously developed linear algorithm for deriving sea surface temperature (SST) from AVHRR-2 data was tested using high-quality in situ data obtained during the ADRIA-84 campaign in the Northern Adriatic Sea. The problems involved in the comparison between satellite and in situ data are considered in detail, including the screening of the data, their preparation, and their matching in space and time. The derived SST, when compared with the in situ measured temperature, showed a standard deviation of 0.2 K after the removal of a bias of 0.1 K. C.D.

A89-39093

ANALYTICAL INDEPENDENT MODEL TRIANGULATION STRIP ADJUSTMENT USING SHORE-LINE CONSTRAINTS

MOHAMED SHAWKI ELGHAZALI (Cairo University, Giza, Egypt) Photogrammetric Engineering and Remote Sensing (ISSN 0099-1112), vol. 55, May 1989, p. 567-571. refs

The effect of adding points on shore lines as absolute constraints to the basic linearized mathematical model of independent model triangulation is studied. A strip of eight aerial photographs having an approximate scale of 1:7500 for part of Kuwait City showing shore line for an area on the Arabian gulf extending over seven stereoscopic models is used. The strip contains five full ground control points, five planimetric check points, and 10 height check points. Eight shore-line points were used, and the strip adjustment was performed twice with and without the additional constraints to compare results, while keeping the check points outside the adjustment procedure to guarantee proper accuracy assessment. Results showed an improvement in the rms errors in height and planimetry of approximately 19.5 percent and 8.5 percent respectively, when adding shore-line points as absolute constraints. Author

A89-39094

A SEMI-AUTOMATIC TERRAIN MEASUREMENT SYSTEM FOR EARTHWORK CONTROL

SUSUMU HATTORI, SHUNJI MURAI (Tokyo, University, Japan), HITOSHI OHTANI (Topcon Co., Tokyo, Japan), and RYOSUKE SHIBASAKI (Ministry of Construction, Public Works Research Institute, Tsukuba, Japan) (International Society for Photogrammetry and Remote Sensing, Congress, 16th, Kyoto, Japan, July 1-10, 1988) Photogrammetric Engineering and Remote Sensing (ISSN 0099-1112), vol. 55, May 1989, p. 573-579.

Less time-consuming and high accuracy DTM production is required for successful management of large scale earthwork construction because efficient control of earthwork requires repeated measurement of cut-and-fill terrain during execution. This paper describes a newly developed semi-automated measurement system for this purpose. Conventional measurement techniques are here replaced by operator-assisted stereo matching by computer. The basic algorithm is based on a sophisticated coarse-to-fine correlation, and the measurement system is implemented on general purpose image processing hardware linked to a newly developed earthwork management system. The paper also describes the outlines of the hardware and software configuration as well as matching precision and processing time. Author

A89-39095

DIGITAL PHOTOGRAMMETRIC PROCESSING SYSTEMS - CURRENT STATUS AND PROSPECTS

ARMIN W. GRUEN (Zuerich, Eidgenoessische Technische Hochschule, Zurich, Switzerland) (International Society for Photogrammetry and Remote Sensing, Congress, 16th, Kyoto, Japan, July 1-10, 1988) Photogrammetric Engineering and Remote Sensing (ISSN 0099-1112), vol. 55, May 1989, p. 581-586. refs

Recent advancements in computer and sensor technology have improved the capabilities and reduced the costs of digital components so drastically that digital processing systems are becoming increasingly available. This paper reviews design concepts of fully digital processing systems, focusing on systems with primarily photogrammetric functions. It addresses potential, characteristics, and operational aspects of Digital Stations. The rapid development in this area also requires an outlook into the near future. The prospects will indicate that the time has come for Digital Stations with truly photogrammetric functions to be used in fully automatic and interactive mode and with high accuracy capabilities. Author

A89-39096

THE NEBRASKA CENTER-PIVOT INVENTORY - AN EXAMPLE OF OPERATIONAL SATELLITE REMOTE SENSING ON A LONG TERM BASIS

DONALD C. RUNDQUIST, RICHARD O. HOFFMAN, MARVIN P. CARLSON, and ALLEN E. COOK (Nebraska, University, Lincoln) Photogrammetric Engineering and Remote Sensing (ISSN 0099-1112), vol. 55, May 1989, p. 587-590. refs

The objective of this paper is to summarize the history, procedures, and results of a long-term program of inventorying center-pivot irrigation systems in Nebraska. Data concerning the location of pivots have been collected each year from 1972 to present, and summarized annually as a map publication. Inventory procedures are simplistic, consisting of identifying and mapping occurrences of the characteristically circular pivot systems as interpreted from photographic enlargements of Landsat imagery. A total of 2,665 pivots were recorded in 1972, and the cumulative total for 1986 was 26,208; nearly a ten-fold increase over 14 years. The temporal periods of greatest increase coincide, as one would expect, with generally dry conditions in the state. While the method for remote detection of irrigation systems is ordinary, we believe that the Nebraska center-pivot inventory provides an excellent example of the practical utility of remote sensing. Author

A89-39097

A METHOD FOR INTEGRATING REMOTE SENSING AND GEOGRAPHIC INFORMATION SYSTEMS

QIMING ZHOU (New South Wales, University, Kensington, Australia) Photogrammetric Engineering and Remote Sensing (ISSN 0099-1112), vol. 55, May 1989, p. 591-596. Research supported by the Department of Administrative Services of Australia. refs

A relational image-based geographic information system (RIGIS) has been developed for interfacing geographic information and remotely sensed data for land resource studies in the arid zone of Australia. The system is composed of two interrelated subsystems: an image data base which handles data sets such as topography and Landsat imagery using spatial modeling techniques, and an aspatial data base which handles attribute data relating to these spatial data coverages. A relational model has been employed for data base management, and interfaces have been developed to allow a high-level view by the user of the spatial and aspatial entities. The paper describes the design of the RIGIS software implementation and its application to land-resource studies. Author

A89-39099

FRACTAL ANALYSIS OF A CLASSIFIED LANDSAT SCENE

LEE DE COLA (Vermont, University, Burlington) Photogrammetric Engineering and Remote Sensing (ISSN 0099-1112), vol. 55, May 1989, p. 601-610. refs

Remotely sensed images tend to be spatially very complicated, revealing regions of homogeneously classified pixels with quite convoluted perimeters. Here, fractal analysis is applied to the patterns created by eight land-cover classes from a Landsat TM image of northwest Vermont. The results suggest that forests manifest high fractal dimension and large regions; agricultural activities have large regions with fractal dimension inversely related

to the intensity of cultivation; and urban land cover yields small regions with relatively high fractal dimension. Author

A89-39100

N-DIMENSIONAL DISPLAY OF CLUSTER MEANS IN FEATURE SPACE

MICHAEL E. HODGSON (Colorado, University, Boulder) and REESE W. PLEWS (Hunter College, New York) Photogrammetric Engineering and Remote Sensing (ISSN 0099-1112), vol. 55, May 1989, p. 613-619. Research supported by the University of Colorado. refs

The visual analysis of cospectral plots of cluster locations is an important tool in the cluster labeling process and in the understanding of the spectral characteristics of land-cover phenomena in general. However, cospectral plots are limited to depicting phenomena locations in only two-band feature space. N-dimensional spectral plots of the location of cluster means in feature space can be created using an X-Y graph and the monocular depth cues of size, thickness, brightness, and color. Methods for implementing these vision cues to depict the multispectral feature locations in two- to six-band feature space are discussed. Graphic examples are provided to illustrate the use of this new method for analyzing feature space. Author

A89-39546

ARCTIC GEODYNAMICS - A SATELLITE ALTIMETER EXPERIMENT FOR THE EUROPEAN SPACE AGENCY EARTH REMOTE-SENSING SATELLITE

ALLEN JOEL ANDERSON, GABRIELE MARQUART, and HANS-GEORG SCHERNECK (Uppsala Universitet, Sweden) EOS (ISSN 0096-3941), vol. 69, Sept. 27, 1988, p. 873, 878-881. Research supported by Naturvetenskapliga Forskningsradet. refs

The use of ERS-1 satellite altimetry data to characterize the formation, evolution, and structure of the Arctic Ocean sea floor (AOSF) is proposed. The orbital parameters, coverage, and instrumentation of ERS-1 are reviewed; current knowledge of the AOSF is summarized; geodynamic modeling methods are explained; and techniques for acquiring and analyzing geodynamic data on specific regions of the AOSF are described in detail and illustrated with maps and diagrams. Also considered is the application of satellite data to studies of Arctic Ocean tides. T.K.

A89-39551* Commonwealth Scientific and Industrial Research Organization, Canberra (Australia).

AUTOCORRELATION AND REGULARIZATION IN DIGITAL IMAGES. II - SIMPLE IMAGE MODELS

DAVID L. B. JUPP (CSIRO, Div. of Water Resources, Canberra, Australia), ALAN H. STRAHLER, and CURTIS E. WOODCOCK (Boston University, MA) IEEE Transactions on Geoscience and Remote Sensing (ISSN 0196-2892), vol. 27, May 1989, p. 247-258. refs

(Contract NAG5-273; NAG5-276; NAGW-735; NAGW-1474; NAS9-16664)

The variogram function used in geostatistical analysis is a useful statistic in the analysis of remotely sensed images. Using the results derived by Jupp et al. (1988), the basic second-order, or covariance, properties of scenes modeled by simple disks of varying size and spacing after imaging into disk-shaped pixels are analyzed to explore the relationship between image variograms and discrete object scene structure. The models provide insight into the nature of real images of the earth's surface and the tools for a complete analysis of the more complex case of three-dimensional illuminated discrete-object images. I.E.

A89-39552* Academia Sinica, Beijing (China).

LAND-SURFACE TEMPERATURE MEASUREMENT FROM SPACE - PHYSICAL PRINCIPLES AND INVERSE MODELING

ZHENGMIN WANG (Chinese Academy of Sciences, Institute of Remote Sensing Applications, Beijing, People's Republic of China) and JEFF DOZIER (California Institute of Technology, Jet Propulsion Laboratory, Pasadena, California, University, Santa

Barbara) IEEE Transactions on Geoscience and Remote Sensing (ISSN 0196-2892), vol. 27, May 1989, p. 268-278. refs (Contract NAS5-28770; NAG5-917)

To apply the multiple-wavelength (split-window) method used for satellite measurement of sea-surface temperature from thermal-infrared data to land-surface temperatures, the authors statistically analyze simulations using an atmospheric radiative transfer model. The range of atmospheric conditions and surface temperatures simulated is wide enough to cover variations in clear atmospheric properties and surface temperatures, both of which are larger over land than over sea. Surface elevation is also included in the simulation as the most important topographic effect. Land covers characterized by measured or modeled spectral emissivities include snow, clay, sands, and tree leaf samples. The empirical inverse model can estimate the surface temperature with a standard deviation less than 0.3 K and a maximum error less than 1 K, for viewing angles up to 40 degrees from nadir under cloud-free conditions, given satellite measurements in three infrared channels. A band in the region from 10.2 to 11.0 microns will usually give the most reliable single-band estimate of surface temperature. In addition, a band in either the 3.5-4.0-micron region or in the 11.5-12.6-micron region must be included for accurate atmospheric correction, and a band below the ozone absorption feature at 9.6 microns (e.g., 8.2-8.8 microns) will increase the accuracy of the estimate of surface temperature. I.E.

A89-39556

SENSITIVITY OF AN ATMOSPHERIC CORRECTION ALGORITHM FOR NON-LAMBERTIAN VEGETATION SURFACES TO ATMOSPHERIC PARAMETERS

ANNEGRET GRATZKI (Koeln, Universitaet, Cologne, Federal Republic of Germany) and SIEGFRIED A. W. GERSTL (Los Alamos National Laboratory, NM) IEEE Transactions on Geoscience and Remote Sensing (ISSN 0196-2892), vol. 27, May 1989, p. 326-331. refs

An atmospheric correction algorithm has been proposed by Gerstl and Simmer (1986) that removes atmospheric perturbations from off-nadir radiances measured at the top of the atmosphere in the visible and near-infrared wavelength regions. The correction formalism requires as minimum information the total optical depth of the atmosphere and the surface albedo. Here, the sensitivity of the model to assumptions about the aerosol scattering phase function, the single scattering albedo, and the vertical profile of the optical depth are tested. The authors find that the forward scattering asymmetry must be known most accurately to perform a reliable atmospheric correction for aerosol-laden atmospheres when high-resolution and off-nadir imagery is considered and the surface bidirectional reflectance distribution function is to be retrieved. I.E.

A89-39650

SYNOPTIC ANALYSIS AND DYNAMICAL ADJUSTMENT OF GEOS 3 AND SEASAT ALTIMETER EDDY FIELDS IN THE NORTHWEST ATLANTIC

PIERRE DE MEY and YVES MENARD (CNES, Groupe de Recherches de Geodesie Spatiale, Toulouse, France) Journal of Geophysical Research (ISSN 0148-0227), vol. 94, May 15, 1989, p. 6221-6230. Research supported by CNRS. refs (Contract N00014-84-C-0461)

Data obtained by the GEOS 3 and Seasat altimeters between May and August 1978 are employed in a synoptic analysis of the dynamic topography of the sea surface in a region including the sites of the Polymode Synoptic Dynamics Experiment and the Local Dynamics Experiment. It is found that the altimeter/in situ correlation is about 0.56, and that the daily mean sea level is measured to within about 2.4 cm. The variance for the altimeter estimate is shown to be no more than 9 percent higher on average than the variance of the in situ estimate. R.R.

A89-39656* Jet Propulsion Lab., California Inst. of Tech., Pasadena.

INFRARED SPECTROSCOPY (2.3-20 MICRONS) FOR THE GEOLOGICAL INTERPRETATION OF REMOTELY-SENSED MULTISPECTRAL THERMAL INFRARED DATA

MARY JANE BARTHOLOMEW, ANNE B. KAHLE, and GORDON HOOVER (California Institute of Technology, Jet Propulsion Laboratory, Pasadena) International Journal of Remote Sensing (ISSN 0143-1161), vol. 10, March 1989, p. 529-544. refs

The spectral radiance and spectral reflectance of natural weathered surfaces of common sedimentary and igneous rocks is determined from in situ and in the laboratory measurements. In situ spectral radiance measurements (5-14 microns) were made with a portable spectral radiometer and were used to derive the spectral emissivity of the rocks. The spectral reflectance measurements (2.3-20 microns) were made in a laboratory with a Fourier transform IR spectrometer with a diffuse reflectance accessory. Good agreement is found between the two techniques. The field portable spectrometer has a larger field of view and the in situ data provide more accurate measurements of the intensity of spectral features related to temperature and atmospheric effects. R.B.

A89-39674

SEA SURFACE SPECTRUM FROM AERIAL PHOTOGRAPHS - LABORATORY MODEL STUDIES

P. S. NAIDU and Y. VENKATRAMI REDDY (Indian Institute of Science, Bangalore, India) Photogrammetria (ISSN 0031-8663), vol. 43, March 1989, p. 181-194. refs

The optical spectrum of daylight photographs of sinusoidal and other complex reflecting surfaces made out of paper coated with a thin layer of plastic is studied. It is shown that the reflecting characteristics of the plastic layer are quite similar to those of the water surface. Hence, the paper models can be conveniently used to model the sea surface undulations. It is also shown that the frequency of a sinusoidal surface is best estimated when the camera angle is about 45 deg and the illumination angle is also 45 deg. Clear skylight illumination produces more accurate estimates than those obtained with diffused illumination. Author

A89-39875

THE POTENTIAL OF INFRARED SATELLITE DATA FOR THE RETRIEVAL OF SAHARAN-DUST OPTICAL DEPTH OVER AFRICA

M. LEGRAND, J. J. BERTRAND (Universite Nationale de Cote d'Ivoire, Abidjan, Ivory Coast), M. DESBOIS, L. MENENGER (Ecole Polytechnique, Palaiseau, France), and Y. FOUQUART (Lille I, Universite, Villeneuve-d'Ascq, France) Journal of Applied Meteorology (ISSN 0894-8763), vol. 28, April 1989, p. 309-318. refs

Optical depth of Saharan dust derived from photometric measurements made during the dry season at a Sahelian site (Niamey, Republic of Niger) is compared with Meteosat-2 radiance in the 10.5-12.5 micron channel for different times of the daily cycle. The ability of retrieving dust optical depth using the outgoing radiance of infrared atmospheric window is clearly demonstrated for the middle of the day. Results obtained with nighttime data through a relation between dust optical depth and visibility are also discussed. The major causes of error are identified and quantitatively estimated. Author

A89-40134

PIXEL AND SUB-PIXEL ACCURACY IN GEOMETRICAL CORRECTION OF AVHRR

A. P. CRACKNELL and K. PAITHOONWATTANAKIJ (Dundee, University, Scotland) (Rutherford Appleton Laboratory, Meteorological Office, ESA, et al., Applications of AVHRR data: European AVHRR Data Users' Meeting, 3rd, Oxford, England, Dec. 16-18, 1987) International Journal of Remote Sensing (ISSN 0143-1161), vol. 10, Apr.-May 1989, p. 661-667.

This paper makes two contributions to the problem of geometrical rectification of AVHRR image data. The first is an automatic procedure for the location of ground control points

(GCPs) without the involvement of operator intervention and using a library of 'chips' of AVHRR data for the GCPs. The second involves the adaptation of a method used by Torlegard (1987) for Landsat MSS data to the case of AVHRR data to attempt to achieve subpixel accuracy in the rectification. An accuracy of 26 percent of the pixel edge has been achieved. Author

A89-40135

AN AVHRR MOSAIC IMAGE OF ANTARCTICA

R. H. MERSON (Royal Aircraft Establishment, National Remote Sensing Centre, Farnborough, England) (Rutherford Appleton Laboratory, Meteorological Office, ESA, et al., Applications of AVHRR data: European AVHRR Data Users' Meeting, 3rd, Oxford, England, Dec. 16-18, 1987) International Journal of Remote Sensing (ISSN 0143-1161), vol. 10, Apr.-May 1989, p. 669-674.

This project was started in October 1985 with the objectives of (1) producing a 1-km-resolution database of Antarctica and (2) producing a 1:5 000 000 scale image map. So far, 28 three-band AVHRR scenes have been corrected for variable Sun reflectance and transformed to a polar stereographic projection using a digitized coastline for control. Relatively cloud-free segments from 18 scenes have been incorporated in a provisional mosaic and further segments are to be included to improve the picture. Author

A89-40139

SATELLITE-DERIVED LOW-LEVEL ATMOSPHERIC WATER VAPOUR CONTENT FROM SYNERGY OF AVHRR WITH HIRS

PETER SCHLUESSEL (GKSS-Forschungszentrum Geesthacht GmbH, Federal Republic of Germany) (Rutherford Appleton Laboratory, Meteorological Office, ESA, et al., Applications of AVHRR data: European AVHRR Data Users' Meeting, 3rd, Oxford, England, Dec. 16-18, 1987) International Journal of Remote Sensing (ISSN 0143-1161), vol. 10, Apr.-May 1989, p. 705-721. refs

(Contract BMFT-KF-10045)

Radiative transfer calculations are used to develop techniques for retrieving atmospheric water vapor profiles from the AVHRR and the High-resolution IR Radiation Sounder. Simulations of radiometer signals are performed for atmospheres from the middle and tropical latitudes. A physical-statistical retrieval method is developed which can derive total column amounts and the amounts in thick (150-200 hPa) layers in the lower troposphere with an accuracy of 5-15 and 15-25 percent, respectively. The amounts in thinner layers (50 hPa) may be estimated with accuracies of 20-30 percent. A case study is presented in which three-dimensional humidity fields are retrieved from NOAA-7 measurements of a region over the North Sea in May, 1982. R.B.

A89-40143

OBSERVATIONS OF VOLCANIC ASH CLOUDS IN THE 10-12 MICRON WINDOW USING AVHRR/2 DATA

A. J. PRATA (CSIRO, Div. of Atmospheric Research, Aspendale, Australia) (Rutherford Appleton Laboratory, Meteorological Office, ESA, et al., Applications of AVHRR data: European AVHRR Data Users' Meeting, 3rd, Oxford, England, Dec. 16-18, 1987) International Journal of Remote Sensing (ISSN 0143-1161), vol. 10, Apr.-May 1989, p. 751-761. refs

The use of thermal data from the AVHRR/2 channels 4 and 5 to detect and discriminate volcanic clouds is studied. It is found that the AVHRR/2 measurements at wavelengths between 10 and 12 microns can be used for detection and discrimination of volcanic clouds during the first few hours of an explosive eruption. Detection becomes more difficult as the eruption cloud spreads and thins out, because of the similarity between a dispersed volcanic cloud and a semitransparent cirrus. If the dispersed volcanic clouds consists of liquid H₂SO₄ droplets, however, they may be discriminated from water/ice clouds. R.B.

A89-40153

AVHRR DATA PROCESSING TO STUDY THE SURFACE CANOPIES IN TEMPERATE REGIONS - FIRST RESULTS OF HAPEX-MOBILHY

T. PHULPIN, J. P. JULLIEN, and D. LASSELIN (Centre National

de Recherches Meteorologiques, Toulouse, France) (Rutherford Appleton Laboratory, Meteorological Office, ESA, et al., Applications of AVHRR data: European AVHRR Data Users' Meeting, 3rd, Oxford, England, Dec. 16-18, 1987) International Journal of Remote Sensing (ISSN 0143-1161), vol. 10, Apr.-May 1989, p. 869-884. refs

Automatic methods to correct vegetation index images from AVHRR are developed and tested. The corrected images are used to plot the temporal variations of the normalized difference vegetation indices in the HAPEX domain for two kinds of vegetation cover. The curves are interpreted differentiating the signal due to phenology from that probably caused by problems of haze or anisotropy. Author

A89-40154

LAKE AREA MEASUREMENT USING AVHRR - A CASE STUDY

A. R. HARRIS and I. M. MASON (London, University College, Dorking, England) (Rutherford Appleton Laboratory, Meteorological Office, ESA, et al., Applications of AVHRR data: European AVHRR Data Users' Meeting, 3rd, Oxford, England, Dec. 16-18, 1987) International Journal of Remote Sensing (ISSN 0143-1161), vol. 10, Apr.-May 1989, p. 885-895.

The importance of remote sensing of lake level and area changes for climate research is discussed. It is noted that ERS-1 will be suitably equipped for the task, carrying a radar altimeter and the Along-Track Scanning Radiometer (ATSR). A simple area measurement technique is investigated and it is shown that the area of Lough Neagh can be measured using data from the AVHRR instrument by using channel-2 in the day and channels-4 and -5 at night, to an accuracy of about 1 percent. Author

A89-40155

AN ALGORITHM FOR SNOW AND ICE DETECTION USING AVHRR DATA - AN EXTENSION TO THE APOLLO SOFTWARE PACKAGE

G. GESELL (DFVLR, Wessling, Federal Republic of Germany) (Rutherford Appleton Laboratory, Meteorological Office, ESA, et al., Applications of AVHRR data: European AVHRR Data Users' Meeting, 3rd, Oxford, England, Dec. 16-18, 1987) International Journal of Remote Sensing (ISSN 0143-1161), vol. 10, Apr.-May 1989, p. 897-905. refs

The Apollo scheme (Saunders and Pescod, 1988) for extracting surface and cloud parameters from AVHRR data is extended for classification in the presence of snow- and ice-contaminated pixels. A daytime algorithm using all five AVHRR channels is developed. The algorithm makes it possible to distinguish between snow/ice and water clouds, detect sea ice, and distinguish between snow-covered and snow-free ice areas. The algorithm is applied to AVHRR data from the Baltic Sea 1987 ice season, showing reasonable classification results, with the exception of a few areas with ice clouds or with ice-topped water clouds. R.B.

A89-40156

MULTI-SPECTRAL CLASSIFICATION OF SNOW USING NOAA AVHRR IMAGERY

ANDREW R. HARRISON and RICHARD M. LUCAS (Bristol, University, England) (Rutherford Appleton Laboratory, Meteorological Office, ESA, et al., Applications of AVHRR data: European AVHRR Data Users' Meeting, 3rd, Oxford, England, Dec. 16-18, 1987) International Journal of Remote Sensing (ISSN 0143-1161), vol. 10, Apr.-May 1989, p. 907-916. Research supported by the Department of the Environment of England. refs

Problems of accurate discrimination between snow and cloud, together with the detection of the snow pack boundary, have handicapped the use of satellite data in operational snow-cover mapping systems. A technique, involving an unsupervised clustering procedure, is described which allows the removal of cloud areas using NOAA-9 Advanced Very High Resolution Radiometer (AVHRR) channel-1, channel-3 and channel-4 data in conditions of recent snow lie and a difference channel (channel-2 - channel-1 with channel-3 and channel-4) during periods of advanced snow melt. Accurate delineation of snow extent is provided by the

techniques if these specified snow conditions are taken into account. A method for the identification of areas of marginal snow melt is also presented, based on comparisons with Landsat Thematic Mapper data. The classifications also enable the determination of snow areas influenced by cloud shadows and conifer forest in addition to separating areas of differing snow depth and percentage cover. Author

A89-40263

COMBINED FILM AND SOFTCOPY PHOTO-INTERPRETATION SYSTEM

FRANZ W. LEBERL and ERWIN KIENEGGER (Vexcel Corp., Boulder, CO) IN: Airborne reconnaissance XII; Proceedings of the Meeting, San Diego, CA, Aug. 16, 17, 1988. Bellingham, WA, Society of Photo-Optical Instrumentation Engineers, 1989, p. 100-106.

The requirements, design features, and performance of a system for the on-line digitization of film and the interactive analysis of digitized pixel arrays are discussed. The digitization method, which can be characterized as 'mensuration frame-grabbing', will maintain an extremely high level of accuracy among pixels that have been 'grabbed' in individual windows. A number of automation tasks supporting the extraction of linear features and areas from aerial photography have been implemented. The true advantages of the approach become evident when data previously collected needs to be revised at a later time. O.C.

A89-40488

AERIAL PHOTOGRAPHY AND SPECIALIZED PHOTOGRAPHIC STUDIES [AEROFOTOGRAFIIA I SPETSIAL'NYE FOTOGRAFICHESKIE ISSLEDOVANIIA]

ALEKSANDR S. KUCHKO Moscow, Izdatel'stvo Nedra, 1988, 240 p. In Russian. refs

The role of aerial photography in obtaining information about the earth surface is examined, and the principal aerial photography processes and materials are reviewed. Topics discussed include the atmospheric-optical conditions of aerial photography, photometric properties and spatial-frequency characteristics of natural formations, optical image formation, and the principal parameters and characteristics of optical systems used in aerial photography. Attention is also given to the principal types and properties of materials for black-and-white and color aerial photography and calibration of aerial cameras. V.L.

A89-40491

SPACE GEOGRAPHY. INVESTIGATIONS ON TEST REGIONS [KOSMICHESKAIA GEOGRAFIIA. POLIGONNYE ISSLEDOVANIIA]

IU. G. SIMONOV, ED. Moscow, Izdatel'stvo Moskovskogo Universiteta, 1988, 128 p. In Russian. No individual items are abstracted in this volume.

Spaceborne remote-sensing systems for acquiring geographical information are discussed. Studies on subsatellite test regions are summarized; methods for obtaining ground data are described; and applications of satellite TV imagery are considered. B.J.

A89-40606

PROPERTIES OF THE EQUATORIAL AND TROPICAL IONOSPHERE ACCORDING TO SOVIET SATELLITE OBSERVATIONS DURING THE IMS [SVOISTVA EKVATORIAL'NOI I TROPICHESKOI IONOSFERY PO DANNYM SOVETSKIKH SPUTNIKOVYKH NABLIUDENII V PERIOD MIM]

N. M. SHIUTTE Magnitosfernye Issledovaniia, no. 10, 1988, p. 85-100. In Russian. refs

Cosmos and Intercosmos satellite data are presented on the characteristic parameters of the ionospheric plasma in the equatorial anomaly zone, and its seasonal, diurnal, and longitudinal variations for various geomagnetic activity levels. Relations between the observed low-latitude distributions of charged-particle parameters and plasma convection due to electric field are examined. Data on daytime and nighttime emissions of the equatorial and low-latitude ionosphere as well as on equatorial F-layer striation are also discussed. B.J.

A89-41076

FURTHER INVESTIGATIONS OF SAMPLING ERRORS IN MEAN TERRAIN HEIGHT ESTIMATION

C. K. CHOW and H. R. RAEMER (Northeastern University, Boston, MA) Franklin Institute, Journal (ISSN 0016-0032), vol. 326, no. 3, 1989, p. 363-379. refs

The modeling of terrain height by multivariate distributions in Gaussian, Exponential and Bessel forms is investigated. The purpose of the modeling is to improve estimation on the electromagnetic wave scattering from rough terrain. The parameters of these distribution models are estimated by using sampled and quantized terrain height data. Of concern here are the effects of sampling and quantization on the estimation error. The paper is limited to the estimation of mean terrain height only and the statistics of sampling error are determined with the help of elliptical distribution properties. Also, the effects of different correlation and sampling frequency are discussed. The effect of quantization will be analyzed in a subsequent paper. Author

A89-41151

1988 ACSM-ASPRS ANNUAL CONVENTION, SAINT LOUIS, MO, MAR. 13-18, 1988, TECHNICAL PAPERS. VOLUME 4 - IMAGE PROCESSING/REMOTE SENSING

Convention sponsored by ACSM and ASPRS. Falls Church, VA, American Congress on Surveying and Mapping and American Society for Photogrammetry and Remote Sensing, 1988, 237 p. For individual items see A89-41152 to A89-41171.

The conference presents papers on techniques for image processing, knowledge-based analysis, hydrographic science applications, geology and soil applications, and forestry applications. Topics include a concept for a satellite-based global reserve monitoring system, crop identification from merged Landsat multispectral scanner and Thematic Mapper data, area sensitivity and feature sensitivity of SPOT 1 data, and a global approach to knowledge-based surface material classification. Consideration is also given to the use of a geographic information system to improve planning for and control of the placement of dredged material, variation of surface water spectral response as a function of in situ sampling technique, and the assessment of forest cover changes using multirate spaceborne imaging radar. K.K.

A89-41152

CONCEPT FOR A SATELLITE-BASED GLOBAL RESERVE MONITORING SYSTEM

DIANA L. MOSSMAN, RALPH W. KIEFER, and BECKY J. BROWN (Wisconsin, University, Madison) IN: 1988 ACSM-ASPRS Annual Convention, Saint Louis, MO, Mar. 13-18, 1988, Technical Papers. Volume 4. Falls Church, VA, American Congress on Surveying and Mapping and American Society for Photogrammetry and Remote Sensing, 1988, p. 1-10. refs

A prototype system is being designed to monitor nature reserves on a global basis using satellite data. This system will have both a central global monitoring facility and a microcomputer-based system that could be used at reserve headquarters for local reserve monitoring. The central system data handling will include monitoring through digital image interpretation. K.K.

A89-41154

AREA SENSITIVITY AND FEATURE SENSITIVITY OF SPOT 1 DATA - A STATISTICAL ANALYSIS

G. VENUGOPAL (Ball State University, Muncie, IN) IN: 1988 ACSM-ASPRS Annual Convention, Saint Louis, MO, Mar. 13-18, 1988, Technical Papers. Volume 4. Falls Church, VA, American Congress on Surveying and Mapping and American Society for Photogrammetry and Remote Sensing, 1988, p. 21-31. refs

The degree of correlation between the original three SPOT bands and three computed principal component bands is analyzed. An attempt was made to determine whether or not the SPOT data were area sensitive, feature sensitive, or both. It was found that there was no relation between the size of the area and the degree of correlation. A relation does exist between the degree of correlation and surface features. K.K.

A89-41156

A GLOBAL APPROACH TO KNOWLEDGE-BASED SURFACE MATERIAL CLASSIFICATION

R. DAVID FLINN and MARK J. CARLOTTO (Analytic Sciences Corp., Reading, MA) IN: 1988 ACSM-ASPRS Annual Convention, Saint Louis, MO, Mar. 13-18, 1988, Technical Papers. Volume 4. Falls Church, VA, American Congress on Surveying and Mapping and American Society for Photogrammetry and Remote Sensing, 1988, p. 50-59. refs

A knowledge-based system for analyzing Landsat Thematic Mapper (TM) imagery is described. The intent of the system is to provide a capability for classifying general surface material categories (SMCs) such as water, trees, sparse vegetation, agriculture, bare soil, and built-up areas across geographically diverse imagery. Standard multispectral classification techniques which use statistical models derived from a training region in one image generally cannot be reliably applied to other images due to the high degree of statistical variability between imagery from different geographical regions. The proposed approach combines statistical methods and artificial intelligence techniques to allow general SMCs to be extracted over a diverse set of imagery. Classification results of work in progress are presented to illustrate the performance of the system on imagery over North and South America. Author

A89-41157

USE OF A GEOGRAPHIC INFORMATION SYSTEM (GIS) TO IMPROVE PLANNING FOR AND CONTROL OF THE PLACEMENT OF DREDGED MATERIAL

CYNTHIA A. ABRAHAMSON, ANDREW J. BRUZEWICZ (U.S. Army, Corps of Engineers, Rock Island, IL), and MARK O. JOHNSON (U.S. Army, Construction Engineering Research Laboratory, Champaign, IL) IN: 1988 ACSM-ASPRS Annual Convention, Saint Louis, MO, Mar. 13-18, 1988, Technical Papers. Volume 4. Falls Church, VA, American Congress on Surveying and Mapping and American Society for Photogrammetry and Remote Sensing, 1988, p. 60-68.

The use of spatial data and a data base management system to plan for the disposal of dredged material has been studied. The geographic resources data analysis support system (GRASS) software developed at the U.S. Army Construction Engineering Research Laboratory was used on a digital data base developed for the Keithsburg lower dredge cut located 20 miles north of Burlington, Iowa, on the Mississippi River. The use of a National High Altitude Program (NHAP) color IR aerial photograph transparency was digitized with 5- by 5-meter pixels and rectified for use as a base map. K.K.

A89-41158* California Univ., Santa Barbara.

KNOWLEDGE-BASED IMAGE DATA MANAGEMENT - AN EXPERT FRONT-END FOR THE BROWSE FACILITY

DAVID M. STOMS, JEFFREY L. STAR, and JOHN E. ESTES (California, University, Santa Barbara) IN: 1988 ACSM-ASPRS Annual Convention, Saint Louis, MO, Mar. 13-18, 1988, Technical Papers. Volume 4. Falls Church, VA, American Congress on Surveying and Mapping and American Society for Photogrammetry and Remote Sensing, 1988, p. 69-78. refs (Contract NAGW-987)

An intelligent user interface being added to the NASA-sponsored BROWSE testbed facility is described. BROWSE is a prototype system designed to explore issues involved in locating image data in distributed archives and displaying low-resolution versions of that imagery at a local terminal. For prototyping, the initial application is the remote sensing of forest and range land. K.K.

A89-41159

THERMAL MODELING OF HEAT DISSIPATION IN THE PEN BRANCH DELTA USING THERMAL INFRARED IMAGERY

JOHN R. JENSEN, ELIJAH RAMSEY, III (South Carolina, University, Columbia), and HALKARD E. MACKEY, JR. (Du Pont de Nemours and Co., Aiken, SC) IN: 1988 ACSM-ASPRS Annual Convention, Saint Louis, MO, Mar. 13-18, 1988, Technical Papers. Volume 4. Falls Church, VA, American Congress on Surveying and Mapping

and American Society for Photogrammetry and Remote Sensing, 1988, p. 79-90. refs
(Contract DE-AC09-76SR-00001)

Thermal infrared imagery of the Pen Branch delta on the Savannah River Plant near Aiken, South Carolina, were obtained on March 12, 1983 and April 6, 1984 during flood and nonflood conditions. These data were registered to one another and then analyzed using digital image processing techniques to: (1) compute the rate of temperature change as the thermal effluent progressed downstream using transect techniques, and (2) mathematically model the spatial distribution of the thermal effluent using fourth and seventh-order trend surfaces. These two mathematical expressions of the thermal data allowed more effective understanding of how the temperature of the thermal effluent changed as it progressed through the Pen Branch delta hydrologic system. Author

A89-41161* National Aeronautics and Space Administration. John C. Stennis Space Center, Bay Saint Louis, MS.

VARIATION OF SURFACE WATER SPECTRAL RESPONSE AS A FUNCTION OF IN SITU SAMPLING TECHNIQUE

BRUCE A. DAVIS (NASA, John C. Stennis Space Center, Bay Saint Louis, MS) and MICHAEL E. HODGSON (Colorado, University, Boulder) IN: 1988 ACSM-ASPRS Annual Convention, Saint Louis, MO, Mar. 13-18, 1988, Technical Papers. Volume 4. Falls Church, VA, American Congress on Surveying and Mapping and American Society for Photogrammetry and Remote Sensing, 1988, p. 112-130. refs

Tests were carried out to determine the spectral variation contributed by a particular sampling technique. A portable radiometer was used to measure the surface water spectral response. Variation due to the reflectance of objects near the radiometer (i.e., the boat side) during data acquisition was studied. Consideration was also given to the variation due to the temporal nature of the phenomena (i.e., wave activity). K.K.

A89-41163* Hydrex Corp., Falls Church, VA.

AIRBORNE TIME-SERIES MEASUREMENT OF SOIL MOISTURE USING TERRESTRIAL GAMMA RADIATION

THOMAS R. CARROLL, DANIEL M. LIPINSKI (NOAA, Office of Hydrology, Minneapolis, MN), and EUGENE L. PECK (Hydrex Corp., Falls Church, VA) IN: 1988 ACSM-ASPRS Annual Convention, Saint Louis, MO, Mar. 13-18, 1988, Technical Papers. Volume 4. Falls Church, VA, American Congress on Surveying and Mapping and American Society for Photogrammetry and Remote Sensing, 1988, p. 141-151. refs
(Contract NAS5-30135)

Terrestrial gamma radiation data and independent ground-based core soil moisture data are analyzed. They reveal the possibility of using natural terrestrial gamma radiation collected from a low-flying aircraft to make reliable real-time soil moisture measurements for the upper 20 cm of soil. The airborne data were compared to the crude ground-based soil moisture data set collected at the core sites. K.K.

A89-41166

SHUTTLE IMAGING RADAR ANALYSIS IN ARID ENVIRONMENTS

BARRY N. HAACK (George Mason University, Fairfax, VA) IN: 1988 ACSM-ASPRS Annual Convention, Saint Louis, MO, Mar. 13-18, 1988, Technical Papers. Volume 4. Falls Church, VA, American Congress on Surveying and Mapping and American Society for Photogrammetry and Remote Sensing, 1988, p. 171-180. refs

Multisensor spaceborne imagery was obtained for areas of co-occurrence in Sudan. This imagery included Shuttle Imaging Radar from missions A and B; Landsat Multispectral Scanner and Thematic Mapper; and stereoscopic photography from the large Format Camera, Metric Camera and Shuttle hand-held cameras. These data were compared to assess the unique attributes and complementarity of the SIR data. The shuttle radar was very useful for form information, drainage patterns, cultural features and in

hyperarid areas provided penetration to subsurface features. The intersection of SIR A and B data at different azimuths provided very little additional information. Author

A89-41168

ASSESSING THE IMPROVEMENT IN SOIL MAPPING USING SPOT HRV OVER LANDSAT MSS IMAGERY (GEOGRAPHY AND LAND USE)

P. A. AYBU and T. D. FRANK (Illinois, University, Urbana) IN: 1988 ACSM-ASPRS Annual Convention, Saint Louis, MO, Mar. 13-18, 1988, Technical Papers. Volume 4. Falls Church, VA, American Congress on Surveying and Mapping and American Society for Photogrammetry and Remote Sensing, 1988, p. 191-197. Research supported by the University of Illinois. refs

Apparent lack of association between soil mapping units and spectral classes derived from satellite imagery have limited the use of remotely sensed data in medium to large soil surveys. This problem results from inadequate spatial resolution of the satellite imagery compared with traditional aerial photography used in soils mapping. Soil patterns derived from Landsat MSS (79 meter resolution) and Spot HRV (20 meter resolution) imagery were compared with field data from a recent soil map of Ford County in eastcentral Illinois. The study demonstrates that there is some improvement in soil mapping unit delineation by using high resolution Spot data over Landsat MSS. Areas of three soil series that were sufficiently discriminated were used to generate error matrices for both data sets. In general Spot HRV performed better than Landsat MSS in accurately assigning most of the soil series. The agreement between Spot HRV classification and the soil map is marginally better than that of the Landsat MSS classification, even though Spot provides higher resolution data. Author

A89-41169* Purdue Univ., West Lafayette, IN.

ASSESSMENT OF FOREST COVER CHANGES USING MULTIDATE SPACEBORNE IMAGING RADAR

KYU-SUNG LEE and ROGER M. HOFFER (Purdue University, West Lafayette, IN) IN: 1988 ACSM-ASPRS Annual Convention, Saint Louis, MO, Mar. 13-18, 1988, Technical Papers. Volume 4. Falls Church, VA, American Congress on Surveying and Mapping and American Society for Photogrammetry and Remote Sensing, 1988, p. 198-211. refs
(Contract JPL-956952; NAS7-918)

Data obtained in 1978 by Seasat and in 1984 by SIR-B over a forested area in northern Florida are analyzed. The objective of the study was to determine the potential for detecting major changes in forest cover utilizing synthetic aperture radar obtained from satellite altitudes, and to define an effective methodology for processing and analyzing digital synthetic aperture radar data obtained on two different dates. It is found that multitemporal synthetic aperture radar data obtained from satellite altitudes can be used to detect major changes in forest cover conditions such as deforestation and reforestation. A surprisingly good level of detectivity was obtained for identifying areas of regrowth after they had been clearcut and replanted. K.K.

A89-41170

REMOTE SENSING OF THE DECIDUOUS VEGETATION OF GREAT SMOKY MOUNTAINS NATIONAL PARK

MARK MACKENZIE (Tennessee, University, Knoxville) IN: 1988 ACSM-ASPRS Annual Convention, Saint Louis, MO, Mar. 13-18, 1988, Technical Papers. Volume 4. Falls Church, VA, American Congress on Surveying and Mapping and American Society for Photogrammetry and Remote Sensing, 1988, p. 212-221. Research supported by the National Park Service and University of Tennessee. refs

The use of Landsat 4 TM digital data to remotely sense the vegetation of the Thunderhead Mountain quadrangle within Great Smoky Mountains National Park is studied. The data were classified into 50 spectral classes using an unsupervised nonhierarchical classification technique. Discriminant analysis was performed to determine the accuracy of the spectral classification, to reclassify the data, and to develop discriminant functions to aid in the classification of other areas in the park. K.K.

A89-41171

ESTIMATING STAND DENSITY OF LOBLOLLY PINE IN NORTHERN LOUISIANA USING AERIAL PHOTOGRAPHS AND PROBABILITY PROPORTIONAL TO SIZE

LAWRENCE R. GERING (Louisiana Tech University, Ruston) and JOHN PAUL MCTAGUE (Northern Arizona University, Flagstaff, AZ) IN: 1988 ACSM-ASPRS Annual Convention, Saint Louis, MO, Mar. 13-18, 1988, Technical Papers. Volume 4. Falls Church, VA, American Congress on Surveying and Mapping and American Society for Photogrammetry and Remote Sensing, 1988, p. 222-228. refs

The dimensions of the aerial-photo angle-gauge were determined to estimate the stand density from aerial photographs of loblolly pine (*Pinus taeda* L.) sites in Louisiana. A ratio of crown diameter to plot limiting distance of 1/2.5735 should be used in the construction of the angle gauge. K.K.

A89-41428* National Aeronautics and Space Administration. Lyndon B. Johnson Space Center, Houston, TX.

EXPANDING THE UTILITY OF MANNED OBSERVATIONS OF EARTH - 70 MM FILM TESTS ON THE SPACE SHUTTLE

DAVID L. AMSBURY (NASA, Johnson Space Flight Center, Houston, TX) Geocarto International (ISSN 1010-6049), vol. 4, March 1989, p. 25-30.

The Space Shuttle Orbiter provides opportunities for testing different ways to record terrestrial scenes using film. Such opportunities are limited by launch schedules and orbital parameters, properties of the Orbiter windows, available astronaut time and equipment stowage, and the necessity for safety qualification of equipment. To date, astronauts have accomplished several successful tests using color-infrared film, plane-polarizing filters, and a faster color emulsion, both on single 70-mm cameras and using a dual camera mount. Author

A89-41429* National Aeronautics and Space Administration. Lyndon B. Johnson Space Center, Houston, TX.

EARTH SCENES IN POLARIZED LIGHT OBSERVED FROM THE SPACE SHUTTLE

VICTOR S. WHITEHEAD (NASA, Johnson Space Flight Center, Houston, TX) and KINSELL L. COULSON (California, University, Davis) Geocarto International (ISSN 1010-6049), vol. 4, March 1989, p. 31-37. Research supported by NASA. refs

By means of a pair of boresighted and synchronized cameras fitted with orthogonally oriented polarizing filters and carried aboard the Space Shuttle, a large number of polarized images of the earth's surface have been obtained from orbital altitude. Selected pairs of images, both in color and in black and white, have been digitized and computer-processed to yield analogous images in each of the three Stokes parameters necessary for characterizing the state of linear polarization of the emergent light. Many of the images show surface properties more distinctly in degree and plane of polarization than in simple intensity alone. It is believed that these are the first, and certainly the most extensive, set of polarized images of the earth ever obtained from space. Selected pairs of the images are presented here along with some early results of analysis. Author

A89-41430

METEOROLOGICAL APPLICATIONS OF SPACE SHUTTLE PHOTOGRAPHY

CARLYLE H. WASH (U.S. Navy, Naval Postgraduate School, Monterey, CA) Geocarto International (ISSN 1010-6049), vol. 4, March 1989, p. 39-48. refs

The meteorological applications of photography by astronauts is demonstrated by both synoptic and mesoscale studies. Shuttle photographs of Hurricane Elena and an extratropical cyclone illustrate the value of high resolution and oblique perspective in describing the circulation of these storms and their associated cloud patterns. Studies of barrier effects, a persistent dry slot pattern and a horizontal roll cloud utilize these photographs to interpret and document mesoscale features. Author

A89-41431* National Aeronautics and Space Administration. Lyndon B. Johnson Space Center, Houston, TX.

GEOLOGIC APPLICATIONS OF SPACE SHUTTLE PHOTOGRAPHY

CHARLES A. WOOD (Johnson Space Flight Center, Houston, TX) Geocarto International (ISSN 1010-6049), vol. 4, March 1989, p. 49-54. refs

Space Shuttle astronauts have used handheld cameras to take about 30,000 photographs of the earth as seen from orbit. These pictures provide valuable, true-color depictions of many geologically significant areas. While the photographs have areal coverages and resolutions similar to the more familiar Landsat MSS and TM images, they differ from the latter in having a wide variety of solar illumination angles and look angles. Astronaut photographs can be used as very small scale aerial photographs for geologic mapping and planning logistical support for field work. Astronaut photography offers unique opportunities, because of the intelligence and training of the on-orbit observer, for documenting dynamic geologic activity such as volcanic eruptions, dust storms, etc. Astronauts have photographed more than 3 dozen volcanic eruption plumes, some of which were not reported otherwise. The stereographic capability of astronaut photography also permits three-dimensional interpretation of geologic landforms which is commonly useful in analysis of structural geology. Astronauts have also photographed about 20 known impact craters as part of project to discover presently unknown examples in Africa, South America, and Australia. Author

A89-41432* National Aeronautics and Space Administration. Lyndon B. Johnson Space Center, Houston, TX.

MONITORING TROPICAL ENVIRONMENTS WITH SPACE SHUTTLE PHOTOGRAPHY

MICHAEL R. HELFERT and KAMLESH P. LULLA (NASA, Johnson Space Flight Center, Houston, TX) Geocarto International (ISSN 1010-6049), vol. 4, March 1989, p. 55-67. refs

Orbital photography from the Space Shuttle missions (1981-88) and earlier manned spaceflight programs (1962-1975) allows remote sensing time series to be constructed for observations of environmental change in selected portions of the global tropics. Particular topics and regions include deforestation, soil erosion, supersedimentation in streams, lacustrine, and estuarine environments, and desertification in the greater Amazon, tropical Africa and Madagascar, South and Southeast Asia, and the Indo-Pacific archipelagoes. Author

A89-41750

A PERFORMANCE COMPARISON FOR TWO LAGRANGIAN DRIFTER DESIGNS

DAVID L. MACKAS, WILLIAM R. CRAWFORD (Institute of Ocean Sciences, Sidney, Canada), and PEARL P. NIILER (California, University, La Jolla) Atmosphere - Ocean (ISSN 0705-5900), vol. 27, June 1989, p. 443-456. refs

The water-parcel-following and position-reporting performances of two recently developed drifter designs, 'TRISTAR' and 'Loran' described, respectively, by Crawford (1988) and Niiler et al. (1987), were compared during a study of an upwelling plume off the outer coast of Vancouver Island, Canada. Over a 78-h joint deployment, the two designs had nearly identical trajectories, with net velocity difference over the full deployment of only 0.1 cm/sec. Little or no downwind slippage was observed during the first third of the deployment, when winds were strongest, and there was no frontal trapping. It was found that, while the initial deployment of the TRISTAR is easier, and its positioning method and lower power requirement allow much longer untended deployments, the Loran design gives more frequent and precise positioning information and, therefore, better resolution of short-time-scale velocity fluctuations. It was also easier to find at sea, and to recover and redeploy. I.S.

A89-41845

MINIMUM CROSS-ENTROPY NOISE REDUCTION IN IMAGES

ROBERT F. MACKINNON (Defence Research Establishment

Pacific, Victoria, Canada) Optical Society of America, Journal, A: Optics and Image Science (ISSN 0740-3232), vol. 6, June 1989, p. 739-747. refs

A method of noise reduction is described that reduces random noise in images through cross-entropy representation under simple constraint bounds placed on linear orthogonal transform variables. The bounds depend on the noise statistics, which must be estimated independently, and on prior knowledge. The bounds may be adjusted through use of a so-called tightness parameter. In practice, solutions represent a compromise between the noisy image and the prior knowledge for which the tightness parameter governs the reduction in the noise variance. The role of the prior knowledge is illustrated by using two examples, one simple and one complicated. Results based on Fourier and Walsh transforms are presented. Examples of speckle noise reduction for synthetic aperture radar images of the ocean surface are given as illustrations of a practical application. Author

A89-42175* Pacific Northwest Labs., Richland, WA.
APPLICATION OF LANDSAT THEMATIC MAPPER DATA FOR COASTAL THERMAL PLUME ANALYSIS AT DIABLO CANYON
 D. E. GIBBONS, G. E. WUKELIC (Pacific Northwest Laboratories, Richland, WA), J. P. LEIGHTON, and M. J. DOYLE (Pacific Gas and Electric Co., San Ramon, CA) Photogrammetric Engineering and Remote Sensing (ISSN 0099-1112), vol. 55, June 1989, p. 903-909. refs
 (Contract NASA ORDER S-56102-D; DE-AC06-76RL-01830)

The possibility of using Landsat Thematic Mapper (TM) thermal data to derive absolute temperature distributions in coastal waters that receive cooling effluent from a power plant is demonstrated. Landsat TM band 6 (thermal) data acquired on June 18, 1986, for the Diablo Canyon power plant in California were compared to ground truth temperatures measured at the same time. Higher-resolution band 5 (reflectance) data were used to locate power plant discharge and intake positions and identify locations of thermal pixels containing only water, no land. Local radiosonde measurements, used in LOWTRAN 6 adjustments for atmospheric effects, produced corrected ocean surface radiances that, when converted to temperatures, gave values within approximately 0.6 C of ground truth. A contour plot was produced that compared power plant plume temperatures with those of the ocean and coastal environment. It is concluded that Landsat can provide good estimates of absolute temperatures of the coastal power plant thermal plume. Moreover, quantitative information on ambient ocean surface temperature conditions (e.g., upwelling) may enhance interpretation of numerical model prediction. Author

A89-42610
MEASUREMENTS OF SPECTRAL RADIANCE AT THE SEA SURFACE FOR THE DEVELOPMENT OF REMOTE SENSING METHODS [IZMERENIIA SPEKTRAL'NOI ENERGETICHESKOI IARKOSTI NA POVERKHNOSTI OKEANA DLIA RAZRABOTKI METODOV DISTANTSIONNOGO ZONDIROVANIYA]
 D. LOMMATZSCH (Akademie der Wissenschaften der DDR, Institut fuer Kosmosforschung, Berlin, German Democratic Republic) Issledovanie Zemli iz Kosmosa (ISSN 0205-9614), Mar.-Apr. 1989, p. 78-83. In Russian. refs

It is shown that spectral radiance measurements at the sea surface can be used to determine concentrations of phytoplankton in water, using the value of chlorophyll absorption in the 443 nm region. Results of synchronized measurements of spectral radiance conducted by research vessels in Atlantic Ocean and on board a spacecraft revealed a relationship between the upwelling spectral radiance and the roughness of the sea. The variation of upwelling radiance vs the content of water chlorophyll in different illumination and sea-surface roughness is described. I.S.

A89-42611
DETERMINATION OF SPECTRAL SIGNATURES FOR REMOTE LASER SENSING OF VEGETATION [OPREDELENIE SPEKTRAL'NYKH PRIZNAKOV DLIA DISTANTSIONNOGO LAZERNOGO ZONDIROVANIYA RASTENII]
 D. V. VLASOV, D. M. MIRKAMILOV, A. A. MUKHAMEDOV, M. M.

MANSUROV, and K. A. NABIEV (Tashkentskii Politekhicheskii Institut, Tashkent, Uzbek SSR) Issledovanie Zemli iz Kosmosa (ISSN 0205-9614), Mar.-Apr. 1989, p. 84-88. In Russian. refs

The potential of the pattern-recognition method for remote laser sensing of green vegetation is discussed. Statistically-processed laboratory data on laser-induced fluorescence in leaves of cotton, corn, and wheat plants in conditions of water stress, nitrogen stress, and water-nitrogen stress are presented. Spectral signatures that are most informative for the generation of a data base for remote sensing of agricultural vegetation are identified. I.S.

A89-42612
CORRECTING ABSOLUTE CALIBRATIONS OF SATELLITE MICROWAVE RADIOMETER USING A PRIORI DATA [KORREKTSIIA ABSOLIUTNYKH KALIBROVOK SPUTNIKOVYKH SVCH-RADIOMETROV PO APRIORNOM DANNYM]

V. P. SAVORSKII (AN SSSR, Institut Radiotekhniki i Elektroniki, Moscow, USSR) Issledovanie Zemli iz Kosmosa (ISSN 0205-9614), Mar.-Apr. 1989, p. 89-94. In Russian. refs

A methodology is described for correcting calibration relationships which relate a priori radio brightness temperatures to data supplied by spaceborne microwave radiometers. Such corrections rely on values of maximum radio brightness temperatures in the region of measurements. The correction method was applied to the ocean/atmosphere system. I.S.

A89-42614
OPTIMAL SATELLITE ORBITS AND THE NETWORK STRUCTURE FOR REGULAR EARTH SURVEYING [OPTIMAL'NYE ORBITY I STRUKTURA SISTEM ISZ DLIA PERIODICHESKOGO OBZORA ZEMLI]

V. K. SAUL'SKII Issledovanie Zemli iz Kosmosa (ISSN 0205-9614), Mar.-Apr. 1989, p. 104-115. In Russian. refs

A method is described for optimizing the satellite orbits and the configuration of the spacecraft network for the round-the-clock earth-surface survey. The method is based on the concept of 'limiting space systems'. Typical features of such systems are described in detail. The relationship between the efficiency of the round-the-clock monitoring system and the orbit inclination of its satellites is determined. I.S.

A89-43024
SPACE COLORISTICS
 VLADIMIR V. VASIUTIN (Akademii Voenno-Vozdushnykh Sil, Moscow, USSR) and ARTUR A. TISHCHENKO (Nauchno-Proizvodstvennoe Ob'edinenie Priroda, Moscow, USSR) Scientific American (ISSN 0036-8733), vol. 261, July 1989, p. 84-90.

Studies to determine the colors of natural formations and phenomena on the earth as seen from outer space are reviewed. An atlas consisting of samples of 1,000 colors observed from space has been compiled using observations from the Salyut orbital station. Consideration is given to the development of a portable visual colorimeter based on a single-lens-reflex camera and an automatic photoelectric colorimeter for use in space. In addition, studies of the characteristics of human color vision during long space flights are examined. R.B.

A89-43316
MONITORING TUNISIA'S STEPPES WITH SPOT
 MIRIAM VAN HEIST (University of Botswana, Gaborone), WILLEM VAN WIJNGAARDEN, and HERMAN HUIZING (International Institute for Aerospace Survey and Earth Sciences, Enschede, Netherlands) ITC Journal (ISSN 0303-2434), no. 3, 1988, p. 232-237. refs

SPOT images were evaluated for their usefulness in mapping vegetation in central Tunisia. The area had been intensively investigated since 1983 in the context of natural resource surveys and land evaluation. The SPOT images were studied to assess their use for mapping land form and land cover, estimating standing crop, and monitoring cereal acreage and production. Author

A89-43541

EM WAVE SCATTERING FROM STATISTICALLY INHOMOGENEOUS AND PERIODIC RANDOM ROUGH SURFACES

D. P. CHRISSOULIDIS IEE Proceedings, Part H - Microwaves, Antennas and Propagation (ISSN 0950-107X), vol. 136, pt. H, no. 3, June 1989, p. 209-214. refs

First-order scatter from statistically inhomogeneous and periodic random rough surfaces is treated by the boundary perturbation technique. The single array of rough strips on a perfectly conducting plane and the complementary arrays of rough strips are examined. Using a sampling approach, it is proved that scatter is produced through a multiple Bragg resonance mechanism. The scattering behavior of the single array of rough strips is investigated numerically. Scatter for the corresponding surface which is covered throughout by roughness is used as reference. The numerical results indicate that the incidence/scattering directions are related to the orientation of the strips while the sensing radio wavelength is related to the strips width and period. Possible applications for this class of scatterers are discussed. Author

N89-20531*# Science and Technology Corp., Hampton, VA.
THE INVESTIGATION OF ADVANCED REMOTE SENSING, RADIATIVE TRANSFER AND INVERSION TECHNIQUES FOR THE MEASUREMENT OF ATMOSPHERIC CONSTITUENTS
Final Report, 15 Dec. 1977 - 15 Mar. 1985

ADARSH DEEPAK and PI-HUAN WANG Mar. 1985 320 p
 (Contract NAS1-15198)
 (NASA-CR-172599; NAS 1.26:172599) Avail: NTIS HC A14/MF A01 CSDL 04A

The research program is documented for developing space and ground-based remote sensing techniques performed during the period from December 15, 1977 to March 15, 1985. The program involved the application of sophisticated radiative transfer codes and inversion methods to various advanced remote sensing concepts for determining atmospheric constituents, particularly aerosols. It covers detailed discussions of the solar aureole technique for monitoring columnar aerosol size distribution, and the multispectral limb scattered radiance and limb attenuated radiance (solar occultation) techniques, as well as the upwelling scattered solar radiance method for determining the aerosol and gaseous characteristics. In addition, analytical models of aerosol size distribution and simulation studies of the limb solar aureole radiance technique and the variability of ozone at high altitudes during satellite sunrise/sunset events are also described in detail. Author

N89-20535# Beleidscommissie Remote Sensing, Delft (Netherlands). Research Inst. for Forestry and Landscape Planning.

THE SUITABILITY OF REMOTE SENSING FOR SURVEYING AND MONITORING LANDSCAPE PATTERNS. VOLUME A: PILOT STUDY - LANDSAT IMAGERY

J. M. J. FARJON, S. I. KAMSTRA, P. G. LENTJES, and W. J. C. HOEFFNAGEL *In its* The Suitability of Remote Sensing for Surveying and Monitoring Landscape Patterns. Volume A: Pilot Study - LANDSAT Imagery. Volume B: PEPS Project No. 73 - SPOT Imagery p 7-47 Feb. 1988 Original contains color illustrations

Avail: NTIS HC A05/MF A01

The utility of satellite imagery and image processing methods, in particular those of RESEDA (REmote SENSing DAta) processing system, was assessed. Ways in which patterns of tree vegetation, watercourses, and land use can be inferred from comparing remote sensing imagery with field inventories were studied. Results show that LANDSAT-TM images are reasonably suitable for area inventories. Problems are due to small units that are heterogeneous in terms of spectral signature, giving rise to many mixed pixels, which are difficult to distinguish as such. The suitability of TM images for the inventory of linear vegetations of trees seems to be limited because there are too many unsuitable classifications (35 pct) and missed lines (50 pct). Using various filters to extract line elements from the image gives less good results than visual interpretation because the computer gives undesired lines that

would be discarded immediately in a visual interpretation. The MAP2 raster-based geographical information system is shown to be useful. ESA

N89-20536# Beleidscommissie Remote Sensing, Delft (Netherlands). Research Inst. for Forestry and Landscape Planning.

THE SUITABILITY OF REMOTE SENSING FOR SURVEYING AND MONITORING LANDSCAPE PATTERNS. VOLUME B: PEPS PROJECT NO. 73 - SPOT IMAGERY

J. M. J. FARJON, P. G. LENTJES, F. B. VANDERLAAN (National Aerospace Lab., Amsterdam, Netherlands), and W. J. C. HOEFFNAGEL *In its* The Suitability of Remote Sensing for Surveying and Monitoring Landscape Patterns. Volume A: Pilot Study - LANDSAT Imagery. Volume B: PEPS Project No. 73 - SPOT Imagery p 49-84 Feb. 1988 Original contains color illustrations

Avail: NTIS HC A05/MF A01

The SPOT spatial, spectral, and temporal resolution for line plantings, watercourses, and major land use classes (grassland, arable land, coniferous forest of different ages, deciduous forest of different ages, orchards and built-up areas) was assessed. The results show that the limit of the spatial resolution is 5 m. Orientation and context influence the spatial resolution only slightly. The reliable distinction of landuse classes is limited to major categories: agricultural land, forests and man-made objects. A further subdivision of landuse categories can presumably be achieved by application of more advanced image-processing software and/or imagery from another period of the year. The most promising applications of SPOT imagery are small-scale mapping and monitoring over large areas of broadly defined classes that correspond with distinct spectral classes: agricultural land, forests and man-made objects. The improvement of the available techniques, i.e., contextual image-processing and the elimination of mixed pixel influence with the aid of geographic information systems improves the accuracy of small-scale mapping of landscape patterns over large areas. Using SPOT for the large-scale mapping of landscape patterns in small areas is not be competitive with aerial photographs because of the higher costs involved and the poorer degree of detection. ESA

N89-20537# Beleidscommissie Remote Sensing, Delft (Netherlands).

LAND USE INVENTORIES USING SATELLITE IMAGES IN THE REGION HAAREN-HELVOIRT-UDENHOUT, NORTH BRABANT (THE NETHERLANDS) [GRONDGEBRUIK SINVENTARISATIES MET SATELLIETOPNAMEN IN HET GEBIED HAAREN-HELVOIRT-UDENHOUT, N-BRABANT]

Apr. 1988 37 p In DUTCH Prepared in cooperation with DHV raadgevend Ingenieursbureau B.V., Amersfoort, The Netherlands and Dienst Ruimtelijkeordening, Natuurbeheer, landschap en Volkshuisvesting, The Netherlands Original contains color illustrations
 (BCRS-88-07; ETN-89-93876) Avail: NTIS HC A03/MF A01

Satellite imagery was investigated as an alternative to aerial photographs for mapping of vegetation and aspects of land use and water management. A methodology for the execution of a vegetation growth type mapping was developed. Land use and water management for a region were mapped, using digital images from LANDSAT Thematic Mapper and SPOT. The results demonstrate the feasibility of satellite pictures for inventories. ESA

N89-20538# Beleidscommissie Remote Sensing, Delft (Netherlands).

PROCESSING AND APPLICATION OF DIGITAL AVHRR-IMAGERY FOR LAND AND SEA SURFACES Final Report

J. N. ROOZEKRANS and G. J. PRANGSMA Aug. 1988 106 p Prepared in cooperation with Royal Netherlands Meteorological Inst., The Hague Original contains color illustrations
 (Contract BCRS-PROJ. TO-3.1)
 (BCRS-88-08; ETN-89-93877) Avail: NTIS HC A06/MF A01

A software-package for reading NOAA AVHRR-data tapes,

calibration of the raw data, cloud detection, calculation of Earth surface parameters, and geometric correction of images was adjusted to perform automatically. Applications of AVHRR data, including observation (and perhaps warning) of damage in the agriculture caused by drought, night-frost etc; monitoring of meteorology related, troublesome situations for traffic like fog, snow and frost; locating fronts in the sea surface temperature, which might be areas with increased occurrence of certain fish-species, and input of sea surface temperature data for meteorological, oceanographic, and climate models were assessed. Results show that the AVHRR is a powerful tool for the monitoring of processes in the Earth-atmosphere system, especially for the monitoring of sea (lake) surface parameters. The coarse spatial resolution renders Advanced Very High Resolution Radiometer (AVHRR) data less suitable for land surfaces. ESA

N89-21162# Army Engineer Topographic Labs., Fort Belvoir, VA. Research Inst.

COMPUTER STRATEGY FOR DETECTING LINE FEATURES ON SIMULATED BINARY ARRAYS IN SUPPORT OF RADAR FEATURE EXTRACTION Technical Report, May - Nov. 1988

FREDERICK W. ROHDE Nov. 1988 27 p
(AD-A203257; ETL-0478) Avail: NTIS HC A03/MF A01 CSCL 17/9

Line search techniques for linear features in digital radar images are developed and described. It is shown that the search techniques can be represented by codes. The codes determine the major directions of search and removal of side branches. The testbed that is necessary to investigate and test the search techniques is described. GRA

N89-21165# La Jolla Inst., CA. Center for the Study of Nonlinear Dynamics.

IMAGING OF OCEAN WAVES BY SAR

R. L. SCHULT, F. S. HENYEY, and J. A. WRIGHT 1988 42 p
(Contract N00014-87-C-0687)
(AD-A203604; LJL-87-P-467) Avail: NTIS HC A03/MF A01 CSCL 17/9

A model is presented for Synthetic Aperture Radar imaging of the ocean surface. The model attempts to avoid making assumptions about the relative importance of various imaging mechanisms. The model is applied to three issues, the focus setting, the asymmetry in the images obtained with obtained with opposite airplane flight directions, and the azimuthal image shift of features on range directed waves. The focus setting depends on a combination of the velocity of the pattern being imaged and on the velocity of the Bragg scatterers. The focus setting does not depend significantly on the imaging mechanism, that is velocity bunching, modulation of Bragg waves, and so on. Comparisons of our model predictions are made with the TOWARD results. A simple analytic prediction is obtained for the complete curve of the observed energy in swell versus the focus setting. The maximum of this curve is predicted to occur at one-half of the phase speed of the swell for azimuthally traveling swell and a simple explanation is provided for this result. The asymmetry in the visibility of the swell obtained by flying with or against the long waves is estimated. The asymmetry arises from competition between velocity bunching and hydrodynamic modulations. GRA

N89-21317*# National Aeronautics and Space Administration. Goddard Space Flight Center, Greenbelt, MD.

GEOLOGICAL REMOTE SENSING SIGNATURES OF TERRESTRIAL IMPACT CRATERS

J. B. GARVIN, C. SCHNETZLER, and R. A. F. GRIEVE /In Lunar and Planetary Inst., Global Catastrophes in Earth History: An Interdisciplinary Conference on Impacts, Volcanism, and Mass Mortality p 52-53 1988 Prepared in cooperation with Geological Survey of Canada, Toronto (Ontario)
Avail: NTIS HC A11/MF A01 CSCL 08/2

Geological remote sensing techniques can be used to investigate structural, depositional, and shock metamorphic effects associated with hypervelocity impact structures, some of which may be linked to global Earth system catastrophes. Although

detailed laboratory and field investigations are necessary to establish conclusive evidence of an impact origin for suspected crater landforms, the synoptic perspective provided by various remote sensing systems can often serve as a pathfinder to key deposits which can then be targeted for intensive field study. In addition, remote sensing imagery can be used as a tool in the search for impact and other catastrophic explosion landforms on the basis of localized disruption and anomaly patterns. In order to reconstruct original dimensions of large, complex impact features in isolated, inaccessible regions, remote sensing imagery can be used to make preliminary estimates in the absence of field geophysical surveys. The experience gained from two decades of planetary remote sensing of impact craters on the terrestrial planets, as well as the techniques developed for recognizing stages of degradation and initial crater morphology, can now be applied to the problem of discovering and studying eroded impact landforms on Earth. Preliminary results of remote sensing analyses of a set of terrestrial impact features in various states of degradation, geologic settings, and for a broad range of diameters and hence energies of formation are summarized. The intention is to develop a database of remote sensing signatures for catastrophic impact landforms which can then be used in EOS-era global surveys as the basis for locating the possibly hundreds of missing impact structures. In addition, refinement of initial dimensions of extremely recent structures such as Zhamanshin and Bosumtwi is an important objective in order to permit re-evaluation of global Earth system responses associated with these types of events. Author

N89-21318*# Geological Survey of Canada, Toronto (Ontario).

THE FRASNIAN-FAMENNIAN MASS KILLING EVENT(S), METHODS OF IDENTIFICATION AND EVALUATION

H. H. J. GELDSETZER /In Lunar and Planetary Inst., Global Catastrophes in Earth History: An Interdisciplinary Conference on Impacts, Volcanism, and Mass Mortality p 54-55 1988
Avail: NTIS HC A11/MF A01 CSCL 13/2

The absence of an abnormally high number of earlier Devonian taxa from Famennian sediments was repeatedly documented and can hardly be questioned. Primary recognition of the event(s) was based on paleontological data, especially common macrofossils. Most paleontologists place the disappearance of these common forms at the gigas/triangularis contact and this boundary was recently proposed as the Frasnian-Famennian (F-F) boundary. Not unexpectedly, alternate F-F positions were suggested caused by temporary Frasnian survivors or sudden post-event radiations of new forms. Secondary supporting evidence for mass killing event(s) is supplied by trace element and stable isotope geochemistry but not with the same success as for the K/T boundary, probably due to additional 300 ma of tectonic and diagenetic overprinting. Another tool is microfacies analysis which is surprisingly rarely used even though it can explain geochemical anomalies or paleontological overlap not detectable by conventional macrofacies analysis. The combination of microfacies analysis and geochemistry was applied at two F-F sections in western Canada and showed how interdependent the two methods are. Additional F-F sections from western Canada, western United States, France, Germany and Australia were sampled or re-sampled and await geochemical/microfacies evaluation. Author

N89-21431# National Geophysical Data Center, Boulder, CO.

SOLAR-GEOPHYSICAL DATA NUMBER 529, SEPTEMBER 1988. PART 1: (PROMPT REPORTS). DATA FOR AUGUST, JULY 1988 AND LATE DATA

HELEN E. COFFEY, ed. and JOHN A. MCKINNON, ed. Sep. 1988 139 p
(Contract N00014-86-F-0049)
(PB89-121305; SGD-529-PT-1; ISSN-0038-0911; LC-79-640375)
Avail: NTIS HC A07/MF A01 CSCL 04/1

Solar-geophysical information is presented in tabular and graphic form. Categories include data for July and August 1988; IUWDS alert periods (advance and worldwide); solar activity indices; solar flares: solar radio emission; solar interferometric charts; and Stanford mean solar magnetic field. B.G.

07 DATA PROCESSING AND DISTRIBUTION SYSTEMS

N89-21452# Naval Postgraduate School, Monterey, CA.
SATELLITE SIGNATURES OF RAPID CYCLOGENESIS M.S. Thesis

JOSE F. H. ATANGAN Dec. 1988 58 p
(AD-A203934) Avail: NTIS HC A04/MF A01 CSCL 04/2

Animation of satellite visual and infrared imagery indicates that rapid cloud growth is a characteristic of explosively deepening cyclones. The working hypothesis in this thesis is that the intense vertical motions responsible for the low-level spin-up will produce rapid cloud expansion in the upper troposphere that can be detected using digital satellite data. Using digital IR data from GOES-West, the cloud growth of three explosive storms that developed over the eastern North Pacific Ocean were measured quantitatively and compared with the cyclone deepening rate. The results indicate that the growth in areal coverage of clouds colder than -45 C is most closely related to the explosive development period while the growth of the warmer cloud tops is related to the open wave stage. This relationship is dependent on the cloud pattern of the maturing cyclone. Correlations between cloud growth and pressure deepening were calculated but provide only a general estimate of the relationship between the two parameters. This study demonstrates the feasibility of using digitized satellite data to quantitatively analyze the cloud growth and structure of explosively developing cyclones. GRA

N89-21460# Defence Research Establishment Pacific, Victoria (British Columbia).

OSRMS (OCEAN SURFACE ROUGHNESS MEASUREMENT SYSTEM): THE DREP (DEFENCE RESEARCH ESTABLISHMENT PACIFIC) NEAR-NADIR SCATTEROMETER
L. C. PEMPEL, B. A. HUGHES, and S. J. HUGHES Aug. 1988 45 p

(AD-A202983; DREP-TM-88-15) Avail: NTIS HC A03/MF A01 CSCL 17/5

The ocean surface roughness measurement system (OSRMS) is a near-nadir-directed infrared (IR) scatterometer. It has been used to measure ocean-surface parameters and particularly for the examination from an aircraft of internal waves. This paper gives a description of the configuration and operation of the OSRMS including the mechanical, electrical, electronic, optical, and software components. A brief overview of the trial, SCATMOD III and the data obtained in that trial are also described. The discussion of the data from this trial contains examples of internal waves, ship wakes, and aircraft attitude compensation, and a description of wind velocity effects on the speckle noise. GRA

N89-21507# Army Engineer Waterways Experiment Station, Vicksburg, MS. Coastal Engineering Research Center.

THE KP EQUATION: A COMPARISON TO LABORATORY GENERATED BIPERIODIC WAVES

NORMAN W. SCHEFFNER In Army Research Office, Transactions of the Fifth Army Conference on Applied Mathematics and Computing p 355-368 Mar. 1988 Presented at the 20th International Conference on Coastal Engineering, Taipei, Taiwan, 9-14 Nov. 1986 Submitted for publication
Avail: NTIS HC A99/MF E03 CSCL 08/3

The propagation of waves in shallow water is a phenomenon of significant practical importance. The ability to realistically predict the complex wave characteristics occurring in shallow water regions has always been an engineering goal which would make the development of solutions to practical engineering problems a reality. The difficulty in making such predictions stems from the fact that the equations governing the complex three-dimensional flow regime can not be solved without linearizing the problem. The linear equations are solvable; however, their solutions do not reflect the nonlinear features of naturally occurring waves. A recent advance (1984) in nonlinear mathematics has resulted in an explicit solution to a nonlinear equation relevant to water waves in shallow water. The solution possesses features found in observed nonlinear three-dimensional wave fields. Author

N89-21521# Army Engineer Waterways Experiment Station, Vicksburg, MS. Geotechnical Lab.

COLUMN MOVEMENT MODEL USED TO SUPPORT AMM

GEORGE B. MCKINLEY In Army Research Office, Transactions of the Fifth Army Conference on Applied Mathematics and Computing p 601-616 Mar. 1988
Avail: NTIS HC A99/MF E03 CSCL 08/2

For many years mobility maps have been created utilizing the Army Mobility Model (AMM). These maps show the maximum speed which a vehicle can attain in off-road terrain and on-road networks. These maps are useful in comparing the performance of vehicles or as an aid in route selection. Three additional computer models have been developed to support the AMM by predicting the performance of military vehicles over digital terrain units along a specified route. These three models are an Acceleration Model, a Traverse Model, and a Column Movement Model. The Acceleration Model produces a time versus speed curve for a vehicle along a specified route across a terrain unit. The Traverse Model uses the Acceleration Model as a building block and predicts a vehicle's performance along a specified route over a series of terrain units. The Column Movement Model uses the Traverse Model as a building block for predicting performance of a column of vehicles along a specified route. The Column Movement Model maintains vehicle spacing within the column in accordance with military doctrine. Author

N89-21568# Air Force Inst. of Tech., Wright-Patterson AFB, OH. School of Engineering.

A SOFTWARE SYSTEM TO CREATE A HIERARCHICAL, MULTIPLE LEVEL OF DETAIL TERRAIN MODEL M.S. Thesis

LEEANNE ROBERTS Dec. 1988 55 p
(AD-A203047; AFIT/GCS/ENG/88D-18) Avail: NTIS HC A04/MF A01 CSCL 08/2

The purpose of this effort was to design and implement a software system that will generate a hierarchical database composed of more than one level of detail of a terrain model and cultural objects from digital elevation and cultural data files. The software system designed and implemented in this effort was written in the C language and implemented on a Digital Equipment GPX Workstation and on a Silicon Graphics Iris 3130 Workstation. Although the primary source of elevation data used in this effort was the Defense Mapping Agencies' (DMA) Digital Terrain Elevation Data (DTED), a method was developed to build a terrain model from non-gridded elevation data. In addition to allowing the use of non-DMA data, this method also makes it possible to build a terrain model from a non-gridded subset of a DMA DTED data file. Two database formats were designed and implemented in this effort. The first database (which was used to generate the terrain model) contains lists of the vertices, exterior edges, interior edges, and polygons (and their interrelations) that form the terrain model. The second database contains polygons (that form the terrain model) and cultural features (such as radio towers) at one or more levels of detail, and a search tree (so that data in a particular area may be retrieved quickly). The list database may be used to generate contours, or non-real-time images of terrain. The hierarchical database may be used in a simulator environment. GRA

N89-21643# Naval Ocean Systems Center, San Diego, CA.
INFRARED SEA-RADIANCE MODELING USING LOWTRAN 6 Final Report

F. G. WOLLENWEBER Sep. 1988 23 p
(AD-A202582; NOSC/TD-1355) Avail: NTIS HC A03/MF A01 CSCL 20/6

This model, based on the Cox-Munk wave-slope statistic and the LOWTRAN 6 radiation model, describes the behavior of the sea as an infrared background. The model addresses atmospheric refraction, aerosol absorption and scattering, molecular scattering, emission, and absorption. Comparisons with measurements of a calibrated thermal-imaging system showed good agreement. GRA

N89-22152*# National Aeronautics and Space Administration. Goddard Space Flight Center, Greenbelt, MD.

NIMBUS-7 DATA PRODUCT SUMMARY

ARNOLD G. OAKES, DAESOO HAN, H. LEE KYLE, GENE CARL FELDMAN, ALBERT J. FLEIG, EDWARD J. HURLEY, and BARBARA A. KAUFMAN (General Sciences Corp., Laurel, MD.) Feb. 1989 103 p

(Contract NAS5-29386)

(NASA-RP-1215; REPT-89B00074; NAS 1.61:1215) Avail: NTIS HC A06/MF A01 CSCL 04/1

Data sets resulting from the first nine years of operations of the Nimbus-7 Satellite are briefly described. After a brief description of the Nimbus-7 Mission, each of the eight experiments on-board the satellite (Coastal Zone Color Scanner (CZCS), Earth Radiation Budget (ERB), Limb Infrared Monitor of the Stratosphere (MIMS), Stratospheric Aerosol Measurement II (SAM II), Stratospheric and Mesospheric Sounder (SAMS), Solar Backscatter Ultraviolet/Total Ozone Mapping Spectrometer (SBUV/TOMS), Scanning Multichannel Microwave Radiometer (SMMR) and the Temperature Humidity Infrared Radiometer (THIR) are introduced and their respective data products are described in terms of media, general format, and suggested applications. Extensive references are provided. Instructions for obtaining further information, and for ordering data products are given. Author

N89-22156*# Jet Propulsion Lab., California Inst. of Tech., Pasadena.

ATMOSPHERIC WATER MAPPING WITH THE AIRBORNE VISIBLE/INFRARED IMAGING SPECTROMETER (AVIRIS), MOUNTAIN PASS, CALIFORNIA

JAMES E. CONEL, ROBERT O. GREEN, VERONIQUE CARRERE, JACK S. MARGOLIS, RONALD E. ALLEY, GREGG VANE, CAROL J. BRUEGGE, and BRUCE L. GARY *In its* Proceedings of the Airborne Visible/Infrared Imaging Spectrometer (AVIRIS) Performance Evaluation Workshop p 21-29 15 Sep. 1988

Avail: NTIS HC A11/MF A01 CSCL 08/2

Observations are given of the spatial variation of atmospheric precipitable water using the Airborne Visible/Infrared Imaging Spectrometer (AVIRIS) over a desert area in eastern California, derived using a band ratio method and the 940 nm atmospheric water band and 870 nm continuum radiances. The ratios yield total path water from curves of growth supplied by the LOWTRAN 7 atmospheric model. An independent validation of the AVIRIS-derived column abundance at a point is supplied by a spectral hygrometer calibrated with respect to radiosonde observations. Water values conform to topography and fall off with surface elevation. The edge of the water vapor boundary layer defined by topography is thought to have been recovered. The ratio method yields column abundance estimates of good precision and high spatial resolution. Author

N89-22157*# Geological Survey, Flagstaff, AZ.

RADIOMETRIC PERFORMANCE OF AVIRIS: ASSESSMENT FOR AN ARID REGION GEOLOGIC TARGET

HUGH H. KIEFFER, ERIC M. ELIASON, KEVIN F. MULLINS, LAURENCE A. SODERBLOM, and JAMES M. TORSON *In* Jet Propulsion Lab., California Inst. of Tech., Proceedings of the Airborne Visible/Infrared Imaging Spectrometer (AVIRIS) Performance Evaluation Workshop p 30-35 15 Sep. 1988

Avail: NTIS HC A11/MF A01 CSCL 08/2

Data from several AVIRIS flight lines were examined to assess instrument stability and response. Both scene and in-flight calibration data were analyzed statistically. The data clearly indicates that, although the instrument output was noisy and unstable at the time of the data acquisition, valuable spectral signatures can still be extracted and analyzed. Some first order calibration corrections can be performed by forcing internal consistency within the data. AVIRIS data are delivered in band-interleaved-by-line format, but high efficiency routines were developed which access the data as either image or spectral planes and enable effective statistical and visual examination of both AVIRIS scenes and ancillary files. Two methods were used to extract spectral information from segment 4 of the Kelso Dunes

flight. Both successfully identified at least three distinct spectral signatures, but neither has positively identified a specific material.

Author

N89-22158*# National Aeronautics and Space Administration. Ames Research Center, Moffett Field, CA.

ZONES OF INFORMATION IN THE AVIRIS SPECTRA

PAUL J. CURRAN and JENNIFER L. DUNGAN (TGS Technology, Inc., Moffett Field, CA.) *In* Jet Propulsion Lab., California Inst. of Tech., Proceedings of the Airborne Visible/Infrared Imaging Spectrometer (AVIRIS) Performance Evaluation Workshop p 36-48 15 Sep. 1988

Avail: NTIS HC A11/MF A01 CSCL 08/2

To make the best use of Airborne Visible/Infrared Imaging Spectrometer (AVIRIS) data an investigator needs to know the ratio of signal to random variability or noise (S/N ratio). The signal is land-cover dependent and decreases with both wavelength and atmospheric absorption and random noise comprises sensor noise and intra-pixel variability. The three existing methods for estimating the S/N ratio are inadequate as typical laboratory methods inflate, while dark current and image methods deflate the S/N ratio. We propose a new procedure called the geostatistical method. It is based on the removal of periodic noise by notch filtering in the frequency domain and the isolation of sensor noise and intra-pixel variability using the semi-variogram. This procedure was applied easily and successfully to five sets of AVIRIS data from the 1987 flying season. Author

N89-22159*# Geological Survey, Denver, CO.

CALIBRATION AND EVALUATION OF AVIRIS DATA: CRIPPLE CREEK IN OCTOBER 1987

ROGER N. CLARK, BARRY J. MIDDLEBROOK, GREGG A. SWAYZE, K. ERIC LIVO, DAN H. KNEPPER, TRUDE V. V. KING, and KEENAN LEE *In* Jet Propulsion Lab., California Inst. of Tech., Proceedings of the Airborne Visible/Infrared Imaging Spectrometer (AVIRIS) Performance Evaluation Workshop p 49-61 15 Sep. 1988

Avail: NTIS HC A11/MF A01 CSCL 08/2

Airborne Visible/Infrared Imaging Spectrometer (AVIRIS) data were obtained over Cripple Creek and Canon City Colorado on October 19, 1987 at local noon. Multiple ground calibration sites were measured within both areas with a field spectrometer and samples were returned to the laboratory for more detailed spectral characterization. The data were used to calibrate the AVIRIS data to ground reflectance. Once calibrated, selected spectra in the image were extracted and examined, and the signal to noise performance was computed. Images of band depth selected to be diagnostic of the presence of certain minerals and vegetation were computed. The AVIRIS data were extremely noisy, but images showing the presence of goethite, kaolinite and lodgepole pine trees agree with ground checks of the area. Author

N89-22160*# Colorado Univ., Boulder. Center for the Study of Earth from Space.

AUTOMATED EXTRACTION OF ABSORPTION FEATURES FROM AIRBORNE VISIBLE/INFRARED IMAGING SPECTROMETER (AVIRIS) AND GEOPHYSICAL AND ENVIRONMENTAL RESEARCH IMAGING SPECTROMETER (GERIS) DATA

FRED A. KRUSE, WENDY M. CALVIN, and OLIVIER SEZNEC *In* Jet Propulsion Lab., California Inst. of Tech., Proceedings of the Airborne Visible/Infrared Imaging Spectrometer (AVIRIS) Performance Evaluation Workshop p 62-75 15 Sep. 1988

Avail: NTIS HC A11/MF A01 CSCL 08/2

Automated techniques were developed for the extraction and characterization of absorption features from reflectance spectra. The absorption feature extraction algorithms were successfully tested on laboratory, field, and aircraft imaging spectrometer data. A suite of laboratory spectra of the most common minerals was analyzed and absorption band characteristics tabulated. A prototype expert system was designed, implemented, and successfully tested to allow identification of minerals based on the extracted absorption band characteristics. AVIRIS spectra for a site in the northern

07 DATA PROCESSING AND DISTRIBUTION SYSTEMS

Grapevine Mountains, Nevada, have been characterized and the minerals sericite (fine grained muscovite) and dolomite were identified. The minerals kaolinite, alunite, and buddingtonite were identified and mapped for a site at Cuprite, Nevada, using the feature extraction algorithms on the new Geophysical and Environmental Research 64 channel imaging spectrometer (GERIS) data. The feature extraction routines (written in FORTRAN and C) were interfaced to the expert system (written in PROLOG) to allow both efficient processing of numerical data and logical spectrum analysis. Author

N89-22164*# TGS Technology, Inc., Moffett Field, CA.
AVIRIS DATA QUALITY FOR CONIFEROUS CANOPY CHEMISTRY

NANCY A. SWANBERG /In Jet Propulsion Lab., California Inst. of Tech., Proceedings of the Airborne Visible/Infrared Imaging Spectrometer (AVIRIS) Performance Evaluation Workshop p 102-108 15 Sep. 1988

Avail: NTIS HC A11/MF A01 CSCL 08/2

An assessment of AVIRIS data quality for studying coniferous canopy chemistry was made. Seven flightlines of AVIRIS data were acquired over a transect of coniferous forest sites in central Oregon. Both geometric and radiometric properties of the data were examined including: pixel size, swath width, spectral position and signal-to-noise ratio. A flat-field correction was applied to AVIRIS data from a coniferous forest site. Future work with this data set will exclude data from spectrometers C and D due to low signal-to-noise ratios. Data from spectrometers A and B will be used to examine the relationship between the canopy chemical composition of the forest sites and AVIRIS spectral response. Author

N89-22165*# Geological Survey, Sioux Falls, SD.
AVIRIS DATA CHARACTERISTICS AND THEIR EFFECTS ON SPECTRAL DISCRIMINATION OF ROCKS EXPOSED IN THE DRUM MOUNTAINS, UTAH: RESULTS OF A PRELIMINARY STUDY

G. B. BAILEY, J. L. DWYER, and D. J. MEYER (TGS Technology, Inc., Sioux Falls, SD.) /In Jet Propulsion Lab., California Inst. of Tech., Proceedings of the Airborne Visible/Infrared Imaging Spectrometer (AVIRIS) Performance Evaluation Workshop p 109-121 15 Sep. 1988

(Contract GS14-08-0001-22521)

Avail: NTIS HC A11/MF A01 CSCL 08/2

Airborne Visible and Infrared Imaging Spectrometer (AVIRIS) data collected over a geologically diverse field site and over a nearby calibration site were analyzed and interpreted in efforts to document radiometric and geometric characteristics of AVIRIS, quantify and correct for detrimental sensor phenomena, and evaluate the utility of AVIRIS data for discriminating rock types and identifying their constituent mineralogy. AVIRIS data acquired for these studies exhibit a variety of detrimental artifacts and have lower signal-to-noise ratios than expected in the longer wavelength bands. Artifacts are both inherent in the image data and introduced during ground processing, but most may be corrected by appropriate processing techniques. Poor signal-to-noise characteristics of this AVIRIS data set limited the usefulness of the data for lithologic discrimination and mineral identification. Various data calibration techniques, based on field-acquired spectral measurements, were applied to the AVIRIS data. Major absorption features of hydroxyl-bearing minerals were resolved in the spectra of the calibrated AVIRIS data, and the presence of hydroxyl-bearing minerals at the corresponding ground locations was confirmed by field data. Author

N89-22166*# Brown Univ., Providence, RI. Dept. of Geological Sciences.

APPLICATION OF IMAGING SPECTROMETER DATA TO THE KINGS-KAWEAH OPHIOLITE MELANGE

JOHN F. MUSTARD and CARLE M. PIETERS /In Jet Propulsion Lab., California Inst. of Tech., Proceedings of the Airborne Visible/Infrared Imaging Spectrometer (AVIRIS) Performance

Evaluation Workshop p 122-127 15 Sep. 1988

Avail: NTIS HC A11/MF A01 CSCL 08/2

The Kings-Kaweah ophiolite melange in east-central California is thought to be an obducted oceanic fracture zone and provides the rare opportunity to examine in detail the complex nature of this type of terrain. It is anticipated that the distribution and abundance of components in the melange can be used to determine the relative importance of geologic processes responsible for the formation of fracture zone crust. Laboratory reflectance spectra of field samples indicate that the melange components have distinct, diagnostic absorptions at visible to near-infrared wavelengths. The spatial and spectral resolution of AVIRIS is ideally suited for addressing important scientific questions concerning the Kings-Kaweah ophiolite melange and fracture zones in general. Author

N89-22168*# California Inst. of Tech., Pasadena.
AN ASSESSMENT OF AVIRIS DATA FOR HYDROTHERMAL ALTERATION MAPPING IN THE GOLDFIELD MINING DISTRICT, NEVADA

VERONIQUE CARRERE and MICHAEL J. ABRAMS /In Jet Propulsion Lab., California Inst. of Tech., Proceedings of the Airborne Visible/Infrared Imaging Spectrometer (AVIRIS) Performance Evaluation Workshop p 134-154 15 Sep. 1988

Avail: NTIS HC A11/MF A01 CSCL 08/2

Airborne Visible and Infrared Imaging Spectrometer (AVIRIS) data were acquired over the Goldfield Mining District, Nevada, in September 1987. Goldfield is one of the group of large epithermal precious metal deposits in Tertiary volcanic rocks, associated with silicic volcanism and caldera formation. Hydrothermal alteration consists of silicification along fractures, advanced argillic and argillic zones further away from veins and more widespread propylitic zones. An evaluation of AVIRIS data quality was performed. Faults in the data, related to engineering problems and a different behavior of the instrument while on-board the U2, were encountered. Consequently, a decision was made to use raw data and correct them only for dark current variations and detector read-out-delays. New software was written to that effect. Atmospheric correction was performed using the flat field correction technique. Analysis of the data was then performed to extract spectral information, mainly concentrating on the 2 to 2.45 micron window, as the alteration minerals of interest have their distinctive spectral reflectance features in this region. Principally kaolinite and alunite spectra were clearly obtained. Mapping of the different minerals and alteration zones was attempted using ratios and clustering techniques. Poor signal-to-noise performance of the instrument and the lack of appropriate software prevented the production of an alteration map of the area. Spectra extracted locally from the AVIRIS data were checked in the field by collecting representative samples of the outcrops. Author

N89-22173# Air Force Inst. of Tech., Wright-Patterson AFB, OH. School of Engineering.

USE OF COMMERCIAL SATELLITE IMAGERY FOR SURVEILLANCE OF THE CANADIAN NORTH BY THE CANADIAN ARMED FORCES M.S. Thesis

ROBERT CHEKAN Dec. 1988 260 p

(AD-A202700; AFIT/GSO/ENS/88D-4) Avail: NTIS HC A12/MF A01 CSCL 17/11

This thesis examines the utility of commercial satellite-acquired imagery for the surveillance of the Canadian North. Analytical performance models are developed for visible and thermal wavelength sensors. These models form the basis for evaluation of an individual sensor's potential contribution to surveillance. The mission of surveillance is sectioned into five separate missions. For each mission, sensor system evaluation algorithms, which combine individual sensor's probabilities of detection and tracking, are proposed and optimization techniques identified. Sample algorithms, using a representative target set, are provided for each mission. Analysis shows that the selection of specific sensors is mission and situation specific. GRA

N89-22293# Colorado State Univ., Fort Collins. Engineering Research Center.

MESOSCALE SEVERE WEATHER DEVELOPMENT UNDER OROGRAPHIC INFLUENCES Final Report, 1 Jul. 1986 - 30 Sep. 1988

ELMAR R. REITER, JOHN D. SHEAFFER, and MARJORIE A. KLITCH Jan. 1989 26 p
(Contract F49620-86-C-0080)
(AD-A205082; AFOSR-89-0095TR) Avail: NTIS HC A03/MF A01 CSCL 04/2

Measurements of surface energy budgets have been carried out at several sites in the Colorado Rocky Mountains, in the Kansas Prairie, in the Gobi Desert and in Tibet. The fluxes of sensible heat, H sub S , from the surface could be estimated as functions of the difference between air temperature and infrared skin surface temperature, as seen by remote sensing instruments. Computations of H_s involve a neutral stability coefficient for turbulent transfer (drag coefficient), C sub T , ranging between 0.0021 (Gobi Desert) and 0.0070 (alpine tundra), and a scaling factor for stability. Latent heat fluxes were estimated either as residual of total energy fluxes or through a Bowen ratio approach. These flux estimates worked well in a mesoscale, nested-grid model over the Rocky Mountains. The model was able to predict with considerable skill flash-flood events such as the Big Thompson flood of 1976 and the Cheyenne flood of 1985. By implanting features such as a vorticity maximum associated with a low-level jet stream, the model without nested grid was able to predict severe cyclogenesis (bomb formation) over the eastern United States. Both model versions run on a desktop workstation. GRA

N89-22344*# National Aeronautics and Space Administration. Goddard Space Flight Center, Greenbelt, MD.

DATA COMPRESSION EXPERIMENTS WITH LANDSAT THEMATIC MAPPER AND NIMBUS-7 COASTAL ZONE COLOR SCANNER DATA

JAMES C. TILTON and H. K. RAMAPRIYAN In its Proceedings of the Scientific Data Compression Workshop p 311-334 Feb. 1989

Avail: NTIS HC A19/MF A01 CSCL 08/2

A case study is presented where an image segmentation based compression technique is applied to LANDSAT Thematic Mapper (TM) and Nimbus-7 Coastal Zone Color Scanner (CZCS) data. The compression technique, called Spatially Constrained Clustering (SCC), can be regarded as an adaptive vector quantization approach. The SCC can be applied to either single or multiple spectral bands of image data. The segmented image resulting from SCC is encoded in small rectangular blocks, with the codebook varying from block to block. Lossless compression potential (LDP) of sample TM and CZCS images are evaluated. For the TM test image, the LCP is 2.79. For the CZCS test image the LCP is 1.89, even though when only a cloud-free section of the image is considered the LCP increases to 3.48. Examples of compressed images are shown at several compression ratios ranging from 4 to 15. In the case of TM data, the compressed data are classified using the Bayes' classifier. The results show an improvement in the similarity between the classification results and ground truth when compressed data are used, thus showing that compression is, in fact, a useful first step in the analysis. Author

N89-22971*# Massachusetts Inst. of Tech., Cambridge. Lab. of Electronics.

REMOTE SENSING OF EARTH TERRAIN Final Report, 1 Sep. 1982 - 31 Mar. 1989

J. A. KONG 31 Mar. 1989 26 p
(Contract NAG5-270)

(NASA-CR-184937; NAS 1.26:184937; OSP-92790) Avail: NTIS HC A03/MF A01 CSCL 08/2

A mathematically rigorous and fully polarimetric radar clutter model used to evaluate the radar backscatter from various types of terrain clutter such as forested areas, vegetation canopies, snow covered terrains, or ice fields is presented. With this model, the radar backscattering coefficients for the multichannel polarimetric radar returns can be calculated, in addition to the complex cross

correlation coefficients between elements of the polarimetric measurement vector. The complete polarization covariance matrix can be computed and the scattering properties of the clutter environment characterized over a broad range of incident angle and frequencies. Author

N89-22972# Freiburg Univ. (Germany, F.R.). Inst. fuer Physische Geographie.

DERIVATION OF A LARGE-SCALE MAP OF HEAT LOAD IN THE REGION FREIBURG-BASEL (GERMANY, F.R.) USING SATELLITE DATA. A CONTRIBUTION TO THE PRODUCTION OF BIOCLIMATE DATA BASED ON A GEOGRAPHIC INFORMATION SYSTEM Ph.D. Thesis [ABLEITUNG EINER GROSSMASSTABEBIGEN KARTE DER WAERMEBELASTUNG IM RAUM FREIBURG-BASEL MIT HILFE VON SATELLITENDATEN. EIN BEITRAG ZUR ERZEUGUNG VON BIOKLIMAKARTEN AUF DER BASIS EINES GEOGRAPHISCHEN INFORMATIONSSYSTEMS]

GUNTER MENZ 1987 222 p In GERMAN Color map as supplement
(REPT-27; ETN-89-93781) Avail: NTIS HC A10/MF A01

The computer-aided production of a map of the heat load on man in the southern Black Forest (West Germany) on the Upper Rhine plane between Freiburg and Basel was investigated. A geographic information system was established using data from a climate model, a digital height model, LANDSAT data, and data from the Heat Capacity Mapping Mission. Using a stochastic model the heat load values were estimated. The form and significance of the estimation equation depends on the data collection. The effect of the local land use on the bioclimate of neighboring locations can only be determined with sufficient environment data. The highest variance information is obtained if the land use is differentiated in 6 classes, allowing a heat load mapping. Heat load mapping on scales 1:200,000, 1:100,000 and 1:50,000 prove to be possible, enabling the transition from a mesoscale to a microscale cartographic determination of climatic effects on human beings. ESA

N89-22973# Technische Univ., Delft (Netherlands). Faculty of Geodesy.

INTEGRATION OF TIE-POINTS IN DIGITAL MOSAICING Thesis

HERMAN RYKS Jun. 1988 79 p
(ETN-89-94147) Avail: NTIS HC A05/MF A01

A mosaicing method which includes the use of tie-points, which are points in the overlap of two or more images that have known image-coordinates in these images, but of which no ground coordinates are necessary, is presented. This enables one to make mosaics, using very few ground control points, or none at all. The FORTRAN program that calculates the transformation parameters of the images to be mosaiced is given. The tests performed are described. Recommendations to achieve an operational mosaicing system are made. ESA

N89-22977# GEC-Marconi Electronics Ltd., Chelmsford (England).

THEORETICAL STUDIES FOR ERS-1 WAVE MODE, VOLUME 1 Final Report

J. T. MACKLIN, R. A. CORDEY, and J. M. PIELOU Paris, France ESA Aug. 1988 130 p
(Contract ESA-6878/87/HGE/I(SC))
(GEC-MTR-87/110-VOL-1; ESA-CR(P)-2750; ETN-89-94471)
Avail: NTIS HC A07/MF A01

The theory of how the sea surface is imaged by synthetic aperture radar (SAR), as well as inverse methods for recovering quantitative information about ocean waves from SAR data are discussed. Short-wave spectra, wave-wave interactions (hydrodynamic modulation) and wave nonlinearities (including breaking waves) are reviewed. Backscattering from breaking waves and the imaging effects due to their motions are considered. An inverse method using complex imagery is developed and is shown to offer improved prediction of the speckle component in the power spectra of SAR intensity images. The possibility of an iterative

07 DATA PROCESSING AND DISTRIBUTION SYSTEMS

inverse method for nonlinear imaging conditions is discussed. The available optimum inverse methods are reviewed, and the potential of the maximum entropy method is considered. The requirements for validating the imaging theory are examined, and recommendations are made for future work, highlighting aspects relevant to the operation of the wave mode of ERS-1. ESA

N89-22978# European Space Agency, Paris (France).
IMAGING RADAR APPLICATIONS IN EUROPE. ILLUSTRATED EXPERIMENTAL RESULTS (1978-1987)

M. G. WOODING, A. J. SIEBER, P. N. CHURCHILL (Joint Research Centre of the European Communities, Ispra, Italy), J. LICHTENEGGER, M. FEA, T.-D. GUYENNE, ed., and N. LONGDON, ed. Oct. 1988 85 p Original contains color illustrations

(ESA-TM-01; ETN-89-94474) Avail: NTIS HC A05/MF A01

The potential of imaging radar for agriculture, forestry, geology, snow and ice, and oceanography applications is illustrated. Image processing techniques and data availability are mentioned. ESA

N89-22979*# California Univ., Santa Barbara.
REMOTE SENSING INFORMATION SCIENCES RESEARCH GROUP: BROWSE IN THE EOS ERA Final Report

JOHN E. ESTES and JEFFREY L. STAR 1 May 1989 155 p (Contract NAGW-987)

(NASA-CR-184637; NAS 1.26:184637) Avail: NTIS HC A06/MF A01 CSCL 08/2

The problem of science data browse was examined. Given the tremendous data volumes that are planned for future space missions, particularly the Earth Observing System in the late 1990's, the need for access to large spatial databases must be understood. Work was continued to refine the concept of data browse. Further, software was developed to provide a testbed of the concepts, both to locate possibly interesting data, as well as view a small portion of the data. Build II was placed on a minicomputer and a PC in the laboratory, and provided accounts for use in the testbed. Consideration of the testbed software as an element of in-house data management plans was begun. Author

N89-23031 Colorado Univ., Boulder.
THE RESPONSE OF THERMOSPHERIC NITRIC OXIDE TO AN AURORAL STORM Ph.D. Thesis

DAVID ERIC SISKIND 1988 189 p

Avail: Univ. Microfilms Order No. DA8902936

The response of thermospheric nitric oxide (NO) to the auroral storm of September 19, 1984 is analyzed. Measurements of nitric oxide from the Solar Mesosphere Explorer (SME) ultraviolet spectrometer are compared with the calculations of a one-dimensional photochemical model of the lower thermosphere. The NCAR thermospheric General Circulation Model (TGCM) is used to calculate the response of the background neutral atmosphere to auroral forcings such as Joule and particle heating. The output of the TGCM is used as input to the photochemical model. The time history of the auroral energy input is assessed using particle data from the NOAA 6 and 7 satellites. Calculations of the mid-latitude NO response show that temperature increases which result from Joule heating lead to NO enhancements. A larger response is initially seen for altitudes greater than 120 km. After several days, downward diffusion leads to NO increases at lower altitudes. Equatorial NO shows little response because the combined effects of temperature enhancements and atomic oxygen enhancements largely cancel. At auroral latitudes the effects of particle precipitation are dominant with Joule heating contributing only 15 percent to the peak NO density. Calculations of the auroral NO response predict an enhancement; however, the amplitude of the response, as well as the absolute magnitude of the calculated NO, greatly exceed the observations. Vertical winds on the order of 1 to 5 m/sec in the E region are proposed as an important loss process. The NO density is sensitive to changes in the O/O₂ ratio, the N(D-2) yield from N₂ dissociative excitation and the quenching of N(D-2) by O. Dissert. Abstr.

N89-23080# SRI International Corp., Menlo Park, CA. Artificial Intelligence Center.

IMAGE UNDERSTANDING RESEARCH AT SRI INTERNATIONAL

MARTIN A. FISCHLER and ROBERT C. BOLLES *In* Science Applications International Corp., Proceedings: Image Understanding Workshop, Volume 1 p 53-61 Apr. 1988

(Contract MDA903-86-C-0084; DACA76-85-C-0004)

Avail: NTIS HC A22/MF A01 CSCL 09/2

The Image Understanding research program is a broad effort spanning the entire range of machine vision research. The progress in two programs is described: the first is concerned with modeling the earth's surface from aerial photographs; the second is concerned with visual interpretation for land navigation. In particular, the following are described: progress in the design of a core knowledge structure; representing, recognizing, and rendering complex natural and man-made objects; recognizing and modeling terrain features and man-made objects in image sequences; interactive techniques for scene modeling and scene generation; automated detection and delineation of cultural objects in aerial imagery; and automated terrain modeling from aerial imagery.

Author

N89-23101# Carnegie-Mellon Univ., Pittsburgh, PA. Digital Mapping Lab.

COOPERATIVE METHODS FOR ROAD TRACKING IN AERIAL IMAGERY

DAVID M. MCKEOWN, JR. and JERRY L. DENLINGER *In* Science Applications International Corp., Proceedings: Image Understanding Workshop, Volume 1 p 327-341 Apr. 1988

(Contract DACA72-84-C-0002; F33615-84-K-1520; DARPA ORDER 4976)

Avail: NTIS HC A22/MF A01 CSCL 08/2

Research in digital mapping and image understanding in the area of automated feature extraction from aerial imagery is described. A system for road tracking, (ARF) A Road Follower that uses multiple cooperative methods for extracting information about road location and structure from complex aerial imagery is discussed. This system is a multi-level architecture for image analysis that allows for cooperation among low-level processes and aggregation of information by high-level analysis components. Two low-level methods were implemented: road surface texture correlation and road edge following. Each low level method works independently to establish a model of the center line of the road, its width, and other local properties. Intermediate-level processes monitor the state of the low-level feature extraction methods and make evaluations concerning the success of each method. They also extract various road properties such as width changes, surface material changes, and overpasses. As a result of these evaluations one tracking method may be suspended due to apparent failure and restarted from the model generated by other successful trackers. Finally a high-level module generates a symbolic description of the road in terms of various attributes of the road such as center line, road width, surface material, overpasses, and an indication of potential vehicles on the road. This description is available in both map and image coordinate systems, and can be used to generate a textual description of the road. Author

N89-23371# Horton (Forest W., Jr.), Washington, DC.

INFORMATION RESOURCES MANAGEMENT

FOREST W. HORTON, JR. *In* AGARD, The Organisation and Functions of Documentation and Information Centres in Defence and Aerospace Environments 5 p Mar. 1989

Avail: NTIS HC A06/MF A01

The transfer of scientific and technical information between and among nations poses increasing challenges because of: larger and larger volumes of data exchanged; the increasing variety of information interchange media; larger and larger numbers of intermediaries and end-users all along the information transfer chain; and increasing incompatibility of bibliographic and telecommunications formatting conventions. The emerging field of Information Resources Management (IRM) offers promise in helping to cope with these serious information exchanges. In particular,

experiments in the U.S. Federal Government with a technique called information mapping, helps information managers identify, describe, inventory/survey, and control their total data, document, and literature flows and holdings, whether automated or manual, more completely. This approach of IRM, and the technique of information mapping, in several organizational contexts - one private (an Australian mineral and mining company), the other public (the U.S. Department of State) are introduced. Author

N89-23946# Institut fuer Angewandte Geodäsie, Frankfurt am Main (Germany, F.R.).

**AUTOMATIC DIGITIZING OF CADASTRAL MAPS
[AUTOMATISCHE DIGITALISIERUNG VON
LIEGENSCHAFTSKARTEN]**

ANDREAS ILLERT *In its Reports on Cartography and Geodesy. Series 1, Number 101 p 37-45 1988 In GERMAN; ENGLISH summary*

Avail: NTIS HC A07/MF A01

Developments in automatic digitizing for cadastral mapping are reviewed. The original map sheet is digitized by a raster-scan device. Data processing continues using the raster-to-vector conversion computer program RAVEL which transforms the raster image into a set of vector features in chains-and-nodes structure. From these data, texts and symbols are extracted using methods of numerical pattern recognition. The whole image is classified by structural techniques. ESA

N89-23947# Institut fuer Angewandte Geodäsie, Frankfurt am Main (Germany, F.R.).

**ARC-INFO: A GEOGRAPHIC INFORMATION SYSTEM
[ARC-INFO: EIN GEOGRAPHISCHES INFORMATIONSSYSTEM]**

HARTWIG JUNIUS *In its Reports on Cartography and Geodesy. Series 1, Number 101 p 47-59 1988 In GERMAN; ENGLISH summary*

Avail: NTIS HC A07/MF A01

The ARC-INFO software package for the establishment of areal information systems is presented. The package contains modules for collecting and managing graphic data, as well as analytic functions and processes for the production of thematic maps. The basic data model can be considered as geo-relational. Dot, line, or areal planimetric reference systems can be selected for application within the system. Specialized data are allocated as attributes to these reference systems in the relational data base INFO. The analytic functions include the various intersection functions which are the outstanding characteristic of this system and which complement the data base evaluation functions. The areas of application are indicated in three examples. ESA

N89-23948# Institut fuer Angewandte Geodäsie, Frankfurt am Main (Germany, F.R.).

**CARTOGRAPHIC SIGNATURES IN PHOCUS
[KARTOGRAPHISCHE SIGNATUREN IN PHOCUS]**

WOLFGANG KRESSE *In its Reports on Cartography and Geodesy. Series 1, Number 101 p 61-67 1988 In GERMAN; ENGLISH summary*

Avail: NTIS HC A07/MF A01

The universal Zeiss photogrammetric-cartographic system PHOCUS is presented. The most important characteristics of the PHOCUS graphics: independence of object geometries stored in the data base and a high level of independency from equipment are described. The usual map specifications can be generated with PHOCUS cartographic signatures. ESA

N89-23949# Institut fuer Angewandte Geodäsie, Frankfurt am Main (Germany, F.R.).

**DIGITIZING OF DRAWINGS AND CADASTRAL MAPS USING A
SCANNER SYSTEM [DIGITALISIERUNG VON ZEICHNUNGEN
UND BESTANDSPLAENEN MIT SCANNERSYSTEM]**

JUERGEN KUNSEMUELLER *In its Reports on Cartography and Geodesy. Series 1, Number 101 p 69-73 1988 In GERMAN; ENGLISH summary*

Avail: NTIS HC A07/MF A01

The ANA Tech system for computer assisted vectorization as

a preliminary stage to CAD map design is presented. The system provides a bridge between the manual drawing and the CAD system. The digitizing of existing drawings is automated and hence substantially simplified. The ANA Tech system uses the high-resolution Eagle scanner. The excellent hard and software technology makes the system cost effective. The system has a broad application domain. ESA

N89-23950# Institut fuer Angewandte Geodäsie, Frankfurt am Main (Germany, F.R.).

GEOCODED DATA SETS OF IMAGING SATELLITES

[GEOCODIERTE DATENSAETZE ABBILDENDER SATELLITEN]

HANS-JOACHIM LOTZ-IWEN and GUNTER SCHREIER *In its Reports on Cartography and Geodesy. Series 1, Number 101 p 75-81 1988 In GERMAN; ENGLISH summary*

Avail: NTIS HC A07/MF A01

The geocoded presentation of data sets of imaging satellites is discussed. Geocoded data sets of imaging satellites are high precision images of thematic information of the Earth surface using cartographic projections. Digital data of the remote sensing system LANDSAT TM is transformed into a cartographic standard projection using digital image processing methods. The data of the synthetic aperture radar sensor are planned to be available in geocoded presentation in the framework of the European ERS-1 remote sensing satellite. ESA

N89-23951# Institut fuer Angewandte Geodäsie, Frankfurt am Main (Germany, F.R.).

**COMPUTER ASSISTED LAYOUT OF GRAPHIC SETTLEMENT
REPRESENTATIONS [RECHNERGESTUETZTE GESTALTUNG
ANSCHAULICHER SIEDLUNGSDARSTELLUNGEN]**

PETER MESENBURG *In its Reports on Cartography and Geodesy. Series 1, Number 101 p 83-90 1988 In GERMAN; ENGLISH summary*

Avail: NTIS HC A07/MF A01

Methods of computer assisted layout of plane representations of areal facts were investigated. Due to the many possibilities of varying representations according to a particular problem, central perspective projection was chosen as the definitive representation method. Aspects of representation geometry and the program concept are described and explained using a concrete example of graphic settlement representation. ESA

N89-23952# Institut fuer Angewandte Geodäsie, Frankfurt am Main (Germany, F.R.).

**TOOLS FOR THE COMPUTER ASSISTED GENERALIZATION
OF SETTLEMENTS FOR THE CONSTRUCTION OF DIGITAL
LANDSCAPE MODELS [BAUSTEINE ZUR
AUTOMATIONSGESTUETZTEN GENERALISIERUNG VON
SIEDLUNGEN FUEER DIE EINRICHTUNG DIGITALER
LANDSCHAFTSMODELLE]**

UWE MEYER *In its Reports on Cartography and Geodesy. Series 1, Number 101 p 91-100 1988 In GERMAN; ENGLISH summary*

Avail: NTIS HC A07/MF A01

The computer assisted generalization of buildings for the construction of digital landscape models (DLM) in the framework of a cartographic information system is discussed. Tools for the computer assisted generalization as well as a method for typifying buildings are presented. Using a building class catalog, all objects are classified by a template-matching procedure and associated to the following DLM. ESA

N89-23953# Institut fuer Angewandte Geodäsie, Frankfurt am Main (Germany, F.R.).

**COMPUTER ASSISTED GENERALIZATION OF TRANSPORT
LINE REPRESENTATIONS [AUTOMATIONSGESTUETZTE
GENERALISIERUNG VON
VERKEHRSWEGEDARSTELLUNGEN]**

BERND M. POWITZ *In its Reports on Cartography and Geodesy. Series 1, Number 101 p 101-110 1988 In GERMAN; ENGLISH summary*

Avail: NTIS HC A07/MF A01

Program modules and algorithms for the automatic generalization and subsequent batch revision of commercial and transport line representations are being developed. The respective middle axes of the transport network are stored as digital object information. These characteristic series of dots, which are independent of scale, form the basis for automated signature deviation. The deviation of double-line transport axes can lead to undesirable line intersections and signature overlapping, in particular at junctions and crossings. The vectorial transport line representations already available are screened and subsequently revised automatically using local and dot-related screening operations. The corrected data are then transformed back into vectorial coordinates, whereby the transport lines are presented at the required scale. The program system supplies a generalized picture of the transport network which requires only minimal manual revision for graphic output. ESA

N89-23954# Institut fuer Angewandte Geodaesie, Frankfurt am Main (Germany, F.R.).

HYBRID CARTOGRAPHIC DATA PROCESSING IN A GEOGRAPHIC INFORMATION SYSTEM [HYBRIDE KARTOGRAPHISCHE DATENVERARBEITUNG IN EINEM LANDESINFORMATIONSSYSTEM]

BERND SONNE *In its Reports on Cartography and Geodesy. Series 1, Number 101 p 111-120 1988 In GERMAN; ENGLISH summary*

Avail: NTIS HC A07/MF A01

Aspects of hybrid graphic information systems are outlined. Hybrid data processing, i.e., the processing and management of vector data, images and their corresponding attributes in a common system, is increasingly important in the field of cartography. Components of the hardware and software configuration which describe the concept of a hybrid information system are presented. ESA

N89-23955# Institut fuer Angewandte Geodaesie, Frankfurt am Main (Germany, F.R.).

AUTOMATIC EXTRACTION OF AREAS FROM OVERLAYS OF THE SERIES DGK 5 (BO) [AUTOMATISCHE EXTRAKTION VON FLAECHEEN AUS DECKFOLIEN DER DGK 5 (BO)]

JUN YANG *In its Reports on Cartography and Geodesy. Series 1, Number 101 p 121-132 1988 In GERMAN; ENGLISH summary*

Avail: NTIS HC A07/MF A01

The automatic digitizing of ground map overlays of the series DGK 5 was investigated. The maps are digitized using a scanner, and the data are then converted into vector format. Dotted boundary lines of areas of utilization are recognized by classification, followed by automatic extraction of the areas indicated by the boundary lines. Recognition of texts, figures, and symbols, necessary to describe the types of utilization, is achieved using numerical and non-numerical classification methods. ESA

N89-23957# Research Inst. of National Defence, Linköping (Sweden). Dept. of Information Technology.

SHORTEST PATHS IN A DIGITIZED MAP USING A TILE-BASED DATA STRUCTURE

PETER HOLMES and ERLAND JUNGERT Oct. 1988 14 p Presented at the 3rd International Conference on Engineering Graphics and Descriptive Geometry, Vienna, 1988 (PB89-143432; FOA-B-30129-3.4; ISSN-0281-0263) Avail: NTIS HC A03/MF A01 CSCL 08/2

The problem addressed here is that of finding the shortest paths between two points within a digitized map. The map contains obstacles which may not be traversed. For this reason, the problem statement is analogous to that of finding shortest paths within a simple polygon containing holes. The approach described herein consists of both heuristic and algorithmic aspects. The heuristic component includes an inference engine for performing spatial reasoning, which operates in tandem with A (*) graph search. The output of the heuristic component is a plan which guides the algorithmic components through final processing states. As a

methodology for system structure, this organization of components forms a powerful framework for exploring various problems encountered in geometrical/spatial analysis. Author

N89-23958# Technische Hogeschool, Delft (Netherlands). Dept. of Geodesy.

ON THE CONNECTION OF GEODETIC POINTFIELDS IN RETRIG

A. J. M. KOSTERS Feb. 1988 109 p (PB89-146112; REPT-88-1) Avail: NTIS HC A06/MF A01 CSCL 08/5

A general view on connection problems in geodesy is presented with worked out practical examples from the Readjustment of the European Triangulation (RETrig). The connection of point fields can be defined as combining different coordinate sets, with limited overlap, which were determined by different point positioning methods and/or with respect to a different datum. Examples of this are numerous in practical geodesy. For the thesis, two types of connection problems related to RETrig are important. The two are: combining two neighboring RETrig-blocks, using their common points; combining satellite derived coordinates (viz. Doppler, SLR, VLBI and GPS) with terrestrial ellipsoidal coordinates. Special attention is paid to the use of 2- and 3-dimensional statistical tests on station coordinates and to the use of substitute covariance matrices for coordinates. Author

N89-23959# Lawrence Livermore National Lab., CA. USE OF THE 1:2,000,000 DIGITAL LINE GRAPH DATA IN EMERGENCY RESPONSE

HOYT WALKER Jan. 1989 13 p Presented at the ASPRS/ACSM Auto-Carto 9th Annual Convention, Baltimore, MD, 2-7 Apr. 1989

(Contract W-7405-ENG-48)

(DE89-006730; UCRL-99435; CONF-8904117-1) Avail: NTIS HC A03/MF A01

Environmental emergencies often have effects that are distributed over the earth's surface. As a result, maps are usually the most effective way to portray the impact of an emergency. The Atmospheric Release Advisory Capability (ARAC) at Lawrence Livermore National Laboratory is an emergency response organization that utilizes computer-assisted cartography. ARAC provides real-time assessments of the consequences of atmospheric releases of radioactive material. The products of this service are isopleths of the material concentration plotted over a base map of geographic features. Because ARAC's commitments encompass the entire United States, the ability to produce base maps anywhere in the United States is very important. At present ARAC is using data derived from the United States Geological Survey's 1:2,000,000 Digital Line Graph (DLG) database to meet its small-scale mapping needs. The DLG data set contains much of the information needed to serve in this emergency response application. However, certain enhancements are required to produce the necessary base maps. To create a data set suitable for ARAC, several preprocessing steps are needed. These include transforming the coordinate system, extracting relevant features as individual entities, correcting coding errors, and matching the edges along adjacent sectional files. DOE

N89-23960# Helsinki Univ. of Technology, Espoo (Finland). Instrument Lab.

DETERMINATION OF AREAL SNOW WATER EQUIVALENT USING SATELLITE IMAGES AND GAMMA RAY SPECTROMETRY Ph.D. Thesis

RISTO KUITTINEN 1988 143 p Sponsored by the Academy of Finland; Imatran Voiman Saatio, Finland; and Maa-ja Vestekniikan Tuki R.Y., Finland (CI-91; ISBN-951-666-275-7; ISSN-0355-2705; ETN-89-94220) Avail: NTIS HC A07/MF A01

A method for near real time estimation of the areal snow water equivalent in the snow melt period is studied. The method involves direct estimation of the areal snow water equivalent and the use of satellite images, gamma ray spectrometry, and field

measurements in estimating snow water equivalent. The method also involves estimation of snow melt by satellite images and field measurements. The areal distribution of the snow and the factors affecting it during the snow melt period are studied. A method for estimating the snow water equivalent on the basis of the area of bare spots on the ground interpreted from satellite images is introduced. The errors in estimating the snow water equivalent are between 20 and 45 mm for point estimates. The accuracy of gamma ray spectrometry and the factors affecting it in snow water equivalent measurements are studied. On the basis of these measurements, the representativeness of point snow water equivalent estimates is evaluated. A snow melt equation based on the degree-days and global radiation is also studied. Daily areal snow water equivalents are estimated for a river basin and the results are compared with measured stream flows. The errors in daily areal snow water equivalents were between 15 and 35 mm. ESA

N89-23962# Naval Civil Engineering Lab., Port Hueneme, CA. Utilities, Process and Geographic Systems Div.
GEOBOTANICAL REMOTE SENSING FOR DETERMINATION OF AGGREGATE SOURCE MATERIAL Final Report, Jul. 1986 - Sep. 1988

TIMOTHY MINOR, DAVID MOUAT, and JEFF MYERS (National Aeronautics and Space Administration. Ames Research Center, Moffett Field, CA.) Dec. 1988 23 p
 (AD-A205943; NCEL-TN-1792) Avail: NTIS HC A03/MF A01 CSCL 08/2

Aggregate source material suitable for facility and roadbed construction is often a very limited and highly valuable resource. The location of suitable source material is crucial to construction operations once facility requirements are established. The application of airborne and spaceborne remote sensing to terrain information requirements has proved attractive because of the rapid processing time and extensive spatial coverage associated with remotely gathered imagery. Source material identification may be improved by the remote sensing of vegetation associated with the material, particularly in areas of high vegetative cover. A research study employing remote sensing techniques was initiated to determine if vegetation could be used to discriminate parent materials for suitability as aggregate source material. Two test sites representing potential alluvial and residual source areas were selected in a semiarid region of Central California. Methods developed for the study included field observations of vegetation characteristics associated with the two parent material types along with the analysis of Thematic Mapper Simulator data flown over the test sites. The most useful images were those composites that included bands from two of the techniques (i.e., a Perpendicular Vegetation Index (PVI) band combined with principal components bands). GRA

N89-23963 Deutsche Geodaetische Kommission, Munich (Germany, F.R.).

ANALYSIS AND OPTIMIZATION OF GEODETIC NETWORKS BY SPECTRAL CRITERIA AND MECHANICAL ANALOGIES Thesis - Karlsruhe Univ. [ANALYSE UND OPTIMIERUNG GEODAETISCHER NETZE NACH SPEKTRALEN KRITERIEN UND MECHANISCHE ANALOGIEN]

REINER JAEGER 1988 136 p In GERMAN; ENGLISH summary

(SER-C-342; ISBN-3-7696-9390-6; ISSN-0065-5325; ETN-89-93998) Avail: Fachinformationszentrum Karlsruhe, 7514 Eggenheim-Leopoldshafen 2, Fed. Republic of Germany

The analysis and optimization of geodetic networks with mathematical models describable as eigenvalue problems connected with the variance-covariance matrix of network coordinates is studied. The eigenvalues and eigenvectors serve as spectral criteria for network analysis and as spectral target functions for network optimization respectively. The analysis is closely linked to the kinetics, especially to the eigen-vibrations of elastic mechanical structures. Proceeding from the elastic continuum, the complete foundation of analogies between elastomechanics and geodetic network-compensation by least

squares can be carried out in the step of its finite element discretization, being based fundamentally on equivalent principles of variations. Optimization leads to solving different associated inverse eigenvalue problems with respect to prescribed target-spectra. ESA

N89-23964# Technische Univ., Delft (Netherlands). Faculty of Geodesy.

THE SEARCH FOR EDGES IN REMOTE SENSING IMAGES USING A DIGITAL POLYGONAL MAP Thesis [HET SOEKEN NAAR RANDEN IN EEN DIGITAAL REMOTE SENSING BEELD MET BEHULP VAN EEN DIGITALE POLYGOON-KAART]

RUUD G. VERWAAL Aug. 1988 107 p In DUTCH; ENGLISH summary
 (ETN-89-94146) Avail: NTIS HC A06/MF A01

Edge detection in digital remote sensing images using an approximate position external information from a digital polygonal map was investigated. The map is transformed in the coordinate system of the digital images, and profiles perpendicular to the polygons are extracted in which the search for edges is performed. The global or local maximum value yields a selection criterion for the magnitude in edge detection. A threshold magnitude is also used. Aerial scanner images are used, and a polygonal map is digitized using aerial pictures. The study shows that the magnitude of the gray value is a primary parameter in edge detection. Texture affects a proper evaluation of line structures. ESA

N89-23965# Technische Univ., Delft (Netherlands). Werkenheid der Fotogrammetrie en Remote Sensing.

INVESTIGATION OF SEVERAL METHODS FOR THE DETECTION OF OUTSTANDING POINTS IN A DIGITAL IMAGE Thesis [HET ONDERZOEKEN VAN VERSCHILLENDE METHODEN VOOR HET OPSPOREN VAN MARKANTE PUNTEN IN EEN DIGITAAL BEELD]

GEERT VANDERMOLLEN Nov. 1988 79 p In DUTCH; ENGLISH summary
 (ETN-89-94148) Avail: NTIS HC A05/MF A01

Methods for the detection of outstanding points in a digital image were investigated, and the point detectors were compared under different circumstances. The investigated point detectors are the Moravec, the Dreschler, and the Foerstner operator; the last one can be combined with the Sobel, the Roberts, or the Prewitt gradient. Operation, reliability, and precision of these five point detectors were determined using a synthetic image in which the points to be detected are exactly known, and which were distorted by several types of noise. Without noise, no large differences in the precision of the detectors are found; the Dreschler operator is the most reliable and the fastest detector. With noise, it is shown that the results depend on the type of noise. The operation of the point detectors depends on the type of smoothing filter. The Foerstner operator gives the best results in many cases, especially in combination with the Sobel or Prewitt gradient. ESA

N89-23967# Technische Univ., Delft (Netherlands). Faculty of Geodesy.

VECTORIZATION OF GRID LINES Thesis [VECTORISEREN VAN RASTERLIJNEN]

P. C. F. LIPS Oct. 1988 77 p In DUTCH; ENGLISH summary
 (ETN-89-94150) Avail: NTIS HC A05/MF A01

The vectorization of grid lines, extracted from gray value images, was investigated with a view to geographic information systems. The operations of edge detection and line following, necessary to extract the grid line structures from digital images are discussed. The artificially created test image on which the final vectorization algorithm is tested, is described. Polygonal approximation methods are presented and compared; nonsequential methods give better results. The algorithm was tested on a synthetic image, i.e., on ideal test data, and submitted to precision analyses. The results of the tests are very positive. ESA

07 DATA PROCESSING AND DISTRIBUTION SYSTEMS

N89-23968# Technische Univ., Delft (Netherlands). Faculty of Geodesy.

DESIGN OF A METHODOLOGY FOR THE DETECTION OF ERRORS IN TERRESTRIAL NETWORKS Thesis [ONTWERP VAN EEN METHODIEK VOOR FOUTDETECTIE IN TERRESTRIE NETWERKEN]

L. V. KOLLAARD Aug. 1988 97 p In DUTCH; ENGLISH summary

(ETN-89-94151) Avail: NTIS HC A05/MF A01

A methodology for the detection of errors in geodetic observations in two-dimensional control networks was developed. Parameter estimation and error detection are outlined. The two stages during the data processing, the measuring stage and the administrative stage, are described. The proposed methodology can easily be implemented on a microcomputer. Some limitations of the methodology are linked with a possible lack of information, namely the singularity and the separability problem. The methodology reduces data production costs, but requires better qualified personnel. ESA

N89-23971# Beleidscommissie Remote Sensing, Delft (Netherlands).

THERMAL ANALYSIS FOR THE MONITORING AND PREDICTION OF FLOOD DYNAMICS IN WETLANDS Final Report [THERMISCHE ANALYSE VOOR DE MONITORING EN VOORSPELLING VAN DE OVERSTROMINGSDYNAMIEK VAN WETLANDS]

J. L. FISELIER and A. ROSEMA (Environmental Analysis and Remote Sensing, Delft, Netherlands) Oct. 1988 55 p In DUTCH; ENGLISH summary (Contract BCRS-PROJ.-OP-3.3)

(BCRS-88-10B; ETN-89-94290) Avail: NTIS HC A04/MF A01

Meteosat-based thermal inertia analysis was used for the mapping of flood dynamics in the Niger inner delta in Mali and the Logone floodplain in northern Cameroon. The remote sensing analysis is based on the heat transfer properties of the surface. Thermal inertia analysis generates a map that shows a more distinct flooding pattern than the visual picture. The maps were used to predict the hydrological impact of planned hydroagricultural schemes. Different weather conditions, especially wind speed, within the area of the image can lead to differences in thermal inertia and false interpretation. Thermal inertia analysis and interpretation are improved by continuous monitoring. Thermal inertia mapping appears a promising tool for monitoring flood dynamics of the larger Sahelian floodplains. ESA

N89-23992# Naval Postgraduate School, Monterey, CA.

THERMAL IMAGES OF SKY AND SEA-SURFACE BACKGROUND INFRARED RADIATION M.S. Thesis

PANAGIOTIS PSIHOGIOS Dec. 1988 157 p

(AD-A205819) Avail: NTIS HC A08/MF A01 CSCL 17/5

Thermal images of the sky and the sea surface background radiance were analyzed using the AGA Thermovision 780 system. Calculated sky radiance was compared with that predicted by the computer code LOWTRAN 6. The Schwartz-Hon computer model for the emissivity of the sea surface was validated using the results from AGA measurements and LOWTRAN 6. The factors which affect the radiance measurements were determined, and the degree of influence they exert was estimated. The radiance emitted from an overcast sky was found to be higher than that emitted from a clear sky. The wind speed reduces significantly the infrared sky radiance. Emissivity of the sea surface depends upon the wave roughness, remaining almost constant with the viewing angle. The whole result showed that LOWTRAN 6 provides a good prediction of the atmospheric radiance with deviation from measurement generally within 10 percent with cases to 15 percent for the elevation angle range from 0 to 19 degrees and that the Schwartz-Hon model agrees well with observation showing deviation varying up to 14 percent in the elevation angle range from 5 to 10 degrees. GRA

N89-24013# GKSS-Forschungszentrum Geesthacht (Germany, F.R.). Inst. fuer Physik.

OPTICAL PROPERTIES OF OCEANIC SUSPENDED MATTER AND THEIR INTERPRETATION FOR REMOTE SENSING OF PHYTOPLANKTON Thesis - Technische Univ., Hamburg [DIE OPTISCHEN EIGENSCHAFTEN DER OZEANISCHEN SCHWEBSTOFFE UND IHRE BEDEUTUNG FÜR DIE FERNERKUNDUNG VON PHYTOPLANKTON]

U. KRONFELD 1988 161 p In GERMAN; ENGLISH summary (GKSS-88/E/40; ISSN-0344-9629; ETN-89-94410) Avail: NTIS HC A08/MF A01

Optical properties of suspended matter and dissolved substances in sea water are studied by remote sensing for the determination of organic and inorganic substances concentration. Model computation is achieved by recording optical absorption of chlorophyll content algae or phytoplankton and of mineral substances such as yellow suspensions. The upward directed radiation spectra are determined by 11 stations of the German MARSEN program. Scattering functions and extinction coefficients are calculated for different algae species from particle size distributions and optical reflection indices. ESA

N89-24686*# California Univ., Santa Barbara. Dept. of Geography.

IMPROVEMENT AND EXTENSION OF A RADAR FOREST BACKSCATTERING MODEL Semiannual Report

DAVID S. SIMONETT and YONG WANG 10 May 1989 18 p (Contract NAG5-1010)

(NASA-CR-184975; NAS 1.26:184975) Avail: NTIS HC A03/MF A01 CSCL 02/6

Radar modeling of mangal forest stands, in the Sundarbans area of Southern Bangladesh, was developed. The modeling employs radar system parameters with forest data on tree height, spacing, biomass, species combinations, and water (including slightly conductive water), content both in leaves and trunks of the mangal. For Sundri and Gewa tropical mangal forests, six model components are proposed, which are required to explain the contributions of various forest species combinations in the attenuation and scattering of mangal vegetated nonflooded or flooded surfaces. Statistical data of simulated images were compared with those of SIR-B images both to refine the modeling procedures and to appropriately characterize the model output. The possibility of delineation of flooded or nonflooded boundaries is discussed. Author

N89-24690# Laboratoire de Meteorologie Dynamique du CNRS, Palaiseau (France).

ON THE FUTURE DEVELOPMENT AND MANAGEMENT OF SPECTROSCOPIC DATABASE FOR RADIATIVE TRANSFER FROM THE ISSUES OF RECENT RELATED WORKSHOPS

N. HUSSON and A. CHEDIN 1988 3 p Presented at the International Radiation Symposium, Lille, France, 18-24 Aug. 1988 (ETN-89-94530) Avail: NTIS HC A02/MF A01

Computer accessible compilations of spectroscopic line parameters, in the infrared to microwave spectral region, are made available in data bases, for molecules of interest in remote sensing or climatic studies. The necessity to create these data bases is summarized as an introduction to future development and management of spectroscopic data bases. ESA

N89-24693# European Space Agency. European Space Research and Technology Center, ESTEC, Noordwijk (Netherlands). Earth Observation Preparatory Program.

ESA'S PLANNED ACTIVITIES IN THE FIELD OF IMAGING SPECTROMETRY FOR EARTH OBSERVATION

M. RAST In *its* Imaging Spectrometry for Land Applications p 7-10 Nov. 1988

Avail: NTIS HC A04/MF A01; ESA Publications Div., ESTEC, Noordwijk, Netherlands, 10 dollars or 25 Dutch guilders

Imaging requirements oriented towards a high resolution imaging spectrometer dedicated to land applications are assessed. A set of recommendations for future action is included. ESA

N89-24696# Natural Environmental Research Council, London (England). British National Space Centre.

THE ACTIVITIES OF THE BRITISH NATIONAL SPACE CENTRE (BNSC) IN THE FIELD OF IMAGING SPECTROMETRY
S. A. BRIGGS, S. J. MACKIN, T. J. MUNDAY, N. J. DRAKE, E. J. MILTON (Southampton Univ., England), and E. M. ROLLIN /in ESA, Imaging Spectrometry for Land Applications p 27-33 Nov. 1988 Original contains color illustrations

Avail: NTIS HC A04/MF A01; ESA Publications Div., ESTEC, Noordwijk, Netherlands, 10 dollars or 25 Dutch guilders

Results obtained with the Airborne Imaging Spectrometer and the GER II scanner in geological applications are discussed. Ground segment activities in terms of data processing and information extraction methods are described and the key role of field spectrometry in the understanding of remotely sensed data is discussed. ESA

N89-24699# Centre National d'Etudes Spatiales, Toulouse (France).

ACTIVITIES OF CNES IN THE FIELD OF IMAGING SPECTROMETRY

P. VERMANDE, D. ALCAYDE, and M. COMBES-DESPA (Observatoire de Paris-Meudon, France) /in ESA, Imaging Spectrometry for Land Applications p 47-49 Nov. 1988

Avail: NTIS HC A04/MF A01; ESA Publications Div., ESTEC, Noordwijk, Netherlands, 10 dollars or 25 Dutch guilders

The CNES Institute's research activities in the field of imaging spectrometry are summarized. The developments include operational field spectroradiometers, transportable imaging spectrometer (TIS), velocity sensors to control image drift in the focal plane (VS), signal compression, balloon flight tests of TIS and VS, and airborne imagery. ESA

N89-24700# Deutsche Forschungs- und Versuchsanstalt fuer Luft- und Raumfahrt, Oberpfaffenhofen (West Germany).

THE EARSLE IMAGING SPECTROMETRY WORKING GROUP

F. LEHMANN /in ESA, Imaging Spectrometry for Land Applications p 51-54 Nov. 1988 Original contains color illustrations

Avail: NTIS HC A04/MF A01; ESA Publications Div., ESTEC, Noordwijk, Netherlands, 10 dollars or 25 Dutch guilders

The activities of an interdisciplinary working group for Earth sciences spectrometry are discussed. The main topic is the development of an infrastructure for the intercommunication of different European laboratories, working in laboratory and field spectroscopy, development, testing and application of airborne high spectral resolution optical sensors, and the definition of future space remote sensing instruments. ESA

N89-24756*# Universities Space Research Association, Boulder, CO. Program Office.

A VISITING SCIENTIST PROGRAM IN ATMOSPHERIC SCIENCES FOR THE GODDARD SPACE FLIGHT CENTER

Final Report, Apr. 1984 - Sep. 1988

M. H. DAVIS Columbia, MD Jan. 1989 36 p

(Contract NAS5-28135)

(NASA-CR-183421; NAS 1.26:183421) Avail: NTIS HC A03/MF A01 CSCL 04/1

A visiting scientist program was conducted in the atmospheric sciences and related areas at the Goddard Laboratory for Atmospheres. Research was performed in mathematical analysis as applied to computer modeling of the atmospheres; development of atmospheric modeling programs; analysis of remotely sensed atmospheric, surface, and oceanic data and its incorporation into atmospheric models; development of advanced remote sensing instrumentation; and related research areas. The specific research efforts are detailed by tasks. B.G.

N89-24784*# Scripps Institution of Oceanography, La Jolla, CA. **BIOOPTICAL VARIABILITY IN THE GREENLAND SEA OBSERVED WITH THE MULTISPECTRAL AIRBORNE RADIOMETER SYSTEM (MARS) Final Technical Report, 21 May - 2 Jun. 1987**

JAMES L. MUELLER and CHARLES C. TREES 31 Mar. 1989

108 p

(Contract NAG5-1022)

(NASA-CR-184856; NAS 1.26:184856; CHORS-TM-89-001)

Avail: NTIS HC A06/MF A01 CSCL 08/6

A site-specific ocean color remote sensing algorithm was developed and used to convert Multispectral Airborne Radiometer System (MARS) spectral radiance measurements to chlorophyll-a concentration profiles along aircraft tracklines in the Greenland Sea. The analysis is described and the results given in graphical or tabular form. Section 2 describes the salient characteristics and history of development of the MARS instrument. Section 3 describes the analyses of MARS flight segments over consolidated sea ice, resulting in a set of altitude dependent ratios used (over water) to estimate radiance reflected by the surface and atmosphere from total radiance measured. Section 4 presents optically weighted pigment concentrations calculated from profile data, and spectral reflectances measured in situ from the top meter of the water column; this data was analyzed to develop an algorithm relating chlorophyll-a concentrations to the ratio of radiance reflectances at 441 and 550 nm (with a selection of coefficients dependent upon whether significant gelvin presence is implied by a low ratio of reflectances at 410 and 550 nm). Section 5 describes the scaling adjustments which were derived to reconcile the MARS upwelled radiance ratios at 410:550 nm and 441:550 nm to in situ reflectance ratios measured simultaneously on the surface. Section 6 graphically presents the locations of MARS data tracklines and positions of the surface monitoring R/V. Section 7 presents stick-plots of MARS tracklines selected to illustrate two-dimensional spatial variability within the box covered by each day's flight. Section 8 presents curves of chlorophyll-a concentration profiles derived from MARS data along survey tracklines. Significant results are summarized in Section 1. A.D.

08

INSTRUMENTATION AND SENSORS

Includes data acquisition and camera systems and remote sensors.

A89-32835#

CALIBRATION COMPARISON FOR THE LANDSAT 4 AND 5 MULTISPECTRAL SCANNERS AND THEMATIC MAPPERS

JOHN C. PRICE (USDA, Beltsville Agricultural Research Center, MD) Applied Optics (ISSN 0003-6935), vol. 28, Feb. 1, 1989, p. 465-471. refs

On March 15, 1984, during the initial orbital corrections of Landsat 5, data were acquired virtually simultaneously by MSSs and TMs on Landsats 4 and 5. A formulation is developed for comparing the calibration of matched instruments (MSS4, MSS5 and TM4, TM5), and spectral interpolation is used to compare the calibration of the nearly equivalent shortwave channels of all four instruments. The MSS instruments are more closely matched in gain with a difference of 6-10 percent vs -2 to 14 percent for the TMs. Radiance comparisons show that the MSSs and TM4 agree reasonably well for a dark surface (water), while TM5 indicates generally lower radiance values in the shortwave channels.

Author

A89-32836#

SHORT- AND LONG-TERM MEMORY EFFECTS IN INTENSIFIED ARRAY DETECTORS - INFLUENCE ON AIRBORNE LASER FLUORESCENCE MEASUREMENTS

MICHAEL P. BRISTOW, CURTIS M. EDMONDS, DONALD H. BUNDY (EPA, Las Vegas, NV), and RUDOLPH M. TURNER (Nevada, University, Las Vegas) Applied Optics (ISSN 0003-6935), vol. 28, Feb. 1, 1989, p. 472-480. refs

Phosphorescence and thermoluminescence memory effects in the phosphors of image intensifiers are investigated, with

08 INSTRUMENTATION AND SENSORS

application to the performance improvement of intensified optical multichannel analyzers. Algorithms have been developed which can be used to remove these effects from airborne measurements of laser-induced fluorescence spectra of aquatic and terrestrial targets. The present method can be adapted to situations involving different gating routines, repetition rates, and diode group sizes.

R.R.

A89-32837

HYPERSPECTRAL INTERACTIONS - INVARIANCE AND SCALING

M. ANN PIECH (New York, State University, Buffalo) and KENNETH R. PIECH (Aspen Analytics, Inc., Buffalo, NY) Applied Optics (ISSN 0003-6935), vol. 28, Feb. 1, 1989, p. 481-489. Research supported by the U.S. Army, Aspen Analytics, Inc., Autometric, Inc., and USAF. refs

Invariance and scaling results were obtained for the scale space filtering of hyperspectral data. It is shown that a hyperspectral curve can be segmented into independent regions by scale space fingerprints, persistent inflection points that precisely locate major atmospheric features that define the regions. It is found that the scale of individual features is independent of the details of feature shape, and depends only on the area of the feature. The bifurcation behavior of the interacting features is described. R.R.

A89-32841

RADIATIVE TRANSFER CALCULATIONS FOR CHARACTERIZING OBSCURED SURFACES USING TIME-DEPENDENT BACKSCATTERED PULSES

T. DURACZ and N. J. MCCORMICK (Washington, University, Seattle) Applied Optics (ISSN 0003-6935), vol. 28, Feb. 1, 1989, p. 544-552. Research supported by the San Diego Supercomputer Center. refs

(Contract DAAL03-86-K-0118)

Numerical calculations for estimating the albedo of a surface and its distance behind an obscuring multiple-scattering atmosphere are performed for the idealized case of an instantaneous pulse uniformly illuminating a plane-geometry atmosphere of known properties. This inverse problem is complicated by the fact that the backscattered irradiance is broadened in time because of purely geometric effects arising from the geometry considered; the broadening increases with an increasing thickness of the obscuring medium and if the medium scatters in a more isotropic manner, such as with Rayleigh scattering. Isocline maps of different observables suggest that graphical inversion maps might be useful for some applications of this type. Author

A89-32848

THE PROGNOSIS OF WEATHER CHANGE LINES OVER THE OCEAN - THE ROLE OF A RECONNAISSANCE AIRCRAFT

B. F. RYAN, J. R. GARRATT, and W. L. PHYSICK (CSIRO, Div. of Atmospheric Research, Mordialloc, Australia) Australian Meteorological Magazine (ISSN 0004-9743), vol. 36, June 1988, p. 69-80. refs

Data collected during the Cold Fronts Research Program (Ryan et al., 1985) are used to study the role of a reconnaissance aircraft in identifying weather change lines over the ocean. It is shown that the mesoscale structure of a change line may be determined from measurements of wind speed, wind direction, and dry and wet bulb temperatures, at time intervals of 2 min or less and a speed of 300 km/h. Three cases are given, showing that most change lines correlate with satellite or radar pictures. Strategies for aircraft reconnaissance flights are proposed, based on meteorological situations that can be identified using simulations with mesoscale models. R.B.

A89-32850

A METEOROLOGICAL OVERVIEW OF THE PRE-AMEX AND AMEX PERIODS OVER THE AUSTRALIAN REGION

G. LOVE and G. GARDEN (Bureau of Meteorology, Darwin, Australia) Australian Meteorological Magazine (ISSN 0004-9743), vol. 36, June 1988, p. 91-100. refs

The tropospheric circulation patterns in the Australian region tropics are analyzed for the month prior to the Australian Monsoon Experiment (AMEX) Phase II (December 14, 1986-January 14, 1987) and the AMEX Phase II period (January 15-February 15, 1987). The analysis shows the rapid evolution from a transition regime to a monsoon regime between the two periods. Data showing the time and space scales of the variability of wind and pressure fields are presented and the major weather systems affecting the region are described. It is found that a high proportion of rainfall received during the AMEX Phase II was produced by mesoscale monsoon squall lines which were parallel to the low-level flow and propagated from the south to the north. R.B.

A89-33505

SATELLITE, AIRBORNE AND RADAR OBSERVATIONS OF AURORAL ARCS

HERBERT C. CARLSON, JR., EDWARD J. WEBER (USAF, Geophysics Laboratory, Hanscom AFB, MA), LARS P. BLOCK (Kungliga Tekniska Hogskolan, Stockholm, Sweden), and SUNANDA BASU (Emmanuel College, Boston, MA) (COSPAR and SCOSTEP, Plenary Meeting, 27th, Symposium on Multipoint Magnetospheric Measurement, 8th, Espoo, Finland, July 18-29, 1988) Advances in Space Research (ISSN 0273-1177), vol. 8, no. 9-10, 1988, p. 49-58. Research supported by DNA. refs (Contract F19628-86-K-0038; AF TASK 2310G9)

The use of a combination of satellite, airborne, and ground-based platforms for in situ and remote sensors to address problems in space physics is discussed. Findings associated with auroral arcs, polar cap F-region stable and sun-aligned arcs, theta auroras, and other auroral features are presented. Consideration is given to the airborne tracking of ionospheric boundaries and polar cap arc and auroral arc electrodynamics. K.K.

A89-33653

MULTISPECTRAL IMAGE PROCESSING AND ENHANCEMENT; PROCEEDINGS OF THE MEETING, ORLANDO, FL, APR. 6-8, 1988

MARSHALL R. WEATHERSBY, ED. (Nichols Research Corp., Ann Arbor, MI) Meeting sponsored by SPIE, Bellingham, WA, Society of Photo-Optical Instrumentation Engineers (SPIE Proceedings, Volume 933), 1988, 297 p. For individual items see A89-33654 to A89-33664, A89-33667, A89-33668. (SPIE-933)

Various papers on multispectral image processing and enhancement are presented. Individual topics addressed include: object detection in multispectral high-resolution images, unification of region and edge information for image segmentation, correlated background adaptive clutter suppression and normalization techniques, multispectral bistatic laser signature generation using monostatic data bases, algorithm for machine-recognizing a river mouth and measuring the sea line from Landsat images, new model for the geometric correction of multispectral scanner data, diffraction effects on IR-system performance, and background signature characterization and prediction in laser scattering phenomenology. Also considered are: a first principles modeling approach to computer-generated IR imagery, first principles deterministic simulation of IR and visible imagery, multispectral terrain background simulation techniques for use in airborne sensor evaluation, earth background scene generation in opaque IR bands, aircraft and cloud sky simulator, synthetic IR cloud image model, and simulating FLIR imaging characteristics in real time. C.D.

A89-33868*# National Aeronautics and Space Administration. John C. Stennis Space Center, Bay Saint Louis, MS.

MODELING SURFACE TEMPERATURE DISTRIBUTIONS IN FOREST LANDSCAPES

H. R. HOLBO and J. C. LUVALL (NASA, Stennis Space Center, Bay Saint Louis, MS) Remote Sensing of Environment (ISSN 0034-4257), vol. 27, Jan. 1989, p. 11-24. refs

A model of the frequency distributions of the spatial variability in surface temperature is presented. Surface temperature data are obtained from two daytime and two nighttime flights of the Thermal IR Multispectral Scanner (TIMS) over forest land in western

Oregon in August, 1985. The temperature values are corrected for atmospheric attenuation and thermal radiation emission with the LOWTRAN-6 algorithm. The temperature distributions were modeled with a two-parameter beta probability density distribution and the fit of the model was evaluated by comparison with the TIMS data set. Use of the model's parameters to identify and classify surface types shows good discrimination among various surfaces for the daytime images, with less distinct discrimination for the nighttime images. R.B.

A89-33869

C-BAND RADAR CROSS SECTION OF THE GUYANA RAIN FOREST - POSSIBLE USE AS A REFERENCE TARGET FOR SPACEBORNE RADARS

R. BERNARD and D. VIDAL-MADJAR (Centre de Recherches en Physique de l'Environnement Terrestre et Planetaire, Issy-les-Moulineaux, France) Remote Sensing of Environment (ISSN 0034-4257), vol. 27, Jan. 1989, p. 25-36. refs (Contract ESTEC-6347/85/NL/MD)

A89-33870

MUNSELL SOIL COLOR AND SOIL REFLECTANCE IN THE VISIBLE SPECTRAL BANDS OF LANDSAT MSS AND TM DATA

RICHARD ESCADAFAL (Office de la Recherche Scientifique et Technique d'Outre-Mer, Bondy, France), MICHEL-CLAUDE GIRARD, and DOMINIQUE COURAULT (Institut National de la Recherche Agronomique, Thiverval-Grignon, France) Remote Sensing of Environment (ISSN 0034-4257), vol. 27, Jan. 1989, p. 37-46. Research supported by CNRS. refs

Color is widely used for soil characterization in the field and for soil classification. Standardized soil color notation is usually achieved by comparison with Munsell color charts. These raw color data are generally not easily related to soil spectral properties. The spectral reflectance curves of 84 soil samples were measured with a spectrophotometer in the laboratory. For each sample, chromaticity coordinates were computed according to CIE standard methods and expressed in RGB (Red, Green, Blue) notation using colorimetric equations. RGB values appear to be strongly correlated with the soil reflectance measured in the corresponding spectral bands of Landsat sensors. RGB coordinates were also estimated from Munsell data using conversion tables. Despite their low precision, the estimated color coordinates are significantly correlated with the reflectance values in the Thematic Mapper visible bands. These results allow the interpretation of published data and further development of soil color remote sensing.

Author

A89-33871* Jet Propulsion Lab., California Inst. of Tech., Pasadena.

SURFACE REFLECTANCE FACTOR RETRIEVAL FROM THEMATIC MAPPER DATA

RONALD G. HOLM (California Institute of Technology, Jet Propulsion Laboratory, Pasadena; Arizona, University, Tucson), RAY D. JACKSON, BENFAN YUAN, M. SUSAN MORAN, PHILIP N. SLATER (Arizona, University, Tucson) et al. Remote Sensing of Environment (ISSN 0034-4257), vol. 27, Jan. 1989, p. 47-57. refs

(Contract NAGW-896)

Based on the absolute radiometric calibration of the TM and the use of a radiative transfer program for atmospheric correction, ground reflectances were retrieved for several fields of crops and bare soil in TM bands 1-4 for six TM scenes acquired over a 12-month period. These reflectances were compared to those measured using ground-based and low-altitude, aircraft-mounted radiometers. When, for four TM acquisitions, the comparison was made between areas that had been carefully selected for their high uniformity, the reflectance factors agreed to \pm or \pm 0.01 over the reflectance range 0.02-0.55. When the comparison was made for two of the above acquisitions and two others on different dates, for larger areas not carefully selected to be of uniform reflectance, the reflectance factors agreed to \pm or \pm 0.02 (1 sigma RMS), over same reflectance range. Author

A89-34002

THE POTENTIAL USE OF REMOTE SENSING TO SOLVE PROBLEMS OF PALEOTECTONIC PREDICTION, GEOLOGIC STRUCTURE, AND EXPLOITATION OF COAL DEPOSITS WITH REFERENCE TO THE MOSCOW-REGION COAL BASIN [VOZMOZHNOSTI ISPOL'ZOVANIYA AERO- I KOSMICHESKOI INFORMATSII DLIA RESHENIIA ZADACH PALEOTEKTONICHESKOGO PROGNOZA, GEOLOGICHESKOGO STROENIIA I EKSPLOATATSII UGOL'NYKH MESTOROZHDENII NA PRIMERE PODMOSKOVNOGO BASSEINA]

L. I. SOLOV'YEV, D. M. TROFIMOV, V. A. BOGOSLOVSKII, K. L. ODINTSOV, and V. K. KHMELEVSKII IN: Remote-sensing studies of present-day tectonic processes. Moscow, Izdatel'stvo Nauka, 1988, p. 5-11. In Russian.

A89-34010

THE USE OF A LINEAMENT-ANALYSIS INSTRUMENT FOR INVESTIGATIONS OF TECTONIC ZONALITY AND THE ELEMENTS OF CONTINENTAL-MARGIN GEODYNAMICS AS APPLIED TO WESTERN ARCTIC [PRIMENENIE APPARATA LINEAMENTNOGO ANALIZA DLIA IZUCHENIIA TEKTONICHESKOI ZONAL'NOSTI I ELEMENTOV GEODINAMIKI KONTINENTAL'NYKH OKRAIN /ZAPADNAIA ARKTIKA/]

B. V. SENIN IN: Remote-sensing studies of present-day tectonic processes. Moscow, Izdatel'stvo Nauka, 1988, p. 63-73. In Russian.

A89-34088

GRAVIMETRIC STUDIES AT SEA [GRAVIMETRICHESKIE ISSLEDOVANIYA NA MORE]

IU. D. BULANZHE, ED. and M. U. SAGITOV, ED. Moscow, Izdatel'stvo Nauka, 1988, 128 p. In Russian. No individual items are abstracted in this volume.

The theory and methods of marine gravimetric measurements are discussed together with the type of instruments used in these measurements and the results of some gravimetric studies. Particular attention is given to methods used to increase the accuracy of gravimetric observations on research vessels, the automation of information processing, the use of radio-navigation instruments and meteorological information in gravimetric studies, and methods for instrument standardization. Papers are presented on statistical models of the anomalous characteristics of the earth's gravity field, a microcomputer-assisted system for studying the dynamic parameters of a gravimeter, and experimental investigations of cross-coupling effects. Other papers are on combined marine gravimetric and seismic studies in Antarctica, the geodynamics of the transition zone in the region of the Sea of Japan, and geophysical investigations of the crust, lithosphere, and upper mantle in the Philippine Sea. I.S.

A89-34267#

GEOSAT ALTIMETER SEA-ICE MAPPING

JEFFREY D. HAWKINS and MATTHEW LYBANON (U.S. Navy, Naval Ocean Research and Development Activity, Bay Saint Louis, MS) IEEE Journal of Oceanic Engineering (ISSN 0364-9059), vol. 14, April 1989, p. 139-148. Research supported by the U.S. Navy. refs

The efforts to use GEOSAT data to refine an ice index that is applicable to widely varying ice conditions are detailed. The sea-ice mapping requirements, the present US Navy ice-index operational utilization, and ongoing and future work that promises to provide additional sea-ice measurement capabilities are discussed. Possibilities include discrimination among water, land, ice, combination water/ice, and water/land, as well as distinguishing various ice concentrations and possibly ice types. Coincident airborne passive microwave and synthetic-aperture-radar (SAR) data have been collected to test several methods which appear to be promising. I.E.

A89-34353

IMPULSE RADAR FOR IDENTIFICATION OF FEATURES IN SOILS

JOHN G. LYON, CHARLES A. MITCHELL (Ohio State University, Columbus), and TED M. ZOBECK (USDA, Soil Science Agricultural Research Service, Big Spring, TX) *Journal of Aerospace Engineering* (ISSN 0893-1321), vol. 1, Jan. 1989, p. 18-27. refs (Contract NOAA-NA-81AAD0095; NOAA-NA-84AAD00079)

In soils developed in loess over glacial till, the presence and depth to clay layers, or fragipans, and other features are identified with radar. Radar evaluation of depths to soil features compares well with the soil pit and core descriptions by traditional methods. Regressions of radar-derived, actual depths of soil features are used to calibrate radar measurements. The calibration approach is verified by evaluation of radar depths and actual depths of soil features in five cores taken on the same transect, away from the pits. Radar measurements of depths to features in soils have several practical applications. Author

A89-34362

USE OF AERIAL PHOTOGRAPHY TO INVENTORY AQUATIC VEGETATION

DONALD W. SCHLOESSER, CHARLES L. BROWN, and BRUCE A. MANNY (U.S. Fish and Wildlife Service, Ann Arbor, MI) *Journal of Aerospace Engineering* (ISSN 0893-1321), vol. 1, July 1988, p. 142-150. refs

The feasibility of low-altitude aerial photography's use to inventory submersed macrophytes in the connecting channels of the Great Lakes is presently demonstrated through the use of five test subjects as interpreters of color transparencies. The interpreters correctly determined the presence or absence of vegetation 80 percent of the time. Determination of the presence of macrophytes partly depended on relative abundances and water clarity; differences among individuals were, however, statistically significant and indicated the importance of careful screening for interpreter trainability. O.C.

A89-34772

DISTRIBUTION OF AURORAL ARCS DURING QUIET GEOMAGNETIC CONDITIONS

K. LASSEN and C. DANIELSEN (Dansk Meteorologisk Institut, Copenhagen, Denmark) *Journal of Geophysical Research* (ISSN 0148-0227), vol. 94, March 1, 1989, p. 2587-2594. refs

A89-34782

THE INTERPLANETARY MAGNETIC FIELD B(Y)-DEPENDENT FIELD-ALIGNED CURRENT IN THE DAYSIDE POLAR CAP UNDER QUIET CONDITIONS

M. YAMAUCHI (Alaska, University, Fairbanks; Kyoto University, Japan) and T. ARAKI (Kyoto University, Japan) *Journal of Geophysical Research* (ISSN 0148-0227), vol. 94, March 1, 1989, p. 2684-2690. refs (Contract NSF ATM-88-03133)

Magnetic data from the Magsat satellite are used to study the spatial distribution and temporal variation of the IMF B(y)-dependent cusp region field-aligned currents (FACs) during quiet periods. It is shown that the FACs are located at about 86-87 deg invariant latitude local noon. The current density of this FAC is found to be greater than 4 $\mu\text{A}/\text{sq m}$ for IMF B(y) = 6nT. The initial rise of the current is on a time scale of about 10 min and is followed by a gradual increase on a time scale of several hours to half a day. R.B.

A89-34876

DROP-SIZE DISTRIBUTIONS ASSOCIATED WITH INTENSE RAINFALL

PAUL T. WILLIS (NOAA, Atlantic Oceanographic and Meteorological Laboratory, Miami, FL) and PAUL TATTELMAN (USAF, Geophysics Laboratory, Hanscom AFB, MA) *Journal of Applied Meteorology* (ISSN 0894-8763), vol. 28, Jan. 1989, p. 3-15. refs

The probability of occurrence of extreme rainfall rates is reviewed. The drop-size distributions associated with a range of

high rainfall rates are examined using data from tropical storms and hurricanes. Mean drop-size distributions are presented for a range of high rainfall rates, as well as a Gamma-distribution fit to the entire set of normalized drop-size distributions. This fit forms the basis for a model drop-size distribution for intense rain. The fit of the model is compared with independent drop-camera measurements of high-rain-rate distributions from several geographic locations. The slope of exponential fits to the distributions are examined for constancy with rainfall rate, and are generally found to decrease with increasing rainfall rate. Author

A89-35687

THE KAP-350 AND KAP-100 SPACE CAMERAS FOR THE REMOTE SENSING OF EARTH RESOURCES [KOSMICHESKIE FOTOAPPARATY KAP-350 I KAP-100 DLIA IPRZ]

IU. K. BUKIN, V. K. EREMIN, and I. S. NENASHEV *Geodeziia i Aerofotos'emka* (ISSN 0536-101X), no. 3, 1988, p. 105-107. In Russian.

A89-35819

PRECIPITATION IN THE CANADIAN ATLANTIC STORMS PROGRAM - MEASUREMENTS OF THE ACOUSTIC SIGNATURE

JEFFREY A. NYSTUEN (U.S. Naval Postgraduate School, Monterey, CA) and DAVID M. FARMER (Institute of Ocean Sciences, Sidney, Canada) *Atmosphere - Ocean* (ISSN 0705-5900), vol. 27, March 1989, p. 237-257. Research supported by the Department of Energy, Mines, and Resources of Canada, U.S. Navy, and NPS Research Foundation. refs

The Canadian Atlantic Storms Program (CASP) allows comparison between radar backscatter and ambient ocean sound approaches to remotely sensed precipitation detection. CASP's radar backscatter record showed a close coincidence with simultaneous acoustic signals; the ambient sound record yielded indications of precipitation from spectral slope shifts. CASP has demonstrated that an identifiable precipitation signal occurs even in strong wind conditions. The surface bubble layer formed during strong winds only partially attenuates the higher frequency acoustic components generated by precipitation. O.C.

A89-35858#

SYNTHETIC APERTURE RADAR DATA FOR MAPPING SUBSURFACE GEOLOGICAL STRUCTURES IN THE NORTHWEST TERRITORIES, CANADA

K. S. MISRA, V. R. SLANEY, J. HARRIS, and D. F. GRAHAM (Canada Centre for Remote Sensing, Ottawa) IN: Thematic Conference on Remote Sensing for Exploration Geology, 6th, Houston, TX, May 16-19, 1988, Proceedings. Volume 1. Ann Arbor, MI, Environmental Research Institute of Michigan, 1988, p. 65-77. refs

A89-35861#

USE OF REMOTELY SENSED DATA IN MATURE BASIN EXPLORATION - CONSIDERATIONS ON CREATING USEFUL IMAGERY

DAVID G. KOGER (Texas Christian University, Fort Worth) and JOHN S. CARTER (Carter Exploration Co.; GeoTrac Energy Corp., Abilene, TX) IN: Thematic Conference on Remote Sensing for Exploration Geology, 6th, Houston, TX, May 16-19, 1988, Proceedings. Volume 1. Ann Arbor, MI, Environmental Research Institute of Michigan, 1988, p. 103-109. refs

The use of Landsat TM and MSS imagery for an exploration program in a mature basin is examined. Images from a study of the Eastern Shelf of the Permian Basin in Texas are presented as examples. The processes for acquiring, analyzing, and interpreting the data are outlined. The features found during the analysis are noted and their use in choosing drilling sites is discussed. R.B.

A89-35862#

THE CONTRIBUTION OF REMOTE SENSING DATA TO EXPLORATION OF FRACTURED RESERVOIRS

D. W. STEARNS (Oklahoma, University, Norman), Z. BERGER, H.

R. HOPKINS (Exxon Production Research Co., Houston, TX), and R. A. NELSON (Amoco Production Co., Houston, TX) IN: Thematic Conference on Remote Sensing for Exploration Geology, 6th, Houston, TX, May 16-19, 1988, Proceedings. Volume 1. Ann Arbor, MI, Environmental Research Institute of Michigan, 1988, p. 113-122. refs

The use of remote sensing data to predict regions of potential fractured reservoirs and trends of fracture permeability is discussed. The parameters that control subsurface fracture spacing and the process of predicting fracture orientation from lineaments are examined. The effects of the in situ stress state are considered. Also, guidelines for using lineaments to predict reservoir-fracture conditions are presented for both lineaments associated with late structural movements and those associated with regional fractures. R.B.

A89-35866#

SPECTRAL INDICES FOR VEGETATION AND ROCK TYPE DISCRIMINATION USING THE OPTICAL SENSOR OF THE JAPANESE ERS-1

YASUSHI YAMAGUCHI (Geological Survey of Japan, Tsukuba) IN: Thematic Conference on Remote Sensing for Exploration Geology, 6th, Houston, TX, May 16-19, 1988, Proceedings. Volume 1. Ann Arbor, MI, Environmental Research Institute of Michigan, 1988, p. 159-168. refs

Spectral indices for vegetation and rock type discrimination have been developed for optical sensor data from the planned Japanese Resources Satellite, ERS-1. Simulations of sensor response patterns from reflectance data and a linear spectral mixing model in a single picture are used to obtain equations for estimating the proportion of vegetation and clay and/or carbonate minerals within a pixel. In addition, a perpendicular vegetation index, a total absorption index, an alunite index, and a calcite index are presented. R.B.

A89-35871#

A FIELD SPECTROMETER AND REMOTE SENSING STUDY OF THE FRESNILLO MINING DISTRICT, MEXICO

JANICE L. GARDINER, RICHARD BIRNIE, and HALF ZANTOP (Dartmouth College, Hanover, NH) IN: Thematic Conference on Remote Sensing for Exploration Geology, 6th, Houston, TX, May 16-19, 1988, Proceedings. Volume 1. Ann Arbor, MI, Environmental Research Institute of Michigan, 1988, p. 229-236. Research supported by Dartmouth College and Sigma Xi. refs

A89-35872#

APPLICATION OF LANDSAT THEMATIC MAPPER DIGITAL DATA TO THE EXPLORATION FOR URANIUM-MINERALIZED BRECCIA PIPES IN NORTHWESTERN ARIZONA

ANDY YAW KWARTENG, PHILIP C. GOODELL (Texas, University, El Paso), PAT S. CHAVEZ, JR. (USGS, Flagstaff, AZ), and KAREN J. WENRICH (USGS, Denver, CO) IN: Thematic Conference on Remote Sensing for Exploration Geology, 6th, Houston, TX, May 16-19, 1988, Proceedings. Volume 1. Ann Arbor, MI, Environmental Research Institute of Michigan, 1988, p. 239-248. Research supported by USGS, Pathfinder Mines Corp., Energy Fuels Corp., and Union Pacific Resources. refs

Northwestern Arizona is actively being explored for uranium-mineralized breccia pipes in spite of the current depressed uranium market. The grade of uranium ore found in the breccia pipes, on the average, is more than ten times the grade of the sandstone-type uranium deposits found elsewhere on the Colorado Plateau. Digital enhancement techniques applied to Landsat Thematic Mapper (TM) data and digitized aerial color-infrared photographs were used to evaluate the utility of the remotely sensed data in the exploration for mineralized breccia pipes. Even though the breccia pipes commonly do not have unique spectral signatures compared to their background, the color composites of TM bands, printed at the scale of 1:100,000, allowed most of the known ore bodies in the study areas to be identified. Detailed structural information which was not apparent in the original color-infrared NHAP photograph was observed in the enhanced NHAP images. Author

A89-35875*# Open Univ., Milton (England).

VOLCANO MONITORING BY SHORT WAVELENGTH INFRARED SATELLITE REMOTE SENSING

D. A. ROTHERY (Open University, Milton Keynes, England), P. W. FRANCIS (Lunar and Planetary Institute, Houston, TX), and C. A. WOOD (NASA, Johnson Space Center, Houston, TX) IN: Thematic Conference on Remote Sensing for Exploration Geology, 6th, Houston, TX, May 16-19, 1988, Proceedings. Volume 1. Ann Arbor, MI, Environmental Research Institute of Michigan, 1988, p. 283-291. Research supported by the Open University. refs (Contract NAS5-28759; NASW-4066)

The use of short wavelength IR Landsat TM data for volcano monitoring is examined. By determining the pixel-integrated from the TM data, it is possible to estimate the temperature and size of hot areas which occupy less than one complete pixel. Examples of volcano monitoring with remote sensing data are discussed. It is suggested that the entire volcanic temperature range (100-1200 C) could be accomplished by decreasing the band 6 gain by just one order of magnitude so that it was sensitive to radiance from 1 to 100 mW/sq cm/sr/micron. R.B.

A89-35878#

SOURCES OF REMOTE SENSING DATA VISIBLE, NEAR INFRARED, AND SHORT WAVE

ORVILLE R. RUSSELL and WILLIAM G. BROONER (Earth Satellite Corp., Chevy Chase, MD) IN: Thematic Conference on Remote Sensing for Exploration Geology, 6th, Houston, TX, May 16-19, 1988, Proceedings. Volume 1. Ann Arbor, MI, Environmental Research Institute of Michigan, 1988, p. 327-336. refs

Descriptions are given for existing and planned airborne and spaceborne remote sensing systems that promise to provide valuable data for geological exploration applications. Advances in remote sensing technology, particularly in the spectral domain, should give geologists of the 1990s new and better data for mineralogical and lithological discrimination. More systems are being designed to acquire stereoscopic coverage which will provide greater reliability in structural mapping. Author

A89-35890#

ANALYSIS OF AIRBORNE IMAGING SPECTROMETER (AIS) DATA FOR GEOBOTANICAL PROSPECTING

C. BANNINGER (Institut fuer digitale Bildverarbeitung und Graphik, Graz, Austria) IN: Thematic Conference on Remote Sensing for Exploration Geology, 6th, Houston, TX, May 16-19, 1988, Proceedings. Volume 2. Ann Arbor, MI, Environmental Research Institute of Michigan, 1988, p. 489-498. refs

Airborne Imaging Spectrometer (AIS) data obtained from a metal-stressed spruce forest in the southeastern Alps of Austria exhibit an overall increase in canopy reflectance in the 800-2400 nanometer spectral region for stressed versus nonstressed trees. Log residual transformed data removed much of the atmospheric, scene, and instrument-related 'noise' contained in the 'raw' canopy data and revealed the presence of broadband absorption-like features centered at 1025 nm, 1185 nm, 1310 nm, and 2185 nm, which coincide with absorption bands of leaf biochemical constituents. Fair to strong statistical relationships exist between the depth of the absorption features at 1185 nm and 2185 nm and the copper, lead, and zinc content of the test site soils. Correlation values for lead and its various linear combinations with zinc and copper range from - 0.80 to - 0.88 for the absorption feature at 2185 nm. This wavelength region may prove to be not only a good indicator, but also a good discriminator of metal stress in coniferous tree stands. Author

A89-35891#

MEIS II AND SURFACE DATA INTEGRATION FOR DETECTION OF GEOBOTANICAL ANOMALIES

G. O. TAPPER and D. A. DEMPSEY (Laurentian University, Sudbury, Canada) IN: Thematic Conference on Remote Sensing for Exploration Geology, 6th, Houston, TX, May 16-19, 1988, Proceedings. Volume 2. Ann Arbor, MI, Environmental Research Institute of Michigan, 1988, p. 499-508. refs

In view of the established display by geochemically stressed

vegetation of an altered spectral response in the 0.5-0.8 micron wavelength range, the detection of such altered spectral reflectance by remote sensors in conjunction with field data acquisition can constitute a viable technique for geological prospecting. This methodology is presently developed by studying the known geochemical anomaly at Katie Lake, Ontario. The results obtained verify the ability of the method to identify the locations of anomalous reflectances in the poplar vegetation; concurrent biogeochemical analysis confirms the presence of base metals both in the soil and in botanical samples. O.C.

A89-35939* National Aeronautics and Space Administration. Langley Research Center, Hampton, VA.

ESTIMATION OF SURFACE INSOLATION USING SUN-SYNCHRONOUS SATELLITE DATA

WAYNE L. DARNELL, W. FRANK STAYLOR (NASA, Langley Research Center, Hampton, VA), SHASHI K. GUPTA, and FRED M. DENN (PRC Kentron, Inc., Hampton, VA) *Journal of Climate* (ISSN 0894-8755), vol. 1, Aug. 1988, p. 820-835. refs

A technique is presented for estimating insolation at the earth's surface using only sun-synchronous satellite data. The technique was tested by comparing the insolation results from year-long satellite data sets with simultaneous ground-measured insolation taken at five continental United States sites. Monthly average insolation values derived from the satellite data showed a standard error of 4.2 W/sq m, or 2.7 percent of the average ground insolation value. Author

A89-35949

EXAMINATION OF USAF NEPHANALYSIS PERFORMANCE IN THE MARGINAL CRYOSPHERE REGION

K. MCGUFFIE (University of Technology, Sydney, Australia) and D. A. ROBINSON (Rutgers University, New Brunswick, NJ) *Journal of Climate* (ISSN 0894-8755), vol. 1, Nov. 1988, p. 1124-1137. refs

(Contract AF-AFOSR-87-0195; AF-AFOSR-86-0053)

This paper investigates the accuracy of one snow-cover data set currently utilized by a global nephanalysis model, the United States Air Force (USAF) RT Nephanalysis, and the effect of inaccuracies in the snow cover information on the derived cloud field. There are found to be situations where the snow model is inaccurate because of the advanced state of the spring melt with respect to climatology, which causes errors in the derived cloud amount. The USAF policy of including surface cloud observations in the RT Nephanalysis leads to correction of the erroneous cloud amount in regions where surface observations are available. Author

A89-35966* National Aeronautics and Space Administration. Goddard Inst. for Space Studies, New York, NY.

GLOBAL, SEASONAL SURFACE VARIATIONS FROM SATELLITE RADIANCE MEASUREMENTS

WILLIAM B. ROSSOW, CHRISTOPHER L. BREST (NASA, Goddard Institute for Space Studies, New York), and LEONID C. GARDER (Columbia University, New York) *Journal of Climate* (ISSN 0894-8755), vol. 2, March 1989, p. 214-247. refs

Global, daily, visible, and infrared radiance measurements from the NOAA-5 Scanning Radiometer (SR) are analyzed for the months of January, April, July, and October 1977 to infer surface radiative properties. A radiative transfer model that simulates the spectral and angular characteristics of the NOAA-5 SR measurements is used to retrieve monthly mean surface visible reflectances and temperature at 25 km resolution. These surface properties were found sufficiently accurate for simulation of clear sky radiances to determine global, seasonal variations in cloudiness. Further comparisons of these results with other data highlight the analysis difficulties and radiative model shortcomings that must be overcome to monitor regional and seasonal variations of earth's surface. These preliminary results also provide an estimate of the magnitude of these variations. Author

A89-36686* Onagawa Magnetic Observatory (Japan).

SOME ASPECTS OF THE RELATION BETWEEN PI 1-2 MAGNETIC PULSATIONS OBSERVED AT L = 1.3-2.1 ON THE GROUND AND SUBSTORM-ASSOCIATED MAGNETIC FIELD VARIATIONS IN THE NEAR-EARTH MAGNETOTAIL OBSERVED BY AMPTE CCE

K. YUMOTO, T. SAITO (Onagawa Magnetic Observatory; Tohoku University, Sendai, Japan), K. TAKAHASHI (Johns Hopkins University, Laurel, MD), F. W. MENK, B. J. FRASER (Newcastle University, Australia) et al. *Journal of Geophysical Research* (ISSN 0148-0227), vol. 94, April 1, 1989, p. 3611-3618. Research supported by NASA. refs

A89-37316

ORE-BEARING STRUCTURES OF CENTRAL KAZAKHSTAN IDENTIFIED ON AERIAL AND SPACE PHOTOGRAPHS IN THE FRAMEWORK OF THE COMPUTER-AIDED PREDICTION OF MINERALS [RUDOKONTSENTRIRUIUSHCHIE STRUKTURY TSENTRAL'NOGO KAZAKHSTANA, VYIAVLENNYE PO AERO-I KOSMICHESKIM SNIMKAM PRI AVTOMATIZIROVANNOM PROGNOZIROVANII]

N. V. SKUBLOVA (Vsesoiuznyi Nauchno-Issledovatel'skii Institut Kosmoaerogeologicheskikh Metodov, Leningrad, USSR) *Issledovanie Zemli iz Kosmosa* (ISSN 0205-9614), Jan.-Feb. 1989, p. 49-54. In Russian. refs

A structure-selective analysis of megafracturing identified on space and high-altitude aerial photographs was carried out using coherent optics. Space geology data were correlated with geological/geophysical and metallogeny predictions to obtain quantitative estimates of their information content for the purpose of mineral prediction in Central Kazakhstan. B.J.

A89-37322

HIGHLY SENSITIVE MICROWAVE RADIOMETER-SCATTEROMETER FOR THE REMOTE SENSING OF THE EARTH'S SURFACE [VYSOKOCHUVSTVITEL'NYI SVCH-RADIOMETR-SKATTEROMETR DLIA DISTANTSIONNOGO ZONDIROVANIYA ZEMNOI POVERKHNOSTI]

N. N. VORSIN, V. B. VENSILAVSKII, A. A. GLOTOV, V. G. MIROVSKII, L. A. SMIRNOVA (Moskovskii Gosudarstvennyi Pedagogicheskii Institut, Moscow, USSR) et al. *Issledovanie Zemli iz Kosmosa* (ISSN 0205-9614), Jan.-Feb. 1989, p. 87-93. In Russian. refs

The design of a high-sensitivity microwave radiometer/scatterometer with a degenerate parametric input amplifier is presented. Possible applications of the system are considered, including the remote sensing of the sea surface. B.J.

A89-37327

REMOTE FOUR-PHOTON RAMAN SPECTROSCOPY OF SEA WATER UNDER NATURAL CONDITIONS [DISTANTSIONNAIA CHETYREKH FOTONNAIA SPEKTROSKOPIA KOMBINATSIONNOGO RASSEIANIYA MORSKOI VODY V NATURNYKH USLOVIYAKH]

A. F. BUNKIN, A. S. GALUMIAN, KH. A. ZHUMANOV, A. V. REZOV, and K. O. SURSKII (AN SSSR, Institut Obshchei Fiziki, Moscow, USSR) *Kvantovaya Elektronika* (Moscow) (ISSN 0368-7147), vol. 16, Jan. 1989, p. 7, 8. In Russian. refs

The possibility of measuring the background concentration of SO₄(2-) ions in sea water using remote Raman induced Kerr effect spectroscopy (RIKES) is demonstrated. SBS was achieved under natural conditions. Its spectroscopy was measured in the region of totally symmetric vibrations of the SO₄(2-) ion. K.K.

A89-37349

THE DISPERSION LIMITATIONS ON THE ACCURACY OF THE INTERNAL REFERENCE METHOD DURING REMOTE LASER SOUNDING OF THE UPPER OCEAN LAYER [O DISPERSSIONNYKH OGRANICHENIYAKH TOCHNOSTI METODA VNUTRENNEGO REPERA PRI DISTANTSIONNOM LAZERNOM ZONDIROVANII VERKHNEGO SLOIA OKEANA]

L. A. APRESIAN and D. V. VLASOV (AN SSSR, Institut Obshchei Fiziki, Moscow, USSR) Kvantovaya Elektronika (Moscow) (ISSN 0368-7147), vol. 16, Jan. 1989, p. 162-164. In Russian. refs

The paper addresses the factors which limit the accuracy of measurements performed with the internal reference method in problems of laser sounding of the upper ocean layer through its rough water surface. Numerical simulation reveals how the use of the internal reference method near the depths of sounding radiation focusing by the rough sea surface can lead to significant errors due to the dispersion of the deep sea refractive index. The effect of refractive index dispersion is significant both for dynamic and static actual measurements. K.K.

A89-37492

COORDINATE REFERENCING OF A TV IMAGE IN THE CASE OF THE REMOTE SENSING OF THE EARTH [KOORDINATNAIA PRIVIAZKA TELEVISIONNOGO IZOBRAZHENIYA PRI DISTANTSIONNOM ISSLEDOVANII ZEMLI]

I. S. SOROKEVICH Radiotekhnika (ISSN 0033-8486), March 1989, p. 7, 8. In Russian.

The different phases of the coordinate referencing of TV images obtained with a remote-sensing system are examined. A method for the realization of coordinate referencing in real time is proposed which is based on the computation of the external-orientation elements using orbital data. B.J.

A89-37549* National Aeronautics and Space Administration. Marshall Space Flight Center, Huntsville, AL.

PRECIPITATION RETRIEVAL OVER LAND AND OCEAN WITH THE SSM/I - IDENTIFICATION AND CHARACTERISTICS OF THE SCATTERING SIGNAL

ROY W. SPENCER, ROBBIE E. HOOD (NASA, Marshall Space Flight Center, Huntsville, AL), and H. MICHAEL GOODMAN (Alabama, University, Huntsville) Journal of Atmospheric and Oceanic Technology (ISSN 0739-0572), vol. 6, April 1989, p. 254-273. refs

Consideration is given to the use of the Defense Meteorological Satellite Program's Special Sensor Microwave/Imager (SSM/I) to identify precipitation in warm and cold land and ocean environments. It is shown that the polarization diversity of the SSM/I operating at 85.5 GHz makes it possible to discriminate between low brightness temperatures due to surface water bodies and those due to precipitation. The theoretical sensitivity of SSM/I between 19.35 and 8.5 GHz and the polarization correction for water surfaces and the effects of cloud water are discussed. Examples are presented of observational studies using SSM/I for the delineation of precipitation over land and oceans. R.B.

A89-37554

FIELD CALIBRATION OF MIXED-LAYER DRIFTERS

W. ROCKWELL GEYER (Woods Hole Oceanographic Institution, MA) Journal of Atmospheric and Oceanic Technology (ISSN 0739-0572), vol. 6, April 1989, p. 333-342. refs (Contract NSF ATM-82-17015)

A set of field experiments was conducted to determine the water-following characteristics of mixed-layer drifters with 'holey-sock' drogues. Through the use of a drifting current meter array, direct estimates of slip velocity (or the difference between the velocity of the drifter and that of the water surrounding the drogue) were obtained with precision of better than + or - 1 cm/s. The range of slip velocities was 1 to 4 cm/s, with the orientation of the slip principally in the downwind direction. The results are consistent with a simple model for slip induced by a wind-drift current assuming a static balance of drag forces.

Author

A89-37627

INFRARED THERMOGRAPHY - A QUANTITATIVE TOOL FOR HEAT STUDY [LA THERMOGRAPHIE INFRAROUGE - UN OUTIL QUANTITATIF A LA DISPOSITION DU THERMICIEN]

D. BALAGEAS, D. BOSCHER, A. DEOM, J. FOURNIER, and R. HENRY (ONERA, Chatillon-sous-Bagneux, France) (Revue Generale Thermique, Oct. 1988, p. 501-510) ONERA, TP no. 1989-3, 1989, 11 p. In French. Research supported by DRET and Service Technique des Programmes Aeronautiques. refs (ONERA, TP NO. 1989-3)

Three applications of infrared thermography for temperature determination are discussed: (1) the detection, localization, and thermal characterization of delamination in carbon-epoxy composite structures; (2) the determination of the heat transfer coefficients for wind tunnel models; and (3) the measurement of temperature in a helicopter blade section during icing/deicing tests performed in an icing wind tunnel. R.R.

A89-37802* Jet Propulsion Lab., California Inst. of Tech., Pasadena.

SEASAT A SATELLITE SCATTEROMETER MEASUREMENTS OF EQUATORIAL SURFACE WINDS

DAVID HALPERN (California Institute of Technology, Jet Propulsion Laboratory, Pasadena) Journal of Geophysical Research (ISSN 0148-0227), vol. 94, April 15, 1989, p. 4829-4833. refs

Seasat A scatterometer measurements of surface wind components made under normal weather conditions during August and September 1978 are examined. The longitudinal distributions of the monthly mean zonal component for each season are described. The average monthly mean slope of the wave number spectra throughout the 550- to 2200-km wavelength band was -1.7. The spectra levels of the zonal wind, but not the meridional component, are substantially different in each equatorial ocean. R.B.

A89-37981#

THE NAVAL RESEARCH LABORATORY'S AIR-SEA INTERACTION BLIMP EXPERIMENT

THEODORE V. BLANC, WILLIAM J. PLANT, and WILLIAM C. KELLER (U.S. Navy, Naval Research Laboratory, Washington, DC) American Meteorological Society, Bulletin (ISSN 0003-0007), vol. 70, April 1989, p. 354-365. Research supported by the U.S. Navy. refs

Microwave scatterometer and surface flux measurements have been conducted from a blimp in order to develop an improved scatterometer model function and, in turn, obtain a more accurate understanding of the relationship between the ocean's surface fluxes and its backscattered microwave power. These scatterometer measurements were conducted in the blimp's gondola, while a sonic anemometer and other flux-measurement instrumentation was suspended 60 m beneath the blimp at a 70-m flight altitude. An Airship Industries Model 600 nonrigid dirigible was used as the experimental platform. O.C.

A89-38290

ARGOS SYSTEM USED FOR BALLOON OBSERVATIONS

SHIGEO OHTA, TAKAMASA YAMAGAMI, JUN NISHIMURA, and HARUTO HIROSAWA (Institute of Space and Astronautical Science, Sagami-hara, Japan) IN: International Symposium on Space Technology and Science, 16th, Sapporo, Japan, May 22-27, 1988, Proceedings. Volume 2. Tokyo, AGNE Publishing, Inc., 1988, p. 1927-1931.

This paper describes a long distance balloon flight over the Pacific Ocean, which performed an observation of electromagnetic fields radiated by electric power lines. The balloon was launched from the Sanriku Balloon Center on October 11, 1986, and terminated 5900 km eastwards of Sanriku on October 13. The ARGOS system located the positions of the balloon along its flight path and collected the data. Author

A89-38330

SEA STATE DETERMINATION BY A REMOTE OPTICAL SENSOR

S. J. MORIZUMI (El Camino College, Torrance, CA) IN: International Symposium on Space Technology and Science, 16th, Sapporo, Japan, May 22-27, 1988, Proceedings. Volume 2. Tokyo, AGNE Publishing, Inc., 1988, p. 2205-2210.

The feasibility of visually detecting the sea state is studied. It is shown that the optical sensor is a possible candidate for sea state determination via the remote sensing technique. Allowance should be made for shadowing due to the presence of steep valleys in the sea surface and the multiple reflections which may be significant in the case of a low sun angle. Other significant factors are those of white caps and water spray near the sea surface in the region of a high wind velocity. K.K.

A89-38966

LOW-RELIEF TOPOGRAPHIC ENHANCEMENT IN A LANDSAT SNOW-COVER SCENE

J. RONALD EYTON (Alberta, University, Edmonton, Canada) Remote Sensing of Environment (ISSN 0034-4257), vol. 27, Feb. 1989, p. 105-118. refs

A Minnaert photometric function was used to model the satellite radiance of low-relief, snow-covered topography visible in a January 12, 1974 Landsat image covering central Illinois. The surface-scattering property (k) for snow was estimated from 43 measurements of the terrain geometry and the corresponding satellite gray-level values. The k value (.72) obtained from a regression analysis showed that snow is a more diffuse reflector relative to the scattering properties of vegetation as indicated by the published k values for various forest cover types. The results of the analysis provided the basis for a simple but effective image enhancement technique that highlighted the systems of glacial moraines dominating the landscape. Author

A89-38967

SEASONAL VISIBLE, NEAR-INFRARED AND MID-INFRARED SPECTRA OF RICE CANOPIES IN RELATION TO LAI AND ABOVE-GROUND DRY PHYTOMASS

MICHIO SHIBAYAMA and TSUYOSHI AKIYAMA (National Institute for Agro-Environmental Sciences, Tsukuba, Japan) Remote Sensing of Environment (ISSN 0034-4257), vol. 27, Feb. 1989, p. 119-127. Research supported by the Ministry of Agriculture, Forestry and Fisheries. refs

A89-39092

HIGH ALTITUDE LASER RANGING OVER RUGGED TERRAIN

N. H. THYER, J. A. R. BLAIS, and M. A. CHAPMAN (Calgary, University, Canada) Photogrammetric Engineering and Remote Sensing (ISSN 0099-1112), vol. 55, May 1989, p. 559-565. Research supported by the Alberta Forestry, Lands and Wildlife, and NSERC. refs

Laser range measurements from aircraft to ground were combined with high-altitude aerial photography in the Rocky Mountains west of Calgary. Estimates of the range from camera stations to ground by laser and photogrammetry initially differed considerably, but compensation for laser beam misalignment drastically reduced the discrepancy. When the laser measurements were combined with measurements of instrument position and orientation by an inertial system between camera stations, analysis showed that the combined system can give a terrain elevation profile with accuracy of a few dm or a few m, depending on the terrain type, vegetation, and slope, provided that the laser alignment is known and photogrammetry using ground control is used to update the inertial system at each end of the profile. Author

A89-39098

CLOSE-RANGE PHOTOGRAMMETRIC MEASUREMENT OF EROSION IN COARSE-GRAINED SOILS

J. SNEDDON and T. A. LUTZE (University College, Campbell, Australia) Photogrammetric Engineering and Remote Sensing (ISSN 0099-1112), vol. 55, May 1989, p. 597-600.

Measurement of soil erosion is difficult if the surface consists of particles whose size is of the same order of magnitude as the erosion. Closer-range photogrammetry can provide high resolution in the determination of coordinates of points on the surface. With

coarse-grained surfaces, a large number of points at close spacing could be observed to define the surface in terms of the size, shape, and position of the individual soil particles. However, tests showed that the experienced observer can, using far fewer observations, define an acceptable representation of the surface. The procedure requires each spot height reading to be estimated mean surface elevation within a zone corresponding to a suitable percentage, e.g., 20 percent of the stereoplotter's field of view. This allows the overall surface to be adequately represented by measurements at spacings indicated by the macrotopographic surface roughness, rather than those associated with individual soil particles. Author

A89-39322

IMPROVING ACCURACY IN RADAR-ALTIMETRY DATA CORRECTION FOR TROPOSPHERIC EFFECTS

P. BASILI, P. CIOTTI, and G. D'AURIA (Roma I, Università, Rome, Italy) Electronics Letters (ISSN 0013-5194), vol. 25, March 30, 1989, p. 458, 459. Research supported by CNR and MPI.

The advantages of using meteorological variables at sea level in regression procedures for correcting radar-altimetry data from satellites are examined. An increase in accuracy is noted when use is made of atmospheric pressure and wind velocity. Meteorological data gathered from radio soundings are used to find retrieval coefficients. C.D.

A89-39555

AN ANALYSIS OF SPECKLE FROM FOREST STANDS WITH PERIODIC STRUCTURES

DIRK H. HOEKMAN (Landbouwhogeschool, Wageningen, Netherlands) IEEE Transactions on Geoscience and Remote Sensing (ISSN 0196-2892), vol. 27, May 1989, p. 316-325. Research supported by the Netherlands Remote Sensing Board. refs

The azimuth time signal of the backscatter measured by an airborne (incoherent or coherent) radar system is known, theoretically, to contain information on the fine-scale spatial arrangement of scatterers, and this information can be revealed by an analysis of speckle. It is shown theoretically that the autocorrelation function of the small-scale (subresolution cell) backscatter signature in azimuth can be estimated from the averaged power density spectrum of azimuth (speckle) signals from homogeneous distributed targets. The accuracy of this estimation is indicated. The minimum size of statistical spatial details that can be resolved from the power spectrum, however, is fundamentally limited to the half-antenna length. The results of experiments conducted with an X-band SLAR over forest plantations with regular tree row spacing are shown to be in good agreement with theory. The row spacing (on the order of several meters) could be estimated accurately (within a few decimeters) using an antenna with an effective length of 2 m and an azimuth spatial resolution on the order of 25 m. I.E.

A89-39557

MESOSPHERIC TEMPERATURE SOUNDING WITH MICROWAVE RADIOMETERS

ALEX STOGRYN (Aerojet ElectroSystems Co., Azusa, CA) IEEE Transactions on Geoscience and Remote Sensing (ISSN 0196-2892), vol. 27, May 1989, p. 332-338. refs

The problem of accounting for the influence of the earth's magnetic field on brightness temperatures in retrieving mesospheric information by use of microwave radiometric measurements is considered. A physically based method for incorporating magnetic field effects within an otherwise linear regression procedure is developed. The resulting algorithm is fast enough to be used operationally for a satellite-borne scanning radiometer system. Error statistics obtained for a small database indicate that considerable improvement over climatological estimates of the state of the mesosphere will be possible up to at least the 0.03-mb level (roughly 73-km altitude). I.E.

A89-39652

GEOLOGICAL USES OF REMOTELY-SENSED REFLECTED AND EMITTED DATA OF LATERITIZED ARCHAEOAN TERRAIN IN WESTERN AUSTRALIA

STEPHEN A. DRURY and GAVIN A. HUNT (Open University, Milton Keynes, England) International Journal of Remote Sensing (ISSN 0143-1161), vol. 10, March 1989, p. 475-497. Research supported by NERC. refs

Strategies and techniques for the use of airborne digital image data equivalent to the Landsat Thematic Mapper (TM) and from the NASA Thermal Infrared Multispectral Scanner (TIMS) in geological mapping are discussed. The test areas are in complex Archaeoan greenstone terrain that has been subject to deep lateritic weathering and subsequent incision. These are spectrally unlike areas that have been covered before, and the analysis is based on new reflected and emitted spectra of natural surfaces. The newly available Landsat TM data over most of Western Australia is seen to have unprecedented potential as an aid to geological mapping in such intractable terrains because of the consistent and clear discrimination of weathered rock surfaces and colluvial soils over a wide range of rock types, particularly in decorrelation stretched three-band and band ratio images. The discrimination is due to the fortuitous association of mixtures of weathering products rather than to the primary mineralogy of the rocks. TIMS data are less useful in bedrock mapping, but offer considerable advantages for mapping the distribution of different types of superficial cover.

Author

A89-39870

RELATING POINT TO AREA AVERAGE RAINFALL IN SEMIARID WEST AFRICA AND THE IMPLICATIONS FOR RAINFALL ESTIMATES DERIVED FROM SATELLITE DATA

I. D. FLITCROFT, J. R. MILFORD, and G. DUGDALE (Reading, University, England) Journal of Applied Meteorology (ISSN 0894-8763), vol. 28, April 1989, p. 252-266. Research supported by the Overseas Development Administration of England. refs

A89-39872* Montana Univ., Missoula.

ESTIMATION OF REGIONAL SURFACE RESISTANCE TO EVAPOTRANSPIRATION FROM NDVI AND THERMAL-IR AVHRR DATA

RAMAKRISHNA R. NEMANI and STEVEN W. RUNNING (Montana, University, Missoula) Journal of Applied Meteorology (ISSN 0894-8763), vol. 28, April 1989, p. 276-284. refs
(Contract NAGW-952; NCA2-138; NCA2-27)

Infrared surface temperatures from satellite sensors have been used to infer evaporation and soil moisture distribution over large areas. However, surface energy partitioning to latent versus sensible heat changes with surface vegetation cover and water availability. The hypothesis that the relationship between surface temperature and canopy density is sensitive to seasonal changes in canopy resistance of conifer forests is presently tested. Surface temperature and canopy density were computed for a 20 x 25 km forested region in Montana, from the NOAA/AVHRR for 8 days during the summer of 1985. A forest ecosystem model, FOREST-BGC, simulated canopy resistance for the same period. For all eight days, surface temperatures had high association with canopy density, measured as Normalized Difference Vegetation Index, implying that latent heat exchange is the major cause of spatial variations in surface radiant temperatures.

Author

A89-40126

APPLICATIONS OF AVHRR DATA; PROCEEDINGS OF THE THIRD EUROPEAN AVHRR DATA USERS' MEETING, UNIVERSITY OF OXFORD, ENGLAND, DEC. 16-18, 1987

I. L. THOMAS, ED. (General Technology Systems, Ltd., Brentford, England), R. W. SAUNDERS, ED. (Oxford, University, England), and D. L. CROOM, ED. (Rutherford Appleton Laboratory, Didcot, England) Meeting sponsored by the Rutherford Appleton Laboratory, Meteorological Office, ESA, et al. International Journal of Remote Sensing (ISSN 0143-1161), vol. 10, Apr.-May 1989, 352 p. For individual items see A89-40127 to A89-40157.

Papers are presented on applications of AVHRR data, covering

applications such as identification of ancient glacier marks, snow and ice detection and classification, monitoring global tropical deforestation, studying the surface canopies in temperate zones, rainfall and evapotranspiration monitoring, and monitoring the phenology of grazing lands and vegetation. Additional applications include assessing water quality, estimating aerosol optical depth, measuring variations in sea surface temperature, and cloud classification. Other topics include the status of the NOAA polar orbiting sensor systems, noise characteristics of AVHRR IR channels, the removal of AVHRR channel-3 noise, geometrical correction of AVHRR imagery, an AVHRR mosaic image of Antarctica, cloud reflectance variations in channel-3, AVHRR image gridding, Earthnet's coordination scheme for AVHRR data, and observations of volcanic ash clouds using AVHRR/2 data. R.B.

A89-40129

ACTIVITIES AT THE NORWEGIAN HYDROTECHNICAL LABORATORY

T. A. MCCLIMANS (Norwegian Hydrotechnical Laboratory, Trondheim, Norway) (Rutherford Appleton Laboratory, Meteorological Office, ESA, et al., Applications of AVHRR data: European AVHRR Data Users' Meeting, 3rd, Oxford, England, Dec. 16-18, 1987) International Journal of Remote Sensing (ISSN 0143-1161), vol. 10, Apr.-May 1989, p. 617-623. refs

Applications of AVHRR and optical satellite data at the Norwegian Hydrotechnical Laboratory are reviewed. The use of AVHRR images to estimate the size and impact of eddies in the Norwegian coastal current is examined. The combined use of AVHRR and Landsat TM data to study the glacial outflow to fjords and AVHRR monitoring of polar lows are discussed. In addition, AVHRR data serves as inputs to a hydrological model to simulate daily snow runoff and to ice-front and ice-drift models used in forecasting.

R.B.

A89-40136

CLOUD REFLECTANCE VARIATIONS IN CHANNEL-3

R. S. SCORER (Imperial College of Science and Technology, London, England) (Rutherford Appleton Laboratory, Meteorological Office, ESA, et al., Applications of AVHRR data: European AVHRR Data Users' Meeting, 3rd, Oxford, England, Dec. 16-18, 1987) International Journal of Remote Sensing (ISSN 0143-1161), vol. 10, Apr.-May 1989, p. 675-686.

Using photographic terminology for channel 3 pictures in sunshine, most ice clouds appear black and cloud shadows are equally dark, but water droplet clouds appear in all shades. These shades also vary greatly with the direction of sunshine relative to the line of sight because scatter is almost entirely by diffraction. Droplets and ice crystals larger than about 10 microns absorb the incident radiation almost completely. The reflection from a water surface is almost metallic in intensity, so that glint completely saturates the radiometer. There is no evidence of comparable reflection from ice. All snow-covered surfaces, including sea ice, appear black.

Author

A89-40148

USING NOAA AVHRR IMAGERY IN ASSESSING WATER QUALITY PARAMETERS

G. J. PRANGSMA and J. N. ROOZEKRANS (Koninklijk Nederlands Meteorologisch Instituut, De Bilt, Netherlands) (Rutherford Appleton Laboratory, Meteorological Office, ESA, et al., Applications of AVHRR data: European AVHRR Data Users' Meeting, 3rd, Oxford, England, Dec. 16-18, 1987) International Journal of Remote Sensing (ISSN 0143-1161), vol. 10, Apr.-May 1989, p. 811-818. Research supported by the Dutch Remote Sensing Board. refs

The Advanced Very High Resolution Radiometer (AVHRR) instrument, carried by the NOAA-TIROS/N series of operational meteorological satellites can, on a routine basis, provide observational data which allow interpretation in terms of parameters related to water quality. In principle, some, though not all of the algorithms applied to Coastal Zone Colour Scanner data, can be transformed for use with AVHRR observations. In combination with the operational character of the NOAA satellites this opens up

08 INSTRUMENTATION AND SENSORS

the way to applications in monitoring of open sea and inland waters. Algorithms and results for some examples of such potential applications are presented. Author

A89-40151* Jet Propulsion Lab., California Inst. of Tech., Pasadena.

NOAA AVHRR AND ITS USES FOR RAINFALL AND EVAPOTRANSPIRATION MONITORING

YANN H. KERR (California Institute of Technology, Jet Propulsion Laboratory, Pasadena), J. IMBERNON (Institut de Recherche en Agronomie Tropicale, Montpellier, France), G. DEDIEU (Laboratoire d'Etudes et de Recherches en Teledetection Spatiale, Toulouse, France), O. HAUTECOEUR (Toulouse, Ecole Nationale Supérieure Agronomique, France), J. P. LAGOUARDE (Institut National de la Recherche Agronomique, Montfavet, France) et al. (Rutherford Appleton Laboratory, Meteorological Office, ESA, et al., Applications of AVHRR data: European AVHRR Data Users' Meeting, 3rd, Oxford, England, Dec. 16-18, 1987) International Journal of Remote Sensing (ISSN 0143-1161), vol. 10, Apr.-May 1989, p. 847-854. Research supported by the Programme Interdisciplinaire de Recherches sur l'Environnement. refs

NOAA-7 Advanced Very High Resolution Radiometer (AVHRR) Global Vegetation Indices (GVI) were used during the 1986 rainy season (June-September) over Senegal to monitor rainfall. The satellite data were used in conjunction with ground-based measurements so as to derive empirical relationships between rainfall and GVI. The regression obtained was then used to map the total rainfall corresponding to the growing season, yielding good results. Normalized Difference Vegetation Indices (NDVI) derived from High Resolution Picture Transmission (HRPT) data were also compared with actual evapotranspiration (ET) data and proved to be closely correlated with it with a time lapse of 20 days. Author

A89-40152* Commission of the European Communities, Ispra (Italy).

AVHRR FOR MONITORING GLOBAL TROPICAL DEFORESTATION

J. P. MALINGREAU, N. LAPORTE (CEC, Joint Research Centre, Ispra, Italy), and C. J. TUCKER (NASA, Goddard Space Flight Center, Greenbelt, MD) (Rutherford Appleton Laboratory, Meteorological Office, ESA, et al., Applications of AVHRR data: European AVHRR Data Users' Meeting, 3rd, Oxford, England, Dec. 16-18, 1987) International Journal of Remote Sensing (ISSN 0143-1161), vol. 10, Apr.-May 1989, p. 855-867. refs

Advanced Very High Resolution Radiometer (AVHRR) data have been used to assess the dynamics of forest transformations in three parts of the tropical belt. A large portion of the Amazon Basin has been systematically covered by Local Area Coverage (LAC) data in the 1985-1987 period. The analysis of the vegetation index and thermal data led to the identification and measurement of large areas of active deforestation. The Kalimantan/Borneo forest fires were monitored and their impact was evaluated using the Global Area Coverage (GAC) 4 km resolution data. Finally, High Resolution Picture Transmission (HRPT) data have provided preliminary information on current activities taking place at the boundary between the savanna and the forest in the Southern part of West Africa. The AVHRR approach is found to be a highly valuable means for carrying out deforestation assessments in regional and global perspectives. Author

A89-41164* National Aeronautics and Space Administration. John C. Stennis Space Center, Bay Saint Louis, MS.

DETECTION TECHNIQUES USING MULTISPECTRAL DATA TO INDEX SOIL EROSIONAL STATUS

R. E. PELLETIER (NASA, John C. Stennis Space Center, Bay Saint Louis, MS) IN: 1988 ACSM-ASPRS Annual Convention, Saint Louis, MO, Mar. 13-18, 1988, Technical Papers. Volume 4. Falls Church, VA, American Congress on Surveying and Mapping and American Society for Photogrammetry and Remote Sensing, 1988, p. 152-161. refs

Indexing techniques that can be used to detect soil erosion utilizing the known band widths of the Landsat MSS and TM sensors

are identified. The indexing techniques focus on iron oxides, clays, and organic matter as properties revealing soil erosional status. For data acquisition, a Collins visible and infrared intelligent spectrometer was used to collect data from 0.4-24 microns. Pressed polytetrafluorethylene was used as the reflectance standard and was acquired at the same time that the sample data were acquired. K.K.

A89-41165

THE APPLICATION OF SPOT RATIO DATA FOR SOIL CLASSIFICATION

G. VENUGOPAL (Ball State University, Muncie, IN) and H. RANDY GIMBLETT (Digital Land Systems Research, Tucson, AZ; Ball State University, Muncie, IN) IN: 1988 ACSM-ASPRS Annual Convention, Saint Louis, MO, Mar. 13-18, 1988, Technical Papers. Volume 4. Falls Church, VA, American Congress on Surveying and Mapping and American Society for Photogrammetry and Remote Sensing, 1988, p. 162-170. refs

The use of SPOT 1 data for soil classification in parts of Henry County, Indiana, is studied. The data used in this study include the original three bands of SPOT 1 and transformed soil indices. Using the original three band data, training samples of various soil types based on color, texture, moisture, and organic water content were selected and a classification map was generated. In the second phase of analysis, generally accepted soil indices were computed and a second classification map was generated. By superimposing the two classification maps, it was possible to understand the discriminative power of the raw SPOT data and the enhanced soil indices. K.K.

A89-41691*# National Aeronautics and Space Administration. Goddard Space Flight Center, Greenbelt, MD.

LASER ALTIMETRY MEASUREMENTS FROM AIRCRAFT AND SPACECRAFT

JACK L. BUFTON (NASA, Goddard Space Flight Center, Greenbelt, MD) IEEE, Proceedings (ISSN 0018-9219), vol. 77, March 1989, p. 463-477. refs

The techniques involved in the design and application of laser altimeter instruments are reviewed, including a description of the instrument subsystems required for the range and waveform measurements. Laser pulse transmitters based on the relatively novel technology of diode-pumped solid-state lasers are considered. Various factors affecting laser altimeter instrument performance are discussed. These include the receiver signal-to-noise ratio, atmospheric propagation, and altimeter platform effects. Some examples of laser altimeter data are presented to illustrate the variety of possible instrument applications. I.E.

A89-41692

SATELLITE-BORNE LIDAR OBSERVATIONS OF THE EARTH - REQUIREMENTS AND ANTICIPATED CAPABILITIES

ROBERT J. CURRAN (SM Systems; Research Corp., Landover, MD) IEEE, Proceedings (ISSN 0018-9219), vol. 77, March 1989, p. 478-490. refs

Satellite observations have relied on passive remote-sensing systems and thereby suffer a fundamental limitation on their accuracy and vertical resolution (2 to 4 km for remote sensing of atmospheric temperature). Lidar systems offer the potential for improved vertical resolution and accuracy, with global coverage. To better understand important processes in the earth system, these higher-resolution observations have now become a basic requirement for the satellite observing system of the 1990s. In this paper, consideration is given to the requirements for lidar observations of the earth's atmosphere, land, and ocean surfaces and the characteristics of the systems which can provide these observations. I.E.

A89-41761* National Aeronautics and Space Administration. Langley Research Center, Hampton, VA.

A PARAMETERIZATION FOR LONGWAVE SURFACE RADIATION FROM SUN-SYNCHRONOUS SATELLITE DATA

SHASHI K. GUPTA (NASA, Langley Research Center; Planning

Research Corp., Aerospace Technologies Div., Hampton, VA) Journal of Climate (ISSN 0894-8755), vol. 2, April 1989, p. 305-320. refs

A parameterization is presented for computing downward, upward, and net longwave radiation at the earth's surface using data from NOAA sun-synchronous satellites. The parameterization is applied to satellite soundings for April, 1982 over a large region of the tropical Pacific Ocean. Sensitivity studies were used to estimate the random and systematic errors in computed fluxes due to probable errors in TOVS-derived parameters. It is suggested that large biases in the results due to errors in TOVS-derived parameters may be corrected with data from the International Satellite Cloud Climatology Project. R.B.

A89-42173

DESIGN OF SPECTRAL AND PANCHROMATIC BANDS FOR THE GERMAN MOMS-02 SENSOR

H. KAUFMANN, F. J. BEHR (Karlsruhe, Universitaet, Federal Republic of Germany), D. MEISSNER (Messerschmitt-Boelkow-Blohm GmbH, Munich, Federal Republic of Germany), and J. BODECHTEL (CEC, Joint Research Centre, Ispra, Italy) Photogrammetric Engineering and Remote Sensing (ISSN 0099-1112), vol. 55, June 1989, p. 875-881. Research supported by BMFT. refs

The process of locating and defining the width of spectral bands in the 0.4 to 1.1 microns range for the MOMS-02 sensor is discussed. Laboratory diffuse reflectance measurements were made for leaves and needles of different deciduous and coniferous trees and for the mineral standards and natural surfaces of rocks and soils containing Fe(2+) and Fe(3+) ions. Band optimization is based on an iterative process, including spectral properties of distinct targets, solar irradiance, atmospheric transmission, calibration standards, and system parameters. The selected spectral bands are 440-505 nm, 530-575 nm, 650-685 nm, and 770-810 nm. The bandpass of the panchromatic nadir and off-nadir viewing stereo modules is defined at 520 and 760 nm. R.B.

A89-42601

REMOTE MEASUREMENTS FROM SALYUT-7 OF THE OPTICAL PARAMETERS OF THE ATMOSPHERE-SURFACE SYSTEM [DISTANTSIONNOE OPREDELENIE OPTICHESKIKH PARAMETROV SISTEMY ATMOSFERA - POVERKHNOST' SO STANTSII 'SALIUT-7']

M. S. MALKEVICH and G. TSIMMERMAN (AN SSSR, Institut Kosmicheskikh Issledovaniy, Moscow, USSR) Issledovanie Zemli iz Kosmosa (ISSN 0205-9614), Mar.-Apr. 1989, p. 3-11. In Russian. refs

Results of remote measurements of optical parameters of the atmosphere and the earth surface, conducted from Salyut-7 by a multichannel spectrometer/multichannel camera (MKS-M/MKF-6M) system, are described together with the principles involved and the methods used. Results presented include data on the height, optical thickness, and reflectance of clouds, and the coefficients of specific absorbance of solar radiation by cloud particles; it is shown that these coefficients are larger (by the factor of 2 to 3) than those of water droplets and ice particles. The MKS-M/MKF-6M measurements of solar occultation were found to correlate with measurements of the ozone and aerosol vertical distributions in lower stratosphere. I.S.

A89-42608

THE SPECTROMETER OF THE SALYUT-7 ORBITAL STATION [SPEKTROMETR ORBITAL'NOI STANTSII 'SALIUT-7']

V. I. SIACHINOV and G. ZIMMERMANN (AN SSSR, Institut Kosmicheskikh Issledovaniy, Moscow, USSR) Issledovanie Zemli iz Kosmosa (ISSN 0205-9614), Mar.-Apr. 1989, p. 65-70. In Russian. refs

The characteristics (such as the spectral range, number of channels, spectral resolution, visual field, recording speed, and measurement error) of instruments used on board the Salyut station for spectrometric measurements of the atmosphere/earth-surface system are discussed. Special attention is given to the principles of operation, the design, and the basic characteristics of the orbital

spectroquantometer MKS-M and its substructures. This spectrometer makes it possible to measure solar radiance reflected by the atmosphere/earth-surface system in 18 spectral ranges between 415 and 880 nm. I.S.

A89-42609

MULTICHANNEL SPETROMETER MKS-M - LABORATORY TESTS, CALIBRATION, AND VERIFICATION OF ITS STABILITY IN FLIGHT [MNOGOKANAL'NYI SPEKTROMETR MKS-M - LABORATORNYE ISSLEDOVANIYA, KALIBROVKA I PROVERKA EE SOKHRANOSTI V POLETE]

K.-H. SUEMNICH (Akademie der Wissenschaften der DDR, Institut fuer Kosmosforschung, Berlin, German Democratic Republic) Issledovanie Zemli iz Kosmosa (ISSN 0205-9614), Mar.-Apr. 1989, p. 71-77. In Russian.

The multichannel spectrometer MKS-M was designed for synchronic measurements of spectral radiance of the atmosphere/earth-surface system and optical parameters of the atmosphere and the clouds. The MKS-M performance characteristics and their stability were tested in laboratory experiments; absolute calibration was performed using standard sources whose radiance values were compared with solar radiation measured in airborne experiments. It is pointed out that, during space flights, the spectrometer can be directly calibrated against solar radiation. I.S.

A89-42684

AN INEXPENSIVE POLARIMETRIC FM RADAR AND POLARIMETRIC SIGNATURES OF ARTIFICIAL SEA ICE

S. P. GOGINENI, J. W. BREDOW, and R. K. MOORE (University of Kansas Center for Research, Inc., Lawrence) IN: 1989 IEEE National Radar Conference, 4th, Dallas, TX, Mar. 29, 30, 1989, Proceedings. New York, Institute of Electrical and Electronics Engineers, Inc., 1989, p. 188-191.

The authors developed an inexpensive FM radar for polarimetric scattering measurements. The system was designed for collecting polarimetric data at 5.3 and 10 GHz over incidence angles from 0 to 60 degrees. The unique features of the system include fine range resolution, phase stabilization, and linearization of the RF oscillator and digital signal processing capability. The system is used for collecting polarimetric scattering data from artificial sea ice at the US Army Cold Regions Research and Engineering Laboratory (CRREL) in Hanover, New Hampshire. The authors discuss the design, construction, and performance of the polarimetric radar and present results from the CRREL experiments. I.E.

A89-42773

1988 CONFERENCE ON PRECISION ELECTROMAGNETIC MEASUREMENTS, TSUKUBA, JAPAN, JUNE 7-10, 1988, PROCEEDINGS

RONALD F. DZIUBA, ED. (NIST, Electricity Div., Washington, DC) Conference sponsored by the Society of Instrument and Control Engineers of Japan, IEEE, URSI, et al. IEEE Transactions on Instrumentation and Measurement (ISSN 0018-9456), vol. 38, April 1989, 572 p. For individual items see A88-42774 to A88-42795.

Various papers on instrumentation and measurement are presented. Some of the individual topics addressed include: precision experiments to search for the fifth force, search for composition-dependent gravity using a beam balance, free-fall interferometer to search for a possible fifth force, industrial experience with an array Josephson junction, precision ac measurement of temperature below 90 K, optical frequency standards, search for the best clock, the NBS time scale algorithm, development of GPS positioning system Prestar, design of Kalman smoothers for GPS data, and time comparisons between KSRJ and CRL via the Geostationary Meteorological Satellite of Japan. Also discussed are: angular navigation on short baselines using phase delay interferometry, millimeter accuracy of geodetic VLBI measurements achieved on a 54-km baseline, short baseline experiments using the highly transportable VLBI station, earth rotation parameters determined by VLBI within Project IRIS, and

baseline length changes of circumpacific VLBI networks and their bearing on global tectonics. C.D.

A89-42941

AIRBORNE IMAGING RADAR SYSTEM FOR MONITORING SEA POLLUTION

C. BOESSWETTER (Messerschmitt-Boelkow-Blohm GmbH, Ottobrunn, Federal Republic of Germany) (International Colloquium on Remote Sensing of Pollution of the Sea, Universitaet Oldenburg, Federal Republic of Germany, Mar. 31-Apr. 3, 1987) IN: Research and development: Technical and scientific publications 1988. Munich, Federal Republic of Germany, Messerschmitt-Boelkow-Blohm GmbH, 1988, p. 215-220. refs (MBB-UK-0016-87-PUB)

An advanced radar imaging concept for airborne and/or helicopter operation monitoring of sea pollution has been developed which satisfies the requirements for near range, narrow swath coverage including the nadir and for long range, wide-swath coverage up to 50 km on both sides. This is achieved by optimally combining a forward-looking imaging radar with a side-looking radar system. The design and performance parameters involved are shown and discussed. C.D.

A89-43026

RETRIEVAL OF MESOSCALE METEOROLOGICAL PARAMETERS FOR POLAR LATITUDES (MIZEX AND ARCTEMIZ CAMPAIGNS)

C. CLAUD, A. CHEDIN, N. A. SCOTT (Ecole Polytechnique, Palaiseau, France), and J. C. GASCARD (Paris VI, Universite, France) Annales Geophysicae (ISSN 0980-8752), vol. 7, June 1989, p. 205-212. Research supported by the Institut Francais de Recherche pour l'Exploitation de la Mer. refs

The '3I' (Improved Initialization Inversion) has been designed for retrieving meteorological parameters from operational satellites for the TIROS-N series. After a brief description of this method, results of its application to high latitude regions in relationship with the MIZEX (Marginal Ice Zone Experiment) and ARCTEMIZ (MIZ of the European ARCTic) campaigns are presented. The particularities of these regions have induced some refinements in the procedure which are described in detail: detection of sea ice, through the use of microwave observations, and its impact on cloud detection, an essential point of the method. Retrieved temperature profiles are compared to conventional data (radiosonde ascents, analyses from different forecasting centers).

Author

A89-43311

SHORT-PERIOD FLUCTUATION OF THE LOWER TROPOSPHERIC WINDS OBSERVED BY MU-RADAR

AKIMASA SUMI (Tokyo, University, Japan) Meteorological Society of Japan, Journal (ISSN 0026-1165), vol. 67, Feb. 1989, p. 167-175. Research supported by Kyoto University. refs

Time-continuous tropospheric wind field observations using a middle and upper atmosphere radar were conducted in July 1986. The observation of a short time-scale fluctuation of the motion field is discussed. It is found that the radar can quickly resolve the wind-field in the middle troposphere, making it possible to describe the temporal behavior of the mesoscale phenomena at a single station. R.B.

A89-43408

MODELLING THE EARTH'S GEOMAGNETIC FIELD TO HIGH DEGREE AND ORDER

DAVE R. SCHMITZ (Univerzita Pavla Jozefa Safarika, Kosice, Czechoslovakia), J. MEYER (Goettingen, Universitaet, Federal Republic of Germany), and JOSEPH C. CAIN (Florida State University, Tallahassee) Geophysical Journal (ISSN 0955-419X), vol. 97, June 1989, p. 421-430. refs

A method is presented to model the earth's magnetic field to very high degree and order in terms of spherical harmonics. The method is based, in part, on the method of Gauss-Legendre quadrature. The Gauss-Legendre technique is compared to the simpler Newton-Cotes quadrature. Both methods are applied to

sets of radial field data computed from an $n = 29$ model simulating Magsat observations. It is shown that the Gauss-Legendre technique is generally more accurate and more efficient than the Newton-Cotes technique. R.B.

A89-43409

DERIVATION OF A GEOMAGNETIC MODEL TO $N = 63$

JOSEPH C. CAIN (Florida State University, Tallahassee), ZHIGANG WANG (State Seismological Bureau, Beijing, People's Republic of China), CHRISTOPHER KLUTH, and DAVE RAY SCHMITZ (USGS, Branch of Geophysics, Denver, CO) Geophysical Journal (ISSN 0955-419X), vol. 97, June 1989, p. 431-441. Research supported by USGS. refs

A high degree model of the geomagnetic field is derived using an integral technique to extend coefficients beyond the limits allowable with least squares approaches. A previously derived model to $n = 29$ was updated with new secular change data for the interval September 1979 to June 1980 combined with the analysis set of Magsat vector data. The reduced $B(r)$ components were averaged over approximately 3×3 deg blocks of latitude and longitude, and coefficients derived using the Neumann method. These coefficients, when combined with those from the least squares solution, show significantly greater detail in the structure of the geomagnetic field which appeared to be realistic to $n = 50$. Author

N89-20430*# National Aeronautics and Space Administration. Marshall Space Flight Center, Huntsville, AL.

IMPROVED CAPABILITIES OF THE MULTISPECTRAL ATMOSPHERIC MAPPING SENSOR (MAMS)

GARY J. JEDLOVEC, K. BRYAN BATSON, ROBERT J. ATKINSON, CHRIS C. MOELLER, W. PAUL MENZEL (National Oceanic and Atmospheric Administration, Madison, WI.), and MARK W. JAMES Jan. 1989 80 p (NASA-TM-100352; NAS 1.15:100352) Avail: NTIS HC A05/MF A01 CSCL 14B

The Multispectral Atmospheric Mapping Sensor (MAMS) is an airborne instrument being investigated as part of NASA's high altitude research program. Findings from work on this and other instruments have been important as the scientific justification of new instrumentation for the Earth Observing System (EOS). This report discusses changes to the instrument which have led to new capabilities, improved data quality, and more accurate calibration methods. In order to provide a summary of the data collected with MAMS, a complete list of flight dates and locations is provided. For many applications, registration of MAMS imagery with landmarks is required. The navigation of this data on the Man-computer Interactive Data Access System (McIDAS) is discussed. Finally, research applications of the data are discussed and specific examples are presented to show the applicability of these measurements to NASA's Earth System Science (ESS) objectives. Author

N89-20532 Hull Univ. (England).

REMOTE SENSING IN REFRACTIVE TURBULENCE Ph.D.

Thesis

JOAO DE LEMOS PINTO 1986 175 p

Avail: Univ. Microfilms Order No. BRDX83208

Atmospheric laser based remote sensing was investigated and developed, using visible and infrared lasers, by various research groups. On the whole, remote sensing is favored when based on infrared lasers. The design of a highly sensitive system has to involve an end-to-end beam control design, i.e., the system designer has to consider carefully the laser system, the propagation path effects and the target characteristics. Of prime import, is the assessment of the limitations imposed by atmospheric turbulence. Depending on its strength, refractive turbulence can cause a wandering in all directions and an eventual breakup of the transmitted beam and a scintillation effect. The sensitivity and accuracy of a remote sensing measurement is also affected by the stability of the laser and the detection system. In a remote sensing system, the laser beam is usually transmitted and received through a telescope in order to reduce the average power density

along the propagation path and the beam divergence, thereby achieving longer ranges or smaller spot sizes in the far field.

Dissert. Abstr.

N89-20539# Beleidscommie Remote Sensing, Delft (Netherlands).

PHASE A STUDY FOR THE EXTENSION OF THE CAESAR SCANNER WITH A SENSOR MODULE FOR THE FAR INFRARED [FASE A STUDIE VOOR DE UITBREIDING VAN DE CAESAR SCANNER MET EEN SENSOR MODULE VOOR HET VERDERE INFRAROOD]

P. BINNENKADE, H. POUWELS, H. BOKHOVEN, and C. SMORENBURG (Technische Physische Dienst TNO-TH, Delft, Netherlands) Aug. 1988 91 p In DUTCH (Contract BCRS-PROJ. TE-1.7) (BCRS-88-09; TPD-733.002; ETN-89-93878) Avail: NTIS HC A05/MF A01

The extension of the CAESAR airborne scanner with a module for measurements in the thermal IR range, using the pushbroom scanning principle, was studied in the project CATS (CAESAR Airborne Thermal Scanner). An inventory of available detector arrays and a first dimensioning of the scanner were made. An optical concept and a preliminary design of electronics for data processing were made. Software aspects and the PARES programming systems are presented. The built-in possibilities of CATS in the METRO aircraft are discussed. The results of the study open the way to a successful development of CATS and demonstrate the feasibility of this scanner. ESA

N89-20542# National Aerospace Lab., Amsterdam (Netherlands). Space Div.

TWELVE YEAR OVERVIEW OF CLOUDFREE LANDSAT IMAGERY OF THE NETHERLANDS

F. B. VANDERLAAN 12 Nov. 1987 31 p In DUTCH; ENGLISH summary Submitted for publication (NLR-MP-87072-U; ETN-89-94045) Avail: NTIS HC A03/MF A01

Twelve years of LANDSAT quick-look images were used to assess the chances of obtaining cloud free imagery from the Netherlands. In 12yr 27 complete cloud free coverages were recorded for which less than 4 recording dates need to be purchased; 18 of these fall in the autumn, winter, spring period in which the image quality is low. Nine cloud free coverages are recorded in summertime. Counting per quarter scene, a cloud free image becomes available on average five times per year. Once every 2yr complete cloud free coverage from a usefull and high quality image can be expected from the whole of the Netherlands. ESA

N89-20543# Massachusetts Inst. of Tech., Cambridge. Lab. of Electronics.

ACTIVE AND PASSIVE REMOTE SENSING OF ICE Final Report, 16 Feb. 1983 - 30 Sep. 1988

JIN AN KONG 2 Feb. 1989 23 p (Contract N00014-83-K-0258) (AD-A203943) Avail: NTIS HC A03/MF A01 CSCL 17/9

Fully polarimetric scattering properties of earth terrain media are studied with three-layer random medium model. The top scattering layer is modeled as an isotropic random medium which is characterized by a scalar permittivity. The middle scattering layer is modeled as an anisotropic random medium with a symmetric permittivity tensor whose optic axis can be tilted depending on the preferred alignment of the embedded scatterers. The bottom layer is considered as a homogeneous half-space. Volume scattering effects of both random media are described by three dimensional correlation functions with variances and correlation lengths corresponding to the strengths of the permittivity fluctuations and the physical sizes of the inhomogeneities, respectively. The strong fluctuation theory is used to derive the mean fields in the random media under the bilocal approximation with singularities of the dyadic Greens's functions properly taken into consideration. With the discrete scatterer concept, effective permittivities of the random media are calculated by two-phase

mixing formulas. Then, the Born approximation is used to calculate the covariance matrix which described the fully polarimetric scattering properties of the remotely sensed media. The polarimetric information is useful in the identification, classification, and radar image simulation of earth terrain media. Author

N89-21218# Air Force Inst. of Tech., Wright-Patterson AFB, OH. School of Engineering.

AN ANALYSIS OF PLATINUM SILICIDE AND INDIUM ANTIMONIDE FOR REMOTE SENSORS IN THE 3 TO 5 MICROMETER WAVELENGTH BAND M.S. Thesis

NEIL F. SCHOON Dec. 1988 126 p (AD-A202663; AFIT/GSO/ENP/88D-4) Avail: NTIS HC A07/MF A01 CSCL 17/5

Platinum Silicide and Indium Antimonide are compared as detector materials in a space based remote sensor using the 3 to 5 micrometer wavelength band. The comparison is based on a scaled count rate involving the material's quantum efficiency, a target's reflected solar and thermal emittances, the atmospheric transmission, and the wavelength. The comparison is made using a baseline scenario and seven sensitivity analysis scenarios. The baseline scenario uses a target at 298K and a vertical line-of-sight from the target to the remote sensor in space. The atmospheric transmission is calculated using the 1962 U.S. Standard atmospheric model resident in LOWTRAN 6, with a 23 kilometer rural visibility and no cloud cover. A sensitivity analysis was performed by varying the target temperature, target reflectance, and finally the atmospheric properties. GRA

N89-21415# National Oceanic and Atmospheric Administration, Washington, DC. Assessment and Information Services Center.

ICE COVER ON CHESAPEAKE BAY FROM AVHRR (ADVANCED VERY HIGH RESOLUTION RADIOMETER) AND LANDSAT IMAGERY, WINTER OF 1987-88

MICHAEL J. DOWGIALLO, MARTIN C. PREDOEHL, and RICHARD P. STUMPF Jun. 1988 36 p (PB89-117261; NOAA-TM-NESDIS-AISC-14) Avail: NTIS HC A03/MF A01 CSCL 08/12

Ice cover on Chesapeake Bay during winter 1987-88 was analyzed using two types of satellite imagery and ice reconnaissance data from the U.S. Coast Guard. Multispectral Scanner (MSS) data from LANDSAT and Advanced Very High Resolution Radiometer (AVHRR) data from the NOAA TIROS-N polar-orbiting satellites were compared for usefulness in detection and evaluation of ice on Chesapeake Bay. Decreases in air temperatures and surface water temperatures in the upper Bay are quantitatively linked to ice formation. Ice conditions during 1987-88, a near-normal winter in the Bay area, were compared to conditions in winter 1981-82, a much colder winter with more ice. Maximum ice cover was 14 percent during winter 1987-88 and 34 percent during winter 1981-82. GRA

N89-22154# Jet Propulsion Lab., California Inst. of Tech., Pasadena.

PROCEEDINGS OF THE AIRBORNE VISIBLE/INFRARED IMAGING SPECTROMETER (AVIRIS) PERFORMANCE EVALUATION WORKSHOP

GREGG VANE, ed. 15 Sep. 1988 241 p Workshop held in Pasadena, CA, 6-8 Jun. 1988 Slides as supplement (Contract NAS7-918) (NASA-CR-184870; JPL-PUBL-88-38; NAS 1.26:184870) Avail: NTIS HC A11/MF A01 CSCL 08/2

The focus of the workshop was the assessment of data quality by the AVIRIS project. Summaries of 16 of the presentations are published. The AVIRIS performance evaluation period began in June 87 with flight data collection in the eastern U.S., and continued in the west until Oct. 87, after which the instrument was returned for post flight calibration. At the beginning, the sensor met all of the spatial, spectral and radiometric performance requirements except in spectrometer D, where the signal to noise ratio was below the required value. By the end, sensor performance had deteriorated due to failure of 2 critical parts and to some design deficiencies. The independent assessment by the NASA

08 INSTRUMENTATION AND SENSORS

investigators confirmed the assessment by the AVIRIS project. Some scientific results were derived and are presented. These include the mapping of the spatial variation of atmospheric precipitable water, detection of shift in chlorophyll red, and mineral identification.

N89-22155*# Jet Propulsion Lab., California Inst. of Tech., Pasadena.

AVIRIS PERFORMANCE DURING THE 1987 FLIGHT SEASON: AN AVIRIS PROJECT ASSESSMENT AND SUMMARY OF THE NASA-SPONSORED PERFORMANCE EVALUATION

GREGG VANE, WALLACE M. PORTER, JOHN H. REIMER, THOMAS G. CHRIEN, and ROBERT O. GREEN *In its* Proceedings of the Airborne Visible/Infrared Imaging Spectrometer (AVIRIS) Performance Evaluation Workshop p 1-20 15 Sep. 1988

Avail: NTIS HC A11/MF A01 CSCL 08/2

Results are presented of the assessment of AVIRIS performance during the 1987 flight season by the AVIRIS project and the earth scientists who were chartered by NASA to conduct an independent data quality and sensor performance evaluation. The AVIRIS evaluation program began in late June 1987 with the sensor meeting most of its design requirements except for signal-to-noise ratio in the fourth spectrometer, which was about half of the required level. Several events related to parts failures and design flaws further reduced sensor performance over the flight season. Substantial agreement was found between the assessments by the project and the independent investigators of the effects of these various factors. A summary of the engineering work that is being done to raise AVIRIS performance to its required level is given. In spite of degrading data quality over the flight season, several exciting scientific results were obtained from the data. These include the mapping of the spatial variation of atmospheric precipitable water, detection of environmentally-induced shifts in the spectral red edge of stressed vegetation, detection of spectral features related to pigment, leaf water and ligno-cellulose absorptions in plants, and the identification of many diagnostic mineral absorption features in a variety of geological settings.

Author

N89-22161*# Colorado Univ., Boulder. Center for the Study of Earth from Space.

PRELIMINARY ANALYSIS OF AIRBORNE VISIBLE/INFRARED IMAGING SPECTROMETER (AVIRIS) FOR MINERALOGIC MAPPING AT SITES IN NEVADA AND COLORADO

FRED A. KRUSE, DAN L. TARANIK, and KATHRYN S. KIEREIN-YOUNG *In* Jet Propulsion Lab., California Inst. of Tech., Proceedings of the Airborne Visible/Infrared Imaging Spectrometer (AVIRIS) Performance Evaluation Workshop p 76-87 15 Sep. 1988

Avail: NTIS HC A11/MF A01 CSCL 08/2

Airborne Visible/Infrared Imaging Spectrometer (AVIRIS) data for sites in Nevada and Colorado were evaluated to determine their utility for mineralogical mapping in support of geologic investigations. Equal energy normalization is commonly used with imaging spectrometer data to reduce albedo effects. Spectra, profiles, and stacked, color-coded spectra were extracted from the AVIRIS data using an interactive analysis program (QLook) and these derivative data were compared to Airborne Imaging Spectrometer (AIS) results, field and laboratory spectra, and geologic maps. A feature extraction algorithm was used to extract and characterize absorption features from AVIRIS and laboratory spectra, allowing direct comparison of the position and shape of absorption features. Both muscovite and carbonate spectra were identified in the Nevada AVIRIS data by comparison with laboratory and AIS spectra, and an image was made that showed the distribution of these minerals for the entire site. Additional, distinctive spectra were located for an unknown mineral. For the two Colorado sites, the signal-to-noise problem was significantly worse and attempts to extract meaningful spectra were unsuccessful. Problems with the Colorado AVIRIS data were accentuated by the IAR reflectance technique because of moderate vegetation cover. Improved signal-to-noise and alternative calibration procedures will be required to produce satisfactory

reflectance spectra from these data. Although the AVIRIS data were useful for mapping strong mineral absorption features and producing mineral maps at the Nevada site, it is clear that significant improvements to the instrument performance are required before AVIRIS will be an operational instrument.

Author

N89-22162*# New Hampshire Univ., Durham. Complex Systems Research Center.

ASSESSMENT OF AVIRIS DATA FROM VEGETATED SITES IN THE OWENS VALLEY, CALIFORNIA

B. N. ROCK, CHRISTOPHER D. ELVIDGE (Desert Research Inst., Reno, NV.), and N. J. DEFEO *In* Jet Propulsion Lab., California Inst. of Tech., Proceedings of the Airborne Visible/Infrared Imaging Spectrometer (AVIRIS) Performance Evaluation Workshop p 88-96 15 Sep. 1988

Avail: NTIS HC A11/MF A01 CSCL 08/2

Airborne Visible/Infrared Imaging Spectrometer (AVIRIS) data were acquired from the Bishop, CA area, located at the northern end of the Owens Valley, on July 30, 1987. Radiometrically-corrected AVIRIS data were flat-field corrected, and spectral curves produced and analyzed for pixels taken from both native and cultivated vegetation sites, using the JPS SPAM software program and PC-based spreadsheet programs. Analyses focussed on the chlorophyll well and red edge portions of the spectral curves. Results include the following: AVIRIS spectral data are acquired at sufficient spectral resolution to allow detection of blue shifts of both the chlorophyll well and red edge in moisture-stressed vegetation when compared with non-stressed vegetation; a normalization of selected parameters (chlorophyll well and near infrared shoulder) may be used to emphasize the shift in red edge position; and the presence of the red edge in AVIRIS spectral curves may be useful in detecting small amounts (20 to 30 pct cover) of semi-arid and arid vegetation ground cover. A discussion of possible causes of AVIRIS red edge shifts in response to stress is presented.

Author

N89-22169*# Geological Survey, Reston, VA.

EVALUATION OF AIRBORNE VISIBLE/INFRARED IMAGING SPECTROMETER DATA OF THE MOUNTAIN PASS, CALIFORNIA CARBONATITE COMPLEX

JAMES CROWLEY, LAWRENCE ROWAN, MELVIN PODWYSOCKI, and DAVID MEYER (EROS Data Center, Sioux Falls, SD.) *In* Jet Propulsion Lab., California Inst. of Tech., Proceedings of the Airborne Visible/Infrared Imaging Spectrometer (AVIRIS) Performance Evaluation Workshop p 155-161 15 Sep. 1988

Avail: NTIS HC A11/MF A01 CSCL 08/2

Airborne Visible/Infrared Imaging Spectrometer (AVIRIS) data of the Mountain Pass, California carbonatite complex were examined to evaluate the AVIRIS instrument performance and to explore alternative methods of data calibration. Although signal-to-noise estimates derived from the data indicated that the A, B, and C spectrometers generally met the original instrument design objectives, the S/N performance of the D spectrometer was below expectations. Signal-to-noise values of 20 to 1 or lower were typical of the D spectrometer and several detectors in the D spectrometer array were shown to have poor electronic stability. The AVIRIS data also exhibited periodic noise, and were occasionally subject to abrupt dark current offsets. Despite these limitations, a number of mineral absorption bands, including CO₃, Al-OH, and unusual rare earth element bands, were observed for mine areas near the main carbonatite body. To discern these bands, two different calibration procedures were applied to remove atmospheric and solar components from the remote sensing data. The two procedures, referred to as the single spectrum and the flat field calibration methods gave distinctly different results. In principle, the single spectrum method should be more accurate; however, additional fieldwork is needed to rigorously determine the degree of calibration success.

Author

N89-22170*# Jet Propulsion Lab., California Inst. of Tech., Pasadena.

DETERMINATION OF IN-FLIGHT AVIRIS SPECTRAL, RADIOMETRIC, SPATIAL AND SIGNAL-TO-NOISE CHARACTERISTICS USING ATMOSPHERIC AND SURFACE MEASUREMENTS FROM THE VICINITY OF THE RARE-EARTH-BEARING CARBONATITE AT MOUNTAIN PASS, CALIFORNIA

ROBERT O. GREEN, GREGG VANE, and JAMES E. CONEL *In its* Proceedings of the Airborne Visible/Infrared Imaging Spectrometer (AVIRIS) Performance Evaluation Workshop p 162-184 15 Sep. 1988

Avail: NTIS HC A11/MF A01 CSCL 08/2

An assessment of the Airborne Visible/Infrared Imaging Spectrometer (AVIRIS) performance was made for a flight over Mountain Pass, California, July 30, 1987. The flight data were reduced to reflectance using an empirical algorithm which compensates for solar, atmospheric and instrument factors. AVIRIS data in conjunction with surface and atmospheric measurements acquired concurrently were used to develop an improved spectral calibration. An accurate in-flight radiometric calibration was also performed using the LOWTRAN 7 radiative transfer code together with measured surface reflectance and atmospheric optical depths. A direct comparison with coincident Thematic Mapper imagery of Mountain Pass was used to demonstrate the high spatial resolution and good geometric performance of AVIRIS. The in-flight instrument noise was independently determined with two methods which showed good agreement. A signal-to-noise ratio was calculated using data from a uniform playa. This ratio was scaled to the AVIRIS reference radiance model, which provided a basis for comparison with laboratory and other in-flight signal-to-noise determinations. Author

N89-22191# Oak Ridge National Lab., TN.

PRELIMINARY DEVELOPMENT OF A SEASHORE-EFFECTS ANALYSIS SYSTEM M.S. Thesis - Miami Univ., Ohio

DENNIS B. MILLER and ROBERT M. CUSHMAN Feb. 1989 130 p

(Contract DE-AC05-84OR-21400)

(DE89-007863; ORNL/CDIAC-23) Avail: NTIS HC A07

A melting of polar ice sheets and mountain glaciers and a thermal expansion of ocean water could lead to a rise in sea level as a result of increasing atmospheric CO₂ concentrations and subsequent global temperature increases. The coastal erosion and inundation caused by this event could create agricultural, economic, demographic, and ecological problems along coastal zones. A preliminary Sea Shore Effects Analysis System (SEAS) data base was developed to answer questions on the effects of global sea level rise. Resources potentially affected by a rise in sea level were identified, resulting in the acquisition of eight data sets. Ten other sources of data were located but are currently unavailable. The data are stored in SAS data sets. This information can be analyzed using the Geographic Information System (GIS) of the Environmental Sciences Division at Oak Ridge National Laboratory and the newly developed Digital Line Graph elevational terrain data of the U.S. Geological Survey. All SEAS data have latitude/longitude locational variables, and, when merged with the terrain data on the GIS, they can be used for a detailed (e.g., 1-m increment) analysis of the effects of sea level rise. Development of the SEAS data base can be continued with an emphasis on locating and obtaining additional data and using the GIS for analysis. DOE

N89-22779*# City Coll. of the City Univ. of New York, NY. Inst. of Marine and Atmospheric Sciences.

PROBABILITIES AND STATISTICS FOR BACKSCATTER ESTIMATES OBTAINED BY A SCATTEROMETER WITH APPLICATIONS TO NEW SCATTEROMETER DESIGN DATA

WILLARD J. PIERSON, JR. Washington NASA Apr. 1989 132 p

(Contract NAGW-690)

(NASA-CR-4228; NAS 1.26:4228) Avail: NTIS HC A07/MF A01 CSCL 20/14

The values of the Normalized Radar Backscattering Cross Section (NRCS), σ (o), obtained by a scatterometer are random variables whose variance is a known function of the expected value. The probability density function can be obtained from the normal distribution. Models for the expected value obtain it as a function of the properties of the waves on the ocean and the winds that generated the waves. Point estimates of the expected value were found from various statistics given the parameters that define the probability density function for each value. Random intervals were derived with a preassigned probability of containing that value. A statistical test to determine whether or not successive values of σ (o) are truly independent was derived. The maximum likelihood estimates for wind speed and direction were found, given a model for backscatter as a function of the properties of the waves on the ocean. These estimates are biased as a result of the terms in the equation that involve natural logarithms, and calculations of the point estimates of the maximum likelihood values are used to show that the contributions of the logarithmic terms are negligible and that the terms can be omitted. Author

N89-22970*# Stanford Univ., CA. Remote Sensing Lab.

EVALUATION OF THE PORTABLE INSTANTANEOUS DISPLAY ANALYSIS SPECTROMETER (PIDAS) Final Report, 1 Oct. 1987 - 30 Nov. 1988

R. J. P. LYON, TOD RUBIN, and MAKOTO OHASHI 3 Jun. 1988 90 p Prepared in cooperation with Pasco Corp. (Japan) (Contract NAGW-1252)

(NASA-CR-184878; NAS 1.26:184878) Avail: NTIS HC A05/MF A01 CSCL 14/2

The Portable Instantaneous Display Analysis System (PIDAS) was evaluated by measuring 125 spectra of mineral specimens and rock samples under the following conditions: in the laboratory under artificial illumination and outdoors, on the building patio, while still using the line voltage electric power supplies. The PIDAS was compared and contrasted with the GEOSCAN PFS, Daedalus-Spectrafax 440, and the Geophysical Environmental Research (GER) IRIS Mark 4. B.G.

N89-22975*# Max-Planck-Inst. fuer Meteorologie, Hamburg (Germany, F.R.).

DEVELOPMENT OF A SATELLITE SAR IMAGE SPECTRA AND ALTIMETER WAVE HEIGHT DATA ASSIMILATION SYSTEM FOR ERS-1

KLAUS HASSELMANN, SUSANNE HASSELMANN, EVA BAUER, CLAUS BRUENING, SUSANNE LEHNER, HANS GRABER, and PIERO LIONELLO (Consiglio Nazionale delle Ricerche, Venice, Italy) Paris, France ESA Jul. 1988 165 p (Contract NAS7-918; JPL-957652; ESA-6875/87/HGE/I(SC); N00014-83-G-0126; ST2J-0044-8-D; BMFT-07-KR-2121) (NASA-CR-182685; NAS 1.26:182685; ESA-CR(P)-2710; ETN-89-94241; REPT-19) Avail: NTIS HC A08/MF A01 CSCL 05/2

The applicability of ERS-1 wind and wave data for wave models was studied using the WAM third generation wave model and SEASAT altimeter, scatterometer and SAR data. A series of global wave hindcasts is made for the surface stress and surface wind fields by assimilation of scatterometer data for the full 96-day SEASAT and also for two wind field analyses for shorter periods by assimilation with the higher resolution ECMWF T63 model and by subjective analysis methods. It is found that wave models respond very sensitively to inconsistencies in wind field analyses and therefore provide a valuable data validation tool. Comparisons between SEASAT SAR image spectra and theoretical SAR spectra derived from the hindcast wave spectra by Monte Carlo simulations yield good overall agreement for 32 cases representing a wide variety of wave conditions. It is concluded that SAR wave imaging is sufficiently well understood to apply SAR image spectra with confidence for wave studies if supported by realistic wave models and theoretical computations of the strongly nonlinear mapping of the wave spectrum into the SAR image spectrum. A closed nonlinear integral expression for this spectral mapping relation is derived which avoids the inherent statistical errors of Monte Carlo

computations and may prove to be more efficient numerically.
ESA

N89-23122# SRI International Corp., Menlo Park, CA. Artificial Intelligence Center.

OVERVIEW OF THE SRI CARTOGRAPHIC MODELING ENVIRONMENT

ANDREW J. HANSON and LYNN H. QUAM *In Science Applications International Corp., Proceedings: Image Understanding Workshop, Volume 2 p 576-582 Apr. 1988*
(Contract MDA903-86-C-0084; NSF IST-85-11751)
Avail: NTIS HC A99/MF E03 CSCL 08/2

Image manipulation capabilities provided to support research on interactive, semiautomated, and automated computer-based cartographic activities are described. The cartographic features and data that can be entered include multiple images, camera models, digital terrain elevation data, point, line, and area cartographic features, and a wide assortment of three-dimensional objects. Interactive capabilities include free-hand feature entry, altering features while constraining them to conform to the terrain and lighting geometry, adjustment of feature parameters, and the adjustment of the camera model to display the scene features from arbitrary viewpoints. Cartographic features are depictable either as wire-frame sketches for interactive purposes or as texture-mapped renderings for realistic scene synthesis. High-quality simulated scenes are created by texture-mapping images onto terrain data and adding renderings of cartographic features using depth-buffering and anti-aliasing techniques. Motion sequences can be created by choosing a series of camera models and rendering the simulated appearance of the scene from each viewpoint.

Author

N89-23287# Swedish Defence Research Establishment, Linköping. Dept. of Information Technology.

ACTIVITIES REPORT OF THE DIVISION OF OPTICAL TECHNOLOGY (FOA 33) Annual Report, fiscal year 1987/88

DIETMAR LETALICK, ed. Nov. 1988 21 p
(FOA-C-30507-3.1; ISSN-0347-3708; ETN-89-94307) Avail: NTIS HC A03/MF A01; Swedish Defence Research Establishment, P.O. Box 1165, S-581 11, Linköping, Sweden, 50 Swedish crowns

Research on hydro-optics; laser remote sensing; coherent CO₂ laser radar; optical signatures; atmospheric transmission; ionizing radiation effects on electronics; fiber optics; optical processing; and terrain models is summarized.
ESA

N89-23942# Institut fuer Angewandte Geodaesie, Frankfurt am Main (Germany, F.R.).

DEFINITION AND FILLING OF INFORMATION SYSTEMS: CHALLENGE FOR A PHOTOGRAMMETRIC SERVICE ENTERPRISE [DEFINITION UND FUELLUNG VON INFORMATIONSSYSTEMEN: HERAUSFORDERUNG AN EIN PHOTOGRAMMETRISCHES

Dienstleistungsunternehmen]

HANS-DIETER ARNOLD and RALF SCHROTH *In its Reports on Cartography and Geodesy. Series 1, Number 101 p 7-16 1988 In GERMAN; ENGLISH summary*
Avail: NTIS HC A07/MF A01

Hardware and software components for graphic data processing and their applications, as well as data acquisition methods are presented. The hardware and software necessary to establish information systems for complex planning aims and decision making in all areas of the economy and administration are discussed; the specific task must first be defined in order to collect the basic data necessary to operate the systems. The equipment necessary for filling of systems, in particular in graphic data processing, is described. A review of aims demonstrates the broad spectrum of ways of obtaining information and shows the differences with traditional photogrammetry. A process for obtaining information is presented and examples are given.
ESA

N89-23956*# Alaska Univ., Fairbanks. Geophysical Inst. **REMOTE SENSING OF GLOBAL SNOWPACK ENERGY AND MASS BALANCE: IN-SITU MEASUREMENTS ON THE SNOW OF INTERIOR AND ARCTIC ALASKA Semiannual Report**
CARL S. BENSON Mar. 1989 11 p
(Contract NAG5-887)
(NASA-CR-180078; NAS 1.26:180078) Avail: NTIS HC A03/MF A01 CSCL 08/12

Observations led to a study of the physical properties of snow and the processes which operate on it. These observations included microwave brightness temperatures in interior Alaska which revealed: (1) up to three times more variability from one cell (1/2 degree latitude x 1/2 degree longitude) to the next in winter than in summer (5 to 15 K in winter and about 5 K in summer); (2) the overall range of temperature from week to week is about seven times greater in winter than in summer; (3) the microwave brightness temperature is about 25 K less than air temperature during summer but 35 to 60 K less during winter; and (4) the presence of snow cover appears to contribute to increasing the difference between air temperature and brightness temperature. The role of irregular substrate under the snow in enhancing convection has been studied with particular attention to variations in snow cover on water surfaces and in forested regions. LANDSAT imagery has been obtained to prepare a classification of ground surface types of the area. The extreme conditions of the 1988 to 1989 winter are discussed with respect to comparing the microwave data sets from 1985, and before, up to the present. The use of the Mt. Wrangell area as aerial photogrammetric controls for glacier measurements is given attention.
A.D.

N89-23970# Beleidscommissie Remote Sensing, Delft (Netherlands).

METEOSAT THERMAL INERTIA MAPPING FOR STUDYING WETLAND DYNAMICS IN THE WEST-AFRICAN SAHEL Final Report

A. ROSEMA, J. L. FISELIER, and W. F. RODENBURG (Leiden Univ., Netherlands) Oct. 1988 45 p Original contains color illustrations
(Contract BCRS-PROJ.-OP-3.3)
(BCRS-88-10A; ETN-89-94289) Avail: NTIS HC A03/MF A01

Meteosat noon and midnight imagery of various dates in 1978, 1983, and 1985 were used to study the dynamics of flooding in the Niger delta and the Lake Chad basin. Infrared imagery was processed to derive images and maps of evapotranspiration (ETP) and thermal inertia (TI). The TI products give the best information on the flooding phase and extension. The ETP images provide valuable supplementary information, in particular on the presence of water in the root zone. The flooded area was quantified by counting pixels, which have a TI above a given threshold; in this way the flooding cycle can be reconstructed and the maximum extension determined for each year. It is shown that Meteosat TI mapping can be used successfully to study the dynamics of flooding in Sahelian wetlands.
ESA

N89-23972# Karlsruhe Univ. (Germany, F.R.). Dept. of Photogrammetry and Remote Sensing.

RESEARCH FOR OPTIMIZATION OF FUTURE MOMS SENSORS Final Report

H. KAUFMANN, F. J. BEHR, R. GEERKEN, H. JACOBS, K. JUNG, T. VOEGTLE, and W. WEISBRICH Apr. 1988 55 p In GERMAN; ENGLISH summary
(Contract BMFT-01-QS-86-206)
(ETN-89-94424) Avail: NTIS HC A04/MF A01

By means of spectroradiometer data and a developed software package for data evaluation, spectral bands and one panchromatic band for the MOMS-02 sensor were defined together with the hardware. The analysis of the relative and absolute geometric quality of MOMS-01 data as compared with LANDSAT Thematic Mapper and SPOT-HRV data is described. Within this context a correlation technique for optimized data merge was developed for combining MOMS data with data of other sensors.
ESA

N89-24589# Interior Dept., Washington, DC.

GEOLOGICAL GYROCOMPASS Patent Application

M. H. MCKEOWN and S. C. BEASON 11 Aug. 1988 9 p
Filed 11 Aug. 1988
(PB89-133086; PAT-APPL-7-231-017) Avail: NTIS HC A02/MF
A01 CSCL 14/2

The geological gyrocompass is an accurate, portable instrument useful for geologic mapping and surveying which employs an aircraft gyrocompass, strike reference bars, a pair of sights and levelling devices for horizontally levelling the instrument. A clinometer graduated in degrees indicates the dip of the surface being measured. GRA

N89-24688# Deutsche Forschungs- und Versuchsanstalt fuer Luft- und Raumfahrt, Oberpfaffenhofen (West Germany).

NECESSITY AND BENEFIT OF THE X-SAR SPACE SHUTTLE EXPERIMENT

WOLFGANG KEYDEL and HERWIG OETTL Oct. 1988 41 p
In GERMAN; ENGLISH summary Original contains color illustrations
(DFVLR-MITT-88-29; ISSN-0176-7736; ETN-89-94375) Avail:
NTIS HC A03/MF A01; DFVLR, VB-PL-DO, Postfach 90 60 58,
5000 Cologne, Federal Republic of Germany, 26.50 deutsche
marks

The X, L, and C-band synthetic aperture radars (SAR) planned to fly in 1992 on space shuttle missions are investigated for their effectiveness in Earth surface vegetation classification and recognition. The scattering of electromagnetic waves by twigs, leaves, branches, and trunks permits vegetation growth length estimation. Earth surface roughness is analyzed by Rayleigh criterion. The SAR sensors are well adapted to Earth surface observation independently of daylight and atmospheric conditions. ESA

N89-24689# Aerospatiale, Cannes La Bocca (France).

THE ADVANCED OCEAN CHLOROPHYLL METER (OCM). A SPECTRAL IMAGING DEVICE FOR THE OBSERVATION OF THE OCEANS [L'ADVANCED OCM: UN SPECTRO-IMAGEUR POUR L'OBSERVATION DES OCEANS]

G. CERUTTI-MAORI 1988 4 p In FRENCH
(REPT-882-440-118; ETN-89-94511) Avail: NTIS HC A02/MF
A01

The main results of a feasibility study are presented. The ESA project concerns an optical multispectral radiometer of the pushbroom type for the study of the oceans in the solar spectrum (0.4 to 1.1 microns). The goal is to establish the space-time distribution of chlorophyll. The instrument choice includes the use of charge coupled devices in mosaic layout. The payload is 62 kg with 90 watts power requirements and a 0.8 reliability. ESA

N89-24691# Laboratoire de Meteorologie Dynamique du CNRS, Palaiseau (France).

REFINEMENTS IN THE CLOUD DETECTION SCHEME OF THE 3I SYSTEM. COMPARISON WITH AVHRR PRODUCTS

CHANTAL CLAUD, NOELLE A. SCOTT, CLAUDE KERGOMARD, and JEAN-CLAUDE GASCARD 1988 3 p Presented at the International Radiation Symposium, Lille, France, 18-24 Aug. 1988 (ETN-89-94531) Avail: NTIS HC A02/MF A01

The improved initialization inversion is designed for retrieving meteorological parameters from operational satellites of the Tiros-N series. Refinements in the cloud detection scheme are presented, and particularly the detection of low clouds over sea ice covered areas. The method is based on the discrimination between open water and sea ice from microwave observation and the detection of clouds by comparing two infrared channels. The results are validated using AVHRR observations. ESA

N89-24692# European Space Agency, Paris (France).

IMAGING SPECTROMETRY FOR LAND APPLICATIONS

T. D. GUYENNE, ed. Nov. 1988 56 p Workshop held in Frascati, Italy, 19-21 Apr. 1988 Original contains color illustrations

(ESA-SP-1101; ISSN-0379-6566; ETN-89-94447) Avail: NTIS HC A04/MF A01; ESA Publications Div., ESTEC, Noordwijk, Netherlands, 10 dollars or 25 Dutch guilders

Airborne fluorescence land imagers, high resolution spectrometers for the Earth Observation System, imaging spectrometers, and ESA programs were discussed.

ESA

N89-24694# Moniteq Ltd., Concord (Ontario).

THE FLI AIRBORNE IMAGING SPECTROMETER: A HIGHLY VERSATILE SENSOR FOR MANY APPLICATIONS

R. A. H. BUXTON In ESA, Imaging Spectrometry for Land Applications p 11-16 Nov. 1988 Original contains color illustrations

Avail: NTIS HC A04/MF A01; ESA Publications Div., ESTEC, Noordwijk, Netherlands, 10 dollars or 25 Dutch guilders

The characteristics and applications of the Fluorescence Line Imager (FLI) are described. The FLI was used to acquire imagery over vegetated land targets during 4.5 yr. The first design was based on sensing the solar-stimulated fluorescence of chlorophyll in plankton in water from space. Images of the chlorophyll red edge in stressed vegetation are applied to evaluate forest decline, mineral and hydrocarbon exploration, and landfill. ESA

N89-24695*# Jet Propulsion Lab., California Inst. of Tech., Pasadena.

HIRIS: NASA'S HIGH-RESOLUTION IMAGING SPECTROMETER FOR THE EARTH OBSERVING SYSTEM (EOS)

J. DOZIER and M. HERRING In ESA, Imaging Spectrometry for Land Applications p 17-25 Nov. 1988 Original contains color illustrations

Avail: NTIS HC A04/MF A01; ESA Publications Div., ESTEC, Noordwijk, Netherlands, 10 dollars or 25 Dutch guilders CSCL 14/2

The HIRIS design includes 10 nm spectral bands from 0.4 to 2.5 micron at 30 m spatial resolution over a 24 or 30 km swath. This resolution allows identification of many minerals in rocks and soils, important algal pigments in oceans and inland water and spectral changes in land canopy. In the 824 km orbit altitude proposed, the cross track pointing capability allows 4 to 5 views during a 16 day revisit cycle. ESA

N89-24697# Deutsche Forschungs- und Versuchsanstalt fuer Luft- und Raumfahrt, Oberpfaffenhofen (West Germany). Inst. fuer Optoelektronik.

DFVLR ACTIVITIES RELATED TO IMAGING SPECTROMETRY

G. KRITIKOS, H. VANDERPIEPEN, and M. SCHROEDER In ESA, Imaging Spectrometry for Land Applications p 35-41 Nov. 1988 Original contains color illustrations

Avail: NTIS HC A04/MF A01; ESA Publications Div., ESTEC, Noordwijk, Netherlands, 10 dollars or 25 Dutch guilders

The institute's research, technologies, and application activities related to imaging spectroscopy are discussed. Special emphasis is given to the development of an airborne programmable imaging spectrometer. The main application is the monitoring of water color and fluorescence for research in marine biology, ecology, water pollution, sediment transport, and climatology. ESA

N89-24698# Institute of Ocean Sciences, Sidney (British Columbia).

DEVELOPMENT OF AN IMAGING SPECTROMETER FOR REMOTE SENSING: THE FLI PROGRAM

J. F. R. GOWER In ESA, Imaging Spectrometry for Land Applications p 43-45 Nov. 1988

Avail: NTIS HC A04/MF A01; ESA Publications Div., ESTEC, Noordwijk, Netherlands, 10 dollars or 25 Dutch guilders

The Fluorescence Line Imager (FLI) spectrometer development is described. The original design intends to detect the near surface distribution of phytoplankton in sea water by imaging the naturally stimulated fluorescence emission from chlorophyll-a. The use of CCD detectors results in flexibility in the positioning of spectral

08 INSTRUMENTATION AND SENSORS

bands in the sensor. The design requirements for sea and land application are outlined. Examples of FLI applications are given.

ESA

N89-24701# Canada Centre for Remote Sensing, Ottawa (Ontario).

IMAGING SPECTROMETRY AT THE CANADA CENTRE FOR REMOTE SENSING

R. A. NEVILLE *In* ESA, Imaging Spectrometry for Land Applications p 55-56 Nov. 1988

Avail: NTIS HC A04/MF A01; ESA Publications Div., ESTEC, Noordwijk, Netherlands, 10 dollars or 25 Dutch guilders

The institute's activities in the field are discussed. The supportive role in the development of the Fluorescence Line Imager, providing calibration facilities and assistance in installations in aircraft is described.

ESA

09

GENERAL

Includes economic analysis.

A89-34703

LANDSAT COMMERCIALIZATION - KEYS TO FUTURE SUCCESS

C. P. WILLIAMS (Earth Observation Satellite Co., Lanham, MD) International Journal of Remote Sensing (ISSN 0143-1161), vol. 10, Feb. 1989, p. 265-274.

The lessons learned over the first thirty-six months of commercialization effort on the Landsat program by Eosat have dictated a change in marketing philosophy and a dramatic rethinking of the strategies necessary to produce an economically viable commercial program. This paper presents EOSAT's philosophy and approach to the commercialization of satellite remote sensing.

Author

A89-34704

COMMERCIALIZATION OF REMOTE SENSING IN THE U.S.A. - THE SPOT PERSPECTIVE

P. BESCOND (SPOT Image Corp., Reston, VA) International Journal of Remote Sensing (ISSN 0143-1161), vol. 10, Feb. 1989, p. 289-293.

Over the past three decades satellite-based remote sensing has developed from experimental programs to a user-oriented commercial industry. The current success and future of the industry are dependent on both the commercial perspective and the advanced technical capabilities as exemplified in the SPOT system. As the U.S. has the largest and most advanced user community in the world, the SPOT programs, commercial experience, and resultant industry trends seen in the U.S. are indicative of, and setting the standards for, industry development in the rest of the world.

Author

A89-34708

ECONOMIC RELATIONS OF THE ALL-UNION TRADE ASSOCIATION SOJUZKARTA AND THE GEODETIC AND CARTOGRAPHIC SERVICES OF THE U.S.S.R. TO FOREIGN COUNTRIES

V. A. PISKULIN (Vsesoiuznoe Ob'edinenie Soiuzkarta, Moscow, USSR) International Journal of Remote Sensing (ISSN 0143-1161), vol. 10, Feb. 1989, p. 319-332.

A89-34712

THE EXPERIENCE OF THE COMMISSION OF THE EUROPEAN COMMUNITIES IN THE USE OF REMOTE SENSING FOR THE IMPLEMENTATION OF COMMUNITY POLICIES

J. P. CONTZEN (CEC, Joint Research Centre, Brussels, Belgium) International Journal of Remote Sensing (ISSN 0143-1161), vol. 10, Feb. 1989, p. 385-394. refs

The integration of remote sensing data in the information used by the services of the European Commission for the preparation and implementation of sectorial EC policies is making rapid progress. The principal areas of application include agricultural statistics, forestry management, and land and sea environmental monitoring. This paper illustrates the growing role of remote sensing within the context of the EC's actions for the protection of the marine environment and resources. It describes the development of remote-sensing-based methods for the surveillance of sea pollution and the study of coastal upwelling.

Author

A89-35685

ANALYSIS OF THE POTENTIAL OF USING SPACE PHOTOGRAPHIC DATA OBTAINED WITH THE PKF-1K CAMERA TO SOLVE SCIENTIFIC, ECONOMIC, AND EDUCATIONAL-METHODOLOGICAL PROBLEMS [ANALIZ VOZMOZHNOSTEI ISPOL'ZOVANIYA KOSMICHESKOI FOTOINFORMATSII, POLUCHENNOI FOTOAPPARATOM PKF-1K DLIA RESHENIYA NAUCHNYKH, KHOZIAISTVENNYKH I UCHEBNO-METODICHESKIKH ZADACH]

A. P. VOROZHEIKIN, S. M. POPOV, P. B. STYSLOVICH, and P. N. IAZEV *Geodeziia i Aerofotos'emka* (ISSN 0536-101X), no. 3, 1988, p. 85-88. In Russian.

A89-35853#

A SURVEY OF THE OPERATIONAL STATUS AND NEEDS OF REMOTE SENSING IN EXPLORATION GEOLOGY

FREDERICK B. HENDERSON, III (Geosat Committee, Inc., Norman, OK) and T. H. LEE WILLIAMS (Cooperative Institute for Applied Remote Sensing, Norman, OK) *IN: Thematic Conference on Remote Sensing for Exploration Geology, 6th, Houston, TX, May 16-19, 1988, Proceedings. Volume 1. Ann Arbor, MI, Environmental Research Institute of Michigan, 1988, p. 11-18.*

Results are presented from a survey of Geosat member companies conducted in 1987 to determine the operational status of remote sensing in exploration geology. It is found that the main use of remote sensing by Geosat companies is reconnaissance photogeology at the front end of exploration, usually for undeveloped areas. In addition, consideration is given to other uses of remote sensing technology, trends in basic and applied research and development, data integration, Geographical Information Systems, and international remote sensing for geological exploration.

R.B.

A89-35899#

THE COMMERCIAL LAND REMOTE SENSING MARKET - CURRENT ASSESSMENT, BASELINE FORECAST AND BASELINE ALTERNATIVES

B. M. REGISTER (Houston, University, TX) *IN: Thematic Conference on Remote Sensing for Exploration Geology, 6th, Houston, TX, May 16-19, 1988, Proceedings. Volume 2. Ann Arbor, MI, Environmental Research Institute of Michigan, 1988, p. 647-651.*

The Space Business Research Center of the University of Houston-Clear Lake has undertaken an evaluation of the current commercial status of satellite remote sensing of land areas in the U.S., with a view to the trends that will govern the future of that marketplace. A baseline market forecast is produced by synergistically extrapolating the effects of those trends. Plausible alternatives to the baseline scenario are also assessed; these involve medium-resolution instruments that can be 'piggybacked' on other payloads in LEO, the use of 'throwaway' satellites, as well as such large, complex remote sensing satellites as the proposed 'Mediasat'.

O.C.

A89-42511

STUDYING THE EARTH FROM MANNED SPACECRAFT [ISSLEDOVANIIE ZEMLI S PILOTIRUEMYKH KOSMICHESKIKH KORABLEI]

ALEKSANDR I. LAZAREV, VLADIMIR V. KOVALENOK, and SERGEI V. AVAKIAN *Leningrad, Gidrometeoizdat, 1987, 400 p. In Russian. refs*

Results of visual and instrumental observations of the earth

conducted from Soviet manned spacecraft and from the Salyut orbital research stations are summarized. In particular, attention is given to the structure of the atmosphere and ionosphere; solar and magnetospheric phenomena; specific characteristics of space-based observations; and optical studies conducted by Soviet cosmonauts. The discussion also covers emissions of the atmosphere and ionosphere; cloud cover, and earth surface observations. V.L.

A89-42549

SPACEBORNE STUDIES RELATED TO NATURE CONSERVATION [KOSMICHESSKIE PRIRODOOKHRANNYE ISSLEDOVANIYA]

ARKADII I. MELUA Leningrad, Izdatel'stvo Nauka, 1988, 176 p. In Russian. refs

The information content of various types of spaceborne measurements, including visual and spectrometric, geomagnetic-field, and radioactivity measurements, is discussed. The most advanced scientific trends applied in the area of nature conservation studies are described together with the instrumental systems used in these investigations; the effect that these studies have on the national economy is examined. Particular attention is given to experiments carried out recently by the Mir, Salyut, Soyuz, Cosmos, and Meteor spacecraft. I.S.

N89-20540# National Aerospace Lab., Amsterdam (Netherlands). Space Div.

A SYSTEMATIC WORLDWIDE LANDCOVER OF SATELLITE MOSAICS

F. B. VANDERLAAN 31 Aug. 1987 7 p Presented at the Willie Nordberg Symposium on Remote Sensing towards Operational Cartographic Application, Graz, Austria, Sep. 1987 (NLR-MP-87062-U; ETN-89-94041) Avail: NTIS HC A02/MF A01

The increasing gap between the number of detailed satellite images (of, e.g., LANDSAT) recorded and the number actually used is discussed. A major cause for limited use of potentially available imagery is the cost. A complete range of national, continental, and worldwide applications has not developed for that reason. Possibilities for a wide use of imagery at affordable cost, particularly in developing regions are outlined. A central role in making satellite imagery available at a large scale is given to printed mosaics, in view of the high printing quality possible. ESA

N89-20558# Radian Corp., Research Triangle Park, NC. Progress Center.

NATIONAL AIR TOXICS INFORMATION CLEARINGHOUSE: ONGOING RESEARCH AND REGULATORY DEVELOPMENT PROJECTS, JULY 1988 Interim Report

SUSAN KAY M. BUCHANAN and THERESA K. MOODY Jul. 1988 194 p

(Contract EPA-68-02-4330)

(PB89-103428; DCN-88-239-001-44-07; EPA/450/5-88/004)

Avail: NTIS HC A09/MF A01 CSCL 13/2

The document is divided into 2 parts and an appendix. The first part lists 365 air toxic projects currently in progress at EPA, NIOSH, and state and local agencies. A brief description of each project and a contact name, office, and telephone number are given. The second part contains the index that allows readers to locate projects of interest. Projects are indexed by agency, project type, chemical name, Chemical Abstract Service number, and source category Standard Industrial Classification Code. The appendix lists regulatory development projects on toxic chemicals underway at the EPA's Office of Drinking Water. Author

N89-22976# Swedish Defence Research Establishment, Linköping. Dept. of Information Technology.

MINIMUM NUMBER OF SATELLITES FOR PERIODIC COVERAGE

ULF EKBLAD Dec. 1988 22 p

(FOA-C-30511-9.4; ISSN-0347-3708; ETN-89-94308) Avail: NTIS

HC A03/MF A01; Swedish Defence Research Establishment, P.O. Box 1165, S-581 Linköping, Sweden, 50 Swedish crowns

The problem of obtaining a periodic coverage of a site by satellites is considered. Periodic coverage is defined as a certain number of observations of a specified site per time interval. This reduces the number of satellites required substantially. One can e.g., obtain periodic coverage of a site from low Earth orbit with as few as one or two satellites if the revisit time is three days or longer. ESA

N89-23969# Beleidscommissie Remote Sensing, Delft (Netherlands).

ON THE INTERNATIONAL COMMERCIALIZATION OF REMOTE SENSING Final Report [INTERNATIONALE COMMERCIALISERING REMOTE SENSING]

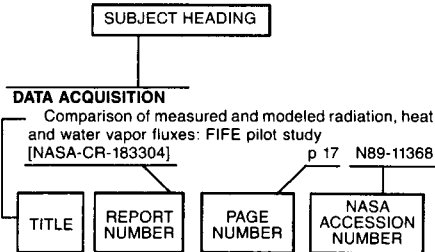
Jan. 1988 81 p In DUTCH Prepared in cooperation with NEDECO, Netherlands; EUROCONSULT B.V., Arnhem, Netherlands; and DHV Raadgevend Ingenieursbureau B.V., Amersfoort, Netherlands

(Contract BCRS-PROJ.-CO-1.3)

(BCRS-88-02; ETN-89-94288) Avail: NTIS HC A05/MF A01

Results of Dutch remote sensing research that have possible commercial applications were inventoried and analyzed. The future demand for remote sensing products by international financing institutions was evaluated and a market analysis was performed. The analysis shows that, if the commercialization criteria are strictly applied to the present products, only a very low percentage can be commercialized. The available expertise can be valuable for the development of the operational use of remote sensing for various applications. ESA

Typical Subject Index Listing



The subject heading is a key to the subject content of the document. The title is used to provide a description of the subject matter. When the title is insufficiently descriptive of document content, a title extension is added, separated from the title by three hyphens. The (NASA or AIAA) accession number and the page number are included in each entry to assist the user in locating the abstract in the abstract section. If applicable, a report number is also included as an aid in identifying the document. Under any one subject heading, the accession numbers are arranged in sequence with the AIAA accession numbers appearing first.

A

ABSORPTION SPECTRA

- Automated extraction of absorption features from Airborne Visible/Infrared Imaging Spectrometer (AVIRIS) and Geophysical and Environmental Research Imaging Spectrometer (GERIS) data p 39 N89-22160
- Evaluation of Airborne Visible/Infrared Imaging Spectrometer Data of the Mountain Pass, California carbonate complex p 60 N89-22169

AIRACTIVITY

- Optical properties of oceanic suspended matter and their interpretation for remote sensing of phytoplankton [GKSS-88/E/40] p 46 N89-24013

ADVANCED VERY HIGH RESOLUTION RADIOMETER

- GEOSAT altimeter sea-ice mapping p 49 A89-34267
- Applications of AVHRR imagery in frontier exploration p 23 A89-35885
- Estimation of regional surface resistance to evapotranspiration from NDVI and thermal-IR AVHRR data --- Normalized Difference Vegetation Index p 55 A89-39872
- Applications of AVHRR data; Proceedings of the Third European AVHRR Data Users' Meeting, University of Oxford, England, Dec. 16-18, 1987 p 55 A89-40126
- Activities at the Norwegian Hydrotechnical Laboratory p 55 A89-40129
- Pixel and sub-pixel accuracy in geometrical correction of AVHRR p 30 A89-40134
- An AVHRR mosaic image of Antarctica p 30 A89-40135
- Satellite-derived low-level atmospheric water vapour content from synergy of AVHRR with HIRS --- High Resolution Infrared Radiation Sounder p 30 A89-40139
- Observations of volcanic ash clouds in the 10-12 micron window using AVHRR/2 data p 30 A89-40143
- Mesoscale variability of sea surface temperature in the North Atlantic p 17 A89-40145

- Using NOAA AVHRR imagery in assessing water quality parameters p 55 A89-40148
- A phenological description of Iberian vegetation using short wave vegetation index imagery p 2 A89-40149
- Monitoring the phenology of Tunisian grazing lands p 3 A89-40150
- NOAA AVHRR and its uses for rainfall and evapotranspiration monitoring p 56 A89-40151
- AVHRR for monitoring global tropical deforestation p 56 A89-40152
- AVHRR data processing to study the surface canopies in temperate regions - First results of HAPEX-MOBILHY p 30 A89-40153
- Lake area measurement using AVHRR - A case study p 31 A89-40154
- An algorithm for snow and ice detection using AVHRR data - An extension to the Apollo software package p 31 A89-40155
- Multi-spectral classification of snow using NOAA AVHRR imagery p 31 A89-40156
- Ice cover on Chesapeake Bay from AVHRR (Advanced Very High Resolution Radiometer) and LANDSAT imagery, winter of 1987-88 p 59 N89-21415
- [PB89-117261]
- NOAA (National Oceanic and Atmospheric Administration) AVHRR (Advanced Very High Resolution Radiometer) observations during the marginal ice zone experiment, between Spitzbergen and Greenland, June 7 to 18 July 1984 [AD-A204911] p 19 N89-22280

AERIAL PHOTOGRAPHY

- Representation and recognition of elongated regions in aerial images p 19 A89-33684
- A raster approach to population estimation using high-altitude aerial and space photographs p 19 A89-33872
- Use of aerial and space photography for the detection of faults and neotectonic movements in Crimea and the Azov Coastal Region p 9 A89-34003
- Dynamics of present-day geological processes from remotely sensed data p 9 A89-34004
- Use of aerial and space methods for observations and studies of the morphology and kinematics of recent movements along some faults of the Baikal Rift Zone p 10 A89-34007
- Methods for investigating seismically active zones using remote imagery p 20 A89-34013
- Use of aerial photography to inventory aquatic vegetation p 50 A89-34362
- Vegetation and landscape of Kora National Reserve, Kenya p 6 A89-34945
- Mapping coastal evolution in Sri Lanka using aerial photographs p 6 A89-34948
- Implication of patterns of faulting and hydrothermal alteration from Landsat TM images and NMAP aerial photos to mineral exploration and tectonics of the Virginia Range, Nevada --- National High Altitude Photography p 11 A89-35868
- From large-scale to small-scale - Economic geologic-geomorphic mapping using aerial photographs and Landsat images p 7 A89-35884
- Conjugate synthetic normal faults around the Gulf of Salwa, southwestern Qatar, the Arabian Gulf p 12 A89-35886
- Radiometric correction of aerial and space remote-sensing images p 25 A89-37323
- A raster approach to topographic map revision p 26 A89-37946
- High altitude laser ranging over rugged terrain p 54 A89-39092
- Analytical independent model triangulation strip adjustment using shore-line constraints p 28 A89-39093
- Digital photogrammetric processing systems - Current status and prospects p 28 A89-39095
- Sea surface spectrum from aerial photographs - Laboratory model studies p 30 A89-39674
- Aerial photography and specialized photographic studies --- Russian book p 31 A89-40488
- Estimating stand density of loblolly pine in northern Louisiana using aerial photographs and probability proportional to size p 34 A89-41171

- Image understanding research at SRI International p 42 N89-23080
- Cooperative methods for road tracking in aerial imagery p 42 N89-23101

AERONOMY

- Comparison of field-aligned currents at ionospheric and magnetospheric altitudes p 9 A89-33540

AEROSOLS

- Aerosol analysis with the Coastal Zone Color Scanner - A simple method for including multiple scattering effects p 25 A89-37291
- Observations of volcanic ash clouds in the 10-12 micron window using AVHRR/2 data p 30 A89-40143
- The investigation of advanced remote sensing, radiative transfer and inversion techniques for the measurement of atmospheric constituents [NASA-CR-172599] p 36 N89-20531
- Correlation between satellite-derived aerosol characteristics and oceanic dimethylsulfide (DMS) [AD-A206179] p 6 N89-24759

AGGREGATES

- Geobotanical determination of aggregate source material using Airborne Thematic Mapper imagery p 1 A89-35865
- Assessing aggregate resource potential in the Canadian Shield - A knowledge-based approach p 23 A89-35877
- Geobotanical remote sensing for determination of aggregate source material [AD-A205943] p 45 N89-23962

AGRICULTURE

- The condition of natural features as related to their intrinsic microwave and IR emission fields p 2 A89-37320
- Microwave X-band radiometric characterization of Brazilian soils by measurement of the complex permittivity [INPE-4588-PRE/1319] p 3 N89-24685

AIR LAND INTERACTIONS

- Mapping freeze/thaw boundaries with SMMR data [NASA-CR-184991] p 9 N89-23961

AIR NAVIGATION

- Loran C field strength contours: Contiguous US [DOT/FAA/CT-TN89/16] p 8 N89-23437

AIR POLLUTION

- Spacelab 2 Upper Atmospheric Modification Experiment over Areibo. II - Plasma dynamics p 4 A89-38897
- National Air Toxics Information Clearinghouse: Ongoing research and regulatory development projects, July 1988 [PB89-103428] p 65 N89-20558
- Air pollution effects field research facility: Ozone flow control and monitoring system p 5 N89-22192
- The relationship between in-lake sulfate concentration and estimates of atmospheric sulfur deposition for subregions of the eastern lake survey [DE89-009868] p 5 N89-24749

AIR SEA ICE INTERACTIONS

- NOAA (National Oceanic and Atmospheric Administration) AVHRR (Advanced Very High Resolution Radiometer) observations during the marginal ice zone experiment, between Spitzbergen and Greenland, June 7 to 18 July 1984 [AD-A204911] p 19 N89-22280

AIR WATER INTERACTIONS

- Interaction between net shortwave flux and sea surface temperature p 15 A89-34878
- Methodology for the remote sensing of fluxes of heat, moisture, and effective radiation in the ocean-atmosphere system p 16 A89-35686
- Precipitation in the Canadian Atlantic Storms Program - Measurements of the acoustic signature p 50 A89-35819
- The rate of gas exchange between the ocean and the atmosphere using microwave radiometer data p 25 A89-37471
- The Naval Research Laboratory's Air-Sea Interaction Blimp Experiment p 53 A89-37981
- OSRMS (Ocean Surface Roughness Measurement System): The DREP (Defence Research Establishment Pacific) near-nadir scatterometer [AD-A202983] p 38 N89-21460

- Nimbus-7 data product summary
[NASA-RP-1215] p 39 N89-22152
- AIRBORNE EQUIPMENT**
- Hyperspectral interactions - Invariance and scaling ---
applied to remote sensing data p 48 A89-32837
- Geobotanical determination of aggregate source
material using Airborne Thematic Mapper imagery
p 1 A89-35865
- Vegetation reflectance features in AVIRIS data
p 22 A89-35867
- Phase A study for the extension of the CAESAR scanner
with a sensor module for the far infrared
[BCRS-88-09] p 59 N89-20539
- Imaging Spectrometry for Land Applications
[ESA-SP-1101] p 63 N89-24692
- The activities of the British National Space Centre
(BNSC) in the field of imaging spectrometry
p 47 N89-24696
- Development of an imaging spectrometer for remote
sensing: The FLI program p 63 N89-24698
- Imaging spectrometry at the Canada Centre for Remote
Sensing p 64 N89-24701
- AIRBORNE LASERS**
- Short- and long-term memory effects in intensified array
detectors - Influence on airborne laser fluorosensor
measurements p 47 A89-32836
- Determination of spectral signatures for remote laser
sensing of vegetation p 35 A89-42611
- AIRBORNE SURVEILLANCE RADAR**
- Airborne imaging radar system for monitoring sea
pollution
[MBB-UK-0016-87-PUB] p 58 A89-42941
- AIRCRAFT INSTRUMENTS**
- Laser altimetry measurements from aircraft and
spacecraft p 56 A89-41691
- ALASKA**
- KRMS (K-band Radiometric Mapping System) SSM/I
validation March 1988 quick look report
[NASA-CR-185320] p 8 N89-23766
- Remote sensing of global snowpack energy and mass
balance: In-situ measurements on the snow of interior and
Arctic Alaska
[NASA-CR-180078] p 62 N89-23956
- ALBEDO**
- Radiative transfer calculations for characterizing
obscured surfaces using time-dependent backscattered
pulses p 48 A89-32841
- Snowmelt increase through albedo reduction
[AD-A204523] p 18 N89-22175
- ALGORITHMS**
- Theoretical algorithms for satellite-derived sea surface
temperatures p 21 A89-35159
- Automated extraction of absorption features from
Airborne Visible/Infrared Imaging Spectrometer (AVIRIS)
and Geophysical and Environmental Research Imaging
Spectrometer (GERIS) data p 39 N89-22160
- Shortest paths in a digitized map using a tile-based data
structure
[PB89-143432] p 44 N89-23957
- ALL SKY PHOTOGRAPHY**
- Distribution of auroral arcs during quiet geomagnetic
conditions p 50 A89-34772
- ALTIMETRY**
- Improving accuracy in radar-altimetry data correction for
tropospheric effects p 54 A89-39322
- ANALOG SIMULATION**
- Image understanding research at SRI International
p 42 N89-23080
- ANALOG TO DIGITAL CONVERTERS**
- Automatic digitizing of cadastral maps
p 43 N89-23946
- ANALYSIS OF VARIANCE**
- Analysis and optimization of geodetic networks by
spectral criteria and mechanical analogies
[SER-C-342] p 45 N89-23963
- ANNUAL VARIATIONS**
- Global, seasonal surface variations from satellite
radiance measurements p 52 A89-35966
- Measuring and modeling spectral characteristics of a
tallgrass prairie p 27 A89-38970
- ANTARCTIC REGIONS**
- Direct ozone depletion in springtime Antarctic lower
stratospheric clouds p 4 A89-32756
- An AVHRR mosaic image of Antarctica
p 30 A89-40135
- Antarctic ozone: Theory and observation
p 4 N89-22189
- Estimating population size of Pygoscelid Penguins from
TM data
[NASA-CR-180081] p 3 N89-24687
- ANTICLINES**
- Structural analysis of fracturing in Sinjar anticline using
remote sensing technique p 13 A89-41167

APPLICATIONS PROGRAMS (COMPUTERS)

- Preliminary analysis of Airborne Visible/Infrared Imaging
Spectrometer (AVIRIS) for mineralogic mapping at sites
in Nevada and Colorado p 60 N89-22161
- AQUATIC PLANTS**
- Use of aerial photography to inventory aquatic
vegetation p 50 A89-34362
- ARCHITECTURE (COMPUTERS)**
- Remote sensing information sciences research group:
Browse in the EOS era
[NASA-CR-184637] p 42 N89-22979
- ARCTIC OCEAN**
- Arctic geodynamics - A satellite altimeter experiment
for the European Space Agency Earth Remote-Sensing
satellite p 29 A89-39546
- Beaufort Sea mesoscale circulation study: Preliminary
results
[PB89-121693] p 17 N89-20597
- Biophysical variability in the Greenland Sea observed with
the Multispectral Airborne Radiometer System (MARS)
[NASA-CR-184856] p 47 N89-24784
- ARCTIC REGIONS**
- The use of a lineament-analysis instrument for
investigations of tectonic zonality and the elements of
continental-margin geodynamics as applied to western
Arctic p 49 A89-34010
- Image-analysis techniques for determination of
morphology and kinematics in arctic sea ice
p 21 A89-34416
- Distribution of auroral arcs during quiet geomagnetic
conditions p 50 A89-34772
- Accuracy assessment of a Landsat-assisted vegetation
map of the coastal plain of the Arctic National Wildlife
Refuge p 6 A89-35840
- NOAA (National Oceanic and Atmospheric
Administration) AVHRR (Advanced Very High Resolution
Radiometer) observations during the marginal ice zone
experiment, between Spitzbergen and Greenland, June 7
to 18 July 1984
[AD-A204911] p 19 N89-22280
- KRMS (K-band Radiometric Mapping System) SSM/I
validation March 1988 quick look report
[NASA-CR-185320] p 8 N89-23766
- Remote sensing of global snowpack energy and mass
balance: In-situ measurements on the snow of interior and
Arctic Alaska
[NASA-CR-180078] p 62 N89-23956
- AREA**
- Automatic extraction of areas from overlays of the series
DGK 5 (Bo) p 44 N89-23955
- ARGOS SYSTEM**
- ARGOS system used for balloon observations
p 53 A89-38290
- A performance comparison for two Lagrangian drifter
designs p 34 A89-41750
- ARID LANDS**
- Application of Landsat Thematic Mapper imagery for
lithological mapping of poorly accessible semi-arid
regions p 7 A89-35879
- Alteration detection using TM imagery - The effects of
supergene weathering in an arid climate
p 12 A89-39655
- Shuttle imaging radar analysis in arid environments
p 33 A89-41166
- Radiometric performance of AVIRIS: Assessment for an
arid region geologic target p 39 N89-22157
- Assessment of AVIRIS data from vegetated sites in the
Owens Valley, California p 60 N89-22162
- ASHES**
- Observations of volcanic ash clouds in the 10-12 micron
window using AVHRR/2 data p 30 A89-40143
- ASIA**
- New data on the morphostructure and geodynamics of
the eastern margin of Eurasia p 10 A89-34012
- ATLANTIC OCEAN**
- Precipitation in the Canadian Atlantic Storms Program
- Measurements of the acoustic signature
p 50 A89-35819
- ATMOSPHERIC ATTENUATION**
- Sensitivity of an atmospheric correction algorithm for
non-Lambertian vegetation surfaces to atmospheric
parameters p 29 A89-39556
- Variation of surface water spectral response as a
function of in situ sampling technique p 33 A89-41161
- ATMOSPHERIC CHEMISTRY**
- Antarctic ozone: Theory and observation
p 4 N89-22189
- ATMOSPHERIC CIRCULATION**
- A meteorological overview of the pre-AMEX and AMEX
periods over the Australian region p 48 A89-32850
- Sensitivity of 30-day dynamical forecasts to continental
snow cover p 17 A89-35937
- Beaufort Sea mesoscale circulation study: Preliminary
results
[PB89-121693] p 17 N89-20597

- Satellite signatures of rapid cyclogenesis
[AD-A203934] p 38 N89-21452
- Mesoscale severe weather development under
orographic influences
[AD-A205082] p 41 N89-22293
- ATMOSPHERIC COMPOSITION**
- The investigation of advanced remote sensing, radiative
transfer and inversion techniques for the measurement
of atmospheric constituents
[NASA-CR-172599] p 36 N89-20531
- Nimbus-7 data product summary
[NASA-RP-1215] p 39 N89-22152
- Antarctic ozone: Theory and observation
p 4 N89-22189
- A visiting scientist program in atmospheric sciences for
the Goddard Space Flight Center
[NASA-CR-183421] p 47 N89-24756
- ATMOSPHERIC CORRECTION**
- Surface reflectance factor retrieval from Thematic
Mapper data p 49 A89-33871
- Evaluating atmospheric correction models for retrieving
surface temperatures from the AVHRR over a tallgrass
prairie p 20 A89-33875
- Atmospheric correction of satellite MSS data in rugged
terrain p 27 A89-38334
- Improving accuracy in radar-altimetry data correction for
tropospheric effects p 54 A89-39322
- Sensitivity of an atmospheric correction algorithm for
non-Lambertian vegetation surfaces to atmospheric
parameters p 29 A89-39556
- ATMOSPHERIC GENERAL CIRCULATION MODELS**
- A comparison of radiation variables calculated in the
UCLA general circulation model to observations
p 24 A89-35926
- The response of thermospheric nitric oxide to an auroral
storm p 42 N89-23031
- A visiting scientist program in atmospheric sciences for
the Goddard Space Flight Center
[NASA-CR-183421] p 47 N89-24756
- ATMOSPHERIC HEATING**
- Monitoring the greenhouse effect from space
p 4 A89-39739
- ATMOSPHERIC MODELS**
- A comparison of radiation variables calculated in the
UCLA general circulation model to observations
p 24 A89-35926
- Antarctic ozone: Theory and observation
p 4 N89-22189
- ATMOSPHERIC MOISTURE**
- Cloud reflectance variations in channel-3
p 55 A89-40136
- Satellite-derived low-level atmospheric water vapour
content from synergy of AVHRR with HIRS --- High
Resolution Infrared Radiation Sounder
p 30 A89-40139
- Improved capabilities of the Multispectral Atmospheric
Mapping Sensor (MAMS)
[NASA-TM-100352] p 58 N89-20430
- Atmospheric water mapping with the Airborne
Visible/Infrared Imaging Spectrometer (AVIRIS), Mountain
Pass, California p 39 N89-22156
- ATMOSPHERIC OPTICS**
- Sensitivity of an atmospheric correction algorithm for
non-Lambertian vegetation surfaces to atmospheric
parameters p 29 A89-39556
- Remote measurements from Salyut-7 of the optical
parameters of the atmosphere-surface system
p 57 A89-42601
- Activities report of the Division of Optical Technology
(FOA 33)
[FOA-C-30507-3.1] p 62 N89-23287
- ATMOSPHERIC PHYSICS**
- Thermal images of sky and sea-surface background
infrared radiation
[AD-A205819] p 46 N89-23992
- ATMOSPHERIC RADIATION**
- A comparison of radiation variables calculated in the
UCLA general circulation model to observations
p 24 A89-35926
- ATMOSPHERIC REFRACTION**
- Remote sensing in refractive turbulence
p 58 N89-20532
- Infrared sea-radiance modeling using LOWTRAN 6
[AD-A202582] p 38 N89-21643
- ATMOSPHERIC SCATTERING**
- Radiative transfer calculations for characterizing
obscured surfaces using time-dependent backscattered
pulses p 48 A89-32841
- ATMOSPHERIC SOUNDING**
- Mesospheric temperature sounding with microwave
radiometers p 54 A89-39557
- Studying the earth from manned spacecraft --- Russian
book p 64 A89-42511
- The spectrometer of the Salyut-7 orbital station
p 57 A89-42608

- Multichannel spectrometer MKS-M - Laboratory tests, calibration, and verification of its stability in flight p 57 A89-42609
- Nimbus-7 data product summary [NASA-RP-1215] p 39 N89-22152
- ATMOSPHERIC STRATIFICATION**
- Aerosol analysis with the Coastal Zone Color Scanner - A simple method for including multiple scattering effects p 25 A89-37291
- ATMOSPHERIC TEMPERATURE**
- Mean temperature in a closed basin by remote sensing p 16 A89-39062
- Mesospheric temperature sounding with microwave radiometers p 54 A89-39557
- Mesoscale severe weather development under orographic influences [AD-A205082] p 41 N89-22293
- Correlation between satellite-derived aerosol characteristics and oceanic dimethylsulfide (DMS) [AD-A206179] p 6 N89-24759
- ATMOSPHERIC TURBULENCE**
- Remote sensing in refractive turbulence p 58 N89-20532
- ATMOSPHERIC WINDOWS**
- Using the radiative temperature difference at 3.7 and 11 microns to track dust outbreaks p 27 A89-38968
- ATMOSPHERICS**
- Loran C field strength contours: Contiguous US [DOT/FAA/CT-TN89/16] p 8 N89-23437
- AURORAL ARCS**
- Satellite, airborne and radar observations of auroral arcs p 48 A89-33505
- Distribution of auroral arcs during quiet geomagnetic conditions p 50 A89-34772
- AURORAL ZONES**
- EXOS-C (Ohzora) observations of polar cap precipitations and inverted V events p 19 A89-33543
- AURORAS**
- The response of thermospheric nitric oxide to an auroral storm p 42 N89-23031
- AUSTRIA**
- Analysis of Airborne Imaging Spectrometer (AIS) data for geobotanical prospecting p 51 A89-35890
- AUTOCORRELATION**
- Autocorrelation and regularization in digital images. II - Simple image models p 29 A89-39551
- AUTOMATIC CONTROL**
- Automatic digitizing of cadastral maps p 43 N89-23946
- AUTONOMOUS SPACECRAFT CLOCKS**
- Observation model and parameter partials for the JPL geodetic GPS modeling software GPSOMC [NASA-CR-185021] p 9 N89-24060

B

- BACKGROUND RADIATION**
- Infrared sea-radiance modeling using LOWTRAN 6 [AD-A202582] p 38 N89-21643
- Thermal images of sky and sea-surface background infrared radiation [AD-A205819] p 46 N89-23992
- BACKSCATTERING**
- Radiative transfer calculations for characterizing obscured surfaces using time-dependent backscattered pulses p 48 A89-32841
- An analysis of speckle from forest stands with periodic structures p 54 A89-39555
- Active and passive remote sensing of ice [AD-A203943] p 59 N89-20543
- Probabilities and statistics for backscatter estimates obtained by a scatterometer with applications to new scatterometer design data p 61 N89-22779
- Improvement and extension of a radar forest backscattering model [NASA-CR-184975] p 46 N89-24686
- BALLOON FLIGHT**
- ARGOS system used for balloon observations p 53 A89-38290
- BAND RATIOING**
- Atmospheric water mapping with the Airborne Visible/Infrared Imaging Spectrometer (AVIRIS), Mountain Pass, California p 39 N89-22156
- BANDSTOP FILTERS**
- Zones of information in the AVIRIS spectra p 39 N89-22158
- BANGLADESH**
- Improvement and extension of a radar forest backscattering model [NASA-CR-184975] p 46 N89-24686
- BATHYMETERS**
- Ground verification method for bathymetric satellite image maps of unsurveyed coral reefs p 6 A89-34949

- Bathymetric mapping with passive multispectral imagery p 16 A89-38766
- BAUXITE**
- Identification of magnesite and bauxite deposits on Landsat imagery, South India p 12 A89-35889
- BAYS (TOPOGRAPHIC FEATURES)**
- Development and verification of Osaka Bay sampling model based on Landsat data p 27 A89-38332
- BEAUFORT SEA (NORTH AMERICA)**
- KRMS (K-band Radiometric Mapping System) SSM/I validation March 1988 quick look report [NASA-CR-185320] p 8 N89-23766
- BEEETLES**
- Cluster analysis of pine crown foliage patterns aid identification of mountain pine beetle current-attack p 26 A89-37950
- BERING SEA**
- KRMS (K-band Radiometric Mapping System) SSM/I validation March 1988 quick look report [NASA-CR-185320] p 8 N89-23766
- BIOGEOCHEMISTRY**
- MEIS II and surface data integration for detection of geobotanical anomalies p 51 A89-35891
- A closer look at the Patrick Draw oil field vegetation anomaly p 1 A89-35893
- BIOLOGICAL EFFECTS**
- Air pollution effects field research facility: Ozone flow control and monitoring system [DE89-007922] p 5 N89-22192
- BIOLOGY**
- New earth observing platforms to study global water, biology p 17 A89-33121
- BIOMETEOROLOGY**
- Derivation of a large-scale map of heat load in the region Freiburg-Basel (Germany, F.R.) using satellite data. A contribution to the production of bioclimate data based on a geographic information system [REPT-27] p 41 N89-22972
- BIOSPHERE**
- Concept for a satellite-based global reserve monitoring system p 32 A89-41152
- BIRDS**
- Estimating population size of Pygoscelid Penguins from TM data [NASA-CR-180081] p 3 N89-24687
- BLACK BODY RADIATION**
- Thermal images of sky and sea-surface background infrared radiation [AD-A205819] p 46 N89-23992
- BRAZIL**
- Microwave X-band radiometric characterization of Brazilian soils by measurement of the complex permittivity [INPE-4588-PRE/1319] p 3 N89-24685
- BRECCIA**
- Application of Landsat Thematic Mapper digital data to the exploration for uranium-mineralized breccia pipes in Northwestern Arizona p 51 A89-35872
- BRIGHTNESS TEMPERATURE**
- Remote sensing of global snowpack energy and mass balance: in-situ measurements on the snow of interior and Arctic Alaska [NASA-CR-180078] p 62 N89-23956

C

- C BAND**
- C-band radar cross section of the Guyana rain forest - Possible use as a reference target for spaceborne radars p 49 A89-33869
- CADASTRAL MAPPING**
- The digital urban map as a basis for a land information system in local administration p 8 N89-23945
- Automatic digitizing of cadastral maps p 43 N89-23946
- Digitizing of drawings and cadastral maps using a scanner system p 43 N89-23949
- CALIBRATING**
- Calibration comparison for the Landsat 4 and 5 Multispectral Scanners and Thematic Mappers p 47 A89-32835
- Methodological aspects of the automation of the calibration and processing of satellite microwave-radiometer data p 25 A89-37324
- Field calibration of mixed-layer drifters p 53 A89-37554
- Multichannel spectrometer MKS-M - Laboratory tests, calibration, and verification of its stability in flight p 57 A89-42609
- Correcting absolute calibrations of satellite microwave radiometer using a priori data p 35 A89-42612
- Improved capabilities of the Multispectral Atmospheric Mapping Sensor (MAMS) [NASA-TM-100352] p 58 N89-20430
- Calibration and evaluation of AVIRIS data: Cripple Creek in October 1987 p 39 N89-22159
- Evaluation of Airborne Visible/Infrared Imaging Spectrometer Data of the Mountain Pass, California carbonate complex p 60 N89-22169
- Determination of in-flight AVIRIS spectral, radiometric, spatial and signal-to-noise characteristics using atmospheric and surface measurements from the vicinity of the rare-earth-bearing carbonate at Mountain Pass, California p 61 N89-22170
- CAMERAS**
- The KAP-350 and KAP-100 space cameras for the remote sensing of earth resources p 50 A89-35687
- CANADA**
- Precipitation in the Canadian Atlantic Storms Program - Measurements of the acoustic signature p 50 A89-35819
- KRMS (K-band Radiometric Mapping System) SSM/I validation March 1988 quick look report [NASA-CR-185320] p 8 N89-23766
- CANADIAN SHIELD**
- Assessing aggregate resource potential in the Canadian Shield - A knowledge-based approach p 23 A89-35877
- CANOPIES (VEGETATION)**
- Measurements of short-term thermal responses of coniferous forest canopies using thermal scanner data p 1 A89-33867
- Seasonal visible, near-infrared and mid-infrared spectra of rice canopies in relation to LAI and above-ground dry phytomass p 54 A89-38967
- A reflectance model for the homogeneous plant canopy and its inversion p 27 A89-38971
- Modeling directional thermal radiance from a forest canopy p 27 A89-38972
- AVHRR data processing to study the surface canopies in temperate regions - First results of HAPEX-MOBILHY p 30 A89-40153
- AVIRIS data quality for coniferous canopy chemistry p 40 N89-22164
- AVIRIS spectra of California wetlands p 3 N89-22167
- Geobotanical remote sensing for determination of aggregate source material [AD-A205943] p 45 N89-23962
- CARBON DIOXIDE CONCENTRATION**
- Preliminary development of a seashore-effects analysis system [DE89-007863] p 61 N89-22191
- CAUCASUS MOUNTAINS (U.S.S.R.)**
- Seismogeological interpretation of space images of the region of Caucasian mineral waters p 10 A89-34018
- CELESTIAL GEODESY**
- Coordinate referencing of a TV image in the case of the remote sensing of the earth p 53 A89-37492
- Seasat altimetry and the South Atlantic geoid. II - Short-wavelength undulations p 16 A89-39659
- CHAD**
- Meteosat thermal inertia mapping for studying wetland dynamics in the West-African Sahel [BCRS-88-10A] p 62 N89-23970
- CHARTS**
- KRMS (K-band Radiometric Mapping System) SSM/I validation March 1988 quick look report [NASA-CR-185320] p 8 N89-23766
- CHEMICAL COMPOSITION**
- AVIRIS data quality for coniferous canopy chemistry p 40 N89-22164
- CHESAPEAKE BAY (US)**
- Ice cover on Chesapeake Bay from AVHRR (Advanced Very High Resolution Radiometer) and LANDSAT imagery, winter of 1987-88 [PB89-117261] p 59 N89-21415
- CHLOROPHYLLS**
- Remote sensing of ocean chlorophyll - Consequence of nonuniform pigment profile p 15 A89-32838
- The advanced Ocean Chlorophyll Meter (OCM). A spectral imaging device for the observation of the oceans [REPT-882-440-118] p 63 N89-24689
- The FLI airborne imaging spectrometer: A highly versatile sensor for many applications p 63 N89-24694
- Development of an imaging spectrometer for remote sensing: The FLI program p 63 N89-24698
- Imaging spectrometry at the Canada Centre for Remote Sensing p 64 N89-24701
- Biooptical variability in the Greenland Sea observed with the Multispectral Airborne Radiometer System (MARS) [NASA-CR-184856] p 47 N89-24784
- CHUKCHI SEA**
- KRMS (K-band Radiometric Mapping System) SSM/I validation March 1988 quick look report [NASA-CR-185320] p 8 N89-23766

CITIES

Comparison of satellite, ground-based, and modeling techniques for analyzing the urban heat island

p 26 A89-37948

Computer aided production of a 1:25,000 relief model of Berlin and surroundings

p 8 N89-23943

The digital urban map as a basis for a land information system in local administration

p 8 N89-23945

CLASSIFICATIONS

Active and passive remote sensing of ice

[AD-A203943] p 59 N89-20543

CLAYS

Visible and near-infrared (0.4- to 2.5-microns) reflectance spectra of selected mixed-layer clays and related minerals

p 12 A89-35897

CLIMATE CHANGE

Greater global warming revealed by satellite-derived sea-surface-temperature trends

p 16 A89-37571

Lake area measurement using AVHRR - A case study

p 31 A89-40154

CLIMATOLOGY

High resolution chronology of late Cretaceous-early Tertiary events determined from 21,000 yr orbital-climatic cycles in marine sediments

p 14 N89-21328

CLOSED ECOLOGICAL SYSTEMS

Advanced space design program to the Universities Space Research Association and the National Aeronautics and Space Administration

[NASA-CR-180450] p 3 N89-24015

CLOUD COVER

Interaction between net shortwave flux and sea surface temperature

p 15 A89-34878

Examination of USAF Nephanalysis performance in the marginal cryosphere region

p 52 A89-35949

Relating point to area average rainfall in semiarid West Africa and the implications for rainfall estimates derived from satellite data

p 55 A89-39870

Twelve year overview of cloudfree LANDSAT imagery of The Netherlands

[NLR-MP-87072-U] p 59 N89-20542

Refinements in the cloud detection scheme of the 3i system. Comparison with AVHRR products

[ETN-89-94531] p 63 N89-24691

CLOUD PHYSICS

Satellite signatures of rapid cyclogenesis

[AD-A203934] p 38 N89-21452

CLOUDS (METEOROLOGY)

Direct ozone depletion in springtime Antarctic lower stratospheric clouds

p 4 A89-32756

Automated recognition of oceanic cloud patterns. I - Methodology and application to cloud climatology

p 24 A89-35906

Cloud reflectance variations in channel-3

p 55 A89-40136

Twelve year overview of cloudfree LANDSAT imagery of The Netherlands

[NLR-MP-87072-U] p 59 N89-20542

Satellite signatures of rapid cyclogenesis

[AD-A203934] p 38 N89-21452

Refinements in the cloud detection scheme of the 3i system. Comparison with AVHRR products

[ETN-89-94531] p 63 N89-24691

CLUSTER ANALYSIS

Cluster analysis of pine crown foliage patterns aid identification of mountain pine beetle current-attack

p 26 A89-37950

N-dimensional display of cluster means in feature space

p 29 A89-39100

Data compression experiments with LANDSAT thematic mapper and Nimbus-7 coastal zone color scanner data

p 41 N89-22344

CLUTTER

Multispectral terrain background simulation techniques for use in airborne sensor evaluation

p 19 A89-33664

Remote sensing of earth terrain

[NASA-CR-184937] p 41 N89-22971

COAL

Lineament analysis for hazard assessment in advance of coal mining

p 11 A89-35873

COASTAL CURRENTS

Use of aerial photography to inventory aquatic vegetation

p 50 A89-34362

COASTAL ECOLOGY

Mapping coastal evolution in Sri Lanka using aerial photographs

p 6 A89-34948

COASTAL PLAINS

Accuracy assessment of a Landsat-assisted vegetation map of the coastal plain of the Arctic National Wildlife Refuge

p 6 A89-35840

COASTAL WATER

Application of Landsat Thematic Mapper data for coastal thermal plume analysis at Diablo Canyon

p 35 A89-42175

Utilizing remote sensing of thematic mapper data to improve our understanding of estuarine processes and their influence on the productivity of estuarine-dependent fisheries

[NASA-CR-183417] p 18 N89-20533

Imaging procedure of underwater bottom topography by air and satellite images in the range of microwave and visible electromagnetic spectra

[GKSS-88/E/41] p 17 N89-24014

COASTAL ZONE COLOR SCANNER

Aerosol analysis with the Coastal Zone Color Scanner - A simple method for including multiple scattering effects

p 25 A89-37291

Data compression experiments with LANDSAT thematic mapper and Nimbus-7 coastal zone color scanner data

p 41 N89-22344

COLOR PHOTOGRAPHY

Expanding the utility of manned observations of earth - 70 mm film tests on the Space Shuttle

p 34 A89-41428

High resolution chronology of late Cretaceous-early Tertiary events determined from 21,000 yr orbital-climatic cycles in marine sediments

p 14 N89-21328

COLOR VISION

Space coloristics --- earth observations from orbital stations

p 35 A89-43024

COMMERCE

On the international commercialization of remote sensing

[BCRS-88-02] p 65 N89-23969

COMMERCIAL SPACECRAFT

Use of commercial satellite imagery for surveillance of the Canadian north by the Canadian armed forces

[AD-A202700] p 40 N89-22173

COMPUTATIONAL GRIDS

Mesoscale severe weather development under orographic influences

[AD-A205082] p 41 N89-22293

COMPUTER AIDED MAPPING

Vegetation and landscape of Kora National Reserve, Kenya

p 6 A89-34945

Monitoring the halfa steppes of central Tunisia using Landsat MSS

p 1 A89-34947

Mapping coastal evolution in Sri Lanka using aerial photographs

p 6 A89-34948

Ground verification method for bathymetric satellite image maps of unsurveyed coral reefs

p 6 A89-34949

Automated DTM validation and progressive sampling algorithm of finite element array relaxation

p 22 A89-35837

A semi-automatic terrain measurement system for earthwork control

p 28 A89-39094

Digital photogrammetric processing systems - Current status and prospects

p 28 A89-39095

Cooperative methods for road tracking in aerial imagery

p 42 N89-23101

Overview of the SRI cartographic modeling environment

p 62 N89-23122

Reports on Cartography and Geodesy. Series 1, number 101

[ISSN-0469-4236] p 8 N89-23941

Computer aided production of a 1:25,000 relief model of Berlin and surroundings

p 8 N89-23943

The Official Topographic-Cartographic Information System (ATKIS) of the Geodesy Group of the Laender of the Federal Republic of Germany: Status after one year of development

p 8 N89-23944

The digital urban map as a basis for a land information system in local administration

p 8 N89-23945

Automatic digitizing of cadastral maps

p 43 N89-23946

Cartographic signatures in PHOCUS

p 43 N89-23948

Digitizing of drawings and cadastral maps using a scanner system

p 43 N89-23949

Computer assisted layout of graphic settlement representations

p 43 N89-23951

Tools for the computer assisted generalization of settlements for the construction of digital landscape models

p 43 N89-23952

Computer assisted generalization of transport line representations

p 43 N89-23953

Hybrid cartographic data processing in a geographic information system

p 44 N89-23954

Automatic extraction of areas from overlays of the series DGK 5 (Bo)

p 44 N89-23955

Shortest paths in a digitized map using a tile-based data structure

[PB89-143432] p 44 N89-23957

Use of the 1:2,000,000 Digital Line Graph data in emergency response

[DE89-006730] p 44 N89-23959

The search for edges in remote sensing images using a digital polygonal map

[ETN-89-94146] p 45 N89-23964

COMPUTER GRAPHICS

Multispectral terrain background simulation techniques for use in airborne sensor evaluation

p 19 A89-33664

N-dimensional display of cluster means in feature space

p 29 A89-39100

Overview of the SRI cartographic modeling environment

p 62 N89-23122

Reports on Cartography and Geodesy. Series 1, number 101

[ISSN-0469-4236] p 8 N89-23941

Definition and filling of information systems: Challenge for a photogrammetric service enterprise

p 62 N89-23942

COMPUTER PROGRAMS

The investigation of advanced remote sensing, radiative transfer and inversion techniques for the measurement of atmospheric constituents

[NASA-CR-172599] p 36 N89-20531

ARC-INFO: A geographic information system

p 43 N89-23947

Thermal images of sky and sea-surface background infrared radiation

[AD-A205819] p 46 N89-23992

COMPUTER SYSTEMS PROGRAMS

ARC-INFO: A geographic information system

p 43 N89-23947

COMPUTER TECHNIQUES

Ore-bearing structures of Central Kazakhstan identified on aerial and space photographs in the framework of the computer-aided prediction of minerals

p 52 A89-37316

A digital mosaicking algorithm allowing for an irregular join 'line'

p 26 A89-37944

COMPUTER VISION

Image understanding research at SRI International

p 42 N89-23080

Cooperative methods for road tracking in aerial imagery

p 42 N89-23101

COMPUTERIZED SIMULATION

Computer-aided synthesis of textures simulating the earth's surface

p 25 A89-37325

Comparison of satellite, ground-based, and modeling techniques for analyzing the urban heat island

p 26 A89-37948

Geological data integration techniques: Proceedings [DE88-705255]

p 14 N89-20868

Computer strategy for detecting line features on simulated binary arrays in support of radar feature extraction

[AD-A203257] p 37 N89-21162

A software system to create a hierarchical, multiple level of detail terrain model

[AD-A203047] p 38 N89-21568

Improvement and extension of a radar forest backscattering model

[NASA-CR-184975] p 46 N89-24686

CONCENTRATION (COMPOSITION)

The relationship between in-lake sulfate concentration and estimates of atmospheric sulfur deposition for subregions of the eastern lake survey

[DE89-009868] p 5 N89-24749

CONFERENCES

Multispectral image processing and enhancement: Proceedings of the Meeting, Orlando, FL, Apr. 6-8, 1988

[SPIE-933] p 48 A89-33653

Remote-sensing studies of present-day tectonic processes --- Russian book

p 20 A89-34001

Thematic Conference on Remote Sensing for Exploration Geology, 6th, Houston, TX, May 16-19, 1988, Proceedings. Volumes 1 & 2

p 10 A89-35851

Applications of AVHRR data; Proceedings of the Third European AVHRR Data Users' Meeting, University of Oxford, England, Dec. 16-18, 1987

p 55 A89-40126

1988 ACSM-ASPRS Annual Convention, Saint Louis, MO, Mar. 13-18, 1988, Technical Papers. Volume 4 - Image processing/remote sensing

p 32 A89-41151

1988 Conference on Precision Electromagnetic Measurements, Tsukuba, Japan, June 7-10, 1988, Proceedings

p 57 A89-42773

Imaging Spectrometry for Land Applications [ESA-SP-1101]

p 63 N89-24692

CONIFERS

Measurements of short-term thermal responses of coniferous forest canopies using thermal scanner data

p 1 A89-33867

A new technique to measure the spectral properties of conifer needles

p 19 A89-33874

Analysis of Airborne Imaging Spectrometer (AIS) data for geobotanical prospecting

p 51 A89-35890

A Landsat Thematic Mapper investigation of the geobotanical relationships in the northern spruce-fir forest, Mt. Moosilauke, New Hampshire

p 2 A89-35894

Estimating stand density of loblolly pine in northern Louisiana using aerial photographs and probability proportional to size

p 34 A89-41171

- AVIRIS data quality for coniferous canopy chemistry p 40 N89-22164
- CONTAMINANTS**
Antarctic ozone: Theory and observation p 4 N89-22189
- CONTINENTS**
The use of a lineament-analysis instrument for investigations of tectonic zonality and the elements of continental-margin geodynamics as applied to western Arctic p 49 A89-34010
- CONTINUUM MECHANICS**
Analysis and optimization of geodetic networks by spectral criteria and mechanical analogies [SER-C-342] p 45 N89-23963
- CONTOUR SENSORS**
Research for optimization of future MOMS sensors [ETN-89-94424] p 62 N89-23972
- CORAL REEFS**
Ground verification method for bathymetric satellite image maps of unsurveyed coral reefs p 6 A89-34949
- CORN**
Large-area crop monitoring with the NOAA AVHRR - Estimating the silking stage of corn development p 1 A89-33873
- COSMOS SATELLITES**
Multispectral space surveys and data processing p 22 A89-35684
- COST REDUCTION**
Lowering the cost of exploration for independents - How remotely sensed data aids in the search for oil and gas p 22 A89-35855
- COVARIANCE**
On the connection of geodetic pointfields in RETrig [PB89-146112] p 44 N89-23958
- CROP IDENTIFICATION**
Sounding of crop fields by nanosecond radio pulses p 1 A89-35584
The discrimination of irrigated orchard and vine crops using remotely sensed data p 2 A89-37949
Crop identification using merged Landsat multispectral scanner and Thematic Mapper data - Preliminary attempts p 3 A89-41153
- CROP INVENTORIES**
Land use inventories using satellite images in the region Haaren-Helvoirt-Udenhout, North Brabant (The Netherlands) [BCRS-88-07] p 36 N89-20537
- CROP VIGOR**
Advanced space design program to the Universities Space Research Association and the National Aeronautics and Space Administration [NASA-CR-180450] p 3 N89-24015
- CRUDE OIL**
Petroleum exploration with airborne radar (SAR) and geologic field work, Sinu Basin of northwest Columbia p 11 A89-35859
The application of high resolution digital elevation models to petroleum and mineral exploration and production p 22 A89-35876
A technique for applying space photographs to search for anticlinal oil- and gas-traps in orogenic structures of the Tien-Shan p 25 A89-37318
- CRUSTAL FRACTURES**
The contribution of remote sensing data to exploration of fractured reservoirs p 50 A89-35862
Structural analysis of fracturing in Sinjar anticline using remote sensing technique p 13 A89-41167
Application of imaging spectrometer data to the Kings-Kaweah ophiolite melange p 40 N89-22166
- CYCLOGENESIS**
Satellite signatures of rapid cyclogenesis [AD-A203934] p 38 N89-21452
- CYCLONES**
Observational analyses of North Atlantic tropical cyclones from NOAA polar-orbiting satellite microwave data p 21 A89-34879
Meteorological applications of Space Shuttle photography p 34 A89-41430

D

- DATA ACQUISITION**
KRMS (K-band Radiometric Mapping System) SSM/I validation March 1988 quick look report [NASA-CR-185320] p 8 N89-23766
- DATA BASE MANAGEMENT SYSTEMS**
Knowledge-based image data management - An expert front-end for the BROWSE facility p 32 A89-41158
On the future development and management of spectroscopic database for radiative transfer from the issues of recent related workshops [ETN-89-94530] p 46 N89-24690

- DATA BASES**
National Air Toxics Information Clearinghouse: Ongoing research and regulatory development projects, July 1988 [PB89-103428] p 65 N89-20558
Beaufort Sea mesoscale circulation study: Preliminary results [PB89-121693] p 17 N89-20597
On the future development and management of spectroscopic database for radiative transfer from the issues of recent related workshops [ETN-89-94530] p 46 N89-24690
- DATA COMPRESSION**
Data compression experiments with LANDSAT thematic mapper and Nimbus-7 coastal zone color scanner data p 41 N89-22344
- DATA CORRELATION**
Area sensitivity and feature sensitivity of SPOT 1 data - A statistical analysis p 32 A89-41154
- DATA FLOW ANALYSIS**
Operational aspects of CASA UNO '88-The first large scale international GPS geodetic network p 7 A89-42787
- DATA INTEGRATION**
Geological data integration techniques: Proceedings [DE88-705255] p 14 N89-20868
Overview of the SRI cartographic modeling environment p 62 N89-23122
- DATA MANAGEMENT**
Information resources management p 42 N89-23371
- DATA PROCESSING**
Accessing remote sensing technology - The microBRIAN example p 21 A89-34706
Methodological aspects of the automation of the calibration and processing of satellite microwave-radiometer data p 25 A89-37324
Operational aspects of CASA UNO '88-The first large scale international GPS geodetic network p 7 A89-42787
Geological data integration techniques: Proceedings [DE88-705255] p 14 N89-20868
Information resources management p 42 N89-23371
Hybrid cartographic data processing in a geographic information system p 44 N89-23954
Investigation of several methods for the detection of outstanding points in a digital image [ETN-89-94148] p 45 N89-23965
- DATA SAMPLING**
Development and verification of Osaka Bay sampling model based on Landsat data p 27 A89-38332
- DATA STORAGE**
A software system to create a hierarchical, multiple level of detail terrain model [AD-A203047] p 38 N89-21568
- DATA STRUCTURES**
Shortest paths in a digitized map using a tile-based data structure [PB89-143432] p 44 N89-23957
- DEEP SPACE NETWORK**
Environmental projects. Volume 3: Environmental compliance audit [NASA-CR-185019] p 5 N89-23985
- DEFORESTATION**
AVHRR for monitoring global tropical deforestation p 56 A89-40152
- DEFORMATION**
The use of space imagery for investigations of recent crustal deformations in southern Yakutia p 20 A89-34015
Plate motions and deformations from geologic and geodetic data [NASA-CR-184987] p 15 N89-24757
- DEPOSITION**
The relationship between in-lake sulfate concentration and estimates of atmospheric sulfur deposition for subregions of the eastern lake survey [DE89-009868] p 5 N89-24749
- DETECTION**
The precedence of global features in the perception of map symbols [AD-A203792] p 7 N89-22174
- DIGITAL DATA**
Digital display of SPOT stereo images p 24 A89-35903
A software system to create a hierarchical, multiple level of detail terrain model [AD-A203047] p 38 N89-21568
Examination of the spectral features of vegetation in 1987 AVIRIS data p 3 N89-22163
The digital urban map as a basis for a land information system in local administration p 8 N89-23945
Investigation of several methods for the detection of outstanding points in a digital image [ETN-89-94148] p 45 N89-23965

- DIGITAL SYSTEMS**
Computer strategy for detecting line features on simulated binary arrays in support of radar feature extraction [AD-A203257] p 37 N89-21162
- DIGITAL TECHNIQUES**
Automated DTM validation and progressive sampling algorithm of finite element array relaxation p 22 A89-35837
Application of Landsat Thematic Mapper digital data to the exploration for uranium-mineralized breccia pipes in Northwestern Arizona p 51 A89-35872
The application of high resolution digital elevation models to petroleum and mineral exploration and production p 22 A89-35876
Uses of the SAS statistical package for digital image analysis p 23 A89-35898
A digital mosaicking algorithm allowing for an irregular join 'line' p 26 A89-37944
Two-dimensional seam-point searching in digital image mosaicking p 26 A89-37945
A raster approach to topographic map revision p 26 A89-37946
Digital photogrammetric processing systems - Current status and prospects p 28 A89-39095
Autocorrelation and regularization in digital images. II - Simple image models p 29 A89-39551
Automatic digitizing of cadastral maps p 43 N89-23946
Digitizing of drawings and cadastral maps using a scanner system p 43 N89-23949
Tools for the computer assisted generalization of settlements for the construction of digital landscape models p 43 N89-23952
Automatic extraction of areas from overlays of the series DGK 5 (Bo) p 44 N89-23955
Shortest paths in a digitized map using a tile-based data structure [PB89-143432] p 44 N89-23957
- DISCRIMINATION**
The precedence of global features in the perception of map symbols [AD-A203792] p 7 N89-22174
- DISTRIBUTION FUNCTIONS**
Further investigations of sampling errors in mean terrain height estimation p 32 A89-41076
- DIURNAL VARIATIONS**
Measuring and modeling spectral characteristics of a tallgrass prairie p 27 A89-38970
- DMSP SATELLITES**
Polar cap deflation during magnetospheric substorms p 24 A89-36704
Precipitation retrieval over land and ocean with the SSM/I - Identification and characteristics of the scattering signal p 53 A89-37549
- DRAWINGS**
Digitizing of drawings and cadastral maps using a scanner system p 43 N89-23949
- DREDGING**
Use of a geographic information system (GIS) to improve planning for and control of the placement of dredged material p 32 A89-41157
- DRIFT (INSTRUMENTATION)**
Field calibration of mixed-layer drifters p 53 A89-37554
- DROP SIZE**
Drop-size distributions associated with intense rainfall p 50 A89-34876
- DUST**
Satellite detection of Saharan dust - Optimized imaging during nighttime p 24 A89-35912
The potential of infrared satellite data for the retrieval of Saharan-dust optical depth over Africa p 30 A89-39875
- DUST STORMS**
Using the radiative temperature difference at 3.7 and 11 microns to track dust outbreaks p 27 A89-38968

E

- EARTH ALBEDO**
Correlation between satellite-derived aerosol characteristics and oceanic dimethylsulfide (DMS) [AD-A206179] p 6 N89-24759
- EARTH ATMOSPHERE**
Monitoring the greenhouse effect from space p 4 A89-39739
A visiting scientist program in atmospheric sciences for the Goddard Space Flight Center [NASA-CR-183421] p 47 N89-24756
- EARTH CORE**
The geomagnetic spectrum for 1980 and core-crustal separation p 13 A89-43410

EARTH CRUST

EARTH CRUST

- Dynamics of present-day geological processes from remotely sensed data p 9 A89-34004
- Structural stresses and the divisibility into blocks of the earth crust as observed on space imagery p 10 A89-34009
- The use of space imagery for investigations of recent crustal deformations in southern Yakutia p 20 A89-34015
- Recent and current geodynamics of the Kyzylkum region as derived from space imagery p 10 A89-34017
- The geomagnetic spectrum for 1980 and core-crustal separation p 13 A89-43410

EARTH ENVIRONMENT

- Earth system science: A program for global change [NASA-TM-101186] p 5 N89-22969

EARTH IONOSPHERE

- Comparison of field-aligned currents at ionospheric and magnetospheric altitudes p 9 A89-33540
- Spacelab 2 Upper Atmospheric Modification Experiment over Areobico, II - Plasma dynamics p 4 A89-38897

EARTH MAGNETOSPHERE

- Comparison of field-aligned currents at ionospheric and magnetospheric altitudes p 9 A89-33540
- Some aspects of the relation between Pi 1-2 magnetic pulsations observed at L = 1.3-2.1 on the ground and substorm-associated magnetic field variations in the near-earth magnetotail observed by AMPTE CCE p 52 A89-36686
- Polar cap deflation during magnetospheric substorms p 24 A89-36704

EARTH MANTLE

- Magnetometer array studies, earth structure, and tectonic processes p 13 A89-42149

EARTH OBSERVATIONS (FROM SPACE)

- Remote-sensing studies of present-day tectonic processes --- Russian book p 20 A89-34001
- Commercialization of remote sensing in the U.S.A. - The SPOT perspective p 64 A89-34704
- Land-surface temperature measurement from space - Physical principles and inverse modeling p 29 A89-39552
- Monitoring the greenhouse effect from space p 4 A89-39739
- Expanding the utility of manned observations of earth - 70 mm film tests on the Space Shuttle p 34 A89-41428
- Earth scenes in polarized light observed from the Space Shuttle p 34 A89-41429
- Satellite-borne lidar observations of the earth - Requirements and anticipated capabilities p 56 A89-41692
- Studying the earth from manned spacecraft --- Russian book p 64 A89-42511
- Spaceborne studies related to nature conservation --- Russian book p 65 A89-42549
- Optimal satellite orbits and the network structure for regular earth surveying p 35 A89-42614
- Space coloristics --- earth observations from orbital stations p 35 A89-43024
- ESA's planned activities in the field of imaging spectrometry for Earth observation p 46 N89-24693

EARTH OBSERVING SYSTEM (EOS)

- Knowledge-based image data management - An expert front-end for the BROWSE facility p 32 A89-41158
- Remote sensing information sciences research group: Browse in the EOS era p 42 N89-22979
- The search for edges in remote sensing images using a digital polygonal map [ETN-89-94146] p 45 N89-23964
- Imaging Spectrometry for Land Applications [ESA-SP-1101] p 63 N89-24692
- HIRIS: NASA's high-resolution imaging spectrometer for the Earth Observing System (EOS) p 63 N89-24695

EARTH PLANETARY STRUCTURE

- Geophysical geodesy - The slow deformations of the earth --- Book p 7 A89-38583
- Magnetometer array studies, earth structure, and tectonic processes p 13 A89-42149

EARTH RADIATION BUDGET

- Nimbus-7 data product summary [NASA-RP-1215] p 39 N89-22152

EARTH RESOURCES

- Landsat commercialization - Keys to future success p 64 A89-34703
- The experience of the Commission of the European Communities in the use of remote sensing for the implementation of community policies p 64 A89-34712
- The KAP-350 and KAP-100 space cameras for the remote sensing of earth resources p 50 A89-35687
- Basic concepts in the use of remotely sensed data for resource exploration p 11 A89-35852

- Lowering the cost of exploration for independents - How remotely sensed data aids in the search for oil and gas p 22 A89-35855

- Identification of Cross Strike discontinuities in the Appalachian basin and implications for hydrocarbon exploration p 11 A89-35860
- Geobotanical determination of aggregate source material using Airborne Thematic Mapper imagery p 1 A89-35865

- Astronaut photography of the earth - Low cost images for resource exploration p 23 A89-35883

- Ore-bearing structures of Central Kazakhstan identified on aerial and space photographs in the framework of the computer-aided prediction of minerals p 52 A89-37316

EARTH SURFACE

- Radiative transfer calculations for characterizing obscured surfaces using time-dependent backscattered pulses p 48 A89-32841
- Laser scattering phenomenology - Background signature characterization and prediction p 6 A89-33661
- Surface reflectance factor retrieval from Thematic Mapper data p 49 A89-33871
- Estimation of surface insolation using sun-synchronous satellite data p 52 A89-35939
- Global, seasonal surface variations from satellite radiance measurements p 52 A89-35966
- Parameter optimization of systems for the thermal microwave mapping of the earth's surface p 25 A89-37321
- Highly sensitive microwave radiometer-scatterometer for the remote sensing of the earth's surface p 52 A89-37322

- Computer-aided synthesis of textures simulating the earth's surface p 25 A89-37325

- The influence of the viewing geometry of bare rough soil surfaces on their spectral response in the visible and near-infrared range p 2 A89-38969

- Combined film and softcopy photo-interpretation system p 31 A89-40263

- Aerial photography and specialized photographic studies --- Russian book p 31 A89-40488

- Geologic applications of Space Shuttle photography p 34 A89-41431

- Laser altimetry measurements from aircraft and spacecraft p 56 A89-41691

- A parameterization for longwave surface radiation from sun-synchronous satellite data p 56 A89-41761

- Remote measurements from Salyut-7 of the optical parameters of the atmosphere-surface system p 57 A89-42601

- The spectrometer of the Salyut-7 orbital station p 57 A89-42608

- Space coloristics --- earth observations from orbital stations p 35 A89-43024

- Remote sensing of earth terrain [NASA-CR-184937] p 41 N89-22971

- Image understanding research at SRI International p 42 N89-23080

EARTHQUAKES

- Methods for investigating seismically active zones using remote imagery p 20 A89-34013

ECONOMIC ANALYSIS

- The commercial land remote sensing market - Current assessment, baseline forecast and baseline alternatives p 64 A89-35899

ECOSYSTEMS

- Estimating population size of Pygoscelid Penguins from TM data [NASA-CR-180081] p 3 N89-24687

EFFLUENTS

- Use of the 1:2,000,000 Digital Line Graph data in emergency response [DE89-006730] p 44 N89-23959

EL NINO

- A comparison of radiation variables calculated in the UCLA general circulation model to observations p 24 A89-35926

ELECTRICAL RESISTIVITY

- Magnetometer array studies, earth structure, and tectonic processes p 13 A89-42149

ELECTROMAGNETIC ABSORPTION

- Imaging procedure of underwater bottom topography by air and satellite images in the range of microwave and visible electromagnetic spectra [GKSS-88/E/41] p 17 N89-24014

ELECTROMAGNETIC MEASUREMENT

- ARGOS system used for balloon observations p 53 A89-38290

ELECTROMAGNETIC SCATTERING

- EM wave scattering from statistically inhomogeneous and periodic random rough surfaces p 36 A89-43541

ELECTRON PRECIPITATION

- EXOS-C (Ohzora) observations of polar cap precipitations and inverted V events p 19 A89-33543

EMERGENCIES

- Use of the 1:2,000,000 Digital Line Graph data in emergency response [DE89-006730] p 44 N89-23959

EMISSIVITY

- Mapping freeze/thaw boundaries with SMMR data [NASA-CR-184991] p 9 N89-23961
- Thermal images of sky and sea-surface background infrared radiation [AD-A205819] p 46 N89-23992
- Microwave X-band radiometric characterization of Brazilian soils by measurement of the complex permittivity [INPE-4588-PRE/1319] p 3 N89-24685

ENDANGERED SPECIES

- Review of wildlife resources of Vandenberg Air Force Base, California [NASA-TM-102146] p 5 N89-23982

ENGLAND

- Integration of Landsat TM, stream sediment geochemistry and regional geophysics for mineral exploration in the English Lake District p 23 A89-35888

ENVIRONMENT MANAGEMENT

- Review of wildlife resources of Vandenberg Air Force Base, California [NASA-TM-102146] p 5 N89-23982

ENVIRONMENT PROTECTION

- The experience of the Commission of the European Communities in the use of remote sensing for the implementation of community policies p 64 A89-34712

- Spaceborne studies related to nature conservation --- Russian book p 65 A89-42549

ENVIRONMENT SIMULATION

- Computer-aided synthesis of textures simulating the earth's surface p 25 A89-37325

ENVIRONMENTAL MONITORING

- New earth observing platforms to study global water, biology p 17 A89-33121
- A Landsat Thematic Mapper investigation of the geobotanical relationships in the northern spruce-fir forest, Mt. Moosilauke, New Hampshire p 2 A89-35894
- AVHRR for monitoring global tropical deforestation p 56 A89-40152
- Concept for a satellite-based global reserve monitoring system p 32 A89-41152
- Monitoring tropical environments with Space Shuttle photography p 34 A89-41432
- National Air Toxics Information Clearinghouse: Ongoing research and regulatory development projects, July 1988 [PB89-103428] p 65 N89-20558
- Review of wildlife resources of Vandenberg Air Force Base, California [NASA-TM-102146] p 5 N89-23982
- Environmental projects. Volume 3: Environmental compliance audit [NASA-CR-185019] p 5 N89-23985

ENVIRONMENTAL SURVEYS

- Correlation between satellite-derived aerosol characteristics and oceanic dimethylsulfide (DMS) [AD-A206179] p 6 N89-24759

EQUATORIAL ATMOSPHERE

- Properties of the equatorial and tropical ionosphere according to Soviet satellite observations during the IMS p 31 A89-40606

EQUATORIAL REGIONS

- Seasat A satellite scatterometer measurements of equatorial surface winds p 53 A89-37802

ERROR ANALYSIS

- Further investigations of sampling errors in mean terrain height estimation p 32 A89-41076

ERROR DETECTION CODES

- Design of a methodology for the detection of errors in terrestrial networks [ETN-89-94151] p 46 N89-23968

ERS-1 (ESA SATELLITE)

- Development of a satellite SAR image spectra and altimeter wave height data assimilation system for ERS-1 [NASA-CR-182685] p 61 N89-22975
- Theoretical studies for ERS-1 wave mode, volume 1 [GEC-MTR-87/110-VOL-1] p 41 N89-22977

ESA SATELLITES

- Design of spectral and panchromatic bands for the German MOMS-02 sensor p 57 A89-42173
- The advanced Ocean Chlorophyll Meter (OCM). A spectral imaging device for the observation of the oceans [REPT-882-440-118] p 63 N89-24689

ESTUARIES

Utilizing remote sensing of thematic mapper data to improve our understanding of estuarine processes and their influence on the productivity of estuarine-dependent fisheries
[NASA-CR-183417] p 18 N89-20533

EUROPEAN SPACE AGENCY

Arctic geodynamics - A satellite altimeter experiment for the European Space Agency Earth Remote-Sensing satellite p 29 A89-39546

EUROPEAN SPACE PROGRAMS

Imaging Spectrometry for Land Applications
[ESA-SP-1101] p 63 N89-24692
ESA's planned activities in the field of imaging spectrometry for Earth observation p 46 N89-24693
DFVLR activities related to imaging spectrometry p 63 N89-24697
Activities of CNES in the field of imaging spectrometry p 47 N89-24699
The EARSSEL Imaging Spectrometry Working Group p 47 N89-24700

EVAPOTRANSPIRATION

Estimation of regional surface resistance to evapotranspiration from NDVI and thermal-IR AVHRR data --- Normalized Difference Vegetation Index p 55 A89-39872
NOAA AVHRR and its uses for rainfall and evapotranspiration monitoring p 56 A89-40151

EXPERIMENT DESIGN

Phase A study for the extension of the CAESAR scanner with a sensor module for the far infrared [BCRS-88-09] p 59 N89-20539

EXPERT SYSTEMS

TAX - Prototype expert system for terrain analysis p 20 A89-34363
Assessing aggregate resource potential in the Canadian Shield - A knowledge-based approach p 23 A89-35877
A global approach to knowledge-based surface material classification p 32 A89-41156
Use of a geographic information system (GIS) to improve planning for and control of the placement of dredged material p 32 A89-41157
Knowledge-based image data management - An expert front-end for the BROWSE facility p 32 A89-41158
Automated extraction of absorption features from Airborne Visible/Infrared Imaging Spectrometer (AVIRIS) and Geophysical and Environmental Research Imaging Spectrometer (GERIS) data p 39 N89-22160

EXTINCTION

The Frasnian-Famennian mass killing event(s), methods of identification and evaluation p 37 N89-21318
High resolution chronology of late Cretaceous-early Tertiary events determined from 21,000 yr orbital-climatic cycles in marine sediments p 14 N89-21328

EXTREMELY HIGH FREQUENCIES

KRMS (K-band Radiometric Mapping System) SSM/I validation March 1988 quick look report [NASA-CR-185320] p 8 N89-23766

F**FAR INFRARED RADIATION**

Phase A study for the extension of the CAESAR scanner with a sensor module for the far infrared [BCRS-88-09] p 59 N89-20539

FARM CROPS

Surface reflectance factor retrieval from Thematic Mapper data p 49 A89-33871
Large-area crop monitoring with the NOAA AVHRR - Estimating the silking stage of corn development p 1 A89-33873
Sounding of crop fields by nanosecond radio pulses p 1 A89-35584
A reflectance model for the homogeneous plant canopy and its inversion p 27 A89-38971

FARMLANDS

EM wave scattering from statistically inhomogeneous and periodic random rough surfaces p 36 A89-43541

FIBER OPTICS

Activities report of the Division of Optical Technology [FOA 33] [FOA-C-30507-3.1] p 62 N89-23287

FIELD ALIGNED CURRENTS

Comparison of field-aligned currents at ionospheric and magnetospheric altitudes p 9 A89-33540
The interplanetary magnetic field B(y)-dependent field-aligned current in the dayside polar cap under quiet conditions p 50 A89-34782

FIELD STRENGTH

Loran C field strength contours: Contiguous US [DOT/FAA/CT-TN89/16] p 8 N89-23437

FINITE ELEMENT METHOD

Automated DTM validation and progressive sampling algorithm of finite element array relaxation p 22 A89-35837

FISHERIES

Utilizing remote sensing of thematic mapper data to improve our understanding of estuarine processes and their influence on the productivity of estuarine-dependent fisheries [NASA-CR-183417] p 18 N89-20533

FLOOD PREDICTIONS

Thermal analysis for the monitoring and prediction of flood dynamics in wetlands [BCRS-88-10B] p 46 N89-23971

FLOODS

Meteosat thermal inertia mapping for studying wetland dynamics in the West-African Sahel [BCRS-88-10A] p 62 N89-23970
Thermal analysis for the monitoring and prediction of flood dynamics in wetlands [BCRS-88-10B] p 46 N89-23971

FLUORESCENCE

The FLI airborne imaging spectrometer: A highly versatile sensor for many applications p 63 N89-24694
DFVLR activities related to imaging spectrometry p 63 N89-24697
Development of an imaging spectrometer for remote sensing: The FLI program p 63 N89-24698
Imaging spectrometry at the Canada Centre for Remote Sensing p 64 N89-24701

FOOD PRODUCTION (IN SPACE)

Advanced space design program to the Universities Space Research Association and the National Aeronautics and Space Administration [NASA-CR-180450] p 3 N89-24015

FOOTPRINTS

Minimum number of satellites for periodic coverage [FOA-C-30511-9.4] p 65 N89-22976

FORESTS

Measurements of short-term thermal responses of coniferous forest canopies using thermal scanner data p 1 A89-33867
Modeling surface temperature distributions in forest landscapes p 48 A89-33868
Reflectance enhancements for the Thematic Mapper - An efficient way to produce images of consistently high quality p 26 A89-37947
Modeling directional thermal radiance from a forest canopy p 27 A89-38972
Modeling and observation of the radar polarization signature of forested areas p 2 A89-39554
An analysis of speckle from forest stands with periodic structures p 54 A89-39555
Assessment of forest cover changes using multistate spaceborne imaging radar p 33 A89-41169
Remote sensing of the deciduous vegetation of Great Smoky Mountains National Park p 33 A89-41170
AVIRIS data quality for coniferous canopy chemistry p 40 N89-22164
Improvement and extension of a radar forest backscattering model [NASA-CR-184975] p 46 N89-24686

FORMAT

A software system to create a hierarchical, multiple level of detail terrain model [AD-A203047] p 38 N89-21568

FRACTALS

Fractal analysis of a classified Landsat scene p 28 A89-39099

FREEZING

Mapping freeze/thaw boundaries with SMMR data [NASA-CR-184991] p 9 N89-23961

FREQUENCY MODULATION

An inexpensive polarimetric FM radar and polarimetric signatures of artificial sea ice p 57 A89-42684

G**GAMMA RAY SPECTROMETERS**

Determination of areal snow water equivalent using satellite images and gamma ray spectrometry [CI-91] p 44 N89-23960

GAMMA RAYS

Airborne time-series measurement of soil moisture using terrestrial gamma radiation p 33 A89-41163

GAS CHROMATOGRAPHY

Gas chromatographic and sonar imaging of hydrocarbon seeps in the marine environment p 22 A89-35863

GAS EXCHANGE

The rate of gas exchange between the ocean and the atmosphere using microwave radiometer data p 25 A89-37471

GEOBOTANY

Geobotanical determination of aggregate source material using Airborne Thematic Mapper imagery p 1 A89-35865

High resolution imaging of geobotanical anomalies associated with subsurface hydrocarbons p 22 A89-35870

Analysis of Airborne Imaging Spectrometer (AIS) data for geobotanical prospecting p 51 A89-35890

MEIS II and surface data integration for detection of geobotanical anomalies p 51 A89-35891

Implementation of background and target geobotanical techniques in mineral exploration p 23 A89-35892

A closer look at the Patrick Draw oil field vegetation anomaly p 1 A89-35893

A Landsat Thematic Mapper investigation of the geobotanical relationships in the northern spruce-fir forest, Mt. Moosilauke, New Hampshire p 2 A89-35894
Geobotanical application of Airborne Thematic Mapper data in Sutherland, north-west Scotland p 2 A89-39657

Geobotanical remote sensing for determination of aggregate source material [AD-A205943] p 45 N89-23962

GEOCHEMISTRY

Combined remote sensing and surface geochemical survey in a drift-covered area in southeastern Saskatchewan p 12 A89-35881
Integration of Landsat TM, stream sediment geochemistry and regional geophysics for mineral exploration in the English Lake District p 23 A89-35888

Geological data integration techniques: Proceedings [DE88-705255] p 14 N89-20868

The Frasnian-Famennian mass killing event(s), methods of identification and evaluation p 37 N89-21318

GEOCHRONOLOGY

The Frasnian-Famennian mass killing event(s), methods of identification and evaluation p 37 N89-21318
High resolution chronology of late Cretaceous-early Tertiary events determined from 21,000 yr orbital-climatic cycles in marine sediments p 14 N89-21328

GEODESY

Economic relations of the all-union trade association Sojuzkart and the geodetic and cartographic services of the U.S.S.R. to foreign countries p 64 A89-34708
Geophysical geodesy - The slow deformations of the earth --- Book p 7 A89-38583
Reports on Cartography and Geodesy. Series 1, number 101 [ISSN-0469-4236] p 8 N89-23941
The Official Topographic-Cartographic Information System (ATKIS) of the Geodesy Group of the Laender of the Federal Republic of Germany: Status after one year of development p 8 N89-23944
On the connection of geodetic pointfields in RETrig [PB89-146112] p 44 N89-23958

GEODETIC COORDINATES

On the connection of geodetic pointfields in RETrig [PB89-146112] p 44 N89-23958
Vectorization of grid lines [ETN-89-94150] p 45 N89-23967
Design of a methodology for the detection of errors in terrestrial networks [ETN-89-94151] p 46 N89-23968

GEODETIC SATELLITES

Geocoded data sets of imaging satellites p 43 N89-23950
Observation model and parameter partials for the JPL geodetic GPS modeling software GPSOMC [NASA-CR-185021] p 9 N89-24060

GEODETIC SURVEYS

Operational aspects of CASA UNO '88-The first large scale international GPS geodetic network p 7 A89-42787

The baseline length changes of circum-Pacific VLBI networks and their bearing on global tectonics p 13 A89-42795

Analysis and optimization of geodetic networks by spectral criteria and mechanical analogies [SER-C-342] p 45 N89-23963

GEODYNAMICS

Remote-sensing studies of present-day tectonic processes --- Russian book p 20 A89-34001
Dynamics of present-day geological processes from remotely sensed data p 9 A89-34004

Morphostructural interpretation of space images and the reconstruction of the recently formed stress field in the Altai-Baikai region p 10 A89-34006

Use of aerial and space methods for observations and studies of the morphology and kinematics of recent movements along some faults of the Baikal Rift Zone p 10 A89-34007

- The use of a lineament-analysis instrument for investigations of tectonic zonality and the elements of continental-margin geodynamics as applied to western Arctic p 49 A89-34010
- New data on the morphostructure and geodynamics of the eastern margin of Eurasia p 10 A89-34012
- Methods for investigating seismically active zones using remote imagery p 20 A89-34013
- Determination of the character of present-day vertical movements from the structure of space imagery p 10 A89-34016
- Recent and current geodynamics of the Kyzylkum region as derived from space imagery p 10 A89-34017
- Arctic geodynamics - A satellite altimeter experiment for the European Space Agency Earth Remote-Sensing satellite p 29 A89-39546
- GEOGRAPHIC INFORMATION SYSTEMS**
- Accessing remote sensing technology - The microBRIAN example p 21 A89-34706
- Economic relations of the all-union trade association Sojuzkarta and the geodetic and cartographic services of the U.S.S.R. to foreign countries p 64 A89-34708
- A method for integrating remote sensing and geographic information systems p 28 A89-39097
- Space geography. Investigations on test regions --- Russian book p 31 A89-40491
- Use of a geographic information system (GIS) to improve planning for and control of the placement of dredged material p 32 A89-41157
- The use of remote sensing and GIS techniques for wetland identification and classification in the Garrison Diversion Unit-North Dakota p 18 A89-41160
- Derivation of a large-scale map of heat load in the region Freiburg-Basel (Germany, F.R.) using satellite data. A contribution to the production of bioclimate data based on a geographic information system [REPT-27] p 41 A89-22972
- Remote sensing information sciences research group: Browse in the EOS era p 42 A89-22979
- [NASA-CR-184637] p 42 A89-22979
- Reports on Cartography and Geodesy. Series 1, number 101 [ISSN-0469-4236] p 8 A89-23941
- The Official Topographic-Cartographic Information System (ATKIS) of the Geodesy Group of the Laender of the Federal Republic of Germany: Status after one year of development p 8 A89-23944
- The digital urban map as a basis for a land information system in local administration p 8 A89-23945
- ARC-INFO: A geographic information system p 43 A89-23947
- Hybrid cartographic data processing in a geographic information system p 44 A89-23954
- Shortest paths in a digitized map using a tile-based data structure p 44 A89-23957
- [PB89-13432] p 44 A89-23957
- The search for edges in remote sensing images using a digital polygonal map p 45 A89-23964
- [ETN-89-94146] p 45 A89-23964
- GEOIDS**
- Satellite altimetry. II - A new prospecting tool p 23 A89-35895
- Seasat altimetry and the South Atlantic geoid. II - Short-wavelength undulations p 16 A89-39659
- GEOLOGICAL FAULTS**
- Use of aerial and space photography for the detection of faults and neotectonic movements in Crimea and the Azov Coastal Region p 9 A89-34003
- Implication of patterns of faulting and hydrothermal alteration from Landsat TM images and NHAP aerial photos to mineral exploration and tectonics of the Virginia Range, Nevada --- National High Altitude Photography p 11 A89-35868
- Conjugate synthetic normal faults around the Gulf of Salwa, southwestern Qatar, the Arabian Gulf p 12 A89-35886
- The Calvin 28 cryptoexplosive disturbance, Cass County, Michigan: Evidence for impact origin p 14 A89-21358
- Neotectonics in Central Mexico from LANDSAT TM data [NASA-CR-183416] p 14 A89-21416
- Kinematics at the intersection of the Garlock and Death Valley fault zones, California: Integration of TM data and field studies [NASA-CR-184854] p 15 A89-22263
- GEOLOGICAL SURVEYS**
- Remote-sensing studies of present-day tectonic processes --- Russian book p 20 A89-34001
- The potential use of remote sensing to solve problems of paleotectonic prediction, geologic structure, and exploitation of coal deposits with reference to the Moscow-Region coal basin p 49 A89-34002
- Dynamics of present-day geological processes from remotely sensed data p 9 A89-34004

- Morphostructural interpretation of space images and the reconstruction of the recently formed stress field in the Altai-Baikai region p 10 A89-34006
- The use of space imagery for investigations of recent crustal deformations in southern Yakutia p 20 A89-34015
- Seismogeological interpretation of space images of the region of Caucasian mineral waters p 10 A89-34018
- Concentric structures in southern Tien-Shan --- Russian book p 10 A89-34196
- Thematic Conference on Remote Sensing for Exploration Geology, 6th, Houston, TX, May 16-19, 1988, Proceedings. Volumes 1 & 2 p 10 A89-35851
- Basic concepts in the use of remotely sensed data for resource exploration p 11 A89-35852
- A survey of the operational status and needs of remote sensing in exploration geology p 64 A89-35853
- Synthetic Aperture Radar data for mapping subsurface geological structures in the Northwest Territories, Canada p 50 A89-35858
- Use of remotely sensed data in mature basin exploration - Considerations on creating useful imagery p 50 A89-35861
- The contribution of remote sensing data to exploration of fractured reservoirs p 50 A89-35862
- Lithologic mapping in East Greenland with Landsat Thematic Mapper imagery p 6 A89-35869
- A field spectrometer and remote sensing study of the Fresnillo mining district, Mexico p 51 A89-35871
- Lineament analysis for hazard assessment in advance of coal mining p 11 A89-35873
- Application of Landsat Thematic Mapper imagery for lithological mapping of poorly accessible semi-arid regions p 7 A89-35879
- Combined remote sensing and surface geochemical survey in a drift-covered area in southeastern Saskatchewan p 12 A89-35881
- Photogeologic-geomorphic mapping provides clues to structural features beneath glacial terrain p 7 A89-35882
- From large-scale to small-scale - Economic geologic-geomorphic mapping using aerial photographs and Landsat images p 7 A89-35884
- Applications of AVHRR imagery in frontier exploration p 23 A89-35885
- The definition of isometric magmatogenic structures on space imagery p 12 A89-37315
- Geologic applications of Space Shuttle photography p 34 A89-41431
- GEOLOGY**
- Geological data integration techniques: Proceedings [DE88-705255] p 14 A89-20868
- Geological remote sensing signatures of terrestrial impact craters p 37 A89-21317
- Geological gyrocompass p 63 A89-24589
- The activities of the British National Space Centre (BNSC) in the field of imaging spectrometry p 47 A89-24696
- GEOLOGIC MICROPULSATIONS**
- Some aspects of the relation between Pi 1-2 magnetic pulsations observed at L = 1.3-2.1 on the ground and substorm-associated magnetic field variations in the near-earth magnetotail observed by AMPTE CCE p 52 A89-36686
- GEOMAGNETISM**
- GEOS 1 observations of low-energy ions in the earth's plasmasphere - A study on composition, and temperature and density structure under quiet geomagnetic conditions p 9 A89-33829
- Distribution of auroral arcs during quiet geomagnetic conditions p 50 A89-34772
- Some aspects of the relation between Pi 1-2 magnetic pulsations observed at L = 1.3-2.1 on the ground and substorm-associated magnetic field variations in the near-earth magnetotail observed by AMPTE CCE p 52 A89-36686
- Magnetometer array studies, earth structure, and tectonic processes p 13 A89-42149
- Modelling the earth's geomagnetic field to high degree and order p 58 A89-43408
- Derivation of a geomagnetic model to n = 63 p 58 A89-43409
- The geomagnetic spectrum for 1980 and core-crustal separation p 13 A89-43410
- GEOMETRIC ACCURACY**
- Pixel and sub-pixel accuracy in geometrical correction of AVHRR p 30 A89-40134
- AVIRIS data characteristics and their effects on spectral discrimination of rocks exposed in the Drum Mountains, Utah: Results of a preliminary study p 40 A89-22165
- GEOMETRIC RECTIFICATION (IMAGERY)**
- Autocorrelation and regularization in digital images. II - Simple image models p 29 A89-39551
- Pixel a. d sub-pixel accuracy in geometrical correction of AVHRR p 30 A89-40134

- GEOMORPHOLOGY**
- Mapping of Landsat satellite and gravity lineaments in west Tennessee p 6 A89-34357
- Photogeologic-geomorphic mapping provides clues to structural features beneath glacial terrain p 7 A89-35882
- GEOPHYSICS**
- Geophysical geodesy - The slow deformations of the earth --- Book p 7 A89-38583
- Geological remote sensing signatures of terrestrial impact craters p 37 A89-21317
- The Calvin 28 cryptoexplosive disturbance, Cass County, Michigan: Evidence for impact origin p 14 A89-21358
- Solar-geophysical data number 529, September 1988, Part 1: (Prompt reports). Data for August, July 1988 and late data [PB89-121305] p 37 A89-21431
- GEOS 1 SATELLITE**
- GEOS 1 observations of low-energy ions in the earth's plasmasphere - A study on composition, and temperature and density structure under quiet geomagnetic conditions p 9 A89-33829
- GEOS 3 SATELLITE**
- Synoptic analysis and dynamical adjustment of GEOS 3 and Seasat altimeter eddy fields in the northwest Atlantic p 29 A89-39650
- GEOSAT SATELLITES**
- GEOSAT altimeter sea-ice mapping p 49 A89-34267
- Evaluation of Geosat altimeter data with application to tropical Pacific sea level variability p 25 A89-37801
- GEOTHERMAL ENERGY EXTRACTION**
- Japan's sunshine project 1987 annual summary of geothermal energy R and D [DE88-756451] p 18 A89-22183
- GEOTHERMAL RESOURCES**
- Japan's sunshine project 1987 annual summary of geothermal energy R and D [DE88-756451] p 18 A89-22183
- GERMANY**
- Computer aided production of a 1:25,000 relief model of Berlin and surroundings p 8 A89-23943
- GLACIERS**
- Preliminary development of a seashore-effects analysis system [DE89-007863] p 61 A89-22191
- Remote sensing of global snowpack energy and mass balance: In-situ measurements on the snow of interior and Arctic Alaska [NASA-CR-180078] p 62 A89-23956
- GLACIOLOGY**
- NOAA (National Oceanic and Atmospheric Administration) AVHRR (Advanced Very High Resolution Radiometer) observations during the marginal ice zone experiment, between Spitzbergen and Greenland, June 7 to 18 July 1984 [AD-A204911] p 19 A89-22280
- GLOBAL POSITIONING SYSTEM**
- Operational aspects of CASA UNO '88-The first large scale international GPS geodetic network p 7 A89-42787
- Observation model and parameter partials for the JPL geodetic GPS modeling software GPSOMC [NASA-CR-185021] p 9 A89-24060
- GNEISS**
- Structural patterns in high grade terrain in parts of Tamil Nadu and Karnataka p 14 A89-22255
- GOLD**
- Implementation of background and target geobotanical techniques in mineral exploration p 23 A89-35892
- GRAINS (FOOD)**
- Advanced space design program to the Universities Space Research Association and the National Aeronautics and Space Administration [NASA-CR-180450] p 3 A89-24015
- GRASSLANDS**
- Evaluating atmospheric correction models for retrieving surface temperatures from the AVHRR over a tallgrass prairie p 20 A89-33875
- Monitoring the halfa steppes of central Tunisia using Landsat MSS p 1 A89-34947
- Measuring and modeling spectral characteristics of a tallgrass prairie p 27 A89-38970
- GRAVIMETRY**
- Gravimetric studies at sea --- Russian book p 49 A89-34088
- GRAVITY ANOMALIES**
- Mapping of Landsat satellite and gravity lineaments in west Tennessee p 6 A89-34357
- GREENHOUSE EFFECT**
- Effect of metal stress on the thermal infrared emission of soybeans: A greenhouse experiment - Possible utility in remote sensing p 2 A89-39658
- Monitoring the greenhouse effect from space p 4 A89-39739

- Preliminary development of a seashore-effects analysis system
[DE89-007863] p 61 N89-22191
- Correlation between satellite-derived aerosol characteristics and oceanic dimethylsulfide (DMS)
[AD-A206179] p 6 N89-24759
- GROUND STATIONS**
- Environmental projects. Volume 3: Environmental compliance audit
[NASA-CR-185019] p 5 N89-23985
- GROUND TRUTH**
- Sea-ice characterization measurements needed for testing of microwave remote sensing models
p 20 A89-34268
- Variation of surface water spectral response as a function of in situ sampling technique
p 33 A89-41161
- Integration of tie-points in digital mosaicing
[ETN-89-94147] p 41 N89-22973
- GYROCOMPASSES**
- Geological gyrocompass
[PB89-133086] p 63 N89-24589

H

- HABITATS**
- Review of wildlife resources of Vandenberg Air Force Base, California
[NASA-TM-102146] p 5 N89-23982
- HAZARDS**
- Lineament analysis for hazard assessment in advance of coal mining
p 11 A89-35873
- HEAT FLUX**
- Methodology for the remote sensing of fluxes of heat, moisture, and effective radiation in the ocean-atmosphere system
p 16 A89-35686
- Mesoscale severe weather development under orographic influences
[AD-A205082] p 41 N89-22293
- HEAT ISLANDS**
- Comparison of satellite, ground-based, and modeling techniques for analyzing the urban heat island
p 26 A89-37948
- HEAT TRANSFER**
- Thermal modeling of heat dissipation in the Pen Branch delta using thermal infrared imagery
p 32 A89-41159
- HEURISTIC METHODS**
- Shortest paths in a digitized map using a tile-based data structure
[PB89-143432] p 44 N89-23957
- HIERARCHIES**
- A software system to create a hierarchical, multiple level of detail terrain model
[AD-A203047] p 38 N89-21568
- HIGH RESOLUTION**
- High resolution chronology of late Cretaceous-early Tertiary events determined from 21,000 yr orbital-climatic cycles in marine sediments
p 14 N89-21328
- HIRIS: NASA's high-resolution imaging spectrometer for the Earth Observing System (EOS)
p 63 N89-24695
- HURRICANES**
- Drop-size distributions associated with intense rainfall
p 50 A89-34876
- Meteorological applications of Space Shuttle photography
p 34 A89-41430

HYDROCARBONS

- Hydrocarbon potential of part of the margin of the Tarim Basin from Landsat - A case history
p 11 A89-35857
- Identification of Cross Strike discontinuities in the Appalachian basin and implications for hydrocarbon exploration
p 11 A89-35860
- Gas chromatographic and sonar imaging of hydrocarbon seeps in the marine environment
p 22 A89-35863
- Use of seabottom magnetic susceptibility measurements in hydrocarbon exploration
p 16 A89-35864
- High resolution imaging of geobotanical anomalies associated with subsurface hydrocarbons
p 22 A89-35870
- Combined remote sensing and surface geochemical survey in a drift-covered area in southeastern Saskatchewan
p 12 A89-35881
- From large-scale to small-scale - Economic geologic-geomorphic mapping using aerial photographs and Landsat images
p 7 A89-35884
- A closer look at the Patrick Draw oil field vegetation anomaly
p 1 A89-35893
- Satellite altimetry. II - A new prospecting tool
p 23 A89-35895
- HYDROCHLORIC ACID**
- Antarctic ozone: Theory and observation
p 4 N89-22189
- HYDRODYNAMICS**
- Imaging of ocean waves by SAR
[AD-A203604] p 37 N89-21165

HYDROLOGICAL CYCLE

- Satellite-borne lidar observations of the earth - Requirements and anticipated capabilities
p 56 A89-41692

HYDROLOGY

- The dispersion limitations on the accuracy of the internal reference method during remote laser sounding of the upper ocean layer
p 53 A89-37349
- Activities at the Norwegian Hydrotechnical Laboratory
p 55 A89-40129
- Using NOAA AVHRR imagery in assessing water quality parameters
p 55 A89-40148
- Thermal modeling of heat dissipation in the Pen Branch delta using thermal infrared imagery
p 32 A89-41159

HYDROLOGY MODELS

- Relating point to area average rainfall in semiarid West Africa and the implications for rainfall estimates derived from satellite data
p 55 A89-39870

HYDROMETEOROLOGY

- Methodology for the remote sensing of fluxes of heat, moisture, and effective radiation in the ocean-atmosphere system
p 16 A89-35686

HYDROTHERMAL STRESS ANALYSIS

- An assessment of AVIRIS data for hydrothermal alteration mapping in the Goldfield Mining District, Nevada
p 40 N89-22168

HYDROTHERMAL SYSTEMS

- Implication of patterns of faulting and hydrothermal alteration from Landsat TM images and NHAP aerial photos to mineral exploration and tectonics of the Virginia Range, Nevada --- National High Altitude Photography
p 11 A89-35868
- Japan's sunshine project 1987 annual summary of geothermal energy R and D
[DE88-756451] p 18 N89-22183

I

ICE

- Active and passive remote sensing of ice
[AD-A203943] p 59 N89-20543
- Ice cover on Chesapeake Bay from AVHRR (Advanced Very High Resolution Radiometer) and LANDSAT imagery, winter of 1987-88
[PB89-117261] p 59 N89-21415
- ICE ENVIRONMENTS**
- Satellite-borne lidar observations of the earth - Requirements and anticipated capabilities
p 56 A89-41692

ICE FORMATION

- Ice cover on Chesapeake Bay from AVHRR (Advanced Very High Resolution Radiometer) and LANDSAT imagery, winter of 1987-88
[PB89-117261] p 59 N89-21415

ICE MAPPING

- GEOSAT altimeter sea-ice mapping
p 49 A89-34267
- Sea-ice characterization measurements needed for testing of microwave remote sensing models
p 20 A89-34268
- Image-analysis techniques for determination of morphology and kinematics in arctic sea ice
p 21 A89-34416
- Lithologic mapping in East Greenland with Landsat Thematic Mapper imagery
p 6 A89-35869
- Ice cover on Chesapeake Bay from AVHRR (Advanced Very High Resolution Radiometer) and LANDSAT imagery, winter of 1987-88
[PB89-117261] p 59 N89-21415
- ICE REPORTING**
- An algorithm for snow and ice detection using AVHRR data - An extension to the Apollo software package
p 31 A89-40155

IGNEOUS ROCKS

- Evaluation of Airborne Visible/Infrared Imaging Spectrometer Data of the Mountain Pass, California carbonate complex
p 60 N89-22169

IMAGE ANALYSIS

- Short- and long-term memory effects in intensified array detectors - Influence on airborne laser fluorosensor measurements
p 47 A89-32836
- An algorithm for machine-recognizing the river mouth and measuring the sealine from the Landsat image
p 19 A89-33658
- Image-analysis techniques for determination of morphology and kinematics in arctic sea ice
p 21 A89-34416
- Multispectral space surveys and data processing
p 22 A89-35684
- Uses of the SAS statistical package for digital image analysis
p 23 A89-35898
- A semi-automatic terrain measurement system for earthwork control
p 28 A89-39094

- Identification and analysis of the alignments of point-like features in remotely-sensed imagery. Volcanic cones in the Pinacate Volcanic Field, Mexico
p 12 A89-39651
- Geological uses of remotely-sensed reflected and emitted data of lateritized Archaean terrain in Western Australia
p 55 A89-39652
- Multi-spectral classification of snow using NOAA AVHRR imagery
p 31 A89-40156
- Combined film and softcopy photo-interpretation system
p 31 A89-40263
- A global approach to knowledge-based surface material classification
p 32 A89-41156
- Knowledge-based image data management - An expert front-end for the BROWSE facility
p 32 A89-41158
- Geological application of SIR-A imagery in southern Iraq
p 13 A89-41162
- AVIRIS performance during the 1987 flight season: An AVIRIS project assessment and summary of the NASA-sponsored performance evaluation
p 60 N89-22155
- Radiometric performance of AVIRIS: Assessment for an arid region geologic target
p 39 N89-22157
- Calibration and evaluation of AVIRIS data: Cripple Creek in October 1987
p 39 N89-22159
- Cooperative methods for road tracking in aerial imagery
p 42 N89-23101
- Investigation of several methods for the detection of outstanding points in a digital image
[ETN-89-94148] p 45 N89-23965
- Biophysical variability in the Greenland Sea observed with the Multispectral Airborne Radiometer System (MARS)
[NASA-CR-184856] p 47 N89-24784

IMAGE CONTRAST

- The definition of isometric magmatogenic structures on space imagery
p 12 A89-37315

IMAGE ENHANCEMENT

- Low-relief topographic enhancement in a Landsat snow-cover scene
p 54 A89-38966
- Zones of information in the AVIRIS spectra
p 39 N89-22158
- Calibration and evaluation of AVIRIS data: Cripple Creek in October 1987
p 39 N89-22159

IMAGE INTENSIFIERS

- Short- and long-term memory effects in intensified array detectors - Influence on airborne laser fluorosensor measurements
p 47 A89-32836

IMAGE PROCESSING

- Multispectral image processing and enhancement: Proceedings of the Meeting, Orlando, FL, Apr. 6-8, 1988
[SPIE-933] p 48 A89-33653
- Representation and recognition of elongated regions in aerial images
p 19 A89-33684
- Accessing remote sensing technology - The microBRIAN example
p 21 A89-34706
- Performance analysis of the DFVLR real time SAR processor for low SNRs
p 28 A89-35336
- A digital mosaicking algorithm allowing for an irregular join 'line'
p 26 A89-37944
- Two-dimensional seam-point searching in digital image mosaicking
p 26 A89-37945
- A raster approach to topographic map revision
p 26 A89-37946
- Digital photogrammetric processing systems - Current status and prospects
p 28 A89-39095
- Autocorrelation and regularization in digital images. II - Simple image models
p 29 A89-39551
- AVHRR data processing to study the surface canopies in temperate regions - First results of HAPEX-MOBILHY
p 30 A89-40153
- 1988 ACSM-ASPRS Annual Convention, Saint Louis, MO, Mar. 13-18, 1988, Technical Papers. Volume 4 - Image processing/remote sensing
p 32 A89-41151
- Earth scenes in polarized light observed from the Space Shuttle
p 34 A89-41429
- Minimum cross-entropy noise reduction in images
p 34 A89-41845
- Computer strategy for detecting line features on simulated binary arrays in support of radar feature extraction
[AD-A203257] p 37 N89-21162
- Preliminary analysis of Airborne Visible/Infrared Imaging Spectrometer (AVIRIS) for mineralogic mapping at sites in Nevada and Colorado
p 60 N89-22161
- Integration of tie-points in digital mosaicing
[ETN-89-94147] p 41 N89-22973
- Geocoded data sets of imaging satellites
p 43 N89-23950
- IMAGE RECONSTRUCTION**
- Reconstruction of imagery of faulted landscapes using a photo-optical technique
p 24 A89-35900
- Overview of the SRI cartographic modeling environment
p 62 N89-23122
- IMAGE RESOLUTION**
- The suitability of remote sensing for surveying and monitoring landscape patterns. Volume B: PEPS Project No. 73 - SPOT Imagery
p 36 N89-20536

IMAGERY

Geological remote sensing signatures of terrestrial impact craters p 37 N89-21317

IMAGING RADAR

Airborne imaging radar system for monitoring sea pollution

[MBB-UK-0016-87-PUB] p 58 A89-42941

Imaging radar applications in Europe. Illustrated experimental results (1978-1987)

[ESA-TM-01] p 42 N89-22978

Geocoded data sets of imaging satellites p 43 N89-23950

Imaging procedure of underwater bottom topography by air and satellite images in the range of microwave and visible electromagnetic spectra

[GKSS-88/E/41] p 17 N89-24014

IMAGING SPECTROMETERS

Analysis of Airborne Imaging Spectrometer (AIS) data for geobotanical prospecting p 51 A89-35890

The spectrometer of the Salyut-7 orbital station

p 57 A89-42608

Proceedings of the Airborne Visible/Infrared Imaging Spectrometer (AVIRIS) Performance Evaluation Workshop

[NASA-CR-184870] p 59 N89-22154

AVIRIS performance during the 1987 flight season: An AVIRIS project assessment and summary of the NASA-sponsored performance evaluation

p 60 N89-22155

Atmospheric water mapping with the Airborne Visible/Infrared Imaging Spectrometer (AVIRIS), Mountain Pass, California p 39 N89-22156

Radiometric performance of AVIRIS: Assessment for an arid region geologic target p 39 N89-22157

Zones of information in the AVIRIS spectra

p 39 N89-22158

Calibration and evaluation of AVIRIS data: Cripple Creek in October 1987 p 39 N89-22159

Automated extraction of absorption features from Airborne Visible/Infrared Imaging Spectrometer (AVIRIS) and Geophysical and Environmental Research Imaging Spectrometer (GERIS) data p 39 N89-22160

Preliminary analysis of Airborne Visible/Infrared Imaging Spectrometer (AVIRIS) for mineralogic mapping at sites in Nevada and Colorado p 60 N89-22161

Assessment of AVIRIS data from vegetated sites in the Owens Valley, California p 60 N89-22162

Examination of the spectral features of vegetation in 1987 AVIRIS data p 3 N89-22163

AVIRIS data quality for coniferous canopy chemistry

p 40 N89-22164

AVIRIS data characteristics and their effects on spectral discrimination of rocks exposed in the Drum Mountains, Utah: Results of a preliminary study p 40 N89-22165

Application of imaging spectrometer data to the Kings-Kaweah ophiolite melange p 40 N89-22166

AVIRIS spectra of California wetlands p 3 N89-22167

An assessment of AVIRIS data for hydrothermal alteration mapping in the Goldfield Mining District, Nevada p 40 N89-22168

Evaluation of Airborne Visible/Infrared Imaging Spectrometer Data of the Mountain Pass, California carbonate complex p 60 N89-22169

Determination of in-flight AVIRIS spectral, radiometric, spatial and signal-to-noise characteristics using atmospheric and surface measurements from the vicinity of the rare-earth-bearing carbonate at Mountain Pass, California p 61 N89-22170

ESA's planned activities in the field of imaging spectrometry for Earth observation p 46 N89-24693

The FLI airborne imaging spectrometer: A highly versatile sensor for many applications p 63 N89-24694

HIRIS: NASA's high-resolution imaging spectrometer for the Earth Observing System (EOS) p 63 N89-24695

The activities of the British National Space Centre (BNSC) in the field of imaging spectrometry p 47 N89-24696

DFVLR activities related to imaging spectrometry p 63 N89-24697

Development of an imaging spectrometer for remote sensing: The FLI program p 63 N89-24698

Activities of CNES in the field of imaging spectrometry p 47 N89-24699

The EARSEL Imaging Spectrometry Working Group p 47 N89-24700

Imaging spectrometry at the Canada Centre for Remote Sensing p 64 N89-24701

IMAGING TECHNIQUES

Automated DTM validation and progressive sampling algorithm of finite element array relaxation

p 22 A89-35837

Using multispectral video imagery for detecting soil surface conditions p 22 A89-35838

Imaging of ocean waves by SAR [AD-A203604] p 37 N89-21165

Data compression experiments with LANDSAT thematic mapper and Nimbus-7 coastal zone color scanner data p 41 N89-22344

Imaging radar applications in Europe. Illustrated experimental results (1978-1987)

[ESA-TM-01] p 42 N89-22978

Imaging Spectrometry for Land Applications

[ESA-SP-1101] p 63 N89-24692

ESA's planned activities in the field of imaging spectrometry for Earth observation p 46 N89-24693

The FLI airborne imaging spectrometer: A highly versatile sensor for many applications p 63 N89-24694

HIRIS: NASA's high-resolution imaging spectrometer for the Earth Observing System (EOS) p 63 N89-24695

The activities of the British National Space Centre (BNSC) in the field of imaging spectrometry p 47 N89-24696

DFVLR activities related to imaging spectrometry p 63 N89-24697

Development of an imaging spectrometer for remote sensing: The FLI program p 63 N89-24698

Activities of CNES in the field of imaging spectrometry p 47 N89-24699

The EARSEL Imaging Spectrometry Working Group p 47 N89-24700

Imaging spectrometry at the Canada Centre for Remote Sensing p 64 N89-24701

INDIA

Identification of magnesite and bauxite deposits on Landsat imagery, South India p 12 A89-35889

Structural patterns in high grade terrain in parts of Tamil Nadu and Karnataka p 14 N89-22255

INDIUM ANTIMONIDES

An analysis of platinum silicide and indium antimonide for remote sensors in the 3 to 5 micrometer wavelength band

[AD-A202663] p 59 N89-21218

INFESTATION

Cluster analysis of pine crown foliage patterns aid identification of mountain pine beetle current-attack

p 26 A89-37950

INFORMATION SYSTEMS

Geological data integration techniques: Proceedings [DE88-705255] p 14 N89-20868

Earth system science: A program for global change [NASA-TM-101186] p 5 N89-22969

Definition and filling of information systems: Challenge for a photogrammetric service enterprise p 62 N89-23942

INFRARED DETECTORS

Review and status of remote sensing of sea ice p 20 A89-34266

INFRARED IMAGERY

Multispectral image processing and enhancement; Proceedings of the Meeting, Orlando, FL, Apr. 6-8, 1988 [SPIE-933] p 48 A89-33653

Multispectral terrain background simulation techniques for use in airborne sensor evaluation p 19 A89-33664

Measurements of short-term thermal responses of coniferous forest canopies using thermal scanner data p 1 A89-33867

GEOSAT altimeter sea-ice mapping p 49 A89-34267

Volcano monitoring by short wavelength infrared satellite remote sensing p 51 A89-35875

Infrared thermography - A quantitative tool for heat study [ONERA, TP NO. 1989-3] p 53 A89-37627

Estimation of regional surface resistance to evapotranspiration from NDVI and thermal-IR AVHRR data --- Normalized Difference Vegetation Index p 55 A89-39872

The potential of infrared satellite data for the retrieval of Saharan-dust optical depth over Africa p 30 A89-39875

Thermal modeling of heat dissipation in the Pen Branch delta using thermal infrared imagery p 32 A89-41159

Satellite signatures of rapid cyclogenesis [AD-A203934] p 38 N89-21452

Infrared sea-radiance modeling using LOWTRAN 6 [AD-A202582] p 38 N89-21643

AVIRIS performance during the 1987 flight season: An AVIRIS project assessment and summary of the NASA-sponsored performance evaluation p 60 N89-22155

Atmospheric water mapping with the Airborne Visible/Infrared Imaging Spectrometer (AVIRIS), Mountain Pass, California p 39 N89-22156

AVIRIS data quality for coniferous canopy chemistry p 40 N89-22164

AVIRIS data characteristics and their effects on spectral discrimination of rocks exposed in the Drum Mountains, Utah: Results of a preliminary study p 40 N89-22165

An assessment of AVIRIS data for hydrothermal alteration mapping in the Goldfield Mining District, Nevada p 40 N89-22168

Evaluation of Airborne Visible/Infrared Imaging Spectrometer Data of the Mountain Pass, California carbonate complex p 60 N89-22169

Determination of in-flight AVIRIS spectral, radiometric, spatial and signal-to-noise characteristics using atmospheric and surface measurements from the vicinity of the rare-earth-bearing carbonate at Mountain Pass, California p 61 N89-22170

Thermal images of sky and sea-surface background infrared radiation [AD-A205819] p 46 N89-23992

INFRARED PHOTOGRAPHY

Expanding the utility of manned observations of earth - 70 mm film tests on the Space Shuttle p 34 A89-41428

Mapping freeze/thaw boundaries with SMMR data [NASA-CR-184991] p 9 N89-23961

INFRARED RADIATION

Global, seasonal surface variations from satellite radiance measurements p 52 A89-35966

The condition of natural features as related to their intrinsic microwave and IR emission fields p 2 A89-37320

Mesoscale severe weather development under orographic influences [AD-A205082] p 41 N89-22293

Thermal images of sky and sea-surface background infrared radiation [AD-A205819] p 46 N89-23992

INFRARED SCANNERS

Modeling surface temperature distributions in forest landscapes p 48 A89-33868

Phase A study for the extension of the CAESAR scanner with a sensor module for the far infrared [BCRS-88-09] p 59 N89-20539

INFRARED SIGNATURES

Satellite signatures of rapid cyclogenesis [AD-A203934] p 38 N89-21452

INFRARED SPECTRA

Visible and near-infrared (0.4- to 2.5-microns) reflectance spectra of selected mixed-layer clays and related minerals p 12 A89-35897

Effect of metal stress on the thermal infrared emission of soybeans: A greenhouse experiment - Possible utility in remote sensing p 2 A89-39658

Proceedings of the Airborne Visible/Infrared Imaging Spectrometer (AVIRIS) Performance Evaluation Workshop [NASA-CR-184870] p 59 N89-22154

Calibration and evaluation of AVIRIS data: Cripple Creek in October 1987 p 39 N89-22159

Preliminary analysis of Airborne Visible/Infrared Imaging Spectrometer (AVIRIS) for mineralogic mapping at sites in Nevada and Colorado p 60 N89-22161

Examination of the spectral features of vegetation in 1987 AVIRIS data p 3 N89-22163

INFRARED SPECTROMETERS

AVIRIS performance during the 1987 flight season: An AVIRIS project assessment and summary of the NASA-sponsored performance evaluation p 60 N89-22155

INFRARED SPECTROSCOPY

Seasonal visible, near-infrared and mid-infrared spectra of rice canopies in relation to LAI and above-ground dry phytomass p 54 A89-38967

Infrared spectroscopy (2.3-20 microns) for the geological interpretation of remotely-sensed multispectral thermal infrared data p 30 A89-39656

INLAND WATERS

Lake area measurement using AVHRR - A case study p 31 A89-40154

INSOLATION

Estimation of surface insolation using sun-synchronous satellite data p 52 A89-35939

The influence of the viewing geometry of bare rough soil surfaces on their spectral response in the visible and near-infrared range p 2 A89-38969

INTERFEROMETRY

Antarctic ozone: Theory and observation p 4 N89-22189

INTERNAL WAVES

OSRMS (Ocean Surface Roughness Measurement System): The DREP (Defence Research Establishment Pacific) near-nadir scatterometer [AD-A202983] p 38 N89-21460

INTERPLANETARY MAGNETIC FIELDS

The interplanetary magnetic field B(y)-dependent field-aligned current in the dayside polar cap under quiet conditions p 50 A89-34782

Polar cap deflation during magnetospheric substorms p 24 A89-36704

INTERPOLATION

Calibration and evaluation of AVIRIS data: Cripple Creek in October 1987 p 39 N89-22159

INVENTORIES

- Land use inventory using LANDSAT Thematic Mapper imagery to study environmental pollution [NLR-MP-87063-U] p 4 N89-20541
- Information resources management p 42 N89-23371

INVERSIONS

- The investigation of advanced remote sensing, radiative transfer and inversion techniques for the measurement of atmospheric constituents [NASA-CR-172599] p 36 N89-20531

IONOSPHERIC ELECTRON DENSITY

- Properties of the equatorial and tropical ionosphere according to Soviet satellite observations during the IMS p 31 A89-40606

IONOSPHERIC SOUNDING

- Satellite, airborne and radar observations of auroral arcs p 48 A89-33505

IRRIGATION

- The Nebraska center-pivot inventory - An example of operational satellite remote sensing on a long term basis p 28 A89-39096

J**JAPAN**

- Japan's sunshine project 1987 annual summary of geothermal energy R and D [DE88-756451] p 18 N89-22183

JAPANESE SPACECRAFT

- Spectral indices for vegetation and rock type discrimination using the optical sensor of the Japanese ERS-1 p 51 A89-35866
- Marine Observation Satellite-1 - First year in orbit p 26 A89-38328

JET STREAMS (METEOROLOGY)

- Mesoscale severe weather development under orographic influences [AD-A205082] p 41 N89-22293

K**KENYA**

- Vegetation and landscape of Kora National Reserve, Kenya p 6 A89-34945

KINEMATICS

- Kinematics at the intersection of the Garlock and Death Valley fault zones, California: Integration of TM data and field studies [NASA-CR-184854] p 15 N89-22263

KNOWLEDGE BASES (ARTIFICIAL INTELLIGENCE)

- A global approach to knowledge-based surface material classification p 32 A89-41156
- Remote sensing information sciences research group: Browse in the EOS era [NASA-CR-184637] p 42 N89-22979
- Image understanding research at SRI International p 42 N89-23080

KNOWLEDGE REPRESENTATION

- Representation and recognition of elongated regions in aerial images p 19 A89-33684

KP INDEX

- Comparison of field-aligned currents at ionospheric and magnetospheric altitudes p 9 A89-33540

L**LAGEOS (SATELLITE)**

- Rate of change of the Quincy-Monument Peak baseline from a translocation analysis of Lageos laser range data p 13 A89-42181

LAKES

- Assessment of the present conditions of lowland lakes of Central Asia using the interpretation of space photographs p 17 A89-37319
- Lake area measurement using AVHRR - A case study p 31 A89-40154
- Analysis of seasonal characteristics of Sambhar Salt Lake, India, from digitized Space Shuttle photography p 18 A89-41433
- The decrease of Lake Chad as documented during twenty years of manned space flight p 18 A89-41434
- The relationship between in-lake sulfate concentration and estimates of atmospheric sulfur deposition for subregions of the eastern lake survey [DE89-009868] p 5 N89-24749

LAND

- Processing and application of digital AVHRR-imagery for land and sea surfaces [BCRS-88-08] p 36 N89-20538

LAND ICE

- Lithologic mapping in East Greenland with Landsat Thematic Mapper imagery p 6 A89-35869

An AVHRR mosaic image of Antarctica

p 30 A89-40135

LAND MANAGEMENT

- Applying remote sensing technology to the Bureau of Land Management's mineral management program p 11 A89-35874
- Concept for a satellite-based global reserve monitoring system p 32 A89-41152
- The use of remote sensing and GIS techniques for wetland identification and classification in the Garrison Diversion Unit-North Dakota p 18 A89-41160

LAND USE

- Rural settlement expansion in Moneragala district, Sri Lanka p 4 A89-34946
- Analysis of seasonal characteristics of Sambhar Salt Lake, India, from digitized Space Shuttle photography p 18 A89-41433
- Monitoring in Moneragala district, Sri Lanka, with SPOT images p 3 A89-43317
- The suitability of remote sensing for surveying and monitoring landscape patterns. Volume A: Pilot study - LANDSAT Imagery. Volume B: PEPS Project No. 73 - SPOT Imagery [BCRS-87-12-VOL-A/B] p 4 N89-20534
- The suitability of remote sensing for surveying and monitoring landscape patterns. Volume A: Pilot study - LANDSAT Imagery p 36 N89-20535
- The suitability of remote sensing for surveying and monitoring landscape patterns. Volume B: PEPS Project No. 73 - SPOT Imagery p 36 N89-20536
- Land use inventories using satellite images in the region Haaren-Helvoirt-Udenhout, North Brabant (The Netherlands) [BCRS-88-07] p 36 N89-20537
- Computer assisted layout of graphic settlement representations p 43 N89-23951

LANDFORMS

- Low-relief topographic enhancement in a Landsat snow-cover scene p 54 A89-38966

LANDSAT SATELLITES

- Mapping of Landsat satellite and gravity lineaments in west Tennessee p 6 A89-34357
- Landsat commercialization - Keys to future success p 64 A89-34703
- Monitoring the halfa steppes of central Tunisia using Landsat MSS p 1 A89-34947
- Accuracy assessment of a Landsat-assisted vegetation map of the coastal plain of the Arctic National Wildlife Refuge p 6 A89-35840
- Landsat interpretation and stratigraphy of the Hugoton gas field (Southwestern Kansas) and surrounding areas p 6 A89-35856
- Hydrocarbon potential of part of the margin of the Tarim Basin from Landsat - A case history p 11 A89-35857
- Integration of Landsat TM, stream sediment geochemistry and regional geophysics for mineral exploration in the English Lake District p 23 A89-35888
- Identification of magnesite and bauxite deposits on Landsat imagery, South India p 12 A89-35889
- The Nebraska center-pivot inventory - An example of operational satellite remote sensing on a long term basis p 28 A89-39096
- Identification and analysis of the alignments of point-like features in remotely-sensed imagery. Volcanic cones in the Pinacate Volcanic Field, Mexico p 12 A89-39651
- Assessing the improvement in soil mapping using spot HRV over Landsat MSS imagery (Geography and land use) p 33 A89-41168

LANDSAT 4

- Calibration comparison for the Landsat 4 and 5 Multispectral Scanners and Thematic Mappers p 47 A89-32835
- Remote sensing of the deciduous vegetation of Great Smoky Mountains National Park p 33 A89-41170

LANDSAT 5

- Calibration comparison for the Landsat 4 and 5 Multispectral Scanners and Thematic Mappers p 47 A89-32835

LASER ALTIMETERS

- Laser altimetry measurements from aircraft and spacecraft p 56 A89-41691

LASER APPLICATIONS

- Laser scattering phenomenology - Background signature characterization and prediction p 6 A89-33661
- The dispersion limitations on the accuracy of the internal reference method during remote laser sounding of the upper ocean layer p 53 A89-37349

LASER BEAMS

- Remote sensing in refractive turbulence p 58 N89-20532

LASER INDUCED FLUORESCENCE

- Determination of spectral signatures for remote laser sensing of vegetation p 35 A89-42611

LASER RANGER/TRACKER

- High altitude laser ranging over rugged terrain p 54 A89-39092

LASER STABILITY

- Remote sensing in refractive turbulence p 58 N89-20532

LATENT HEAT

- Mesoscale severe weather development under orographic influences [AD-A205082] p 41 N89-22293

LAYOUTS

- Computer assisted layout of graphic settlement representations p 43 N89-23951

LEAF AREA INDEX

- Seasonal visible, near-infrared and mid-infrared spectra of rice canopies in relation to LAI and above-ground dry phytomass p 54 A89-38967

LEAVES

- A new technique to measure the spectral properties of conifer needles p 19 A89-33874

LIGHT SCATTERING

- Remote four-photon Raman spectroscopy of sea water under natural conditions p 52 A89-37327

LIMNOLOGY

- Assessment of the present conditions of lowland lakes of Central Asia using the interpretation of space photographs p 17 A89-37319

LINE SPECTRA

- The FLI airborne imaging spectrometer: A highly versatile sensor for many applications p 63 N89-24694
- HIRIS: NASA's high-resolution imaging spectrometer for the Earth Observing System (EOS) p 63 N89-24695
- Imaging spectrometry at the Canada Centre for Remote Sensing p 64 N89-24701

LITHOLOGY

- Lithologic mapping in East Greenland with Landsat Thematic Mapper imagery p 6 A89-35869
- Application of Landsat Thematic Mapper imagery for lithological mapping of poorly accessible semi-arid regions p 7 A89-35879
- Discrimination of rocks and hydrothermal altered areas based on Landsat TM data p 27 A89-38333

LONG WAVE RADIATION

- A parameterization for longwave surface radiation from sun-synchronous satellite data p 56 A89-41761

LORAN C

- Loran C field strength contours: Contiguous US [DOT/FAA/CT-TN89/16] p 8 N89-23437

LOW LEVEL TURBULENCE

- Mesoscale severe weather development under orographic influences [AD-A205082] p 41 N89-22293

LUNAR SURFACE

- Laser altimetry measurements from aircraft and spacecraft p 56 A89-41691

M**MAGMA**

- Discriminating late volcanic differentiates commonly associated with precious metal deposits, using Landsat Thematic Mapper imagery p 12 A89-35896
- The definition of isometric magmatogenic structures on space imagery p 12 A89-37315

MAGNETIC FIELD CONFIGURATIONS

- The interplanetary magnetic field B(y)-dependent field-aligned current in the dayside polar cap under quiet conditions p 50 A89-34782
- Modelling the earth's geomagnetic field to high degree and order p 58 A89-43408
- Derivation of a geomagnetic model to n = 63 p 58 A89-43409
- The geomagnetic spectrum for 1980 and core-crustal separation p 13 A89-43410

MAGNETIC FIELDS

- Solar-geophysical data number 529, September 1988. Part 1: (Prompt reports). Data for August, July 1988 and late data [PB89-121305] p 37 N89-21431

MAGNETIC PERMEABILITY

- Use of seabottom magnetic susceptibility measurements in hydrocarbon exploration p 16 A89-35864

MAGNETIC STORMS

- Polar cap deflation during magnetospheric substorms p 24 A89-36704
- The response of thermospheric nitric oxide to an auroral storm p 42 N89-23031

MAGNETIC VARIATIONS

- Some aspects of the relation between Pi 1-2 magnetic pulsations observed at L = 1.3-2.1 on the ground and substorm-associated magnetic field variations in the near-earth magnetotail observed by AMPTE CCE p 52 A89-36686

MAGNETOMETERS

- Magnetometer array studies, earth structure, and tectonic processes p 13 A89-42149

MAGNETOSPHERIC INSTABILITY

- Polar cap deflation during magnetospheric substorms p 24 A89-36704

MANNED SPACE FLIGHT

- Monitoring tropical environments with Space Shuttle photography p 34 A89-41432
The decrease of Lake Chad as documented during twenty years of manned space flight p 18 A89-41434

MANNED SPACECRAFT

- Studying the earth from manned spacecraft --- Russian book p 64 A89-42511

MAPPING

- High altitude laser ranging over rugged terrain p 54 A89-39092
Information resources management p 42 N89-23371
KRMS (K-band Radiometric Mapping System) SSM/I validation March 1988 quick look report [NASA-CR-185320] p 8 N89-23766
Geological gyrocompass [PB89-133086] p 63 N89-24589

MAPS

- Geological data integration techniques: Proceedings [DE88-705255] p 14 N89-20868
Column movement model used to support AMM p 38 N89-21521
The precedence of global features in the perception of map symbols [AD-A203792] p 7 N89-22174

MARINE BIOLOGY

- Remote sensing of ocean chlorophyll - Consequence of nonuniform pigment profile p 15 A89-32838
Development and verification of Osaka Bay sampling model based on Landsat data p 27 A89-38332
Measurements of spectral radiance at the sea surface for the development of remote sensing methods p 35 A89-42610
High resolution chronology of late Cretaceous-early Tertiary events determined from 21,000 yr orbital-climatic cycles in marine sediments p 14 N89-21328

MARINE ENVIRONMENTS

- Gravimetric studies at sea --- Russian book p 49 A89-34088
The experience of the Commission of the European Communities in the use of remote sensing for the implementation of community policies p 64 A89-34712
Infrared sea-radiance modeling using LOWTRAN 6 [AD-A202582] p 38 N89-21643

MARINE METEOROLOGY

- The prognosis of weather change lines over the ocean - The role of a reconnaissance aircraft p 48 A89-32848
Theoretical algorithms for satellite-derived sea surface temperatures p 21 A89-35159
Automated recognition of oceanic cloud patterns. I - Methodology and application to cloud climatology p 24 A89-35906

MARINE RESOURCES

- Gas chromatographic and sonar imaging of hydrocarbon seeps in the marine environment p 22 A89-35863
Use of seabottom magnetic susceptibility measurements in hydrocarbon exploration p 16 A89-35864
Nimbus-7 data product summary [NASA-RP-1215] p 39 N89-22152

MARKET RESEARCH

- On the international commercialization of remote sensing [BCRS-88-02] p 65 N89-23969

MARKETING

- A systematic worldwide landcover of satellite mosaics [NLR-MP-87062-U] p 65 N89-20540

MARSHLANDS

- Utilizing remote sensing of thematic mapper data to improve our understanding of estuarine processes and their influence on the productivity of estuarine-dependent fisheries [NASA-CR-183417] p 18 N89-20533

MATHEMATICAL MODELS

- Active and passive remote sensing of ice [AD-A203943] p 59 N89-20543
Infrared sea-radiance modeling using LOWTRAN 6 [AD-A202582] p 38 N89-21643
Remote sensing of earth terrain [NASA-CR-184937] p 41 N89-22971
On the connection of geodetic pointfields in RETrig [PB89-146112] p 44 N89-23958
Improvement and extension of a radar forest backscattering model [NASA-CR-184975] p 46 N89-24686

MATHEMATICAL PROGRAMMING

- Analysis and optimization of geodetic networks by spectral criteria and mechanical analogies [SER-C-342] p 45 N89-23963

MEASURING INSTRUMENTS

- 1988 Conference on Precision Electromagnetic Measurements, Tsukuba, Japan, June 7-10, 1988, Proceedings p 57 A89-42773

MELTING

- Snowmelt increase through albedo reduction [AD-A204523] p 18 N89-22175
Mapping freeze/thaw boundaries with SMMR data [NASA-CR-184991] p 9 N89-23961

MESOMETEOROLOGY

- Retrieval of mesoscale meteorological parameters for polar latitudes (MIZEX and ARCTEMIZ campaigns) p 58 A89-43026
Short-period fluctuation of the lower tropospheric winds observed by MU-radar p 58 A89-43311
Mesoscale severe weather development under orographic influences [AD-A205082] p 41 N89-22293

MESOSCALE PHENOMENA

- A meteorological overview of the pre-AMEX and AMEX periods over the Australian region p 48 A89-32850
Observing oceanic mesoscale eddies from Geosat altimetry - Preliminary results p 16 A89-39372
Mesoscale variability of sea surface temperature in the North Atlantic p 17 A89-40145
Meteorological applications of Space Shuttle photography p 34 A89-41430
Beaufort Sea mesoscale circulation study: Preliminary results [PB89-121693] p 17 N89-20597

MESOSPHERE

- Mesospheric temperature sounding with microwave radiometers p 54 A89-39557

METAMORPHISM (GEOLOGY)

- The Calvin 28 cryptoexplosive disturbance, Cass County, Michigan: Evidence for impact origin p 14 N89-21358

METEORITE COLLISIONS

- Geological remote sensing signatures of terrestrial impact craters p 37 N89-21317
The Calvin 28 cryptoexplosive disturbance, Cass County, Michigan: Evidence for impact origin p 14 N89-21358

METEORITE CRATERS

- Geological remote sensing signatures of terrestrial impact craters p 37 N89-21317

METEOROLOGICAL PARAMETERS

- Retrieval of mesoscale meteorological parameters for polar latitudes (MIZEX and ARCTEMIZ campaigns) p 58 A89-43026

METEOROLOGICAL RESEARCH AIRCRAFT

- The prognosis of weather change lines over the ocean - The role of a reconnaissance aircraft p 48 A89-32848

METEOROLOGY

- Beaufort Sea mesoscale circulation study: Preliminary results [PB89-121693] p 17 N89-20597

METEOSAT SATELLITE

- Meteosat thermal inertia mapping for studying wetland dynamics in the West-African Sahel [BCRS-88-10A] p 62 N89-23970

METHODOLOGY

- Design of a methodology for the detection of errors in terrestrial networks [ETN-89-94151] p 46 N89-23968

MICROWAVE EMISSION

- The condition of natural features as related to their intrinsic microwave and IR emission fields p 2 A89-37320
Parameter optimization of systems for the thermal microwave mapping of the earth's surface p 25 A89-37321

MICROWAVE IMAGERY

- Precipitation retrieval over land and ocean with the SSM/I - Identification and characteristics of the scattering signal p 53 A89-37549
Remote sensing of global snowpack energy and mass balance: In-situ measurements on the snow of interior and Arctic Alaska [NASA-CR-180078] p 62 N89-23956

MICROWAVE RADIOMETERS

- Highly sensitive microwave radiometer-scatterometer for the remote sensing of the earth's surface p 52 A89-37322
Methodological aspects of the automation of the calibration and processing of satellite microwave-radiometer data p 25 A89-37324
The rate of gas exchange between the ocean and the atmosphere using microwave radiometer data p 25 A89-37471
Mesospheric temperature sounding with microwave radiometers p 54 A89-39557

- Correcting absolute calibrations of satellite microwave radiometer using a priori data p 35 A89-42612
Processing and application of digital AVHRR-imagery for land and sea surfaces [BCRS-88-08] p 36 N89-20538

- Microwave X-band radiometric characterization of Brazilian soils by measurement of the complex permittivity [INPE-4588-PRE/1319] p 3 N89-24685

MICROWAVE SCATTERING

- Sea-ice characterization measurements needed for testing of microwave remote sensing models p 20 A89-34268
Precipitation retrieval over land and ocean with the SSM/I - Identification and characteristics of the scattering signal p 53 A89-37549

MICROWAVE SENSORS

- GEOSAT altimeter sea-ice mapping p 49 A89-34267
Sea-ice characterization measurements needed for testing of microwave remote sensing models p 20 A89-34268
Precipitation retrieval over land and ocean with the SSM/I - Identification and characteristics of the scattering signal p 53 A89-37549
Remote sensing of earth terrain [NASA-CR-184937] p 41 N89-22971

MICROWAVE SOUNDING

- Observational analyses of North Atlantic tropical cyclones from NOAA polar-orbiting satellite microwave data p 21 A89-34879

MICROWAVE TRANSMISSION

- Improving accuracy in radar-altimetry data correction for tropospheric effects p 54 A89-39322

MICROWAVES

- An analysis of platinum silicide and indium antimonide for remote sensors in the 3 to 5 micrometer wavelength band [AD-A202663] p 59 N89-21218
KRMS (K-band Radiometric Mapping System) SSM/I validation March 1988 quick look report [NASA-CR-185320] p 8 N89-23766

MINERAL DEPOSITS

- Identification of magnesite and bauxite deposits on Landsat imagery, South India p 12 A89-35889
Discriminating late volcanic differentiates commonly associated with precious metal deposits, using Landsat Thematic Mapper imagery p 12 A89-35896

MINERAL EXPLORATION

- Thematic Conference on Remote Sensing for Exploration Geology, 6th, Houston, TX, May 16-19, 1988, Proceedings. Volumes 1 & 2 p 10 A89-35851
Basic concepts in the use of remotely sensed data for resource exploration p 11 A89-35852
A survey of the operational status and needs of remote sensing in exploration geology p 64 A89-35853
Hydrocarbon potential of part of the margin of the Tarim Basin from Landsat - A case history p 11 A89-35857
Identification of Cross Strike discontinuities in the Appalachian basin and implications for hydrocarbon exploration p 11 A89-35860
Gas chromatographic and sonar imaging of hydrocarbon seeps in the marine environment p 22 A89-35863
Use of seabottom magnetic susceptibility measurements in hydrocarbon exploration p 16 A89-35864
Geobotanical determination of aggregate source material using Airborne Thematic Mapper imagery p 1 A89-35865
Application of Landsat Thematic Mapper digital data to the exploration for uranium-mineralized breccia pipes in Northwestern Arizona p 51 A89-35872
Applying remote sensing technology to the Bureau of Land Management's mineral management program p 11 A89-35874
The application of high resolution digital elevation models to petroleum and mineral exploration and production p 22 A89-35876
Assessing aggregate resource potential in the Canadian Shield - A knowledge-based approach p 23 A89-35877

- Combined remote sensing and surface geochemical survey in a drift-covered area in southeastern Saskatchewan p 12 A89-35881
Astronaut photography of the earth - Low cost images for resource exploration p 23 A89-35883
From large-scale to small-scale - Economic geologic-geomorphic mapping using aerial photographs and Landsat images p 7 A89-35884
Applications of AVHRR imagery in frontier exploration p 23 A89-35885
Integration of Landsat TM, stream sediment geochemistry and regional geophysics for mineral exploration in the English Lake District p 23 A89-35888

- Analysis of Airborne Imaging Spectrometer (AIS) data for geobotanical prospecting p 51 A89-35890

- MEIS II and surface data integration for detection of geobotanical anomalies p 51 A89-35891
Implementation of background and target geobotanical techniques in mineral exploration p 23 A89-35892
Ore-bearing structures of Central Kazakhstan identified on aerial and space photographs in the framework of the computer-aided prediction of minerals p 52 A89-37316
Preliminary analysis of Airborne Visible/Infrared Imaging Spectrometer (AVIRIS) for mineralogic mapping at sites in Nevada and Colorado p 60 N89-22161
AVIRIS data characteristics and their effects on spectral discrimination of rocks exposed in the Drum Mountains, Utah: Results of a preliminary study p 40 N89-22165
An assessment of AVIRIS data for hydrothermal alteration mapping in the Goldfield Mining District, Nevada p 40 N89-22168
- MINERALOGY**
Calibration and evaluation of AVIRIS data: Cripple Creek in October 1987 p 39 N89-22159
AVIRIS data characteristics and their effects on spectral discrimination of rocks exposed in the Drum Mountains, Utah: Results of a preliminary study p 40 N89-22165
Application of imaging spectrometer data to the Kings-Kaweah ophiolite melange p 40 N89-22166
- MINERALS**
Visible and near-infrared (0.4- to 2.5-microns) reflectance spectra of selected mixed-layer clays and related minerals p 12 A89-35897
- MINES (EXCAVATIONS)**
A field spectrometer and remote sensing study of the Fresno mining district, Mexico p 51 A89-35871
Lineament analysis for hazard assessment in advance of coal mining p 11 A89-35873
- MINIMUM ENTROPY METHOD**
Minimum cross-entropy noise reduction in images p 34 A89-41845
- MIXING LAYERS (FLUIDS)**
Field calibration of mixed-layer drifters p 53 A89-37554
- MODELS**
A software system to create a hierarchical, multiple level of detail terrain model [AD-A203047] p 38 N89-21568
- MOISTURE CONTENT**
Satellite-derived low-level atmospheric water vapour content from synergy of AVHRR with HIRS --- High Resolution Infrared Radiation Sounder p 30 A89-40139
Determination of areal snow water equivalent using satellite images and gamma ray spectrometry [CI-91] p 44 N89-23960
- MOLECULAR SPECTRA**
On the future development and management of spectroscopic database for radiative transfer from the issues of recent related workshops [ETN-89-94530] p 46 N89-24690
- MOLECULAR SPECTROSCOPY**
Remote four-photon Raman spectroscopy of sea water under natural conditions p 52 A89-37327
- MONSOONS**
A meteorological overview of the pre-AMEX and AMEX periods over the Australian region p 48 A89-32850
- MORPHOLOGY**
Geological remote sensing signatures of terrestrial impact craters p 37 N89-21317
- MOSAICS**
Reconstruction of imagery of faulted landscapes using a photo-optical technique p 24 A89-35900
A digital mosaicking algorithm allowing for an irregular join 'line' p 26 A89-37944
Two-dimensional seam-point searching in digital image mosaicking p 26 A89-37945
A systematic worldwide landcover of satellite mosaics [NLR-MP-87062-U] p 65 N89-20540
Integration of tie-points in digital mosaicking [ETN-89-94147] p 41 N89-22973
- MOTOR VEHICLES**
Column movement model used to support AMM p 38 N89-21521
- MOUNTAINS**
Structural analysis of the Wichita Mountains using TM data for lineament mapping p 12 A89-35887
- MULTISPECTRAL BAND CAMERAS**
Infrared spectroscopy (2.3-20 microns) for the geological interpretation of remotely-sensed multispectral thermal infrared data p 30 A89-39656
- MULTISPECTRAL BAND SCANNERS**
Calibration comparison for the Landsat 4 and 5 Multispectral Scanners and Thematic Mappers p 47 A89-32835
Multispectral image processing and enhancement; Proceedings of the Meeting, Orlando, FL, Apr. 6-8, 1988 [SPIE-933] p 48 A89-33653
Multispectral terrain background simulation techniques for use in airborne sensor evaluation p 19 A89-33664
- Measurements of short-term thermal responses of coniferous forest canopies using thermal scanner data p 1 A89-33867
Accuracy assessment of a Landsat-assisted vegetation map of the coastal plain of the Arctic National Wildlife Refuge p 6 A89-35840
Reflectance enhancements for the Thematic Mapper - An efficient way to produce images of consistently high quality p 26 A89-37947
Atmospheric correction of satellite MSS data in rugged terrain p 27 A89-38334
Crop identification using merged Landsat multispectral scanner and Thematic Mapper data - Preliminary attempts p 3 A89-41153
Detection techniques using multispectral data to index soil erosional status p 56 A89-41164
Assessing the improvement in soil mapping using spot HRV over Landsat MSS imagery (Geography and land use) p 33 A89-41168
Design of spectral and panchromatic bands for the German MOMS-02 sensor p 57 A89-42173
Improved capabilities of the Multispectral Atmospheric Mapping Sensor (MAMS) [NASA-TM-100352] p 58 N89-20430
Ice cover on Chesapeake Bay from AVHRR (Advanced Very High Resolution Radiometer) and LANDSAT imagery, winter of 1987-88 [PB89-117261] p 59 N89-21415
Geobotanical remote sensing for determination of aggregate source material [AD-A205943] p 45 N89-23962
Research for optimization of future MOMS sensors [ETN-89-94424] p 62 N89-23972
- MULTISPECTRAL PHOTOGRAPHY**
Multispectral space surveys and data processing p 22 A89-35684
Using multispectral video imagery for detecting soil surface conditions p 22 A89-35838
High resolution imaging of geobotanical anomalies associated with subsurface hydrocarbons p 22 A89-35870
- N**
- NASA PROGRAMS**
Earth system science: A program for global change [NASA-TM-101186] p 5 N89-22969
- NASA SPACE PROGRAMS**
HIRIS: NASA's high-resolution imaging spectrometer for the Earth Observing System (EOS) p 63 N89-24695
- NATURAL GAS**
Successful applications of remotely sensed data for oil and gas exploration p 22 A89-35854
Lowering the cost of exploration for independents - How remotely sensed data aids in the search for oil and gas p 22 A89-35855
Landsat interpretation and stratigraphy of the Hugoton gas field (Southwestern Kansas) and surrounding areas p 6 A89-35856
A technique for applying space photographs to search for anticlinal oil- and gas-traps in orogenic structures of the Tien-Shan p 25 A89-37318
- NAVIGATION AIDS**
Loran C field strength contours: Contiguous US [DOT/FAA/CT-TN89/16] p 8 N89-23437
- NEAR INFRARED RADIATION**
Sources of remote sensing data visible, near infrared, and short wave p 51 A89-35878
Visible and near-infrared (0.4- to 2.5-microns) reflectance spectra of selected mixed-layer clays and related minerals p 12 A89-35897
- NEPHANALYSIS**
Examination of USAF Nephanalysis performance in the marginal cryosphere region p 52 A89-35949
- NETHERLANDS**
Twelve year overview of cloudfree LANDSAT imagery of The Netherlands [NLR-MP-87072-U] p 59 N89-20542
- NEUMANN PROBLEM**
Derivation of a geomagnetic model to $n = 63$ p 58 A89-43409
- NEUTRAL GASES**
Spacelab 2 Upper Atmospheric Modification Experiment over Areibo. II - Plasma dynamics p 4 A89-38897
- NIGER**
Meteosat thermal inertia mapping for studying wetland dynamics in the West-African Sahel [BCRS-88-10A] p 62 N89-23970
- NIGHT SKY**
Satellite detection of Saharan dust - Optimized imaging during nighttime p 24 A89-35912
- NIMBUS 7 SATELLITE**
Nimbus-7 data product summary [NASA-RP-1215] p 39 N89-22152
- NITRIC ACID**
Antarctic ozone: Theory and observation p 4 N89-22189
- NITRIC OXIDE**
The response of thermospheric nitric oxide to an auroral storm p 42 N89-23031
- NOAA SATELLITES**
Review and status of remote sensing of sea ice p 20 A89-34266
Sensitivity of 30-day dynamical forecasts to continental snow cover p 17 A89-35937
Greater global warming revealed by satellite-derived sea-surface-temperature trends p 16 A89-37571
A parameterization for longwave surface radiation from sun-synchronous satellite data p 56 A89-41761
Processing and application of digital AVHRR-imagery for land and sea surfaces [BCRS-88-08] p 36 N89-20538
- NOBLE METALS**
Discriminating late volcanic differentiates commonly associated with precious metal deposits, using Landsat Thematic Mapper imagery p 12 A89-35896
- NOISE REDUCTION**
Minimum cross-entropy noise reduction in images p 34 A89-41845
- NONDESTRUCTIVE TESTS**
Infrared thermography - A quantitative tool for heat study [ONERA, TP NO. 1989-3] p 53 A89-37627
- NONLINEAR EQUATIONS**
The KP equation: A comparison to laboratory generated bi-periodic waves p 38 N89-21507
- NONLINEARITY**
The KP equation: A comparison to laboratory generated bi-periodic waves p 38 N89-21507
- O**
- OCCULTATION**
The investigation of advanced remote sensing, radiative transfer and inversion techniques for the measurement of atmospheric constituents [NASA-CR-172599] p 36 N89-20531
- OCEAN BOTTOM**
Identification of tectonic dislocations underneath large water areas using space images p 15 A89-34011
Use of seabottom magnetic susceptibility measurements in hydrocarbon exploration p 16 A89-35864
Bathymetric mapping with passive multispectral imagery p 16 A89-38766
Imaging procedure of underwater bottom topography by air and satellite images in the range of microwave and visible electromagnetic spectra [GKSS-88/E/41] p 17 N89-24014
- OCEAN CURRENTS**
Field calibration of mixed-layer drifters p 53 A89-37554
Observing oceanic mesoscale eddies from Geosat altimetry - Preliminary results p 16 A89-39372
A performance comparison for two Lagrangian drifter designs p 34 A89-41750
Development of a satellite SAR image spectra and altimeter wave height data assimilation system for ERS-1 [NASA-CR-182685] p 61 N89-22975
- OCEAN DATA ACQUISITIONS SYSTEMS**
Field calibration of mixed-layer drifters p 53 A89-37554
A performance comparison for two Lagrangian drifter designs p 34 A89-41750
- OCEAN MODELS**
The Naval Research Laboratory's Air-Sea Interaction Blimp Experiment p 53 A89-37981
Development of a satellite SAR image spectra and altimeter wave height data assimilation system for ERS-1 [NASA-CR-182685] p 61 N89-22975
Observation model and parameter partials for the JPL geodetic GPS modeling software GPSOMC [NASA-CR-185021] p 9 N89-24060
- OCEAN SURFACE**
Surface solar irradiance in the central Pacific during tropic heat - Comparisons between in situ measurements and satellite estimates p 16 A89-35931
Aerosol analysis with the Coastal Zone Color Scanner - A simple method for including multiple scattering effects p 25 A89-37291
The dispersion limitations on the accuracy of the internal reference method during remote laser sounding of the upper ocean layer p 53 A89-37349
Field calibration of mixed-layer drifters p 53 A89-37554
Seasat A satellite scatterometer measurements of equatorial surface winds p 53 A89-37802

- Statistical geometry of a small surface patch in a developed sea p 26 A89-37808
- The Naval Research Laboratory's Air-Sea Interaction Blimp Experiment p 53 A89-37981
- Sea surface spectrum from aerial photographs - Laboratory model studies p 30 A89-39674
- Measurements of spectral radiance at the sea surface for the development of remote sensing methods p 35 A89-42610
- Processing and application of digital AVHRR-imagery for land and sea surfaces [BCRS-88-08] p 36 N89-20538
- Imaging of ocean waves by SAR [AD-A203604] p 37 N89-21165
- OSRMS (Ocean Surface Roughness Measurement System): The DREP (Defence Research Establishment Pacific) near-nadir scatterometer [AD-A202983] p 38 N89-21460
- Theoretical studies for ERS-1 wave mode, volume 1 [GEC-MTR-87/110-VOL-1] p 41 N89-22977
- The advanced Ocean Chlorophyll Meter (OCM). A spectral imaging device for the observation of the oceans [REPT-882-440-118] p 63 N89-24689
- Correlation between satellite-derived aerosol characteristics and oceanic dimethylsulfide (DMS) [AD-A206179] p 6 N89-24759
- Biophysical variability in the Greenland Sea observed with the Multispectral Airborne Radiometer System (MARS) [NASA-CR-184856] p 47 N89-24784

OCEAN TEMPERATURE

- Application of Landsat Thematic Mapper data for coastal thermal plume analysis at Diablo Canyon p 35 A89-42175

OCEANOGRAPHIC PARAMETERS

- Evaluation of Geosat altimeter data with application to tropical Pacific sea level variability p 25 A89-37801
- Marine Observation Satellite-1 - First year in orbit p 26 A89-38328
- NOAA (National Oceanic and Atmospheric Administration) AVHRR (Advanced Very High Resolution Radiometer) observations during the marginal ice zone experiment, between Spitzbergen and Greenland, June 7 to 18 July 1984 [AD-A204911] p 19 N89-22280

OCEANOGRAPHY

- Gravimetric studies at sea --- Russian book p 49 A89-34088
- Greater global warming revealed by satellite-derived sea-surface-temperature trends p 16 A89-37571

OCEANS

- The prognosis of weather change lines over the ocean - The role of a reconnaissance aircraft p 48 A89-32848

- Infrared sea-radiance modeling using LOWTRAN 6 [AD-A202582] p 38 N89-21643

OIL EXPLORATION

- Successful applications of remotely sensed data for oil and gas exploration p 22 A89-35854
- Lowering the cost of exploration for independents - How remotely sensed data aids in the search for oil and gas p 22 A89-35855
- Petroleum exploration with airborne radar (SAR) and geologic field work, Sinu Basin of northwest Columbia p 11 A89-35859
- High resolution imaging of geobotanical anomalies associated with subsurface hydrocarbons p 22 A89-35870
- The application of high resolution digital elevation models to petroleum and mineral exploration and production p 22 A89-35876
- Satellite altimetry. II - A new prospecting tool p 23 A89-35895
- A technique for applying space photographs to search for anticlinal oil- and gas-traps in orogenic structures of the Tien-Shan p 25 A89-37318

OIL FIELDS

- A closer look at the Patrick Draw oil field vegetation anomaly p 1 A89-35893

OKLAHOMA

- Structural analysis of the Wichita Mountains using TM data for lineament mapping p 12 A89-35887

OPTICAL PROPERTIES

- Optical properties of oceanic suspended matter and their interpretation for remote sensing of phytoplankton [GKSS-88/E/40] p 46 N89-24013

OPTICAL RADAR

- Laser scattering phenomenology - Background signature characterization and prediction p 6 A89-33661
- Satellite-borne lidar observations of the earth - Requirements and anticipated capabilities p 56 A89-41692

OPTICAL REFLECTION

- Cloud reflectance variations in channel-3 p 55 A89-40136

OPTICAL THICKNESS

- Using the radiative temperature difference at 3.7 and 11 microns to track dust outbreaks p 27 A89-38968
- The potential of infrared satellite data for the retrieval of Saharan-dust optical depth over Africa p 30 A89-39875

OPTIMIZATION

- Snowmelt increase through albedo reduction [AD-A204523] p 18 N89-22175
- Analysis and optimization of geodetic networks by spectral criteria and mechanical analogies [SER-C-342] p 45 N89-23963

ORBITAL MECHANICS

- Minimum number of satellites for periodic coverage [FOA-C-30511-9.4] p 65 N89-22976

ORBITAL POSITION ESTIMATION

- Coordinate referencing of a TV image in the case of the remote sensing of the earth p 53 A89-37492

ORCHARDS

- The discrimination of irrigated orchard and vine crops using remotely sensed data p 2 A89-37949

OROGRAPHY

- Investigation of the recently formed imbricate structure of the southern Tien-Shan using space photographs p 10 A89-34005
- Topographic analysis of the Andean Highlands using the Large Format Camera p 7 A89-35880

OZONE

- Air pollution effects field research facility: Ozone flow control and monitoring system [DE89-007922] p 5 N89-22192

OZONE DEPLETION

- Direct ozone depletion in springtime Antarctic lower stratospheric clouds p 4 A89-32756
- Monitoring the greenhouse effect from space p 4 A89-39739
- Antarctic ozone: Theory and observation p 4 N89-22189

OZONOSPHERE

- Nimbus-7 data product summary [NASA-RP-1215] p 39 N89-22152

P**PALEOMAGNETISM**

- High resolution chronology of late Cretaceous-early Tertiary events determined from 21,000 yr orbital-climatic cycles in marine sediments p 14 N89-21328

PALEONTOLOGY

- The Frasnian-Famennian mass killing event(s), methods of identification and evaluation p 37 N89-21318

PARTIAL DIFFERENTIAL EQUATIONS

- Observation model and parameter partials for the JPL geodetic GPS modeling software GPSOMC [NASA-CR-185021] p 9 N89-24060

PATTERN RECOGNITION

- An algorithm for machine-recognizing the river mouth and measuring the sealine from the Landsat image p 19 A89-33658
- Representation and recognition of elongated regions in aerial images p 19 A89-33684
- Automated recognition of oceanic cloud patterns. I - Methodology and application to cloud climatology p 24 A89-35906
- N-dimensional display of cluster means in feature space p 29 A89-39100
- Identification and analysis of the alignments of point-like features in remotely-sensed imagery. Volcanic cones in the Pinacate Volcanic Field, Mexico p 12 A89-39651
- The suitability of remote sensing for surveying and monitoring landscape patterns. Volume A: Pilot study - LANDSAT imagery p 36 N89-20535
- The suitability of remote sensing for surveying and monitoring landscape patterns. Volume B: PEPS Project No. 73 - SPOT Imagery p 36 N89-20536
- Computer strategy for detecting line features on simulated binary arrays in support of radar feature extraction [AD-A203257] p 37 N89-21162
- Automated extraction of absorption features from Airborne Visible/Infrared Imaging Spectrometer (AVIRIS) and Geophysical and Environmental Research Imaging Spectrometer (GERIS) data p 39 N89-22160
- AVIRIS spectra of California wetlands p 3 N89-22167
- Image understanding research at SRI International p 42 N89-23080
- Cooperative methods for road tracking in aerial imagery p 42 N89-23101
- Automatic extraction of areas from overlays of the series DGK 5 (Bo) p 44 N89-23955
- The search for edges in remote sensing images using a digital polygonal map [ETN-89-94146] p 45 N89-23964

PERFORMANCE PREDICTION

- Column movement model used to support AMM p 38 N89-21521

PERFORMANCE TESTS

- Evaluation of the Portable Instantaneous Display Analysis Spectrometer (PIDAS) [NASA-CR-184878] p 61 N89-22970

PERMITTIVITY

- Microwave X-band radiometric characterization of Brazilian soils by measurement of the complex permittivity [INPE-4588-PRE/1319] p 3 N89-24685

PETROLOGY

- Spectral indices for vegetation and rock type discrimination using the optical sensor of the Japanese ERS-1 p 51 A89-35866

PHENOLOGY

- A phenological description of Iberian vegetation using short wave vegetation index imagery p 2 A89-40149
- Monitoring the phenology of Tunisian grazing lands p 3 A89-40150

PHOSPHORESCENCE

- Short- and long-term memory effects in intensified array detectors - Influence on airborne laser fluorosensor measurements p 47 A89-32836

PHOTOCHEMICAL REACTIONS

- The response of thermospheric nitric oxide to an auroral storm p 42 N89-23031

PHOTO GEOLOGY

- The potential use of remote sensing to solve problems of paleotectonic prediction, geologic structure, and exploitation of coal deposits with reference to the Moscow-Region coal basin p 49 A89-34002
- Use of aerial and space photography for the detection of faults and neotectonic movements in Crimea and the Azov Coastal Region p 9 A89-34003
- Investigation of the recently formed imbricate structure of the southern Tien-Shan using space photographs p 10 A89-34005
- Use of aerial and space methods for observations and studies of the morphology and kinematics of recent movements along some faults of the Baikal Rift Zone p 10 A89-34007
- Identification of tectonic dislocations underneath large water areas using space images p 15 A89-34011
- Recent and current geodynamics of the Kyzylkum region as derived from space imagery p 10 A89-34017
- Thematic Conference on Remote Sensing for Exploration Geology, 6th, Houston, TX, May 16-19, 1988, Proceedings, Volumes 1 & 2 p 10 A89-35851
- Identification of Cross Strike discontinuities in the Appalachian basin and implications for hydrocarbon exploration p 11 A89-35860
- Use of remotely sensed data in mature basin exploration - Considerations on creating useful imagery p 50 A89-35861

- A field spectrometer and remote sensing study of the Fresno mining district, Mexico p 51 A89-35871
- Sources of remote sensing data visible, near infrared, and short wave p 51 A89-35878
- Photogeologic-geomorphic mapping provides clues to structural features beneath glacial terrain p 7 A89-35882
- Reconstruction of imagery of faulted landscapes using a photo-optical technique p 24 A89-35900
- Geological applications of the Space Station core platform p 24 A89-35902
- Digital display of SPOT stereo images p 24 A89-35903
- The definition of isometric magmatogenic structures on space imagery p 12 A89-37315
- A technique for applying space photographs to search for anticlinal oil- and gas-traps in orogenic structures of the Tien-Shan p 25 A89-37318
- Infrared spectroscopy (2.3-20 microns) for the geological interpretation of remotely-sensed multispectral thermal infrared data p 30 A89-39656
- Geological application of SIR-A imagery in southern Iraq p 13 A89-41162
- Geologic applications of Space Shuttle photography p 34 A89-41431

- Proceedings of the Airborne Visible/Infrared Imaging Spectrometer (AVIRIS) Performance Evaluation Workshop [NASA-CR-184870] p 59 N89-22154

PHOTOGRAMMETRY

- A semi-automatic terrain measurement system for earthwork control p 28 A89-39094
- Close-range photogrammetric measurement of erosion in coarse-grained soils p 54 A89-39098
- Combined film and softcopy photo-interpretation system p 31 A89-40263
- Aerial photography and specialized photographic studies --- Russian book p 31 A89-40488

- Reports on Cartography and Geodesy. Series 1, number 101
[ISSN-0469-4236] p 8 N89-23941
Definition and filling of information systems: Challenge for a photogrammetric service enterprise p 62 N89-23942
Cartographic signatures in PHOCUS p 43 N89-23948
Remote sensing of global snowpack energy and mass balance: In-situ measurements on the snow of interior and Arctic Alaska
[NASA-CR-180078] p 62 N89-23956
- PHOTOGRAPHIC FILM**
Combined film and softcopy photo-interpretation system p 31 A89-40263
- PHOTOGRAPHIC PROCESSING**
Combined film and softcopy photo-interpretation system p 31 A89-40263
- PHOTOINTERPRETATION**
A raster approach to population estimation using high-altitude aerial and space photographs p 19 A89-33872
Morphostructural interpretation of space images and the reconstruction of the recently formed stress field in the Altai-Baikal region p 10 A89-34006
Seismogeological interpretation of space images of the region of Caucasian mineral waters p 10 A89-34018
Analysis of the potential of using space photographic data obtained with the PKF-1K camera to solve scientific, economic, and educational-methodological problems p 64 A89-35685
Landsat interpretation and stratigraphy of the Hugoton gas field (Southwestern Kansas) and surrounding areas p 6 A89-35856
Ore-bearing structures of Central Kazakhstan identified on aerial and space photographs in the framework of the computer-aided prediction of minerals p 52 A89-37316
Assessment of the present conditions of lowland lakes of Central Asia using the interpretation of space photographs p 17 A89-37319
Combined film and softcopy photo-interpretation system p 31 A89-40263
Estimating stand density of loblolly pine in northern Louisiana using aerial photographs and probability proportional to size p 34 A89-41171
Analysis of seasonal characteristics of Sambhar Salt Lake, India, from digitized Space Shuttle photography p 18 A89-41433
Image understanding research at SRI International p 42 N89-23080
Cooperative methods for road tracking in aerial imagery p 42 N89-23101
- PHOTOMAPPING**
Economic relations of the all-union trade association Sojuzkart and the geodetic and cartographic services of the U.S.S.R. to foreign countries p 64 A89-34708
Mapping coastal evolution in Sri Lanka using aerial photographs p 6 A89-34948
From large-scale to small-scale - Economic geologic-geomorphic mapping using aerial photographs and Landsat images p 7 A89-35884
Two-dimensional seam-point searching in digital image mosaicking p 26 A89-37945
A raster approach to topographic map revision p 26 A89-37946
The discrimination of irrigated orchard and vine crops using remotely sensed data p 2 A89-37949
The decrease of Lake Chad as documented during twenty years of manned space flight p 18 A89-41434
The search for edges in remote sensing images using a digital polygonal map [ETN-89-94146] p 45 N89-23964
- PHYTOPLANKTON**
Remote sensing of ocean chlorophyll - Consequence of nonuniform pigment profile p 15 A89-32838
Biophysical variability in the Greenland Sea observed with the Multispectral Airborne Radiometer System (MARS) [NASA-CR-184856] p 47 N89-24784
- PLAINS**
Assessment of the present conditions of lowland lakes of Central Asia using the interpretation of space photographs p 17 A89-37319
- PLANETARY EVOLUTION**
Earth system science: A program for global change [NASA-TM-101186] p 5 N89-22969
- PLANETARY MAPPING**
Mapping of Landsat satellite and gravity lineaments in west Tennessee p 6 A89-34357
- PLANETARY STRUCTURE**
Earth system science: A program for global change [NASA-TM-101186] p 5 N89-22969
- PLANETARY SURFACES**
Laser altimetry measurements from aircraft and spacecraft p 56 A89-41691
- PLANT STRESS**
Analysis of Airborne Imaging Spectrometer (AIS) data for geobotanical prospecting p 51 A89-35890
MEIS II and surface data integration for detection of geobotanical anomalies p 51 A89-35891
A closer look at the Patrick Draw oil field vegetation anomaly p 1 A89-35893
A Landsat Thematic Mapper investigation of the geobotanical relationships in the northern spruce-fir forest, Mt. Moosilauke, New Hampshire p 2 A89-35894
Assessment of AVIRIS data from vegetated sites in the Owens Valley, California p 60 N89-22162
- PLASMA DYNAMICS**
Spacelab 2 Upper Atmospheric Modification Experiment over Arecibo. II - Plasma dynamics p 4 A89-38897
- PLASMA TEMPERATURE**
GEOS 1 observations of low-energy ions in the earth's plasmasphere - A study on composition, and temperature and density structure under quiet geomagnetic conditions p 9 A89-33829
- PLASMASPHERE**
GEOS 1 observations of low-energy ions in the earth's plasmasphere - A study on composition, and temperature and density structure under quiet geomagnetic conditions p 9 A89-33829
- PLATES (TECTONICS)**
Investigation of the recently formed imbricate structure of the southern Tien-Shan using space photographs p 10 A89-34005
Rate of change of the Quincy-Monument Peak baseline from a translocation analysis of Lageos laser range data p 13 A89-42181
The baseline length changes of circumpacific VLBI networks and their bearing on global tectonics p 13 A89-42795
Plate motions and deformations from geologic and geodetic data [NASA-CR-184987] p 15 N89-24757
- PLATINUM COMPOUNDS**
An analysis of platinum silicide and indium antimonide for remote sensors in the 3 to 5 micrometer wavelength band [AD-A202663] p 59 N89-21218
- PLUMES**
Application of Landsat Thematic Mapper data for coastal thermal plume analysis at Diablo Canyon p 35 A89-42175
- POLAR CAPS**
EXOS-C (Ohzora) observations of polar cap precipitations and inverted V events p 19 A89-33543
Polar cap deflation during magnetospheric substorms p 24 A89-36704
Correlation between satellite-derived aerosol characteristics and oceanic dimethylsulfide (DMS) [AD-A206179] p 6 N89-24759
- POLAR CUSPS**
The interplanetary magnetic field B(y)-dependent field-aligned current in the dayside polar cap under quiet conditions p 50 A89-34782
- POLAR ORBITS**
Observational analyses of North Atlantic tropical cyclones from NOAA polar-orbiting satellite microwave data p 21 A89-34879
- POLAR REGIONS**
Examination of USAF Nephelometer performance in the marginal cryosphere region p 52 A89-35949
Retrieval of mesoscale meteorological parameters for polar latitudes (MIZEX and ARCTEMIZ campaigns) p 58 A89-43026
Beaufort Sea mesoscale circulation study: Preliminary results [PB89-121693] p 17 N89-20597
- POLARIMETRY**
Modeling and observation of the radar polarization signature of forested areas p 2 A89-39554
An inexpensive polarimetric FM radar and polarimetric signatures of artificial sea ice p 57 A89-42684
Active and passive remote sensing of ice [AD-A203943] p 59 N89-20543
- POLARIZED ELECTROMAGNETIC RADIATION**
Modeling and observation of the radar polarization signature of forested areas p 2 A89-39554
- POLARIZED LIGHT**
Earth scenes in polarized light observed from the Space Shuttle p 34 A89-41429
- POLLUTION CONTROL**
Environmental projects. Volume 3: Environmental compliance audit [NASA-CR-185019] p 5 N89-23985
- POLLUTION MONITORING**
Performance analysis of the DFVLR real time SAR processor for low SNRs p 21 A89-35336
Monitoring the greenhouse effect from space p 4 A89-39739
- Air pollution effects field research facility: Ozone flow control and monitoring system [DE89-007922] p 5 N89-22192
- POPULATION THEORY**
Rural settlement expansion in Moneragala district, Sri Lanka p 4 A89-34946
- POPULATIONS**
A raster approach to population estimation using high-altitude aerial and space photographs p 19 A89-33872
The Frasnian-Famennian mass killing event(s), methods of identification and evaluation p 37 N89-21318
Estimating population size of Pygoscelid Penguins from TM data [NASA-CR-180081] p 3 N89-24687
- PORTABLE EQUIPMENT**
Evaluation of the Portable Instantaneous Display Analysis Spectrometer (PIDAS) [NASA-CR-184878] p 61 N89-22970
Geological gyrocompass [PB89-133086] p 63 N89-24589
- POSITION (LOCATION)**
Investigation of several methods for the detection of outstanding points in a digital image [ETN-89-94148] p 45 N89-23965
- PRECIPITATION (METEOROLOGY)**
Precipitation in the Canadian Atlantic Storms Program - Measurements of the acoustic signature p 50 A89-35819
Precipitation retrieval over land and ocean with the SSM/I - Identification and characteristics of the scattering signal p 53 A89-37549
- PRECIPITATION PARTICLE MEASUREMENT**
Drop-size distributions associated with intense rainfall p 50 A89-34876
- PREDICTION ANALYSIS TECHNIQUES**
Imaging of ocean waves by SAR [AD-A203604] p 37 N89-21165
- PREDICTIONS**
The KP equation: A comparison to laboratory generated bi-periodic waves p 38 N89-21507
- PROBABILITY DENSITY FUNCTIONS**
Probabilities and statistics for backscatter estimates obtained by a scatterometer with applications to new scatterometer design data [NASA-CR-4228] p 61 N89-22779
- PROGRAMMING LANGUAGES**
A software system to create a hierarchical, multiple level of detail terrain model [AD-A203047] p 38 N89-21568
- PROTOTYPES**
TAX - Prototype expert system for terrain analysis p 20 A89-34363
- PUBLIC HEALTH**
National Air Toxics Information Clearinghouse: Ongoing research and regulatory development projects, July 1988 [PB89-103428] p 65 N89-20558
- PULSE CODE MODULATION**
Data compression experiments with LANDSAT thematic mapper and Nimbus-7 coastal zone color scanner data p 41 N89-22344
- PULSE RADAR**
Impulse radar for identification of features in soils p 50 A89-34353
- PUSHBROOM SENSOR MODES**
Design of spectral and panchromatic bands for the German MOMS-02 sensor p 57 A89-42173

Q

QATAR

- Conjugate synthetic normal faults around the Gulf of Salwa, southwestern Qatar, the Arabian Gulf p 12 A89-35886

QUANTITATIVE ANALYSIS

- Infrared thermography - A quantitative tool for heat study [ONERA, TP NO. 1989-3] p 53 A89-37627

QUANTUM EFFICIENCY

- An analysis of platinum silicide and indium antimonide for remote sensors in the 3 to 5 micrometer wavelength band [AD-A202663] p 59 N89-21218

QUARTZITE

- Structural patterns in high grade terrain in parts of Tamil Nadu and Karnataka p 14 N89-22255

R

RADAR CROSS SECTIONS

- C-band radar cross section of the Guyana rain forest - Possible use as a reference target for spaceborne radars p 49 A89-33869

- Probabilities and statistics for backscatter estimates obtained by a scatterometer with applications to new scatterometer design data [NASA-CR-4228] p 61 N89-22779
- RADAR DATA**
- Satellite, airborne and radar observations of auroral arcs p 48 A89-33505
- Improving accuracy in radar-altimetry data correction for tropospheric effects p 54 A89-39322
- Short-period fluctuation of the lower tropospheric winds observed by MU-radar p 58 A89-43311
- Development of a satellite SAR image spectra and altimeter wave height data assimilation system for ERS-1 [NASA-CR-182685] p 61 N89-22975
- RADAR IMAGERY**
- Image-analysis techniques for determination of morphology and kinematics in arctic sea ice p 21 A89-34416
- Research on speckle behavior in SAR images p 21 A89-35335
- Petroleum exploration with airborne radar (SAR) and geologic field work, Sinu Basin of northwest Columbia p 11 A89-35859
- Minimum cross-entropy noise reduction in images p 34 A89-41845
- Active and passive remote sensing of ice [AD-A203943] p 59 N89-20543
- Computer strategy for detecting line features on simulated binary arrays in support of radar feature extraction [AD-A203257] p 37 N89-21162
- Imaging of ocean waves by SAR [AD-A203604] p 37 N89-21165
- Development of a satellite SAR image spectra and altimeter wave height data assimilation system for ERS-1 [NASA-CR-182685] p 61 N89-22975
- Theoretical studies for ERS-1 wave mode, volume 1 [GEC-MTR-87/110-VOL-1] p 41 N89-22977
- Imaging radar applications in Europe. Illustrated experimental results (1978-1987) [ESA-TM-01] p 42 N89-22978
- Improvement and extension of a radar forest backscattering model [NASA-CR-184975] p 46 N89-24686
- Necessity and benefit of the X-SAR space shuttle experiment [DFVLR-MITT-88-29] p 63 N89-24688
- RADAR MAPS**
- Synthetic Aperture Radar data for mapping subsurface geological structures in the Northwest Territories, Canada p 50 A89-35858
- RADAR MEASUREMENT**
- Impulse radar for identification of features in soils p 50 A89-34353
- RADAR PHOTOGRAPHY**
- Imaging radar applications in Europe. Illustrated experimental results (1978-1987) [ESA-TM-01] p 42 N89-22978
- RADAR SCATTERING**
- An analysis of speckle from forest stands with periodic structures p 54 A89-39555
- An inexpensive polarimetric FM radar and polarimetric signatures of artificial sea ice p 57 A89-42684
- Probabilities and statistics for backscatter estimates obtained by a scatterometer with applications to new scatterometer design data [NASA-CR-4228] p 61 N89-22779
- RADAR SIGNATURES**
- Modeling and observation of the radar polarization signature of forested areas p 2 A89-39554
- An inexpensive polarimetric FM radar and polarimetric signatures of artificial sea ice p 57 A89-42684
- Imaging procedure of underwater bottom topography by air and satellite images in the range of microwave and visible electromagnetic spectra [GKSS-88/E/41] p 17 N89-24014
- RADIANCE**
- Modeling directional thermal radiance from a forest canopy p 27 A89-38972
- Infrared sea-radiance modeling using LOWTRAN 6 [AD-A202582] p 38 N89-21643
- Atmospheric water mapping with the Airborne Visible/Infrared Imaging Spectrometer (AVIRIS), Mountain Pass, California p 39 N89-22156
- Biophysical variability in the Greenland Sea observed with the Multispectral Airborne Radiometer System (MARS) [NASA-CR-184856] p 47 N89-24784
- RADIANT FLUX DENSITY**
- Measuring thermal budgets of active volcanoes by satellite remote sensing p 9 A89-32988
- RADIATION MEASUREMENT**
- Global, seasonal surface variations from satellite radiance measurements p 52 A89-35966

RADIATIVE TRANSFER

Radiative transfer calculations for characterizing obscured surfaces using time-dependent backscattered pulses p 48 A89-32841

The investigation of advanced remote sensing, radiative transfer and inversion techniques for the measurement of atmospheric constituents [NASA-CR-172599] p 36 N89-20531

RADIO ALTIMETERS

Improving accuracy in radar-altimetry data correction for tropospheric effects p 54 A89-39322

RADIO EMISSION

Parameter optimization of systems for the thermal microwave mapping of the earth's surface p 25 A89-37321

RADIO PROBING

Sounding of crop fields by nanosecond radio pulses p 1 A89-35584

RADIO TRANSMISSION

Loran C field strength contours: Contiguous US [DOT/FAA/CT-TN89/16] p 8 N89-23437

RADIOACTIVE CONTAMINANTS

Use of the 1:2,000,000 Digital Line Graph data in emergency response [DE89-006730] p 44 N89-23959

RADIOMETERS

Biophysical variability in the Greenland Sea observed with the Multispectral Airborne Radiometer System (MARS) [NASA-CR-184856] p 47 N89-24784

RADIOMETRIC CORRECTION

Radiometric correction of aerial and space remote-sensing images p 25 A89-37323

AVIRIS data characteristics and their effects on spectral discrimination of rocks exposed in the Drum Mountains, Utah: Results of a preliminary study p 40 N89-22165

RADIOMETRIC RESOLUTION

Pixel and sub-pixel accuracy in geometrical correction of AVHRR p 30 A89-40134

AVIRIS performance during the 1987 flight season: An AVIRIS project assessment and summary of the NASA-sponsored performance evaluation p 60 N89-22155

Radiometric performance of AVIRIS: Assessment for an arid region geologic target p 39 N89-22157

Assessment of AVIRIS data from vegetated sites in the Owens Valley, California p 60 N89-22162

Determination of in-flight AVIRIS spectral, radiometric, spatial and signal-to-noise characteristics using atmospheric and surface measurements from the vicinity of the rare-earth-bearing carbonatite at Mountain Pass, California p 61 N89-22170

RAIN

A meteorological overview of the pre-AMEX and AMEX periods over the Australian region p 48 A89-32850

Relating point to area average rainfall in semiarid West Africa and the implications for rainfall estimates derived from satellite data p 55 A89-39870

NOAA AVHRR and its uses for rainfall and evapotranspiration monitoring p 56 A89-40151

RAIN FORESTS

C-band radar cross section of the Guyana rain forest - Possible use as a reference target for spaceborne radars p 49 A89-33869

RAIN IMPACT DAMAGE

Drop-size distributions associated with intense rainfall p 50 A89-34876

RANDOM NOISE

Zones of information in the AVIRIS spectra p 39 N89-22158

RANDOM PROCESSES

EM wave scattering from statistically inhomogeneous and periodic random rough surfaces p 36 A89-43541

RANGELANDS

Monitoring the phenology of Tunisian grazing lands p 3 A89-40150

RARE EARTH ELEMENTS

Evaluation of Airborne Visible/Infrared Imaging Spectrometer Data of the Mountain Pass, California carbonatite complex p 60 N89-22169

RAYLEIGH SCATTERING

Aerosol analysis with the Coastal Zone Color Scanner - A simple method for including multiple scattering effects p 25 A89-37291

REAL TIME OPERATION

A real-time global sea surface temperature analysis p 16 A89-35907

RECONNAISSANCE AIRCRAFT

The prognosis of weather change lines over the ocean - The role of a reconnaissance aircraft p 48 A89-32848

REDUCED GRAVITY

Advanced space design program to the Universities Space Research Association and the National Aeronautics and Space Administration [NASA-CR-180450] p 3 N89-24015

REFLECTANCE

Infrared sea-radiance modeling using LOWTRAN 6 [AD-A202582] p 38 N89-21643

REGULATIONS

Environmental projects. Volume 3: Environmental compliance audit [NASA-CR-185019] p 5 N89-23985

RELAXATION METHOD (MATHEMATICS)

Automated DTM validation and progressive sampling algorithm of finite element array relaxation p 22 A89-35837

RELIEF MAPS

Computer aided production of a 1:25,000 relief model of Berlin and surroundings p 8 N89-23943

REMOTE REGIONS

Application of Landsat Thematic Mapper imagery for lithological mapping of poorly accessible semi-arid regions p 7 A89-35879

An AVHRR mosaic image of Antarctica p 30 A89-40135

REMOTE SENSING

Hyperspectral interactions - Invariance and scaling --- applied to remote sensing data p 48 A89-32837

Remote sensing of ocean chlorophyll - Consequence of nonuniform pigment profile p 15 A89-32838

Radiative transfer calculations for characterizing obscured surfaces using time-dependent backscattered pulses p 48 A89-32841

Measuring thermal budgets of active volcanoes by satellite remote sensing p 9 A89-32988

New earth observing platforms to study global water, biology p 17 A89-33121

Multispectral image processing and enhancement: Proceedings of the Meeting, Orlando, FL, Apr. 6-8, 1988 [SPIE-933] p 48 A89-33653

Laser scattering phenomenology - Background signature characterization and prediction p 6 A89-33661

Measurements of short-term thermal responses of coniferous forest canopies using thermal scanner data p 1 A89-33867

Modeling surface temperature distributions in forest landscapes p 48 A89-33868

Large-area crop monitoring with the NOAA AVHRR - Estimating the silking stage of corn development p 1 A89-33873

A new technique to measure the spectral properties of conifer needles p 19 A89-33874

Remote-sensing studies of present-day tectonic processes --- Russian book p 20 A89-34001

The potential use of remote sensing to solve problems of paleotectonic prediction, geologic structure, and exploitation of coal deposits with reference to the Moscow-Region coal basin p 49 A89-34002

Dynamics of present-day geological processes from remotely sensed data p 9 A89-34004

New data on the morphostructure and geodynamics of the eastern margin of Eurasia p 10 A89-34012

Methods for investigating seismically active zones using remote imagery p 20 A89-34013

Review and status of remote sensing of sea ice p 20 A89-34266

Sea-ice characterization measurements needed for testing of microwave remote sensing models p 20 A89-34268

Impulse radar for identification of features in soils p 50 A89-34353

Use of aerial photography to inventory aquatic vegetation p 50 A89-34362

TAX - Prototype expert system for terrain analysis p 20 A89-34363

Landsat commercialization - Keys to future success p 64 A89-34703

Accessing remote sensing technology - The microBRIAN example p 21 A89-34706

Economic relations of the all-union trade association Sojuzkarta and the geodetic and cartographic services of the U.S.S.R. to foreign countries p 64 A89-34708

Ground verification method for bathymetric satellite image maps of unsurveyed coral reefs p 6 A89-34949

Sounding of crop fields by nanosecond radio pulses p 1 A89-35584

Analysis of the potential of using space photographic data obtained with the PKF-1K camera to solve scientific, economic, and educational-methodological problems p 64 A89-35685

Methodology for the remote sensing of fluxes of heat, moisture, and effective radiation in the ocean-atmosphere system p 16 A89-35686

The KAP-350 and KAP-100 space cameras for the remote sensing of earth resources p 50 A89-35687

Precipitation in the Canadian Atlantic Storms Program - Measurements of the acoustic signature p 50 A89-35819

Thematic Conference on Remote Sensing for Exploration Geology, 6th, Houston, TX, May 16-19, 1988, Proceedings. Volumes 1 & 2 p 10 A89-35851

- Basic concepts in the use of remotely sensed data for resource exploration p 11 A89-35852
- A survey of the operational status and needs of remote sensing in exploration geology p 64 A89-35853
- Successful applications of remotely sensed data for oil and gas exploration p 22 A89-35854
- Use of remotely sensed data in mature basin exploration - Considerations on creating useful imagery p 50 A89-35861
- The contribution of remote sensing data to exploration of fractured reservoirs p 50 A89-35862
- Applying remote sensing technology to the Bureau of Land Management's mineral management program p 11 A89-35874
- Volcano monitoring by short wavelength infrared satellite remote sensing p 51 A89-35875
- Assessing aggregate resource potential in the Canadian Shield - A knowledge-based approach p 23 A89-35877
- Sources of remote sensing data visible, near infrared, and short wave p 51 A89-35878
- Combined remote sensing and surface geochemical survey in a drift-covered area in southeastern Saskatchewan p 12 A89-35881
- Applications of AVHRR imagery in frontier exploration p 23 A89-35885
- MEIS II and surface data integration for detection of geobotanical anomalies p 51 A89-35891
- Implementation of background and target geobotanical techniques in mineral exploration p 23 A89-35892
- Satellite altimetry. II - A new prospecting tool p 23 A89-35895
- Uses of the SAS statistical package for digital image analysis p 23 A89-35898
- The commercial land remote sensing market - Current assessment, baseline forecast and baseline alternatives p 64 A89-35899
- Geological applications of the Space Station core platform p 24 A89-35902
- Ore-bearing structures of Central Kazakhstan identified on aerial and space photographs in the framework of the computer-aided prediction of minerals p 52 A89-37316
- The condition of natural features as related to their intrinsic microwave and IR emission fields p 2 A89-37320
- Parameter optimization of systems for the thermal microwave mapping of the earth's surface p 25 A89-37321
- Radiometric correction of aerial and space remote-sensing images p 25 A89-37323
- Remote four-photon Raman spectroscopy of sea water under natural conditions p 52 A89-37327
- The dispersion limitations on the accuracy of the internal reference method during remote laser sounding of the upper ocean layer p 53 A89-37349
- Coordinate referencing of a TV image in the case of the remote sensing of the earth p 53 A89-37492
- Comparison of satellite, ground-based, and modeling techniques for analyzing the urban heat island p 26 A89-37948
- The discrimination of irrigated orchard and vine crops using remotely sensed data p 2 A89-37949
- Cluster analysis of pine crown foliage patterns aid identification of mountain pine beetle current-attack p 26 A89-37950
- Sea state determination by a remote optical sensor p 53 A89-38330
- Development and verification of Osaka Bay sampling model based on Landsat data p 27 A89-38332
- Bathymetric mapping with passive multispectral imagery p 16 A89-38766
- Seasonal visible, near-infrared and mid-infrared spectra of rice canopies in relation to LAI and above-ground dry phytomass p 54 A89-38967
- Using the radiative temperature difference at 3.7 and 11 microns to track dust outbreaks p 27 A89-38968
- The influence of the viewing geometry of bare rough soil surfaces on their spectral response in the visible and near-infrared range p 2 A89-38969
- Measuring and modeling spectral characteristics of a tallgrass prairie p 27 A89-38970
- A reflectance model for the homogeneous plant canopy and its inversion p 27 A89-38971
- Modeling directional thermal radiance from a forest canopy p 27 A89-38972
- Mean temperature in a closed basin by remote sensing p 16 A89-39062
- Validation problems for remotely sensed sea surface temperature p 28 A89-39063
- A semi-automatic terrain measurement system for earthwork control p 28 A89-39094
- The Nebraska center-pivot inventory - An example of operational satellite remote sensing on a long term basis p 28 A89-39096
- A method for integrating remote sensing and geographic information systems p 28 A89-39097
- Fractal analysis of a classified Landsat scene p 28 A89-39099
- N-dimensional display of cluster means in feature space p 29 A89-39100
- Arctic geodynamics - A satellite altimeter experiment for the European Space Agency Earth Remote-Sensing satellite p 29 A89-39546
- Geological uses of remotely-sensed reflected and emitted data of lateritized Archean terrain in Western Australia p 55 A89-39652
- Infrared spectroscopy (2.3-20 microns) for the geological interpretation of remotely-sensed multispectral thermal infrared data p 30 A89-39656
- Geobotanical application of Airborne Thematic Mapper data in Sutherland, north-west Scotland p 2 A89-39657
- Effect of metal stress on the thermal infrared emission of soybeans: A greenhouse experiment - Possible utility in remote sensing p 2 A89-39658
- Applications of AVHRR data; Proceedings of the Third European AVHRR Data Users' Meeting, University of Oxford, England, Dec. 16-18, 1987 p 55 A89-40126
- Activities at the Norwegian Hydrotechnical Laboratory p 55 A89-40129
- Cloud reflectance variations in channel-3 p 55 A89-40136
- Lake area measurement using AVHRR - A case study p 31 A89-40154
- Space geography. Investigations on test regions --- Russian book p 31 A89-40491
- 1988 ACSM-ASPRS Annual Convention, Saint Louis, MO, Mar. 13-18, 1988, Technical Papers, Volume 4 - Image processing/remote sensing p 32 A89-41151
- Concept for a satellite-based global reserve monitoring system p 32 A89-41152
- The use of remote sensing and GIS techniques for wetland identification and classification in the Garrison Diversion Unit-North Dakota p 18 A89-41160
- Earth scenes in polarized light observed from the Space Shuttle p 34 A89-41429
- Monitoring tropical environments with Space Shuttle photography p 34 A89-41432
- Design of spectral and panchromatic bands for the German MOMS-02 sensor p 57 A89-42173
- Spaceborne studies related to nature conservation --- Russian book p 65 A89-42549
- Remote measurements from Salyut-7 of the optical parameters of the atmosphere-surface system p 57 A89-42601
- Measurements of spectral radiance at the sea surface for the development of remote sensing methods p 35 A89-42610
- Determination of spectral signatures for remote laser sensing of vegetation p 35 A89-42611
- Airborne imaging radar system for monitoring sea pollution [MBB-UK-0016-87-PUB] p 58 A89-42941
- Space coloristics --- earth observations from orbital stations p 35 A89-43024
- Retrieval of mesoscale meteorological parameters for polar latitudes (MIZEX and ARCTEMIZ campaigns) p 58 A89-43026
- Monitoring Tunisia's steppes with SPOT p 35 A89-43316
- Monitoring in Moneragala district, Sri Lanka, with SPOT images p 3 A89-43317
- EM wave scattering from statistically inhomogeneous and periodic random rough surfaces p 36 A89-43541
- The investigation of advanced remote sensing, radiative transfer and inversion techniques for the measurement of atmospheric constituents [NASA-CR-172599] p 36 A89-20531
- Remote sensing in refractive turbulence p 58 A89-20532
- Utilizing remote sensing of thematic mapper data to improve our understanding of estuarine processes and their influence on the productivity of estuarine-dependent fisheries [NASA-CR-183417] p 18 A89-20533
- The suitability of remote sensing for surveying and monitoring landscape patterns. Volume A: Pilot study - LANDSAT Imagery. Volume B: PEPS Project No. 73 - SPOT Imagery [BCRS-87-12-VOL-A/B] p 4 A89-20534
- The suitability of remote sensing for surveying and monitoring landscape patterns. Volume A: Pilot study - LANDSAT imagery p 36 A89-20535
- The suitability of remote sensing for surveying and monitoring landscape patterns. Volume B: PEPS Project No. 73 - SPOT Imagery p 36 A89-20536
- Land use inventories using satellite images in the region Haaren-Helvoirt-Udenhout, North Brabant (The Netherlands) [BCRS-88-07] p 36 A89-20537
- Phase A study for the extension of the CAESAR scanner with a sensor module for the far infrared [BCRS-88-09] p 59 A89-20539
- Land use inventory using LANDSAT Thematic Mapper imagery to study environmental pollution [NLR-MP-87063-U] p 4 A89-20541
- Geological remote sensing signatures of terrestrial impact craters p 37 A89-21317
- The Frasnian-Famennian mass killing event(s), methods of identification and evaluation p 37 A89-21318
- AVIRIS data characteristics and their effects on spectral discrimination of rocks exposed in the Drum Mountains, Utah: Results of a preliminary study p 40 A89-22165
- Earth system science: A program for global change [NASA-TM-101186] p 5 A89-22969
- Evaluation of the Portable Instantaneous Display Analysis Spectrometer (PIDAS) [NASA-CR-184878] p 61 A89-22970
- Remote sensing of earth terrain [NASA-CR-184937] p 41 A89-22971
- Imaging radar applications in Europe. Illustrated experimental results (1978-1987) [ESA-TM-01] p 42 A89-22978
- Remote sensing information sciences research group: Browse in the EOS era [NASA-CR-184637] p 42 A89-22979
- Remote sensing of global snowpack energy and mass balance: In-situ measurements on the snow of interior and Arctic Alaska [NASA-CR-180078] p 62 A89-23956
- Determination of areal snow water equivalent using satellite images and gamma ray spectrometry [CI-91] p 44 A89-23960
- Geobotanical remote sensing for determination of aggregate source material [AD-A205943] p 45 A89-23962
- The search for edges in remote sensing images using a digital polygonal map [ETN-89-94146] p 45 A89-23964
- Investigation of several methods for the detection of outstanding points in a digital image [ETN-89-94148] p 45 A89-23965
- Vectorization of grid lines [ETN-89-94150] p 45 A89-23967
- On the international commercialization of remote sensing [BCRS-88-02] p 65 A89-23969
- Optical properties of oceanic suspended matter and their interpretation for remote sensing of phytoplankton [GKSS-88/E/40] p 46 A89-24013
- Microwave X-band radiometric characterization of Brazilian soils by measurement of the complex permittivity [INPE-4588-PRE/1319] p 3 A89-24685
- Estimating population size of Pygoscelid Penguins from TM data [NASA-CR-180081] p 3 A89-24687
- The activities of the British National Space Centre (BNSC) in the field of imaging spectrometry p 47 A89-24696
- A visiting scientist program in atmospheric sciences for the Goddard Space Flight Center [NASA-CR-183421] p 47 A89-24756
- Biooptical variability in the Greenland Sea observed with the Multispectral Airborne Radiometer System (MARS) [NASA-CR-184856] p 47 A89-24784
- ### REMOTE SENSORS
- Short- and long-term memory effects in intensified array detectors - Influence on airborne laser fluorosensor measurements p 47 A89-32836
- Multispectral terrain background simulation techniques for use in airborne sensor evaluation p 19 A89-33664
- Highly sensitive microwave radiometer-scatterometer for the remote sensing of the earth's surface p 52 A89-37322
- Improved capabilities of the Multispectral Atmospheric Mapping Sensor (MAMS) [NASA-TM-100352] p 58 A89-20430
- Phase A study for the extension of the CAESAR scanner with a sensor module for the far infrared [BCRS-88-09] p 59 A89-20539
- An analysis of platinum silicide and indium antimonide for remote sensors in the 3 to 5 micrometer wavelength band [AD-A202663] p 59 A89-21218
- Research for optimization of future MOMS sensors [ETN-89-94424] p 62 A89-23972
- ### RESEARCH
- Earth system science: A program for global change [NASA-TM-101186] p 5 A89-22969
- A visiting scientist program in atmospheric sciences for the Goddard Space Flight Center [NASA-CR-183421] p 47 A89-24756
- ### RESEARCH FACILITIES
- Activities at the Norwegian Hydrotechnical Laboratory p 55 A89-40129

- Air pollution effects field research facility: Ozone flow control and monitoring system
[DE89-007922] p 5 N89-22192
- RESOURCES MANAGEMENT**
Information resources management p 42 N89-23371
- RICE**
Seasonal visible, near-infrared and mid-infrared spectra of rice canopies in relation to LAI and above-ground dry phytomass p 54 A89-38967
- RING STRUCTURES**
Concentric structures in southern Tien-Shan --- Russian book p 10 A89-34196
- RIVERS**
An algorithm for machine-recognizing the river mouth and measuring the sealine from the Landsat image p 19 A89-33658
- ROADS**
Cooperative methods for road tracking in aerial imagery p 42 N89-23101
- ROCK MECHANICS**
The contribution of remote sensing data to exploration of fractured reservoirs p 50 A89-35862
- RURAL AREAS**
Rural settlement expansion in Moneragala district, Sri Lanka p 4 A89-34946
The condition of natural features as related to their intrinsic microwave and IR emission fields p 2 A89-37320
- RURAL LAND USE**
Land use inventory using LANDSAT Thematic Mapper imagery to study environmental pollution [NLR-MP-87063-U] p 4 N89-20541
- S**
- SAHARA DESERT (AFRICA)**
Satellite detection of Saharan dust - Optimized imaging during nighttime p 24 A89-35912
The potential of infrared satellite data for the retrieval of Saharan-dust optical depth over Africa p 30 A89-39875
- SALINITY**
Analysis of seasonal characteristics of Sambhar Salt Lake, India, from digitized Space Shuttle photography p 18 A89-41433
- SALYUT SPACE STATION**
Remote measurements from Salyut-7 of the optical parameters of the atmosphere-surface system p 57 A89-42601
The spectrometer of the Salyut-7 orbital station p 57 A89-42608
- SAMPLING**
Further investigations of sampling errors in mean terrain height estimation p 32 A89-41076
Evaluation of the Portable Instantaneous Display Analysis Spectrometer (PIDAS) [NASA-CR-184878] p 61 N89-22970
- SAN ANDREAS FAULT**
Rate of change of the Quincy-Monument Peak baseline from a translocation analysis of Lageos laser range data p 13 A89-42181
- SATELLITE ALTIMETRY**
GEOSAT altimeter sea-ice mapping p 49 A89-34267
Satellite altimetry. II - A new prospecting tool p 23 A89-35895
Evaluation of Geosat altimeter data with application to tropical Pacific sea level variability p 25 A89-37801
Arctic geodynamics - A satellite altimeter experiment for the European Space Agency Earth Remote-Sensing satellite p 29 A89-39546
Synoptic analysis and dynamical adjustment of GEOS 3 and Seasat altimeter eddy fields in the northwest Atlantic p 29 A89-39650
Seasat altimetry and the South Atlantic geoid. II - Short-wavelength undulations p 16 A89-39659
Development of a satellite SAR image spectra and altimeter wave height data assimilation system for ERS-1 [NASA-CR-182685] p 61 N89-22975
- SATELLITE DOPPLER POSITIONING**
On the connection of geodetic pointfields in RETrig [PB89-146112] p 44 N89-23958
- SATELLITE IMAGERY**
New earth observing platforms to study global water, biology p 17 A89-33121
Satellite, airborne and radar observations of auroral arcs p 48 A89-33505
An algorithm for machine-recognizing the river mouth and measuring the sealine from the Landsat image p 19 A89-33658
Munsell soil color and soil reflectance in the visible spectral bands of Landsat MSS and TM data p 49 A89-33870

- Large-area crop monitoring with the NOAA AVHRR - Estimating the silking stage of corn development p 1 A89-33873
- Mapping of Landsat satellite and gravity lineaments in west Tennessee p 6 A89-34357
- Image-analysis techniques for determination of morphology and kinematics in arctic sea ice p 21 A89-34416
- Commercialization of remote sensing in the U.S.A. - The SPOT perspective p 64 A89-34704
- Monitoring the halfa steppes of central Tunisia using Landsat MSS p 1 A89-34947
- Ground verification method for bathymetric satellite image maps of unsurveyed coral reefs p 6 A89-34949
- Research on speckle behavior in SAR images p 21 A89-35335
- A survey of the operational status and needs of remote sensing in exploration geology p 64 A89-35853
- Successful applications of remotely sensed data for oil and gas exploration p 22 A89-35854
- Lowering the cost of exploration for independents - How remotely sensed data aids in the search for oil and gas p 22 A89-35855
- Hydrocarbon potential of part of the margin of the Tarim Basin from Landsat - A case history p 11 A89-35857
- Identification of Cross Strike discontinuities in the Appalachian basin and implications for hydrocarbon exploration p 11 A89-35860
- Application of Landsat Thematic Mapper digital data to the exploration for uranium-mineralized breccia pipes in Northwestern Arizona p 51 A89-35872
- Applying remote sensing technology to the Bureau of Land Management's mineral management program p 11 A89-35874
- Volcano monitoring by short wavelength infrared satellite remote sensing p 51 A89-35875
- Topographic analysis of the Andean Highlands using the Large Format Camera p 7 A89-35880
- From large-scale to small-scale - Economic geologic-geomorphic mapping using aerial photographs and Landsat images p 7 A89-35884
- Conjugate synthetic normal faults around the Gulf of Salwa, southwestern Qatar, the Arabian Gulf p 12 A89-35886
- Structural analysis of the Wichita Mountains using TM data for lineament mapping p 12 A89-35887
- Integration of Landsat TM, stream sediment geochemistry and regional geophysics for mineral exploration in the English Lake District p 23 A89-35888
- Identification of magnesite and bauxite deposits on Landsat imagery, South India p 12 A89-35889
- Discriminating late volcanic differentiates commonly associated with precious metal deposits, using Landsat Thematic Mapper imagery p 12 A89-35896
- Reconstruction of imagery of faulted landscapes using a photo-optical technique p 24 A89-35900
- Geological applications of the Space Station core platform p 24 A89-35902
- Digital display of SPOT stereo images p 24 A89-35903
- Satellite detection of Saharan dust - Optimized imaging during nighttime p 24 A89-35912
- Aerosol analysis with the Coastal Zone Color Scanner - A simple method for including multiple scattering effects p 25 A89-37291
- Radiometric correction of aerial and space remote-sensing images p 25 A89-37323
- A digital mosaicking algorithm allowing for an irregular join 'line' p 26 A89-37944
- Reflectance enhancements for the Thematic Mapper - An efficient way to produce images of consistently high quality p 26 A89-37947
- Low-relief topographic enhancement in a Landsat snow-cover scene p 54 A89-38966
- The Nebraska center-pivot inventory - An example of operational satellite remote sensing on a long term basis p 28 A89-39096
- Fractal analysis of a classified Landsat scene p 28 A89-39099
- Observing oceanic mesoscale eddies from Geosat altimetry - Preliminary results p 16 A89-39372
- Identification and analysis of the alignments of point-like features in remotely-sensed imagery. Volcanic cones in the Pinacate Volcanic Field, Mexico p 12 A89-39651
- Alteration detection using TM imagery - The effects of supergene weathering in an arid climate p 12 A89-39655
- An AVHRR mosaic image of Antarctica p 30 A89-40135
- A phenological description of Iberian vegetation using short wave vegetation index imagery p 2 A89-40149
- Monitoring the phenology of Tunisian grazing lands p 3 A89-40150

- AVHRR data processing to study the surface canopies in temperate regions - First results of HAPEX-MOBILHY p 30 A89-40153
- An algorithm for snow and ice detection using AVHRR data - An extension to the Apollo software package p 31 A89-40155
- Multi-spectral classification of snow using NOAA AVHRR imagery p 31 A89-40156
- Space geography. Investigations on test regions --- Russian book p 31 A89-40491
- 1988 ACSM-ASPRS Annual Convention, Saint Louis, MO, Mar. 13-18, 1988, Technical Papers. Volume 4 - Image processing/remote sensing p 32 A89-41151
- Shuttle imaging radar analysis in arid environments p 33 A89-41166
- Assessing the improvement in soil mapping using spot HRV over Landsat MSS imagery (Geography and land use) p 33 A89-41168
- Monitoring Tunisia's steppes with SPOT p 35 A89-43316
- Monitoring in Moneragala district, Sri Lanka, with SPOT images p 3 A89-43317
- The suitability of remote sensing for surveying and monitoring landscape patterns. Volume A: Pilot study - LANDSAT imagery. Volume B: PEPS Project No. 73 - SPOT imagery [BCRS-87-12-VOL-A/B] p 4 N89-20534
- The suitability of remote sensing for surveying and monitoring landscape patterns. Volume A: Pilot study - LANDSAT imagery p 36 N89-20535
- The suitability of remote sensing for surveying and monitoring landscape patterns. Volume B: PEPS Project No. 73 - SPOT imagery p 36 N89-20536
- Land use inventories using satellite images in the region Haaren-Helvoirt-Udenhout, North Brabant (The Netherlands) p 36 N89-20537
- Processing and application of digital AVHRR-imagery for land and sea surfaces p 36 N89-20538
- A systematic worldwide landcover of satellite mosaics [NLR-MP-87062-U] p 65 N89-20540
- Land use inventory using LANDSAT Thematic Mapper imagery to study environmental pollution [NLR-MP-87063-U] p 4 N89-20541
- Twelve year overview of cloudfree LANDSAT imagery of The Netherlands [NLR-MP-87072-U] p 59 N89-20542
- Use of commercial satellite imagery for surveillance of the Canadian north by the Canadian armed forces [AD-A202700] p 40 N89-22173
- Theoretical studies for ERS-1 wave mode, volume 1 [GEC-MTR-87/110-VOL-1] p 41 N89-22977
- Imaging radar applications in Europe. Illustrated experimental results (1978-1987) p 42 N89-22978
- The response of thermospheric nitric oxide to an auroral storm p 42 N89-23031
- Geocoded data sets of imaging satellites p 43 N89-23950
- Remote sensing of global snowpack energy and mass balance: In-situ measurements on the snow of interior and Arctic Alaska [NASA-CR-180078] p 62 N89-23956
- Determination of areal snow water equivalent using satellite images and gamma ray spectrometry [CI-91] p 44 N89-23960
- SATELLITE INSTRUMENTS**
Design of spectral and panchromatic bands for the German MOMS-02 sensor p 57 A89-42173
- SATELLITE NAVIGATION SYSTEMS**
A performance comparison for two Lagrangian drifter designs p 34 A89-41750
- Observation model and parameter partials for the JPL geodetic GPS modeling software GPSOMC [NASA-CR-185021] p 9 N89-24060
- SATELLITE NETWORKS**
Minimum number of satellites for periodic coverage [FOA-C-30511-9.4] p 65 N89-22976
- SATELLITE OBSERVATION**
EXOS-C (Ohzora) observations of polar cap precipitations and inverted V events p 19 A89-33543
- Review and status of remote sensing of sea ice p 20 A89-34266
- The experience of the Commission of the European Communities in the use of remote sensing for the implementation of community policies p 64 A89-34712
- Observational analyses of North Atlantic tropical cyclones from NOAA polar-orbiting satellite microwave data p 21 A89-34879
- A comparison of radiation variables calculated in the UCLA general circulation model to observations p 24 A89-35926
- Global, seasonal surface variations from satellite radiance measurements p 52 A89-35966

- Some aspects of the relation between Pi 1-2 magnetic pulsations observed at L = 1.3-2.1 on the ground and substorm-associated magnetic field variations in the near-earth magnetotail observed by AMPTE CCE
p 52 A89-36686
- Marine Observation Satellite-1 - First year in orbit
p 26 A89-38328
- Development and verification of Osaka Bay sampling model based on Landsat data
p 27 A89-38332
- Discrimination of rocks and hydrothermal altered areas based on Landsat TM data
p 27 A89-38333
- Atmospheric correction of satellite MSS data in rugged terrain
p 27 A89-38334
- Land-surface temperature measurement from space - Physical principles and inverse modeling
p 29 A89-39552
- Relating point to area average rainfall in semiarid West Africa and the implications for rainfall estimates derived from satellite data
p 55 A89-39870
- The potential of infrared satellite data for the retrieval of Saharan-dust optical depth over Africa
p 30 A89-39875
- Properties of the equatorial and tropical ionosphere according to Soviet satellite observations during the IMS
p 31 A89-40606
- 1988 ACSM-ASPRS Annual Convention, Saint Louis, MO, Mar. 13-18, 1988, Technical Papers, Volume 4 - Image processing/remote sensing
p 32 A89-41151
- Concept for a satellite-based global reserve monitoring system
p 32 A89-41152
- Processing and application of digital AVHRR imagery for land and sea surfaces
[BCRS-88-08]
p 36 A89-20538
- NOAA (National Oceanic and Atmospheric Administration) AVHRR (Advanced Very High Resolution Radiometer) observations during the marginal ice zone experiment, between Spitzbergen and Greenland, June 7 to 18 July 1984
[AD-A204911]
p 19 A89-22280
- Derivation of a large-scale map of heat load in the region Freiburg-Basel (Germany, F.R.) using satellite data. A contribution to the production of bioclimate data based on a geographic information system
[REPT-27]
p 41 A89-22972
- The advanced Ocean Chlorophyll Meter (OCM). A spectral imaging device for the observation of the oceans
[REPT-882-440-118]
p 63 A89-24689
- On the future development and management of spectroscopic database for radiative transfer from the issues of recent related workshops
[ETN-89-94530]
p 46 A89-24690
- Refinements in the cloud detection scheme of the 3I system. Comparison with AVHRR products
[ETN-89-94531]
p 63 A89-24691
- ESA's planned activities in the field of imaging spectrometry for Earth observation
p 46 A89-24693
- HIRS: NASA's high-resolution imaging spectrometer for the Earth Observing System (EOS)
p 63 A89-24695
- DFVLR activities related to imaging spectrometry
p 63 A89-24697
- Activities of CNES in the field of imaging spectrometry
p 47 A89-24699
- The EARSEL Imaging Spectrometry Working Group
p 47 A89-24700
- SATELLITE ORBITS**
- Optimal satellite orbits and the network structure for regular earth surveying
p 35 A89-42614
- Operational aspects of CASA UNO '88-The first large scale international GPS geodetic network
p 7 A89-42787
- SATELLITE SOUNDING**
- Measuring thermal budgets of active volcanoes by satellite remote sensing
p 9 A89-32988
- Munsell soil color and soil reflectance in the visible spectral bands of Landsat MSS and TM data
p 49 A89-33870
- Evaluating atmospheric correction models for retrieving surface temperatures from the AVHRR over a tallgrass prairie
p 20 A89-33875
- Theoretical algorithms for satellite-derived sea surface temperatures
p 21 A89-35159
- Applications of AVHRR data; Proceedings of the Third European AVHRR Data Users' Meeting, University of Oxford, England, Dec. 16-18, 1987
p 55 A89-40126
- Satellite-derived low-level atmospheric water vapour content from synergy of AVHRR with HIRS --- High Resolution Infrared Radiation Sounder
p 30 A89-40139
- Observations of volcanic ash clouds in the 10-12 micron window using AVHRR/2 data
p 30 A89-40143
- Mesoscale variability of sea surface temperature in the North Atlantic
p 17 A89-40145
- Using NOAA AVHRR imagery in assessing water quality parameters
p 55 A89-40148
- NOAA AVHRR and its uses for rainfall and evapotranspiration monitoring
p 56 A89-40151
- AVHRR for monitoring global tropical deforestation
p 56 A89-40152
- Spaceborne studies related to nature conservation --- Russian book
p 65 A89-42549
- Measurements of spectral radiance at the sea surface for the development of remote sensing methods
p 35 A89-42610
- SATELLITE TRACKING**
- Operational aspects of CASA UNO '88-The first large scale international GPS geodetic network
p 7 A89-42787
- SATELLITE-BORNE INSTRUMENTS**
- Spectral indices for vegetation and rock type discrimination using the optical sensor of the Japanese ERS-1
p 51 A89-35866
- Methodological aspects of the automation of the calibration and processing of satellite microwave-radiometer data
p 25 A89-37324
- Comparison of satellite, ground-based, and modeling techniques for analyzing the urban heat island
p 26 A89-37948
- Bathymetric mapping with passive multispectral imagery
p 16 A89-38766
- Satellite-borne lidar observations of the earth - Requirements and anticipated capabilities
p 56 A89-41692
- Multichannel spectrometer MKS-M - Laboratory tests, calibration, and verification of its stability in flight
p 57 A89-42609
- Correcting absolute calibrations of satellite microwave radiometer using a priori data
p 35 A89-42612
- SATELLITE-BORNE PHOTOGRAPHY**
- A raster approach to population estimation using high-altitude aerial and space photographs
p 19 A89-33872
- The potential use of remote sensing to solve problems of paleotectonic prediction, geologic structure, and exploitation of coal deposits with reference to the Moscow-Region coal basin
p 49 A89-34002
- Use of aerial and space photography for the detection of faults and neotectonic movements in Crimea and the Azov Coastal Region
p 9 A89-34003
- Dynamics of present-day geological processes from remotely sensed data
p 9 A89-34004
- Investigation of the recently formed imbricate structure of the southern Tien-Shan using space photographs
p 10 A89-34005
- Morphostructural interpretation of space images and the reconstruction of the recently formed stress field in the Altai-Baikal region
p 10 A89-34006
- Use of aerial and space methods for observations and studies of the morphology and kinematics of recent movements along some faults of the Baikal Rift Zone
p 10 A89-34007
- Structural stresses and the divisibility into blocks of the earth crust as observed on space imagery
p 10 A89-34009
- The use of a lineament-analysis instrument for investigations of tectonic zonality and the elements of continental-margin geodynamics as applied to western Arctic
p 49 A89-34010
- Identification of tectonic dislocations underneath large water areas using space images
p 15 A89-34011
- Methods for investigating seismically active zones using remote imagery
p 20 A89-34013
- Automated analysis of lineaments from space imagery obtained during seismic studies of central Tien-Shan
p 20 A89-34014
- The use of space imagery for investigations of recent crustal deformations in southern Sakhalin
p 20 A89-34015
- Determination of the character of present-day vertical movements from the structure of space imagery
p 10 A89-34016
- Recent and current geodynamics of the Kyzylkum region as derived from space imagery
p 10 A89-34017
- Seismogeological interpretation of space images of the region of Caucasian mineral waters
p 10 A89-34018
- Multispectral space surveys and data processing
p 22 A89-35684
- Analysis of the potential of using space photographic data obtained with the PKF-1K camera to solve scientific, economic, and educational-methodological problems
p 64 A89-35685
- The KAP-350 and KAP-100 space cameras for the remote sensing of earth resources
p 50 A89-35687
- Astronaut photography of the earth - Low cost images for resource exploration
p 23 A89-35883
- The definition of isometric magmatogenic structures on space imagery
p 12 A89-37315
- A technique for applying space photographs to search for anticlinal oil- and gas-traps in orogenic structures of the Tien-Shan
p 25 A89-37318
- Assessment of the present conditions of lowland lakes of Central Asia using the interpretation of space photographs
p 17 A89-37319
- Studying the earth from manned spacecraft --- Russian book
p 64 A89-42511
- Use of commercial satellite imagery for surveillance of the Canadian north by the Canadian armed forces
[AD-A202700]
p 40 A89-22173
- SCANNING**
- Digitizing of drawings and cadastral maps using a scanner system
p 43 A89-23949
- SCATTERING CROSS SECTIONS**
- EM wave scattering from statistically inhomogeneous and periodic random rough surfaces
p 36 A89-43541
- SCATTEROMETERS**
- Highly sensitive microwave radiometer-scatterometer for the remote sensing of the earth's surface
p 52 A89-37322
- OSRMS (Ocean Surface Roughness Measurement System): The DREP (Defence Research Establishment Pacific) near-nadir scatterometer
[AD-A202983]
p 38 A89-21460
- SCENE ANALYSIS**
- Automated analysis of lineaments from space imagery obtained during seismic studies of central Tien-Shan
p 20 A89-34014
- Earth scenes in polarized light observed from the Space Shuttle
p 34 A89-41429
- Image understanding research at SRI International
p 42 A89-23080
- SCIENTISTS**
- A visiting scientist program in atmospheric sciences for the Goddard Space Flight Center
[NASA-CR-183421]
p 47 A89-24756
- SEA BREEZE**
- Seasat A satellite scatterometer measurements of equatorial surface winds
p 53 A89-37802
- SEA ICE**
- Review and status of remote sensing of sea ice
p 20 A89-34266
- GEOSAT altimeter sea-ice mapping
p 49 A89-34267
- Sea-ice characterization measurements needed for testing of microwave remote sensing models
p 20 A89-34268
- Image-analysis techniques for determination of morphology and kinematics in arctic sea ice
p 21 A89-34416
- Examination of USAF Nephelometer performance in the marginal cryosphere region
p 52 A89-35949
- An inexpensive polarimetric FM radar and polarimetric signatures of artificial sea ice
p 57 A89-42684
- Refinements in the cloud detection scheme of the 3I system. Comparison with AVHRR products
[ETN-89-94531]
p 63 A89-24691
- SEA LEVEL**
- Satellite altimetry. II - A new prospecting tool
p 23 A89-35895
- Evaluation of Geosat altimeter data with application to tropical Pacific sea level variability
p 25 A89-37801
- Preliminary development of a seashore-effects analysis system
[DE89-007863]
p 61 A89-22191
- SEA STATES**
- Sea state determination by a remote optical sensor
p 53 A89-38330
- SEA SURFACE TEMPERATURE**
- Interaction between net shortwave flux and sea surface temperature
p 15 A89-34878
- Theoretical algorithms for satellite-derived sea surface temperatures
p 21 A89-35159
- Methodology for the remote sensing of fluxes of heat, moisture, and effective radiation in the ocean-atmosphere system
p 16 A89-35686
- A real-time global sea surface temperature analysis
p 16 A89-35907
- Greater global warming revealed by satellite-derived sea-surface-temperature trends
p 16 A89-37571
- Validation problems for remotely sensed sea surface temperature
p 28 A89-39063
- Land-surface temperature measurement from space - Physical principles and inverse modeling
p 29 A89-39552
- Mesoscale variability of sea surface temperature in the North Atlantic
p 17 A89-40145
- Improved capabilities of the Multispectral Atmospheric Mapping Sensor (MAMS)
[NASA-TM-100352]
p 58 A89-20430
- SEA WATER**
- Remote four-photon Raman spectroscopy of sea water under natural conditions
p 52 A89-37327
- Optical properties of oceanic suspended matter and their interpretation for remote sensing of phytoplankton
[GKSS-88/E/40]
p 46 A89-24013

SEASAT SATELLITES

- Seasat A satellite scatterometer measurements of equatorial surface winds p 53 A89-37802
 Synoptic analysis and dynamical adjustment of GEOS 3 and Seasat altimeter eddy fields in the northwest Atlantic p 29 A89-39650
 Seasat altimetry and the South Atlantic geoid. II - Short-wavelength undulations p 16 A89-39659
 Assessment of forest cover changes using multistate spaceborne imaging radar p 33 A89-41169

SEDIMENTARY ROCKS

- Discrimination of rocks and hydrothermal altered areas based on Landsat TM data p 27 A89-38333

SEDIMENTS

- Integration of Landsat TM, stream sediment geochemistry and regional geophysics for mineral exploration in the English Lake District p 23 A89-35888

- Structural patterns in high grade terrain in parts of Tamil Nadu and Karnataka p 14 A89-22255

SEISMOLOGY

- Methods for investigating seismically active zones using remote imagery p 20 A89-34013
 Automated analysis of lineaments from space imagery obtained during seismic studies of central Tien-Shan p 20 A89-34014

- Seismogeological interpretation of space images of the region of Caucasian mineral waters p 10 A89-34018
 The Calvin 28 cryptoexplosive disturbance, Cass County, Michigan: Evidence for impact origin p 14 A89-21358

SHALLOW WATER

- Bathymetric mapping with passive multispectral imagery p 16 A89-38766
 The KP equation: A comparison to laboratory generated biperiodic waves p 38 A89-21507

SHEAR STRAIN

- Plate motions and deformations from geologic and geodetic data [NASA-CR-184987] p 15 A89-24757

SHORELINES

- Analytical independent model triangulation strip adjustment using shore-line constraints p 28 A89-39093

- Preliminary development of a seashore-effects analysis system [DE89-007863] p 61 A89-22191

SHORT WAVE RADIATION

- Interaction between net shortwave flux and sea surface temperature p 15 A89-34878
 Sources of remote sensing data visible, near infrared, and short wave p 51 A89-35878

SHUTTLE IMAGING RADAR

- Geological application of SIR-A imagery in southern Iraq p 13 A89-41162
 Shuttle imaging radar analysis in arid environments p 33 A89-41166

- Assessment of forest cover changes using multistate spaceborne imaging radar p 33 A89-41169
 Necessity and benefit of the X-SAR space shuttle experiment [DFVLR-MITT-88-29] p 63 A89-24688

SIGNAL TO NOISE RATIOS

- Performance analysis of the DFVLR real time SAR processor for low SNRs p 21 A89-35336

- Zones of information in the AVIRIS spectra p 39 A89-22158

- Evaluation of Airborne Visible/Infrared Imaging Spectrometer Data of the Mountain Pass, California carbonate complex p 60 A89-22169

- Determination of in-flight AVIRIS spectral, radiometric, spatial and signal-to-noise characteristics using atmospheric and surface measurements from the vicinity of the rare-earth-bearing carbonate at Mountain Pass, California p 61 A89-22170

SIGNATURE ANALYSIS

- Laser scattering phenomenon - Background signature characterization and prediction p 6 A89-33661
 Modeling and observation of the radar polarization signature of forested areas p 2 A89-39554

SIGNATURES

- Geological remote sensing signatures of terrestrial impact craters p 37 A89-21317
 Cartographic signatures in PHOCUS p 43 A89-23948

SILICIDES

- An analysis of platinum silicide and indium antimonide for remote sensors in the 3 to 5 micrometer wavelength band [AD-A202663] p 59 A89-21218

SKY RADIATION

- Thermal images of sky and sea-surface background infrared radiation [AD-A205819] p 46 A89-23992

SNOW

- Snowmelt increase through albedo reduction [AD-A204523] p 18 A89-22175

- Determination of areal snow water equivalent using satellite images and gamma ray spectrometry [CI-91] p 44 A89-23960

SNOW COVER

- Sensitivity of 30-day dynamical forecasts to continental snow cover p 17 A89-35937

- Examination of USAF Nephanalysis performance in the marginal cryosphere region p 52 A89-35949
 Low-relief topographic enhancement in a Landsat snow-cover scene p 54 A89-38966

- An algorithm for snow and ice detection using AVHRR data - An extension to the Apollo software package p 31 A89-40155

- Multi-spectral classification of snow using NOAA AVHRR imagery p 31 A89-40156

- Snowmelt increase through albedo reduction [AD-A204523] p 18 A89-22175

- Remote sensing of global snowpack energy and mass balance: In-situ measurements on the snow of interior and Arctic Alaska [NASA-CR-180078] p 62 A89-23956

SODIUM COMPOUNDS

- Remote four-photon Raman spectroscopy of sea water under natural conditions p 52 A89-37327

SOFTWARE TOOLS

- An algorithm for snow and ice detection using AVHRR data - An extension to the Apollo software package p 31 A89-40155

SOIL EROSION

- Close-range photogrammetric measurement of erosion in coarse-grained soils p 54 A89-39098
 Detection techniques using multispectral data to index soil erosional status p 56 A89-41164

SOIL MAPPING

- Munsell soil color and soil reflectance in the visible spectral bands of Landsat MSS and TM data p 49 A89-33870

- Using multispectral video imagery for detecting soil surface conditions p 22 A89-35838

- Detection techniques using multispectral data to index soil erosional status p 56 A89-41164

- The application of SPOT ratio data for soil classification p 56 A89-41165

- Assessing the improvement in soil mapping using spot HRV over Landsat MSS imagery (Geography and land use) p 33 A89-41168

SOIL MECHANICS

- Impulse radar for identification of features in soils p 50 A89-34353

SOIL MOISTURE

- Estimation of regional surface resistance to evapotranspiration from NDVI and thermal-IR AVHRR data --- Normalized Difference Vegetation Index p 55 A89-39872

- Airborne time-series measurement of soil moisture using terrestrial gamma radiation p 33 A89-41163

- Mapping freeze/thaw boundaries with SMMR data [NASA-CR-184991] p 9 A89-23961

SOILS

- The influence of the viewing geometry of bare rough soil surfaces on their spectral response in the visible and near-infrared range p 2 A89-38969

- AVIRIS spectra of California wetlands p 3 A89-22167

SOLAR ACTIVITY

- Solar-geophysical data number 529, September 1988. Part 1: (Prompt reports). Data for August, July 1988 and late data [PB89-121305] p 37 A89-21431

SOLAR ENERGY

- Nimbus-7 data product summary [NASA-RP-1215] p 39 A89-22152

SOLAR FLUX DENSITY

- Surface solar irradiance in the central Pacific during tropic heat - Comparisons between in situ measurements and satellite estimates p 16 A89-35931

SOLAR PHYSICS

- Solar-geophysical data number 529, September 1988. Part 1: (Prompt reports). Data for August, July 1988 and late data [PB89-121305] p 37 A89-21431

SOLAR RADIATION

- Surface solar irradiance in the central Pacific during tropic heat - Comparisons between in situ measurements and satellite estimates p 16 A89-35931

- Nimbus-7 data product summary [NASA-RP-1215] p 39 A89-22152

SOLAR RADIO EMISSION

- Solar-geophysical data number 529, September 1988. Part 1: (Prompt reports). Data for August, July 1988 and late data [PB89-121305] p 37 A89-21431

SOLAR WIND

- EXOS-C (Ohzora) observations of polar cap precipitations and inverted V events p 19 A89-33543

SONAR

- Gas chromatographic and sonar imaging of hydrocarbon seeps in the marine environment p 22 A89-35863

SOVIET SPACECRAFT

- Properties of the equatorial and tropical ionosphere according to Soviet satellite observations during the IMS p 31 A89-40606

- Studying the earth from manned spacecraft --- Russian book p 64 A89-42511

SOYBEANS

- Effect of metal stress on the thermal infrared emission of soybeans: A greenhouse experiment - Possible utility in remote sensing p 2 A89-39658

SPACE BASED RADAR

- C-band radar cross section of the Guyana rain forest - Possible use as a reference target for spaceborne radars p 49 A89-33869

SPACE COMMERCIALIZATION

- Landsat commercialization - Keys to future success p 64 A89-34703

- Commercialization of remote sensing in the U.S.A. - The SPOT perspective p 64 A89-34704

- Economic relations of the all-union trade association Sojuzkarta and the geodetic and cartographic services of the U.S.S.R. to foreign countries p 64 A89-34708

- The commercial land remote sensing market - Current assessment, baseline forecast and baseline alternatives p 64 A89-35899

SPACE PLASMAS

- GEOS 1 observations of low-energy ions in the earth's plasmasphere - A study on composition, and temperature and density structure under quiet geomagnetic conditions p 9 A89-33829

SPACE PLATFORMS

- New earth observing platforms to study global water, biology p 17 A89-33121

- Geological applications of the Space Station core platform p 24 A89-35902

SPACE SHUTTLE ORBITERS

- Spacelab 2 Upper Atmospheric Modification Experiment over Arecibo. II - Plasma dynamics p 4 A89-38897

- Expanding the utility of manned observations of earth - 70 mm film tests on the Space Shuttle p 34 A89-41428

SPACE SHUTTLES

- Astronaut photography of the earth - Low cost images for resource exploration p 23 A89-35883

- Earth scenes in polarized light observed from the Space Shuttle p 34 A89-41429

- Meteorological applications of Space Shuttle photography p 34 A89-41430

- Geologic applications of Space Shuttle photography p 34 A89-41431

- Monitoring tropical environments with Space Shuttle photography p 34 A89-41432

- Analysis of seasonal characteristics of Sambhar Salt Lake, India, from digitized Space Shuttle photography p 18 A89-41433

SPACE STATION PAYLOADS

- The spectrometer of the Salyut-7 orbital station p 57 A89-42608

SPACE STATIONS

- Geological applications of the Space Station core platform p 24 A89-35902

SPACEBORNE LASERS

- Rate of change of the Quincy-Monument Peak baseline from a translocation analysis of Lageos laser range data p 13 A89-42181

SPACEBORNE PHOTOGRAPHY

- Topographic analysis of the Andean Highlands using the Large Format Camera p 7 A89-35880

- Shuttle imaging radar analysis in arid environments p 33 A89-41166

- Expanding the utility of manned observations of earth - 70 mm film tests on the Space Shuttle p 34 A89-41428

- Earth scenes in polarized light observed from the Space Shuttle p 34 A89-41429

- Meteorological applications of Space Shuttle photography p 34 A89-41430

- Geologic applications of Space Shuttle photography p 34 A89-41431

- Monitoring tropical environments with Space Shuttle photography p 34 A89-41432

- Analysis of seasonal characteristics of Sambhar Salt Lake, India, from digitized Space Shuttle photography p 18 A89-41433

- The decrease of Lake Chad as documented during twenty years of manned space flight p 18 A89-41434

SPACECRAFT INSTRUMENTS

- Laser altimetry measurements from aircraft and spacecraft p 56 A89-41691

SPACELAB

- Spacelab 2 Upper Atmospheric Modification Experiment over Arecibo. II - Plasma dynamics p 4 A89-38897

SPATIAL DEPENDENCIES

- Shortest paths in a digitized map using a tile-based data structure
[PB89-143432] p 44 N89-23957

SPATIAL RESOLUTION

- Area sensitivity and feature sensitivity of SPOT 1 data
- A statistical analysis p 32 A89-41154
Atmospheric water mapping with the Airborne Visible/Infrared Imaging Spectrometer (AVIRIS), Mountain Pass, California p 39 N89-22156
Determination of in-flight AVIRIS spectral, radiometric, spatial and signal-to-noise characteristics using atmospheric and surface measurements from the vicinity of the rare-earth-bearing carbonate at Mountain Pass, California p 61 N89-22170

SPECKLE PATTERNS

- Research on speckle behavior in SAR images p 21 A89-35335
An analysis of speckle from forest stands with periodic structures p 54 A89-39555

SPECTRAL BANDS

- Geobotanical remote sensing for determination of aggregate source material [AD-A205943] p 45 N89-23962
Research for optimization of future MOMS sensors [ETN-89-94424] p 62 N89-23972

SPECTRAL EMISSION

- Measurements of spectral radiance at the sea surface for the development of remote sensing methods p 35 A89-42610
Mapping freeze/thaw boundaries with SMMR data [NASA-CR-184991] p 9 N89-23961

SPECTRAL METHODS

- A new technique to measure the spectral properties of conifer needles p 19 A89-33874
Spectral indices for vegetation and rock type discrimination using the optical sensor of the Japanese ERS-1 p 51 A89-35866

SPECTRAL REFLECTANCE

- Hyperspectral interactions - Invariance and scaling --- applied to remote sensing data p 48 A89-32837
Munsell soil color and soil reflectance in the visible spectral bands of Landsat MSS and TM data p 49 A89-33870
Surface reflectance factor retrieval from Thematic Mapper data p 49 A89-33871
Vegetation reflectance features in AVIRIS data p 22 A89-35867
Visible and near-infrared (0.4- to 2.5-microns) reflectance spectra of selected mixed-layer clays and related minerals p 12 A89-35897
Reflectance enhancements for the Thematic Mapper - An efficient way to produce images of consistently high quality p 26 A89-37947
The influence of the viewing geometry of bare rough soil surfaces on their spectral response in the visible and near-infrared range p 2 A89-38969
Measuring and modeling spectral characteristics of a tallgrass prairie p 27 A89-38970
A reflectance model for the homogeneous plant canopy and its inversion p 27 A89-38971
Using textural measures to distinguish spectrally similar vegetation p 3 A89-41155
Proceedings of the Airborne Visible/Infrared Imaging Spectrometer (AVIRIS) Performance Evaluation Workshop [NASA-CR-184870] p 59 N89-22154
Automated extraction of absorption features from Airborne Visible/Infrared Imaging Spectrometer (AVIRIS) and Geophysical and Environmental Research Imaging Spectrometer (GERIS) data p 39 N89-22160
Preliminary analysis of Airborne Visible/Infrared Imaging Spectrometer (AVIRIS) for mineralogic mapping at sites in Nevada and Colorado p 60 N89-22161
Assessment of AVIRIS data from vegetated sites in the Owens Valley, California p 60 N89-22162
Examination of the spectral features of vegetation in 1987 AVIRIS data p 3 N89-22163
Application of imaging spectrometer data to the Kings-Kaweah ophiolite melange p 40 N89-22166
An assessment of AVIRIS data for hydrothermal alteration mapping in the Goldfield Mining District, Nevada p 40 N89-22168
Biophysical variability in the Greenland Sea observed with the Multispectral Airborne Radiometer System (MARS) [NASA-CR-184856] p 47 N89-24784

SPECTRAL RESOLUTION

- Radiometric performance of AVIRIS: Assessment for an arid region geologic target p 39 N89-22157
Determination of in-flight AVIRIS spectral, radiometric, spatial and signal-to-noise characteristics using atmospheric and surface measurements from the vicinity of the rare-earth-bearing carbonate at Mountain Pass, California p 61 N89-22170
Research for optimization of future MOMS sensors [ETN-89-94424] p 62 N89-23972

SPECTRAL SIGNATURES

- Multi-spectral classification of snow using NOAA AVHRR imagery p 31 A89-40156
Using textural measures to distinguish spectrally similar vegetation p 3 A89-41155
Variation of surface water spectral response as a function of in situ sampling technique p 33 A89-41161
Determination of spectral signatures for remote laser sensing of vegetation p 35 A89-42611
Radiometric performance of AVIRIS: Assessment for an arid region geologic target p 39 N89-22157
Research for optimization of future MOMS sensors [ETN-89-94424] p 62 N89-23972

SPECTROMETERS

- Hyperspectral interactions - Invariance and scaling --- applied to remote sensing data p 48 A89-32837
Vegetation reflectance features in AVIRIS data p 22 A89-35867
Multichannel spectrometer MKS-M - Laboratory tests, calibration, and verification of its stability in flight p 57 A89-42609
Evaluation of the Portable Instantaneous Display Analysis Spectrometer (PIDAS) [NASA-CR-184878] p 61 N89-22970
Imaging Spectrometry for Land Applications [ESA-SP-1101] p 63 N89-24692

SPECTROPHOTOMETERS

- Examination of the spectral features of vegetation in 1987 AVIRIS data p 3 N89-22163

SPECTRODIAMETERS

- Research for optimization of future MOMS sensors [ETN-89-94424] p 62 N89-23972
The advanced Ocean Chlorophyll Meter (OCM), A spectral imaging device for the observation of the oceans [REPT-882-440-118] p 63 N89-24689
Activities of CNES in the field of imaging spectrometry p 47 N89-24699

SPECTROSCOPIC ANALYSIS

- A field spectrometer and remote sensing study of the Fresnillo mining district, Mexico p 51 A89-35871
On the future development and management of spectroscopic database for radiative transfer from the issues of recent related workshops [ETN-89-94530] p 46 N89-24690

SPECTRUM ANALYSIS

- High resolution chronology of late Cretaceous-early Tertiary events determined from 21,000 yr orbital-climatic cycles in marine sediments p 14 N89-21328
Proceedings of the Airborne Visible/Infrared Imaging Spectrometer (AVIRIS) Performance Evaluation Workshop [NASA-CR-184870] p 59 N89-22154

SPHERICAL HARMONICS

- Modelling the earth's geomagnetic field to high degree and order p 58 A89-43408

SPOT (FRENCH SATELLITE)

- Commercialization of remote sensing in the U.S.A. - The SPOT perspective p 64 A89-34704
Digital display of SPOT stereo images p 24 A89-35903
Area sensitivity and feature sensitivity of SPOT 1 data - A statistical analysis p 32 A89-41154
The application of SPOT ratio data for soil classification p 56 A89-41165
Assessing the improvement in soil mapping using spot HRV over Landsat MSS imagery (Geography and land use) p 33 A89-41168
Monitoring Tunisia's steppes with SPOT p 35 A89-43316
Monitoring in Moneragala district, Sri Lanka, with SPOT images p 3 A89-43317
The suitability of remote sensing for surveying and monitoring landscape patterns. Volume A: Pilot study - LANDSAT Imagery. Volume B: PEPS Project No. 73 - SPOT Imagery [BCRS-87-12-VOL-A/B] p 4 N89-20534
The suitability of remote sensing for surveying and monitoring landscape patterns. Volume B: PEPS Project No. 73 - SPOT Imagery p 36 N89-20536

SPRING (SEASON)

- Direct ozone depletion in springtime Antarctic lower stratospheric clouds p 4 A89-32756

SRI LANKA

- Rural settlement expansion in Moneragala district, Sri Lanka p 4 A89-34946
Mapping coastal evolution in Sri Lanka using aerial photographs p 6 A89-34948
Monitoring in Moneragala district, Sri Lanka, with SPOT images p 3 A89-43317

STATISTICAL ANALYSIS

- Statistical geometry of a small surface patch in a developed sea p 26 A89-37808
Area sensitivity and feature sensitivity of SPOT 1 data - A statistical analysis p 32 A89-41154

STRUCTURAL PROPERTIES (GEOLOGY)**STEPPIES**

- Monitoring Tunisia's steppes with SPOT p 35 A89-43316

STEREOPHOTOGRAPHY

- Topographic analysis of the Andean Highlands using the Large Format Camera p 7 A89-35880

STEREOSCOPY

- Digital display of SPOT stereo images p 24 A89-35903

STORMS (METEOROLOGY)

- Precipitation in the Canadian Atlantic Storms Program - Measurements of the acoustic signature p 50 A89-35819

STRAIN RATE

- Plate motions and deformations from geologic and geodetic data [NASA-CR-184987] p 15 N89-24757

STRATEGY

- Computer strategy for detecting line features on simulated binary arrays in support of radar feature extraction [AD-A203257] p 37 N89-21162

STRATIGRAPHY

- Landsat interpretation and stratigraphy of the Hugoton gas field (Southwestern Kansas) and surrounding areas p 6 A89-35856
The Calvin 28 cryptoexplosive disturbance, Cass County, Michigan: Evidence for impact origin p 14 N89-21358

STRATOSPHERE

- Direct ozone depletion in springtime Antarctic lower stratospheric clouds p 4 A89-32756

STRATOSPHERIC WARMING

- Preliminary development of a seashore-effects analysis system [DE89-007863] p 61 N89-22191

STRUCTURAL BASINS

- Use of remotely sensed data in mature basin exploration - Considerations on creating useful imagery p 50 A89-35861

- Mean temperature in a closed basin by remote sensing p 16 A89-39062

STRUCTURAL PROPERTIES (GEOLOGY)

- Investigation of the recently formed imbricate structure of the southern Tien-Shan using space photographs p 10 A89-34005
Morphostructural interpretation of space images and the reconstruction of the recently formed stress field in the Altai-Baikal region p 10 A89-34006
Structural stresses and the divisibility into blocks of the earth crust as observed on space imagery p 10 A89-34009
The use of a lineament-analysis instrument for investigations of tectonic zonality and the elements of continental-margin geodynamics as applied to western Arctic p 49 A89-34010
New data on the morphostructure and geodynamics of the eastern margin of Eurasia p 10 A89-34012
Automated analysis of lineaments from space imagery obtained during seismic studies of central Tien-Shan p 20 A89-34014
The use of space imagery for investigations of recent crustal deformations in southern Yakutia p 20 A89-34015

- Determination of the character of present-day vertical movements from the structure of space imagery p 10 A89-34016

- Concentric structures in southern Tien-Shan --- Russian book p 10 A89-34196

- Mapping of Landsat satellite and gravity lineaments in west Tennessee p 6 A89-34357

- Hydrocarbon potential of part of the margin of the Tarim Basin from Landsat - A case history p 11 A89-35857
Synthetic Aperture Radar data for mapping subsurface geological structures in the Northwest Territories, Canada p 50 A89-35858

- The contribution of remote sensing data to exploration of fractured reservoirs p 50 A89-35862

- Implication of patterns of faulting and hydrothermal alteration from Landsat TM images and NHAAP aerial photos to mineral exploration and tectonics of the Virginia Range, Nevada --- National High Altitude Photography p 11 A89-35868

- Lineament analysis for hazard assessment in advance of coal mining p 11 A89-35873

- Photogeologic-geomorphic mapping provides clues to structural features beneath glacial terrain p 7 A89-35882

- Structural analysis of the Wichita Mountains using TM data for lineament mapping p 12 A89-35887

- Discrimination of rocks and hydrothermal altered areas based on Landsat TM data p 27 A89-38333

- Structural analysis of fracturing in Sinjar anticline using remote sensing technique p 13 A89-41167
The Frasnian-Famennian mass killing event(s), methods of identification and evaluation p 37 N89-21318

Kinematics at the intersection of the Garlock and Death Valley fault zones, California: Integration of TM data and field studies
[NASA-CR-184854] p 15 N89-22263

SULFATES

The relationship between in-lake sulfate concentration and estimates of atmospheric sulfur deposition for subregions of the eastern lake survey
[DE89-009868] p 5 N89-24749

SURFACE NAVIGATION

Image understanding research at SRI International
p 42 N89-23080

SURFACE PROPERTIES

Statistical geometry of a small surface patch in a developed sea
p 26 A89-37808

SURFACE ROUGHNESS

OSRMS (Ocean Surface Roughness Measurement System): The DREP (Defence Research Establishment Pacific) near-nadir scatterometer
[AD-A202983] p 38 N89-21460

SURFACE ROUGHNESS EFFECTS

The influence of the viewing geometry of bare rough soil surfaces on their spectral response in the visible and near-infrared range
p 2 A89-38969
EM wave scattering from statistically inhomogeneous and periodic random rough surfaces
p 36 A89-43541

SURFACE TEMPERATURE

Modeling surface temperature distributions in forest landscapes
p 48 A89-33868
Evaluating atmospheric correction models for retrieving surface temperatures from the AVHRR over a tallgrass prairie
p 20 A89-33875
Land-surface temperature measurement from space - Physical principles and inverse modeling
p 29 A89-39552

Estimation of regional surface resistance to evapotranspiration from NDVI and thermal-IR AVHRR data --- Normalized Difference Vegetation Index
p 55 A89-39872

Improved capabilities of the Multispectral Atmospheric Mapping Sensor (MAMS)
[NASA-TM-100352] p 58 N89-20430

Ice cover on Chesapeake Bay from AVHRR (Advanced Very High Resolution Radiometer) and LANDSAT imagery, winter of 1987-88
[PB89-117261] p 59 N89-21415

Mapping freeze/thaw boundaries with SMMR data
[NASA-CR-184991] p 9 N89-23961

SURFACE WATER

Variation of surface water spectral response as a function of in situ sampling technique
p 33 A89-41161

SURFACE WAVES

A performance comparison for two Lagrangian drifter designs
p 34 A89-41750

SURVEILLANCE

Use of commercial satellite imagery for surveillance of the Canadian north by the Canadian armed forces
[AD-A202700] p 40 N89-22173

SWATH WIDTH

Minimum number of satellites for periodic coverage
[FOA-C-30511-9.4] p 65 N89-22976

SYMBOLS

The precedence of global features in the perception of map symbols
[AD-A203792] p 7 N89-22174

SYNCHRONOUS SATELLITES

Estimation of surface insolation using sun-synchronous satellite data
p 52 A89-35939
A parameterization for longwave surface radiation from sun-synchronous satellite data
p 56 A89-41761

SYNOPTIC METEOROLOGY

A meteorological overview of the pre-AMEX and AMEX periods over the Australian region
p 48 A89-32850
Synoptic analysis and dynamical adjustment of GEOS 3 and Seasat altimeter eddy fields in the northwest Atlantic
p 29 A89-39650

Meteorological applications of Space Shuttle photography
p 34 A89-41430

SYNTHETIC APERTURE RADAR

Review and status of remote sensing of sea ice
p 20 A89-34266
Research on speckle behavior in SAR images
p 21 A89-35335

Performance analysis of the DFVLR real time SAR processor for low SNRs
p 21 A89-35336

Synthetic Aperture Radar data for mapping subsurface geological structures in the Northwest Territories, Canada
p 50 A89-35858

Petroleum exploration with airborne radar (SAR) and geologic field work, Sinu Basin of northwest Columbia
p 11 A89-35859

An inexpensive polarimetric FM radar and polarimetric signatures of artificial sea ice
p 57 A89-42684

Imaging of ocean waves by SAR
[AD-A203604] p 37 N89-21165

Theoretical studies for ERS-1 wave mode, volume 1
[GEC-MTR-87/110-VOL-1] p 41 N89-22977

Imaging radar applications in Europe. Illustrated experimental results (1978-1987)
[ESA-TM-01] p 42 N89-22978

Imaging procedure of underwater bottom topography by air and satellite images in the range of microwave and visible electromagnetic spectra
[GKSS-88/E/41] p 17 N89-24014

Necessity and benefit of the X-SAR space shuttle experiment
[DFVLR-MITT-88-29] p 63 N89-24688

SYSTEMS STABILITY

Radiometric performance of AVIRIS: Assessment for an arid region geologic target
p 39 N89-22157

T**TASKS**

A visiting scientist program in atmospheric sciences for the Goddard Space Flight Center
[NASA-CR-183421] p 47 N89-24756

TECHNOLOGY TRANSFER

Information resources management
p 42 N89-23371

TECHNOLOGY UTILIZATION

Successful applications of remotely sensed data for oil and gas exploration
p 22 A89-35854

Applications of AVHRR imagery in frontier exploration
p 23 A89-35885

TECTONICS

Remote-sensing studies of present-day tectonic processes --- Russian book
p 20 A89-34001

The potential use of remote sensing to solve problems of paleotectonic prediction, geologic structure, and exploitation of coal deposits with reference to the Moscow-Region coal basin
p 49 A89-34002

Use of aerial and space photography for the detection of faults and neotectonic movements in Crimea and the Azov Coastal Region
p 9 A89-34003

Structural stresses and the divisibility into blocks of the earth crust as observed on space imagery
p 10 A89-34009

The use of a lineament-analysis instrument for investigations of tectonic zonality and the elements of continental-margin geodynamics as applied to western Arctic
p 49 A89-34010

Identification of tectonic dislocations underneath large water areas using space images
p 15 A89-34011

New data on the morphostructure and geodynamics of the eastern margin of Eurasia
p 10 A89-34012

Automated analysis of lineaments from space imagery obtained during seismic studies of central Tien-Shan
p 20 A89-34014

Reconstruction of imagery of faulted landscapes using a photo-optical technique
p 24 A89-35900

Structural analysis of fracturing in Sinjar anticline using remote sensing technique
p 13 A89-41167

Satellite-borne lidar observations of the earth - Requirements and anticipated capabilities
p 56 A89-41692

Magnetometer array studies, earth structure, and tectonic processes
p 13 A89-42149

Neotectonics in Central Mexico from LANDSAT TM data
[NASA-CR-183416] p 14 N89-21416

Application of imaging spectrometer data to the Kings-Kaweah ophiolite melange
p 40 N89-22166

Structural patterns in high grade terrain in parts of Tamil Nadu and Karnataka
p 14 N89-22255

Kinematics at the intersection of the Garlock and Death Valley fault zones, California: Integration of TM data and field studies
[NASA-CR-184854] p 15 N89-22263

Plate motions and deformations from geologic and geodetic data
[NASA-CR-184987] p 15 N89-24757

TELEMETRY
Satellite signatures of rapid cyclogenesis
[AD-A203934] p 38 N89-21452

TELEVISION SYSTEMS
Coordinate referencing of a TV image in the case of the remote sensing of the earth
p 53 A89-37492

TEMPERATE REGIONS
AVHRR data processing to study the surface canopies in temperate regions - First results of HAPEX-MOBILHY
p 30 A89-40153

TEMPERATURE MEASUREMENT
Evaluating atmospheric correction models for retrieving surface temperatures from the AVHRR over a tallgrass prairie
p 20 A89-33875

A real-time global sea surface temperature analysis
p 16 A89-35907

Mean temperature in a closed basin by remote sensing
p 16 A89-39062

Validation problems for remotely sensed sea surface temperature
p 28 A89-39063

Land-surface temperature measurement from space - Physical principles and inverse modeling
p 29 A89-39552

TERRAIN
Active and passive remote sensing of ice
[AD-A203943] p 59 N89-20543

Column movement model used to support AMM
p 38 N89-21521

A software system to create a hierarchical, multiple level of detail terrain model
[AD-A203047] p 38 N89-21568

Structural patterns in high grade terrain in parts of Tamil Nadu and Karnataka
p 14 N89-22255

The Official Topographic-Cartographic Information System (ATKIS) of the Geodesy Group of the Laender of the Federal Republic of Germany: Status after one year of development
p 8 N89-23944

Tools for the computer assisted generalization of settlements for the construction of digital landscape models
p 43 N89-23952

TERRAIN ANALYSIS
Laser scattering phenomenology - Background signature characterization and prediction
p 6 A89-33661

Multispectral terrain background simulation techniques for use in airborne sensor evaluation
p 19 A89-33664

TAX - Prototype expert system for terrain analysis
p 20 A89-34363

Vegetation and landscape of Kora National Reserve, Kenya
p 6 A89-34945

Automated DTM validation and progressive sampling algorithm of finite element array relaxation
p 22 A89-35837

The application of high resolution digital elevation models to petroleum and mineral exploration and production
p 22 A89-35876

Atmospheric correction of satellite MSS data in rugged terrain
p 27 A89-38334

High altitude laser ranging over rugged terrain
p 54 A89-39092

A semi-automatic terrain measurement system for earthwork control
p 28 A89-39094

Geological uses of remotely-sensed reflected and emitted data of latitized Archaean terrain in Western Australia
p 55 A89-39652

Further investigations of sampling errors in mean terrain height estimation
p 32 A89-41076

Geological application of SIR-A imagery in southern Iraq
p 13 A89-41162

Computer strategy for detecting line features on simulated binary arrays in support of radar feature extraction
[AD-A203257] p 37 N89-21162

A software system to create a hierarchical, multiple level of detail terrain model
[AD-A203047] p 38 N89-21568

Remote sensing of earth terrain
[NASA-CR-184937] p 41 N89-22971

Image understanding research at SRI International
p 42 N89-23080

Overview of the SRI cartographic modeling environment
p 62 N89-23122

TERRESTRIAL RADIATION
Parameter optimization of systems for the thermal microwave mapping of the earth's surface
p 25 A89-37321

Airborne time-series measurement of soil moisture using terrestrial gamma radiation
p 33 A89-41163

TEXTURES
Computer-aided synthesis of textures simulating the earth's surface
p 25 A89-37325

Using textural measures to distinguish spectrally similar vegetation
p 3 A89-41155

THEMATIC MAPPERS (LANDSAT)
Calibration comparison for the Landsat 4 and 5 Multispectral Scanners and Thematic Mappers
p 47 A89-32835

Measuring thermal budgets of active volcanoes by satellite remote sensing
p 9 A89-32988

Surface reflectance factor retrieval from Thematic Mapper data
p 49 A89-33871

Implication of patterns of faulting and hydrothermal alteration from Landsat TM images and NHP aerial photos to mineral exploration and tectonics of the Virginia Range, Nevada --- National High Altitude Photography
p 11 A89-35868

- Lithologic mapping in East Greenland with Landsat Thematic Mapper imagery p 6 A89-35869
- A field spectrometer and remote sensing study of the Fresno mining district, Mexico p 51 A89-35871
- Application of Landsat Thematic Mapper digital data to the exploration for uranium-mineralized breccia pipes in Northwestern Arizona p 51 A89-35872
- Application of Landsat Thematic Mapper imagery for lithological mapping of poorly accessible semi-arid regions p 7 A89-35879
- Structural analysis of the Wichita Mountains using TM data for lineament mapping p 12 A89-35887
- A Landsat Thematic Mapper investigation of the geobotanical relationships in the northern spruce-fir forest, Mt. Moosilauke, New Hampshire p 2 A89-35894
- Discriminating late volcanic differentiates commonly associated with precious metal deposits, using Landsat Thematic Mapper imagery p 12 A89-35896
- Reflectance enhancements for the Thematic Mapper - An efficient way to produce images of consistently high quality p 26 A89-37947
- Discrimination of rocks and hydrothermal altered areas based on Landsat TM data p 27 A89-38333
- Fractal analysis of a classified Landsat scene p 28 A89-39099
- Geological uses of remotely-sensed reflected and emitted data of lateritized Archean terrain in Western Australia p 55 A89-39652
- Alteration detection using TM imagery - The effects of supergene weathering in an arid climate p 12 A89-39655
- Crop identification using merged Landsat multispectral scanner and Thematic Mapper data - Preliminary attempts p 3 A89-41153
- A global approach to knowledge-based surface material classification p 32 A89-41156
- Remote sensing of the deciduous vegetation of Great Smoky Mountains National Park p 33 A89-41170
- Application of Landsat Thematic Mapper data for coastal thermal plume analysis at Diablo Canyon p 35 A89-42175
- Utilizing remote sensing of thematic mapper data to improve our understanding of estuarine processes and their influence on the productivity of estuarine-dependent fisheries [NASA-CR-183417] p 18 A89-20533
- The suitability of remote sensing for surveying and monitoring landscape patterns. Volume A: Pilot study - LANDSAT Imagery. Volume B: PEPS Project No. 73 - SPOT Imagery [BCRS-87-12-VOL-A/B] p 4 A89-20534
- The suitability of remote sensing for surveying and monitoring landscape patterns. Volume A: Pilot study - LANDSAT imagery p 36 A89-20535
- Land use inventory using LANDSAT Thematic Mapper imagery to study environmental pollution [NLR-MP-87063-U] p 4 A89-20541
- Neotectonics in Central Mexico from LANDSAT TM data [NASA-CR-183416] p 14 A89-21416
- Data compression experiments with LANDSAT thematic mapper and Nimbus-7 coastal zone color scanner data p 41 A89-22344
- THEMATIC MAPPING**
- Geobotanical application of Airborne Thematic Mapper data in Sutherland, north-west Scotland p 2 A89-39657
- The suitability of remote sensing for surveying and monitoring landscape patterns. Volume A: Pilot study - LANDSAT Imagery. Volume B: PEPS Project No. 73 - SPOT Imagery [BCRS-87-12-VOL-A/B] p 4 A89-20534
- The suitability of remote sensing for surveying and monitoring landscape patterns. Volume A: Pilot study - LANDSAT imagery p 36 A89-20535
- The suitability of remote sensing for surveying and monitoring landscape patterns. Volume B: PEPS Project No. 73 - SPOT Imagery p 36 A89-20536
- Neotectonics in Central Mexico from LANDSAT TM data [NASA-CR-183416] p 14 A89-21416
- Proceedings of the Airborne Visible/Infrared Imaging Spectrometer (AVIRIS) Performance Evaluation Workshop [NASA-CR-184870] p 59 A89-22154
- Atmospheric water mapping with the Airborne Visible/Infrared Imaging Spectrometer (AVIRIS), Mountain Pass, California p 39 A89-22156
- Automated extraction of absorption features from Airborne Visible/Infrared Imaging Spectrometer (AVIRIS) and Geophysical and Environmental Research Imaging Spectrometer (GERIS) data p 39 A89-22160
- Preliminary analysis of Airborne Visible/Infrared Imaging Spectrometer (AVIRIS) for mineralogic mapping at sites in Nevada and Colorado p 60 A89-22161
- Application of imaging spectrometer data to the Kings-Kaweah ophiolite melange p 40 A89-22166
- An assessment of AVIRIS data for hydrothermal alteration mapping in the Goldfield Mining District, Nevada p 40 A89-22168
- Structural patterns in high grade terrain in parts of Tamil Nadu and Karnataka p 14 A89-22255
- Geocoded data sets of imaging satellites p 43 A89-23950
- Mapping freeze/thaw boundaries with SMMR data [NASA-CR-184991] p 9 A89-23961
- Geobotanical remote sensing for determination of aggregate source material [AD-A205943] p 45 A89-23962
- Meteosat thermal inertia mapping for studying wetland dynamics in the West-African Sahel [BCRS-88-10A] p 62 A89-23970
- Estimating population size of Pygoscelid Penguins from TM data [NASA-CR-180081] p 3 A89-24687
- THERMAL EMISSION**
- Effect of metal stress on the thermal infrared emission of soybeans: A greenhouse experiment - Possible utility in remote sensing p 2 A89-39658
- THERMAL MAPPING**
- Modeling surface temperature distributions in forest landscapes p 48 A89-33868
- Parameter optimization of systems for the thermal microwave mapping of the earth's surface p 25 A89-37321
- Infrared spectroscopy (2.3-20 microns) for the geological interpretation of remotely-sensed multispectral thermal infrared data p 30 A89-39656
- Derivation of a large-scale map of heat load in the region Freiburg-Basel (Germany, F.R.) using satellite data. A contribution to the production of bioclimate data based on a geographic information system [REPT-27] p 41 A89-22972
- Meteosat thermal inertia mapping for studying wetland dynamics in the West-African Sahel [BCRS-88-10A] p 62 A89-23970
- Thermal analysis for the monitoring and prediction of flood dynamics in wetlands [BCRS-108B] p 46 A89-23971
- THERMAL POLLUTION**
- Application of Landsat Thematic Mapper data for coastal thermal plume analysis at Diablo Canyon p 35 A89-42175
- Correlation between satellite-derived aerosol characteristics and oceanic dimethylsulfide (DMS) [AD-A206179] p 6 A89-24759
- THERMAL RADIATION**
- Modeling directional thermal radiance from a forest canopy p 27 A89-38972
- THERMOGRAPHY**
- Infrared thermography - A quantitative tool for heat study [ONERA, TP NO. 1989-3] p 53 A89-37627
- Thermal modeling of heat dissipation in the Pen Branch delta using thermal infrared imagery p 32 A89-41159
- THERMOLUMINESCENCE**
- Short- and long-term memory effects in intensified array detectors - Influence on airborne laser fluorosensor measurements p 47 A89-32836
- THERMOSPHERE**
- The response of thermospheric nitric oxide to an auroral storm p 42 A89-23031
- THREE DIMENSIONAL FLOW**
- The KP equation: A comparison to laboratory generated bi-periodic waves p 38 A89-21507
- TIMBER IDENTIFICATION**
- Remote sensing of the deciduous vegetation of Great Smoky Mountains National Park p 33 A89-41170
- TIMBER INVENTORY**
- Assessment of forest cover changes using multitemporal spaceborne imaging radar p 33 A89-41169
- Estimating stand density of loblolly pine in northern Louisiana using aerial photographs and probability proportional to size p 34 A89-41171
- TIMBER VIGOR**
- Cluster analysis of pine crown foliage patterns aid identification of mountain pine beetle current-attack p 26 A89-37950
- TIME SERIES ANALYSIS**
- Airborne time-series measurement of soil moisture using terrestrial gamma radiation p 33 A89-41163
- High resolution chronology of late Cretaceous-early Tertiary events determined from 21,000 yr orbital-climatic cycles in marine sediments p 14 A89-21328
- TIROS SATELLITES**
- Retrieval of mesoscale meteorological parameters for polar latitudes (MIZEX and ARCTEMIZ campaigns) p 58 A89-43026
- Refinements in the cloud detection scheme of the 3I system. Comparison with AVHRR products [ETN-89-94531] p 63 A89-24691
- TOPOGRAPHY**
- Topographic analysis of the Andean Highlands using the Large Format Camera p 7 A89-35880
- Atmospheric correction of satellite MSS data in rugged terrain p 27 A89-38334
- Low-relief topographic enhancement in a Landsat snow-cover scene p 54 A89-38966
- Tools for the computer assisted generalization of settlements for the construction of digital landscape models p 43 A89-23952
- Computer assisted generalization of transport line representations p 43 A89-23953
- TOXICITY**
- National Air Toxics Information Clearinghouse: Ongoing research and regulatory development projects, July 1988 [PB89-103428] p 65 A89-20558
- TRACKING (POSITION)**
- Use of commercial satellite imagery for surveillance of the Canadian north by the Canadian armed forces [AD-A202700] p 40 A89-22173
- Cooperative methods for road tracking in aerial imagery p 42 A89-23101
- TRAJECTORY OPTIMIZATION**
- Optimal satellite orbits and the network structure for regular earth surveying p 35 A89-42614
- TRANSMISSION LINES**
- ARGOS system used for balloon observations p 53 A89-38290
- TRANSPORTATION NETWORKS**
- Computer assisted generalization of transport line representations p 43 A89-23953
- TRIANGULATION**
- Analytical independent model triangulation strip adjustment using shore-line constraints p 28 A89-39093
- TROPICAL REGIONS**
- Geological applications of the Space Station core platform p 24 A89-35902
- AVHRR for monitoring global tropical deforestation p 56 A89-40152
- Properties of the equatorial and tropical ionosphere according to Soviet satellite observations during the IMS p 31 A89-40606
- Monitoring tropical environments with Space Shuttle photography p 34 A89-41432
- TROPICAL STORMS**
- Drop-size distributions associated with intense rainfall p 50 A89-34876
- Observational analyses of North Atlantic tropical cyclones from NOAA polar-orbiting satellite microwave data p 21 A89-34879
- TROPOSPHERE**
- A meteorological overview of the pre-AMEX and AMEX periods over the Australian region p 48 A89-32850
- Improving accuracy in radar-altimetry data correction for tropospheric effects p 54 A89-39322
- Observation model and parameter partials for the JPL geodetic GPS modeling software GPSOMC [NASA-CR-185021] p 9 A89-24060
- TROPOSPHERIC WAVES**
- Short-period fluctuation of the lower tropospheric winds observed by MU-radar p 58 A89-43311
- TUNISIA**
- Monitoring the halfa steppes of central Tunisia using Landsat MSS p 1 A89-34947
- Monitoring Tunisia's steppes with SPOT p 35 A89-43316
- U**
- U.S.S.R.**
- Concentric structures in southern Tien-Shan --- Russian book p 10 A89-34196
- UK SPACE PROGRAM**
- The activities of the British National Space Centre (BNSC) in the field of imaging spectrometry p 47 A89-24696
- UNDERWATER OPTICS**
- The dispersion limitations on the accuracy of the internal reference method during remote laser sounding of the upper ocean layer p 53 A89-37349
- Activities report of the Division of Optical Technology (FOA 33) [FOA-C-30507-3.1] p 62 A89-23287
- UNITED STATES**
- The commercial land remote sensing market - Current assessment, baseline forecast and baseline alternatives p 64 A89-35899
- Loran C field strength contours: Contiguous US [DOT/FAA/CT-TN89/16] p 8 A89-23437
- URBAN RESEARCH**
- A raster approach to population estimation using high-altitude aerial and space photographs p 19 A89-33872

USER REQUIREMENTS

Minimum number of satellites for periodic coverage
[FOA-C-30511-9.4] p 85 N89-22976

V

VECTORS (MATHEMATICS)

Data compression experiments with LANDSAT thematic mapper and Nimbus-7 coastal zone color scanner data
p 41 N89-22344

Vectorization of grid lines
[ETN-89-94150] p 45 N89-23967

VEGETATION

Accuracy assessment of a Landsat-assisted vegetation map of the coastal plain of the Arctic National Wildlife Refuge
p 6 A89-35840

Vegetation reflectance features in AVIRIS data
p 22 A89-35867

Using textural measures to distinguish spectrally similar vegetation
p 3 A89-41155

Determination of spectral signatures for remote laser sensing of vegetation
p 35 A89-42611

Assessment of AVIRIS data from vegetated sites in the Owens Valley, California
p 60 N89-22162

AVIRIS spectra of California wetlands
p 3 N89-22167

VEGETATION GROWTH

Use of aerial photography to inventory aquatic vegetation
p 50 A89-34362

A Landsat Thematic Mapper investigation of the geobotanical relationships in the northern spruce-fir forest, Mt. Moosilauke, New Hampshire
p 2 A89-35894

VEGETATIVE INDEX

Vegetation and landscape of Kora National Reserve, Kenya
p 6 A89-34945

Spectral indices for vegetation and rock type discrimination using the optical sensor of the Japanese ERS-1
p 51 A89-35866

Sensitivity of an atmospheric correction algorithm for non-Lambertian vegetation surfaces to atmospheric parameters
p 29 A89-39556

Estimation of regional surface resistance to evapotranspiration from NDVI and thermal-IR AVHRR data --- Normalized Difference Vegetation Index
p 55 A89-39872

A phenological description of Iberian vegetation using short wave vegetation index imagery
p 2 A89-40149

Monitoring the phenology of Tunisian grazing lands
p 3 A89-40150

The application of SPOT ratio data for soil classification
p 56 A89-41165

Examination of the spectral features of vegetation in 1987 AVIRIS data
p 3 N89-22163

Necessity and benefit of the X-SAR space shuttle experiment
[DFVLR-MITT-88-29] p 63 N89-24688

The FLI airborne imaging spectrometer: A highly versatile sensor for many applications
p 63 N89-24694

VELOCITY

Column movement model used to support AMM
p 38 N89-21521

VERTICAL MOTION

Determination of the character of present-day vertical movements from the structure of space imagery
p 10 A89-34016

VERY LONG BASE INTERFEROMETRY

Rate of change of the Quincy-Monument Peak baseline from a translocation analysis of Lageos laser range data
p 13 A89-42181

The baseline length changes of circum-Pacific VLBI networks and their bearing on global tectonics
p 13 A89-42795

VIDEO EQUIPMENT

Using multispectral video imagery for detecting soil surface conditions
p 22 A89-35838

VINEYARDS

The discrimination of irrigated orchard and vine crops using remotely sensed data
p 2 A89-37949

VISIBLE SPECTRUM

Munsell soil color and soil reflectance in the visible spectral bands of Landsat MSS and TM data
p 49 A89-33870

Sources of remote sensing data visible, near infrared, and short wave
p 51 A89-35878

Visible and near-infrared (0.4- to 2.5-microns) reflectance spectra of selected mixed-layer clays and related minerals
p 12 A89-35897

Seasonal visible, near-infrared and mid-infrared spectra of rice canopies in relation to LAI and above-ground dry phytomass
p 54 A89-38967

Sea surface spectrum from aerial photographs - Laboratory model studies
p 30 A89-39674

Assessment of AVIRIS data from vegetated sites in the Owens Valley, California
p 60 N89-22162

VISUAL OBSERVATION

Sea state determination by a remote optical sensor
p 53 A89-38330

VISUAL PERCEPTION

The precedence of global features in the perception of map symbols
[AD-A203792] p 7 N89-22174

VOLCANOES

Measuring thermal budgets of active volcanoes by satellite remote sensing
p 9 A89-32988

Volcano monitoring by short wavelength infrared satellite remote sensing
p 51 A89-35875

Discriminating late volcanic differentiates commonly associated with precious metal deposits, using Landsat Thematic Mapper imagery
p 12 A89-35896

Identification and analysis of the alignments of point-like features in remotely-sensed imagery. Volcanic cones in the Pinacate Volcanic Field, Mexico
p 12 A89-39651

Observations of volcanic ash clouds in the 10-12 micron window using AVHRR/2 data
p 30 A89-40143

VOLCANOLOGY

Neotectonics in Central Mexico from LANDSAT TM data
[NASA-CR-183416] p 14 N89-21416

VORTICES

Observing oceanic mesoscale eddies from Geosat altimetry - Preliminary results
p 16 A89-39372

W

WATER COLOR

Nimbus-7 data product summary
[NASA-RP-1215] p 39 N89-22152

Optical properties of oceanic suspended matter and their interpretation for remote sensing of phytoplankton
[GKSS-88/E/40] p 46 N89-24013

DFVLR activities related to imaging spectrometry
p 63 N89-24697

Biooptical variability in the Greenland Sea observed with the Multispectral Airborne Radiometer System (MARS)
[NASA-CR-184856] p 47 N89-24784

WATER MANAGEMENT

Use of a geographic information system (GIS) to improve planning for and control of the placement of dredged material
p 32 A89-41157

WATER POLLUTION

Airborne imaging radar system for monitoring sea pollution
[MBB-UK-0016-87-PUB] p 58 A89-42941

WATER QUALITY

New earth observing platforms to study global water, biology
p 17 A89-33121

Development and verification of Osaka Bay sampling model based on Landsat data
p 27 A89-38332

Using NOAA AVHRR imagery in assessing water quality parameters
p 55 A89-40148

WATER VAPOR

Satellite-derived low-level atmospheric water vapour content from synergy of AVHRR with HIRS --- High Resolution Infrared Radiation Sounder
p 30 A89-40139

WATER WAVES

Statistical geometry of a small surface patch in a developed sea
p 26 A89-37808

Imaging of ocean waves by SAR
[AD-A203604] p 37 N89-21165

The KP equation: A comparison to laboratory generated bi-periodic waves
p 38 N89-21507

Probabilities and statistics for backscatter estimates obtained by a scatterometer with applications to new scatterometer design data
[NASA-CR-4228] p 61 N89-22779

Theoretical studies for ERS-1 wave mode, volume 1
[GEC-MTR-87/110-VOL-1] p 41 N89-22977

WAVE INTERACTION

Interaction between net shortwave flux and sea surface temperature
p 15 A89-34878

WAVE PROPAGATION

The KP equation: A comparison to laboratory generated bi-periodic waves
p 38 N89-21507

WEATHER

Beaufort Sea mesoscale circulation study: Preliminary results
[PB89-121693] p 17 N89-20597

Use of the 1:2,000,000 Digital Line Graph data in emergency response
[DE89-006730] p 44 N89-23959

WEATHER FORECASTING

The prognosis of weather change lines over the ocean - The role of a reconnaissance aircraft
p 48 A89-32848

Sensitivity of 20-day dynamical forecasts to continental snow cover
p 17 A89-35937

WEATHERING

Alteration detection using TM imagery - The effects of superegene weathering in an arid climate
p 12 A89-39655

WETLANDS

The use of remote sensing and GIS techniques for wetland identification and classification in the Garrison Diversion Unit-North Dakota
p 18 A89-41160

Utilizing remote sensing of thematic mapper data to improve our understanding of estuarine processes and their influence on the productivity of estuarine-dependent fisheries
[NASA-CR-183417] p 18 N89-20533

AVIRIS spectra of California wetlands
p 3 N89-22167

Meteosat thermal inertia mapping for studying wetland dynamics in the West-African Sahel
[BCRS-88-10A] p 62 N89-23970

Thermal analysis for the monitoring and prediction of flood dynamics in wetlands
[BCRS-88-10B] p 46 N89-23971

WILDLIFE

Accuracy assessment of a Landsat-assisted vegetation map of the coastal plain of the Arctic National Wildlife Refuge
p 6 A89-35840

Review of wildlife resources of Vandenberg Air Force Base, California
[NASA-TM-102146] p 5 N89-23982

WIND DIRECTION

The prognosis of weather change lines over the ocean - The role of a reconnaissance aircraft
p 48 A89-32848

WIND MEASUREMENT

Seasat A satellite scatterometer measurements of equatorial surface winds
p 53 A89-37802

Short-period fluctuation of the lower tropospheric winds observed by MU-radar
p 58 A89-43311

WIND TUNNEL TESTS

Infrared thermography - A quantitative tool for heat study
[ONERA, TP NO. 1989-3] p 53 A89-37627

WIND VELOCITY MEASUREMENT

Probabilities and statistics for backscatter estimates obtained by a scatterometer with applications to new scatterometer design data
[NASA-CR-4228] p 61 N89-22779

WRANGELL MOUNTAINS (AK)

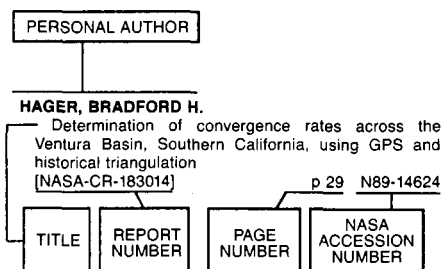
Remote sensing of global snowpack energy and mass balance: In-situ measurements on the snow of interior and Arctic Alaska
[NASA-CR-180078] p 62 N89-23956

Z

ZINC

Implementation of background and target geobotanical techniques in mineral exploration
p 23 A89-35892

Typical Personal Author Index Listing



Listings in this index are arranged alphabetically by personal author. The title of the document provides the user with a brief description of the subject matter. The report number helps to indicate the type of document listed (e.g., NASA report, translation, NASA contractor report). The page and accession numbers are located beneath and to the right of the title. Under any one author's name the accession numbers are arranged in sequence with the AIAA accession numbers appearing first.

A

- AAGAARD, A.**
Beaufort Sea mesoscale circulation study: Preliminary results
[PB89-121693] p 17 N89-20597
- ABDULLAH, QASSIM A.**
Geological application of SIR-A imagery in southern Iraq p 13 A89-41162
- ABRAHAMSON, CYNTHIA A.**
Use of a geographic information system (GIS) to improve planning for and control of the placement of dredged material p 32 A89-41157
- ABRAMS, MICHAEL**
Kinematics at the intersection of the Garlock and Death Valley fault zones, California: Integration of TM data and field studies
[NASA-CR-184854] p 15 N89-22263
- ABRAMS, MICHAEL J.**
An assessment of AVIRIS data for hydrothermal alteration mapping in the Goldfield Mining District, Nevada p 40 N89-22168
- ACKERMAN, STEVEN A.**
Using the radiative temperature difference at 3.7 and 11 microns to track dust outbreaks p 27 A89-38968
- AHERN, F. J.**
Reflectance enhancements for the Thematic Mapper - An efficient way to produce images of consistently high quality p 26 A89-37947
- AKIYAMA, TSUYOSHI**
Seasonal visible, near-infrared and mid-infrared spectra of rice canopies in relation to LAI and above-ground dry phytomass p 54 A89-38967
- AKSENOV, V. T.**
Automated analysis of lineaments from space imagery obtained during seismic studies of central Tien-Shan p 20 A89-34014
- AKVILONOVA, A. B.**
Methodological aspects of the automation of the calibration and processing of satellite microwave-radiometer data p 25 A89-37324
- ALANIZ, M. A.**
Using multispectral video imagery for detecting soil surface conditions p 22 A89-35838

- ALCAYDE, D.**
Activities of CNES in the field of imaging spectrometry p 47 N89-24699
- ALLEY, RONALD E.**
Atmospheric water mapping with the Airborne Visible/Infrared Imaging Spectrometer (AVIRIS), Mountain Pass, California p 39 N89-22156
- AMOS, B. J.**
Alteration detection using TM imagery - The effects of supergene weathering in an arid climate p 12 A89-39655
- AMSBURY, DAVID L.**
Geological applications of the Space Station core platform p 24 A89-35902
Expanding the utility of manned observations of earth - 70 mm film tests on the Space Shuttle p 34 A89-41428
- ANDERSON, ALLEN JOEL**
Arctic geodynamics - A satellite altimeter experiment for the European Space Agency Earth Remote-Sensing satellite p 29 A89-39546
- ANDERSON, R. L.**
Reconstruction of imagery of faulted landscapes using a photo-optical technique p 24 A89-35900
- ANDREEV, G. A.**
Computer-aided synthesis of textures simulating the earth's surface p 25 A89-37325
- APRESIAN, L. A.**
The dispersion limitations on the accuracy of the internal reference method during remote laser sounding of the upper ocean layer p 53 A89-37349
- ARAKI, T.**
The interplanetary magnetic field B(y)-dependent field-aligned current in the dayside polar cap under quiet conditions p 50 A89-34782
- ARGIALAS, DEMETRE P.**
Mapping of Landsat satellite and gravity lineaments in west Tennessee p 6 A89-34357
TAX - Prototype expert system for terrain analysis p 20 A89-34363
- ARNOLD, HANS-DIETER**
Definition and filling of information systems: Challenge for a photogrammetric service enterprise p 62 N89-23942
- ASRAR, G.**
Evaluating atmospheric correction models for retrieving surface temperatures from the AVHRR over a tallgrass prairie p 20 A89-33875
Measuring and modeling spectral characteristics of a tallgrass prairie p 27 A89-38970
- ATANGAN, JOSE F. H.**
Satellite signatures of rapid cyclogenesis
[AD-A203934] p 38 N89-21452
- ATKINSON, ROBERT J.**
Improved capabilities of the Multispectral Atmospheric Mapping Sensor (MAMS)
[NASA-TM-100352] p 58 N89-20430
- AVAKIAN, SERGEI V.**
Studying the earth from manned spacecraft p 64 A89-42511
- AVENARIUS, I. G.**
Identification of tectonic dislocations underneath large water areas using space images p 15 A89-34011
- AYBU, P. A.**
Assessing the improvement in soil mapping using spot HRV over Landsat MSS imagery (Geography and land use) p 33 A89-41168

B

- BAILEY, G. B.**
AVIRIS data characteristics and their effects on spectral discrimination of rocks exposed in the Drum Mountains, Utah: Results of a preliminary study p 40 N89-22165
- BAKER, KEN**
Automated DTM validation and progressive sampling algorithm of finite element array relaxation p 22 A89-35837

- BAKLANOV, A. D.**
A technique for applying space photographs to search for anticlinal oil- and gas-traps in orogenic structures of the Tien-Shan p 25 A89-37318
- BALAGEAS, D.**
Infrared thermography - A quantitative tool for heat study
[ONERA, TP NO. 1989-3] p 53 A89-37627
- BALICK, L. K.**
Modeling directional thermal radiance from a forest canopy p 27 A89-38972
- BALSIGER, H.**
GEOS 1 observations of low-energy ions in the earth's plasmasphere - A study on composition, and temperature and density structure under quiet geomagnetic conditions p 9 A89-33829
- BANNINGER, C.**
Analysis of Airborne Imaging Spectrometer (AIS) data for geobotanical prospecting p 51 A89-35890
- BARTHEL, K.**
NOAA (National Oceanic and Atmospheric Administration) AVHRR (Advanced Very High Resolution Radiometer) observations during the marginal ice zone experiment, between Spitzbergen and Greenland, June 7 to 18 July 1984
[AD-A204911] p 19 N89-22280
- BARTHOLOMEW, MARY JANE**
Infrared spectroscopy (2.3-20 microns) for the geological interpretation of remotely-sensed multispectral thermal infrared data p 30 A89-39656
- BARTINGTON, G. W.**
Use of seabottom magnetic susceptibility measurements in hydrocarbon exploration p 16 A89-35864
- BARTON, I. J.**
Theoretical algorithms for satellite-derived sea surface temperatures p 21 A89-35159
- BARTON, R. H.**
Use of seabottom magnetic susceptibility measurements in hydrocarbon exploration p 16 A89-35864
- BARYKIN, A. S.**
Radiometric correction of aerial and space remote-sensing images p 25 A89-37323
- BASILI, P.**
Improving accuracy in radar-altimetry data correction for tropospheric effects p 54 A89-39322
- BASU, SUNANDA**
Satellite, airborne and radar observations of auroral arcs p 48 A89-33505
- BATES, JOHN**
Interaction between net shortwave flux and sea surface temperature p 15 A89-34878
- BATSON, K. BRYAN**
Improved capabilities of the Multispectral Atmospheric Mapping Sensor (MAMS)
[NASA-TM-100352] p 58 N89-20430
- BAUER, EVA**
Development of a satellite SAR image spectra and altimeter wave height data assimilation system for ERS-1
[NASA-CR-182685] p 61 N89-22975
- BAUMANN, ROBERT H.**
Utilizing remote sensing of thematic mapper data to improve our understanding of estuarine processes and their influence on the productivity of estuarine-dependent fisheries
[NASA-CR-183417] p 18 N89-20533
- BEASON, S. C.**
Geological gyrocompass
[PB89-133086] p 63 N89-24589
- BEHR, F. J.**
Design of spectral and panchromatic bands for the German MOMS-02 sensor p 57 A89-42173
Research for optimization of future MOMS sensors
[ETN-89-94424] p 62 N89-23972
- BELOUSOV, V. V.**
Concentric structures in southern Tien-Shan p 10 A89-34196
- BENDER, P. L.**
Rate of change of the Quincy-Monument Peak baseline from a translocation analysis of Lageos laser range data p 13 A89-42181

- BENSON, CARL S.**
Remote sensing of global snowpack energy and mass balance: In-situ measurements on the snow of interior and Arctic Alaska
[NASA-CR-180078] p 62 N89-23956
- BERGER, Z.**
The contribution of remote sensing data to exploration of fractured reservoirs p 50 A89-35862
- BERNARD, R.**
C-band radar cross section of the Guyana rain forest - Possible use as a reference target for spaceborne radars p 49 A89-33869
- BERNHARDT, P. A.**
Spacelab 2 Upper Atmospheric Modification Experiment over Arecibo. II - Plasma dynamics p 4 A89-38897
- BERRY, JOHN L.**
Hydrocarbon potential of part of the margin of the Tarim Basin from Landsat - A case history p 11 A89-35857
- BERTRAND, J. J.**
The potential of infrared satellite data for the retrieval of Saharan-dust optical depth over Africa p 30 A89-39875
- BESCOND, P.**
Commercialization of remote sensing in the U.S.A. - The SPOT perspective p 64 A89-34704
- BIEHL, L. L.**
A new technique to measure the spectral properties of conifer needles p 19 A89-33874
- BINNENKADE, P.**
Phase A study for the extension of the CAESAR scanner with a sensor module for the far infrared [BCRS-88-09] p 59 N89-20539
- BINNEY, DARYL L.**
Accuracy assessment of a Landsat-assisted vegetation map of the coastal plain of the Arctic National Wildlife Refuge p 6 A89-35840
- BIRNIE, RICHARD**
A field spectrometer and remote sensing study of the Fresno mining district, Mexico p 51 A89-35871
- BIRNIE, RICHARD W.**
Lithologic mapping in East Greenland with Landsat Thematic Mapper imagery p 6 A89-35869
A Landsat Thematic Mapper investigation of the geobotanical relationships in the northern spruce-fir forest, Mt. Moosilauke, New Hampshire p 2 A89-35894
- BLAIS, J. A. R.**
High altitude laser ranging over rugged terrain p 54 A89-39092
- BLANC, THEODORE V.**
The Naval Research Laboratory's Air-Sea Interaction Blimp Experiment p 53 A89-37981
- BLOCK, LARS P.**
Satellite, airborne and radar observations of auroral arcs p 48 A89-33505
- BOCHAROV, G. V.**
The use of space imagery for investigations of recent crustal deformations in southern Yakutia p 20 A89-34015
- BODECHTEL, J.**
Design of spectral and panchromatic bands for the German MOMS-02 sensor p 57 A89-42173
- BOESSWETTER, C.**
Airborne imaging radar system for monitoring sea pollution [MBB-UK-0016-87-PUB] p 58 A89-42941
- BOGOSLOVSKII, V. A.**
The potential use of remote sensing to solve problems of paleotectonic prediction, geologic structure, and exploitation of coal deposits with reference to the Moscow-Region coal basin p 49 A89-34002
- BOKHOVEN, H.**
Phase A study for the extension of the CAESAR scanner with a sensor module for the far infrared [BCRS-88-09] p 59 N89-20539
- BOLLES, ROBERT C.**
Image understanding research at SRI International p 42 N89-23080
- BORDER, J. S.**
Observation model and parameter partials for the JPL geodetic GPS modeling software GPSOMC [NASA-CR-185021] p 9 N89-24060
- BORISENKO, L. S.**
Use of aerial and space photography for the detection of faults and neotectonic movements in Crimea and the Azov Coastal Region p 9 A89-34003
- BORISIUK, A. P.**
The definition of isometric magmatogenic structures on space imagery p 12 A89-37315
- BORISIUK, M. V.**
The definition of isometric magmatogenic structures on space imagery p 12 A89-37315
- BORISOV, O. M.**
Determination of the character of present-day vertical movements from the structure of space imagery p 10 A89-34016
- BOSCHER, D.**
Infrared thermography - A quantitative tool for heat study [ONERA, TP NO. 1989-3] p 53 A89-37627
- BOUR, WILLIAM**
Ground verification method for bathymetric satellite image maps of unsurveyed coral reefs p 6 A89-34949
- BOWERS, TERRY L.**
Air pollution effects field research facility: Ozone flow control and monitoring system [DE89-007922] p 5 N89-22192
- BRADY, ROLAND H., III**
Kinematics at the intersection of the Garlock and Death Valley fault zones, California: Integration of TM data and field studies [NASA-CR-184854] p 15 N89-22263
- BREDOW, J. W.**
An inexpensive polarimetric FM radar and polarimetric signatures of artificial sea ice p 57 A89-42684
- BREININGER, DAVID R.**
Review of wildlife resources of Vandenberg Air Force Base, California [NASA-TM-102146] p 5 N89-23982
- BREST, CHRISTOPHER L.**
Global, seasonal surface variations from satellite radiance measurements p 52 A89-35966
- BRIGGS, S. A.**
The activities of the British National Space Centre (BNSC) in the field of imaging spectrometry p 47 N89-24696
- BRISTOW, MICHAEL P.**
Short- and long-term memory effects in intensified array detectors - Influence on airborne laser fluorosensor measurements p 47 A89-32836
- BRONNER, WILLIAM G.**
Sources of remote sensing data visible, near infrared, and short wave p 51 A89-35878
- BROWDER, JOAN A.**
Utilizing remote sensing of thematic mapper data to improve our understanding of estuarine processes and their influence on the productivity of estuarine-dependent fisheries [NASA-CR-183417] p 18 N89-20533
- BROWN, BECKY J.**
Concept for a satellite-based global reserve monitoring system p 32 A89-41152
- BROWN, CHARLES L.**
Use of aerial photography to inventory aquatic vegetation p 50 A89-34362
- BRUCE, B.**
Implementation of background and target geobotanical techniques in mineral exploration p 23 A89-35892
- BRUCE, BILL**
Assessing aggregate resource potential in the Canadian Shield - A knowledge-based approach p 23 A89-35877
- BRUEGGE, CAROL J.**
Atmospheric water mapping with the Airborne Visible/Infrared Imaging Spectrometer (AVIRIS), Mountain Pass, California p 39 N89-22156
- BRUENING, CLAUS**
Development of a satellite SAR image spectra and altimeter wave height data assimilation system for ERS-1 [NASA-CR-182685] p 61 N89-22975
- BRUZEWICZ, ANDREW J.**
Use of a geographic information system (GIS) to improve planning for and control of the placement of dredged material p 32 A89-41157
- BUCHANAN, SUSAN KAY M.**
National Air Toxics Information Clearinghouse: Ongoing research and regulatory development projects, July 1988 [PB89-103428] p 65 N89-20558
- BUFTON, JACK L.**
Laser altimetry measurements from aircraft and spacecraft p 56 A89-41691
- BUKIN, IU. K.**
The KAP-350 and KAP-100 space cameras for the remote sensing of earth resources p 50 A89-35687
- BULANZHE, IU. D.**
Gravimetric studies at sea p 49 A89-34088
- BUNDY, DONALD H.**
Short- and long-term memory effects in intensified array detectors - Influence on airborne laser fluorosensor measurements p 47 A89-32836
- BUNKIN, A. F.**
Remote four-photon Raman spectroscopy of sea water under natural conditions p 52 A89-37327
- BUXTON, R. A. H.**
The FLI airborne imaging spectrometer: A highly versatile sensor for many applications p 63 N89-24694
- CAIN, JOSEPH C.**
Modelling the earth's geomagnetic field to high degree and order p 58 A89-43408
Derivation of a geomagnetic model to $n = 63$ p 58 A89-43409
The geomagnetic spectrum for 1980 and core-crustal separation p 13 A89-43410
- CALVIN, WENDY M.**
Automated extraction of absorption features from Airborne Visible/Infrared Imaging Spectrometer (AVIRIS) and Geophysical and Environmental Research Imaging Spectrometer (GERIS) data p 39 N89-22160
- CARLOTTO, MARK J.**
A global approach to knowledge-based surface material classification p 32 A89-41156
- CARLSON, HERBERT C., JR.**
Satellite, airborne and radar observations of auroral arcs p 48 A89-33505
- CARLSON, MARVIN P.**
The Nebraska center-pivot inventory - An example of operational satellite remote sensing on a long term basis p 28 A89-39096
- CARRERE, VERONIQUE**
Atmospheric water mapping with the Airborne Visible/Infrared Imaging Spectrometer (AVIRIS), Mountain Pass, California p 39 N89-22156
An assessment of AVIRIS data for hydrothermal alteration mapping in the Goldfield Mining District, Nevada p 40 N89-22168
- CARROLL, THOMAS R.**
Airborne time-series measurement of soil moisture using terrestrial gamma radiation p 33 A89-41163
- CARSEY, FRANK**
Review and status of remote sensing of sea ice p 20 A89-34266
- CARTER, JOHN S.**
Successful applications of remotely sensed data for oil and gas exploration p 22 A89-35854
Use of remotely sensed data in mature basin exploration - Considerations on creating useful imagery p 50 A89-35861
- CASTANO, DIEGO J.**
Aerosol analysis with the Coastal Zone Color Scanner - A simple method for including multiple scattering effects p 25 A89-37291
- CERUTTI-MAORI, G.**
The advanced Ocean Chlorophyll Meter (OCM). A spectral imaging device for the observation of the oceans [REPT-882-440-118] p 63 N89-24689
- CHAPMAN, M. A.**
High altitude laser ranging over rugged terrain p 54 A89-39092
- CHAVEZ, PAT S., JR.**
Application of Landsat Thematic Mapper digital data to the exploration for uranium-mineralized breccia pipes in Northwestern Arizona p 51 A89-35872
- CHEBANENKO, I. I.**
Use of aerial and space photography for the detection of faults and neotectonic movements in Crimea and the Azov Coastal Region p 9 A89-34003
- CHEDIN, A.**
Retrieval of mesoscale meteorological parameters for polar latitudes (MIZEX and ARCTEMIZ campaigns) p 58 A89-43026
On the future development and management of spectroscopic database for radiative transfer from the issues of recent related workshops [ETN-89-94530] p 46 N89-24690
- CHEKAN, ROBERT**
Use of commercial satellite imagery for surveillance of the Canadian north by the Canadian armed forces [AD-A202700] p 40 N89-22173
- CHEN, WENYI**
An algorithm for machine-recognizing the river mouth and measuring the sealine from the Landsat image p 19 A89-33658
- CHENEY, ROBERT E.**
Evaluation of Geosat altimeter data with application to tropical Pacific sea level variability p 25 A89-37801
- CHI, KWANG HOON**
Discrimination of rocks and hydrothermal altered areas based on Landsat TM data p 27 A89-38333
- CHOW, C. K.**
Further investigations of sampling errors in mean terrain height estimation p 32 A89-41076
- CHRIEN, THOMAS G.**
AVIRIS performance during the 1987 flight season: An AVIRIS project assessment and summary of the NASA-sponsored performance evaluation p 60 N89-22155
- CHRISSOULIDIS, D. P.**
EM wave scattering from statistically inhomogeneous and periodic random rough surfaces p 36 A89-43541

- CHRIST, FRED**
Computer aided production of a 1:25,000 relief model of Berlin and surroundings p 8 N89-23943
- CHURCHILL, P. N.**
Imaging radar applications in Europe. Illustrated experimental results (1978-1987) [ESA-TM-01] p 42 N89-22978
- CIERNIEWSKI, JERZY**
The influence of the viewing geometry of bare rough soil surfaces on their spectral response in the visible and near-infrared range p 2 A89-38969
- CIOTTI, P.**
Improving accuracy in radar-altimetry data correction for tropospheric effects p 54 A89-39322
- CLARK, RICHARD C.**
The use of remote sensing and GIS techniques for wetland identification and classification in the Garrison Division Unit-North Dakota p 18 A89-41160
- CLARK, ROGER N.**
Calibration and evaluation of AVIRIS data: Cripple Creek in October 1987 p 39 N89-22159
- CLAUD, C.**
Retrieval of mesoscale meteorological parameters for polar latitudes (MIZEX and ARCTEMIZ campaigns) p 58 A89-43026
- CLAUD, CHANTAL**
Refinements in the cloud detection scheme of the 3I system. Comparison with AVHRR products [ETN-89-94531] p 63 N89-24691
- COFFEY, HELEN E.**
Solar-geophysical data number 529, September 1988. Part 1: (Prompt reports). Data for August, July 1988 and late data [PB89-121305] p 37 N89-21431
- COLBECK, SAMUEL C.**
Snowmelt increase through albedo reduction [AD-A204523] p 18 N89-22175
- COLLINS, AMY HUTSINPILLER**
Implication of patterns of faulting and hydrothermal alteration from Landsat TM images and NHAP aerial photos to mineral exploration and tectonics of the Virginia Range, Nevada p 11 A89-35868
- COMBES-DESPA, M.**
Activities of CNES in the field of imaging spectrometry p 47 N89-24699
- CONANT, JOHN**
Multispectral terrain background simulation techniques for use in airborne sensor evaluation p 19 A89-33664
- CONEL, JAMES E.**
Atmospheric water mapping with the Airborne Visible/Infrared Imaging Spectrometer (AVIRIS), Mountain Pass, California p 39 N89-22156
Determination of in-flight AVIRIS spectral, radiometric, spatial and signal-to-noise characteristics using atmospheric and surface measurements from the vicinity of the rare-earth-bearing carbonatite at Mountain Pass, California p 61 N89-22170
- CONTZEN, J. P.**
The experience of the Commission of the European Communities in the use of remote sensing for the implementation of community policies p 64 A89-34712
- COOK, ALLEN E.**
The Nebraska center-pivot inventory - An example of operational satellite remote sensing on a long term basis p 28 A89-39096
- COOPER, D. I.**
Evaluating atmospheric correction models for retrieving surface temperatures from the AVHRR over a tallgrass prairie p 20 A89-33875
- CORDEY, R. A.**
Theoretical studies for ERS-1 wave mode, volume 1 [GEC-MTR-87/110-VOL-1] p 41 N89-22977
- COULSON, KINSELL L.**
Earth scenes in polarized light observed from the Space Shuttle p 34 A89-41429
- COURAULT, DOMINIQUE**
Munsell soil color and soil reflectance in the visible spectral bands of Landsat MSS and TM data p 49 A89-33870
- COURTILLOT, VINCENT**
Seasat altimetry and the South Atlantic geoid. II - Short-wavelength undulations p 16 A89-39659
- COX, JULIE A.**
Monitoring in Moneragala district, Sri Lanka, with SPOT images p 3 A89-43317
- CRACKNELL, A. P.**
Geobotanical application of Airborne Thematic Mapper data in Sutherland, north-west Scotland p 2 A89-39657
Pixel and sub-pixel accuracy in geometrical correction of AVHRR p 30 A89-40134
- CRAWFORD, WILLIAM R.**
A performance comparison for two Lagrangian drifter designs p 34 A89-41750
- CROOM, D. L.**
Applications of AVHRR data; Proceedings of the Third European AVHRR Data Users' Meeting, University of Oxford, England, Dec. 16-18, 1987 p 55 A89-40126
- CROSS, A. M.**
Identification and analysis of the alignments of point-like features in remotely-sensed imagery. Volcanic cones in the Pinacate Volcanic Field, Mexico p 12 A89-39651
- CROWLEY, J. K.**
Visible and near-infrared (0.4- to 2.5-microns) reflectance spectra of selected mixed-layer clays and related minerals p 12 A89-35897
- CROWLEY, JAMES**
Evaluation of Airborne Visible/Infrared Imaging Spectrometer Data of the Mountain Pass, California carbonatite complex p 60 N89-22169
- CURRAN, PAUL J.**
Zones of information in the AVIRIS spectra p 39 N89-22158
- CURRAN, ROBERT J.**
Satellite-borne lidar observations of the earth - Requirements and anticipated capabilities p 56 A89-41692
- CUSHMAN, ROBERT M.**
Preliminary development of a seashore-effects analysis system [DE89-007863] p 61 N89-22191
- CUTTEN, D. R.**
Theoretical algorithms for satellite-derived sea surface temperatures p 21 A89-35159

D

- D'AURIA, G.**
Improving accuracy in radar-altimetry data correction for tropospheric effects p 54 A89-39322
- DAHMER, PAUL A.**
Estimating population size of Pygoscelid Penguins from TM data [NASA-CR-180081] p 3 N89-24687
- DALU, G.**
Validation problems for remotely sensed sea surface temperature p 28 A89-39063
- DANIELSEN, C.**
Distribution of auroral arcs during quiet geomagnetic conditions p 50 A89-34772
- DARNELL, WAYNE L.**
Estimation of surface insolation using sun-synchronous satellite data p 52 A89-35939
- DAUGHTRY, C. S. T.**
A new technique to measure the spectral properties of conifer needles p 19 A89-33874
- DAVIS, BRUCE A.**
Variation of surface water spectral response as a function of in situ sampling technique p 33 A89-41161
- DAVIS, DON**
Automated DTM validation and progressive sampling algorithm of finite element array relaxation p 22 A89-35837
- DAVIS, M. H.**
A visiting scientist program in atmospheric sciences for the Goddard Space Flight Center [NASA-CR-183421] p 47 N89-24756
- DAVIS, M. R.**
Using multispectral video imagery for detecting soil surface conditions p 22 A89-35838
- DE COLA, LEE**
Fractal analysis of a classified Landsat scene p 28 A89-39099
- DE MEY, PIERRE**
Synoptic analysis and dynamical adjustment of GEOS 3 and Seasat altimeter eddy fields in the northwest Atlantic p 29 A89-39650
- DEDIEU, G.**
NOAA AVHRR and its uses for rainfall and evapotranspiration monitoring p 56 A89-40151
- DEEPAK, ADARSH**
The investigation of advanced remote sensing, radiative transfer and inversion techniques for the measurement of atmospheric constituents [NASA-CR-172599] p 36 N89-20531
- DEFEO, N. J.**
Assessment of AVIRIS data from vegetated sites in the Owens Valley, California p 60 N89-22162
- DEKKER, LARRY L.**
Petroleum exploration with airborne radar (SAR) and geologic field work, Sinu Basin of northwest Columbia p 11 A89-35859
- DEMPSEY, D. A.**
MEIS II and surface data integration for detection of geobotanical anomalies p 51 A89-35891
- DENLINGER, JERRY L.**
Cooperative methods for road tracking in aerial imagery p 42 N89-23101
- DENN, FRED M.**
Estimation of surface insolation using sun-synchronous satellite data p 52 A89-35939
- DEOM, A.**
Infrared thermography - A quantitative tool for heat study [ONERA, TP NO. 1989-3] p 53 A89-37627
- DESBOIS, M.**
The potential of infrared satellite data for the retrieval of Saharan-dust optical depth over Africa p 30 A89-39875
- DESBOIS, MICHEL**
Satellite detection of Saharan dust - Optimized imaging during nighttime p 24 A89-35912
- DHONDT, STEVEN**
High resolution chronology of late Cretaceous-early Tertiary events determined from 21,000 yr orbital-climatic cycles in marine sediments p 14 N89-21328
- DICKS, STEVEN E.**
Comparison of satellite, ground-based, and modeling techniques for analyzing the urban heat island p 26 A89-37948
- DIXON, T. H.**
Operational aspects of CASA UNO '88-The first large scale international GPS geodetic network p 7 A89-42787
- DOBSON, M. C.**
Mapping freeze/thaw boundaries with SMMR data [NASA-CR-184991] p 9 N89-23961
- DOUGLAS, BRUCE C.**
Evaluation of Geosat altimeter data with application to tropical Pacific sea level variability p 25 A89-37801
- DOUILLET, PASCAL**
Ground verification method for bathymetric satellite image maps of unsurveyed coral reefs p 6 A89-34949
- DOWGIALLO, MICHAEL J.**
Ice cover on Chesapeake Bay from AVHRR (Advanced Very High Resolution Radiometer) and LANDSAT imagery, winter of 1987-88 [PB89-117261] p 59 N89-21415
- DOYLE, M. J.**
Application of Landsat Thematic Mapper data for coastal thermal plume analysis at Diablo Canyon p 35 A89-42175
- DOZIER, J.**
HIRIS: NASA's high-resolution imaging spectrometer for the Earth Observing System (EOS) p 63 N89-24695
- DOZIER, JEFF**
Land-surface temperature measurement from space - Physical principles and inverse modeling p 29 A89-39552
- DRAKE, N. J.**
The activities of the British National Space Centre (BNSC) in the field of imaging spectrometry p 47 N89-24696
- DRURY, STEPHEN A.**
Geological uses of remotely-sensed reflected and emitted data of lateritized Archaean terrain in Western Australia p 55 A89-39652
- DUGDALE, G.**
Relating point to area average rainfall in semiarid West Africa and the implications for rainfall estimates derived from satellite data p 55 A89-39870
- DUNGAN, JENNIFER L.**
Zones of information in the AVIRIS spectra p 39 N89-22158
- DURACZ, T.**
Radiative transfer calculations for characterizing obscured surfaces using time-dependent backscattered pulses p 48 A89-32841
- DURDEN, STEPHEN L.**
Modeling and observation of the radar polarization signature of forested areas p 2 A89-39554
- DWYER, J. L.**
AVIRIS data characteristics and their effects on spectral discrimination of rocks exposed in the Drum Mountains, Utah: Results of a preliminary study p 40 N89-22165
- DZIUBA, RONALD F.**
1988 Conference on Precision Electromagnetic Measurements, Tsukuba, Japan, June 7-10, 1988, Proceedings p 57 A89-42773

E

- EAGLE, THOMAS C.**
Uses of the SAS statistical package for digital image analysis p 23 A89-35898
- EANES, R. J.**
Rate of change of the Quincy-Monument Peak baseline from a translocation analysis of Lageos laser range data p 13 A89-42181
- EDMONDS, CURTIS M.**
Short- and long-term memory effects in intensified array detectors - Influence on airborne laser fluorosensor measurements p 47 A89-32836

EDWARDS, NELSON

Air pollution effects field research facility: Ozone flow control and monitoring system
[DE89-007922] p 5 N89-22192

EKBLAD, ULF

Minimum number of satellites for periodic coverage
[FOA-C-30511-9.4] p 65 N89-22976

EL-KASSAS, I. A.

Conjugate synthetic normal faults around the Gulf of Salwa, southwestern Qatar, the Arabian Gulf
p 12 A89-35886

ELGHAZALI, MOHAMED SHAWKI

Analytical independent model triangulation strip adjustment using shore-line constraints
p 28 A89-39093

ELIASON, ERIC M.

Radiometric performance of AVIRIS: Assessment for an arid region geologic target
p 39 N89-22157

ELLIS, JAMES M.

Petroleum exploration with airborne radar (SAR) and geologic field work, Sinu Basin of northwest Columbia
p 11 A89-35859

ELVIDGE, CHRISTOPHER D.

Vegetation reflectance features in AVIRIS data
p 22 A89-35867
Assessment of AVIRIS data from vegetated sites in the Owens Valley, California
p 60 N89-22162
Examination of the spectral features of vegetation in 1987 AVIRIS data
p 3 N89-22163

ENGLAND, A. W.

Mapping freeze/thaw boundaries with SMMR data
[NASA-CR-184991] p 9 N89-23961

EPPLER, DUANE T.

KRMS (K-band Radiometric Mapping System) SSM/I validation March 1988 quick look report
[NASA-CR-185320] p 8 N89-23766

EREMIN, V. K.

The KAP-350 and KAP-100 space cameras for the remote sensing of earth resources
p 50 A89-35687

ESCADAFAL, RICHARD

Munsell soil color and soil reflectance in the visible spectral bands of Landsat MSS and TM data
p 49 A89-33870

ESCOBAR, D. E.

Using multispectral video imagery for detecting soil surface conditions
p 22 A89-35838

ESTES, JOHN E.

Knowledge-based image data management - An expert front-end for the BROWSE facility
p 32 A89-41158
Remote sensing information sciences research group: Browse in the EOS era
[NASA-CR-184637] p 42 N89-22979

EVERITT, J. H.

Using multispectral video imagery for detecting soil surface conditions
p 22 A89-35838

EYTON, J. RONALD

Low-relief topographic enhancement in a Landsat snow-cover scene
p 54 A89-38966

F

FALCONER, A.

Reconstruction of imagery of faulted landscapes using a photo-optical technique
p 24 A89-35900

FARJON, J. M. J.

The suitability of remote sensing for surveying and monitoring landscape patterns. Volume A: Pilot study - LANDSAT Imagery. Volume B: PEPS Project No. 73 - SPOT Imagery
[BCRS-87-12-VOL-A/B] p 4 N89-20534

The suitability of remote sensing for surveying and monitoring landscape patterns. Volume A: Pilot study - LANDSAT imagery
p 36 N89-20535
The suitability of remote sensing for surveying and monitoring landscape patterns. Volume B: PEPS Project No. 73 - SPOT Imagery
p 36 N89-20536

FARMER, DAVID M.

Precipitation in the Canadian Atlantic Storms Program - Measurements of the acoustic signature
p 50 A89-35819

FARMER, L. DENNIS

KRMS (K-band Radiometric Mapping System) SSM/I validation March 1988 quick look report
[NASA-CR-185320] p 8 N89-23766

FARRUGIA, C. J.

GEOS 1 observations of low-energy ions in the earth's plasmasphere - A study on composition, and temperature and density structure under quiet geomagnetic conditions
p 9 A89-33829

FEA, M.

Imaging radar applications in Europe. Illustrated experimental results (1978-1987)
[ESA-TM-01] p 42 N89-22978

FELDMAN, GENE CARL

Nimbus-7 data product summary
[NASA-RP-1215] p 39 N89-22152

FELIX, NANCY A.

Accuracy assessment of a Landsat-assisted vegetation map of the coastal plain of the Arctic National Wildlife Refuge
p 6 A89-35840

FINKEL'SHTEIN, M. I.

Sounding of crop fields by nanosecond radio pulses
p 1 A89-35584

FISCHLER, MARTIN A.

Image understanding research at SRI International
p 42 N89-23080

FISLIER, J. L.

Meteosat thermal inertia mapping for studying wetland dynamics in the West-African Sahel
[BCRS-88-10A] p 62 N89-23970
Thermal analysis for the monitoring and prediction of flood dynamics in wetlands
[BCRS-88-10B] p 46 N89-23971

FLEIG, ALBERT J.

Nimbus-7 data product summary
[NASA-RP-1215] p 39 N89-22152

FLESCH, T. K.

Large-area crop monitoring with the NOAA AVHRR - Estimating the silking stage of corn development
p 1 A89-33873

FLINN, R. DAVID

A global approach to knowledge-based surface material classification
p 32 A89-41156

FLITCROFT, I. D.

Relating point to area average rainfall in semiarid West Africa and the implications for rainfall estimates derived from satellite data
p 55 A89-39870

FORREST, M. D.

Integration of Landsat TM, stream sediment geochemistry and regional geophysics for mineral exploration in the English Lake District
p 23 A89-35888

FOUQUART, Y.

The potential of infrared satellite data for the retrieval of Saharan-dust optical depth over Africa
p 30 A89-39875

FOURNIER, J.

Infrared thermography - A quantitative tool for heat study
[ONERA, TP NO. 1989-3] p 53 A89-37627

FOY, C. D.

Effect of metal stress on the thermal infrared emission of soybeans: A greenhouse experiment - Possible utility in remote sensing
p 2 A89-39658

FRANCIS, P. W.

Measuring thermal budgets of active volcanoes by satellite remote sensing
p 9 A89-32988
Volcano monitoring by short wavelength infrared satellite remote sensing
p 51 A89-35875

FRANK, T. D.

Assessing the improvement in soil mapping using spot HRV over Landsat MSS imagery (Geography and land use)
p 33 A89-41168

FRASER, B. J.

Some aspects of the relation between Pi 1-2 magnetic pulsations observed at L = 1.3-2.1 on the ground and substorm-associated magnetic field variations in the near-earth magnetotail observed by AMPTE CCE
p 52 A89-36686

FU, LEE-LUENG

Observing oceanic mesoscale eddies from Geosat altimetry - Preliminary results
p 16 A89-39372

G

GALKINA, T. V.

Computer-aided synthesis of textures simulating the earth's surface
p 25 A89-37325

GALLO, K. P.

Large-area crop monitoring with the NOAA AVHRR - Estimating the silking stage of corn development
p 1 A89-33873

GALUMIAN, A. S.

Remote four-photon Raman spectroscopy of sea water under natural conditions
p 52 A89-37327

GAO, PENG

Two-dimensional seam-point searching in digital image mosaicking
p 26 A89-37945

GARAND, LOUIS

Automated recognition of oceanic cloud patterns. I - Methodology and application to cloud climatology
p 24 A89-35906

GARDEN, G.

A meteorological overview of the pre-AMEX and AMEX periods over the Australian region
p 48 A89-32850

GARDER, LEONID C.

Global, seasonal surface variations from satellite radiance measurements
p 52 A89-35966

GARDINER, JANICE L.

A field spectrometer and remote sensing study of the Fresno mining district, Mexico
p 51 A89-35871

GARRATT, J. R.

The prognosis of weather change lines over the ocean - The role of a reconnaissance aircraft
p 48 A89-32848

GARUFI, FRANK

Loran C field strength contours: Contiguous US
[DOT/FAA/CT-TN89/16] p 8 N89-23437

GARVIN, J. B.

Geological remote sensing signatures of terrestrial impact craters
p 37 N89-21317

GARY, BRUCE L.

Atmospheric water mapping with the Airborne Visible/Infrared Imaging Spectrometer (AVIRIS), Mountain Pass, California
p 39 N89-22156

GASCARD, J. C.

Retrieval of mesoscale meteorological parameters for polar latitudes (MIZEX and ARCTEMIZ campaigns)
p 58 A89-43026

GASCARD, JEAN-CLAUDE

Refinements in the cloud detection scheme of the 3I system. Comparison with AVHRR products
[ETN-89-94531] p 63 N89-24691

GAUTIER, CATHERINE

Interaction between net shortwave flux and sea surface temperature
p 15 A89-34878
Surface solar irradiance in the central Pacific during tropic heat - Comparisons between in situ measurements and satellite estimates
p 16 A89-35931

GEERKEN, R.

Research for optimization of future MOMS sensors
[ETN-89-94424] p 62 N89-23972

GEISS, J.

GEOS 1 observations of low-energy ions in the earth's plasmasphere - A study on composition, and temperature and density structure under quiet geomagnetic conditions
p 9 A89-33829

GELDSETZER, H. H. J.

The Frasnian-Famennian mass killing event(s), methods of identification and evaluation
p 37 N89-21318

GERING, LAWRENCE R.

Estimating stand density of loblolly pine in northern Louisiana using aerial photographs and probability proportional to size
p 34 A89-41171

GERSTL, SIEGFRIED A. W.

Sensitivity of an atmospheric correction algorithm for non-Lambertian vegetation surfaces to atmospheric parameters
p 29 A89-39556

GESELL, G.

An algorithm for snow and ice detection using AVHRR data - An extension to the Apollo software package
p 31 A89-40155

GEYER, W. ROCKWELL

Field calibration of mixed-layer drifters
p 53 A89-37554

GIARDINO, JOHN R.

The decrease of Lake Chad as documented during twenty years of manned space flight
p 18 A89-41434

GIBBONS, D. E.

Application of Landsat Thematic Mapper data for coastal thermal plume analysis at Diablo Canyon
p 35 A89-42175

GIBERT, DOMINIQUE

Seasat altimetry and the South Atlantic geoid. II - Short-wavelength undulations
p 16 A89-39659

GIMBLETT, H. RANDY

The application of SPOT ratio data for soil classification
p 56 A89-41165

GIRARD, MICHEL-CLAUDE

Munsell soil color and soil reflectance in the visible spectral bands of Landsat MSS and TM data
p 49 A89-33870

GLAZE, L.

Measuring thermal budgets of active volcanoes by satellite remote sensing
p 9 A89-32988

GLAZMAN, ROMAN E.

Statistical geometry of a small surface patch in a developed sea
p 26 A89-37808

GLOTOV, A. A.

Highly sensitive microwave radiometer-scatterometer for the remote sensing of the earth's surface
p 52 A89-37322

GOBLIRSCH, W.

Research on speckle behavior in SAR images
p 21 A89-35335

GOGININI, S. P.

An inexpensive polarimetric FM radar and polarimetric signatures of artificial sea ice
p 57 A89-42684

GONIKBERG, V. E.

Morphostructural interpretation of space images and the reconstruction of the recently formed stress field in the Altai-Baikal region
p 10 A89-34006

- GOODELL, PHILIP C.**
Application of Landsat Thematic Mapper digital data to the exploration for uranium-mineralized breccia pipes in Northwestern Arizona p 51 A89-35872
- GOODMAN, H. MICHAEL**
Precipitation retrieval over land and ocean with the SSM/I - Identification and characteristics of the scattering signal p 53 A89-37549
- GORDIENKO, I. G.**
Automated analysis of lineaments from space imagery obtained during seismic studies of central Tien-Shan p 20 A89-34014
- GORDON, HOWARD R.**
Aerosol analysis with the Coastal Zone Color Scanner - A simple method for including multiple scattering effects p 25 A89-37291
- GOSSELINK, JAMES G.**
Utilizing remote sensing of thematic mapper data to improve our understanding of estuarine processes and their influence on the productivity of estuarine-dependent fisheries [NASA-CR-183417] p 18 N89-20533
- GOUGH, D. IAN**
Magnetometer array studies, earth structure, and tectonic processes p 13 A89-42149
- GOWER, J. F. R.**
Development of an imaging spectrometer for remote sensing: The FLI program p 63 N89-24698
- GRABER, HANS**
Development of a satellite SAR image spectra and altimeter wave height data assimilation system for ERS-1 [NASA-CR-182685] p 61 N89-22975
- GRADENKO, S. I.**
Automated analysis of lineaments from space imagery obtained during seismic studies of central Tien-Shan p 20 A89-34014
- GRAHAM, D. F.**
Synthetic Aperture Radar data for mapping subsurface geological structures in the Northwest Territories, Canada p 50 A89-35858
- GRATZKI, ANNEGRET**
Sensitivity of an atmospheric correction algorithm for non-Lambertian vegetation surfaces to atmospheric parameters p 29 A89-39556
- GREEN, ROBERT O.**
AVIRIS performance during the 1987 flight season: An AVIRIS project assessment and summary of the NASA-sponsored performance evaluation p 60 N89-22155
Atmospheric water mapping with the Airborne Visible/Infrared Imaging Spectrometer (AVIRIS), Mountain Pass, California p 39 N89-22156
Determination of in-flight AVIRIS spectral, radiometric, spatial and signal-to-noise characteristics using atmospheric and surface measurements from the vicinity of the rare-earth-bearing carbonate at Mountain Pass, California p 61 N89-22170
- GREENBAUM, D.**
Alteration detection using TM imagery - The effects of supergene weathering in an arid climate p 12 A89-39655
- GRIEVE, R. A. F.**
Geological remote sensing signatures of terrestrial impact craters p 37 N89-21317
- GROSS, MICHAEL F.**
AVIRIS spectra of California wetlands p 3 N89-22167
- GRUEN, ARMIN W.**
Digital photogrammetric processing systems - Current status and prospects p 28 A89-39095
- GUPTA, SHASHI K.**
Estimation of surface insolation using sun-synchronous satellite data p 52 A89-35939
A parameterization for longwave surface radiation from sun-synchronous satellite data p 56 A89-41761
- GUYENNE, T. D.**
Imaging Spectrometry for Land Applications [ESA-SP-1101] p 63 N89-24692
- GUYENNE, T.-D.**
Imaging radar applications in Europe. Illustrated experimental results (1978-1987) [ESA-TM-01] p 42 N89-22978
- H**
- HAACK, BARRY N.**
Shuttle imaging radar analysis in arid environments p 33 A89-41166
- HALL, LAURA B.**
The use of remote sensing and GIS techniques for wetland identification and classification in the Garrison Diversion Unit-North Dakota p 18 A89-41160
- HALLS, JOANNE N.**
The use of remote sensing and GIS techniques for wetland identification and classification in the Garrison Diversion Unit-North Dakota p 18 A89-41160
- HALPERN, DAVID**
Seasat A satellite scatterometer measurements of equatorial surface winds p 53 A89-37802
- HAN, DAESOO**
Nimbus-7 data product summary [NASA-RP-1215] p 39 N89-22152
- HANSON, ANDREW J.**
Overview of the SRI cartographic modeling environment p 62 N89-23122
- HARBECK, ROLF**
The Official Topographic-Cartographic Information System (ATKIS) of the Geodesy Group of the Laender of the Federal Republic of Germany: Status after one year of development p 8 N89-23944
- HARDING, A. E.**
Integration of Landsat TM, stream sediment geochemistry and regional geophysics for mineral exploration in the English Lake District p 23 A89-35888
- HARLOW, CHARLES A.**
Representation and recognition of elongated regions in aerial images p 19 A89-33684
- HARRIS, A. R.**
Lake area measurement using AVHRR - A case study p 31 A89-40154
- HARRIS, J.**
Synthetic Aperture Radar data for mapping subsurface geological structures in the Northwest Territories, Canada p 50 A89-35858
Implementation of background and target geobotanical techniques in mineral exploration p 23 A89-35892
- HARRISON, ANDREW R.**
Multi-spectral classification of snow using NOAA AVHRR imagery p 31 A89-40156
- HARRISON, B. A.**
Accessing remote sensing technology - The microBRIAN example p 21 A89-34706
- HARRISON, CHRISTOPHER G. A.**
Neotectonics in Central Mexico from LANDSAT TM data [NASA-CR-183416] p 14 N89-21416
- HASHIM, MAZLAN**
Crop identification using merged Landsat multispectral scanner and Thematic Mapper data - Preliminary attempts p 3 A89-41153
- HASLINGER, KARL**
The digital urban map as a basis for a land information system in local administration p 8 N89-23945
- HASSELMANN, KLAUS**
Development of a satellite SAR image spectra and altimeter wave height data assimilation system for ERS-1 [NASA-CR-182685] p 61 N89-22975
- HASSELMANN, SUSANNE**
Development of a satellite SAR image spectra and altimeter wave height data assimilation system for ERS-1 [NASA-CR-182685] p 61 N89-22975
- HATTORI, SUSUMU**
A semi-automatic terrain measurement system for earthwork control p 28 A89-39094
- HAUTECOEUR, O.**
NOAA AVHRR and its uses for rainfall and evapotranspiration monitoring p 56 A89-40151
- HAWKINS, JEFFREY D.**
GEOSAT altimeter sea-ice mapping p 49 A89-34267
- HEEL, F.**
Research on speckle behavior in SAR images p 21 A89-35335
- HEELIS, R. A.**
Polar cap deflation during magnetospheric substorms p 24 A89-36704
- HEKI, KOSUKE**
The baseline length changes of circumpacific VLBI networks and their bearing on global tectonics p 13 A89-42795
- HELFERT, MICHAEL R.**
Monitoring tropical environments with Space Shuttle photography p 34 A89-41432
Analysis of seasonal characteristics of Sambhar Salt Lake, India, from digitized Space Shuttle photography p 18 A89-41433
- HENDERSON, FREDERICK B., III**
A survey of the operational status and needs of remote sensing in exploration geology p 64 A89-35853
- HENNINGS, I.**
Imaging procedure of underwater bottom topography by air and satellite images in the range of microwave and visible electromagnetic spectra [GKSS-88/E/41] p 17 N89-24014
- HENRY, JAMES A.**
Comparison of satellite, ground-based, and modeling techniques for analyzing the urban heat island p 26 A89-37948
- HENRY, R.**
Infrared thermography - A quantitative tool for heat study [ONERA, TP NO. 1989-3] p 53 A89-37627
- HENRY, RODNEY L.**
The application of high resolution digital elevation models to petroleum and mineral exploration and production p 22 A89-35876
- HENYEF, F. S.**
Imaging of ocean waves by SAR [AD-A203604] p 37 N89-21165
- HERBERT, TIMOTHY D.**
High resolution chronology of late Cretaceous-early Tertiary events determined from 21,000 yr orbital-climatic cycles in marine sediments p 14 N89-21328
- HERIC, MATTHEW**
Topographic analysis of the Andean Highlands using the Large Format Camera p 7 A89-35880
- HERMAN, JOHN D.**
The application of high resolution digital elevation models to petroleum and mineral exploration and production p 22 A89-35876
- HERRING, M.**
HIRIS: NASA's high-resolution imaging spectrometer for the Earth Observing System (EOS) p 63 N89-24695
- HEYDLAUFF, BRUCE**
KRMS (K-band Radiometric Mapping System) SSM/I validation March 1988 quick look report [NASA-CR-185320] p 8 N89-23766
- HIROSAWA, HARUTO**
ARGOS system used for balloon observations p 53 A89-38290
- HODGSON, MICHAEL E.**
N-dimensional display of cluster means in feature space p 29 A89-39100
Variation of surface water spectral response as a function of in situ sampling technique p 33 A89-41161
- HODGSON, ROBERT A.**
Combined remote sensing and surface geochemical survey in a drift-covered area in southeastern Saskatchewan p 12 A89-35881
- HOEFFNAGEL, W. J. C.**
The suitability of remote sensing for surveying and monitoring landscape patterns. Volume A: Pilot study - LANDSAT imagery p 36 N89-20535
The suitability of remote sensing for surveying and monitoring landscape patterns. Volume B: PEPS Project No. 73 - SPOT imagery p 36 N89-20536
- HOEKMAN, DIRK H.**
An analysis of speckle from forest stands with periodic structures p 54 A89-39555
- HOFFER, ROGER M.**
Assessment of forest cover changes using multirate spaceborne imaging radar p 33 A89-41169
- HOFFMAN, RICHARD O.**
The Nebraska center-pivot inventory - An example of operational satellite remote sensing on a long term basis p 28 A89-39096
- HOFMANN, D. J.**
Direct ozone depletion in springtime Antarctic lower stratospheric clouds p 4 A89-32756
- HOLBO, H. R.**
Measurements of short-term thermal responses of coniferous forest canopies using thermal scanner data p 1 A89-33867
Modeling surface temperature distributions in forest landscapes p 48 A89-33868
- HOLM, RONALD G.**
Surface reflectance factor retrieval from Thematic Mapper data p 49 A89-33871
- HOLMES, PETER**
Shortest paths in a digitized map using a tile-based data structure [PB89-143432] p 44 N89-23957
- HOOD, ROBBIE E.**
Precipitation retrieval over land and ocean with the SSM/I - Identification and characteristics of the scattering signal p 53 A89-37549
- HOOVER, GORDON**
Infrared spectroscopy (2.3-20 microns) for the geological interpretation of remotely-sensed multispectral thermal infrared data p 30 A89-39656
- HOPKINS, H. R.**
The contribution of remote sensing data to exploration of fractured reservoirs p 50 A89-35862

HORIGUCHI, HIROSHI

Marine Observation Satellite-1 - First year in orbit
p 26 A89-38328

HORNSBY, J. K.

Assessing aggregate resource potential in the Canadian
Shield - A knowledge-based approach p 23 A89-35877

Implementation of background and target geobotanical
techniques in mineral exploration p 23 A89-35892

HORTON, FOREST W., JR.

Information resources management p 42 N89-23371

HUANG, XIANFANG

Structural analysis of the Wichita Mountains using TM
data for lineament mapping p 12 A89-35887

HUGHES, B. A.

OSRMS (Ocean Surface Roughness Measurement
System): The DREP (Defence Research Establishment
Pacific) near-nadir scatterometer [AD-A202983] p 38 N89-21460

HUGHES, S. J.

OSRMS (Ocean Surface Roughness Measurement
System): The DREP (Defence Research Establishment
Pacific) near-nadir scatterometer [AD-A202983] p 38 N89-21460

HUISING, HERMAN

Monitoring Tunisia's steppes with SPOT p 35 A89-43316

HUMMER-MILLER, SUSANNE

A digital mosaicking algorithm allowing for an irregular
join 'line' p 26 A89-37944

HUNT, GAVIN A.

Geological uses of remotely-sensed reflected and
emitted data of lateritized Archaean terrain in Western
Australia p 55 A89-39652

HURLEY, EDWARD J.

Nimbus-7 data product summary
[NASA-RP-1215] p 39 N89-22152

HUSSON, N.

On the future development and management of
spectroscopic database for radiative transfer from the
issues of recent related workshops [ETN-89-94530] p 46 N89-24690

HUTCHISON, B. A.

Modeling directional thermal radiance from a forest
canopy p 27 A89-38972

HUTTON, P. G.

Accessing remote sensing technology - The microBRIAN
example p 21 A89-34706

IABLONSKAIA, N. A.

Investigation of the recently formed imbricate structure
of the southern Tien-Shan using space photographs p 10 A89-34005

IAZEV, P. N.

Analysis of the potential of using space photographic
data obtained with the PKF-1K camera to solve scientific,
economic, and educational-methodological problems p 64 A89-35685

IL'IN, IU. A.

Methodology for the remote sensing of fluxes of heat,
moisture, and effective radiation in the ocean-atmosphere
system p 16 A89-35686

ILLEERT, ANDREAS

Automatic digitizing of cadastral maps p 43 N89-23946

IMBERNON, J.

NOAA AVHRR and its uses for rainfall and
evapotranspiration monitoring p 56 A89-40151

IUDIN, V. S.

Recent and current geodynamics of the Kyzylkum region
as derived from space imagery p 10 A89-34017

IVANCHENKO, G. N.

Automated analysis of lineaments from space imagery
obtained during seismic studies of central Tien-Shan p 20 A89-34014

IVANOVA, T. P.

Seismogeological interpretation of space images of the
region of Caucasian mineral waters p 10 A89-34018

IWASHITA, A.

High resolution imaging of geobotanical anomalies
associated with subsurface hydrocarbons p 22 A89-35870

J

JACKSON, RAY D.

Surface reflectance factor retrieval from Thematic
Mapper data p 49 A89-33871

JACOBS, H.

Research for optimization of future MOMS sensors
[ETN-89-94424] p 62 N89-23972

JAEGER, REINER

Analysis and optimization of geodetic networks by
spectral criteria and mechanical analogies [SER-C-342] p 45 N89-23963

JAMES, MARK W.

Improved capabilities of the Multispectral Atmospheric
Mapping Sensor (MAMS) [NASA-TM-100352] p 58 N89-20430

JASANI, BHUPENDRA

Monitoring the greenhouse effect from space p 4 A89-39739

JEDLOVEC, GARY J.

Improved capabilities of the Multispectral Atmospheric
Mapping Sensor (MAMS) [NASA-TM-100352] p 58 N89-20430

JENSEN, JOHN R.

Thermal modeling of heat dissipation in the Pen Branch
delta using thermal infrared imagery p 32 A89-41159

JOHANNESSEN, O.

NOAA (National Oceanic and Atmospheric
Administration) AVHRR (Advanced Very High Resolution
Radiometer) observations during the marginal ice zone
experiment, between Spitzbergen and Greenland, June 7
to 18 July 1984 [AD-A204911] p 19 N89-22280

JOHNSON, CHRISTOPHER A.

Neotectonics in Central Mexico from LANDSAT TM
data [NASA-CR-183416] p 14 N89-21416

JOHNSON, MARK O.

Use of a geographic information system (GIS) to improve
planning for and control of the placement of dredged
material p 32 A89-41157

JONES, V. T.

Gas chromatographic and sonar imaging of hydrocarbon
seeps in the marine environment p 22 A89-35863

JORDAN, THOMAS H.

Plate motions and deformations from geologic and
geodetic data [NASA-CR-184987] p 15 N89-24757

JOSHI, ASHOK KUMAR

Identification of magnesite and bauxite deposits on
Landsat imagery, South India p 12 A89-35889

JULLIEN, J. P.

AVHRR data processing to study the surface canopies
in temperate regions - First results of HAPEX-MOBILHY p 30 A89-40153

JUNG, K.

Research for optimization of future MOMS sensors
[ETN-89-94424] p 62 N89-23972

JUNGERT, ERLAND

Shortest paths in a digitized map using a tile-based data
structure [PB89-143432] p 44 N89-23957

JUNIUS, HARTWIG

ARC-INFO: A geographic information system p 43 N89-23947

JUPP, D. L. B.

Accessing remote sensing technology - The microBRIAN
example p 21 A89-34706

JUPP, DAVID L. B.

Autocorrelation and regularization in digital images. II -
Simple image models p 29 A89-39551

K

KAHLE, ANNE B.

Infrared spectroscopy (2.3-20 microns) for the geological
interpretation of remotely-sensed multispectral thermal
infrared data p 30 A89-39656

KAMSTRA, S. I.

The suitability of remote sensing for surveying and
monitoring landscape patterns. Volume A: Pilot study -
LANDSAT imagery p 36 N89-20535

KANEMASU, E. T.

Measuring and modeling spectral characteristics of a
tallgrass prairie p 27 A89-38970

KANG, PIL CHONG

Discrimination of rocks and hydrothermal altered areas
based on Landsat TM data p 27 A89-38333

KARPUKHIN, V. I.

Sounding of crop fields by nanosecond radio pulses p 1 A89-35584

KATS, IA. G.

Dynamics of present-day geological processes from
remotely sensed data p 9 A89-34004

KAUFMAN, BARBARA A.

Nimbus-7 data product summary
[NASA-RP-1215] p 39 N89-22152

KAUFMANN, H.

Design of spectral and panchromatic bands for the
German MOMS-02 sensor p 57 A89-42173

Research for optimization of future MOMS sensors
[ETN-89-94424] p 62 N89-23972

KAWATA, Y.

Atmospheric correction of satellite MSS data in rugged
terrain p 27 A89-38334

KAYA, N.

EXOS-C (Ohzora) observations of polar cap
precipitations and inverted V events p 19 A89-33543

KELLER, WILLIAM C.

The Naval Research Laboratory's Air-Sea Interaction
Blimp Experiment p 53 A89-37981

KELLOGG, J. N.

Operational aspects of CASA UNO '88-The first large
scale international GPS geodetic network p 7 A89-42787

KELLY, M. C.

Spacelab 2 Upper Atmospheric Modification Experiment
over Arecibo. II - Plasma dynamics p 4 A89-38897

KENNEDY, P. J.

Monitoring the phenology of Tunisian grazing lands p 3 A89-40150

KERGOMARD, CLAUDE

Refinements in the cloud detection scheme of the 3I
system. Comparison with AVHRR products [ETN-89-94531] p 63 N89-24691

KERR, YANN H.

NOAA AVHRR and its uses for rainfall and
evapotranspiration monitoring p 56 A89-40151

KEYDEL, WOLFGANG

Necessity and benefit of the X-SAR space shuttle
experiment [DFVLR-MITT-88-29] p 63 N89-24688

KHMELEVSKII, V. K.

The potential use of remote sensing to solve problems
of paleotectonic prediction, geologic structure, and
exploitation of coal deposits with reference to the
Moscow-Region coal basin p 49 A89-34002

KIEFER, RALPH W.

Concept for a satellite-based global reserve monitoring
system p 32 A89-41152

KIEFFER, HUGH H.

Radiometric performance of AVIRIS: Assessment for an
arid region geologic target p 39 N89-22157

KIENEGGER, ERWIN

Combined film and softcopy photo-interpretation
system p 31 A89-40263

KIEREIN-YOUNG, KATHRYN S.

Preliminary analysis of Airborne Visible/Infrared Imaging
Spectrometer (AVIRIS) for mineralogic mapping at sites
in Nevada and Colorado p 60 N89-22161

KIETZMANN, H.

Research on speckle behavior in SAR images p 21 A89-35335

KING, TRUDE V. V.

Calibration and evaluation of AVIRIS data: Cripple Creek
in October 1987 p 39 N89-22159

KISELEV, V. V.

Multispectral space surveys and data processing p 22 A89-35684

KITAYAMA, M.

EXOS-C (Ohzora) observations of polar cap
precipitations and inverted V events p 19 A89-33543

KIVELSON, M. G.

Comparison of field-aligned currents at ionospheric and
magnetospheric altitudes p 9 A89-33540

KLEMAS, VYTAUTAS

AVIRIS spectra of California wetlands p 3 N89-22167

KLITCH, MARJORIE A.

Mesoscale severe weather development under
orographic influences [AD-A205082] p 41 N89-22293

KLOSTER, K.

NOAA (National Oceanic and Atmospheric
Administration) AVHRR (Advanced Very High Resolution
Radiometer) observations during the marginal ice zone
experiment, between Spitzbergen and Greenland, June 7
to 18 July 1984 [AD-A204911] p 19 N89-22280

KLUTH, CHRISTOPHER

Derivation of a geomagnetic model to $n = 63$ p 58 A89-43409

KNAPP, BEVERLY G.

The precedence of global features in the perception
of map symbols [AD-A203792] p 7 N89-22174

KNEPPER, DAN H.

Calibration and evaluation of AVIRIS data: Cripple Creek
in October 1987 p 39 N89-22159

KOGER, DAVID

Structural analysis of the Wichita Mountains using TM
data for lineament mapping p 12 A89-35887

KOGER, DAVID G.

Successful applications of remotely sensed data for oil
and gas exploration p 22 A89-35854

Use of remotely sensed data in mature basin exploration
- Considerations on creating useful imagery p 50 A89-35861

- KOLESNIKOV, A. I.**
Computer-aided synthesis of textures simulating the earth's surface p 25 A89-37325
- KOLLAARD, L. V.**
Design of a methodology for the detection of errors in terrestrial networks [ETN-89-94151] p 46 N89-23968
- KONDO, TETSURO**
The baseline length changes of circumpacific VLBI networks and their bearing on global tectonics p 13 A89-42795
- KONG, J. A.**
Remote sensing of earth terrain [NASA-CR-184937] p 41 N89-22971
- KONG, JIN AN**
Active and passive remote sensing of ice [AD-A203943] p 59 N89-20543
- KOSTERS, A. J. M.**
On the connection of geodetic pointfields in RETrig [PB89-146112] p 44 N89-23958
- KOUZAI, KATSUTOSHI**
Development and verification of Osaka Bay sampling model based on Landsat data p 27 A89-38332
- KOVALENOK, VLADIMIR V.**
Studying the earth from manned spacecraft p 64 A89-42511
- KRESSE, WOLFGANG**
Cartographic signatures in PHOCUS p 43 N89-23948
- KRITIKOS, G.**
DFVLR activities related to imaging spectrometry p 63 N89-24697
- KRONFELD, U.**
Optical properties of oceanic suspended matter and their interpretation for remote sensing of phytoplankton [GKSS-88/E/40] p 46 N89-24013
- KRUSE, FRED A.**
Automated extraction of absorption features from Airborne Visible/Infrared Imaging Spectrometer (AVIRIS) and Geophysical and Environmental Research Imaging Spectrometer (GERIS) data p 39 N89-22160
Preliminary analysis of Airborne Visible/Infrared Imaging Spectrometer (AVIRIS) for mineralogic mapping at sites in Nevada and Colorado p 60 N89-22161
- KRYLOVA, M. S.**
Methodological aspects of the automation of the calibration and processing of satellite microwave-radiometer data p 25 A89-37324
- KUCHKO, ALEKSANDR S.**
Aerial photography and specialized photographic studies p 31 A89-40488
- KUCHLER, DEBORAH**
Ground verification method for bathymetric satellite image maps of unsurveyed coral reefs p 6 A89-34949
- KUITTINEN, RISTO**
Determination of areal snow water equivalent using satellite images and gamma ray spectrometry [CI-91] p 44 N89-23960
- KULAKOV, A. P.**
New data on the morphostructure and geodynamics of the eastern margin of Eurasia p 10 A89-34012
- KUNSEMUELLER, JUERGEN**
Digitizing of drawings and cadastral maps using a scanner system p 43 N89-23949
- KUTUZA, B. G.**
Methodological aspects of the automation of the calibration and processing of satellite microwave-radiometer data p 25 A89-37324
- KUUSK, ANDRES**
A reflectance model for the homogeneous plant canopy and its inversion p 27 A89-38971
- KUZNETSOV, A. A.**
Methodology for the remote sensing of fluxes of heat, moisture, and effective radiation in the ocean-atmosphere system p 16 A89-35686
- KWARTENG, ANDY YAW**
Application of Landsat Thematic Mapper digital data to the exploration for uranium-mineralized breccia pipes in Northwestern Arizona p 51 A89-35872
- KYLE, H. LEE**
Nimbus-7 data product summary [NASA-RP-1215] p 39 N89-22152
- L**
- LAGOUARDE, J. P.**
NOAA AVHRR and its uses for rainfall and evapotranspiration monitoring p 56 A89-40151
- LAMBECK, KURT**
Geophysical geodesy - The slow deformations of the earth p 7 A89-38583
- LAPORTE, N.**
AVHRR for monitoring global tropical deforestation p 56 A89-40152
- LAPSHIN, V. B.**
The rate of gas exchange between the ocean and the atmosphere using microwave radiometer data p 25 A89-37471
- LASSELIN, D.**
AVHRR data processing to study the surface canopies in temperate regions - First results of HAPEX-MOBILHY p 30 A89-40153
- LASSEN, K.**
Distribution of auroral arcs during quiet geomagnetic conditions p 50 A89-34772
- LAZAREV, ALEKSANDR I.**
Studying the earth from manned spacecraft p 64 A89-42511
- LEBERL, FRANZ W.**
Combined film and softcopy photo-interpretation system p 31 A89-40263
- LEE, KEENAN**
Calibration and evaluation of AVIRIS data: Cripple Creek in October 1987 p 39 N89-22159
- LEE, KYU-SUNG**
Assessment of forest cover changes using multirate spaceborne imaging radar p 33 A89-41169
- LEE, MEEMONG**
Image-analysis techniques for determination of morphology and kinematics in arctic sea ice p 21 A89-34416
- LEGG, CHRISTOPHER A.**
Applications of AVHRR imagery in frontier exploration p 23 A89-35885
- LEGRAND, M.**
The potential of infrared satellite data for the retrieval of Saharan-dust optical depth over Africa p 30 A89-39875
- LEGRAND, MICHEL**
Satellite detection of Saharan dust - Optimized imaging during nighttime p 24 A89-35912
- LEHMAN, WILLIAM T.**
The application of high resolution digital elevation models to petroleum and mineral exploration and production p 22 A89-35876
- LEHMANN, F.**
The EARSEL Imaging Spectrometry Working Group p 47 N89-24700
- LEHNER, SUSANNE**
Development of a satellite SAR image spectra and altimeter wave height data assimilation system for ERS-1 [NASA-CR-182685] p 61 N89-22975
- LEIGHTON, J. P.**
Application of Landsat Thematic Mapper data for coastal thermal plume analysis at Diablo Canyon p 35 A89-42175
- LENTJES, P. G.**
The suitability of remote sensing for surveying and monitoring landscape patterns. Volume A: Pilot study - LANDSAT imagery p 36 N89-20535
The suitability of remote sensing for surveying and monitoring landscape patterns. Volume B: PEPS Project No. 73 - SPOT Imagery p 36 N89-20536
- LESHT, BARRY M.**
The relationship between in-lake sulfate concentration and estimates of atmospheric sulfur deposition for subregions of the eastern lake survey [DE89-009688] p 5 N89-24749
- LETALICK, DIETMAR**
Activities report of the Division of Optical Technology (FOA 33) [FOA-C-30507-3.1] p 62 N89-23287
- LI, LI**
Two-dimensional seam-point searching in digital image mosaicking p 26 A89-37945
- LI, Y.**
Measuring and modeling spectral characteristics of a tallgrass prairie p 27 A89-38970
- LIBERTI, G. L.**
Validation problems for remotely sensed sea surface temperature p 28 A89-39063
- LICHTENEGGER, J.**
Imaging radar applications in Europe. Illustrated experimental results (1978-1987) [ESA-TM-01] p 42 N89-22978
- LIONELLO, PIERO**
Development of a satellite SAR image spectra and altimeter wave height data assimilation system for ERS-1 [NASA-CR-182685] p 61 N89-22975
- LIPARI, CHARLES A.**
Representation and recognition of elongated regions in aerial images p 19 A89-33684
- LIPINSKI, DANIEL M.**
Airborne time-series measurement of soil moisture using terrestrial gamma radiation p 33 A89-41163
- LIPS, P. C. F.**
Vectorization of grid lines [ETN-89-94150] p 45 N89-23967
- LIVO, K. ERIC**
Calibration and evaluation of AVIRIS data: Cripple Creek in October 1987 p 39 N89-22159
- LLOYD, DANIEL**
A phenological description of Iberian vegetation using short wave vegetation index imagery p 2 A89-40149
- LO, C. P.**
A raster approach to population estimation using high-altitude aerial and space photographs p 19 A89-33872
- LOMMATZSCH, D.**
Measurements of spectral radiance at the sea surface for the development of remote sensing methods p 35 A89-42610
- LONGDON, N.**
Imaging radar applications in Europe. Illustrated experimental results (1978-1987) [ESA-TM-01] p 42 N89-22978
- LORIA, A.**
Mean temperature in a closed basin by remote sensing p 16 A89-39062
- LOTH, PAUL E.**
Vegetation and landscape of Kora National Reserve, Kenya p 6 A89-34945
- LOTZ-IWEN, HANS-JOACHIM**
Geocoded data sets of imaging satellites p 43 N89-23950
- LOVE, G.**
A meteorological overview of the pre-AMEX and AMEX periods over the Australian region p 48 A89-32850
- LUCAS, RICHARD M.**
Multi-spectral classification of snow using NOAA AVHRR imagery p 31 A89-40156
- LUKINA, N. V.**
Use of aerial and space methods for observations and studies of the morphology and kinematics of recent movements along some faults of the Baikal Rift Zone p 10 A89-34007
- LULLA, KAMLESH P.**
Monitoring tropical environments with Space Shuttle photography p 34 A89-41432
Analysis of seasonal characteristics of Sambhar Salt Lake, India, from digitized Space Shuttle photography p 18 A89-41433
- LUNDGREN, BERT**
Satellite altimetry. II - A new prospecting tool p 23 A89-35895
- LUTZE, T. A.**
Close-range photogrammetric measurement of erosion in coarse-grained soils p 54 A89-39098
- LUVALL, J. C.**
Measurements of short-term thermal responses of coniferous forest canopies using thermal scanner data p 1 A89-33867
Modeling surface temperature distributions in forest landscapes p 48 A89-33868
- LYBANON, MATTHEW**
GEOSAT altimeter sea-ice mapping p 49 A89-34267
- LYON, JOHN G.**
Impulse radar for identification of features in soils p 50 A89-34353
- LYON, R. J. P.**
Evaluation of the Portable Instantaneous Display Analysis Spectrometer (PIDAS) [NASA-CR-184878] p 61 N89-22970
- M**
- MACKAS, DAVID L.**
A performance comparison for two Lagrangian drifter designs p 34 A89-41750
- MACKENZIE, MARK**
Remote sensing of the deciduous vegetation of Great Smoky Mountains National Park p 33 A89-41170
- MACKEY, HALKARD E., JR.**
Thermal modeling of heat dissipation in the Pen Branch delta using thermal infrared imagery p 32 A89-41159
- MACKIN, S. J.**
The activities of the British National Space Centre (BNSC) in the field of imaging spectrometry p 47 N89-24696
- MACKINNON, ROBERT F.**
Minimum cross-entropy noise reduction in images p 34 A89-41845
- MACKLIN, J. T.**
Theoretical studies for ERS-1 wave mode, volume 1 [GEC-MTR-87/110-VOL-1] p 41 N89-22977
- MAGZUMOVA, D. A.**
Determination of the character of present-day vertical movements from the structure of space imagery p 10 A89-34016
- MAJEED, BALSAM S.**
Structural analysis of fracturing in Sinjar anticline using remote sensing technique p 13 A89-41167

MAJEED, TAHREER A.

Geological application of SIR-A imagery in southern Iraq p 13 A89-41162

MAKAROV, V. I.

Methods for investigating seismically active zones using remote imagery p 20 A89-34013

MALHOTRA, R. VEENA

Uses of the SAS statistical package for digital image analysis p 23 A89-35898

MALINGREAU, J. P.

AVHRR for monitoring global tropical deforestation p 56 A89-40152

MALINNIKOV, V. A.

Methodology for the remote sensing of fluxes of heat, moisture, and effective radiation in the ocean-atmosphere system p 16 A89-35886

MALKEVICH, M. S.

Remote measurements from Salyut-7 of the optical parameters of the atmosphere-surface system p 57 A89-42601

MANN, BRUCE A.

Use of aerial photography to inventory aquatic vegetation p 50 A89-34362

MANSUROV, M. M.

Determination of spectral signatures for remote laser sensing of vegetation p 35 A89-42611

MANTOVANI, F.

Mean temperature in a closed basin by remote sensing p 16 A89-39062

MARGOLIS, JACK S.

Atmospheric water mapping with the Airborne Visible/Infrared Imaging Spectrometer (AVIRIS), Mountain Pass, California p 39 N89-22156

MARQUART, GABRIELE

Arctic geodynamics - A satellite altimeter experiment for the European Space Agency Earth Remote-Sensing satellite p 29 A89-39546

MASON, I. M.

Lake area measurement using AVHRR - A case study p 31 A89-40154

MASUDA, TAKESHI

Marine Observation Satellite-1 - First year in orbit p 26 A89-38328

MATSUEDA, TATSUO

Marine Observation Satellite-1 - First year in orbit p 26 A89-38328

MAY, L. NELSON

Utilizing remote sensing of thematic mapper data to improve our understanding of estuarine processes and their influence on the productivity of estuarine-dependent fisheries [NASA-CR-183417] p 18 N89-20533

MAYO, K. K.

Accessing remote sensing technology - The microBRIAN example p 21 A89-34706

MCCLEIMANS, T. A.

Activities at the Norwegian Hydrotechnical Laboratory p 55 A89-40129

MCCORMICK, N. J.

Radiative transfer calculations for characterizing obscured surfaces using time-dependent backscattered pulses p 48 A89-32841

MCCOY, R. M.

A closer look at the Patrick Draw oil field vegetation anomaly p 1 A89-35893

MCEEVERS, JIM A.

Air pollution effects field research facility: Ozone flow control and monitoring system [DE89-007922] p 5 N89-22192

MCUFFIE, K.

Examination of USAF Nephelometer performance in the marginal cryosphere region p 52 A89-35949

MCQUIRE, M. J.

Modeling directional thermal radiance from a forest canopy p 27 A89-38972

MCKEOWN, DAVID M., JR.

Cooperative methods for road tracking in aerial imagery p 42 N89-23101

MCKEOWN, M. H.

Geological gyrocompass [PB89-133086] p 63 N89-24589

MCKINLEY, GEORGE B.

Column movement model used to support AMM p 38 N89-21521

MCKINNON, JOHN A.

Solar-geophysical data number 529, September 1988. Part 1: (Prompt reports). Data for August, July 1988 and late data [PB89-121305] p 37 N89-21431

MCMANUS, J.

Geobotanical application of Airborne Thematic Mapper data in Sutherland, north-west Scotland p 2 A89-39657

MCTAGUE, JOHN PAUL

Estimating stand density of loblolly pine in northern Louisiana using aerial photographs and probability proportional to size p 34 A89-41171

MEEHAN, THOMAS K.

Operational aspects of CASA UNO '88-The first large scale international GPS geodetic network p 7 A89-42787

MEEKER, DAVID L.

Laser scattering phenomenology - Background signature characterization and prediction p 6 A89-33661

MEISSNER, D.

Design of spectral and panchromatic bands for the German MOMS-02 sensor p 57 A89-42173

MELBOURNE, WILLIAM G.

Operational aspects of CASA UNO '88-The first large scale international GPS geodetic network p 7 A89-42787

MELUA, ARKADII I.

Spaceborne studies related to nature conservation p 65 A89-42549

MENARD, YVES

Synoptic analysis and dynamical adjustment of GEOS 3 and Seasat altimeter eddy fields in the northwest Atlantic p 29 A89-39650

MENENGER, L.

The potential of infrared satellite data for the retrieval of Saharan-dust optical depth over Africa p 30 A89-39875

MENK, F. W.

Some aspects of the relation between Pi 1-2 magnetic pulsations observed at L = 1.3-2.1 on the ground and substorm-associated magnetic field variations in the near-earth magnetotail observed by AMPTE CCE p 52 A89-36686

MENZ, GUNTER

Derivation of a large-scale map of heat load in the region Freiburg-Basel (Germany, F.R.) using satellite data. A contribution to the production of bioclimate data based on a geographic information system [REPT-27] p 41 N89-22972

MENZEL, W. PAUL

Improved capabilities of the Multispectral Atmospheric Mapping Sensor (MAMS) [NASA-TM-100352] p 58 N89-20430

MERIN, IRA S.

Identification of Cross Strike discontinuities in the Appalachian basin and implications for hydrocarbon exploration p 11 A89-35860

MERSON, R. H.

An AVHRR mosaic image of Antarctica p 30 A89-40135

MESENBURG, PETER

Computer assisted layout of graphic settlement representations p 43 N89-23951

MEYER, D. J.

AVIRIS data characteristics and their effects on spectral discrimination of rocks exposed in the Drum Mountains, Utah: Results of a preliminary study p 40 N89-22165

MEYER, DAVID

Evaluation of Airborne Visible/Infrared Imaging Spectrometer Data of the Mountain Pass, California carbonate complex p 60 N89-22169

MEYER, J.

Modelling the earth's geomagnetic field to high degree and order p 58 A89-43408

The geomagnetic spectrum for 1980 and core-crustal separation p 13 A89-43410

MEYER, UWE

Tools for the computer assisted generalization of settlements for the construction of digital landscape models p 43 N89-23952

MIDDLEBROOK, BARRY J.

Calibration and evaluation of AVIRIS data: Cripple Creek in October 1987 p 39 N89-22159

MILFORD, J. R.

Relating point to area average rainfall in semiarid West Africa and the implications for rainfall estimates derived from satellite data p 55 A89-39870

MILLER, DENNIS B.

Preliminary development of a seashore-effects analysis system [DE89-007863] p 61 N89-22191

MILLER, LAURY

Evaluation of Geosat altimeter data with application to tropical Pacific sea level variability p 25 A89-37801

MILSTEIN, RANDALL L.

The Calvin 28 cryptoexplosive disturbance, Cass County, Michigan: Evidence for impact origin p 14 N89-21358

MILTON, E. J.

The activities of the British National Space Centre (BNSC) in the field of imaging spectrometry p 47 N89-24696

MINOR, TIMOTHY

Geobotanical determination of aggregate source material using Airborne Thematic Mapper imagery p 1 A89-35865

Geobotanical remote sensing for determination of aggregate source material [AD-A205943] p 45 N89-23962

MIRKAMLOV, D. M.

Determination of spectral signatures for remote laser sensing of vegetation p 35 A89-42611

MIROVSKII, V. G.

Highly sensitive microwave radiometer-scatterometer for the remote sensing of the earth's surface p 52 A89-37322

MISRA, K. S.

Synthetic Aperture Radar data for mapping subsurface geological structures in the Northwest Territories, Canada p 50 A89-35858

MITCHELL, CHARLES A.

Impulse radar for identification of features in soils p 50 A89-34353

MOELLER, CHRIS C.

Improved capabilities of the Multispectral Atmospheric Mapping Sensor (MAMS) [NASA-TM-100352] p 58 N89-20430

MOHLER, ROBERT R. J.

The decrease of Lake Chad as documented during twenty years of manned space flight p 18 A89-41434

MOLLARD, J. D.

Combined remote sensing and surface geochemical survey in a drift-covered area in southeastern Saskatchewan p 12 A89-35881

MOODY, THERESA K.

National Air Toxics Information Clearinghouse: Ongoing research and regulatory development projects, July 1988 [PB89-103428] p 65 N89-20558

MOORE, R. K.

An inexpensive polarimetric FM radar and polarimetric signatures of artificial sea ice p 57 A89-42684

MORAN, M. SUSAN

Surface reflectance factor retrieval from Thematic Mapper data p 49 A89-33871

MOREIRA, ALBERTO

Performance analysis of the DFLVR real time SAR processor for low SNRs p 21 A89-35336

MORGAN, KEN

Structural analysis of the Wichita Mountains using TM data for lineament mapping p 12 A89-35887

MORGAN, KEN M.

Basic concepts in the use of remotely sensed data for resource exploration p 11 A89-35852

MORIZUMI, S. J.

Sea state determination by a remote optical sensor p 53 A89-38330

MOSES, J. J.

Polar cap deflation during magnetospheric substorms p 24 A89-36704

MOSSMAN, DIANA L.

Concept for a satellite-based global reserve monitoring system p 32 A89-41152

MOUAT, DAVID

Geobotanical determination of aggregate source material using Airborne Thematic Mapper imagery p 1 A89-35865

Geobotanical remote sensing for determination of aggregate source material [AD-A205943] p 45 N89-23962

MOUSSEAU, R. J.

Gas chromatographic and sonar imaging of hydrocarbon seeps in the marine environment p 22 A89-35863

MUELLER, JAMES L.

Biooptical variability in the Greenland Sea observed with the Multispectral Airborne Radiometer System (MARS) [NASA-CR-184856] p 47 N89-24784

MUKAI, T.

EXOS-C (Ohzora) observations of polar cap precipitations and inverted V events p 19 A89-33543

MUKHAMEDOV, A. A.

Determination of spectral signatures for remote laser sensing of vegetation p 35 A89-42611

MULLINS, KEVIN F.

Radiometric performance of AVIRIS: Assessment for an arid region geologic target p 39 N89-22157

MUNDAY, T. J.

The activities of the British National Space Centre (BNSC) in the field of imaging spectrometry p 47 N89-24696

MURAI, SHUNJI

A semi-automatic terrain measurement system for earthwork control p 28 A89-39094

MURTHA, PETER A.

Cluster analysis of pine crown foliage patterns aid identification of mountain pine beetle current-attack p 26 A89-37950

O

MUSTARD, JOHN F.

Application of imaging spectrometer data to the Kings-Kaweah ophiolite melange p 40 N89-22166

MYERS, JEFF

Geobotanical determination of aggregate source material using Airborne Thematic Mapper imagery p 1 A89-35865

Geobotanical remote sensing for determination of aggregate source material [AD-A205943] p 45 N89-23962

MYNENI, R. B.

Measuring and modeling spectral characteristics of a tallgrass prairie p 27 A89-38970

N

NABIEV, K. A.

Determination of spectral signatures for remote laser sensing of vegetation p 35 A89-42611

NAIDU, P. S.

Sea surface spectrum from aerial photographs - Laboratory model studies p 30 A89-39674

NARASIMHAN, RAVI

TAX - Prototype expert system for terrain analysis p 20 A89-34363

NASLUND, H. RICHARD

Lithologic mapping in East Greenland with Landsat Thematic Mapper imagery p 6 A89-35869

NEILAN, RUTH E.

Operational aspects of CASA UNO '88-The first large scale international GPS geodetic network p 7 A89-42787

NELSON, R. A.

The contribution of remote sensing data to exploration of fractured reservoirs p 50 A89-35862

NEMANI, RAMAKRISHNA R.

Estimation of regional surface resistance to evapotranspiration from NDVI and thermal-IR AVHRR data p 55 A89-39872

NENASHEV, I. S.

Multispectral space surveys and data processing p 22 A89-35684

The KAP-350 and KAP-100 space cameras for the remote sensing of earth resources p 50 A89-35687

NEVILL, GALE E., JR.

Advanced space design program to the Universities Space Research Association and the National Aeronautics and Space Administration [NASA-CR-180450] p 3 N89-24015

NEVILLE, R. A.

Imaging spectrometry at the Canada Centre for Remote Sensing p 64 N89-24701

NICHOLS, JENNIFER D.

Lithologic mapping in East Greenland with Landsat Thematic Mapper imagery p 6 A89-35869

NILER, PEARL P.

A performance comparison for two Lagrangian drifter designs p 4 A89-35870

NILSON, TIIT

A reflectance model for the homogeneous plant canopy and its inversion p 27 A89-38971

NISHIDA, A.

EXOS-C (Ohzora) observations of polar cap precipitations and inverted V events p 19 A89-33543

NISHIDA, TAKASHI

Hydrocarbon potential of part of the margin of the Tarim Basin from Landsat - A case history p 11 A89-35857

NISHIMURA, JUN

ARGOS system used for balloon observations p 53 A89-38290

NOBLE, S. T.

Spacelab 2 Upper Atmospheric Modification Experiment over Arecibo. II - Plasma dynamics p 4 A89-38897

NORDIN, PER

Satellite altimetry. II - A new prospecting tool p 23 A89-35895

NOVIK, N. N.

Use of aerial and space photography for the detection of faults and neotectonic movements in Crimea and the Azov Coastal Region p 9 A89-34003

NOWEIR, A. M.

Conjugate synthetic normal faults around the Gulf of Salwa, southwestern Qatar, the Arabian Gulf p 12 A89-35886

NURIDDINOV, O. S.

Assessment of the present conditions of lowland lakes of Central Asia using the interpretation of space photographs p 17 A89-37319

NYSTUEN, JEFFREY A.

Precipitation in the Canadian Atlantic Storms Program - Measurements of the acoustic signature p 50 A89-35819

O'BRIEN, D. M.

Theoretical algorithms for satellite-derived sea surface temperatures p 21 A89-35159

OAKES, ARNOLD G.

Nimbus-7 data product summary [NASA-RP-1215] p 39 N89-22152

OBARA, T.

EXOS-C (Ohzora) observations of polar cap precipitations and inverted V events p 19 A89-33543

ODINTSOV, K. L.

The potential use of remote sensing to solve problems of paleotectonic prediction, geologic structure, and exploitation of coal deposits with reference to the Moscow-Region coal basin p 49 A89-34002

OETTL, HERWIG

Necessity and benefit of the X-SAR space shuttle experiment [DFVLR-MITT-88-29] p 63 N89-24688

OHASHI, MAKOTO

Evaluation of the Portable Instantaneous Display Analysis Spectrometer (PIDAS) [NASA-CR-184878] p 61 N89-22970

OHTA, SHIGEO

ARGOS system used for balloon observations p 53 A89-38290

OHTANI, HITOSHI

A semi-automatic terrain measurement system for earthwork control p 28 A89-39094

OLIVET, JEAN-LOUIS

Seasat altimetry and the South Atlantic geoid. II - Short-wavelength undulations p 16 A89-39659

OLSEN, DAVID

KRMS (K-band Radiometric Mapping System) SSM/I validation March 1988 quick look report [NASA-CR-185320] p 8 N89-23766

OLSON, CHARLES E., JR.

Estimating population size of Pygoscelid Penguins from TM data [NASA-CR-180081] p 3 N89-24687

ORLOV, I. K.

Multispectral space surveys and data processing p 22 A89-35684

ORLOVA, T. I.

Computer-aided synthesis of textures simulating the earth's surface p 25 A89-37325

P

PAITHOONWATTANAKIJ, K.

Pixel and sub-pixel accuracy in geometrical correction of AVHRR p 30 A89-40134

PALME, ULF WALTER

Microwave X-band radiometric characterization of Brazilian soils by measurement of the complex permittivity [INPE-4588-PRE/1319] p 3 N89-24685

PARR, J. THOMAS

Lithologic mapping in East Greenland with Landsat Thematic Mapper imagery p 6 A89-35869

PEASE, C. H.

Beaufort Sea mesoscale circulation study: Preliminary results [PB89-121693] p 17 N89-20597

PECK, EUGENE L.

Airborne time-series measurement of soil moisture using terrestrial gamma radiation p 33 A89-41163

PELLETIER, R. E.

Detection techniques using multispectral data to index soil erosional status p 56 A89-41164

PEMPEL, L. C.

OSRMS (Ocean Surface Roughness Measurement System): The DREP (Defence Research Establishment Pacific) near-nadir scatterometer [AD-A202983] p 38 N89-21460

PENNER, LYNDEN

Combined remote sensing and surface geochemical survey in a drift-covered area in southeastern Saskatchewan p 12 A89-35881

PESHKOV, A. N.

Sounding of crop fields by nanosecond radio pulses p 1 A89-35584

PETERS, DOUGLAS C.

Lineament analysis for hazard assessment in advance of coal mining p 11 A89-35873

PETRENKO, B. Z.

Methodological aspects of the automation of the calibration and processing of satellite microwave-radiometer data p 25 A89-37324

PETROV, A. F.

The use of space imagery for investigations of recent crustal deformations in southern Yakutia p 20 A89-34015

PHILPOT, WILLIAM D.

Bathymetric mapping with passive multispectral imagery p 16 A89-38766

PHULPIN, T.

AVHRR data processing to study the surface canopies in temperate regions - First results of HAPEX-MOBILHY p 30 A89-40153

PHYSICK, W. L.

The prognosis of weather change lines over the ocean - The role of a reconnaissance aircraft p 48 A89-32848

PICHUGIN, A. P.

Parameter optimization of systems for the thermal microwave mapping of the earth's surface p 25 A89-37321

PIECH, KENNETH R.

Hyperspectral interactions - Invariance and scaling p 48 A89-32837

PIECH, M. ANN

Hyperspectral interactions - Invariance and scaling p 48 A89-32837

PIELOU, J. M.

Theoretical studies for ERS-1 wave mode, volume 1 [GEC-MTR-87/110-VOL-1] p 41 N89-22977

PIERSON, WILLARD J., JR.

Probabilities and statistics for backscatter estimates obtained by a scatterometer with applications to new scatterometer design data [NASA-CR-4228] p 61 N89-22779

PIETERS, CARLE M.

Application of imaging spectrometer data to the Kings-Kaweah ophiolite melange p 40 N89-22166

PILAN, L.

Mean temperature in a closed basin by remote sensing p 16 A89-39062

PINTO, JOAO DE LEMOS

Remote sensing in refractive turbulence p 58 N89-20532

PISKULIN, V. A.

Economic relations of the all-union trade association Sojuzkarta and the geodetic and cartographic services of the U.S.S.R. to foreign countries p 64 A89-34708

PLANT, WILLIAM J.

The Naval Research Laboratory's Air-Sea Interaction Blimp Experiment p 53 A89-37981

PLATT, TREVOR

Remote sensing of ocean chlorophyll - Consequence of nonuniform pigment profile p 15 A89-32838

PLEWS, REESE W.

N-dimensional display of cluster means in feature space p 29 A89-39100

PODWYSOCKI, MELVIN

Evaluation of Airborne Visible/Infrared Imaging Spectrometer Data of the Mountain Pass, California carbonate complex p 60 N89-22169

POLETAEV, A. I.

Dynamics of present-day geological processes from remotely sensed data p 9 A89-34004

PONOMAREV, V. S.

Structural stresses and the divisibility into blocks of the earth crust as observed on space imagery p 10 A89-34009

PONTUAL, A.

Application of Landsat Thematic Mapper imagery for lithological mapping of poorly accessible semi-arid regions p 7 A89-35879

POPOV, S. M.

Analysis of the potential of using space photographic data obtained with the PKF-1K camera to solve scientific, economic, and educational-methodological problems p 64 A89-35865

PORTER, WALLACE M.

AVIRIS performance during the 1987 flight season: An AVIRIS project assessment and summary of the NASA-sponsored performance evaluation p 60 N89-22155

POTAPOV, A. A.

Computer-aided synthesis of textures simulating the earth's surface p 25 A89-37325

POUWELS, H.

Phase A study for the extension of the CAESAR scanner with a sensor module for the far infrared [BCRS-88-09] p 59 N89-20539

POWERS, EDWARD

Multispectral terrain background simulation techniques for use in airborne sensor evaluation p 19 A89-33664

POWITZ, BERND M.

Computer assisted generalization of transport line representations p 43 N89-23953

PRANGSMA, G. J.

Using NOAA AVHRR imagery in assessing water quality parameters p 55 A89-40148

Processing and application of digital AVHRR-imagery for land and sea surfaces [BCRS-88-08] p 36 N89-20538

PRATA, A. J.

Observations of volcanic ash clouds in the 10-12 micron window using AVHRR/2 data p 30 A89-40143

PREDOEHL, MARTIN C.

Ice cover on Chesapeake Bay from AVHRR (Advanced Very High Resolution Radiometer) and LANDSAT imagery, winter of 1987-88 [PB89-117261] p 59 N89-21415

PRICE, JOHN C.

Calibration comparison for the Landsat 4 and 5 Multispectral Scanners and Thematic Mappers p 47 A89-32835

PSIHOGIOS, PANAGIOTIS

Thermal images of sky and sea-surface background infrared radiation [AD-A205819] p 46 N89-23992

PUCHERELLI, MICHAEL J.

The use of remote sensing and GIS techniques for wetland identification and classification in the Garrison Diversion Unit-North Dakota p 18 A89-41160

PUGNAGHI, S.

Mean temperature in a closed basin by remote sensing p 16 A89-39062

PYRON, ARTHUR J.

Lowering the cost of exploration for independents - How remotely sensed data aids in the search for oil and gas p 22 A89-35855

Q**QUAM, LYNN H.**

Overview of the SRI cartographic modeling environment p 62 N89-23122

R**RAEMER, H. R.**

Further investigations of sampling errors in mean terrain height estimation p 32 A89-41076

RAGULIN, I. G.

The rate of gas exchange between the ocean and the atmosphere using microwave radiometer data p 25 A89-37471

RAMAPRIYAN, H. K.

Data compression experiments with LANDSAT thematic mapper and Nimbus-7 coastal zone color scanner data p 41 N89-22344

RAMSEY, ELIJAH, III

Thermal modeling of heat dissipation in the Pen Branch delta using thermal infrared imagery p 32 A89-41159

RANSON, K. J.

A new technique to measure the spectral properties of conifer needles p 19 A89-33874

RAST, M.

ESA's planned activities in the field of imaging spectrometry for Earth observation p 46 N89-24693

RAUHALA, URHO A.

Automated DTM validation and progressive sampling algorithm of finite element array relaxation p 22 A89-35837

REED, BRADLEY C.

Using textural measures to distinguish spectrally similar vegetation p 3 A89-41155

REGISTER, B. M.

The commercial land remote sensing market - Current assessment, baseline forecast and baseline alternatives p 64 A89-35899

REID, NICHOLAS

High resolution imaging of geobotanical anomalies associated with subsurface hydrocarbons p 22 A89-35870

REIMER, JOHN H.

AVIRIS performance during the 1987 flight season: An AVIRIS project assessment and summary of the NASA-sponsored performance evaluation p 60 N89-22155

REITER, ELMAR R.

Mesoscale severe weather development under orographic influences [AD-A205082] p 41 N89-22293

RENCZ, A. N.

Implementation of background and target geobotanical techniques in mineral exploration p 23 A89-35892

REUTOV, E. A.

The condition of natural features as related to their intrinsic microwave and IR emission fields p 2 A89-37320

REYNOLDS, RICHARD W.

A real-time global sea surface temperature analysis p 16 A89-35907

REZOV, A. V.

Remote four-photon Raman spectroscopy of sea water under natural conditions p 52 A89-37327

ROBERTS, LEEANNE

A software system to create a hierarchical, multiple level of detail terrain model [AD-A203047] p 38 N89-21568

ROBINSON, D. A.

Examination of USAF Nephanalysis performance in the marginal cryosphere region p 52 A89-35949

ROCK, B. N.

Assessment of AVIRIS data from vegetated sites in the Owens Valley, California p 60 N89-22162

RODENBURG, W. F.

Meteosat thermal inertia mapping for studying wetland dynamics in the West-African Sahel [BCRS-88-10A] p 62 N89-23970

ROGUSKI, STEPHEN J.

Comparison of satellite, ground-based, and modeling techniques for analyzing the urban heat island p 26 A89-37948

ROHDE, FREDERICK W.

Computer strategy for detecting line features on simulated binary arrays in support of radar feature extraction [AD-A203257] p 37 N89-21162

ROLLIN, E. M.

The activities of the British National Space Centre (BNSC) in the field of imaging spectrometry p 47 N89-24696

ROOZEKRANS, J. N.

Using NOAA AVHRR imagery in assessing water quality parameters p 55 A89-40148

Processing and application of digital AVHRR-imagery for land and sea surfaces [BCRS-88-08] p 36 N89-20538

ROSEMA, A.

Meteosat thermal inertia mapping for studying wetland dynamics in the West-African Sahel [BCRS-88-10A] p 62 N89-23970

Thermal analysis for the monitoring and prediction of flood dynamics in wetlands [BCRS-88-10B] p 46 N89-23971

ROSENTHAL, ALAN

Utilizing remote sensing of thematic mapper data to improve our understanding of estuarine processes and their influence on the productivity of estuarine-dependent fisheries [NASA-CR-183417] p 18 N89-20533

ROSS, BECKY

Sensitivity of 30-day dynamical forecasts to continental snow cover p 17 A89-35937

ROSSOW, WILLIAM B.

Global, seasonal surface variations from satellite radiance measurements p 52 A89-35966

ROTHERY, D. A.

Measuring thermal budgets of active volcanoes by satellite remote sensing p 9 A89-32988

Volcano monitoring by short wavelength infrared satellite remote sensing p 51 A89-35875

ROWAN, LAWRENCE

Evaluation of Airborne Visible/Infrared Imaging Spectrometer Data of the Mountain Pass, California carbonate complex p 60 N89-22169

RUBIN, TOD

Evaluation of the Portable Instantaneous Display Analysis Spectrometer (PIDAS) [NASA-CR-184878] p 61 N89-22970

RUMIANTSEVA, E. F.

Dynamics of present-day geological processes from remotely sensed data p 9 A89-34004

RUNDQUIST, DONALD C.

The Nebraska center-pivot inventory - An example of operational satellite remote sensing on a long term basis p 28 A89-39096

RUNNING, STEVEN W.

Estimation of regional surface resistance to evapotranspiration from NDVI and thermal-IR AVHRR data p 55 A89-39872

RUSSELL, ORVILLE R.

Sources of remote sensing data visible, near infrared, and short wave p 51 A89-35878

RYAN, B. F.

The prognosis of weather change lines over the ocean - The role of a reconnaissance aircraft p 48 A89-32848

RYKS, HERMAN

Integration of tie-points in digital mosaicing [ETN-89-94147] p 41 N89-22973

S**SAGITOV, M. U.**

Gravimetric studies at sea p 49 A89-34088

SAITO, T.

Some aspects of the relation between Pi 1-2 magnetic pulsations observed at L = 1.3-2.1 on the ground and substorm-associated magnetic field variations in the near-earth magnetotail observed by AMPTE CCE p 52 A89-36686

SALAWITCH, ROSS JAY

Antarctic ozone: Theory and observation p 4 N89-22189

SALO, S. A.

Beaufort Sea mesoscale circulation study: Preliminary results [PB89-121693] p 17 N89-20597

SARAF, A. K.

Geobotanical application of Airborne Thematic Mapper data in Sutherland, north-west Scotland p 2 A89-39657

SATHYENDRANATH, SHUBHA

Remote sensing of ocean chlorophyll - Consequence of nonuniform pigment profile p 15 A89-32838

SAUL'SKII, V. K.

Optimal satellite orbits and the network structure for regular earth surveying p 35 A89-42614

SAUNDERS, R. W.

Theoretical algorithms for satellite-derived sea surface temperatures p 21 A89-35159

Applications of AVHRR data; Proceedings of the Third European AVHRR Data Users' Meeting, University of Oxford, England, Dec. 16-18, 1987 p 55 A89-40126

SAVIN, G. A.

Multispectral space surveys and data processing p 22 A89-35684

SAVORSKII, V. P.

Methodological aspects of the automation of the calibration and processing of satellite microwave-radiometer data p 25 A89-37324

Correcting absolute calibrations of satellite microwave radiometer using a priori data p 35 A89-42612

SCHIEFFNER, NORMAN W.

The KP equation: A comparison to laboratory generated biperiodic waves p 38 N89-21507

SCHEID, JOHN A.

Operational aspects of CASA UNO '88-The first large scale international GPS geodetic network p 7 A89-42787

SCHERNECK, HANS-GEORG

Arctic geodynamics - A satellite altimeter experiment for the European Space Agency Earth Remote-Sensing satellite p 29 A89-39546

SCHLOSSER, DONALD W.

Use of aerial photography to inventory aquatic vegetation p 50 A89-34362

SCHLUESSEL, PETER

Satellite-derived low-level atmospheric water vapour content from synergy of AVHRR with HIRS p 30 A89-40139

SCHMITZ, DAVE R.

Modelling the earth's geomagnetic field to high degree and order p 58 A89-43408

The geomagnetic spectrum for 1980 and core-crustal separation p 13 A89-43410

SCHMITZ, DAVE RAY

Derivation of a geomagnetic model to n = 63 p 58 A89-43409

SCHNETZLER, C.

Geological remote sensing signatures of terrestrial impact craters p 37 N89-21317

SCHNETZLER, C. S.

Effect of metal stress on the thermal infrared emission of soybeans: A greenhouse experiment - Possible utility in remote sensing p 2 A89-39658

SCHOON, NEIL F.

An analysis of platinum silicide and indium antimonide for remote sensors in the 3 to 5 micrometer wavelength band [AD-A202663] p 59 N89-21218

SCHOUIMANS, O. F.

Land use inventory using LANDSAT Thematic Mapper imagery to study environmental pollution [NLR-MP-87063-U] p 4 N89-20541

SCHREIER, GUNTER

Geocoded data sets of imaging satellites p 43 N89-23950

SCHROEDER, M.

DFVLR activities related to imaging spectrometry p 63 N89-24697

SCHROTH, RALF

Definition and filling of information systems: Challenge for a photogrammetric service enterprise p 62 N89-23942

SCHULT, R. L.

Imaging of ocean waves by SAR [AD-A203604] p 37 N89-21165

- SCHWALLER, M. R.**
Effect of metal stress on the thermal infrared emission of soybeans: A greenhouse experiment - Possible utility in remote sensing p 2 A89-39658
- SCHWALLER, MATHEW R.**
Estimating population size of Pygoscelid Penguins from TM data [NASA-CR-180081] p 3 N89-24687
- SCORER, R. S.**
Cloud reflectance variations in channel-3 p 55 A89-40136
- SCOTT, L. F.**
A closer look at the Patrick Draw oil field vegetation anomaly p 1 A89-35893
- SCOTT, N. A.**
Retrieval of mesoscale meteorological parameters for polar latitudes (MIZEX and ARCTEMIZ campaigns) p 58 A89-43026
- SCOTT, NOELLE A.**
Refinements in the cloud detection scheme of the 3I system. Comparison with AVHRR products [ETN-89-94531] p 63 N89-24691
- SENIN, B. V.**
The use of a lineament-analysis instrument for investigations of tectonic zonality and the elements of continental-margin geodynamics as applied to western Arctic p 49 A89-34010
- SEZNEC, OLIVIER**
Automated extraction of absorption features from Airborne Visible/Infrared Imaging Spectrometer (AVIRIS) and Geophysical and Environmental Research Imaging Spectrometer (GERIS) data p 39 N89-22160
- SHAHROKHI, FIROUZ**
Mapping of Landsat satellite and gravity lineaments in west Tennessee p 6 A89-34357
- SHANNON, JACK D.**
The relationship between in-lake sulfate concentration and estimates of atmospheric sulfur deposition for subregions of the eastern lake survey [DE89-009868] p 5 N89-24749
- SHANNON, PATRICK J.**
Landsat interpretation and stratigraphy of the Hugoton gas field (Southwestern Kansas) and surrounding areas p 6 A89-35856
- SHATALOV, N. N.**
Use of aerial and space photography for the detection of faults and neotectonic movements in Crimea and the Azov Coastal Region p 9 A89-34003
- SHEA, VALOIS R.**
Lineament analysis for hazard assessment in advance of coal mining p 11 A89-35873
- SHEAFFER, JOHN D.**
Mesoscale severe weather development under orographic influences [AD-A205082] p 41 N89-22293
- SHEMA, RICHARD A.**
Correlation between satellite-derived aerosol characteristics and oceanic dimethylsulfide (DMS) [AD-A206179] p 6 N89-24759
- SHIBASAKI, RYOSUKE**
A semi-automatic terrain measurement system for earthwork control p 28 A89-39094
- SHIBAYAMA, MICHIO**
Seasonal visible, near-infrared and mid-infrared spectra of rice canopies in relation to LAI and above-ground dry phytomass p 54 A89-38967
- SHILO, S. A.**
Parameter optimization of systems for the thermal microwave mapping of the earth's surface p 25 A89-37321
- SHIUTTE, N. M.**
Properties of the equatorial and tropical ionosphere according to Soviet satellite observations during the IMS p 31 A89-40606
- SIACHINOV, V. I.**
The spectrometer of the Salyut-7 orbital station p 57 A89-42608
- SIEBER, A. J.**
Imaging radar applications in Europe. Illustrated experimental results (1978-1987) [ESA-TM-01] p 42 N89-22978
- SIMONETT, DAVID S.**
Improvement and extension of a radar forest backscattering model [NASA-CR-184975] p 46 N89-24686
- SIMONOV, I. G.**
Space geography. Investigations on test regions p 31 A89-40491
- SIROIS, J.**
Reflectance enhancements for the Thematic Mapper - An efficient way to produce images of consistently high quality p 26 A89-37947
- SISCOE, G. L.**
Polar cap deflation during magnetospheric substorms p 24 A89-36704
- SISKIND, DAVID ERIC**
The response of thermospheric nitric oxide to an auroral storm p 42 N89-23031
- SKAGSETH, OEASTEIN**
NOAA (National Oceanic and Atmospheric Administration) AVHRR (Advanced Very High Resolution Radiometer) observations during the marginal ice zone experiment, between Spitzbergen and Greenland, June 7 to 18 July 1984 [AD-A204911] p 19 N89-22280
- SKOBELEV, S. F.**
Methods for investigating seismically active zones using remote imagery p 20 A89-34013
- SKUBLOVA, N. V.**
Ore-bearing structures of Central Kazakhstan identified on aerial and space photographs in the framework of the computer-aided prediction of minerals p 52 A89-37316
- SLANEY, V. R.**
Synthetic Aperture Radar data for mapping subsurface geological structures in the Northwest Territories, Canada p 50 A89-35858
- SLATER, PHILIP N.**
Surface reflectance factor retrieval from Thematic Mapper data p 49 A89-33871
- SMIRNOVA, L. A.**
Highly sensitive microwave radiometer-scatterometer for the remote sensing of the earth's surface p 52 A89-37322
- SMITH, J. A.**
Modeling directional thermal radiance from a forest canopy p 27 A89-38972
- SMITH, KAYNE**
Topographic analysis of the Andean Highlands using the Large Format Camera p 7 A89-35880
- SMITH, W. L.**
Reconstruction of imagery of faulted landscapes using a photo-optical technique p 24 A89-35900
- SMORENBURG, C.**
Phase A study for the extension of the CAESAR scanner with a sensor module for the far infrared [BCRS-88-09] p 59 N89-20539
- SNEDDON, J.**
Close-range photogrammetric measurement of erosion in coarse-grained soils p 54 A89-39098
- SODERBLOM, LAURENCE A.**
Radiometric performance of AVIRIS: Assessment for an arid region geologic target p 39 N89-22157
- SOLOMATIN, M. E.**
Multispectral space surveys and data processing p 22 A89-35684
- SOLOVEVA, L. I.**
The potential use of remote sensing to solve problems of paleotectonic prediction, geologic structure, and exploitation of coal deposits with reference to the Moscow-Region coal basin p 49 A89-34002
- SONNE, BERND**
Hybrid cartographic data processing in a geographic information system p 44 N89-23954
- SOROKEVICH, I. S.**
Coordinate referencing of a TV image in the case of the remote sensing of the earth p 53 A89-37492
- SOVERS, O. J.**
Observation model and parameter partials for the JPL geodetic GPS modeling software GPSOMC [NASA-CR-185021] p 9 N89-24060
- SPATZ, DAVID M.**
Discriminating late volcanic differentiates commonly associated with precious metal deposits, using Landsat Thematic Mapper imagery p 12 A89-35896
- SPEIRER, ROBERT A.**
Lineament analysis for hazard assessment in advance of coal mining p 11 A89-35873
- SPENCE, H. E.**
Comparison of field-aligned currents at ionospheric and magnetospheric altitudes p 9 A89-33540
- SPENCER, ROY W.**
Precipitation retrieval over land and ocean with the SSM/I - Identification and characteristics of the scattering signal p 53 A89-37549
- STAR, JEFFREY L.**
Knowledge-based image data management - An expert front-end for the BROWSE facility p 32 A89-41158
- STAYLOR, W. FRANK**
Remote sensing information sciences research group: Browse in the EOS era [NASA-CR-184637] p 42 N89-22979
- STEARN, D. W.**
The contribution of remote sensing data to exploration of fractured reservoirs p 50 A89-35862
- STEARN, RICHARD G.**
Mapping of Landsat satellite and gravity lineaments in west Tennessee p 6 A89-34357
- STIVERS, MARK E.**
The application of high resolution digital elevation models to petroleum and mineral exploration and production p 22 A89-35876
- STOGRYN, ALEX**
Mesospheric temperature sounding with microwave radiometers p 54 A89-39557
- STOHL, L. PAUL**
Photogeologic-geomorphic mapping provides clues to structural features beneath glacial terrain p 7 A89-35882
- STOLZ, A.**
Rate of change of the Quincy-Monument Peak baseline from a translocation analysis of Lageos laser range data p 13 A89-42181
- STOMS, DAVID M.**
Knowledge-based image data management - An expert front-end for the BROWSE facility p 32 A89-41158
- STOWELL, J. L.**
Operational aspects of CASA UNO '88-The first large scale international GPS geodetic network p 7 A89-42787
- STRAHLER, ALAN H.**
Autocorrelation and regularization in digital images. II - Simple image models p 29 A89-39551
- STRONG, A. E.**
Greater global warming revealed by satellite-derived sea-surface-temperature trends p 16 A89-37571
- STUMPF, RICHARD P.**
Ice cover on Chesapeake Bay from AVHRR (Advanced Very High Resolution Radiometer) and LANDSAT imagery, winter of 1987-88 [PB89-117261] p 59 N89-21415
- STYSLOVICH, P. B.**
Analysis of the potential of using space photographic data obtained with the PKF-1K camera to solve scientific, economic, and educational-methodological problems p 64 A89-35685
- SUEMNICH, K.-H.**
Multichannel spectrometer MKS-M - Laboratory tests, calibration, and verification of its stability in flight p 57 A89-42609
- SUGAVANAM, E. B.**
Structural patterns in high grade terrain in parts of Tamil Nadu and Karnataka p 14 N89-22255
- SULZER, M. P.**
Spacelab 2 Upper Atmospheric Modification Experiment over Arecibo. II - Plasma dynamics p 4 A89-38897
- SUMI, AKIMASA**
Short-period fluctuation of the lower tropospheric winds observed by MU-radar p 58 A89-43311
- SURESH, R.**
Effect of metal stress on the thermal infrared emission of soybeans: A greenhouse experiment - Possible utility in remote sensing p 2 A89-39658
- SURSKII, K. O.**
Remote four-photon Raman spectroscopy of sea water under natural conditions p 52 A89-37327
- SWANBERG, NANCY A.**
AVIRIS data quality for coniferous canopy chemistry p 40 N89-22164
- SWANSON, DONALD C.**
Landsat interpretation and stratigraphy of the Hugoton gas field (Southwestern Kansas) and surrounding areas p 6 A89-35856
- SWARTZ, W. E.**
Spacelab 2 Upper Atmospheric Modification Experiment over Arecibo. II - Plasma dynamics p 4 A89-38897
- SWAYZE, GREGG A.**
Calibration and evaluation of AVIRIS data: Cripple Creek in October 1987 p 39 N89-22159

T

- TADZHIEV, T. T.**
A technique for applying space photographs to search for anticlinal oil- and gas-traps in orogenic structures of the Tien-Shan p 25 A89-37318
- TAKAHASHI, K.**
Some aspects of the relation between Pi 1-2 magnetic pulsations observed at L = 1.3-2.1 on the ground and substorm-associated magnetic field variations in the near-earth magnetotail observed by AMPTE CCE p 52 A89-36686
- TAKAHASHI, YUKIO**
The baseline length changes of circumpacific VLBI networks and their bearing on global tectonics p 13 A89-42795
- TAPPER, G. O.**
MEIS II and surface data integration for detection of geobotanical anomalies p 51 A89-35891
- TARANIK, DAN L.**
Preliminary analysis of Airborne Visible/Infrared Imaging Spectrometer (AVIRIS) for mineralogic mapping at sites in Nevada and Colorado p 60 N89-22161

TARANIK, JAMES V.

TARANIK, JAMES V.

Discriminating late volcanic differentiates commonly associated with precious metal deposits, using Landsat Thematic Mapper imagery p 12 A89-35896

TASHKHODZHAIEV, D. A.

A technique for applying space photographs to search for anticlinal oil- and gas-traps in orogenic structures of the Tien-Shan p 25 A89-37318

TATTELMAN, PAUL

Drop-size distributions associated with intense rainfall p 50 A89-34876

TEVELEV, A. V.

Dynamics of present-day geological processes from remotely sensed data p 9 A89-34004

THOMAS, I. L.

Applications of AVHRR data; Proceedings of the Third European AVHRR Data Users' Meeting, University of Oxford, England, Dec. 16-18, 1987 p 55 A89-40126

THOMPSON, KEITH

High resolution imaging of geobotanical anomalies associated with subsurface hydrocarbons p 22 A89-35870

THOMPSON, VIRGINIA

Digital display of SPOT stereo images p 24 A89-35903

THUNNISSEN, H. A. M.

Land use inventory using LANDSAT Thematic Mapper imagery to study environmental pollution [NLR-MP-87063-U] p 4 A89-20541

THYER, N. H.

High altitude laser ranging over rugged terrain p 54 A89-39092

TILTON, JAMES C.

Data compression experiments with LANDSAT thematic mapper and Nimbus-7 coastal zone color scanner data p 41 A89-22344

TISHCHENKO, ARTUR A.

Space coloristics p 35 A89-43024

TOMLINSON, W. D.

Use of seabottom magnetic susceptibility measurements in hydrocarbon exploration p 16 A89-35864

TORCOLETTI, PAUL J.

A Landsat Thematic Mapper investigation of the geobotanical relationships in the northern spruce-fir forest, Mt. Moosilauke, New Hampshire p 2 A89-35894

TORSON, JAMES M.

Radiometric performance of AVIRIS: Assessment for an arid region geologic target p 39 A89-22157

TREES, CHARLES C.

Biophysical variability in the Greenland Sea observed with the Multispectral Airborne Radiometer System (MARS) [NASA-CR-184856] p 47 A89-24784

TRESHCHOV, A. A.

Identification of tectonic dislocations underneath large water areas using space images p 15 A89-34011

TRIFONOV, V. G.

Remote-sensing studies of present-day tectonic processes p 20 A89-34001
Methods for investigating seismically active zones using remote imagery p 20 A89-34013

TRIVEDI, MOHAN M.

Representation and recognition of elongated regions in aerial images p 19 A89-33684

TROFIMOV, D. M.

The potential use of remote sensing to solve problems of paleotectonic prediction, geologic structure, and exploitation of coal deposits with reference to the Moscow-Region coal basin p 49 A89-34002
The definition of isometric magmatogenic structures on space imagery p 12 A89-37315

TSANG, LEUNG

Sea-ice characterization measurements needed for testing of microwave remote sensing models p 20 A89-34268

TSIMMERMAN, G.

Remote measurements from Salyut-7 of the optical parameters of the atmosphere-surface system p 57 A89-42601

TSUCHIYA, KIYOSHI

Development and verification of Osaka Bay sampling model based on Landsat data p 27 A89-38332
Discrimination of rocks and hydrothermal altered areas based on Landsat TM data p 27 A89-38333

TUCKER, C. J.

AVHRR for monitoring global tropical deforestation p 56 A89-40152

TURNER, JAMES A.

Applying remote sensing technology to the Bureau of Land Management's mineral management program p 11 A89-35874

TURNER, PATRICIA A.

Lithologic mapping in East Greenland with Landsat Thematic Mapper imagery p 6 A89-35869

TURNER, RUDOLPH A. M.

Short- and long-term memory effects in intensified array detectors - Influence on airborne laser fluorosensor measurements p 47 A89-32836

U

UENO, S.

Atmospheric correction of satellite MSS data in rugged terrain p 27 A89-38334

ULABY, F. T.

Mapping freeze/thaw boundaries with SMMR data [NASA-CR-184991] p 9 A89-23961

URBAN, STEPHANIE B.

From large-scale to small-scale - Economic geologic-geomorphic mapping using aerial photographs and Landsat images p 7 A89-35884

USERY, E. LYNN

A raster approach to topographic map revision p 26 A89-37946

USTIN, SUSAN L.

AVIRIS spectra of California wetlands p 3 A89-22167

V

VAN DER ZEE, DICK

Rural settlement expansion in Moneragala district, Sri Lanka p 4 A89-34946
Monitoring in Moneragala district, Sri Lanka, with SPOT images p 3 A89-43317

VAN HEIST, MIRIAM

Monitoring Tunisia's steppes with SPOT p 35 A89-43316

VAN WIJNGAARDEN, WILLEM

Monitoring Tunisia's steppes with SPOT p 35 A89-43316

VAN ZYL, JAKOB J.

Modeling and observation of the radar polarization signature of forested areas p 2 A89-39554

VANDERLAAN, F. B.

The suitability of remote sensing for surveying and monitoring landscape patterns. Volume B: PEPS Project No. 73 - SPOT imagery p 36 A89-20536
A systematic worldwide landcover of satellite mosaics [NLR-MP-87062-U] p 65 A89-20540
Land use inventory using LANDSAT Thematic Mapper imagery to study environmental pollution [NLR-MP-87063-U] p 4 A89-20541
Twelve year overview of cloudfree LANDSAT imagery of The Netherlands [NLR-MP-87072-U] p 59 A89-20542

VANDERMOLEN, GEERT

Investigation of several methods for the detection of outstanding points in a digital image [ETN-89-94148] p 45 A89-23965

VANDERPIEPEN, H.

DFVLR activities related to imaging spectrometry p 63 A89-24697

VANE, GREGG

Proceedings of the Airborne Visible/Infrared Imaging Spectrometer (AVIRIS) Performance Evaluation Workshop [NASA-CR-184870] p 59 A89-22154
AVIRIS performance during the 1987 flight season: An AVIRIS project assessment and summary of the NASA-sponsored performance evaluation p 60 A89-22155

Atmospheric water mapping with the Airborne Visible/Infrared Imaging Spectrometer (AVIRIS), Mountain Pass, California p 39 A89-22156

Determination of in-flight AVIRIS spectral, radiometric, spatial and signal-to-noise characteristics using atmospheric and surface measurements from the vicinity of the rare-earth-bearing carbonatite at Mountain Pass, California p 61 A89-22170

VASIUTIN, VLADIMIR V.

Space coloristics p 35 A89-43024

VELDEN, CHRISTOPHER S.

Observational analyses of North Atlantic tropical cyclones from NOAA polar-orbiting satellite microwave data p 21 A89-34879

VENKATRAMI REDDY, Y.

Sea surface spectrum from aerial photographs - Laboratory model studies p 30 A89-39674

VENSLAVSKII, V. B.

Highly sensitive microwave radiometer-scatterometer for the remote sensing of the earth's surface p 52 A89-37322

VENUGOPAL, G.

Area sensitivity and feature sensitivity of SPOT 1 data - A statistical analysis p 32 A89-41154
The application of SPOT ratio data for soil classification p 56 A89-41165

VERGO, N.

Visible and near-infrared (0.4- to 2.5-microns) reflectance spectra of selected mixed-layer clays and related minerals p 12 A89-35897

VERKHOVTSSEV, V. G.

Use of aerial and space photography for the detection of faults and neotectonic movements in Crimea and the Azov Coastal Region p 9 A89-34003

VERMANDE, P.

Activities of CNES in the field of imaging spectrometry p 47 A89-24699

VEROSUB, KENNETH L.

Kinematics at the intersection of the Garlock and Death Valley fault zones, California: Integration of TM data and field studies [NASA-CR-184854] p 15 A89-22263

VERWAAL, RUUD G.

The search for edges in remote sensing images using a digital polygonal map [ETN-89-94146] p 45 A89-23964

VIDAL-MADJAR, D.

C-band radar cross section of the Guyana rain forest - Possible use as a reference target for spaceborne radars p 49 A89-33869

VIDYADHARAN, K. T.

Structural patterns in high grade terrain in parts of Tamil Nadu and Karnataka p 14 A89-22255

VIEHOFF, THOMAS

Mesoscale variability of sea surface temperature in the North Atlantic p 17 A89-40145

VINCENT, M. A.

Rate of change of the Quincy-Monument Peak baseline from a translocation analysis of Lagoos laser range data p 13 A89-42181

VINCENT, ROBERT K.

The application of high resolution digital elevation models to petroleum and mineral exploration and production p 22 A89-35876

VINCENZI, S.

Mean temperature in a closed basin by remote sensing p 16 A89-39062

VLASOV, D. V.

The dispersion limitations on the accuracy of the internal reference method during remote laser sounding of the upper ocean layer p 53 A89-37349
Determination of spectral signatures for remote laser sensing of vegetation p 35 A89-20541

VOEGTLE, T.

Research for optimization of future MOMS sensors [ETN-89-94424] p 62 A89-23972

VOGT, JUERGEN

Monitoring the halfa steppes of central Tunisia using Landsat MSS p 1 A89-34947

VON LOH, JAMES D.

The use of remote sensing and GIS techniques for wetland identification and classification in the Garrison Diversion Unit-North Dakota p 18 A89-41160

VOROZHEIKIN, A. P.

Analysis of the potential of using space photographic data obtained with the PKF-1K camera to solve scientific, economic, and educational-methodological problems p 64 A89-35685

VORSIN, N. N.

Highly sensitive microwave radiometer-scatterometer for the remote sensing of the earth's surface p 52 A89-37322

VOVOR, KWAMI

Satellite detection of Saharan dust - Optimized imaging during nighttime p 24 A89-35912

W

WADGE, G.

Identification and analysis of the alignments of point-like features in remotely-sensed imagery. Volcanic cones in the Pinacate Volcanic Field, Mexico p 12 A89-39651

WALKER, HOYT

Use of the 1:2,000,000 Digital Line Graph data in emergency response [DE89-006730] p 44 A89-23959

WALKER, R. J.

Comparison of field-aligned currents at ionospheric and magnetospheric altitudes p 9 A89-33540

WALSH, JOHN E.

Sensitivity of 30-day dynamical forecasts to continental snow cover p 17 A89-35937

WAN, ZHENGMING

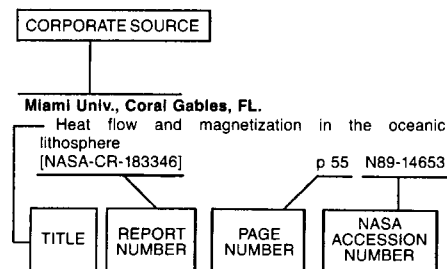
Land-surface temperature measurement from space - Physical principles and inverse modeling p 29 A89-39552

WANG, PI-HUAN

The investigation of advanced remote sensing, radiative transfer and inversion techniques for the measurement of atmospheric constituents [NASA-CR-172599] p 36 A89-20531

- WANG, YONG**
Improvement and extension of a radar forest backscattering model
[NASA-CR-184975] p 46 N89-24686
- WANG, ZHIGANG**
Derivation of a geomagnetic model to $n = 63$
p 58 A89-43409
The geomagnetic spectrum for 1980 and core-crustal separation p 13 A89-43410
- WASH, CARLYLE H.**
Meteorological applications of Space Shuttle photography p 34 A89-41430
- WATKINS, M. M.**
Rate of change of the Quincy-Monument Peak baseline from a translocation analysis of Lageos laser range data p 13 A89-42181
- WEARE, BRYAN C.**
A comparison of radiation variables calculated in the UCLA general circulation model to observations p 24 A89-35926
- WEATHERSBY, MARSHALL R.**
Multispectral image processing and enhancement; Proceedings of the Meeting, Orlando, FL, Apr. 6-8, 1988 [SPIE-933] p 48 A89-33653
- WEBER, EDWARD J.**
Satellite, airborne and radar observations of auroral arcs p 48 A89-33505
- WEERAKKODY, UPALI**
Mapping coastal evolution in Sri Lanka using aerial photographs p 6 A89-34948
- WEICHMAN, PETER B.**
Statistical geometry of a small surface patch in a developed sea p 26 A89-37808
- WEIDNER, J. R.**
Effect of metal stress on the thermal infrared emission of soybeans: A greenhouse experiment - Possible utility in remote sensing p 2 A89-39658
- WEINBERG, MICHAEL**
Multispectral terrain background simulation techniques for use in airborne sensor evaluation p 19 A89-33664
- WEISBRICH, W.**
Research for optimization of future MOMS sensors [ETN-89-94424] p 62 N89-23972
- WELCH, R.**
A raster approach to topographic map revision p 26 A89-37946
- WEN, BOHENG**
Sea-ice characterization measurements needed for testing of microwave remote sensing models p 20 A89-34268
- WENRICH, KAREN J.**
Application of Landsat Thematic Mapper digital data to the exploration for uranium-mineralized breccia pipes in Northwestern Arizona p 51 A89-35872
- WEST, RICHARD**
Sea-ice characterization measurements needed for testing of microwave remote sensing models p 20 A89-34268
- WETTERQVIST, ORJAN F.**
Comparison of satellite, ground-based, and modeling techniques for analyzing the urban heat island p 26 A89-37948
- WHITEHEAD, VICTOR S.**
Earth scenes in polarized light observed from the Space Shuttle p 34 A89-41429
- WIART, RAOUL J.**
Cluster analysis of pine crown foliage patterns aid identification of mountain pine beetle current-attack p 26 A89-37950
- WILLIAMS, C. P.**
Landsat commercialization - Keys to future success p 64 A89-34703
- WILLIAMS, J. C.**
Gas chromatographic and sonar imaging of hydrocarbon seeps in the marine environment p 22 A89-35863
- WILLIAMS, T. H. LEE**
A survey of the operational status and needs of remote sensing in exploration geology p 64 A89-35853
Digital display of SPOT stereo images p 24 A89-35903
- WILLIAMSON, H. D.**
The discrimination of irrigated orchard and vine crops using remotely sensed data p 2 A89-37949
- WILLIS, PAUL T.**
Drop-size distributions associated with intense rainfall p 50 A89-34876
- WINEBRENNER, DALE P.**
Sea-ice characterization measurements needed for testing of microwave remote sensing models p 20 A89-34268
- WINNINGHAM, J. D.**
Polar cap deflation during magnetospheric substorms p 24 A89-36704
- WOHLERS, RONALD**
Multispectral terrain background simulation techniques for use in airborne sensor evaluation p 19 A89-33664
- WOLLENWEBER, F. G.**
Infrared sea-radiance modeling using LOWTRAN 6 [AD-A202582] p 38 N89-21643
- WOOD, C. A.**
Volcano monitoring by short wavelength infrared satellite remote sensing p 51 A89-35875
- WOOD, CHARLES A.**
Astronaut photography of the earth - Low cost images for resource exploration p 23 A89-35883
Geologic applications of Space Shuttle photography p 34 A89-41431
- WOODCOCK, CURTIS E.**
Autocorrelation and regularization in digital images. II - Simple image models p 29 A89-39551
- WOODING, M. G.**
Imaging radar applications in Europe. Illustrated experimental results (1978-1987) [ESA-TM-01] p 42 N89-22978
- WRIGHT, J. A.**
Imaging of ocean waves by SAR [AD-A203604] p 37 N89-21165
- WUKELIC, G. E.**
Application of Landsat Thematic Mapper data for coastal thermal plume analysis at Diablo Canyon p 35 A89-42175
- WULLSTEIN, L. H.**
A closer look at the Patrick Draw oil field vegetation anomaly p 1 A89-35893
- Y**
- YAMAGAMI, TAKAMASA**
ARGOS system used for balloon observations p 53 A89-38290
- YAMAGUCHI, YASUSHI**
Spectral indices for vegetation and rock type discrimination using the optical sensor of the Japanese ERS-1 p 51 A89-35866
- YAMASHITA, YOICHIRO**
High resolution imaging of geobotanical anomalies associated with subsurface hydrocarbons p 22 A89-35870
- YAMAUCHI, M.**
The interplanetary magnetic field $B(y)$ -dependent field-aligned current in the dayside polar cap under quiet conditions p 50 A89-34782
- YANG, JUN**
Automatic extraction of areas from overlays of the series DGK 5 (Bo) p 44 N89-23955
- YANG, SHIREN**
Two-dimensional seam-point searching in digital image mosaicking p 26 A89-37945
- YANG, WEI-LIANG**
Image-analysis techniques for determination of morphology and kinematics in arctic sea ice p 21 A89-34416
- YOSHITOMI, SUSUMU**
Marine Observation Satellite-1 - First year in orbit p 26 A89-38328
- YOUNG, D. T.**
GEOS 1 observations of low-energy ions in the earth's plasmasphere - A study on composition, and temperature and density structure under quiet geomagnetic conditions p 9 A89-33829
- YUAN, BENFAN**
Surface reflectance factor retrieval from Thematic Mapper data p 49 A89-33871
- YUMOTO, K.**
Some aspects of the relation between Pi 1-2 magnetic pulsations observed at $L = 1.3-2.1$ on the ground and substorm-associated magnetic field variations in the near-earth magnetotail observed by AMPTE CCE p 52 A89-36686
- Z**
- ZAMARAEV, N. N.**
The use of space imagery for investigations of recent crustal deformations in southern Yakutia p 20 A89-34015
- ZANTOP, HALF**
A field spectrometer and remote sensing study of the Fresno mining district, Mexico p 51 A89-35871
- ZAVODY, A. M.**
Theoretical algorithms for satellite-derived sea surface temperatures p 21 A89-35159
- ZEBKER, HOWARD A.**
Modeling and observation of the radar polarization signature of forested areas p 2 A89-39554
- ZHOU, QIMING**
A method for integrating remote sensing and geographic information systems p 28 A89-39097
- ZHUMANOV, KH. A.**
Remote four-photon Raman spectroscopy of sea water under natural conditions p 52 A89-37327
- ZIMMERMANN, G.**
The spectrometer of the Salyut-7 orbital station p 57 A89-42608
- ZINK, M.**
Research on speckle behavior in SAR images p 21 A89-35335
- ZLATOPOL'SKII, A. A.**
Automated analysis of lineaments from space imagery obtained during seismic studies of central Tien-Shan p 20 A89-34014
- ZLOTNICKI, VICTOR**
Observing oceanic mesoscale eddies from Geosat altimetry - Preliminary results p 16 A89-39372
- ZOBECK, TED M.**
Impulse radar for identification of features in soils p 50 A89-34353
- ZUERNDORFER, B. W.**
Mapping freeze/thaw boundaries with SMMR data [NASA-CR-184991] p 9 N89-23961
- ZWAIN, JAWAD A.**
Geological application of SIR-A imagery in southern Iraq p 13 A89-41162
Structural analysis of fracturing in Sinjar anticline using remote sensing technique p 13 A89-41167

Typical Corporate Source Index Listing



Listings in this index are arranged alphabetically by corporate source. The title of the document is used to provide a brief description of the subject matter. The page number and the accession number are included in each entry to assist the user in locating the abstract in the abstract section. If applicable, a report number is also included as an aid in identifying the document.

A

Academia Sinica, Beijing (China).

Land-surface temperature measurement from space - Physical principles and inverse modeling p 29 A89-39552

Aerospatiale, Cannes La Bocca (France).

The advanced Ocean Chlorophyll Meter (OCM). A spectral imaging device for the observation of the oceans [REPT-882-440-118] p 63 N89-24689

Agricultural Research Service, Beltsville, MD.

Effect of metal stress on the thermal infrared emission of soybeans: A greenhouse experiment - Possible utility in remote sensing p 2 A89-39658

Air Force Inst. of Tech., Wright-Patterson AFB, OH.

An analysis of platinum silicide and indium antimonide for remote sensors in the 3 to 5 micrometer wavelength band [AD-A202663] p 59 N89-21218

A software system to create a hierarchical, multiple level of detail terrain model [AD-A203047] p 38 N89-21568

Use of commercial satellite imagery for surveillance of the Canadian north by the Canadian armed forces [AD-A202700] p 40 N89-22173

Alabama Univ., Huntsville.

Precipitation retrieval over land and ocean with the SSM/I - Identification and characteristics of the scattering signal p 53 A89-37549

Alaska Univ., Fairbanks.

Remote sensing of global snowpack energy and mass balance: In-situ measurements on the snow of interior and Arctic Alaska [NASA-CR-180078] p 62 N89-23956

Arecibo Ionospheric Observatory, Puerto Rico.

Spacelab 2 Upper Atmospheric Modification Experiment over Arecibo. II - Plasma dynamics p 4 A89-38897

Argonne National Lab., IL.

The relationship between in-lake sulfate concentration and estimates of atmospheric sulfur deposition for subregions of the eastern lake survey [DE89-009868] p 5 N89-24749

Arizona Univ., Tucson.

Surface reflectance factor retrieval from Thematic Mapper data p 49 A89-33871
Evaluating atmospheric correction models for retrieving surface temperatures from the AVHRR over a tallgrass prairie p 20 A89-33875

Army Cold Regions Research and Engineering Lab., Hanover, NH.

Snowmelt increase through albedo reduction [AD-A204523] p 18 N89-22175

Army Engineer Topographic Labs., Fort Belvoir, VA.

Computer strategy for detecting line features on simulated binary arrays in support of radar feature extraction [AD-A203257] p 37 N89-21162

Army Engineer Waterways Experiment Station, Vicksburg, MS.

The KP equation: A comparison to laboratory generated bi-periodic waves p 38 N89-21507
Column movement model used to support AMM p 38 N89-21521

Army Research Inst. Field Unit, Fort Huachuca, AZ.

The precedence of global features in the perception of map symbols [AD-A203792] p 7 N89-22174

Army Research Inst. for the Behavioral and Social Sciences, Alexandria, VA.

The precedence of global features in the perception of map symbols [AD-A203792] p 7 N89-22174

B

Beleidscommissie Remote Sensing, Delft (Netherlands).

The suitability of remote sensing for surveying and monitoring landscape patterns. Volume A: Pilot study - LANDSAT Imagery. Volume B: PEPS Project No. 73 - SPOT Imagery [BCRS-87-12-VOL-A/B] p 4 N89-20534

The suitability of remote sensing for surveying and monitoring landscape patterns. Volume A: Pilot study - LANDSAT Imagery p 36 N89-20535

The suitability of remote sensing for surveying and monitoring landscape patterns. Volume B: PEPS Project No. 73 - SPOT Imagery p 36 N89-20536

Land use inventories using satellite images in the region Haaren-Helvoirt-Udenhout, North Brabant (The Netherlands) [BCRS-88-07] p 36 N89-20537

Processing and application of digital AVHRR-imagery for land and sea surfaces [BCRS-88-08] p 36 N89-20538

Phase A study for the extension of the CAESAR scanner with a sensor module for the far infrared [BCRS-88-09] p 59 N89-20539

On the international commercialization of remote sensing [BCRS-88-02] p 65 N89-23969

Meteosat thermal inertia mapping for studying wetland dynamics in the West-African Sahel [BCRS-88-10A] p 62 N89-23970

Thermal analysis for the monitoring and prediction of flood dynamics in wetlands [BCRS-88-10B] p 46 N89-23971

Boston Univ., MA.

Autocorrelation and regularization in digital images. II - Simple image models p 29 A89-39551

Brown Univ., Providence, RI.

Application of imaging spectrometer data to the Kings-Kaweah ophiolite melange p 40 N89-22166

C

California Inst. of Tech., Pasadena.

Statistical geometry of a small surface patch in a developed sea p 26 A89-37808

An assessment of AVIRIS data for hydrothermal alteration mapping in the Goldfield Mining District, Nevada p 40 N89-22168

California Univ., Berkeley.

AVIRIS spectra of California wetlands p 3 N89-22167

California Univ., Davis.

Earth scenes in polarized light observed from the Space Shuttle p 34 A89-41429

Kinematics at the intersection of the Garlock and Death Valley fault zones, California: Integration of TM data and field studies [NASA-CR-184854] p 15 N89-22263

California Univ., Los Angeles.

Comparison of field-aligned currents at ionospheric and magnetospheric altitudes p 9 A89-33540

Polar cap deflation during magnetospheric substorms p 24 A89-36704

California Univ., Santa Barbara.

Land-surface temperature measurement from space - Physical principles and inverse modeling p 29 A89-39552

Knowledge-based image data management - An expert front-end for the BROWSE facility p 32 A89-41158

Remote sensing information sciences research group: Browse in the EOS era [NASA-CR-184637] p 42 N89-22979

Improvement and extension of a radar forest backscattering model [NASA-CR-184975] p 46 N89-24686

Canada Centre for Remote Sensing, Ottawa (Ontario).

Imaging spectrometry at the Canada Centre for Remote Sensing p 64 N89-24701

Carnegie-Mellon Univ., Pittsburgh, PA.

Cooperative methods for road tracking in aerial imagery p 42 N89-23101

Centre National d'Etudes Spatiales, Toulouse (France).

Activities of CNES in the field of imaging spectrometry p 47 N89-24699

City Coll. of the City Univ. of New York, NY.

Probabilities and statistics for backscatter estimates obtained by a scatterometer with applications to new scatterometer design data [NASA-CR-4228] p 61 N89-22779

Colorado State Univ., Fort Collins.

Mesoscale severe weather development under orographic influences [AD-A205082] p 41 N89-22293

Colorado Univ., Boulder.

Variation of surface water spectral response as a function of in situ sampling technique p 33 A89-41161

Automated extraction of absorption features from Airborne Visible/Infrared Imaging Spectrometer (AVIRIS) and Geophysical and Environmental Research Imaging Spectrometer (GERIS) data p 39 N89-22160

Preliminary analysis of Airborne Visible/Infrared Imaging Spectrometer (AVIRIS) for mineralogic mapping at sites in Nevada and Colorado p 60 N89-22161

The response of thermospheric nitric oxide to an auroral storm p 42 N89-23031

Columbia Univ., New York, NY.

Global, seasonal surface variations from satellite radiance measurements p 52 A89-35966

Commission of the European Communities, Ispra (Italy).

AVHRR for monitoring global tropical deforestation p 56 A89-40152

Commonwealth Scientific and Industrial Research Organization, Canberra (Australia).

Autocorrelation and regularization in digital images. II - Simple image models p 29 A89-39551

Cornell Univ., Ithaca, NY.

Spacelab 2 Upper Atmospheric Modification Experiment over Arecibo. II - Plasma dynamics p 4 A89-38897

D

Dartmouth Coll., Hanover, NH.

A Landsat Thematic Mapper investigation of the geobotanical relationships in the northern spruce-fir forest, Mt. Moosilauke, New Hampshire p 2 A89-35894

Defence Research Establishment Pacific, Victoria (British Columbia).

OSRMS (Ocean Surface Roughness Measurement System): The DREP (Defence Research Establishment Pacific) near-nadir scatterometer [AD-A202983] p 38 N89-21460

Delaware Univ., Newark.

AVIRIS spectra of California wetlands p 3 N89-22167

Department of Agriculture, Beltsville, MD.

A new technique to measure the spectral properties of conifer needles p 19 A89-33874

Desert Research Inst., Reno, NV.

Examination of the spectral features of vegetation in 1987 AVIRIS data p 3 N89-22163

Deutsche Forschungs- und Versuchsanstalt fuer Luft- und Raumfahrt, Oberpfaffenhofen (West Germany).

Necessity and benefit of the X-SAR space shuttle experiment [DFVLR-MITT-88-29] p 63 N89-24688

DFVLR activities related to imaging spectrometry p 63 N89-24697

The EARSSEL Imaging Spectrometry Working Group p 47 N89-24700

Deutsche Geodaetische Kommission, Munich (Germany, F.R.).

Analysis and optimization of geodetic networks by spectral criteria and mechanical analogies [SER-C-342] p 45 N89-23963

DHV Raadgevend Ingenieursbureau B.V., Amersfoort (Netherlands).

Land use inventories using satellite images in the region Haaren-Helvoirt-Udenhout, North Brabant (The Netherlands) [BCRS-88-07] p 36 N89-20537

On the international commercialization of remote sensing [BCRS-88-02] p 65 N89-23969

Dienst Ruimtelijkeoordening Natuurbeheer, Landschapen Volkshuisvesting (Netherlands).

Land use inventories using satellite images in the region Haaren-Helvoirt-Udenhout, North Brabant (The Netherlands) [BCRS-88-07] p 36 N89-20537

E

EG and G Energy Measurements, Inc., Las Vegas, NV.

Modeling directional thermal radiance from a forest canopy p 27 A89-38972

EUROCONSULT B.V., Arnhem (Netherlands).

On the international commercialization of remote sensing [BCRS-88-02] p 65 N89-23969

European Space Agency, Paris (France).

Imaging radar applications in Europe. Illustrated experimental results (1978-1987) [ESA-TM-01] p 42 N89-22978

Imaging Spectrometry for Land Applications [ESA-SP-1101] p 63 N89-24692

European Space Agency. European Space Research and Technology Center, ESTEC, Noordwijk (Netherlands).

ESA's planned activities in the field of imaging spectrometry for Earth observation p 46 N89-24693

F

Federal Aviation Administration, Atlantic City, NJ.

Loran C field strength contours: Contiguous US [DOT/FAA/CT-TN89/16] p 8 N89-23437

Florida Univ., Gainesville.

Advanced space design program to the Universities Space Research Association and the National Aeronautics and Space Administration [NASA-CR-180450] p 3 N89-24015

Freiburg Univ. (Germany, F.R.).

Derivation of a large-scale map of heat load in the region Freiburg-Basel (Germany, F.R.) using satellite data. A contribution to the production of climate data based on a geographic information system [REPT-27] p 41 N89-22972

G

GEC-Marconi Electronics Ltd., Chelmsford (England).

Theoretical studies for ERS-1 wave mode, volume 1 [GEC-MTR-87/110-VOL-1] p 41 N89-22977

Geological Survey, Denver, CO.

Calibration and evaluation of AVIRIS data: Cripple Creek in October 1987 p 39 N89-22159

Geological Survey, Flagstaff, AZ.

Radiometric performance of AVIRIS: Assessment for an arid region geologic target p 39 N89-22157

Geological Survey, Lansing, MI.

The Calvin 28 cryptoexplosive disturbance, Cass County, Michigan: Evidence for impact origin p 14 N89-21358

Geological Survey, Reston, VA.

Evaluation of Airborne Visible/Infrared Imaging Spectrometer Data of the Mountain Pass, California carbonatite complex p 60 N89-22169

Geological Survey, Sioux Falls, SD.

AVIRIS data characteristics and their effects on spectral discrimination of rocks exposed in the Drum Mountains, Utah: Results of a preliminary study p 40 N89-22165

Geological Survey of Canada, Toronto (Ontario).

Geological remote sensing signatures of terrestrial impact craters p 37 N89-21317
The Frasnian-Famennian mass killing event(s), methods of identification and evaluation p 37 N89-21318

Geological Survey of India, Bangalore.

Structural patterns in high grade terrain in parts of Tamil Nadu and Karnataka p 14 N89-22255

GKSS-Forschungszentrum Geesthacht (Germany, F.R.).

Optical properties of oceanic suspended matter and their interpretation for remote sensing of phytoplankton [GKSS-88/E/40] p 46 N89-24013
Imaging procedure of underwater bottom topography by air and satellite images in the range of microwave and visible electromagnetic spectra [GKSS-88/E/41] p 17 N89-24014

H

Harvard Univ., Cambridge, MA.

Antarctic ozone: Theory and observation p 4 N89-22189

Helsinki Univ. of Technology, Espoo (Finland).

Determination of areal snow water equivalent using satellite images and gamma ray spectrometry [CI-91] p 44 N89-23960

Horton (Forest W., Jr.), Washington, DC.

Information resources management p 42 N89-23371

Hull Univ. (England).

Remote sensing in refractive turbulence p 58 N89-20532

Hydex Corp., Falls Church, VA.

Airborne time-series measurement of soil moisture using terrestrial gamma radiation p 33 A89-41163

I

Industrial Science and Technology Agency, Tokyo (Japan).

Japan's sunshine project 1987 annual summary of geothermal energy R and D [DE88-756451] p 18 N89-22183

Institut fuer Angewandte Geodasie, Frankfurt am Main (Germany, F.R.).

Reports on Cartography and Geodesy. Series 1, number 101 [ISSN-0469-4236] p 8 N89-23941

Definition and filling of information systems: Challenge for a photogrammetric service enterprise p 62 N89-23942

Computer aided production of a 1:25,000 relief model of Berlin and surroundings p 8 N89-23943

The Official Topographic-Cartographic Information System (ATKIS) of the Geodesy Group of the Laender of the Federal Republic of Germany: Status after one year of development p 8 N89-23944

The digital urban map as a basis for a land information system in local administration p 8 N89-23945

Automatic digitizing of cadastral maps p 43 N89-23946

ARC-INFO: A geographic information system p 43 N89-23947

Cartographic signatures in PHOCUS p 43 N89-23948

Digitizing of drawings and cadastral maps using a scanner system p 43 N89-23949

Geocoded data sets of imaging satellites p 43 N89-23950

Computer assisted layout of graphic settlement representations p 43 N89-23951

Tools for the computer assisted generalization of settlements for the construction of digital landscape models p 43 N89-23952

Computer assisted generalization of transport line representations p 43 N89-23953

Hybrid cartographic data processing in a geographic information system p 44 N89-23954

Automatic extraction of areas from overlays of the series DGK 5 (Bo) p 44 N89-23955

Institut National de la Recherche Agronomique, Montfavet (France).

NOAA AVHRR and its uses for rainfall and evapotranspiration monitoring p 56 A89-40151

Institute of Ocean Sciences, Sidney (British Columbia).

Development of an imaging spectrometer for remote sensing: The FLI program p 63 N89-24698

Instituto de Pesquisas Espaciais, Sao Jose dos Campos (Brazil).

Microwave X-band radiometric characterization of Brazilian soils by measurement of the complex permittivity [INPE-4588-PRE/1319] p 3 N89-24685

Interior Dept., Washington, DC.

Geological gyrocompass [PB89-133086] p 63 N89-24589

International Atomic Energy Agency, Vienna (Austria).

Geological data integration techniques: Proceedings [DE88-705255] p 14 N89-20868

J

Jet Propulsion Lab., California Inst. of Tech., Pasadena.

Surface reflectance factor retrieval from Thematic Mapper data p 49 A89-33871

Review and status of remote sensing of sea ice p 20 A89-34266

Image-analysis techniques for determination of morphology and kinematics in arctic sea ice p 21 A89-34416

Seasat A satellite scatterometer measurements of equatorial surface winds p 53 A89-37802

Statistical geometry of a small surface patch in a developed sea p 26 A89-37808

Observing oceanic mesoscale eddies from Geosat altimetry - Preliminary results p 16 A89-39372

Land-surface temperature measurement from space - Physical principles and inverse modeling p 29 A89-39552

Modeling and observation of the radar polarization signature of forested areas p 2 A89-39554

Infrared spectroscopy (2.3-20 microns) for the geological interpretation of remotely-sensed multispectral thermal infrared data p 30 A89-39656

NOAA AVHRR and its uses for rainfall and evapotranspiration monitoring p 56 A89-40151

Rate of change of the Quincy-Monument Peak baseline from a translocation analysis of Lageos laser range data p 13 A89-42181

Operational aspects of CASA UNO '88-The first large scale international GPS geodetic network p 7 A89-42787

Proceedings of the Airborne Visible/Infrared Imaging Spectrometer (AVIRIS) Performance Evaluation Workshop [NASA-CR-184870] p 59 N89-22154

AVIRIS performance during the 1987 flight season: An AVIRIS project assessment and summary of the NASA-sponsored performance evaluation p 60 N89-22155

Atmospheric water mapping with the Airborne Visible/Infrared Imaging Spectrometer (AVIRIS), Mountain Pass, California p 39 N89-22156

Determination of in-flight AVIRIS spectral, radiometric, spatial and signal-to-noise characteristics using atmospheric and surface measurements from the vicinity of the rare-earth-bearing carbonatite at Mountain Pass, California p 61 N89-22170

Environmental projects. Volume 3: Environmental compliance audit [NASA-CR-185019] p 5 N89-23985

Observation model and parameter partials for the JPL geodetic GPS modeling software GPSOMC [NASA-CR-185021] p 9 N89-24060

HIRIS: NASA's high-resolution imaging spectrometer for the Earth Observing System (EOS) p 63 N89-24695

Johns Hopkins Univ., Laurel, MD.

Some aspects of the relation between Pi 1-2 magnetic pulsations observed at L = 1.3-2.1 on the ground and substorm-associated magnetic field variations in the near-earth magnetotail observed by AMPTE CCE p 52 A89-36886

Joint Inst. for Lab. Astrophysics, Boulder, CO.

Rate of change of the Quincy-Monument Peak baseline from a translocation analysis of Lageos laser range data p 13 A89-42181

K

Kansas State Univ., Manhattan.

Measuring and modeling spectral characteristics of a tallgrass prairie p 27 A89-38970

Karlsruhe Univ. (Germany, F.R.).

Research for optimization of future MOMS sensors [ETN-89-94424] p 62 N89-23972

L

La Jolla Inst., CA.

Imaging of ocean waves by SAR [AD-A203604] p 37 N89-21165

Laboratoire de Meteorologie Dynamique du CNRS, Palaiseau (France).

On the future development and management of spectroscopic database for radiative transfer from the issues of recent related workshops [ETN-89-94530] p 46 N89-24690

Refinements in the cloud detection scheme of the 3I system. Comparison with AVHRR products [ETN-89-94531] p 63 N89-24691

Lawrence Livermore National Lab., CA.

Use of the 1:2,000,000 Digital Line Graph data in emergency response [DE89-006730] p 44 N89-23959

Lockheed Engineering and Sciences Co., Houston, TX.

The decrease of Lake Chad as documented during twenty years of manned space flight p 18 A89-41434

Los Alamos National Lab., NM.

Spacelab 2 Upper Atmospheric Modification Experiment over Arecibo. II - Plasma dynamics p 4 A89-38897

Louisiana State Univ., Baton Rouge.

Mapping of Landsat satellite and gravity lineaments in west Tennessee p 6 A89-34357

Utilizing remote sensing of thematic mapper data to improve our understanding of estuarine processes and their influence on the productivity of estuarine-dependent fisheries [NASA-CR-183417] p 18 N89-20533

Lunar and Planetary Inst., Houston, TX.

Measuring thermal budgets of active volcanoes by satellite remote sensing p 9 A89-32988

Volcano monitoring by short wavelength infrared satellite remote sensing p 51 A89-35875

M

Maryland Univ., College Park.

Effect of metal stress on the thermal infrared emission of soybeans: A greenhouse experiment - Possible utility in remote sensing p 2 A89-39658

Massachusetts Inst. of Tech., Cambridge.

Active and passive remote sensing of ice [AD-A203943] p 59 N89-20543

Remote sensing of earth terrain [NASA-CR-184937] p 41 N89-22971

Plate motions and deformations from geologic and geodetic data [NASA-CR-184987] p 15 N89-24757

Max-Planck-Inst. fuer Meteorologie, Hamburg (Germany, F.R.).

Development of a satellite SAR image spectra and altimeter wave height data assimilation system for ERS-1 [NASA-CR-182685] p 61 N89-22975

Miami Univ., Coral Gables, FL.

Aerosol analysis with the Coastal Zone Color Scanner - A simple method for including multiple scattering effects p 25 A89-37291

Miami Univ., FL.

Neotectonics in Central Mexico from LANDSAT TM data [NASA-CR-183416] p 14 N89-21416

Michigan Univ., Ann Arbor.

Mapping freeze/thaw boundaries with SMMR data [NASA-CR-184991] p 9 N89-23961

Estimating population size of Pygoscelid Penguins from TM data [NASA-CR-180081] p 3 N89-24687

Moniteq Ltd., Concord (Ontario).

The FLI airborne imaging spectrometer: A highly versatile sensor for many applications p 63 N89-24694

Montana Univ., Missoula.

Estimation of regional surface resistance to evapotranspiration from NDVI and thermal-IR AVHRR data p 55 A89-39872

N

Nansen Ocean and Remote Sensing Center,**Solheimsvik (Norway).**

NOAA (National Oceanic and Atmospheric Administration) AVHRR (Advanced Very High Resolution Radiometer) observations during the marginal ice zone experiment, between Spitzbergen and Greenland, June 7 to 18 July 1984 [AD-A204911] p 19 N89-22280

National Aeronautics and Space Administration, Washington, DC.

Evaluating atmospheric correction models for retrieving surface temperatures from the AVHRR over a tallgrass prairie p 20 A89-33875

Earth system science: A program for global change [NASA-TM-101186] p 5 N89-22969

National Aeronautics and Space Administration. Ames Research Center, Moffett Field, CA.

Geobotanical determination of aggregate source material using Airborne Thematic Mapper imagery p 1 A89-35865

Zones of information in the AVIRIS spectra p 39 N89-22158

National Aeronautics and Space Administration.**Goddard Inst. for Space Studies, New York, NY.**

Global, seasonal surface variations from satellite radiance measurements p 52 A89-35966

National Aeronautics and Space Administration.**Goddard Space Flight Center, Greenbelt, MD.**

A new technique to measure the spectral properties of conifer needles p 19 A89-33874

Modeling directional thermal radiance from a forest canopy p 27 A89-38972

Effect of metal stress on the thermal infrared emission of soybeans: A greenhouse experiment - Possible utility in remote sensing p 2 A89-39658

AVHRR for monitoring global tropical deforestation p 56 A89-40152

Laser altimetry measurements from aircraft and spacecraft p 56 A89-41691

Geological remote sensing signatures of terrestrial impact craters p 37 N89-21317

Nimbus-7 data product summary [NASA-RP-1215] p 39 N89-22152

Data compression experiments with LANDSAT thematic mapper and Nimbus-7 coastal zone color scanner data p 41 N89-22344

National Aeronautics and Space Administration. John C. Stennis Space Center, Bay Saint Louis, MS.

Measurements of short-term thermal responses of coniferous forest canopies using thermal scanner data p 1 A89-33867

Modeling surface temperature distributions in forest landscapes p 48 A89-33868

Variation of surface water spectral response as a function of in situ sampling technique p 33 A89-41161

Detection techniques using multispectral data to index soil erosional status p 56 A89-41164

National Aeronautics and Space Administration. John F. Kennedy Space Center, Cocoa Beach, FL.

Review of wildlife resources of Vandenberg Air Force Base, California [NASA-TM-102146] p 5 N89-23982

National Aeronautics and Space Administration.**Lyndon B. Johnson Space Center, Houston, TX.**

Volcano monitoring by short wavelength infrared satellite remote sensing p 51 A89-35875

Astronaut photography of the earth - Low cost images for resource exploration p 23 A89-35883

Geological applications of the Space Station core platform p 24 A89-35902

Expanding the utility of manned observations of earth - 70 mm film tests on the Space Shuttle p 34 A89-41428

Earth scenes in polarized light observed from the Space Shuttle p 34 A89-41429

Geologic applications of Space Shuttle photography p 34 A89-41431

Monitoring tropical environments with Space Shuttle photography p 34 A89-41432

Analysis of seasonal characteristics of Sambhar Salt Lake, India, from digitized Space Shuttle photography p 18 A89-41433

The decrease of Lake Chad as documented during twenty years of manned space flight p 18 A89-41434

National Aeronautics and Space Administration.**Langley Research Center, Hampton, VA.**

Estimation of surface insolation using sun-synchronous satellite data p 52 A89-35939

A parameterization for longwave surface radiation from sun-synchronous satellite data p 56 A89-41761

National Aeronautics and Space Administration.**Marshall Space Flight Center, Huntsville, AL.**

Precipitation retrieval over land and ocean with the SSM/I - Identification and characteristics of the scattering signal p 53 A89-37549

Improved capabilities of the Multispectral Atmospheric Mapping Sensor (MAMS) [NASA-TM-100352] p 58 N89-20430

National Aerospace Lab., Amsterdam (Netherlands).

A systematic worldwide landcover of satellite mosaics [NLR-MP-87062-U] p 65 N89-20540

Land use inventory using LANDSAT Thematic Mapper imagery to study environmental pollution [NLR-MP-87063-U] p 4 N89-20541

Twelve year overview of cloudfree LANDSAT imagery of The Netherlands [NLR-MP-87072-U] p 59 N89-20542

National Center for Atmospheric Research, Boulder, CO.

Polar cap deflation during magnetospheric substorms p 24 A89-36704

National Geophysical Data Center, Boulder, CO.

Solar-geophysical data number 529, September 1988. Part 1: (Prompt reports). Data for August, July 1988 and late data [PB89-121305] p 37 N89-21431

National Oceanic and Atmospheric Administration, Seattle, WA.

Beaufort Sea mesoscale circulation study: Preliminary results [PB89-121693] p 17 N89-20597

National Oceanic and Atmospheric Administration, Washington, DC.

Ice cover on Chesapeake Bay from AVHRR (Advanced Very High Resolution Radiometer) and LANDSAT imagery, winter of 1987-88 [PB89-117261] p 59 N89-21415

Natural Environmental Research Council, London (England).

The activities of the British National Space Centre (BNSC) in the field of imaging spectrometry p 47 N89-24696

Naval Civil Engineering Lab., Port Hueneme, CA.

Geobotanical determination of aggregate source material using Airborne Thematic Mapper imagery p 1 A89-35865

Geobotanical remote sensing for determination of aggregate source material [AD-A205943] p 45 N89-23962

Naval Ocean Research and Development Activity, Bay Saint Louis, MS.

KRMS (K-band Radiometric Mapping System) SSM/I validation March 1988 quick look report [NASA-CR-185320] p 8 N89-23766

Naval Ocean Research and Development Activity, Hanover, NH.

KRMS (K-band Radiometric Mapping System) SSM/I validation March 1988 quick look report [NASA-CR-185320] p 8 N89-23766

Naval Ocean Systems Center, San Diego, CA.

Infrared sea-radiance modeling using LOWTRAN 6 [AD-A202582] p 38 N89-21643

Naval Polar Oceanography Center, Suitland, MD.

KRMS (K-band Radiometric Mapping System) SSM/I validation March 1988 quick look report [NASA-CR-185320] p 8 N89-23766

Naval Postgraduate School, Monterey, CA.

Satellite signatures of rapid cyclogenesis [AD-A203934] p 38 N89-21452

Thermal images of sky and sea-surface background infrared radiation [AD-A205819] p 46 N89-23992

Correlation between satellite-derived aerosol characteristics and oceanic dimethylsulfide (DMS) [AD-A206179] p 6 N89-24759

Naval Weapons Center, China Lake, CA.

KRMS (K-band Radiometric Mapping System) SSM/I validation March 1988 quick look report [NASA-CR-185320] p 8 N89-23766

NEDECO (Netherlands).

On the international commercialization of remote sensing [BCRS-88-02] p 65 N89-23969

Nevada Univ., Reno.

Geobotanical determination of aggregate source material using Airborne Thematic Mapper imagery p 1 A89-35865

Vegetation reflectance features in AVIRIS data p 22 A89-35867

Discriminating late volcanic differentiates commonly associated with precious metal deposits, using Landsat Thematic Mapper imagery p 12 A89-35896

New Hampshire Univ., Durham.

Modeling directional thermal radiance from a forest canopy p 27 A89-38972

- Assessment of AVIRIS data from vegetated sites in the Owens Valley, California p 60 N89-22162
- Newcastle Univ. (Australia).**
Some aspects of the relation between Pi 1-2 magnetic pulsations observed at L = 1.3-2.1 on the ground and substorm-associated magnetic field variations in the near-earth magnetotail observed by AMPTE CCE p 52 A89-36686

O

- Oak Ridge National Lab., TN.**
Preliminary development of a seashore-effects analysis system [DE89-007863] p 61 N89-22191
Air pollution effects field research facility: Ozone flow control and monitoring system [DE89-007922] p 5 N89-22192
- Onagawa Magnetic Observatory (Japan).**
Some aspects of the relation between Pi 1-2 magnetic pulsations observed at L = 1.3-2.1 on the ground and substorm-associated magnetic field variations in the near-earth magnetotail observed by AMPTE CCE p 52 A89-36686
- Open Univ., Milton (England).**
Measuring thermal budgets of active volcanoes by satellite remote sensing p 9 A89-32988
Volcano monitoring by short wavelength infrared satellite remote sensing p 51 A89-35875

P

- Pacific Gas and Electric Co., San Ramon, CA.**
Application of Landsat Thematic Mapper data for coastal thermal plume analysis at Diablo Canyon p 35 A89-42175
- Pacific Northwest Labs., Richland, WA.**
Application of Landsat Thematic Mapper data for coastal thermal plume analysis at Diablo Canyon p 35 A89-42175
- Pasco Corp. (Japan).**
Evaluation of the Portable Instantaneous Display Analysis Spectrometer (PIDAS) [NASA-CR-184878] p 61 N89-22970
- Planning Research Corp., Hampton, VA.**
A parameterization for longwave surface radiation from sun-synchronous satellite data p 56 A89-41761
- PRC Kentron, Inc., Hampton, VA.**
Estimation of surface insolation using sun-synchronous satellite data p 52 A89-35939
- Princeton Univ., NJ.**
High resolution chronology of late Cretaceous-early Tertiary events determined from 21,000 yr orbital-climatic cycles in marine sediments p 14 N89-21328
- Purdue Univ., West Lafayette, IN.**
A new technique to measure the spectral properties of conifer needles p 19 A89-33874
Assessment of forest cover changes using multistate spaceborne imaging radar p 33 A89-41169

R

- Radian Corp., Research Triangle Park, NC.**
National Air Toxics Information Clearinghouse: Ongoing research and regulatory development projects, July 1988 [PB89-103428] p 65 N89-20558
- Research Inst. of National Defence, Linköping (Sweden).**
Shortest paths in a digitized map using a tile-based data structure [PB89-143432] p 44 N89-23957
- Rice Univ., Houston, TX.**
Spacelab 2 Upper Atmospheric Modification Experiment over Arecibo. II - Plasma dynamics p 4 A89-38897
- Royal Netherlands Meteorological Inst., The Hague.**
Processing and application of digital AVHRR imagery for land and sea surfaces [BCRS-88-08] p 36 N89-20538

S

- Science and Technology Corp., Hampton, VA.**
The investigation of advanced remote sensing, radiative transfer and inversion techniques for the measurement of atmospheric constituents [NASA-CR-172599] p 36 N89-20531
- Science Applications International Corp., Washington, DC.**
Effect of metal stress on the thermal infrared emission of soybeans: A greenhouse experiment - Possible utility in remote sensing p 2 A89-39658

- Scripps Institution of Oceanography, La Jolla, CA.**
Biooptical variability in the Greenland Sea observed with the Multispectral Airborne Radiometer System (MARS) [NASA-CR-184856] p 47 N89-24784
- Southwest Research Inst., San Antonio, TX.**
Polar cap deflation during magnetospheric substorms p 24 A89-36704
- SRI International Corp., Menlo Park, CA.**
Image understanding research at SRI International p 42 N89-23080
Overview of the SRI cartographic modeling environment p 62 N89-23122
- Stanford Univ., CA.**
Evaluation of the Portable Instantaneous Display Analysis Spectrometer (PIDAS) [NASA-CR-184878] p 61 N89-22970
- Swedish Defence Research Establishment, Linköping.**
Minimum number of satellites for periodic coverage [FOA-C-30511-9.4] p 65 N89-22976
Activities report of the Division of Optical Technology (FOA 33) [FOA-C-30507-3.1] p 62 N89-23287

T

- Technische Hogeschool, Delft (Netherlands).**
On the connection of geodetic pointfields in RETrig [PB89-146112] p 44 N89-23958
- Technische Univ., Delft (Netherlands).**
Integration of tie-points in digital mosaicing [ETN-89-94147] p 41 N89-22973
The search for edges in remote sensing images using a digital polygonal map [ETN-89-94146] p 45 N89-23964
Investigation of several methods for the detection of outstanding points in a digital image [ETN-89-94148] p 45 N89-23965
Vectorization of grid lines [ETN-89-94150] p 45 N89-23967
Design of a methodology for the detection of errors in terrestrial networks [ETN-89-94151] p 46 N89-23968
- Tennessee Univ., Tullahoma.**
Mapping of Landsat satellite and gravity lineaments in west Tennessee p 6 A89-34357
- Texas A&M Univ., College Station.**
The decrease of Lake Chad as documented during twenty years of manned space flight p 18 A89-41434
- Texas Univ., Austin.**
Rate of change of the Quincy-Monument Peak baseline from a translocation analysis of Lageos laser range data p 13 A89-42181
- Texas Univ. at Dallas, Richardson.**
Polar cap deflation during magnetospheric substorms p 24 A89-36704
- TGS Technology, Inc., Moffett Field, CA.**
AVIRIS data quality for coniferous canopy chemistry p 40 N89-22164
- Tohoku Univ., Sendai (Japan).**
Some aspects of the relation between Pi 1-2 magnetic pulsations observed at L = 1.3-2.1 on the ground and substorm-associated magnetic field variations in the near-earth magnetotail observed by AMPTE CCE p 52 A89-36686

U

- Universities Space Research Association, Boulder, CO.**
A visiting scientist program in atmospheric sciences for the Goddard Space Flight Center [NASA-CR-183421] p 47 N89-24756

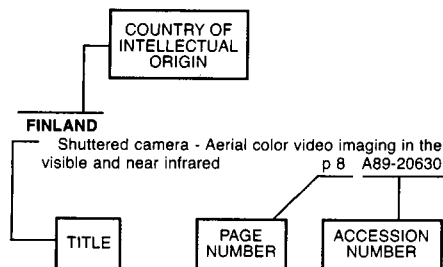
V

- Vanderbilt Univ., Nashville, TN.**
Mapping of Landsat satellite and gravity lineaments in west Tennessee p 6 A89-34357

W

- Wisconsin Univ., Madison.**
Using the radiative temperature difference at 3.7 and 11 microns to track dust outbreaks p 27 A89-38968

Typical Foreign Technology Index Listing



Listings in this index are arranged alphabetically by country of intellectual origin. The title of the document is used to provide a brief description of the subject matter. The page number and the accession number are included in each entry to assist the user in locating the citation in the abstract section. If applicable, a report number is also included as an aid in identifying the document.

A

AUSTRALIA

- The prognosis of weather change lines over the ocean - The role of a reconnaissance aircraft p 48 A89-32848
- A meteorological overview of the pre-AMEX and AMEX periods over the Australian region p 48 A89-32850
- Accessing remote sensing technology - The microBRIAN example p 21 A89-34706
- Ground verification method for bathymetric satellite image maps of unsurveyed coral reefs p 6 A89-34949
- Theoretical algorithms for satellite-derived sea surface temperatures p 21 A89-35159
- Examination of USAF Nephanalysis performance in the marginal cryosphere region p 52 A89-35949
- The discrimination of irrigated orchard and vine crops using remotely sensed data p 2 A89-37949
- Geophysical geodesy - The slow deformations of the earth p 7 A89-38583
- A method for integrating remote sensing and geographic information systems p 28 A89-39097
- Close-range photogrammetric measurement of erosion in coarse-grained soils p 54 A89-39098
- Autocorrelation and regularization in digital images. II - Simple image models p 29 A89-39551
- Observations of volcanic ash clouds in the 10-12 micron window using AVHRR/2 data p 30 A89-40143

AUSTRIA

- Analysis of Airborne Imaging Spectrometer (AIS) data for geobotanical prospecting p 51 A89-35890

B

BOTSWANA

- Monitoring Tunisia's steppes with SPOT p 35 A89-43316

- OSRMS (Ocean Surface Roughness Measurement System): The DREP (Defence Research Establishment Pacific) near-nadir scatterometer [AD-A202983] p 38 A89-21460

BRAZIL

- Microwave X-band radiometric characterization of Brazilian soils by measurement of the complex permittivity [INPE-4588-PRE/1319] p 3 A89-24685

C

CANADA

- Remote sensing of ocean chlorophyll - Consequence of nonuniform pigment profile p 15 A89-32838
- Synthetic Aperture Radar data for mapping subsurface geological structures in the Northwest Territories, Canada p 50 A89-35858
- High resolution imaging of geobotanical anomalies associated with subsurface hydrocarbons p 22 A89-35870
- Assessing aggregate resource potential in the Canadian Shield - A knowledge-based approach p 23 A89-35877
- MEIS II and surface data integration for detection of geobotanical anomalies p 51 A89-35891
- Implementation of background and target geobotanical techniques in mineral exploration p 23 A89-35892
- Automated recognition of oceanic cloud patterns. I - Methodology and application to cloud climatology p 24 A89-35906
- Reflectance enhancements for the Thematic Mapper - An efficient way to produce images of consistently high quality p 26 A89-37947
- Cluster analysis of pine crown foliage patterns aid identification of mountain pine beetle current-attack p 26 A89-37950
- Low-relief topographic enhancement in a Landsat snow-cover scene p 54 A89-38966
- High altitude laser ranging over rugged terrain p 54 A89-39092
- A performance comparison for two Lagrangian drifter designs p 34 A89-41750
- Minimum cross-entropy noise reduction in images p 34 A89-41845
- Magnetometer array studies, earth structure, and tectonic processes p 13 A89-42149
- The FLI airborne imaging spectrometer: A highly versatile sensor for many applications p 63 A89-24694
- Development of an imaging spectrometer for remote sensing: The FLI program p 63 A89-24698
- Imaging spectrometry at the Canada Centre for Remote Sensing p 64 A89-24701

CHINA, PEOPLE'S REPUBLIC OF

- An algorithm for machine-recognizing the river mouth and measuring the sealine from the Landsat image p 19 A89-33658
- Structural analysis of the Wichita Mountains using TM data for lineament mapping p 12 A89-35887
- Two-dimensional seam-point searching in digital image mosaicking p 26 A89-37945
- Land-surface temperature measurement from space - Physical principles and inverse modeling p 29 A89-39552

CZECHOSLOVAKIA

- Modelling the earth's geomagnetic field to high degree and order p 58 A89-43408

D

DENMARK

- Distribution of auroral arcs during quiet geomagnetic conditions p 50 A89-34772

E

EGYPT

- Analytical independent model triangulation strip adjustment using shore-line constraints p 28 A89-39093

ESTONIA

- A reflectance model for the homogeneous plant canopy and its inversion p 27 A89-38971

F

FINLAND

- Determination of areal snow water equivalent using satellite images and gamma ray spectrometry [CI-91] p 44 A89-23960

FRANCE

- C-band radar cross section of the Guyana rain forest - Possible use as a reference target for spaceborne radars p 49 A89-33869
- Munsell soil color and soil reflectance in the visible spectral bands of Landsat MSS and TM data p 49 A89-33870
- Infrared thermography - A quantitative tool for heat study [ONERA, TP NO. 1989-3] p 53 A89-37627
- Synoptic analysis and dynamical adjustment of GEOS 3 and Seasat altimeter eddy fields in the northwest Atlantic p 29 A89-39650
- Seasat altimetry and the South Atlantic geoid. II - Short-wavelength undulations p 16 A89-39659
- AVHRR data processing to study the surface canopies in temperate regions - First results of HAPEX-MOBILHY p 30 A89-40153
- Retrieval of mesoscale meteorological parameters for polar latitudes (MIZEX and ARCTEMIZ campaigns) p 58 A89-43026
- Imaging radar applications in Europe. Illustrated experimental results (1978-1987) [ESA-TM-01] p 42 A89-22978
- The advanced Ocean Chlorophyll Meter (OCM). A spectral imaging device for the observation of the oceans [REPT-882-440-118] p 63 A89-24689
- On the future development and management of spectroscopic database for radiative transfer from the issues of recent related workshops [ETN-89-94530] p 46 A89-24690
- Refinements in the cloud detection scheme of the 3I system. Comparison with AVHRR products [ETN-89-94531] p 63 A89-24691
- Imaging Spectrometry for Land Applications [ESA-SP-1101] p 63 A89-24692
- Activities of CNES in the field of imaging spectrometry p 47 A89-24699

G

GERMANY DEMOCRATIC REPUBLIC

- Multichannel spectrometer MKS-M - Laboratory tests, calibration, and verification of its stability in flight p 57 A89-42609
- Measurements of spectral radiance at the sea surface for the development of remote sensing methods p 35 A89-42610

GERMANY, FEDERAL REPUBLIC OF

- Monitoring the halfa steppes of central Tunisia using Landsat MSS p 1 A89-34947
- Research on speckle behavior in SAR images p 21 A89-35335
- Performance analysis of the DFVLR real time SAR processor for low SNRs p 21 A89-35336
- Sensitivity of an atmospheric correction algorithm for non-Lambertian vegetation surfaces to atmospheric parameters p 29 A89-39556
- Satellite-derived low-level atmospheric water vapour content from synergy of AVHRR with HIRS p 30 A89-40139
- Mesoscale variability of sea surface temperature in the North Atlantic p 17 A89-40145
- Design of spectral and panchromatic bands for the German MOMS-02 sensor p 57 A89-42173
- Airborne imaging radar system for monitoring sea pollution [MBB-UK-0016-87-PUB] p 58 A89-42941

Derivation of a large-scale map of heat load in the region Freiburg-Basel (Germany, F.R.) using satellite data. A contribution to the production of bioclimate data based on a geographic information system [REPT-27] p 41 N89-22972

Development of a satellite SAR image spectra and altimeter wave height data assimilation system for ERS-1 [NASA-CR-182685] p 61 N89-22975

Reports on Cartography and Geodesy. Series 1, number 101 [ISSN-0469-4236] p 8 N89-23941

Definition and filling of information systems: Challenge for a photogrammetric service enterprise p 62 N89-23942

Computer aided production of a 1:25,000 relief model of Berlin and surroundings p 8 N89-23943

The Official Topographic-Cartographic Information System (ATKIS) of the Geodesy Group of the Laender of the Federal Republic of Germany: Status after one year of development p 8 N89-23944

The digital urban map as a basis for a land information system in local administration p 8 N89-23945

Automatic digitizing of cadastral maps p 43 N89-23946

ARC-INFO: A geographic information system p 43 N89-23947

Cartographic signatures in PHOCUS p 43 N89-23948

Digitizing of drawings and cadastral maps using a scanner system p 43 N89-23949

Geocoded data sets of imaging satellites p 43 N89-23950

Computer assisted layout of graphic settlement representations p 43 N89-23951

Tools for the computer assisted generalization of settlements for the construction of digital landscape models p 43 N89-23952

Computer assisted generalization of transport line representations p 43 N89-23953

Hybrid cartographic data processing in a geographic information system p 44 N89-23954

Automatic extraction of areas from overlays of the series DGK 5 (Bo) p 44 N89-23955

Analysis and optimization of geodetic networks by spectral criteria and mechanical analogies [SER-C-342] p 45 N89-23963

Research for optimization of future MOMS sensors [ETN-89-94424] p 62 N89-23972

Optical properties of oceanic suspended matter and their interpretation for remote sensing of phytoplankton [GKSS-88/E/40] p 46 N89-24013

Imaging procedure of underwater bottom topography by air and satellite images in the range of microwave and visible electromagnetic spectra [GKSS-88/E/41] p 17 N89-24014

Necessity and benefit of the X-SAR space shuttle experiment [DFVLR-MITT-88-29] p 63 N89-24688

DFVLR activities related to imaging spectrometry p 63 N89-24697

The EARSEL Imaging Spectrometry Working Group p 47 N89-24700

GREECE

An algorithm for snow and ice detection using AVHRR data - An extension to the Apollo software package p 31 A89-40155

EM wave scattering from statistically inhomogeneous and periodic random rough surfaces p 36 A89-43541

I

INDIA

Sea surface spectrum from aerial photographs - Laboratory model studies p 30 A89-39674

Structural patterns in high grade terrain in parts of Tamil Nadu and Karnataka p 14 N89-22255

INTERNATIONAL ORGANIZATION

The experience of the Commission of the European Communities in the use of remote sensing for the implementation of community policies p 64 A89-34712

Vegetation and landscape of Kora National Reserve, Kenya p 6 A89-34945

AVHRR for monitoring global tropical deforestation p 56 A89-40152

Monitoring in Moneragala district, Sri Lanka, with SPOT images p 3 A89-43317

IRAQ

Geological application of SIR-A imagery in southern Iraq p 13 A89-41162

Structural analysis of fracturing in Sinjar anticline using remote sensing technique p 13 A89-41167

ITALY

Mean temperature in a closed basin by remote sensing p 16 A89-39062

Validation problems for remotely sensed sea surface temperature p 28 A89-39063

Improving accuracy in radar-altimetry data correction for tropospheric effects p 54 A89-39322

Geological data integration techniques: Proceedings [DE88-705255] p 14 N89-20868

IVORY COAST

Satellite detection of Saharan dust - Optimized imaging during nighttime p 24 A89-35912

The potential of infrared satellite data for the retrieval of Saharan-dust optical depth over Africa p 30 A89-39875

J

JAPAN

EXOS-C (Ohzora) observations of polar cap precipitations and inverted V events p 19 A89-33543

Spectral indices for vegetation and rock type discrimination using the optical sensor of the Japanese ERS-1 p 51 A89-35866

Some aspects of the relation between Pi 1-2 magnetic pulsations observed at L = 1.3-2.1 on the ground and substorm-associated magnetic field variations in the near-earth magnetotail observed by AMPTE CCE p 52 A89-36686

ARGOS system used for balloon observations p 53 A89-38290

Marine Observation Satellite-1 - First year in orbit p 26 A89-38328

Development and verification of Osaka Bay sampling model based on Landsat data p 27 A89-38332

Atmospheric correction of satellite MSS data in rugged terrain p 27 A89-38334

Seasonal visible, near-infrared and mid-infrared spectra of rice canopies in relation to LAI and above-ground dry phytomass p 54 A89-38967

A semi-automatic terrain measurement system for earthwork control p 28 A89-39094

The baseline length changes of circumpacific VLBL networks and their bearing on global tectonics p 13 A89-42795

Short-period fluctuation of the lower tropospheric winds observed by MU-radar p 58 A89-43311

Japan's sunshine project 1987 annual summary of geothermal energy R and D [DE88-756451] p 18 N89-22183

K

KENYA

Reconstruction of imagery of faulted landscapes using a photo-optical technique p 24 A89-35900

KOREA(SOUTH)

Discrimination of rocks and hydrothermal altered areas based on Landsat TM data p 27 A89-38333

M

MALAYSIA

Crop identification using merged Landsat multispectral scanner and Thematic Mapper data - Preliminary attempts p 3 A89-41153

N

NETHERLANDS

Rural settlement expansion in Moneragala district, Sri Lanka p 4 A89-34946

An analysis of speckle from forest stands with periodic structures p 54 A89-39555

Using NOAA AVHRR imagery in assessing water quality parameters p 55 A89-40148

The suitability of remote sensing for surveying and monitoring landscape patterns. Volume A: Pilot study - LANDSAT Imagery. Volume B: PEPS Project No. 73 - SPOT Imagery [BCRS-87-12-VOL-A/B] p 4 N89-20534

The suitability of remote sensing for surveying and monitoring landscape patterns. Volume A: Pilot study - LANDSAT Imagery p 36 N89-20535

The suitability of remote sensing for surveying and monitoring landscape patterns. Volume B: PEPS Project No. 73 - SPOT Imagery p 36 N89-20536

Land use inventories using satellite images in the region Haaren-Helvoirt-Udenhout, North Brabant (The Netherlands) [BCRS-88-07] p 36 N89-20537

Processing and application of digital AVHRR-imagery for land and sea surfaces [BCRS-88-08] p 36 N89-20538

Phase A study for the extension of the CAESAR scanner with a sensor module for the far infrared [BCRS-88-09] p 59 N89-20539

A systematic worldwide landcover of satellite mosaics [NLR-MP-87062-U] p 65 N89-20540

Land use inventory using LANDSAT Thematic Mapper imagery to study environmental pollution [NLR-MP-87063-U] p 4 N89-20541

Twelve year overview of cloudfree LANDSAT imagery of The Netherlands [NLR-MP-87072-U] p 59 N89-20542

Integration of tie-points in digital mosaicing [ETN-89-94147] p 41 N89-22973

On the connection of geodetic pointfields in RETrig [PB89-146112] p 44 N89-23958

The search for edges in remote sensing images using a digital polygonal map [ETN-89-94146] p 45 N89-23964

Investigation of several methods for the detection of outstanding points in a digital image [ETN-89-94148] p 45 N89-23965

Vectorization of grid lines [ETN-89-94150] p 45 N89-23967

Design of a methodology for the detection of errors in terrestrial networks [ETN-89-94151] p 46 N89-23968

On the international commercialization of remote sensing [BCRS-88-02] p 65 N89-23969

Meteosat thermal inertia mapping for studying wetland dynamics in the West-African Sahel [BCRS-88-10A] p 62 N89-23970

Thermal analysis for the monitoring and prediction of flood dynamics in wetlands [BCRS-88-10B] p 46 N89-23971

ESA's planned activities in the field of imaging spectrometry for Earth observation p 46 N89-24693

NORWAY

Activities at the Norwegian Hydrotechnical Laboratory p 55 A89-40129

O

OTHER

Conjugate synthetic normal faults around the Gulf of Salwa, southwestern Qatar, the Arabian Gulf p 12 A89-35886

P

POLAND

The influence of the viewing geometry of bare rough soil surfaces on their spectral response in the visible and near-infrared range p 2 A89-38969

S

SRI LANKA

Mapping coastal evolution in Sri Lanka using aerial photographs p 6 A89-34948

SWEDEN

Satellite altimetry. II - A new prospecting tool p 23 A89-35895

Arctic geodynamics - A satellite altimeter experiment for the European Space Agency Earth Remote-Sensing satellite p 29 A89-39546

Minimum number of satellites for periodic coverage [FOA-C-30511-9.4] p 65 N89-22976

Activities report of the Division of Optical Technology (FOA 33) p 62 N89-23287

Shortest paths in a digitized map using a tile-based data structure [PB89-143432] p 44 N89-23957

SWITZERLAND

Digital photogrammetric processing systems - Current status and prospects p 28 A89-39095

U

U.S.S.R.

Remote-sensing studies of present-day tectonic processes p 20 A89-34001

The potential use of remote sensing to solve problems of paleotectonic prediction, geologic structure, and exploitation of coal deposits with reference to the Moscow-Region coal basin p 49 A89-34002

Use of aerial and space photography for the detection of faults and neotectonic movements in Crimea and the Azov Coastal Region p 9 A89-34003

- Dynamics of present-day geological processes from remotely sensed data p 9 A89-34004
- Investigation of the recently formed imbricate structure of the southern Tien-Shan using space photographs p 10 A89-34005
- Morphostructural interpretation of space images and the reconstruction of the recently formed stress field in the Altai-Baikal region p 10 A89-34006
- Use of aerial and space methods for observations and studies of the morphology and kinematics of recent movements along some faults of the Baikal Rift Zone p 10 A89-34007
- Structural stresses and the divisibility into blocks of the earth crust as observed on space imagery p 10 A89-34009
- The use of a lineament-analysis instrument for investigations of tectonic zonality and the elements of continental-margin geodynamics as applied to western Arctic p 49 A89-34010
- Identification of tectonic dislocations underneath large water areas using space images p 15 A89-34011
- New data on the morphostructure and geodynamics of the eastern margin of Eurasia p 10 A89-34012
- Methods for investigating seismically active zones using remote imagery p 20 A89-34013
- Automated analysis of lineaments from space imagery obtained during seismic studies of central Tien-Shan p 20 A89-34014
- The use of space imagery for investigations of recent crustal deformations in southern Yakutia p 20 A89-34015
- Determination of the character of present-day vertical movements from the structure of space imagery p 10 A89-34016
- Recent and current geodynamics of the Kyzylkum region as derived from space imagery p 10 A89-34017
- Seismogeological interpretation of space images of the region of Caucasian mineral waters p 10 A89-34018
- Gravimetric studies at sea p 49 A89-34088
- Concentric structures in southern Tien-Shan p 10 A89-34196
- Economic relations of the all-union trade association Sojuzkarta and the geodetic and cartographic services of the U.S.S.R. to foreign countries p 64 A89-34708
- Sounding of crop fields by nanosecond radio pulses p 1 A89-35584
- Multispectral space surveys and data processing p 22 A89-35684
- Analysis of the potential of using space photographic data obtained with the PKF-1K camera to solve scientific, economic, and educational-methodological problems p 64 A89-35685
- Methodology for the remote sensing of fluxes of heat, moisture, and effective radiation in the ocean-atmosphere system p 16 A89-35686
- The KAP-350 and KAP-100 space cameras for the remote sensing of earth resources p 50 A89-35687
- The definition of isometric magmatogenic structures on space imagery p 12 A89-37315
- Ore-bearing structures of Central Kazakhstan identified on aerial and space photographs in the framework of the computer-aided prediction of minerals p 52 A89-37316
- A technique for applying space photographs to search for anticlinal oil- and gas-traps in orogenic structures of the Tien-Shan p 25 A89-37318
- Assessment of the present conditions of lowland lakes of Central Asia using the interpretation of space photographs p 17 A89-37319
- The condition of natural features as related to their intrinsic microwave and IR emission fields p 2 A89-37320
- Parameter optimization of systems for the thermal microwave mapping of the earth's surface p 25 A89-37321
- Highly sensitive microwave radiometer-scatterometer for the remote sensing of the earth's surface p 52 A89-37322
- Radiometric correction of aerial and space remote-sensing images p 25 A89-37323
- Methodological aspects of the automation of the calibration and processing of satellite microwave-radiometer data p 25 A89-37324
- Computer-aided synthesis of textures simulating the earth's surface p 25 A89-37325
- Remote four-photon Raman spectroscopy of sea water under natural conditions p 52 A89-37327
- The dispersion limitations on the accuracy of the internal reference method during remote laser sounding of the upper ocean layer p 53 A89-37349
- The rate of gas exchange between the ocean and the atmosphere using microwave radiometer data p 25 A89-37471
- Coordinate referencing of a TV image in the case of the remote sensing of the earth p 53 A89-37492
- Aerial photography and specialized photographic studies p 31 A89-40488
- Space geography. Investigations on test regions p 31 A89-40491
- Properties of the equatorial and tropical ionosphere according to Soviet satellite observations during the IMS p 31 A89-40606
- Studying the earth from manned spacecraft p 64 A89-42511
- Spaceborne studies related to nature conservation p 65 A89-42549
- Remote measurements from Salyut-7 of the optical parameters of the atmosphere-surface system p 57 A89-42601
- The spectrometer of the Salyut-7 orbital station p 57 A89-42608
- Determination of spectral signatures for remote laser sensing of vegetation p 35 A89-42611
- Correcting absolute calibrations of satellite microwave radiometer using a priori data p 35 A89-42612
- Optimal satellite orbits and the network structure for regular earth surveying p 35 A89-42614
- Space coloristics p 35 A89-43024

UNITED KINGDOM

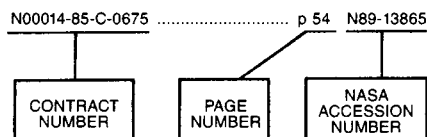
- GEOS 1 observations of low-energy ions in the earth's plasmasphere - A study on composition, and temperature and density structure under quiet geomagnetic conditions p 9 A89-33829
- Volcano monitoring by short wavelength infrared satellite remote sensing p 51 A89-35875
- Application of Landsat Thematic Mapper imagery for lithological mapping of poorly accessible semi-arid regions p 7 A89-35879
- Applications of AVHRR imagery in frontier exploration p 23 A89-35885
- Integration of Landsat TM, stream sediment geochemistry and regional geophysics for mineral exploration in the English Lake District p 23 A89-35888
- Identification and analysis of the alignments of point-like features in remotely-sensed imagery. Volcanic cones in the Pinacate Volcanic Field, Mexico p 12 A89-39651
- Geological uses of remotely-sensed reflected and emitted data of lateritized Archean terrain in Western Australia p 55 A89-39652
- Alteration detection using TM imagery - The effects of supergene weathering in an arid climate p 12 A89-39655
- Geobotanical application of Airborne Thematic Mapper data in Sutherland, north-west Scotland p 2 A89-39657
- Monitoring the greenhouse effect from space p 4 A89-39739
- Relating point to area average rainfall in semiarid West Africa and the implications for rainfall estimates derived from satellite data p 55 A89-39870
- Applications of AVHRR data; Proceedings of the Third European AVHRR Data Users' Meeting, University of Oxford, England, Dec. 16-18, 1987 p 55 A89-40126
- Pixel and sub-pixel accuracy in geometrical correction of AVHRR p 30 A89-40134
- An AVHRR mosaic image of Antarctica p 30 A89-40135
- Cloud reflectance variations in channel-3 p 55 A89-40136
- A phenological description of Iberian vegetation using short wave vegetation index imagery p 2 A89-40149
- Monitoring the phenology of Tunisian grazing lands p 3 A89-40150
- Lake area measurement using AVHRR - A case study p 31 A89-40154
- Multi-spectral classification of snow using NOAA AVHRR imagery p 31 A89-40156
- Remote sensing in refractive turbulence p 58 A89-20532
- Theoretical studies for ERS-1 wave mode, volume 1 [GEC-MTR-87/110-VOL-1] p 41 A89-22977
- The activities of the British National Space Centre (BNSC) in the field of imaging spectrometry p 47 A89-24696

CONTRACT NUMBER INDEX

EARTH RESOURCES / A Continuing Bibliography (Issue 63)

OCTOBER 1989

Typical Contract Number Index Listing



Listings in this index are arranged alphanumerically by contract number. Under each contract number, the accession numbers denoting documents that have been produced as a result of research done under the contract are arranged in ascending order with the AIAA accession numbers appearing first. The accession number denotes the number by which the citation is identified in the abstract section. Preceding the accession number is the page number on which the citation may be found.

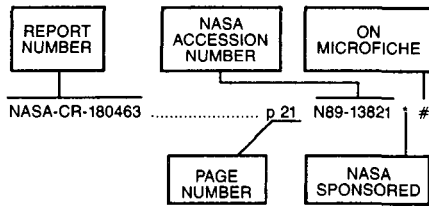
AF TASK 2310G9	p 48	A89-33505
AF-AFOSR-86-0053	p 52	A89-35949
AF-AFOSR-87-0195	p 52	A89-35949
BCRS-PROJ. TE-1.7	p 59	N89-20539
BCRS-PROJ. TO-3.1	p 36	N89-20538
BCRS-PROJ.-CO-1.3	p 65	N89-23969
BCRS-PROJ.-OP-3.3	p 62	N89-23970
	p 46	N89-23971
BMFT-KF-10045	p 30	A89-40139
BMFT-01-QS-86-206	p 62	N89-23972
BMFT-07-KR-2121	p 61	N89-22975
DAAL03-86-K-0118	p 48	A89-32841
DACA72-84-C-0002	p 42	N89-23101
DACA76-85-C-0004	p 42	N89-23080
DARPA ORDER 4976	p 42	N89-23101
DE-AC05-84OR-21400	p 61	N89-22191
	p 5	N89-22192
DE-AC06-76RL-01830	p 35	A89-42175
DE-AC09-76SR-00001	p 32	A89-41159
DFG-SFB-133	p 17	A89-40145
EPA-68-02-4330	p 65	N89-20558
ESA-6875/87/HGE/I(SC)	p 61	N89-22975
ESA-6878/87/HGE/I(SC)	p 41	N89-22977
ESTEC-6347/85/NL/MD	p 49	A89-33869
FAA-T0702-N	p 8	N89-23437
F19628-84-N-0006	p 24	A89-36704
F19628-86-K-0038	p 48	A89-33505
F33615-84-K-1520	p 42	N89-23101
F49620-86-C-0080	p 41	N89-22293
GS14-08-0001-22521	p 40	N89-22165
JPL-956952	p 33	A89-41169
JPL-957652	p 61	N89-22975
MDA903-86-C-0084	p 42	N89-23080
	p 62	N89-23122
NAGW-1252	p 61	N89-22970
NAGW-1474	p 29	A89-39551
NAGW-273	p 25	A89-37291
NAGW-690	p 61	N89-22779
NAGW-735	p 29	A89-39551
NAGW-799	p 19	A89-33874
NAGW-896	p 49	A89-33871
NAGW-952	p 55	A89-39872
NAGW-987	p 32	A89-41158
	p 42	N89-22979
NAG5-1010	p 46	N89-24686
NAG5-1022	p 47	N89-24784
NAG5-270	p 41	N89-22971
NAG5-273	p 29	A89-39551
NAG5-276	p 29	A89-39551
NAG5-305	p 24	A89-36704
NAG5-306	p 24	A89-36704
NAG5-389	p 20	A89-33875
	p 27	A89-38970
NAG5-459	p 15	N89-24757
NAG5-852	p 9	N89-23961
NAG5-887	p 62	N89-23956
NAG5-917	p 29	A89-39552
NASA ORDER S-56102-D	p 35	A89-42175
NASA ORDER W-16320	p 24	A89-36704
NASW-4049	p 2	A89-35894
NASW-4066	p 51	A89-35875
NAS1-15198	p 36	N89-20531
NAS1-18272	p 27	A89-38968
NAS10-10285	p 5	N89-23982
NAS5-28135	p 47	N89-24756
NAS5-28712	p 24	A89-36704
NAS5-28745	p 14	N89-21416
NAS5-28754	p 15	N89-22263
NAS5-28755	p 3	N89-24687
NAS5-28756	p 18	N89-20533
NAS5-28759	p 51	A89-35875
NAS5-28770	p 29	A89-39552
NAS5-28798	p 25	A89-37291
NAS5-29386	p 39	N89-22152
NAS5-30135	p 33	A89-41163
NAS7-918	p 33	A89-41169
	p 59	N89-22154
	p 61	N89-22975
NAS8-33218	p 6	A89-34357
NAS9-16664	p 29	A89-39551
NCA2-138	p 55	A89-39872
NCA2-27	p 55	A89-39872
NERC-F60/G6/12	p 12	A89-39651
NERC-GT/4/83/TLS/6/	p 2	A89-40149
NGL-05-007-004	p 9	A89-33540
NGT-21-002-080	p 3	N89-24015
NOAA-NA-81AAD0095	p 50	A89-34353
NOAA-NA-84AAD00079	p 50	A89-34353
NOAA-NA-84DGC0155	p 21	A89-34879
NSF ATM-82-17015	p 53	A89-37554
NSF ATM-84-14467	p 24	A89-35906
NSF ATM-85-07782	p 17	A89-35937
NSF ATM-85-21180	p 4	A89-38897
NSF ATM-85-21214	p 27	A89-38968
NSF ATM-86-10858	p 9	A89-33540
NSF ATM-87-22962	p 24	A89-36704
NSF ATM-88-03133	p 50	A89-34782
NSF IST-85-11751	p 62	N89-23122
NSF OCE-82-14791	p 16	A89-35931
N00014-80-G-0003	p 19	N89-22280
N00014-83-G-0126	p 61	N89-22975
N00014-83-K-0258	p 59	N89-20543
N00014-84-C-0461	p 29	A89-39650
N00014-84-K-0451	p 25	A89-37291
N00014-86-F-0049	p 37	N89-21431
N00014-87-C-0687	p 37	N89-21165
N00014-87-K-6006	p 16	A89-38766
ST2J-0044-8-D	p 61	N89-22975
USDA-A647-SCS00210	p 6	A89-34357
W-31-109-ENG-38	p 5	N89-24749
W-7405-ENG-48	p 44	N89-23959
677-21-35	p 39	N89-22158
677-80-25-02	p 59	N89-22154

REPORT NUMBER INDEX

EARTH RESOURCES / A Continuing Bibliography (Issue 63)

OCTOBER 1989

Typical Report Number Index Listing



Listings in this index are arranged alphanumerically by report number. The page number indicates the page on which the citation is located. The accession number denotes the number by which the citation is identified. An asterisk (*) indicates that the item is a NASA report. A pound sign (#) indicates that the item is available on microfiche.

AD-A202582 p 38 N89-21643 #
 AD-A202663 p 59 N89-21218 #
 AD-A202700 p 40 N89-22173 #
 AD-A202983 p 38 N89-21460 #
 AD-A203047 p 38 N89-21568 #
 AD-A203257 p 37 N89-21162 #
 AD-A203604 p 37 N89-21165 #
 AD-A203792 p 7 N89-22174 #
 AD-A203934 p 38 N89-21452 #
 AD-A203943 p 59 N89-20543 #
 AD-A204523 p 18 N89-22175 #
 AD-A204911 p 19 N89-22280 #
 AD-A205082 p 41 N89-22293 #
 AD-A205606 p 8 N89-23766 *
 AD-A205819 p 46 N89-23992 #
 AD-A205943 p 45 N89-23962 #
 AD-A206179 p 6 N89-24759 #
 AFIT/GCS/ENG/88D-18 p 38 N89-21568 #
 AFIT/GSO/ENP/88D-4 p 59 N89-21218 #
 AFIT/GSO/ENS/88D-4 p 40 N89-22173 #
 AFOSR-89-0095TR p 41 N89-22293 #
 AIST-8804 p 18 N89-22183 #
 ANL-9009868 p 5 N89-24749 #
 ARI-TR-803 p 7 N89-22174 #
 BCRS-87-12-VOL-A/B p 4 N89-20534 #
 BCRS-88-02 p 65 N89-23969 #
 BCRS-88-07 p 36 N89-20537 #
 BCRS-88-08 p 36 N89-20538 #
 BCRS-88-09 p 59 N89-20539 #
 BCRS-88-10A p 62 N89-23970 #
 BCRS-88-10B p 46 N89-23971 #
 CHORS-TM-89-001 p 47 N89-24784 *
 CI-91 p 44 N89-23960 #
 CONF-8610449 p 14 N89-20868 #
 CONF-8904117-1 p 44 N89-23959 #
 CONTRIB-1040 p 17 N89-20597 #
 CRREL-SR-88-26 p 18 N89-22175 #
 DCN-88-239-001-44-07 p 65 N89-20558 #
 DE88-705255 p 14 N89-20868 #
 DE88-756451 p 18 N89-22183 #

DE89-006730 p 44 N89-23959 #
 DE89-007863 p 61 N89-22191 #
 DE89-007922 p 5 N89-22192 #
 DE89-009868 p 5 N89-24749 #
 DFLVR-MITT-88-29 p 63 N89-24688 #
 DOT/FAA/CT-TN89/16 p 8 N89-23437 #
 DREP-TM-88-15 p 38 N89-21460 #
 EPA/450/5-88/004 p 65 N89-20558 #
 ESA-CR(P)-2710 p 61 N89-22975 *
 ESA-CR(P)-2750 p 41 N89-22977 #
 ESA-SP-1101 p 63 N89-24692 #
 ESA-TM-01 p 42 N89-22978 #
 ETL-0478 p 37 N89-21162 #
 ETN-89-93779 p 8 N89-23941 #
 ETN-89-93781 p 41 N89-22972 #
 ETN-89-93871 p 4 N89-20534 #
 ETN-89-93876 p 36 N89-20537 #
 ETN-89-93877 p 36 N89-20538 #
 ETN-89-93878 p 59 N89-20539 #
 ETN-89-93998 p 45 N89-23963 #
 ETN-89-94041 p 65 N89-20540 #
 ETN-89-94042 p 4 N89-20541 #
 ETN-89-94045 p 59 N89-20542 #
 ETN-89-94146 p 45 N89-23964 #
 ETN-89-94147 p 41 N89-22973 #
 ETN-89-94148 p 45 N89-23965 #
 ETN-89-94150 p 45 N89-23967 #
 ETN-89-94151 p 46 N89-23968 #
 ETN-89-94220 p 44 N89-23960 #
 ETN-89-94241 p 61 N89-22975 *
 ETN-89-94288 p 65 N89-23969 #
 ETN-89-94289 p 62 N89-23970 #
 ETN-89-94290 p 46 N89-23971 #
 ETN-89-94307 p 62 N89-23287 #
 ETN-89-94308 p 65 N89-22976 #
 ETN-89-94375 p 63 N89-24688 #
 ETN-89-94410 p 46 N89-24013 #
 ETN-89-94411 p 17 N89-24014 #
 ETN-89-94424 p 62 N89-23972 #
 ETN-89-94447 p 63 N89-24692 #
 ETN-89-94471 p 41 N89-22977 #
 ETN-89-94474 p 42 N89-22978 #
 ETN-89-94511 p 63 N89-24689 #
 ETN-89-94530 p 46 N89-24690 #
 ETN-89-94531 p 63 N89-24691 #
 FOA-B-30129-3.4 p 44 N89-23957 #
 FOA-C-30507-3.1 p 62 N89-23287 #
 FOA-C-30511-9.4 p 65 N89-22976 #
 GEC-MTR-87/110-VOL-1 p 41 N89-22977 #
 GKSS-88/E/40 p 46 N89-24013 #
 GKSS-88/E/41 p 17 N89-24014 #
 IAEA-TECDOC-472 p 14 N89-20868 #
 INPE-4588-PRE/1319 p 3 N89-24685 #
 ISBN-3-7696-9390-6 p 45 N89-23963 #
 ISBN-951-666-275-7 p 44 N89-23960 #
 ISSN-0038-0911 p 37 N89-21431 #
 ISSN-0065-5325 p 45 N89-23963 #
 ISSN-0176-7736 p 63 N89-24688 #
 ISSN-0281-0263 p 44 N89-23957 #
 ISSN-0344-9629 p 46 N89-24013 #
 ISSN-0344-9629 p 17 N89-24014 #
 ISSN-0347-3708 p 65 N89-22976 #
 ISSN-0347-3708 p 62 N89-23287 #
 ISSN-0355-2705 p 44 N89-23960 #
 ISSN-0379-6566 p 63 N89-24692 #
 ISSN-0469-4236 p 8 N89-23941 #

JPL-PUBL-87-21-REV-1 p 9 N89-24060 *
 JPL-PUBL-87-4 p 5 N89-23985 *
 JPL-PUBL-88-38 p 59 N89-22154 *
 LC-79-640375 p 37 N89-21431 #
 LJI-87-P-467 p 37 N89-21165 #
 MBB-UK-0016-87-PUB p 58 A89-42941
 NAS 1.15:100352 p 58 N89-20430 *
 NAS 1.15:101186 p 5 N89-22969 *
 NAS 1.15:102146 p 5 N89-23982 *
 NAS 1.26:172599 p 36 N89-20531 *
 NAS 1.26:180078 p 62 N89-23956 *
 NAS 1.26:180081 p 3 N89-24687 *
 NAS 1.26:180450 p 3 N89-24015 *
 NAS 1.26:182685 p 61 N89-22975 *
 NAS 1.26:183416 p 14 N89-21416 *
 NAS 1.26:183417 p 18 N89-20533 *
 NAS 1.26:183421 p 47 N89-24756 *
 NAS 1.26:184637 p 42 N89-22979 *
 NAS 1.26:184854 p 15 N89-22263 *
 NAS 1.26:184856 p 47 N89-24784 *
 NAS 1.26:184870 p 59 N89-22154 *
 NAS 1.26:184878 p 61 N89-22970 *
 NAS 1.26:184937 p 41 N89-22971 *
 NAS 1.26:184975 p 46 N89-24686 *
 NAS 1.26:184987 p 15 N89-24757 *
 NAS 1.26:184991 p 9 N89-23961 *
 NAS 1.26:185019 p 5 N89-23985 *
 NAS 1.26:185021 p 9 N89-24060 *
 NAS 1.26:185320 p 8 N89-23766 *
 NAS 1.26:4228 p 61 N89-22779 *
 NAS 1.61:1215 p 39 N89-22152 *
 NASA-CR-172599 p 36 N89-20531 *
 NASA-CR-180078 p 62 N89-23956 *
 NASA-CR-180081 p 3 N89-24687 *
 NASA-CR-180450 p 3 N89-24015 *
 NASA-CR-182685 p 61 N89-22975 *
 NASA-CR-183416 p 14 N89-21416 *
 NASA-CR-183417 p 18 N89-20533 *
 NASA-CR-183421 p 47 N89-24756 *
 NASA-CR-184637 p 42 N89-22979 *
 NASA-CR-184854 p 15 N89-22263 *
 NASA-CR-184856 p 47 N89-24784 *
 NASA-CR-184870 p 59 N89-22154 *
 NASA-CR-184878 p 61 N89-22970 *
 NASA-CR-184937 p 41 N89-22971 *
 NASA-CR-184975 p 46 N89-24686 *
 NASA-CR-184987 p 15 N89-24757 *
 NASA-CR-184991 p 9 N89-23961 *
 NASA-CR-185019 p 5 N89-23985 *
 NASA-CR-185021 p 9 N89-24060 *
 NASA-CR-185320 p 8 N89-23766 *
 NASA-CR-4228 p 61 N89-22779 *
 NASA-RP-1215 p 39 N89-22152 *
 NASA-TM-100352 p 58 N89-20430 *
 NASA-TM-101186 p 5 N89-22969 *
 NASA-TM-102146 p 5 N89-23982 *
 NCEL-TN-1792 p 45 N89-23962 #
 NEPRF-CR-88-10 p 19 N89-22280 #
 NLR-MP-87062-U p 65 N89-20540 #
 NLR-MP-87063-U p 4 N89-20541 #
 NLR-MP-87072-U p 59 N89-20542 #
 NOAA-TM-ERL-PMEL-82 p 17 N89-20597 #
 NOAA-TM-NESDIS-AISC-14 p 59 N89-21415 #
 NORDA-TN-385 p 8 N89-23766 *
 NOSC/TD-1355 p 38 N89-21643 #
 NRSCTR-6 p 19 N89-22280 #
 ONERA, TP NO. 1989-3 p 53 A89-37627

REPORT

ORNL/CDIAC-23**REPORT NUMBER INDEX**

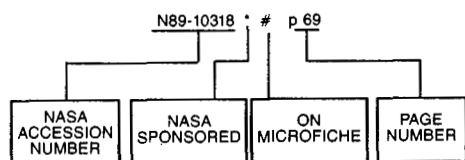
ORNL/CDIAC-23	p 61	N89-22191	#
ORNL/TM-10758	p 5	N89-22192	#
OSP-92790	p 41	N89-22971 *	#
PAT-APPL-7-231-017	p 63	N89-24589	#
PB89-103428	p 65	N89-20558	#
PB89-117261	p 59	N89-21415	#
PB89-121305	p 37	N89-21431	#
PB89-121693	p 17	N89-20597	#
PB89-133086	p 63	N89-24589	#
PB89-143432	p 44	N89-23957	#
PB89-146112	p 44	N89-23958	#
REPT-19	p 61	N89-22975 *	#
REPT-27	p 41	N89-22972	#
REPT-88-1	p 44	N89-23958	#
REPT-882-440-118	p 63	N89-24689	#
REPT-89B00074	p 39	N89-22152 *	#
SER-C-342	p 45	N89-23963	
SGD-529-PT-1	p 37	N89-21431	#
SPIE-933	p 48	A89-33653	
TPD-733.002	p 59	N89-20539	#
UCRL-99435	p 44	N89-23959	#

ACCESSION NUMBER INDEX

EARTH RESOURCES / A Continuing Bibliography (Issue 63)

OCTOBER 1989

Typical Accession Number Index Listing



Listings in this index are arranged alphanumerically by accession number. The page number listed to the right indicates the page on which the citation is located. An asterisk (*) indicates that the item is a NASA report. A pound sign (#) indicates that the item is available on microfiche.

A89-32756	p 4	A89-34703	p 64
A89-32835 #	p 47	A89-34704	p 64
A89-32836 #	p 47	A89-34706	p 21
A89-32837	p 48	A89-34708	p 64
A89-32838	p 15	A89-34712	p 64
A89-32841	p 48	A89-34772	p 50
A89-32848	p 48	A89-34782	p 50
A89-32850	p 48	A89-34876	p 50
A89-32988 *	p 9	A89-34878	p 15
A89-33121	p 17	A89-34879	p 21
A89-33505	p 48	A89-34945	p 6
A89-33540 *	p 9	A89-34946	p 4
A89-33543	p 19	A89-34947	p 1
A89-33653	p 48	A89-34948	p 6
A89-33658	p 19	A89-34949	p 6
A89-33661	p 6	A89-35159	p 21
A89-33664	p 19	A89-35335 #	p 21
A89-33684	p 19	A89-35336 #	p 21
A89-33829	p 9	A89-35584	p 1
A89-33867 *	p 1	A89-35684	p 22
A89-33868 *	p 48	A89-35685	p 64
A89-33869	p 49	A89-35686	p 16
A89-33870	p 49	A89-35687	p 50
A89-33871 *	p 49	A89-35819	p 50
A89-33872	p 19	A89-35837	p 22
A89-33873 #	p 1	A89-35838	p 22
A89-33874 *	p 19	A89-35840	p 6
A89-33875 *	p 20	A89-35851 *	p 10
A89-34001	p 20	A89-35852 #	p 11
A89-34002	p 49	A89-35853 #	p 64
A89-34003	p 9	A89-35854 #	p 22
A89-34004	p 9	A89-35855 #	p 22
A89-34005	p 10	A89-35856 #	p 6
A89-34006	p 10	A89-35857 #	p 11
A89-34007	p 10	A89-35858 #	p 50
A89-34009	p 10	A89-35859 #	p 11
A89-34010	p 49	A89-35860 #	p 11
A89-34011	p 15	A89-35861 #	p 50
A89-34012	p 10	A89-35862 #	p 50
A89-34013	p 20	A89-35863 #	p 22
A89-34014	p 20	A89-35864 #	p 16
A89-34015	p 20	A89-35865 *	p 1
A89-34016	p 10	A89-35866 #	p 51
A89-34017	p 10	A89-35867 *	p 22
A89-34018	p 10	A89-35868 #	p 11
A89-34088	p 49	A89-35869 #	p 6
A89-34196	p 10	A89-35870 #	p 22
A89-34266 *	p 20	A89-35871 #	p 51
A89-34267 #	p 49	A89-35872 #	p 11
A89-34268	p 20	A89-35873 #	p 11
A89-34353	p 50	A89-35874 #	p 11
A89-34357 *	p 6	A89-35875 *	p 51
A89-34362	p 50	A89-35876 #	p 22
A89-34363	p 20	A89-35877 #	p 23
A89-34416 *	p 21	A89-35878 #	p 51

A89-35879	#	p 7	A89-39092	p 54	A89-41750	p 34
A89-35880	#	p 7	A89-39093	p 28	A89-41761	p 56
A89-35881	#	p 12	A89-39094	p 28	A89-41845	p 34
A89-35882	#	p 7	A89-39095	p 28	A89-42149	p 13
A89-35883	*	p 23	A89-39096	p 28	A89-42173	p 57
A89-35884	#	p 7	A89-39097	p 28	A89-42175	p 35
A89-35885	#	p 23	A89-39098	p 54	A89-42181	p 13
A89-35886	#	p 12	A89-39099	p 28	A89-42511	p 64
A89-35887	#	p 12	A89-39100	p 29	A89-42549	p 65
A89-35888	#	p 12	A89-39322	p 54	A89-42601	p 57
A89-35889	#	p 23	A89-39372	p 16	A89-42608	p 57
A89-35890	#	p 51	A89-39546	p 29	A89-42609	p 57
A89-35891	#	p 51	A89-39551	p 29	A89-42610	p 35
A89-35892	#	p 23	A89-39552	p 29	A89-42611	p 35
A89-35893	#	p 1	A89-39554	p 2	A89-42612	p 35
A89-35894	*	p 2	A89-39555	p 54	A89-42614	p 35
A89-35895	#	p 23	A89-39556	p 29	A89-42684	p 57
A89-35896	#	p 12	A89-39557	p 54	A89-42773	p 57
A89-35897	#	p 12	A89-39650	p 29	A89-42787	p 7
A89-35898	#	p 23	A89-39651	p 12	A89-42795	p 13
A89-35899	#	p 64	A89-39652	p 55	A89-42941	p 58
A89-35900	#	p 24	A89-39655	p 12	A89-43024	p 35
A89-35902	*	p 24	A89-39656	p 30	A89-43026	p 58
A89-35903	#	p 24	A89-39657	p 2	A89-43311	p 58
A89-35906	#	p 24	A89-39658	p 2	A89-43316	p 35
A89-35907	#	p 16	A89-39659	p 16	A89-43317	p 3
A89-35912	#	p 24	A89-39674	p 30	A89-43408	p 58
A89-35926	#	p 24	A89-39739	p 4	A89-43409	p 58
A89-35931	#	p 16	A89-39870	p 55	A89-43410	p 13
A89-35937	#	p 17	A89-39872	p 55	A89-43541	p 36
A89-35939	*	p 52	A89-39875	p 30		
A89-35949	*	p 52	A89-40126	p 55	N89-20430	p 58
A89-35966	*	p 52	A89-40129	p 55	N89-20531	p 36
A89-36686	*	p 52	A89-40134	p 30	N89-20532	p 58
A89-36704	*	p 24	A89-40135	p 30	N89-20533	p 18
A89-37291	*	p 25	A89-40136	p 55	N89-20534	p 4
A89-37315	#	p 12	A89-40139	p 30	N89-20535	p 36
A89-37316	#	p 52	A89-40143	p 30	N89-20536	p 36
A89-37318	#	p 25	A89-40145	p 17	N89-20537	p 36
A89-37319	#	p 17	A89-40148	p 55	N89-20538	p 36
A89-37320	#	p 2	A89-40149	p 2	N89-20539	p 59
A89-37321	#	p 25	A89-40150	p 3	N89-20540	p 65
A89-37322	#	p 52	A89-40151	p 56	N89-20541	p 4
A89-37323	#	p 25	A89-40152	p 56	N89-20542	p 59
A89-37324	#	p 25	A89-40153	p 30	N89-20543	p 59
A89-37325	#	p 25	A89-40154	p 31	N89-20544	p 65
A89-37327	#	p 52	A89-40155	p 31	N89-20545	p 17
A89-37349	#	p 53	A89-40156	p 31	N89-20868	p 14
A89-37471	#	p 25	A89-40263	p 31	N89-21162	p 37
A89-37492	#	p 53	A89-40488	p 31	N89-21165	p 37
A89-37549	*	p 53	A89-40491	p 31	N89-21218	p 59
A89-37554	*	p 53	A89-40606	p 31	N89-21317	p 37
A89-37571	*	p 16	A89-41076	p 32	N89-21318	p 37
A89-37627	*	p 53	A89-41151	p 32	N89-21328	p 14
A89-37801	#	p 25	A89-41152	p 32	N89-21358	p 59
A89-37802	*	p 53	A89-41153	p 3	N89-21415	p 14
A89-37808	*	p 26	A89-41154	p 32	N89-21416	p 14
A89-37944	*	p 26	A89-41155	p 3	N89-21431	p 37
A89-37945	*	p 26	A89-41156	p 32	N89-21452	p 38
A89-37946	*	p 26	A89-41157	p 32	N89-21480	p 38
A89-37947	*	p 26	A89-41158	p 32	N89-21507	p 38
A89-37948	*	p 26	A89-41159	p 32	N89-21521	p 38
A89-37949	*	p 2	A89-41160	p 18	N89-21568	p 38
A89-37950	*	p 26	A89-41161	p 33	N89-21643	p 38
A89-37981	#	p 53	A89-41162	p 13	N89-22152	p 39
A89-38290	#	p 53	A89-41163	p 33	N89-22154	p 59
A89-38328	#	p 26	A89-41164	p 56	N89-22155	p 60
A89-38330	#	p 53	A89-41165	p 56	N89-22156	p 39
A89-38332	#	p 27	A89-41166	p 33	N89-22157	p 39
A89-38333	#	p 27	A89-41167	p 13	N89-22158	p 39
A89-38334	#	p 27	A89-41168	p 33	N89-22159	p 39
A89-38583	#	p 7	A89-41169	p 33	N89-22160	p 39
A89-38766	#	p 16	A89-41170	p 33	N89-22161	p 60
A89-38897	#	p 4	A89-41171	p 34	N89-22162	p 60
A89-38966	#	p 54	A89-41172	p 34	N89-22163	p 3
A89-38967	#	p 54	A89-41173	p 34	N89-22164	p 40
A89-38968	*	p 27	A89-41174	p 34	N89-22165	p 40
A89-38969	*	p 2	A89-41175	p 34	N89-22166	p 40
A89-38970	*	p 27	A89-41176	p 34	N89-22167	p 3
A89-38971	*	p 27	A89-41177	p 18	N89-22168	p 40
A89-38972	*	p 27	A89-41178	p 18	N89-22169	p 60
A89-39062	*	p 16	A89-41179	p 56	N89-22170	p 61
A89-39063	*	p 28	A89-41692	p 56	N89-22173	p 40

N89-22174**ACCESSION NUMBER INDEX**

N89-22174 # p 7
N89-22175 # p 18
N89-22183 # p 18
N89-22189 # p 4
N89-22191 # p 61
N89-22192 # p 5
N89-22255 * # p 14
N89-22263 * # p 15
N89-22280 # p 19
N89-22293 # p 41
N89-22344 * # p 41
N89-22779 * # p 61
N89-22969 * # p 5
N89-22970 * # p 61
N89-22971 * # p 41
N89-22972 # p 41
N89-22973 # p 41
N89-22975 * # p 61
N89-22976 # p 65
N89-22977 # p 41
N89-22978 # p 42
N89-22979 * # p 42
N89-23031 # p 42
N89-23080 # p 42
N89-23101 # p 42
N89-23122 # p 62
N89-23287 # p 62
N89-23371 # p 42
N89-23437 # p 8
N89-23766 * # p 8
N89-23941 # p 8
N89-23942 # p 62
N89-23943 # p 8
N89-23944 # p 8
N89-23945 # p 8
N89-23946 # p 43
N89-23947 # p 43
N89-23948 # p 43
N89-23949 # p 43
N89-23950 # p 43
N89-23951 # p 43
N89-23952 # p 43
N89-23953 # p 43
N89-23954 # p 44
N89-23955 # p 44
N89-23956 * # p 62
N89-23957 # p 44
N89-23958 # p 44
N89-23959 # p 44
N89-23960 # p 44
N89-23961 * # p 9
N89-23962 # p 45
N89-23963 # p 45
N89-23964 # p 45
N89-23965 # p 45
N89-23967 # p 45
N89-23968 # p 46
N89-23969 # p 65
N89-23970 # p 62
N89-23971 # p 46
N89-23972 # p 62
N89-23982 * # p 5
N89-23985 * # p 5
N89-23992 # p 46
N89-24013 # p 46
N89-24014 # p 17
N89-24015 * # p 3
N89-24060 * # p 9
N89-24589 # p 63
N89-24685 # p 3
N89-24686 * # p 46
N89-24687 * # p 3
N89-24688 # p 63
N89-24689 # p 63
N89-24690 # p 46
N89-24691 # p 63
N89-24692 # p 63
N89-24693 # p 46
N89-24694 # p 63
N89-24695 * # p 63
N89-24696 # p 47
N89-24697 # p 63
N89-24698 # p 63
N89-24699 # p 47
N89-24700 # p 47
N89-24701 # p 64
N89-24749 # p 5
N89-24756 * # p 47
N89-24757 * # p 15
N89-24759 # p 6
N89-24784 * # p 47

AVAILABILITY OF CITED PUBLICATIONS

IAA ENTRIES (A89-10000 Series)

Publications announced in *IAA* are available from the AIAA Technical Information Service as follows: Paper copies of accessions are available at \$10.00 per document (up to 50 pages), additional pages \$0.25 each. Microfiche⁽¹⁾ of documents announced in *IAA* are available at the rate of \$4.00 per microfiche on demand. Standing order microfiche are available at the rate of \$1.45 per microfiche for *IAA* source documents and \$1.75 per microfiche for AIAA meeting papers.

Minimum air-mail postage to foreign countries is \$2.50. All foreign orders are shipped on payment of pro-forma invoices.

All inquiries and requests should be addressed to: Technical Information Service, American Institute of Aeronautics and Astronautics, 555 West 57th Street, New York, NY 10019. Please refer to the accession number when requesting publications.

STAR ENTRIES (N89-10000 Series)

One or more sources from which a document announced in *STAR* is available to the public is ordinarily given on the last line of the citation. The most commonly indicated sources and their acronyms or abbreviations are listed below. If the publication is available from a source other than those listed, the publisher and his address will be displayed on the availability line or in combination with the corporate source line.

Avail: NTIS. Sold by the National Technical Information Service. Prices for hard copy (HC) and microfiche (MF) are indicated by a price code preceded by the letters HC or MF in the *STAR* citation. Current values for the price codes are given in the tables on NTIS PRICE SCHEDULES.

Documents on microfiche are designated by a pound sign (#) following the accession number. The pound sign is used without regard to the source or quality of the microfiche.

Initially distributed microfiche under the NTIS SRIM (Selected Research in Microfiche) is available at greatly reduced unit prices. For this service and for information concerning subscription to NASA printed reports, consult the NTIS Subscription Section, Springfield, Va. 22161.

NOTE ON ORDERING DOCUMENTS: When ordering NASA publications (those followed by the * symbol), use the N accession number. NASA patent applications (only the specifications are offered) should be ordered by the US-Patent-Appl-SN number. Non-NASA publications (no asterisk) should be ordered by the AD, PB, or other *report number* shown on the last line of the citation, not by the N accession number. It is also advisable to cite the title and other bibliographic identification.

Avail: SOD (or GPO). Sold by the Superintendent of Documents, U.S. Government Printing Office, in hard copy. The current price and order number are given following the availability line. (NTIS will fill microfiche requests, as indicated above, for those documents identified by a # symbol.)

(1) A microfiche is a transparent sheet of film, 105 by 148 mm in size containing as many as 60 to 98 pages of information reduced to micro images (not to exceed 26.1 reduction).

- Avail: BLL (formerly NLL): British Library Lending Division, Boston Spa, Wetherby, Yorkshire, England. Photocopies available from this organization at the price shown. (If none is given, inquiry should be addressed to the BLL.)
- Avail: DOE Depository Libraries. Organizations in U.S. cities and abroad that maintain collections of Department of Energy reports, usually in microfiche form, are listed in *Energy Research Abstracts*. Services available from the DOE and its depositories are described in a booklet, *DOE Technical Information Center - Its Functions and Services* (TID-4660), which may be obtained without charge from the DOE Technical Information Center.
- Avail: ESDU. Pricing information on specific data, computer programs, and details on ESDU topic categories can be obtained from ESDU International Ltd. Requesters in North America should use the Virginia address while all other requesters should use the London address, both of which are on the page titled ADDRESSES OF ORGANIZATIONS.
- Avail: Fachinformationszentrum, Karlsruhe. Sold by the Fachinformationszentrum Energie, Physik, Mathematik GMBH, Eggenstein Leopoldshafen, Federal Republic of Germany, at the price shown in deutschmarks (DM).
- Avail: HMSO. Publications of Her Majesty's Stationery Office are sold in the U.S. by Pendragon House, Inc. (PHI), Redwood City, California. The U.S. price (including a service and mailing charge) is given, or a conversion table may be obtained from PHI.
- Avail: NASA Public Document Rooms. Documents so indicated may be examined at or purchased from the National Aeronautics and Space Administration, Public Documents Room (Room 126), 600 Independence Ave., S.W., Washington, D.C. 20546, or public document rooms located at each of the NASA research centers, the NASA Space Technology Laboratories, and the NASA Pasadena Office at the Jet Propulsion Laboratory.
- Avail: Univ. Microfilms. Documents so indicated are dissertations selected from *Dissertation Abstracts* and are sold by University Microfilms as xerographic copy (HC) and microfilm. All requests should cite the author and the Order Number as they appear in the citation.
- Avail: US Patent and Trademark Office. Sold by Commissioner of Patents and Trademarks, U.S. Patent and Trademark Office, at the standard price of \$1.50 each, postage free. (See discussion of NASA patents and patent applications below.)
- Avail: (US Sales Only). These foreign documents are available to users within the United States from the National Technical Information Service (NTIS). They are available to users outside the United States through the International Nuclear Information Service (INIS) representative in their country, or by applying directly to the issuing organization.
- Avail: USGS. Originals of many reports from the U.S. Geological Survey, which may contain color illustrations, or otherwise may not have the quality of illustrations preserved in the microfiche or facsimile reproduction, may be examined by the public at the libraries of the USGS field offices whose addresses are listed in this Introduction. The libraries may be queried concerning the availability of specific documents and the possible utilization of local copying services, such as color reproduction.
- Avail: Issuing Activity, or Corporate Author, or no indication of availability. Inquiries as to the availability of these documents should be addressed to the organization shown in the citation as the corporate author of the document.

PUBLIC COLLECTIONS OF NASA DOCUMENTS

DOMESTIC: NASA and NASA-sponsored documents and a large number of aerospace publications are available to the public for reference purposes at the library maintained by the American Institute of Aeronautics and Astronautics, Technical Information Service, 555 West 57th Street, 12th Floor, New York, New York 10019.

EUROPEAN: An extensive collection of NASA and NASA-sponsored publications is maintained by the British Library Lending Division, Boston Spa, Wetherby, Yorkshire, England for public access. The British Library Lending Division also has available many of the non-NASA publications cited in *STAR*. European requesters may purchase facsimile copy or microfiche of NASA and NASA-sponsored documents, those identified by both the symbols # and * from ESA – Information Retrieval Service European Space Agency, 8-10 rue Mario-Nikis, 75738 CEDEX 15, France.

FEDERAL DEPOSITORY LIBRARY PROGRAM

In order to provide the general public with greater access to U.S. Government publications, Congress established the Federal Depository Library Program under the Government Printing Office (GPO), with 50 regional depositories responsible for permanent retention of material, inter-library loan, and reference services. At least one copy of nearly every NASA and NASA-sponsored publication, either in printed or microfiche format, is received and retained by the 50 regional depositories. A list of the regional GPO libraries, arranged alphabetically by state, appears on the inside back cover. These libraries are *not* sales outlets. A local library can contact a Regional Depository to help locate specific reports, or direct contact may be made by an individual.

STANDING ORDER SUBSCRIPTIONS

NASA SP-7041 and its supplements are available from the National Technical Information Service (NTIS) on standing order subscription as PB 89-903800 at the price of \$15.50 domestic and \$31.00 foreign. Standing order subscriptions do not terminate at the end of a year, as do regular subscriptions, but continue indefinitely unless specifically terminated by the subscriber.

ADDRESSES OF ORGANIZATIONS

American Institute of Aeronautics and
Astronautics
Technical Information Service
555 West 57th Street, 12th Floor
New York, New York 10019

British Library Lending Division,
Boston Spa, Wetherby, Yorkshire,
England

Commissioner of Patents and
Trademarks
U.S. Patent and Trademark Office
Washington, D.C. 20231

Department of Energy
Technical Information Center
P.O. Box 62
Oak Ridge, Tennessee 37830

ESA-Information Retrieval Service
ESRIN
Via Galileo Galilei
00044 Frascati (Rome) Italy

ESDU International, Ltd.
1495 Chain Bridge Road
McLean, Virginia 22101

ESDU International, Ltd.
251-259 Regent Street
London, W1R 7AD, England

Fachinformationszentrum Energie, Physik,
Mathematik GMBH
7514 Eggenstein Leopoldshafen
Federal Republic of Germany

Her Majesty's Stationery Office
P.O. Box 569, S.E. 1
London, England

NASA Scientific and Technical Information
Facility
P.O. Box 8757
B.W.I. Airport, Maryland 21240

National Aeronautics and Space
Administration
Scientific and Technical Information
Branch (NTT)
Washington, D.C. 20546

National Technical Information Service
5285 Port Royal Road
Springfield, Virginia 22161

Pendragon House, Inc.
899 Broadway Avenue
Redwood City, California 94063

Superintendent of Documents
U.S. Government Printing Office
Washington, D.C. 20402

University Microfilms
A Xerox Company
300 North Zeeb Road
Ann Arbor, Michigan 48106

University Microfilms, Ltd.
Tylers Green
London, England

U.S. Geological Survey Library
National Center - MS 950
12201 Sunrise Valley Drive
Reston, Virginia 22092

U.S. Geological Survey Library
2255 North Gemini Drive
Flagstaff, Arizona 86001

U.S. Geological Survey
345 Middlefield Road
Menlo Park, California 94025

U.S. Geological Survey Library
Box 25046
Denver Federal Center, MS914
Denver, Colorado 80225

NTIS PRICE SCHEDULES

(Effective January 1, 1989)

Schedule A STANDARD PRICE DOCUMENTS AND MICROFICHE

PRICE CODE	NORTH AMERICAN PRICE	FOREIGN PRICE
A01	\$ 6.95	\$13.90
A02	10.95	21.90
A03	13.95	27.90
A04-A05	15.95	31.90
A06-A09	21.95	43.90
A10-A13	28.95	57.90
A14-A17	36.95	73.90
A18-A21	42.95	85.90
A22-A25	49.95	99.90
A99	*	*
NO1	55.00	70.00
NO2	55.00	80.00

Schedule E EXCEPTION PRICE DOCUMENTS AND MICROFICHE

PRICE CODE	NORTH AMERICAN PRICE	FOREIGN PRICE
E01	\$ 9.00	\$ 18.00
E02	11.50	23.00
E03	13.00	26.00
E04	15.50	31.00
E05	17.50	35.00
E06	20.50	41.00
E07	23.00	46.00
E08	25.50	51.00
E09	28.00	56.00
E10	31.00	62.00
E11	33.50	67.00
E12	36.50	73.00
E13	39.00	78.00
E14	42.50	85.00
E15	46.00	92.00
E16	50.50	101.00
E17	54.50	109.00
E18	59.00	118.00
E19	65.50	131.00
E20	76.00	152.00
E99	*	*

*Contact NTIS for price quote.

IMPORTANT NOTICE

NTIS Shipping and Handling Charges

U.S., Canada, Mexico — ADD \$3.00 per TOTAL ORDER

All Other Countries — ADD \$4.00 per TOTAL ORDER

Exceptions — Does NOT apply to:

ORDERS REQUESTING NTIS RUSH HANDLING
ORDERS FOR SUBSCRIPTION OR STANDING ORDER PRODUCTS *ONLY*

NOTE: Each additional delivery address on an order
requires a separate shipping and handling charge.

1. Report No. NASA SP-7041 (63)		2. Government Accession No.		3. Recipient's Catalog No.	
4. Title and Subtitle EARTH RESOURCES A Continuing Bibliography with Indexes (Issue 63)				5. Report Date October 1989	
				6. Performing Organization Code	
7. Author(s)				8. Performing Organization Report No.	
9. Performing Organization Name and Address National Aeronautics and Space Administration Washington, DC 20546				10. Work Unit No.	
				11. Contract or Grant No.	
12. Sponsoring Agency Name and Address				13. Type of Report and Period Covered	
				14. Sponsoring Agency Code	
15. Supplementary Notes					
16. Abstract <p>This bibliography lists 449 reports, articles and other documents introduced into the NASA scientific and technical information system between July 1 and September 30, 1989. Emphasis is placed on the use of remote sensing and geophysical instrumentation in spacecraft and aircraft to survey and inventory natural resources and urban areas. Subject matter is grouped according to agriculture and forestry, environmental changes and cultural resources, geodesy and cartography, geology and mineral resources, hydrology and water management, data processing and distribution systems, instrumentation and sensors, and economic analysis.</p>					
17. Key Words (Suggested by Authors(s)) Bibliographies Earth Resources Remote Sensors			18. Distribution Statement Unclassified - Unlimited		
19. Security Classif. (of this report) Unclassified		20. Security Classif. (of this page) Unclassified		21. No. of Pages 130	
				22. Price * A07/HC	

*For sale by the National Technical Information Service, Springfield, Virginia 22161